МІНІСТЕРСТВО ОСВІТИ І НАУКИ УКРАЇНИ

ДВНЗ «Прикарпатський національний університет імені Василя Стефаника»
Кафедра фізики і хімії твердого тіла
Фізико-хімічний інститут
Навчально-дослідний центр напівпровідникового матеріалознавства

АКАДЕМІЯ НАУК ВИЩОЇ ШКОЛИ УКРАЇНИ

НАЦІОНАЛЬНА АКАДЕМІЯ НАУК УКРАЇНИ
Інститут фізики напівпровідників ім. В.Є. Лашкарьова
Інститут хімії поверхні ім. О.О. Чуйка
Інститут металофізики ім. Г.В. Курдюмова
Інститут загальної і неорганічної хімії ім. В.І. Вернадського
Українське фізичне товариство
Інститут інноваційних досліджень (Івано-Франківськ, Україна)
Університет Цзілінь (Чанчунь, Китай)

XVII МІЖНАРОДНА ФРЕЇКІВСЬКА КОНФЕРЕНЦІЯ З ФІЗИКИ І ТЕХНОЛОГІЇ ТОНКИХ ПЛІВОК ТА НАНОСИСТЕМ

Збірник тез

Івано-Франківськ, 20-25 травня, 2019

Ivano-Frankivsk, May 20-25, 2019

Abstract book

XVII INTERNATIONAL FREIK CONFERENCE ON PHYSICS AND TECHNOLOGY OF THIN FILMS AND NANOSYSTEMS

MINISTRY OF EDUCATION AND SCIENCE OF UKRAINE
Vasyl Stefanyk Precarpathian National University
Physics and Chemistry of Solids Department
Physical-Chemical Institute
Educational Research Centre for Semiconductor Material

ACADEMY OF SCIENCE OF HIGH SCHOOL OF UKRAINE

NATIONAL ACADEMY OF SCIENCE OF UKRAINE
V.E. Lashkarev Institute of Semiconductor Physics
Chuiko Institute of Surface Chemistry
G.V. Kurdyumov Institute of the Physics of Metals
V.I. Vernadsky Institute of General and Inorganic Chemistry
Ukraine Physics Society
Institute of Innovation Research (Ivano-Frankivsk, Ukraine)
Jilin University (Changchun, P. R. China)

УДК 539.2
ББК 22.373.1

П 80

XVII Міжнародна Фреїківська конференція з фізики і технології тонких плівок та наносистем. ***Збірник тез.*** / За заг. ред. проф. В.В. Прокопіва. Івано-Франківськ : Видавництво Прикарпатського національного університету імені Василя Стефаника, 2019. 376 с.

Представлено сучасні результати теоретичних і експериментальних досліджень з питань фізики і технології тонких плівок та наносистем: метали, напівпровідники, діелектрики, провідні полімери; методи отримання та дослідження; фізико-хімічні властивості; нанотехнології і наноматеріали, квантово-розмірні структури, наноелектроніка, тощо. Матеріали підготовлено до друку Програмним комітетом конференції і подано в авторській редакції.

Для наукових та інженерних працівників, що займаються проблемами тонкоплівкового матеріалознавства, мікро- та наноелектроніки.

Рекомендовано до друку науково-технічною радою Фізико-хімічного інституту ДВНЗ «Прикарпатський національний університет імені Василя Стефаника»

XVII International Freik Conference Physics and Technology of Thin Films and Nanosystems. ***Abstract book.*** / Ed. by Prof. V.V. Prokopiv. Ivano-Frankivsk : Publisher Vasyl Stefanyk Precarpathian National University, 2019. 376 c.

The results of theoretical and experimental researches in directions of the physics and technology of thin films and nanosystems: metals, semiconductors, dielectrics, and polymers; and methods of their investigation; physic-chemical properties of thin films; nanotechnology and nanomaterials, quantum-size structures; thin-film devices of electronics, are presented. The materials preformed for printing by Conference's Organizational Committee and Editorial Board, are conveyed in authoring edition.

For scientists and reserchers on the field of thin-film material sciences, micro- and nanoelectronics.

PROGRAM COMMITTEE / EDITORAL BOARD

PLENARY SESSIONS

Photon Counting X-ray Image Sensor by Laser Doping Process

Aoki Toru[1,2], Takagi Katsuyuki[1,2], Takagi Toshiyuki[1], Terao Tsuyoshi[1,2], Kase Hiroki [1,2], Gnatyuk Volodymyr [1,3], Koike Akifumi [1,2]

[1]*Research Institute of Electronics, Shizuoka University, Hamamatsu, Japan,*
aoki.toru@shizuoka.ac.jp
[2]*ANSeeN Inc. Hamamatsu, Japan*
[3]*V.E. Lashkaryov Institute of Semiconductor Physics of the NAS of Ukraine, Kyiv, Ukraine*

Laser processing of the CdTe-In semiconductor-metal interface has been studied by irradiation through the CdTe crystal in water using nanosecond pulses with λ= 1064 nm. A thin In-doped CdTe layer adjoining to the In film was formed after direct laser impact on the CdTe-In interface (Fig.1). The fabricated In/CdTe/Au diode detectors with a p-n junction exhibited steep rectification and sensitivity to X/γ-ray radiation. The simulation of laser-induced heating of the In film deposited on the CdTe crystal surface and irradiated through the CdTe in water was performed and temperature distribution in the three layer CdTe-In-Water structure at different moments after laser irradiation was calculated.

The main application of this laser doping is fabrication of high-energy radiation detector, but this method also effective for making solar-cells, sensors and so on. In this paper, we will show the detail data and discussion of mechanism of this laser doping process by using both results of irradiated by top (In-side) and back (through CdTe wafer) side.

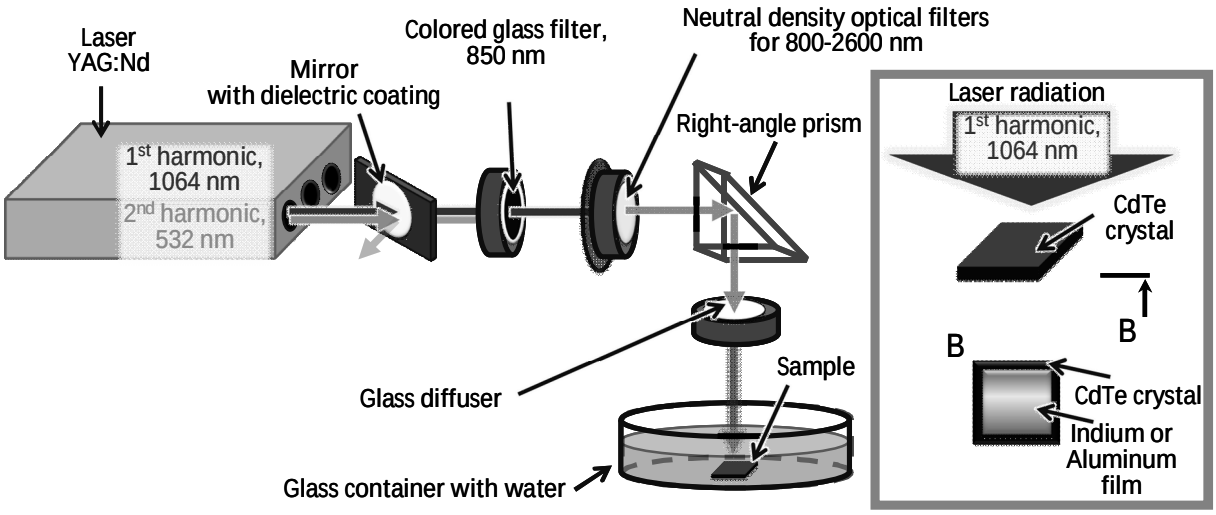

Fig.1 Experimental setup of the optical equipment for irradiation of the CdTe-metal structure in water with pulses of the 1st harmonic of a YAG:Nd laser (λ = 1064 nm, τ = 8 ns).
Insert shows a CdTe crystal with a deposited metal film (In or Al electrode) and irradiation of the CdTe-metal interface through the CdTe).

Investigation of the Dislocation Structure of CdTe Crystals and Its Influence on the Characteristics of Barrier Structures Constructed on Their Basis

Fodchuk I.M.[1], Kuzmin A.R[1], Gutsuliak I.I[1], Solodkyi M.S.[1], Maslyanchuk O.L.[1], Kazemirskiy T.A.[1], Gudymenko O.[2], Kladko V.P.[2]

[1] *Chernivtsi National University, Chernivtsi, Ukraine*
[2] *Institute of Semiconductor Physics of NASU, Kyiv, Ukraine, ifodchuk@ukr.net*

The research objects are a set of high resistive ($\rho=(2\text{-}4)\cdot10^9$ Ohm·cm at 300 K) CdTe single crystals (111) and barrier structures made of them. Methods of high-resolution X-ray diffraction were used to investigate dislocation structure in CdTe bulk samples, search for new contact materials and study their influence on electrical and physical properties of X- and γ-radiation detectors made based on MoO_x/p-CdTe heterostructures [1].

Experimental investigations with different diffraction sets (symmetric 333 and asymmetric 331 reflections of Cu$K_{\alpha1}$-radiation) were performed on Philips X'Pert PRO diffractometer. The influence of possible dislocation system in CdTe is analyzed based on Krivoglaz kinematic theory and Monte-Carlo method [2].

The samples have several types of defects, including dislocation loops, Lomer-Cottrell locks and inclusions of different phase. Estimated dislocation densities are within ~10^5 – 10^6 cm^{-2}. The dislocation pattern was represented as two possible sets of full 60^0 dislocations with lines perpendicular to the surface and Burgers vectors $b_1 = a/2[\bar{1}10]$, $b_F = a/2[011]$ in (111) plane.

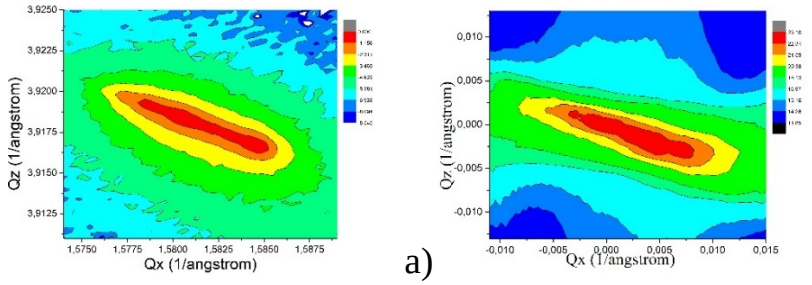

a) b)

Fig. 1. Experimental (a) and simulated (b) RSMs, 331, Cu$K_{\alpha1}$.

Correlation between the defect (dislocation) system in CdTe, mismatch deformations in transition layers of Mo-MoO_x/p-CdTe/MoO_x-Mo Schottky barrier structures and their electrical and physical properties is established.

1. O. L. Maslyanchuk, M. M. Solovan, V. V. Brus, et al., Capabilities of CdTe-based Detectors with MoOx Contacts for Detection of X-and γ-radiation // *IEEE Transactions on Nuclear*. 2017. V.64,№5. P. 1168-1172
2. Vladimir M. Kaganer, Karl K. Sabelfeld, X-ray diffraction peaks from partially ordered misfit dislocations // *Physical Review B.* 2009. V.80. P.184105.

Use of the Seebeck Effect for Converging of the Thermal Energy of Sun into Electricity

Halushchak M.O.

Ivano-Frankivsk National Technical University of Oil and Gas,
Ivano-Frankivsk, Ukraine, galuschak@nung.edu.ua

Due to the growing of environmental tasks and due to the gradual exhaustion of existing natural resources, the need for alternative energy sources becomes increasingly tangible.

Solar radiation is one of the most promising types of renewable energy sources. The annual amount of solar energy in thousands of times exceeds the needs of the population for our planet, but only small part of it is used to solve these needs. The use of the classical approach to solving power supply problems with the use of solar cells is the most well-known and simple, but it is ineffective under conditions of low solar insolation. It is also known that solar cells can only absorb 18% of the solar radiation that falls on them. Most of the energy of the sun, which is approximately 70%, is dissipated in the form of thermal energy, which can not be used by photovoltaic. Therefore, it is expedient to use the heat energy itself to convert it into electricity. Therefore, solar energy, combined with thermoelectricity, today has all the prerequisites to partially solve the energy problems of Ukraine.

We have been developed new method and technology for the production of thermoelectric semiconductor materials on the base of high thermoelectric figure of merit lead telluride and confirmed the promise of their use in the range of operating temperatures 400-850 K. We note that thermoelectric materials (TE) are characterized by a number of parameters that determine the effectiveness of their practical use, namely: the specific electrical resistance (r), the coefficient of thermo-e.m.f. (a), coefficient of thermal conductivity (c), thermoelectric figure of merit ($Z = \frac{a^2}{rc}$), dimensionless thermoelectric figure of merit (ZT). Thermoelectric materials for which ZT ≈ 1 are considered to be promising for practical application.

The main ways of improving the thermoelectric parameters of the semiconductor material through optimization by reducing the thermal conductivity and increasing the electrical conductivity are established. It is confirmed that the thermal conductivity of the material is determined by the nature of the scattering of phonons, which can be made more effective when doped with isovalent or heterovalent impurities in solid solutions. Also, a confirmation of the growth of specific conductivity with an increase in the amount of impurity has been obtained, which leads to increase the carriers concentration and next increases of the electrical conductivity.

The construction of a thermoelectric generator (TEG) for the transformation of solar thermal energy accumulated by liquid moving through a cylindrical tube into an electricity is proposed. A system of developed TEG consisting of twenty thermoelements in the size of 5x5x0.4 cm is placed around a pipe with a heated fluid, which at difference temperature of 150°C between cold and hot planes yields a useful power of 237.3 W.

Consequently, the direct way of solar thermal energy transforming into electricity with use of thermoelectric energy converters is most suitable, despite the fact that for thermoelectric transformation, a rather low efficiency, which is up to 10%, is characteristic. At the same time, investigation on obtaining of the new thermoelectric materials will increase it to 15-20%, which will significantly increase the economic efficiency of this method.

1. Kim, R. Y., Lai, J. S., York, B., and Koran, A.: ‘Analysis and design of maximum power point tracking scheme for thermoelectric battery energy storage system’, IEEE T.Instrum. Meas., 2009, 56, (9), pp. 3709–3716.
2. Niu, X., Yu, J., and Wang, S.: ‘Experimental study on low–temperature waste heat thermoelectric generator, J. Power Sources, 2009, 188, (2), pp. 621–626.

The Development of Technology CdTe and CdS Layers for Thin-Film Soilar Cells Creation

Khrypunov G.S., Kudii D.A., Kovtun N.A., Khrypunov M.G.

National Technical University "Kharkiv Polytechnic Institute", Kharkiv, Ukraine,
khrip@ukr.net, klochko.np16@gmail.com

The CdTe thin film solar cells have now reached long-term stable performance, high efficiency and easy scale-up for large area production. The highest efficiencies in CdTe solar cells have been obtained using close space sublimation CSS deposition method, which requires a high substrate temperature (~550 °C). Unfortunately the development of flexible CdTe solar cells on polymers is difficult with the CSS process because of the high substrate temperatures encountered during sublimation process. On the other hand, conventional physical vapor deposition (PVD) process where CdTe is evaporated in a high vacuum evaporation (HVE) system at lower substrate temperatures (typically 300°C) has also provided solar cells with efficiencies exceeding 12% on low cost soda-lime glass substrates . For these reasons HVE process is attractive for a very simple in-line deposition of large area CdTe solar modules on soda-lime glass substrates, as well as on polymer foils thereby facilitating the roll-to-roll manufacturing of flexible solar modules. Therefore, optimization of the technology for cadmium sulfide and cadmium telluride films production is an actual task.

Under optimization of the cadmium telluride base layers deposited by thermal vacuum evaporation it has been established that the main defects of the structure, namely twins and stacking faults, accompany to the <111> axial texture in CdTe face-centered cubic lattice and to the layerwise film growth.

It has been shown that the optimal thickness of the "chloride treated" base layer in the thin film ITO/CdS/CdTe/Cu/Au solar cells (SC) equals 4 μm. The decreasing of CdTe film thickness leads to the SC efficiency decreasing as a result of the shunting resistance reduction, saturation diode current density and series resistance increasing. The CdTe film thickness growth leads to the SC efficiency decreasing because of the shunting resistance reduction and series resistance increasing.

Experimentally approved the possibility of the deposition by close box method of the high-quality from the point of view of their structure CdTe base layers at the substrate temperatures in the range 300 - 450°C.

It has been shown that for thin film glass/ITO/CdS/CdTe/Cu/Au SC optimal cadmium sulfide thickness equals 0.4 μm because of two competitive physical processes, namely, simultaneous variation of the diode saturation current density and the photocurrent density

It has been experimentally demonstrated that the maximal efficiency of ITO/CdS/CdTe/Cu/Au SC corresponds to the 0,35 μm $CdCl_2$ thickness at "chloride treatment". In this case both minimal series resistance and lowest diode saturation current density are achieved simultaneously

Physical and Technical Bases of Functional Thin Film Solid-State Structures Constructive-Technological Solution for Combined Photovoltaic Systems

Khrypunov G.S., Zaitsev R.V.

[1]*National Technical University "Kharkiv Polytechnic Institute", Kharkiv, Ukraine,*
klochko.np16@gmail.com

The development of the physicotechnical foundations of design and technology solutions of functional thin-filmed solid-state structures of economical and efficient combined photovoltaic energetic systems suitable for large-scale production was carried out.

The paper formulates the physic-technical patterns of functional solid-state structures creation, including thin-filmed layers, multilayer systems and systems with a developed surface, for the realization with their help of combined photovoltaic energetic systems with increased efficiency in thermal and electrical energy.

The innovative measuring stands for determining the photovoltaic parameters of solar cells and modules were developed. A study of working temperature influence on the efficiency of photovoltaic converters was made, the optimal functional layers were selected, and on their basis, samples of highly efficient combined photovoltaic systems were created and tested.

As a result of carrying out complex experimental and theoretical studies, the problem of developing the physic-technical foundations of design and technology solutions of functional solid-state device structures for combined photovoltaic energetic systems, which allow significantly increase the efficiency of complex conversion of solar irradiation into electrical and thermal energy, was solved.

When conducting research, combined photovoltaic installations were implemented in the form of low-concentration systems based on uninjunction silicon photovoltaic devices, highly concentrated systems based on multi-junction silicon solar modules and InGaP/InGaAs/Ge micromodules and solar collectors with integrated flexible solar cells based on cadmium telluride into their structure.

Carbon Rich Silicon Carbide and Silicon Carbonitride Films: New Protective and Antireflection Coatings

Klyui N.I.[1,2]

[1]*College of Physics, Jilin University, Changchun, People's Republic of China*
[2]*V. Lashkaryov Institute of Semiconductor Physics, National Academy of Sciences of Ukraine, Kyiv, Ukraine,* klyuini@ukr.net

A technology for preparation of amorphous carbon rich hydrogenated silicon carbide (a-Si_xC_{1-x}:H) and silicon carbonitride (a-$Si_xC_{1-x}N_y$:H) films by PE-CVD method has been developed.

The films were deposited by PE-CVD technique using Sentech Depolab 200 system with capacitively coupled electrodes. The films were deposited using the gas mixture of hydrogen, argon, methane, silane, and, in some cases, nitrogen. RF discharge power and silane flow rate were changed to vary the film properties.

In the work optical and mechanical properties of a-Si_xC_{1-x}:H films prepared by the PECVD technique from the mixture of CH_4, SiH_4, H_2, and *Ar* were studied.

It was shown that variation of silane flow rate (10, 20 sccm) and discharge power in the 100-300 W range allow us to obtain films with the following characteristics: optical bandgap 2.5-4.1 eV; refractive index of 1.8-2.4; hardness (*H*) 2.3-18.3 GPa; Young modulus (*E*) of 21-162 GPa. The film deposition rate varied from 10 to 35 nm/min.

By selecting deposition regimes, we deposited films with high ratio between film hardness and Young modulus (*H/E* = 0.13). The variations of optical and mechanical properties of the films by changing discharge power and silane flow are interpreted within a model taking into consideration the film composition and phase-structural transformations in them.

The unique feature of the developed films is good combination of optical and mechanical properties that makes them promising for application as protective, passivation and anti-reflection coatings for different materials.

The conclusion has been practically supported by results of the films applications as the antireflection and protective coatings for germanium. silicon, CdZnTe, InSb, and other materials in IR spectral range. Another prospective application is to improve Si-based solar cells properties and to create new efficient HIT solar cells.

This work was supported by the national long-term project No WQ20142200205 of "Thousand Talents Plan of Bureau of Foreign Experts Affairs" of the People's Republic of China as well as by III-10-19 and III-4-19 scientific theme of NAS of Ukraine.

The Formation and Propagation of Cracks in Thin Films of Chalcogenide Glasses

Kozak M.I.[1], Loya V.Yu.[2], Zhikharev V.N.[1], Fedelesh V.I.[1]

[1] *Uzhhorod National University, Uzhhorod, Ukraine, kozakmi@ukr.net*
[2]*Institute of electron physics of NASU, Uzhhorod, Ukraine, vasyl.loya@gmail.com*

Chalcogenide glasses have a number of unique properties, for example, such as high transparency in the IR region, photosensitivity, etc., which makes them an indispensable material in instrument making, electronics, etc. Some of their properties also stimulate fundamental research. This report presents the results of studies of the mechanical properties of thin films of some compositions of chalcogenide glasses (As – S, As – Se, As – Ge – Se). The patterns of formation of a grid of cracks (mud cracks, straight and sinusoidal cracks, spirals, sawtooth cracks) are shown depending on the composition during thermal hardening of films in air [1]. An important result was the discovery of slow cracks in the films of composition As_2S_3. As it turned out, the formation of cracks in the films can occur at a rate that makes it possible to investigate the dynamics of the propagation of cracks using conventional video recording and determine the crack velocity. In Fig. 1 shows an example of determining the crack velocity in a 2 μm thick film on a fused quartz substrate.

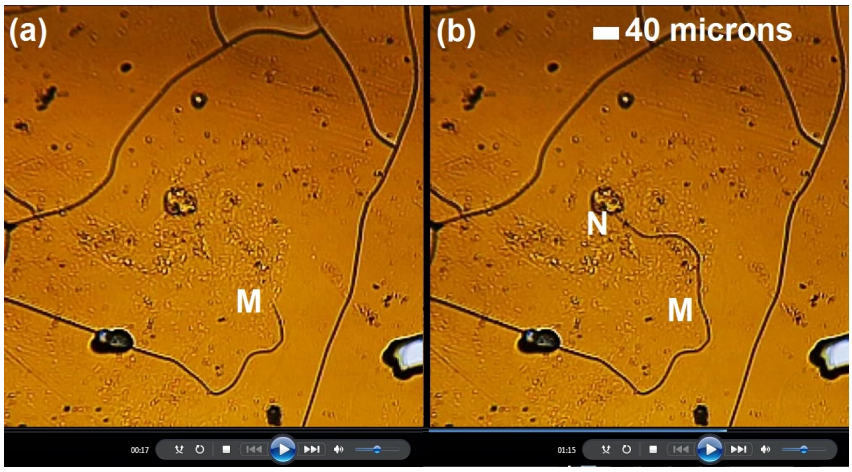

Fig.1. The initial (a) and final (b) footage of the crack propagation. Spread time 58 s. The crack length is determined according to the scale of the image in an optical microscope as the length of the MN curve.

The report is illustrated with a variety of photos and videos. It also considers the proposed model of mechanical cracking of a plastic-elastic film.

1. M.I. Kozak, V.N. Zhickarev, V.I. Fedelesh, A.M. Solomon, V.Y. Loya, Advanced Photonics 2018 OSA, Tech. Digest (online), paper JTu2A.26. Optical Society of America (2018). https://doi.org/10.1364/BGPPM.2018.JTu2A.26.

Magnetic Dielectric - Graphene - Ferroelectric System as a Promising non-Volatile Device for a Spin Filter and a Spin Valve

Kurchak Anatolii I.[1], Morozovska Anna N.[2, 3] and Strikha Maksym V.[4]

[1]*V.Lashkariov Institute of Semiconductor Physics, NAS of Ukraine,*
[2]*Institute of Physics, NAS of Ukraine,*
[3]*Bogolyubov Institute for Theoretical Physics, NAS of Ukraine,*
[4] *Taras Shevchenko Kyiv National University, Faculty of Radiophysics, Electronics and Computer Systems, maksym.strikha@gmail.com*

The conductivity of the system magnetic dielectric (EuO) - graphene channel - ferroelectric substrate was considered. The magnetic dielectric locally transforms the band spectrum of graphene by inducing an energy gap in it and making it spin-asymmetric with respect to the free electrons. The range of spontaneous polarization (2 – 5)mC/m^2 that can be easily realized in thin films of proper and incipient ferroelectrics, was under examination. It was demonstrated, that if the Fermi level in the graphene channel belongs to energy intervals where the graphene band spectrum, modified by EuO, becomes sharply spin-asymmetric, such a device can be an ideal non-volatile spin filter.

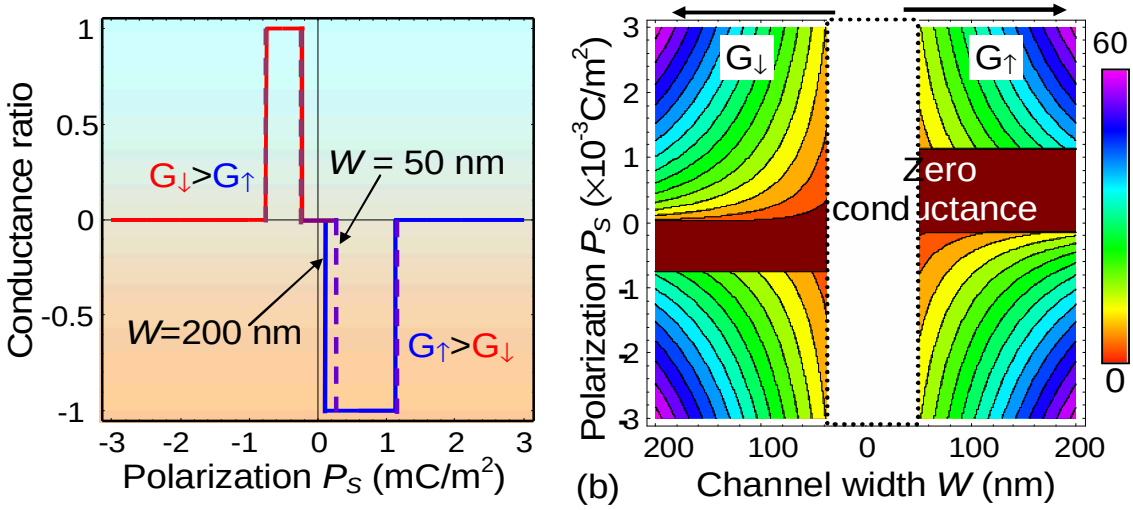

Fig. (a) presents the calculated dependence of the ratio $\frac{G_\uparrow - G_\downarrow}{G_\uparrow + G_\downarrow}$ ($G_\uparrow$ and $G_\downarrow$ are conductances for electrons with spin up and down correspondingly) on the ferroelectric polarization P_S calculated for channel width $W = 50$ nm and 200 nm. **Fig. (b)** presents the dependences of the normalized $G_\downarrow$ (left side) and $G_\uparrow$ (right side) on W and P_S. The conductance is normalized on Klitzing constant $e^2/2\pi\mathbf{h}$. The practical application of the system under consideration would be restricted by a low Curie temperature of EuO, $T_C = 77K$. However, alternative magnetic insulators with high Curie temperature (e.g. $Y_3Fe_5O_{12}$ with $T_C = 550K$) can be used for a system operating under ambient conditions. Controlling of the Fermi level (e.g. by temperature that changes ferroelectric polarization) can convert a spin filter to a spin valve.

Non-Stoichiometric Amorphous Silicon Carbonitride Films as Antireflective and Protective Coatings for IR Photosensors

Lukianov A.M.[1,2], Klyui N.I.[1,2], Lozinskii V.B.[2], Sapon S.V.[2], Rashkovetskyi L.V.[2], Temchenko V.P.[2], Dusheiko M.G.[2,3], Gorbulik V.I.[2]

[1]*College of Physics, Jilin University, Changchun, People's Republic of China*
[2]*V. Lashkaryov Institute of Semiconductor Physics, NationalAcademy of Sciences of Ukraine, Kyiv, Ukraine*
[3]*National Technical University of Ukraine "Igor Sikorsky Kyiv Polytechnic Institute",*
lukianov@isp.kiev.ua

The non-stoichiometric a-SiCHN films were prepared by PECVD deposition from gas mixture of CH_4, SiH_4, H_2, and N_2 on InSb and CdZnTe substrates. The additional silicon wafer, quartz plates, aluminium foil substrates were used for characterization of the optical and mechanical properties of the deposited films. The properties of the a-SiCHN films were analyzed from spectra of reflection and transmission in the UV-VIS-NIR and mid-IR wavelength ranges by spectrophotometry, laser ellipsometry and FTIR. The mechanical properties of the films were characterized by nanoindentation method and the Young modulus and nano-hardness measurements. The SEM and EDS analysis were used for estimation of films content. The single-layer ARC coatings with thickness 875 nm and refractive index close to 1.99 on front and rear side of CdZnTe substrate increased the transmittance up to 92.6% at wavelength 6.0 μm (Fig. 1a). The deposition of the single-layer ARC film with thickness about 520 nm and refractive index about 2.45 on InSb reduced the reflectance to 1.33% at wavelength 5.2 μm (Fig. 1b). The hardness of such films is 7,26 GPa with Young modulus 54,1 GPa. Thus, the studied films are suitable for application as antireflective coatings in the wide wavelength range (from 0.5 to 10 μm) and have excellent protective properties.

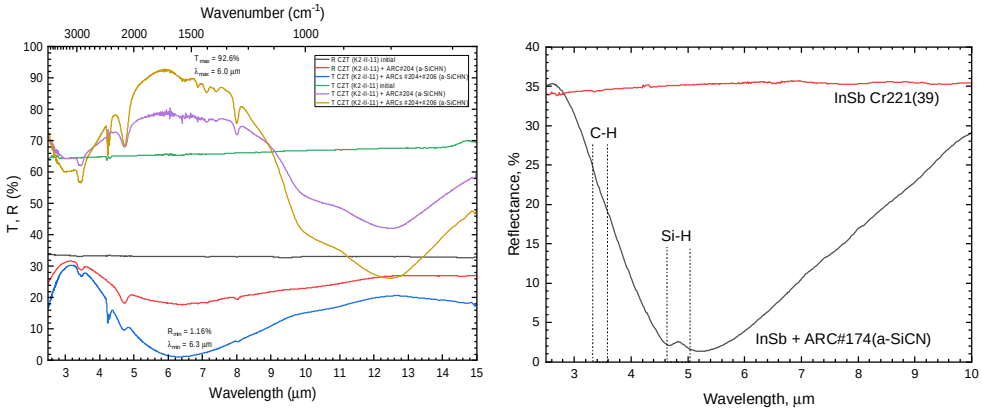

a **b**

Fig. 1. T and R spectra for CdZnTe (a) and InSb (b) with and without a-SiCN films.

Ferroelectric Nano-Structures for Ultrafast THz Communications, Low-Dissipation Electronics, and Multi-Logic Computing Circuits

Lukyanchuk I.[1], Mezanne D.[2], Razumnaya A.[3]

[1]*University of Picardie, Amiens, France, e-mail: lukyanc@ferroix.net*
[2] *University Cadi Ayyad, Marrakech, Morocco*
[3]*Southern Federal University, Rostov-on-Don, Russia*

Formation of unusual textures of polarization is imminent for nano-scale ferroelectric samples, films, rods, and granules, where the depolarization surface effects play the crucial role. The topologically protected stability of such textures and security of information storage is coming from polarization vorticity, provided by condition of absence of the energetically-unfavorable depolarization charge. The endurance of ferroelectric formations with respect to high-energy irradiation makes them ideal for the aerospace industry, and the periodic domain walls structures can be used as platform for terahertz radiation generators and detection devices.

Polarization domains that alternate the surface charge distribution can be formed in ferroelectric thin films as an effective mechanism to confine the depolarization field to the near-surface layer and diminish the depolarization energy. However their existence have long been considered as barely possible until the direct theoretical predictions [1,2] and experimental evidences [3,4] in thin oxide-based superlattices. Very recently we have demonstrated that the effective capacitance of ferroelectric layers with domains is negative [5]. This effect is explained by the opposite orientation of the depolarizing field with respect to the field-induced averaged polarization. This phenomenon is currently considered as the platform for realization of the dissipation-free high performance nano-circuits [6]. Moreover, in sub-THz region the resonance plasmonic effect can be induced by oscillating domain walls [7] and can be suitable for design of the ultra-small low-energy THz chips.

Multi-vortex [8] and skyrmion [9] states can be formed inside ferroelectric cylindrical nano-dots and nanorods to reduce the depolarization energy. We study the topological stability of such states and target the multi-domain and topological excitations in FE nanodots as a platform for IT-secured multivalued logic units, breaking ground for neuromorphic computing [10,11].

1. A. M. Bratkovsky and A. P. Levanyuk, *Phys. Rev. Lett.* 84, 3177 (2000).
2. I. A. Luk'yanchuk, et al. *Phys. Rev. Lett.*, 94, 047601 (2005), ibid. 102, 147601 (2009)
3. S. K. Streiffer, J. A. Eastman, D. D. Fong et al., *Phys. Rev. Lett.* 89, 067601 (2002);
4. S. O. Hruszkewycz, M. J. Highland, et al., *Phys. Rev. Lett.*110, 177601 (2013).

5. P. Zubko, A. Sen, I. Luk’yanchuk, J.-M. Triscone & J.Iniguez, *Nature*, 534, 524 (2016).
6. Khan, A. I., Chatterjee, K., Wang B. et al. *Nature Materials* 14, 182–186 (2015).
7. I. Luk'yanchuk, A.Pakhomov, A.Sene, A. Sidorkin, V. Vinokur, arXiv: 1410.3124
8. G. Pascoli L. Lahoche, I. Luk'yanchuk, *Integrated Ferroelectrics*, 99, 60 (2008).
9. L Baudry, A Sene, IA Luk'yanchuk, L Lahoche, and JF Scott, *Phys. Rev*. B 90, 024102 (2014).
10. P.-W. Martelli, S. M. Mefire, I. Luk'yanchuk, *Europhys. Lett*. 111, 50001 (2015).
11. Baudry, L., Lukyanchuk, I. & Vinokur, V. M. *Sci. Rep*. 7: 42196 (2017).

Extrusion Methods Used to Estimate the Density and Anti-Friction Properties of Polymer Composites

Martynyuk M.I., Sirenko H.O., Grinevich R.V.

Vasyl Stefanyk Precarpathian National University,
Ivano-Frankivsk, Ukraine, mar.martinyuk2904@gmail.com

1. Polymer composites of anti-frictional purpose were obtained on the basis of polytetrafluoroethylene, carbon fiber, coke, molybdenum disulphide, talc. Polymer compositions were obtained from the powders by the chemo-mechano-activation technology, which provided the chemo-thermal effect on the powders and the fiber of the filler and the powder of the polymer, and then on the mechanical crushing composition in the crusher MRP-1 and MPP-1M for 7000 revolutions per minute of the workers organs (knives) within 10-20 minutes. The composition was compressed into tablets of 30 mm in diameter and it was heat treated at 360-370 °C.

2. The resulting tablets were examined by the extruding through a filter a 30 mm diameter that is made of steel 45 (HRC 45-48), with the evenly spaced 13 holes (3 mm in diameter) on a plane with a diameter of 18 mm. In the mold there were a solid bottom lower punch, the tablet of a polymeric composite, the filter and a top punch in the form of a sleeve, which was loaded with a hydraulic press.

3. Investigating the following dependencies:

a) the mass flow rate of the material (G, g/min) from the applied pressure (P, kgs/cm^2) for 0,5 and 5 minutes;

b) the critical pressure load ($P_{кр}$, kgs/cm^2) from the concentration of the filler (c, mass %) in the material;

c) the critical pressure load by the number of passes of the material through the filter (number of tablets N).

The results of the study are summarized in Table.

Table

Dependence of the critical pressure load *on the number of passes through the* filter *(number of tablets) of materials based on polytetrafluoroethylene.*

	Filler	Number of passes through the filter (number of tablets)		
		1	4	9
		Critical load, kgs/cm^2		
	-	2362	2079	2080
	20% of coke	4200	3825	3792
	20% of graphite fiber	4586	4000	3884

Reversible Direct Surface Relief Formation on Nanomultilayer Structures Based on Chalcogenide Glasses

Meshalkin A.[1], Paiuk O.[2], Prisacar A.[1], Triduh G.[1], Achimova E.[1], Stronski A.[2]

[1]*Institute of Applied Physics, Chisinau, Moldova, alexei@asm.md*
[2]*V.Lashkaryov Institute of Semiconductor Physics NAS of Ukraine, Kyiv, Ukraine, paiuk@ua.fm*

Chalcogenide glasses (CGs) are distinguished by a number of unique properties, i.e., various photostimulated changes in the physical and chemical characteristics, which have a complex nature and include different effects, such as photodarkening/photobleaching (absorption edge shift), photorefraction, photoinduced solubility change, photoinduced anisotropy, photocrystallization, etc. The most interesting property of CGs is the possibility of forming a surface relief with a high lateral resolution up to 100 nm. First found on glasslike As_2S_3, the photoselective etching using the photolithographic interference process is often applied to produce relief diffraction structures.

First, using of multilayer nanostructures based on CGs as a recording medium for the direct holographic recording of relief structures was proposed by Kikineshi A. Galstian T. was the first who found giant formation of relief during holographic recording with intensified exposure in the amorphous As_2S_3 layers. In our work direct surface relief formation using holographic recording and subsequent erasure have been investigated on As_2S_3–Se multilayer nanostructure.

The work investigates how pre-exposure to actinic laser radiation up to complete photoinduced changes in the optical properties affects the formation of diffraction gratings in the studied structure. It is shown that the pre-exposure of an As_2S_3–Se multilayer nanostructure leads to photobleaching, and the maximum achievable diffraction efficiency (DE) of 35% does not change; however, the required exposure value is increased. It is also shown that exposure using one laser beam results in complete erasure of the diffraction grating recorded up to the maximum. Several recording–erasure cycles show that the kinetics of the increase in diffraction efficiency and its maximum value do not change, which indicates that the As_2S_3–Se multilayer structure is capable of reversible holographic recording under orthogonal circular polarization. Study of the gratings recorded with an atomic-force microscope shows that the main factor determining the diffraction efficiency value is modulation of the relief, the depth of which is greater than 200 nm.

1. Meshalkin A. Reversible polarization recording in As_2S_3–Se multilayer nanostructures. *Surface Engineering and Applied Electrochemistry*. 2018. V. 54, No. 4. P. 407–414.

Deviation from Stoichiometry and Temperature Dependences of Thermoelectric Properties of Bi_2Te_3 Crystals and Thin Films

Rogacheva E.I., Novak K.V., Budnik A.V., Men'shov Yu.V.

National Technical University "KhPI", Kharkiv, Ukraine,
rogachova.olena@gmail.com

Bi_2Te_3-based alloys are among the best low-temperature thermoelectric (TE) materials. At present, interest in Bi_2Te_3 in the thin-film state is becoming ever more intense, due to the possibility of increasing the TE figure of merit in low-dimensional structures and reducing the size of TE converters. The discovery of 3D-topological insulator properties in Bi_2Te_3 crystals and films in recent years has further increased interest in these objects.

One of the methods of controlling the conductivity type and properties of Bi_2Te_3 is changing the stoichiometry of this compound. In [1], it was shown that the room-temperature dependence of the properties of Bi_2Te_3 polycrystals on the deviation from stoichiometry is non-monotonic. It is of interest to investigate the behavior of such dependences at other temperatures, as well as in the thin-film state. Earlier we have shown that the composition of Bi_2Te_3 crystals is fairly well reproduced in thin films [2,3].

The purpose of this work was to prepare crystals and thin films of Bi_2Te_3 with different stoichiometry and films with different thicknesses d, to measure the temperature dependences of TE parameters, and to build isotherms of properties. Polycrystals with compositions in the range of 59.5–67.5 at.% Te were prepared by the ampoule method. Using the synthesized crystals as a charge, thin films with thicknesses d = 45 - 620 nm were grown by thermal evaporation in vacuum from a single source on mica. For all the prepared crystals and films, the Seebeck coefficient, Hall coefficient, electrical conductivity were measured in the temperature range of 77–300 K, charge carrier concentration and mobility, as well as TE power factor, the exponent in the temperature dependence of charge carrier mobility were calculated. The obtained experimental results are analyzed with a view to establishing the role of non-stoichiometry in determining the properties of Bi_2Te_3 crystals and films at different temperatures and showing the possibility of their practical application.

1. E.I. Rogacheva, A.V. Budnik, O.S. Vodorez, J. Thermoelectricity.6, 48 (2014).
2. E.I. Rogacheva, A.V. Budnik, A.Yu. Sipatov, O.N. Nashchekina, M.S. Dresselhaus, Appl. Phys. Lett. 106, 053103 (2015).
3. E.I. Rogacheva, A.V. Budnik, A. Sipatov, O.N. Nashchekina, A.G. Fedorov, M.S. Dresselhaus, S. Tang, Thin Solid Films – 2015. – V. 594. – P. 109–114.

Photosensitive Plasmon Structures Based on Chalcogenide Amorphous Films and Noble Metal Nanoparticles

Rubish V.M.[1], Trunov M.L.[1], Lytvyn P.M.[2], Durkot M.O. [1], Horvat Yu.A. [1], Kyrylenko V.K.[1], Pisak R.P.[1], Tarnaj A.A.[1]

[1] *Institute for Information Recording, NAS of Ukraine, Uzhhorod, Ukraine,* center.uzh@gmail.com

[2] *V. Lashkaryov Institute of Semiconductor Physics, NAS of Ukraine, Kyiv, Ukraine*

The goal of our investigation is the development of a novel type of photosensitive materials that use spontaneous or coherent plasmonic signal generation by noble metal nanoparticles (NPs) integrated into the chalcogenide film (ChFs) matrix or into the “noble metal /NPs/ ChFs” composites.

In the present report we demonstrated the results of investigation influence of near-field illumination on the formation of surface relief (SR) produced by photoinduced mass transport in ChFs deposities on the ordered arrays and arrays of randomly distributed gold and silver nanoparticles under the appropriate photoexcitation of surface plasmon resonance (SPR).

The arrays of randomly distributed gold and silver NPs are formed by the method of rapid (20-25 K/s) radiation heating in the air of thin Au (2-25 nm) and Ag (4-20 nm) films deposited on glass substrates. The size of NPs and the maximum position of the SPR band are 10-100 nm and 520-580 nm for Au NPs arrays and 20-100 nm and 480-510 nm for Ag NPs arrays. The ordered arrays of gold nanoslits are formed by etching with a focused beam of a gallium ions in a scanning electron microscope and ordered arrays of gold triangles arrangered hexagonally – by colloidal nanolithography. Studies have shown that intensive Ag photodiffusion into a ChFs of “Ag NPs/ ChFs” composite structures occurs, and leads to the formation of an intermediate layer enriched with silver ions. To block the photodiffusion phenomenon the design of composite structures was changed by the introduction of a buffer anti-diffusion SiO layer between the Ag NPs and the ChFs. The spectral position of the SPR band after deposition of the ChFs with thickness 30-200 nm is shifted toward the red region by 70-150 nm. The shift values depend on the thickness of this ChFs and geometrical characteristics of noble metal nanostructures.

The resulting “noble metal NPs/ ChFs” plasmon composites are sensitive to band gap laser irradiation and simultaneously excite SPR. The changes of surface topography of these composities were investigated *in situ* using AFM. It is shown that the rate of SR formation in “noble metal NPs/ ChFs” composities is much higher than in nominally pure chalcogenide films. The near-field illumination leads to nanostructurization of the ChFs. The shape of resultant relief of studied plasmon composities depends on the chemical composition and thickness of the ChFs, the NPs arrays morphology, polarization of laser beams and illumination regimes.

About the History of Formation and Development of Theoretical Physics in the Institute of Physics of the National Academy of Sciences of Ukraine

Shenderovsky V.A.

Institute of Physics NAS of Ukraine, Kyiv, Ukraine, schender@iop.kiev.ua

This material is devoted to the 100th anniversary of the foundation of the National Academy of Sciences of Ukraine and to the 90th anniversary of the establishment of the Institute of Physics of the National Academy of Sciences of Ukraine, which consisted on the first period of two divisions: the Department of Experimental Physics and the Department of Theoretical Physics. Most interesting are the first steps of the formation and development of theoretical physics at the St. Volodymyr Kiev University, at the Emperor Alexander II Kiev Polytechnic Institute and at the Institute of Physics of the Ukrainian Academy of Sciences (UAS).

The paper attempts to trace organization methods, places of the relevant studies in the direction of theoretical physics conducted and headed. We are tracing the history of the Department of Theoretical Physics of the University and the Department of Theoretical Physics of the Ukrainian Academy of Sciences in cross of the names of distinguished scientists, in their biographies and scientific achievements.

In paper mention the theoretical physicists, namely, Professor Nikolay Schiller, as the first head of the Department of Physics at the Kyiv University, and Professor Leon Kardish, as the first head of the Theoretical Physics Department in the Institute of Physics. After death of him, the theoretical department was headed by Professor Lev Strum, and later headed by Nathan Rosen (he was an assistant to Albert Einstein at the Princeton Institute of Advanced Studies (1934-36) at the beginning of his scientific career). Since 1944, after the return of the Institute to Kiev from the evacuation, until 1960, the department was led by Professor Solomon Pekar (from 1961 - academician of the Academy of Sciences of the USSR). The well-known theoretical physicists O. Davydov, M. Deigen, I. Dikman, K. Tolpigo, E. Rashba worked at the department at that time.

In 1964 the Department of Theoretical Physics of the Institute headed by Olexander Davydov. After him, since 1973, Corresponding Member of the Academy of Sciences of Ukraine Professor Petro Tomchuk heads the department.

In the paper the most significant achievements during the existence of the theoretical department, the present members of the department and the main directions of scientific activity of the Department of Theoretical Physics of the Institute of Physics of the National Academy of Sciences of Ukraine highlighted.

The Transition from Ballistic to Classical Electron Transport in Thin Metal Films

Stasyuk Z.V., Bihun R.I.

Ivan Franko Lviv national university, Lviv, Ukraine, bihun28@ukr.net

Properties of ultrathin slabs is essentially differ to bulk material due to dimensional effect which are used in nowadays engineering. This difference first of all is caused by prevailing influence of the surface phenomena on ultrathin layer structure and electric parameters. Current theoretical and experimental researches on electron charge transport in ultrathin (layer thickness are 2-10 nm) electrically continuous metal films (temperature coefficient of resistance $\beta > 0$) under the condition $d < l$ were analyzed and reviewed, where d is the film thickness, l is the charge mean free path. With reduction of metal layer thickness when the electron mean free path satisfies the condition $d < l$, the ballistic electron transport in film (without changes of electron energy spectrum in metal film) is presented. Thus charge carriers surface scattering in metal film becomes dominating. The contribution of surface scattering has essentially influenced on macroscopic surface inhomogeneity because the mean linear grain sizes are commensurable to film thickness. When the film thickness does not exceed 5 - 8 nm the ballistic dimensional effect is observed. Quantum size effects are most brightly displayed in semimetal films because of electron de-Brogle wave length in 10 times exceeds interatomic distances in contrast to metal and consequently the interference of electronic waves is influenced poorly by imperfections of film surface. In metal films the situation is essentially different as a de-Brogle electron wave length is commensurable to interatomic distances. If we want to observe oscillations of the kinetic coefficients in thin metal layers, it is necessary to provide high perfection surface structure. The ballistic electron transport is under thickness law of residual conductivity size dependences: $\sigma_{res}=1/[\rho(d)-\rho_\infty] \sim d^{\alpha}$ takes place (under classical electron transport thickness law $\sigma_{res} \sim d$ is observed). Modern theoretical approaches of quantum size effect in kinetic phenomena of metal films are based on assumption that the metal electronic structure is identical to bulk materials, but it is not correct due to real film structure. That is why, we proposed one dimension model of metal films conductivity with Boltzmann approach. The fluctuation of film boundary has dramatic impact on electron spectra. In the frame work of developed model size dependences of metal films conductivity were calculated. The developed model was successfully applied for quantitative description of size dependencies of electrical resistivity of monocrystalline $CoSi_2$ films and fine-grained films of varies metal films. The developed quantum model of charge transport in films with metallic conductivity can more successfully describe the transition from ballistic to classical charge transport with comparison to existed quantum approach [1]. It was possible because proposed model considers the perturbation energy states in the whole volume of the film due to the existence of macroscopic asperities on the metal film surface.

[1] R.I. Bihun, Z.V. Stasyuk, O.A. Balitskii. *Physica B.* 2016. Vol. 487. P. 73-77.

Effects of Defect Pattern and External Magnetic or Mechanical Fields on Electronic and Transport Properties of Graphene Layer

Tatarenko V.A., Radchenko T.M.

G.V. Kurdyumov Institute for Metal Physics, N.A.S. of Ukraine, Kyiv, Ukraine,
tatar@imp.kiev.ua

We study numerically the effects of structural imperfections (point and line defects) and external magnetic or mechanical fields on electronic and transport properties of graphene sheet comprising millions of atoms, *i.e.* layer of several hundred nanometres in size. Point defects are modelled as resonant (neutral) adsorbed atoms or molecules, charged impurities, vacancies, basing local distortions. Line defects are attributed to atomic steps and terraces in epitaxial graphene or nanoripples, wrinkles and grain boundaries in polycrystalline graphene. Results are obtained numerically using the quantum-mechanical Kubo–Greenwood formalism and tight-binding approach. Calculated behaviours of electron density of states and conductivity indicate that deviations from perfection can be useful: they make possible tailoring graphene electrotransport properties for achievement of new functionalities. Particularly, the ordering of point defects can open a band gap in the energy spectrum of graphene, enhance its conductivity up to dozens (10–30) of times, and orientation correlation of linear defects can increase the conductivity up to 4–5 times. If there are both types of defects, their ordering and correlation may improve the conductivity up to hundreds of times as compared with their random distribution [1].

Observed non-equidistant Landau levels in the energy spectrum of defect-free graphene subjected to the external magnetic field undergo the displacement towards the non-shiftable zero-energy Landau level. Thus, they get contraction as the uniaxial tension is applied independently along the stretching direction. The presence of both point and extended defects reduces Landau-level peaks, broadens, smears, and even suppresses the Landau levels, depending on a degree of disorders, their strength, and largely effective ranges [1].

The utilizing of the combination of both the shear strain and the uniaxial tensile deformation is found to be the easy and adjustable way for the band-gap opening and tuning. Results of our numerical calculations demonstrate that shear strains can induce the band gap up to 3 eV at the most extreme elastic deformations, while combination of both the shear strain and the uniaxial one can provide the energy gap up to 6 eV that is substantially higher than for some materials (including silicon) typically used in (nano)electronic devices [1].

1. Radchenko T.M., Sahalianov I.Y., Tatarenko V.A., Prylutskyy Y.I., Szroeder P., Kempiński M., Kempiński W. The impact of uniaxial strain and defect pattern on ***magnetoelectronic*** and transport properties of graphene, *Handbook of Graphene, Vol. 1: Growth, Synthesis, and Functionalization* (Eds. E. Celasco, A. Chaika) (Beverly: Scrivener Publishing LLC: 2019), Ch. 14, pp. 451–502.

The Strategy of Formation and Tuning Properties the Metal Oxide Dielectric and Semiconductor Hybrid Sol–Gel Films

Telbiz German, Stronski Alexander

L.V. Pisarzhevsky Institute of Physical Chemistry NASU, Kyiv, Ukraine, gtelbiz@yahoo.com
V.Lashkaryov Institute of Semiconductor Physics NASU, Kyiv, Ukraine, stronski@isp.kiev.ua

Rapid developments of thin film science and technologies are induced by the growing development of microelectronics and have been increasingly in the direction of devices utilizing thin film materials, which offer the advantages over 3D materials in many aspects and in terms of material requirements. Recently, metal oxide and semiconductors have received considerable attention because of their excellent optical transparency, high carrier mobility, and decent environmental stability. Research efforts are concentrated on developing solution deposition techniques for formation of the large-area metal oxides and semiconductor - based films. While the majority of methods for processing these materials rely on vacuum-based deposition, the solution-based deposition of sol-gel MOx materials can ideally reduce both material and processing costs

This presentation reviews recent advances in solution-based hybrid dielectric mesostructured MOx (M=Si,Ti) sol-gel materials, with a specific focus on the extensive tuning of their compositions for advanced approaches for realizing ultimate material properties. The existing methods for the preparation of semiconductor doped sol-gel films and amorphous semiconductor films for applications in nonlinear optics, have been critically reviewed and compared. Development of a simple sol-gel based method for producing high quality inorganic/organic composite film is reported. A distribution of dye molecules within the body of film corresponded to three extreme configurations. The formation of fluorescent aggregates most probably can be promoted by the presence of the amphiphilic triblock copolymers that favor the formation hybrid micelles. The constrained environment favors the formation within hybrid micelles and gives rise to oblique aggregates that coexist in film. Variation of values of refractive index, absorption coefficient and optical conductivity can be evidence of various spatial organizations of dye molecules within the body of generated films, subject to method of deposition on substrates.

Scanning Electron Microscopic (SEM) Analysis Showing Monazite and Xenotime Content in Materials for Rare Earth Element Extraction

Uhrin Robert[1], Leone Edgar[2], Preuss Thomas [2]

[1]*XLight Corporation, Mendham, NJ, USA, ruhrin@aol.com*
[2]*Exel Laboratory Services, Dover, NJ, USA*

Rare earth (Lanthanide) elements were placed on the United States Critical Materials List in 2018 as a concern for a domestic supply of rare earth compounds. Efforts were spearheaded by the US Department of Energy to develop sources obtained from scrap and coal-associated materials, for example. One project discussed herein evaluated materials associated with bituminous and anthracite coal deposits in eastern and western Pennsylvania.* An interesting observation was that at least one sample contained both monazite and xenotime crystals among other crystalline compounds interspersed within the selected sample.

The search for rare earth elements in coal-associated materials derives from the identification of fairly high (100 ppm) rare earth element concentrations in coal ash. This was interpreted to result from the types of material that accompany coal mining. These include materials like fire clay, muscovite and zircon, compounds that contain rare earth elements as substituted impurities. Techniques of SEM coupled with energy dispersive x-ray analysis (EDX), and wavelength dispersive x-ray (WDX) analysis were used to identify individual particles as monazite and xenotime. This was found to be unusual, since monazite and xenotime ore deposits exist primarily as one or the other compound.

Detailed analyses of the observed compounds will be presented along with suggestions for additional analysis of other coal-associated materials containing >300 ppm rare earth elements.

**A portion of this work was supported by DOE/NETL under Contract No. DE-FE-0026527*

Physics and Technology of Thin Films (Ge + Ga) on GaAs Substrates

Venger E.F., Kolyadina E.Yu., Kholevchuk V.V., Matveeva L.A., Mitin V.F.

V. Lashkaryov Institute of Semiconductor Physics NAS of Ukraine,
Kyiv, Ukraine, matveeva@isp.kiev.ua

The physical properties of the heterosystems are not simple sum of the properties of the film and the substrate. Internal mechanical stresses arise at the interface of the film-substrate. They change the band structure, the electronic properties of the film surface and the substrate at the interface. Ge/GaAs heterosystems are used in sensor technics. Temperature sensors, magnetic fields and bolometers are made on this basis. The addition of metal to films of fullerenes C_{60} changes their band structure and electronic properties [1]. The purpose of this work was a comprehensive study of heterosystems with films of Ge + Ga on gallium arsenide substrates.

Heterosystems were obtained by thermal deposition in a vacuum of 10^{-4} Pa of a (Ge + Ga) mixture on GaAs (100). The substrate temperature was 300 ºC, the substrate thickness was 300 μm, the film thickness was 1 μm. Before deposition, the mixture Ga: Ge = 1.05 % was annealed for 15 minutes at 500 ºC. After opening the flap, films were deposited at a speed of 1.75 Å/s and annealed for 30 minutes at 500 ºC. The thermal probe showed that the films had a *p*-type conductivity.

Electroreflection of the films was measured in an electrolytic cell with a 0.1 normal solution of KCl in water at room temperature in the low-field electroreflection mode. The modulating voltage did not exceed 0.3 V. The band gap E_g and the parameters of the broadening of the spectra Γ were determined by the Aspnes method. The parameter Γ and the time of energy relaxation of light-excited charge carriers $\tau = \hbar/\Gamma$ characterize the structural perfection of the surface under study. The sign and value of the mechanical stresses in the films were determined from the change in the transition energy in a germanium crystal, as well as from the bend profile of the heterosystem recorded on the profilometer - profilograph. Bending with a film upwards corresponds to the appearance of compression stresses in it. Their value σ was determined by the Stony formula $\sigma = Ed^2/6(1 - \nu)Rt$, where E, d, ν is Young's modulus, thickness and Poisson's ratio of the substrate, t is the film thickness, R is the bend radius of the heterosystem.

The physical properties of the films are different from the properties of the crystal. The elastic deformation that arises in the films changes their band structure, shifts the absorption edge and removes the degeneration of the zones of light and heavy holes in the E_0 transition region. We observed these effects in Ge/GaAs and Ge/InP heterosystems. In the spectra of Ge films on GaAs, compressive stresses appeared, the absorption edge shifted to higher energies. In

Ge films on InP tensile stresses occurred, and the absorption edge shifted to lower energies. Under the action of internal mechanical stresses in Ge films on GaAs and InP substrates, the degeneration of the zones of light and heavy holes was lifted. An additional signal with a higher energy than the band gap width E_g in germanium single crystals appeared in the spectra of electroreflection.

In the (Ge + Ga)/GaAs heterosystems, the value of the mechanical stresses, determined by the bending of the heterosystems, differed from the values determined by the electroreflectance method by the shift of the transition energy. Electroreflectance spectra were measured in the E_1 (2.14 eV) and $E_1 + \Delta_1$ (2.34 eV) transition regions. In this region, there is no degeneration of the zones of light and heavy holes in the semiconductor, and in metals, electroreflectance signal never occurs. But for both transitions, the splitting of the electroreflectance signal was registered. The value of the internal mechanical stresses, determined from the spectra of electroreflectance, did not coincide with that measured from the curvature of the heterosystems. The value and sign of the stresses in the films (Ge + Ga) on GaAs substrates were also determined by the change in the energy of the E_1 and $E_1 + \Delta_1$ transitions. The broadening parameter of the spectra Γ and the energy relaxation time of charge-excited light carriers τ characterize the perfection of the surface of the films and substrate at the interface of the film-substrate. Γ and τ were determined by the position of the signal maxima and the ratio of their intensities.

In molecular crystals of C_{60} fullerenes transitions occur in the same point of the Brillouin zone at different energy levels. In C_{60} films on different substrates, compression stresses always occurred. Their lattice constant ($\approx$ 1 nm) is almost 2 times more then lattice constant of any semiconductor. Heterosystems (Ti + C_{60})/Si and (Cu + C_{60})/glass were bent down with films. Consequently, tensile stresses of greater value than compressive stresses occurred in the films. We explained the obtained result by the presence of two interfaces in the metalfullerene films: fullerenes-substrate and fullerenes-metal grains. The planar photograph of the metalfullerene films in the atomic force microscope confirmed this assumption [1]. A similar result was obtained for (Ge + Ga)/GaAs heterosystems. Two signals also appeared in them with energy above and below the band gap for transitions in the E_1 and $E_1 + \Delta_1$ regions. The compressive stresses were $2.6 \cdot 10^8$ Pa, and the tensile stresses of $6.8 \cdot 10^8$ Pa exceeded the compressive stresses in the films.

1. Венгер Е.Ф., Литвин П.М., Матвеева Л.А., Матиюк И.Н., Нелюба П.Л., Шпилевский Э.М. Электроотражение металлофулуреновых плёнок // Фуллерены и наноструктуры в конденсированных средах. Сборник научных статей. – Минск 2018, Институт Тепло- и массообмена им. А.В. Лыкова НАН Беларуси. – С. 279-283.

Obtaining, Structure and Gas Sensor Properties of Nanopowder Metal Oxides

Venhryn Yu.I., Savka S.S., Bovhyra R.V., Zhyrovetsky V.M., Serednytski A.S., Popovych D.I.

Pidstryhach Institute for Applied Problems of Mechanics and Mathematics of National Academy of Sciencies of Ukraine, Lviv, Ukraine, popovych@iapmm.lviv.ua, http://dpmm.iapmm.lviv.ua

The theoretical and experimental researches of formation processes of the nanopowder metal oxides by means of pulsed laser ablation in chemically active environment and studied their properties were carried for the purpose of gas sensor. Molecular dynamics simulations of the oxidation of zinc nanoclusters to investigate the process of the formation of *ZnO* nanocluster or *Zn-ZnO* "core-shell" nanostructures were carried. It established that the structure, shape and oxide layer thickness of the obtained particles directly depends on the initial oxygen density and initial temperature of the system. Density-functional theory studies of the structural and electronic properties of $(ZnO)_n$ (n = 34, 60) nanoclusters with native point defects were performed. It was determined that the most favorable defects of the clusters structure were Zn and O vacancies. The study of the features of photoluminescence in different gas environment (vacuum, air, O_2, N_2, H_2, CO, CO_2) of nanopowder metal oxides obtained by pulsed laser reactive technology [1] has been carried out. Correlation between chemical composition, microstructure and electronic properties of initial, laser-modified and doped metal oxides and structures on their basis and their gas sensitivity are established. The peculiarities of the influence of surface doping by impurities (*Mg*, *Pt*, *Cu*, *Ge*, *In*, *Si*, *Ni*, *Sn*) on the sensitivity and selectivity of the signal response during adsorption of gases are established. The optimal luminescent gas-sensitive materials (initial and doped ZnO and also the complex metal oxides $ZnSiO_4$*:Mn*, $ZnTiO_3$, $ZnGa_2O_4$, $ZnGa_2O_4$*:Mn*, KGa_5O_8*:Mn*, $ZnGdO_3$*:Eu*) were selected to build a multielement gas sensory matrix, the color of its light is determined by the composition of the gas environment [2]. Measurement of the signals of all cells of the gas sensory matrix at once and digital processing make it possible to determine simultaneously the concentration and type of many gas particles.

1. Gafiychuk V.V., Ostafiychuk B.K., Popovych D.I., Popovych I.D., Serednytski A.S. ZnO nanoparticles produced by reactive laser ablation. *Applied Surface Science.* 2011. V.257, №20. P.8396–8401.
2. Zhyrovetsky V.M., Popovych D.I., Savka S.S., Serednytski A.S. Nanopowder Metal Oxide for Photoluminescent Gas Sensing. *Nanoscale Research Letters*. 2017. 12. -P.132(5).

Testing of Lead, Tin and Germanium Tellurides by Means of Secondary Neutral Mass Spectrometry: Features, Problems and Possibilities

Zayachuk D.M.[1], Slynko V.E.[2], and Csik A.[3]

[1]*Lviv Polytechnic National University, Lviv, Ukraine, zayachuk@polynet.lviv.ua*
[2]*Institute for Problems of Materials Science NASU, Chernivtsy branch, Chernivtsy, Ukraine, slynko_vasily@yahoo.com*
[3]*Institute for Nuclear Research, Hungarian Academy of Sciences (ATOMKI), Debrecen, Hungary, csik.attila@atomki.mta.hu*

Complete characterization of any samples for their practical applications requires a sensitive chemical analysis including identification of compounds and quantitative determination of elements. Secondary Neutral Mass Spectrometry (SNMS) are usually used for such analysis. In SNMS method the neutral particles are sputtered from the surface and post-ionized via interaction with energetic electrons. The neutral particles make up approximately 99% of the species removed during the target bombardment therefore their flux reflects the true surface composition.

The flux intensity of a sputtered chemical element measured in the SNMS conditions depends on its absolute sensitivity factor, which, in turn, depends on the different characteristics of the detected element, the plasma, and the mass spectrometer and is not known in advance. As a result, for straightforward quantification of SNMS data for a multicomponent solid it is necessary to know the relative detection factor (RDF) of the sputtered species. Knowing RDF and having determined experimentally the ratio of the intensities of the sputtered species, one can establish the ratio of their sputter yields and further convert it into the concentrations of the sputtered species.

In this report we present the generalized results of our studies of the peculiarities of using the SNMS method for testing of the crystals and thin layers of PbTe, SnTe, and GeTe caused by the preferential sputtering of their constituents, the large differences in the atomic masses of the constituents, as well as the formation of a dimple texture and various types of three-dimensional structures on the sample surface under conditions of its sputtering by Ar^+ beams of different energies in the range from 50 to 500 eV.

We suggest a method for determination of the RDF of the intrinsic components for the studied materials. Also we obtained the empirical relationship for its dependence on a sputtering energy, which may be used for straightforward quantification of SNMS data for any PbTe, SnTe, and GeTe samples if the sample surface remains practically flat after sputtering, regardless of whether it is a thin layer or a bulk crystal. We show that if the surface of the sputtered sample is covered by surface structures in the process of its sputtering, it is necessary to introduce an adjustment to the value of RDF, which must be determined individually in each particular case.

ORAL REPORTS

Session 1

Thin films technology (metals, semiconductors, dielectrics, conductive polymers) and their research methods

The Role of Depositing Conditions of Cu_2ZnSnS_4 Colloidal Nanocrystals and Flash-Lamp Annealing of the Thin-Films Based on Them

Havryliuk Ye., Mazur N., Dzhagan V., Yukhymchuk V., Valakh M.Ya.

V.E. Lashkaryov Institute of Semiconductor Physics NAS of Ukraine, Kyiv, Ukraine,
evgenko93@isp.kiev.ua

In recent decades, an increasing demand for electricity has led to the search for new alternative sources. One of the areas of development is the search for affordable and non-toxic solar energy materials having a high absorption coefficient and direct bandgap in the solar range. One of such materials is Cu_2ZnSnS_4 (CZTS) and related compounds. This class of compounds can be used in the promising technology of "printing" solar cells using inks based on CZTS nanocrystals (NCs).

However, due to complexity of these compounds, they contain numerous structural defects and secondary phases of the binary and ternary compounds of the constituent elements. That is why an important question is possible improvement of the quality of the NC material after synthesis. In this sense, the information about the peculiarities of the film formation is very important and the technologies of rapid annealing by the thermal heating, and intensive pulse light radiation turned out to be a very promising. The effectiveness of the method of using flash lamp annealing (FLA) has been demonstrated for various compounds, including quaternary metal chalcogenides.

Here we report striking differences in the Raman spectra of CZTS NCs with size of 2-6 nm deposited on different substrates. This fact is usually overlooked in the literature and makes the comparison of different reports quite questionable. We established that the exposure of CZTS NCs to ambient moisture in air results in a partial hydrolysis/oxidation of CZTS with the formation of $Cu_{2-x}S$ as a secondary phase and transformation of the remaining CZTS phase into a disordered kesterite one. According to our findings, the latter transition may be additionally stimulated by the laser illumination during Raman measurements. Consequently, we established the combination of the drying rate and environment as well as measurement conditions which do not lead to a deterioration of the CZTS NCs.

Also we investigate the effect of FLA on CZTS NCs. We investigated the effect of various doses of irradiation energy, up to 60 J/cm^2, on NC films deposited on a glass substrate by drop-casting. The influence of the film thickness and crystallinity of initial NCs (before FLA) was also studied. Raman scattering was chosen as a main characterization method in this work, because it has already proved to be very efficient diagnostic tool of the structure and composition of CZTS and relative compounds

Synthesis and Investigation of the Thermoelectric Parameters of PbSnAgTe Film

Ivakin E.[1], Nykyruy L.[2], Kisialiou I.[1], Yavorskiy Y.[2]

[1]*Belarusian State University, Minsk, Belarus, ivakin@ifanbel.bas-net.by*
[2] *Vasyl Stefanyk Precarpathian National University, Ivano-Frankivsk, Ukraine*

PbTe-based compounds are characterized by a wide range of modifications of their properties by doping. High efficiency thermoelectric (TE) materials can obtain by smooth change of composition. The perspective such materials for the production of thermoelectric energy are the multicomponent compounds like as LAST (PbAgSbTe) and LATT (PbSnAgTe). On the other hand, modern research shows that thin film technology significantly improves TE properties.

The studying thin films were obtained by the vapor phase method. To improve thermoelectric properties, the dynamics of electrons in polycrystalline films was studied, which is determined both by crystallites and intergrain barriers. The size of the grains can significantly effect on the processes of electrons and phonons scattering.

Heat transfer in films was investigated by laser pulse excitation and subsequent CW laser probe of surface diffraction gratings caused by the formation of surface thermal relief and thermal change in the complex dielectric constant in the layer. The diffraction signal was observed in reflected light. In-plane thermal diffusivity χ was determined from the time of its attenuation. To improve the accuracy of the measurements, the principle of homodyne amplification and phase selection of the diffraction signal has been developed and used. Typical kinetics of diffraction is shown in the figure.

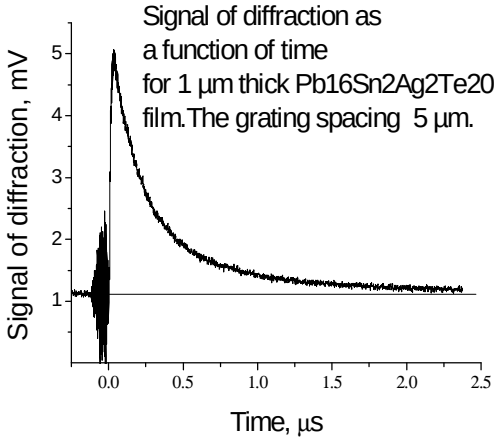

In-plane thermal diffusivity of PbSnAgTe films on glass and muscovite substrate

Film type	χ 10^{-2} cm^2/s
PbTe	1.4-1.5
$Pb_{18}Ag_2Te_{20}$	0.9 -1.0
$Pb_{14}Sn_4Ag_2Te_{20}$	0.8-0.9
$Pb_{16}Sn_2Ag_2Te_{20}$	0.6-0.8

It is shown that the thermal diffusivity decreases when binary compounds are interchanged by the multicomponent systems, as well as in a case of transition from bulk materials application to low-dimensional films. For example, the value of the dimensionless TE figure of merit ZT was ~0.7 at 570°C and ~1.17 at 670°C for $Pb_{14}Sn_4Ag_2Te_{20}$ thin film, which is greater than that for bulk materials.

The Structural-Phase State and Diffusion Process in Film Structures Based on Co and Ru

Lohvynov A., Cheshko I., Odnodvorets K.

Sumy State University, Sumy, Ukraine, andreylogvinovsumdu@gmail.com

A necessary condition for obtaining a simple metal spin-valve-type device structures according scheme «magnetic working layer 1 / non-magnetic layer / magnetic working layer 2» for the needs of modern functional solid-state and flexible electronics is to ensure the stability of the interface between magnetism and nonmagnetic layers. According to the data [1, 2] reliable layer separation possible by using thin layers with Ru thickness from 0.2 ÷ 3 nm. In the study received film system in a single-layer films Ru / S (S – substrate) and Co / S, two-layer Ru / Co / S and three-layer systems Co / Ru / Co / S and multi-layers [Ru (2) / Co (2)]$_5$ / S. The thickness of individual layers was 5 ÷ 60 nm and controlled by the quartz resonator method in the process of samples forming. Layers metals condense on the substrate by electron-beam gun in a vacuum (pressure of the residual atmosphere 10^{-5} Pa).

The crystalline structure of single-layer Ru films essentially depends on the thickness. Before annealing in the whole range of film thicknesses the average size of crystallites is of order 2 ÷ 3 nm. After annealing, the average crystallite size is significantly increased for samples thicker than 30 nm. For Co films before and after annealing can observe homogeneous hexagonal structure with average crystallite size 5 ÷ 7 nm. Only for relatively thin Co layers with thickness near 5 nm samples have a nanodispersed structure. Only in the case of a three-layer sample Co (30) / Ru (5) / Co (30) / S nanodispersion of Ru layer cannot be traced. A clear electronogram corresponding to hcp-Ru without oxide trace can be obtained at $d > 20$ nm with annealing to $T_a = 600$ K. The calculated values of the mean values of the lattice parameters are $a = 0.270 \pm 0.001$ nm and $c = 0.430 \pm 0.001$ nm. The two-layer Co / Ru / S and three-layer film systems Co / Ru / Co / S consist of phases hcp-Co + hcp-Ru. Investigation of diffusion profiles of two-layer film systems Co / Ru / S showed that before and after annealing the individuality of the layers remains. The best conditions in terms of stability performance characteristics synthetic antiferromagnetic film functional layers based on Ru and Co for metal spin-valves there is a choice of Ru layer thickness 5 ÷ 30 nm and the thickness of the Co layers 30 nm and followed annealing up to 600 K.

The work has been performed under the partial financial support of the Ministry of Education and Science of Ukraine (project № 117U003925).

1. P. H. Chan, X. Li, P. W. T. Pong, *Vacuum* **140**, 111 (2017).
2. A. G. Kolesnikov, V. S. Plotnikov, *Sci. Reports* **8**, 15794 (2018).

Methods of Planning Processes Growing of Thin Films and $A^{II}B^{VI}$ and $A^{IV}B^{VI}$ from the Vapor Phase

Lopyanko M.A.

Vasyl Stefanyk Precarpathian National University, Ivano-Frankivsk, Ukraine,
lopyanko@gmail.com

It is known that semiconductors groups AIIBVI and AIVBVI have unique features number that allows them to apply for production of photodetectors and lasers with spectral range of 3-50 microns. Advances for reduce the size of photonic devices closely related with the use of controlled growing of epitaxial thin layers. Despite numerous studies of thin films and nanostructures compounds of AIIBVI and AIVBVI, still not fully clarified the impact of growing conditions on the electrical parameters of thin-layer material.

For factors which vary (k=3) were selected substrate temperature (T_S), evaporator temperature (T_V) and chamber walls temperature (T_C) technologically acceptable change range of which are respectively:

$$473\ К \le T_S \le 623\ К,\ 758\ К \le T_V \le 878\ К,\ 833\ К \le T_C \le 983\ К.$$

Optimization parameters are: charge carrier mobility (μ), concentration (n), Seebeck coefficient (α), conductivity (σ), thermoelectric power ($\alpha^2\sigma$), and value:

$$Z=\mu/\mu_{max} +(n/n_{min})^{-1} + (\alpha^2\sigma)/(\alpha^2\sigma)_{max},$$

which is a complex optimization parameter.

The data presented shown in the form of hypersurfaces of response.

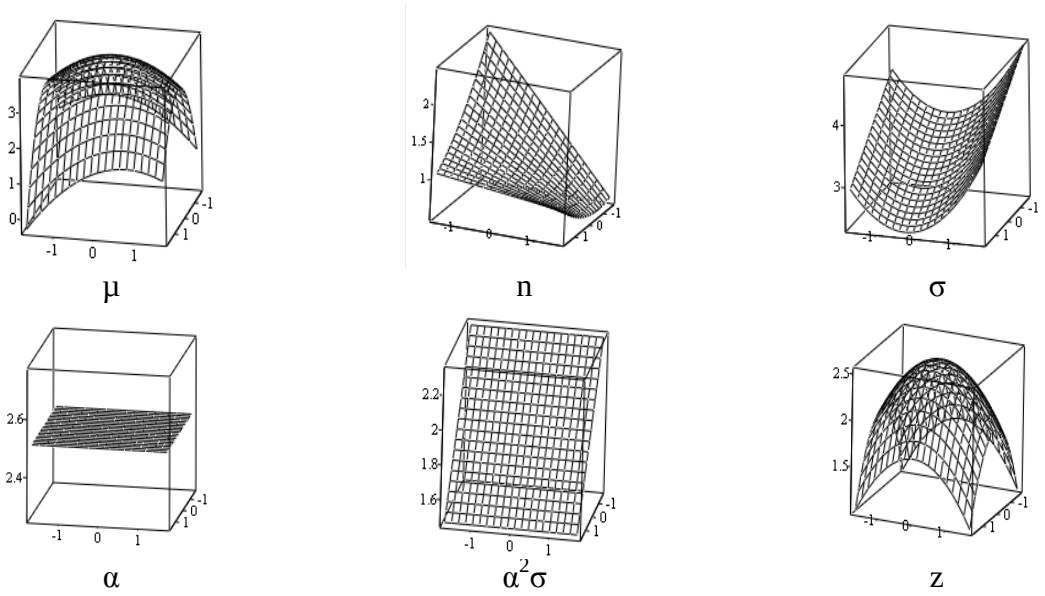

Fig. *Response hypersurfaces at a fixed value $x_3=0$.*

1. Налимов В. В., Чернова Н. А. Статистические методы планирования эксперимента. – М., 1965. – 339 с.
2. Хартман К., Лецкий Э., Шефер В. Планирование эксперимента в исследовании технологических процессов. – М.: Мир, 1977. – 246 с.

Voltammetric Analysis of Phase Composition of Zn-Ni-Cu Alloy Thin Films

Maizelis A.A., Kolupaieva Z.I., Bairachniy B.I.

National Technical University «Kharkiv Polytechnic Institute», Kharkiv, Ukraine,
a.maizelis@gmail.com

Zn-Ni alloy coatings containing 10–15 wt. % of Ni are recommended to replace the environmentally hazardous cadmium coatings. Though these coatings possess higher corrosion resistance and better mechanical properties than Zn they are more electronegative than Cd and dissolve rapidly in highly corrosive environments. It is known that the addition of a more positive metal to the alloy leads to the increase in its corrosion potential.

The aim of the study is to establish the influence of Cu^{2+} ions in electrolyte on the composition of Zn-Ni alloy thin films using anodic stripping voltammetry.

The Zn-Ni and Zn-Ni-Cu alloy films of 40–200 nm thickness and coatings of up to 10 μm thickness were electrochemically deposited in potentiostatic and galvanostatic regimes on the Pt substrate from weak alkaline ammonia-glycinate poliligand electrolyte. Cupric ions were added to in electrolyte in concentration of 5 mmol L^{-1}. Phase and elemental composition of thin films was analyzed by anodic stripping voltammetry in solution containing 0.5 mol L^{-1} of Gly^- and $NH_3(NH_4^+)$ each [1]. Phase composition of thick coatings was analyzed by XRD. Chemical composition of alloys was determined by X-ray fluorescence analysis.

On the voltamperogramms of films deposited from the electrolyte containing cupric ions the height of peak of of Zn dissolution from η-phase decreases, the peak of Zn dissolution from the γ-phase increases and a sharp peak of Cu dissolution appears as compared to voltamerogramm of Zn-Ni alloy dissolution. As the thickness of Zn-Ni alloy films increases, the peak of Zn dissolution from the η-phase decreases, and last peak of Ni-enriched residue dissolution shifts indicating a change in composition of the residue. In the presence of Cu in the alloy, increase of film thickness leads to the increase in the height of the residue dissolution peak and decrease in the height of the sharp peak of Cu dissolution. This is in accordance with the fact that the XRD of both Zn-Ni alloy and Zn-Ni-Cu alloy coatings (6.5 % of Cu) of much higher thickness (10 μm) reveal the presence of only γ-phase.

The γ-phase has more electronegative potential as compared to steel substrate and it has high anti-corrosion properties. The increase in the content of γ-phase in films when Cu^{2+} ions are present in the electrolyte for the deposition of Zn-Ni alloy is a prerequisite for increase in anti-corrosion properties of multilayer coatings consisting of these alloys.

Structural-Phase Features of the Formation of Ti-Zr-Ni Quasicrystalline Thin Films

Malykhin S.V., Kondratenko V.V., Kopylets I.A., Surovitskiy S.V., Borisova S.S., Bogdanov Yu.S.

NTU "Kharkiv Polytechnic Institute", Kharkiv, Ukraine

Since the discovery of quasicrystals by D. Shechtman [1] in 1984, it has now become known about the existence of stable quasicrystalline phases in more than 200 double and triple metallic systems. Quasicrystals (quasi-periodic crystals) are a new class of condensed matter which possesses a strict long-range order at the disposal of atoms and fifth-order symmetry in the absence of translational invariance. The unusual structure generates a number of unusual properties: low thermal and electrical conductivity, corrosion resistance, high hardness, low surface energy, corrosion resistance, low friction coefficient, high strength at high temperatures, etc. [2]. Since many practical applications of thin films are based on their specific properties, developing the technology of thin films of quasicrystals and compositions based on them provides creation of new functional materials with a combination of attractive properties [3, 4].

The interest in Ti-Zr-Ni quasicrystals is primarily due to their ability to accumulate hydrogen up to the atomic ratio 2H/1Me as a solid solution. The ability to hold a significant amount of hydrogen and its isotopes can be also used to create a neutron generator.

The Ti-Zr-Ni films were prepared by the method of direct-current magnetron sputtering the target of corresponding alloys. In the experiments, alloys of two compositions were used, for which the formation of icosahedral *i*-phase was typical for the preparation of ribbon and bulk samples. The composition Ti53Zr30Ni18 (e/a = 1.245) was selected near the electron concentration e/a = 1.25 corresponded to the stable *i*-phase; and the composition Ti41Zr38.3Ni20.7 (e/a = 1.19) was close to the cross section of a stable concentration e/a=1.20). The alloys were prepared in the NSC KIPT from nickel, titanium and zirconium taken in nominal concentrations; the components were refined by the method of double electron-beam melting in an ultrahigh-vacuum not worse than 10^{-4} Pa. The thickness of the Ti53Zr30Ni18 films was 14.6 and 6 μm, and that of the Ti41Zr38.3Ni20.7 films was 2.5 μm. Single-crystalline silicon and sapphire, glass and polished steel were used as substrates. The substrate was not specifically heated; its temperature during the deposition did not exceed 40-50° C. Sputtering was carried out in purified argon at a pressure of $2 \cdot 10^{-1}$ Pa. The elemental composition of the targets and films was monitored by X-ray fluorescence analysis. Note that the chemical composition of the grown films corresponded to the composition of the target. Structural and phase analysis was performed by X-ray diffraction method. The measurements were carried out with a DRON-type apparatus in filtered Cu-Kα radiation.

Spectra processing was performed using the New_Profile 3.5 software package. The identification of the quasicrystalline phase and the determination of its quasicrystalline parameter a_q were carried out according to Cahn J.W. [6], using the original software package. The samples were studied in the initial state and after isothermal annealing in vacuum for 1 hour at temperatures from 373 K to 1023 K with a step of 50 ... 100 degrees.

The formation peculiarities of phase composition, structure and thermal stability of quasi-crystalline thin films were studied. It was established that in initial state the films were X-ray-amorphous or nano-crystalline with coherence lengths (according to Scherrer) near 1.6 – 1.8 nm independently on the element composition of the sputtered target. This structure is relatively stable up to the temperature 400°C when the formation of the quasi-crystalline phase begins. In the films with the Ti53Zr30Ni18 composition, the largest quantity of the quasi-crystalline phase with a characteristic parameter a_q=0.517 nm was observed after annealing at the temperature 600°C; in the samples, an admixture of the 1/1 W-crystal approximant was revealed. In the films with Ti41Zr38.3Ni20.7 composition, an optimal annealing temperature was 500° C; the quasi-crystalline phase was characterized by the quasi-crystallinity parameter a_q=0.5205 – 0.5209 nm. For the first time, the 2/1 approximant crystal as an admixture phase in this system was found. Under annealing at the temperatures higher than 700 – 750°C, the decomposition of the quasi-crystalline and approximant phases into crystalline phases stable at higher temperatures was established according to the equilibrium phase diagram.

[1] Shechtman D., Blech I., Gratias D., Cahn J. W. Physical review Letters.– 1984. – Vol. 53. – P. 1951–1953.
[2] Stadnik Z.M. Physical properties of quasicrystals: Berlin: Springer, 1999.- 365 p.
[3] Palatnik L.S., Fuks M.Ya., Kosevich V.M. The Mechanism of Formation and Substructure of Condensed Films.- M.: Nauka. – 1972. – 319 p. (In Russian)
[4] Yu.V. Milman, N.A. Yefimov. Quasicrystals and Nano-Quasicrystals are New Promising Materials. In the book: Promising Materials. Vitebsk UO „VSTU” . – 2009. – P. 31-60 (In Russian).
[5] Huang H., Meng D., Lai X. et al. Vacuum. – 2015. – Vol.122. – P.147 –153.
[6] Cahn J.W., Shechtman D., Gratias J. Mater. Res. – 1986. – Vol.1. – P. 13.

Peculiarities of SIMS Analysis of Interfaces in Nanoscale Mo/Si Multilayer Periodic Structures

Oberemok O.C, Sabov T.M, Dubikovskyi O.V, Melnik V.P, Romanyuk B.M, Popov V.G., Kosulya O.V.

V. Lashkaryov Institute of Semiconductor Physics of NAS of Ukraine, Kyiv, Ukraine,
ober@isp.kiev.ua

The nanoscale multilayer periodic Mo/Si structures (MPS) are widely used as mirrors for the extreme ultraviolet lithography and soft X-rays diffraction devices. The mirror reflection quality is determined by the elemental and component composition, the thickness, the homogeneity and structure of deposited layers, etcetera. The presence of mechanical stress and structural defects at the interfaces lead to the roughness evolution, compound formation and layer interdiffusion at the heating of Mo/Si structure already at temperature of 150°C. Thin layers of a-$MoSi_2$ are formed at each interface yet during fabrication at the room temperature. The prolonged exposure to elevated temperatures will lead to crystallize of this layer and additional Mo and Si interdiffusion as result. $MoSi_2$ interlayers have different thicknesses for the Mo-on-Si and Si-on-Mo depositions. This is due to easier penetration Mo in Si layer during deposition that resulting in a thicker a-$MoSi_2$ layer. Development of the MPS production technology requires the stepwise control of structure parameters by the analytical methods that have the high depth resolution and also to provide the quantitative information about the elemental composition [1]. One of the methods of such control is Secondary Ion Mass Spectrometry (SIMS) with a depth resolution of less than one nanometer. However, the nanoscale thickness of Mo/Si MPS, the high energy of primary ions and the large difference in the density of molybdenum and silicon materials lead to different penetration depths of the primary ions at the sputtering. It leads to a distortion of the real picture of molybdenum and silicon distributions in the Mo/Si MPS during SIMS analysis. In present study, the distortions of SIMS profiles caused by the accumulation of oxygen [2] at the Mo/Si interfaces at the different energies of primary ions were investigated.

1. Efremov A.A., Litovchenko V.G., Melnik V.P., Oberemok O.S., Popov V.G., Romanyuk B.M. Mechanisms of dopant depth profile modification during mass spectrometric analysis of multilayer nanostructures. *Ukrainian Journal of Physics.* 60(6), p.p. 511-520 (2015).
2. Oberemok O., Kladko V., Litovchenko V., Romanyuk B., Popov V., Melnik V., Sarikov A., Gudymenko O. and Vanhellemont J. Stimulated oxygen impurity gettering under ultra-shallow junction formation in silicon. *Semiconductor Science and Technology*. 29(5), p. 055008(7) (2014).

ORAL REPORTS

Session 2

Nanotechnologies and nanomaterials, quantum-size structures

Surface phases of the 2D Honeycomb BeO Nanostructures on the Mo(112) Surface: ab Initio Thermodynamics Calculations and LEED/AES Investigations

Afanasieva T.V., Fedorus A.G., Naumovets A.G., Rumiantsev D.V.

Institute of Physics National Academy of Sciences of Ukraine, Kyiv, Ukraine,
rumiantsevdmytro@gmail.com

Two-dimensional graphen-like structures are now attracting a broad interest. In this work, we have studied atomic structure and stability of one-monolayer and submonolayer films of Be+O coadsorbed on the Mo(112) surface. We used the density functional theory (DFT) calculations to obtain the formation energies, ΔE_{form}, of various Be_uO_v phases on Mo(112) and computed the difference in Gibbs surface free energy, ΔG, as a function of the changes in O and Be chemical potentials, $\Delta\mu_O$ and $\Delta\mu_{Be}$ accordingly:

$$\Delta G(\Delta\mu_O, \Delta\mu_{Be}) = (1/A)(\Delta E_{\text{form}} - u\Delta\mu_{Be} - v(1/2)\Delta\mu_O).$$

Here A is the surface area and the coefficient (1/2) takes account of the initial molecular state of oxygen. As a result, the ranges of $\Delta\mu_O$, $\Delta\mu_{Be}$ have been found that minimize the surface free energy at various compositions of the Be_uO_v phases. In particular, the honeycomb nanosheet BeO/Mo(112) phase occurs absolutely stable at low temperature in a wide range of Be and O coverages. However, the honeycomb nanoribbon phases Be_uO_v with $u = v = 3, 5, 7, 9$ and $u + 1 = v = 3, 5, 7, 9$ can exist at decreasing local coverages and rising temperatures.

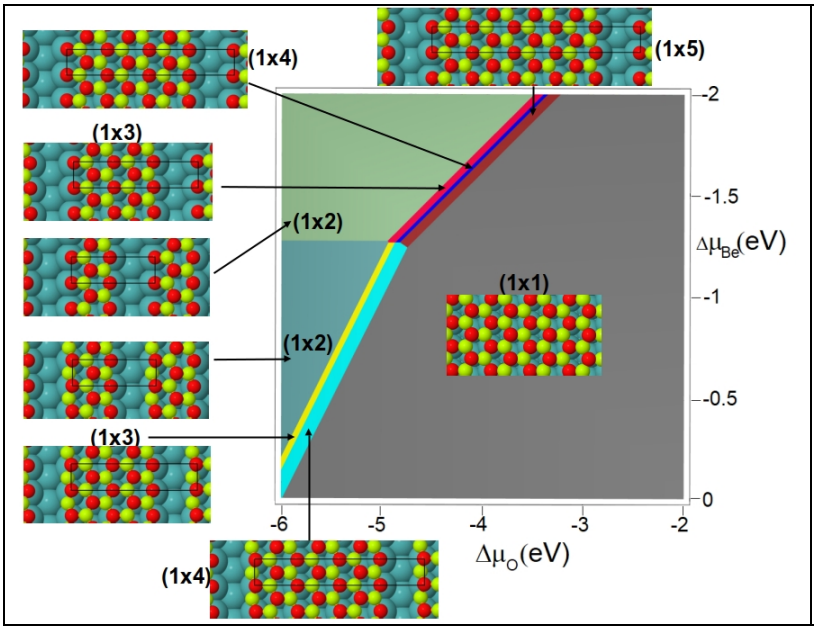

Phase diagram of the (Be + O)/Mo(112) system presented as a projection to the plane of $\Delta\mu_O$, $\Delta\mu_{Be}$. Be atoms are depicted in light, O in dark.

Experimental investigations, performed by low-energy electron diffraction (LEED) and Auger electron spectroscopy (AES) methods in ultra-high vacuum, have verified formation of the both-type honeycomb structures, nanosheet, and nanoribbon.

Micro/Nanocrystalline Cellulose and Expanded Graphite for Development of New Nanostructured Composite Materials

Alekseev O.M.[1], Ivanenko K.O.[1], Nedilko S.G.[1], Revo S.L.[1], Scherbatskii V.P.[1], Teselko P.O.[1], Boyko V.V.[2], Chornii V.P.[2], Barbash V.A.[3], Yaschenko O.V[3], Hamamda S.[4]

[1]Taras Shevchenko National University of Kyiv, Kyiv, Ukraine
[2]National University of Life and Environmental Sciences of Ukraine,Kyiv, Ukraine
[3]National Technical University of Ukraine "Igor Sikorsky Kyiv Polytechnic Institute" Kyiv, Ukraine, s_revo@i.ua
[4]University Frères Mentouri, Constantine, Algeria

It is not surprising that today there is a rising demand for new nanostructured materials and their composites. It should be noted that new materials are needed both for high-tech manufacturing industries and for those which are traditionally considered as material for "primitive" routine production processes.

Here, we would like to draw attention to two types of new ("old") materials that can be useful in both directions. Such are (1) cellulose-based materials and (2) graphite-based materials.

Both the first and the second are such that without them it is even hard to imagine the mankind development. Among the first we undertake here micro, or nanocrystalline cellulose (MCC, or NCC, respectively), and among others - thermo-expandable graphite (TEG). Both types of materials were considered by us as matrices for the introduction to their composition some fillers, which provide these materials important and useful functions. The incorporation of such fillers not only provides the composites "MCC-oxide" and "TEG-oxide" new optical qualities, but also changes the electrical and mechanical properties of the matrix.

Some oxide dielectric compounds which exhibit luminescent properties under certain conditions (composition, concentration, temperature) were used as fillers in this work.

A review of today's data on similar systems is presented, a series of new experimental and theoretical results concerning structure, morphology, hardness, dielectric permittivity, temperature behavior of their dilatometric characteristics, heat capacity, optical reflection and luminescence are given.

The presented data and the results of their analysis have manifested the prospects of these nanostructured materials in both bulk and film form application in science and technology.

Optical Properties of Quantum Dots Arrays

Bilynskyi I., Leshko R., Metsan H.

Drohobych Ivan Franko State Pedagogical University
Physics Departmant, Drohobych, iv.bilynskyi@gmail.com

Resent development of nanotechnologies and science give possibility to create systems composed of many nanodimensional building blocks with extremely different structures. One of the most promising types of those blocks includes semiconductor quantum dots (QDs), which are called “artificial atoms” because of their discrete energy spectrum for electrons, holes and excitons.

Many experimental technologies give possibility to produce arrays of QDs which are one-, two and three-dimentional systems. In those systems there are often observed the ordered arrays of DQs. Due to that, all optical properties of that systems will depend on the energy spectrum which are presented as allowed and forbidden minibands. In our and other works [1-3] those minibands has been defined for different 1D 2D and 3D systems. It was showed that the widths of the allowed and forbidden minibands depend on the thicknesses and heights of potential barriers. Those calculation were made for electrons and obtain electon minibands.

Very often for calculate hole minibands the single bandmodel of valence ban has been used. It give possibility to determine hole minibands and calculate the absorption coefficients caused by transition of hole between minibands. Also transition from hole miniband to electron miniband can be defined too. For better convergence results the Luttinger multiband hole model should be used. Those problems are studied in this work in framework of the spherical QD approximation. Due to degeneracy of the hole ground state of the spherical QD within multiband model some feature has been observer in the absortion spactra, which are differ from singleband model. This results are presented too.

[1] V.A. Holovatsky, V.I. Gutsul, O.M. Makhanets. Energy spectrum of electron in superlattice along the elliptic nanowire. Rom. J. Phys. 52 , 327 (2007).

[2] O.L. Lazarenkova, A.A. Balandin. Miniband formation in a quantum dot crystal. J. Appl. Phys. 89 , 5509 (2001)

[3] В.І. Бойчук, І.В. Білинський, Р.І. Пазюк. Мінізонна електропровідність у надґратках сферичних квантових точок гетеросистеми InAs/GaAs, УФЖ, 62, 335 (2017).

The Important Thermal and Kinetic Properties of Crystals and Their Calculations with the Use of the Gibbs Potentials

Budzhak Ya.S., Druzhinin A.O., Waclawski T.K.

State University Lvivska Polytechnica, Lviv, Ukraine, jabudjak@ukr.net

Semiconductor crystals are composed of the structural particles – these are located within their volume. These particles create the crystal lattice that it has a symmetry. The particles are located in points which are called the lattice sites, and the space between them is called the interstitial site. In such crystals there are the free charge carriers (electrons with the charge –e or positive holes with the charge +e) and these carriers are moving chaotically or in ordered way in the interstitial sites of the crystals. This set of the charge carriers in the crystal is called the electron or hole gas, but also as the gas of charge carriers. In statistical theory of the kinetic properties of crystals [1-4], the ensembles of the structural particles and ensembles of the gases of charge carriers are described respectively by the following Gibbs thermodynamic potentials:

$$\Omega_D = 9NkT\left(\frac{T}{\theta}\right)^3 \int_0^{\theta/T} x^2 \ln\left(1-\exp(-x)\right)dx = 3NkT\left[3\ln\left(1-\exp\left(-\frac{\theta}{T}\right)\right) - D\left(\frac{\theta}{T}\right)\right], \quad (1)$$

$$\Omega = -2kT\sum_{\vec{p}} \ln\left\{1+\exp\left(\frac{m+\Delta m_{\vec{p}}-e_{\vec{p}}}{kT}\right)\right\}. \quad (2)$$

The quantities in the above formulas were described thoroughly in the cited works. In formula (2), $\Delta m_{\vec{p}}$ is the change of the one particle's chemical potential (i. e., free energy per particle) that is produced by the action of the perturbations which force the crystal out of its thermal equilibrium state. When these perturbations are absent, $\Delta m_{\vec{p}} = 0$. It is clear from this condition that the thermodynamic potential (2) describes the thermal characteristics of the charge carriers gas.

The successive statistical calculations of the properties of $3D, 2D$ and $1D$ crystals, with the use of potentials (1) and (2), show that these crystals have considerably large set of the thermal and kinetic properties. These properties are described in the cited works.

[1]. J. S. Budjak, Gibbs Grand Thermodynamic Potential in the Theory of Kinetic Crystal Properties, PCSS, 18(1), 7-14, (2017).

[2]. Ya.S. Budzhak, T. Waclawski, The Important Thermal Characteristics of Matter and Their Computations with the Use of the Gibbs Potentials, PCSS, 19(2), 134-138, (2018).

[3]. J. Budjak, V. Chaban, Energetic and Kinetic Properties of Semiconductors Crystals, Lviv, ProstirM, 190 p. (2018).

[4]. Ya. S. Budzhak, A.O. Druzhinin, T. K. Waclawski, Modern Statistical Methods of Investigations of Properties of Crystals as Micro- and Nanoelectronics Materials, Lviv, Publishing House of Lviv Polytechnic, 230 p. (2018).

Radiation-Stimulated Ordering of the Defect Structure of Si Crystals Under Irradiated with Alpha Particles

Gaidar G.P., Starchyk M.I., Pinkovska M.B.

Institute for Nuclear Research of the National Academy of Sciences of Ukraine, Kyiv, Ukraine, gaydar@kinr.kiev.ua

It is known [1] that radiation-stimulated processes include structural ordering, self-organization, and, consequently, modification of the properties of irradiated crystals. The result of these processes is the formation of periodic structures, the phase transformations etc. Theoretical models of the interaction of radiation with crystals, which describe the behavior of radiation defects in solids quite well, do not adequately explain a number of effects in the case of prolonged irradiation and significant ion beams, when in limited volume the large number of defects is accumulated, and the peculiarities of collective interaction must be taken into account [2]. It turned out that the range of light ions with energies of tens of MeV remains the least studied in this regard. This range has become the object of our research. The interest in the behavior of helium implanted into silicon is due to the possibility of orderly introducing nanopores into the crystal, which have clean internal surfaces, can getter unwanted impurities from the crystal bulk, and be centers of stress relaxation in the surrounding lattice.

The structural properties of the irradiated samples were studied using a number of techniques: X-ray topography, selective etching, metallography, scanning electron microscopy, multi-angle monochromatic ellipsometry, microprofilometry, atomic-force microscopy.

The propagation of periodic defect structure, located perpendicular to the ion flux, into the region beyond the ion path was found when Si was irradiated with the high-energy alpha particles. It was established that for large fluences ($\geq 10^{16}$ cm^{-2}), the formation of defects passes the stage of ordering (the layered linear structures from pores) as a result of their self-organization in the range of ion path. At currents of 0.25–0.45 μA these structures were observed in Si both in the ion path region and beyond the ion path region, and with increasing current to 1 μA they were observed only in the ion path region.

The use of high-energy (MeV) light ions makes it possible to form in the Si bulk at the depths up to 760 μm the linear structures of different widths associated with defects, and this makes it possible to change the layer-by-layer properties of Si to meet the urgent needs of micro- and nanoelectronics.

1. Ovchinnikov V.V. Radiation-dynamics effects. Potential for producing condensed media with unique properties and structural states // Phys. Usp. – 2008. – V. 51. – P. 955–964.
2. Selischev P.A. Self-organization in radiation physics. – Kiev: Aspekt-Poligraf, 2004. – 239 c. (in Russian).

Effect of Doping Methods and Cooling Conditions after High-Temperature Annealing on the Strain Resistance of n-Si

Gaidar G.P.

Institute for Nuclear Research of the National Academy of Sciences of Ukraine, Kyiv, Ukraine, gaydar@kinr.kiev.ua

Analyzing the results, obtained in [1] for the ordinary and transmutation doped Si crystals, it can be concluded that the features of the strain resistance, characteristic for transmutation doped crystals, such as the lack of the complete saturation r (X) at large uniaxial mechanical compression stress X, are directly related with the lack of the complete "depletion" of impurity centres in the temperature region of 77–150 K and with some dependence on the elastic deformation of the energy gap between the donor levels and the bottom of the conduction band. However, in [1], where studied the effect of high-temperature annealing and the cooling conditions on the strain resistance and Hall effect in transmutation doped Si crystals, in the initial state of investigated samples the deep donor levels did not appeared neither at measurements $n_0 = n_0$ ($1/T$) nor at $r = r$ (X). By insignificant deviations from the saturation of the strain resistance effect (in the region of high X), their presence was detected only in the bulk of crystals cooled with rate of 15 K/min after annealing at 1473 K during 2 h.

The assumption, that a similar thermal treatment may lead to the increased concentration of deep centers in those transmutation doped crystals, in which their traces appear in the initial state (after the standard technological annealing), was experimentally confirmed. The prerequisites emerged for studying the influence of these levels on the strain resistance effect under such unusual conditions, when the depth of their occurrence in the crystal under uniaxial load may not remain constant. As a result, it was established that two competing mechanism of resistivity changes under the influence of X are responsible for the formation of strain resistance. One of these mechanisms, represented by the typical redistribution of the charge carriers between the minima with increasing X, leads to the decrease in the effective mobility of carriers along the current direction $\vec{J} \parallel \vec{X} \parallel [001]$, and the second one ensures an increase in the total concentration of charge carriers in the conduction band due to a decrease in the occurrence depth of impurity levels during the elastic deformation of the crystal. The last of the effects in the studied transmutation-doped n-Si is so strongly pronounced that in the region of $X > 0.5$ GPa the strain resistance effect (unlike the usual increase r with X) becomes negative, since in this case $\Delta r_X / r_0 = (r_X / r_0) - 1 < 0$, that almost never occurs, at least, on the Si crystals lightly doped with typical impurities through the melt.

Gaidar G.P., Baranskii P.I. Thermoelectric properties of transmutation doped silicon crystals // Physica B. – 2014. – V. 441. – P. 80–88.

The Effect of Nonparabolicity Described by the Fivaz Model on the Electrical Contact Resistance "Thermoelectric Material-Metal"

Gorskyi P.V.

Institute of Thermoelectricity of NAS and MES of Ukraine, gena.grim@gmail.com

It is known that the layered semiconductor materials, including thermoelectric, tend to formation of superlattices. The energy spectrum of charge carriers in these materials is very often described by the Fivaz model. Within this model, the motion of electrons or holes along the layers is described by the effective mass approximation, and across the layers – by the tight-binding method. It can be represented as follows:

$$e(k_x,k_y,k_z)=\frac{\mathbf{h}^2}{2m^*}\left(k_x^2+k_y^2\right)+\Delta(1-\cos ak_z), \qquad (1)$$

where k_x,k_y,k_z – the components of the quasimomentum of electron (hole), m^* – the effective mass of electron (hole) in the plane of the layers, Δ – the half-width of the minizone describing the motion of electrons (holes) in the direction perpendicular to the layers, a – the distance between the traditionally equivalent layers.

Within this model, the specific electrical conductivity of a "superlattice" thermoelectric material (SLTEM) in the plane of the layers is determined as follows [1]:

$$s_s = s_{0l}\int_0^{\infty}\int_0^{p}\frac{y\exp\left\{\left[y+K^{-1}(1-\cos x)-g^*\right]/t_{2D}\right\}}{\left\{\exp\left\{\left[y+K^{-1}(1-\cos x)-g^*\right]/t_{2D}\right\}+1\right\}^2\sqrt{2y+4pK^{-2}n_0a^3\sin^2 x}}dxdy, \qquad (2)$$

where $s_{0l}=8p^{5/2}e^2l\sqrt{n_0a}/(aht_{2D})$, l – the mean free path of electrons (holes), n_0 – the concentration of electrons (holes), $t_{2D}=kT/z_{02D}$, z_{02D} – the Fermi energy of an ideal two-dimensional Fermi gas with a quadratic dispersion law at absolute zero temperature, $K=z_{02D}/\Delta$, $g^*=z/z_{02D}$, z – the chemical potential of electron (hole) gas in SLTEM. Parameter K characterizes the degree of quasi-two-dimensionality of SLTEM, or, in other words, the degree of openness of its electron (hole) Fermi surface.

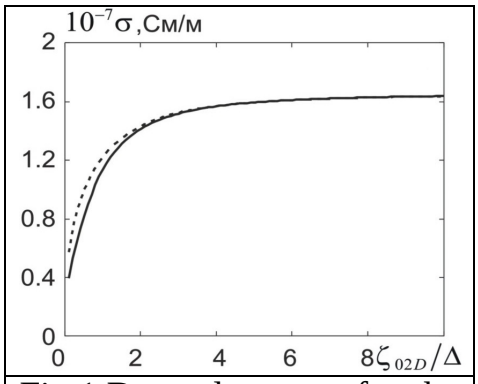

Fig.1.Dependence of the specific electrical conductivity of SLTEM on the degree of openness of its Fermi surface

The chemical potential is determined from the following equation:

$$\frac{t_{2D}}{p}\int_0^{p}\ln\left[1+\exp\left(\frac{g^*-K^{-1}(1-\cos x)}{t_{2D}}\right)\right]-1=0. \qquad (3)$$

The results of calculations of the specific electrical conductivity of SLTEM in the plane of the layers depending on parameter z_{02D}/Δ are represented in Fig.1.

In the construction of the plot, the following parameter values were taken: $n_0=3\cdot10^{19}\,\text{cm}^{-3}$, $a=3\,\text{nm}$, $m^*=m_0$, $T=300\,\text{K}$, $l=20\,\text{nm}$. It is seen from the figure

that with an increase in the degree of openness of the Fermi surface of SLTEM, its electrical conductivity rises sharply enough, tending to the asymptotic limit, which, for the accepted parameters values, is $1.61 \cdot 10^7$ Sm/m.

We now turn to the calculation of the electrical contact resistance of SLTEM-metal. To do this, we use an exponential model of the distribution of conductivity across the thickness of the transient layer. Analysis shows that such a model is acceptable in at least two cases. The first of these is realized when the transient layer consists of SLTEM, in which the concentration of diffused atoms of the contact metal decreases linearly with the depth, and they are "suppliers" of free charge carriers. The second is realized when the transient layer is caused by the deviation of the surface of the SLTEM, on which the contact metal is applied, from ideal flatness, and the true rough surface consists of evenly distributed holes (humps) with random depths (heights), as shown, for example, in Fig. 2. In this case, the thickness of the transient layer should be considered as the distance between the horizontal planes, one of which passes through the top of the highest "hump", and the second through the bottom of the deepest "depression". In this case, the statistical description of a rough surface seems more reasonable than its simulation as a set of objects of a specific geometric shape, for example, hemispheres.

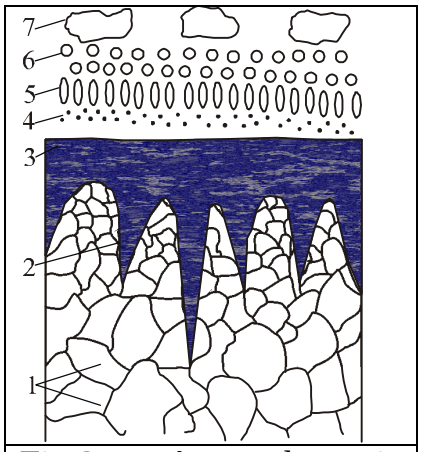

Fig.2. A schematic representation of the real surface of a SLTEM with a metal layer deposited on it: 1 - a broken layer with cracks; 2 - surface irregularities of TEM, 3 - metal layer, 4-7 - fragments of SLTEM, formed due to the presence of cracks

The transient layer, as can be seen from Fig. 2, can be "constructed" by filling with metal the voids formed after drawing the above-mentioned horizontal planes.

In both cases, the electrical contact resistance is determined by the formula [2]:

$$R_c = \frac{d(s_m - s_s)}{s_m s_s \ln(s_m / s_s)}. \qquad (4)$$

where s_m – the specific electrical resistance of contact metal, d – the thickness of transient layer.

Therefore, in the asymptotic limit, the electrical contact resistance for the SLTEM-nickel couple at $s_m = 1.67 \cdot 10^7$ Sm/m will be $1.22 \cdot 10^{-8}$ Ohm·cm^2, at $d = 20$ μm and $9.15 \cdot 10^{-8}$ Ohm·cm^2 at $d = 150$ μm.

Thus, we see that SLTEM with open Fermi surfaces, other things being equal, not only have a higher figure of merit value compared to traditional materials [1], but also yield significantly lower electrical contact resistances even for contacts with anti-diffusion layers.

1. Gorskyi P.V. (2017). Fivaz model and prediction of thermoelectric materials. *J.Thermoelectricity*, 1, 22-34.
2. Gorskyi P.V. (2018). Estimation of the electrical and thermal contact resistances and thermoemf of thermoelectric material-metal transient contact layer due to semiconductor surface roughness. *arXiv. 1809.02504v1 [cond-mat.mes-hall]*. 6p.

Light-Emitting Characteristics of Nanoparticles of Zinc Oxide in Biocompatible Polymeric Matrixes

Isaieva O.F.[1], Rudko G.Yu.[1], Fediv V.I.[2], Gule E.G.[1], Olar O.I.[2]

[1]*V. Lashkaryov Institute of Semiconductor Physics of National Academy of Sciences of Ukraine, Ukraine, info@isp.kiev.ua.*

[2]*Department of Biophysics and Medical Informatics, Bukovinian State Medical University, Chernivtsi, Ukraine, vfediv@ukr.net*

At present organic-inorganic nanocomposites are becoming a commonly used functional materials for light-emitting devices. Considerable interest to these materials is caused by the fact that their properties are not only a combination of the properties of matrix and filler; new properties emerge as a result of the presence of a thin layer at the boundary between the two phases, processes of charge exchange between the components of the nanocomposite, energy transfer from nanoparticles to a matrix and vice versa.

Nanosized zinc oxide is a promising material for use in light-emitting devices, in medicine, in cosmetology. ZnO attracts attention due to large band gap, high exciton binding energy and optical transparency.

To study and use nanoparticles, one has to start with nanoparticles synthesis and then place them into a matrix with appropriate physical properties. Thus, it is necessary to develop a cheap, environmentally friendly, low-temperature synthesis method, to investigate optical properties of the synthesized composite, and to analyze the effect of the matrix on the PL nanocomposite.

In the present study, we synthesize zinc oxide nanoparticles (*in situ*) in three different optically transparent biocompatible matrixes (polyvinyl alcohol, polyvinylpyrrolidone, and gelatin) and analyze their light-emitting properties. All of these polymers are highly soluble in water and other polar solvents, are optical-transparent and biocompatible. For the syntheses of zinc oxide nanoparticles, we used the following precursors: zinc acetate ($Zn(CH_3COO)_2$), tetramethyl hydroxide ($(CH_3)_4NOH$) (TMAH), urotropin and biocompatible polymers, which play a role of passivation agents and matrix of nanocomposite. We added TMAH to the zinc acetate/polymer solution at 1^oC, heated this solution to 80 ^oC and mixed it. The obtained colloidal solutions of zinc oxide nanoparticles in polymers were dried and, thus, thin films of nanocomposites were formed.

We compare light-emitting properties nanocomposites, obtained by the above method in three polymer matrixes. The obtained nanocomposites emit intense light which is perceived by the naked eye as blue-green. We studied photoluminescence spectra of nanocomposites at different excitation wavelengths as well as photoluminescence excitation spectra. The spectra of emission are almost the same irrespective of the matrix. Moreover, irrespective of the matrix, only one dominating band is seen in the photoluminescence excitation spectra. Based on the results obtained the nature of light-emitting properties of the synthesized nanocomposites was analyzed and the scheme of corresponding processes was proposed.

Hydrothermally Synthesized MoO_2, MoO_2/rGO та MoO_2/C: Structure, Morphology and Electrical Conductivity

Kachmar A., Boichuk V., Kotsyubynsky V., Bandura Kh., Khatsevych O.

Vasyl Stefanyk Precarpathian National University, Ivano-Frankivsk, Ukraine,
kotsuybynsky@gmail.com

Ultrafine molybdenum oxide is successfully tested as a catalyst, gas sensors, optoelectronics due to their crystal and electronic structure peculiarities. The successful application of MoO_2 as a pseudocapacitive electrode for hybrid supercapacitors implies the possibility of fast redox reactions on the material surface. The use of nanostructured MoO_2 / carbon systems reduces ion diffusion paths and increases the electrode material / electrolyte interface and the reactive redox response. Ultrafine MoO_2 and CM with reduced graphene oxide (MoO_2 / rGO) and nanoporous carbon (MoO_2/C) were obtained by hydrothermal route. All the samples are characterized by broadening of (211) and (312) reflexes of MoO_2 monoclinic structure (JCPDS 65-5787). Average sizes of coherent scattering domains for MoO_2, MoO_2/rGO and MoO_2/C materials are 5.2, 6.0 and 6.4 nm, respectively. The initial MoO_2 is a complex of spherical agglomerates with the sizes of about 14-17 nm. MoO_2/rGO has comparatively smaller particles sizes (12-13 nm). For MoO_2/rGO average thickness of stacked graphene planes in packets is about 1.8±0.3 nm (XRD data) so it consists of 2-3 graphene planes. The MoO_2/C material is more homogeneous and small carbon fragments form "shells" around MoO_2 particles. Pore distribution (low-temperature nitrogen adsorption (LTNA) data, DFT method) for MoO_2 are in the range of 7-20 nm. The contribution of graphene and oxide components was separated. Graphene component is characterized by micro- and mesopores with maximum diameters of 1.45 and 3.25 nm. There is a «narrowing» of the pore distribution range for the oxide component of MoO_2/rGO composite, compared to the «pure» MoO_2 that is the result of filling the interparticle pores with reduced graphene oxide. A similar «narrowing» is observed for the MoO_2/C system, moreover in this case the effect of filling the interparticle pores is relatively stronger. The electrical conductivity (EC) of the obtained materials was investigated by impedance spectroscopy (IS) in the temperature range of 25-200 ^oC and was fitted with Johnsher model. The calculated activation energy of the EC for MoO_2 is 0,146 ±0,015 eV. The presence of two conduction mechanisms (activation energies of about 0.10±0.01 eV and 0.23±0.01 eV) for MoO_2/rGO dominating at different temperatures is observed. EC of the graphene decreases with the frequency increasing and vice versa for the oxide component. An increase in the temperature causes the redistribution of the EC contributions for the oxide and graphene components. Frequency dependence of EC of MoO_2/C was fitted with Drude-Smith formalism. The models of MoO_2/rGO and MoO_2/C CM were proposed on the base of XRD, LTNA, SEM and IS.

Synthesis and Optical Properties of Cadmium Telluride Nanocrystals with Paramagnetic Doping

Kapush O.A [1], Budzulyak S.I.[1], Korbutyak D.V.[1], Dremlyuzhenko K.S.[1], Hatilov S.E.[1], Trishchuk L.I.[1], Tomashik V.M.[1], Yemets A.I.[2], Dzhagan V.M.[1]

[1]*V.Ye. Laskaryov Institute of Semiconductor Physics of NAS of Ukraine, Kyiv, Ukraine, savchuk-olja@ukr.net*
Institute of Food Biotechnology and Genomics NAS of Ukraine, Kyiv, Ukraine

One of the leading research directions of modern semiconductor physics is solving the problem of a controllable change of the properties of semiconductors nanocrystals (NCs), expanding their functionality for various applications (medicine, spintronics, sonotrons, optoelectronics, etc.). Additional functionality in semiconductor NCs can be obtained by introducing into their crystalline lattice of impurity atoms, in particular, ions of 3d-transition elements (Mn, Fe, Co, Ni, etc.). The main feature of these materials, known as dilute magnetic semiconductors (DMS), is the manifestation of strong s, p-d exchange interaction of band carriers with magnetic ions. This leads to a large Zeeman splitting of band and excitonic states, a giant magneto-optical Faraday effect, and the formation of magnetic polarons. In quantum-sized structures, these magneto-optical properties undergo transformation due to the superposition of quantum-size effect and exchange interactions.

In this paper we consider a simple way of room-temperature synthesis of CdTe NC doped with 3d-elements. CdTe NCs capped with thioglycolic acid and, thus, carrying a negative charge were synthesized in aqueous medium by means of colloidal synthesis in a semi-periodic reactor. The PL spectrum of freshly synthesized NCs CdTe, obtained in the presence of Mn dopant, is a narrow symmetric band with a maximum at 538 nm, only slightly red-shifted with respect to PL of undoped CdTe NCs (532 nm). Importantly, the presence of Mn ions in the reaction medium causes an extremely large increase in the PL intensity. It can be assumed that positively charged manganese ions are adsorbed on the surface of formed CdTe NCs with a negative surface charge. As a result of energy transfer between the CdTe NCs and the Mn ions, blocking of non-radiative recombination channels can take place.

Thus obtained NCs doped with manganese ions, possessing high efficiency of PL emission and magnetic moment, are very attractive for application as multimodal nanoparticle imaging probes in complex PL-MRT investigations.

Fermi Energy of a Thin Metal Nanotube with Elliptical Cross-Section

Karandas Ya.V.[1], Korotun A.V.[1], Titov I.M.[2]

[1]*Zaporizhzhya National Technical University, Zaporizhzhya, Ukraine, andko@zntu.edu.ua*
[2]*UAD Systems, Zaporizhzhya, Ukraine*

There are composite nanostructures that are commonly used in modern Hi-Tech, among which the metal nanotubes can be distinguished. Due to the effect of the radial mechanical stresses during the fusion process, in practice, the nanotubes are most often obtained with the cross-section form close to elliptical. One of the main characteristics of the electronic properties of the metallic nanosystems is the Fermi energy, which, in particular, makes the major contribution to the optical absorption. Therefore, the aim of this work is to study the effect of the cross-section's geometry of a metal nanotube on the behavior of its energy characteristics.

The size dependence of the Fermi energy of a metal nanotube is determined by solving the transcendental equation [1]:

$$\overline{n} = \frac{2}{\pi^2\left(b^2 - a^2\right)} \sum_{m,n} \sqrt{k_{\mathrm{F}}^2 - \left(\frac{x_{mn}}{b-a}\right)^2}\,, \qquad (1)$$

where $\overline{n}$ is the concentration of the conduction electrons in the 3*D*-metal; a and b are the effective internal and external radii, respectively; $x_{mn} = k_{mn}\left(b-a\right)$ are the roots of the equation:

$$\begin{aligned}(1+\varepsilon)\mathrm{i}_{mn} k_{mn}\left(J_{m+1}(\mathrm{i}_{mn}a)K_m(\mathrm{i}_{mn}a) - J_m(\mathrm{i}_{mn}a)K_{m+1}(\mathrm{i}_{mn}a)\right) = \\ = (b-a)k_{mn}\left(\mathrm{i}_{mn}^2 - k_{mn}^2\right)J_m(\mathrm{i}_{mn}a)K_m(\mathrm{i}_{mn}a).\end{aligned} \qquad (2)$$

Here $J_m(x)$ and $K_m(x)$ are the Infeld and McDonald functions; ε is the eccentricity which is the same for both internal and external ellipses; $\mathbf{h}k_{mn} = \sqrt{2m_e\varepsilon_{mn}}$; $\mathbf{h}\mathrm{i}_{mn} = \sqrt{2m_e\left(U_0 - \varepsilon_{mn}\right)}$; U_0 is the depth of the potential energy well.

It is shown that with the oscillating character of the size dependence of the Fermi energy, the relation $\varepsilon_{\mathrm{F}}/\varepsilon_{\mathrm{F}}^0 < 1$ ($\varepsilon_{\mathrm{F}}^0$ is the value of the Fermi energy in the 3*D*-metal) is satisfied, which is explained by the "extrusion" of the energy levels due to the decrease in the effective width of the potential energy well.

1. Korotun A.V., Karandas Ya.V., Babich A.V., Titov I.M. Oscillations of Fermi's energy of a Cylindrical Metal Nanoparticle // Nanosystems, Nanomaterials, Nanotechnologies. – 2018. – V.16, No. 3. – P. 451–463.

Complexing Properties of Nitrogen-Doped Nanomesh Graphene

Karpenko O.S., Demianenko E.M., Lobanov V.V., Kartel M.T.

Chuiko Institute of Surface Chemistry of National Academy of Sciences of Ukraine, Kyiv, Ukraine, karpenkooksana@ukr.net

Nanomesh graphene is an important representative of the graphene with intrinsic defects. They are produced by creating periodically ordered finite-size holes in a graphene sheet using electron-beam lithography or template techniques. A relaxation of electronic states along the edges of those holes is accompanied by local modifications of the graphene lattice and is followed by a number of important effects related to the conductivity and magnetism. Among the latter, one can distinguish complexing properties of thus obtained nanomesh graphene. To simulate a sample of the nanomesh graphene, we have chosen $C_{90}H_{24}$ cluster that has been formed by cutting six central carbon atoms from the hexagonal polyaromatic molecule (PAM) $C_{96}H_{24}$. Our calculations have been performed within the density functional theory (B3LYP, 6-31G**). To enhance electron-donor properties of such a perforated system, several two-coordinated carbon atoms ($C^{(2)}$) on the edge of the hole have been replaced by nitrogen atoms. The hole is formed as the result of breaking six C-C bonds, each having bond order of 1.5 and binding energy of 499 kJ/mol (similar to those in the benzene molecule). The electronic ground state (EGS) of the $C_{90}H_{24}$ system is a triplet which is significantly separated by energy from the lowest excited triplet and quintet states (2.9 and 1.1 eV, respectively). Each peripheral $C^{(2)}$ atom carries a relatively small positive charge (+0.015 a. u.) that makes no obstacle to bind cations. To investigate the ability of $C_{90}H_{24}$ derivatives to bind cations, we have created several model systems by a sequential substitution of one, two or six $C^{(2)}$ atoms in $C_{90}H_{24}$ by nitrogen atoms. To calculate corresponding energetic effects, we have employed the following model reactions: $C_{90}H_{24}$ + N **à** $C_{89}NH_{24}$ + C + 94.3 kJ/mol, $C_{89}NH_{24}$ + N **à** $C_{88}N_2H_{24}$ + C + 74.0 kJ/mol, and $C_{88}N_2H_{24}$ + N **à** $C_{87}N_3H_{24}$ + C + 65.0 kJ/mol, respectively. The EGS multiplicity (M) of nitrogen-substituted clusters is the following: M=6 for $C_{89}NH_{24}$, M=3 for $C_{88}N_2H_{24}$, and M=4 for $C_{87}N_3H_{24}$ (one has to note that the EGSs of $C_{89}NH_{24}$ and $C_{87}N_3H_{24}$ are not doublets). The energy of formation of the $[C_{87}N_3H_{24}Fe]^{+3}$ complex in its EGS (M=3) out of Fe^{+3} ion (M=6) and $C_{87}N_3H_{24}$ cluster (M=4) amounts 633 kJ/mol. Obviously, as the $[C_{87}N_3H_{24}Fe]^{+3}$ complex is formed, eight initially unpaired electrons of the interacting particles are re-arranged within three doubly occupied molecular orbitals, while two remaining unpaired electrons give rise to its triplet state. From the multiplicity considerations for EGSs of $C_{87}N_3H_{24}$ cluster and $[C_{87}N_3H_{24}Fe]^{+3}$ complex, one can conclude that the binding of Fe^{+2} cation is impossible.

Conductivity of β-$Ni(OH)_2$/C Composites Exposed to Ultrasound

Khemii O.M., Budzulyak I.M, Yablon L.S., Khemii M.M., Popovych O.V.

Vasyl Stefanyk Precarpathian University, Ivano-Frankivsk, Ukraine, khemiiolha@gmail.com

Ultrafine nickel hydroxide is attractive for investigations due to peculiarities of its structural and electronic properties. Creation of composites based on nickel hydroxides and activated carbon allows to increase the specific capacities of materials several times. It is known that β-$Ni(OH)_2$ is a p-type semiconductor with low conductivity and a band gap of 4 eV [1], whereas in atomic amorphous carbon materials, atoms form mostly sp^2 and sp^3 hybridized bonds, as a result of which they are bad conductors [2]. From the obtained results, it was established (Table 1) that the electrical conductivity of β-$Ni(OH)_2$ after exposure to ultrasound was $2.95 \cdot 10^{-4}$ $\Omega^{-1}m^{-1}$, whereas the non-dispersed β-$Ni(OH)_2$ was $1.24 \cdot 10^{-4}$ $\Omega^{-1}m^{-1}$. Ultrasonic dispersion results in the grinding of material particles, which reduces the resistance of the material. For investigated materials, the growth of conductivity with increasing frequency is observed, which is probably due to the jumping mechanism of charge transfer. The conductivity of the β-$Ni(OH)_2$ / C composite exposed to ultrasound at a mass ratio of 9: 1 reaches 0.75 $\Omega^{-1}m^{-1}$. With increasing content of nanoporous carbon in composites, conductivity increases. However, this negatively affects the value of the specific capacity of composites, since it is established [3] that the optimum carbon content in composites based on nickel hydroxide is 10% of the total mass.

Table 1

Conductivity of β-$Ni(OH)_2$ and β-$Ni(OH)_2$ / C composites

Sample	Conductivity, $\Omega^{-1}m^{-1}$
β-$Ni(OH)_2$	$2{,}95 \cdot 10^{-4}$
β-$Ni(OH)_2$/C (9:1)	0,75
β-$Ni(OH)_2$/C (5:5)	20
β-$Ni(OH)_2$/C (1:9)	38

1. Nickel foam-supported porous $Ni(OH)_2$/NiOOH composite film as advanced pseudocapacitor material / [Y.F. Yuan, X.H. Xia, J.B. Wu et al.] // Electrochim. Acta. – 2011. – V. 56. – P. 2627–2632.
2. Electrical Conductivity of Nitrogen-Containing Nanoporous CarbonMaterials / [M.M. Kuzyshyn, B.K. Ostafiychuk, I.M. Budzulyak et al.] // PHYSICS AND CHEMISTRY OF SOLID STATE. – 2014. – V. 15, № 3. - P. 497-503.
3. Electrochemical Properties of Nanocomposite Nanoporous Carbon / Nickel Hydroxide / [O.M. Hemiy, L.S. Yablon, I.M. Budzulyak et al.] // J. Nano-Electron. Phys. – 2016. – V. 8. – P. 04074.

More on the Size Dependence of Surface Plasmons Frequency of Metal Nanoparticle

Koval' A.O., Korotun A.V., Pogosov V.V.

Zaporizhzhya National Technical University, Zaporizhzhya, Ukraine, andko@zntu.edu.ua

As is known, the optical properties of metal-dielectric nanocomposites are due to the surface plasmon resonance of small metal particles, the position and shape of the line of which depend on the dielectric constant of the host matrices, the concentration and size of the nanoparticles. Therefore, the aim of the work is a derivation of size asymptotics for the surface plasmons (SP) frequency of metal nanoparticles in dielectric host.

It is well known that the poles of the scattering amplitude of Mie's solution determine the SP frequency of an isolated sphere with taking retardation exactly into account. Taking into account the plasmon resonance condition in the nonstationary case [1] and using the Drude formula for the dielectric function of metal sphere, we obtain the equation

$$\grave{o}^{\infty} - \frac{\omega_{\mathrm{p}}^2\left(\tau_{\mathrm{bulk}}^{-1} + 3v_{\mathrm{F}}/4R\right)^2}{1+\omega_{\mathrm{sp}}^2\left(\tau_{\mathrm{bulk}}^{-1} + 3v_{\mathrm{F}}/4R\right)^2} = -2\grave{o}_{\mathrm{m}}\left(1+\frac{6}{5}\grave{o}_{\mathrm{m}}\left(\frac{\omega_{\mathrm{sp}}R}{c}\right)^2\right), \qquad (1)$$

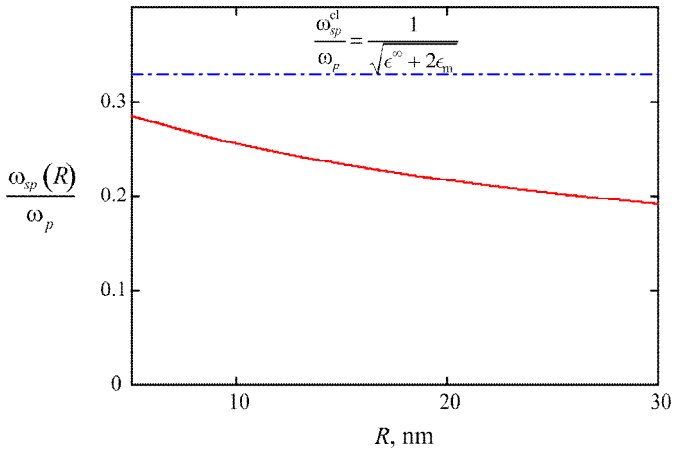

Fig.1. Size dependence of the SP frequency for Ag nanospheres, embedded in Teflon ($\grave{o}_{\mathrm{m}} = 2.3$)

where ω_{p}, v_{F}, $\grave{o}^{\infty}$, τ_{bulk}, $\grave{o}_{\mathrm{m}}$, R and c are the plasma frequency, the lattice contribution, the relaxation time, the Fermi electron velocity for the 3*D*-metal, the host dielectric, the particle radius, and the speed of light.

The size dependence of the SP frequency, calculated from Eq. (1), is shown in Fig. 1. One can see, that $\lim\limits_{R\to\infty}\omega_{\mathrm{sp}}(R) \to \omega_{\mathrm{sp}}^{\mathrm{cl}}$ (blue dash-dotted line) and $\lim\limits_{R\to\infty}\omega_{\mathrm{sp}}(R) \to 0$ (red solid line) without and with light lag.

Thus, it is shown that the effect of the finiteness of the speed of light is the reason for the decrease in the SP frequency with an increase in the radius of the metal nanoparticle.

1. Bohren C.F., Huffman D.R. Absorption and scattering of light by small particles. – John Wiley & Sons, 2008 – 530 p.

Modification of Surface of ZnO:Mn Nanocrystals Synthesized by Cryochemical Method

Kovalenko A.V., Vorovsky V.Yu., Bulaniy M.F., Khmelenko O.V.

Oles Honchar Dnipro National University, Dnipro, Ukraine,
kovalenko.dnu@gmail.com

The method of cryochemical synthesis (CCS) is based on the thermal decomposition of salts of initial components, which solutions were frozen before it as tiny drops and dried up by a sublimation method. The nanocrystals (NC) obtained by this method have a chemically inactive surface which diminishes the possibility of their practical use as chemical catalysts, gas sensors and other functional materials. Therefore the development of surface modification methods of NC is an actual task. The influence of organic admixture – polyvinyl alcohol (PVA) – on physical properties of ZnO:Mn NC obtained by the CCS method was investigated in this work. ZnO:Mn NC were synthesized at T = 850 °C from water solutions of zinc sulfates and manganese sulfates with the concentration of manganese 4 at % at different conditions of thermal decomposition of initial components: in the first case without PVA, and in the second one with PVA in ratio 1:1.

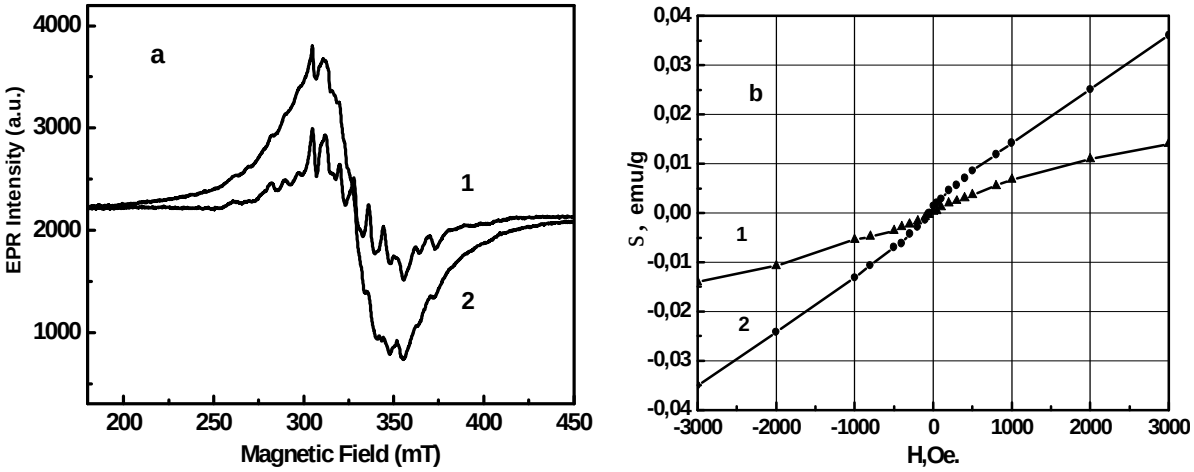

Fig. 1 EPR spectra (a) and the magnetization curves (b) of NC ZnO:Mn patterns with concentration of Mn 4 at % , synthesized without PVA – (1) and with PVA (2).

It was ascertained by EPR method that there is an increase of amount of paramagnetic admixture of Mn2+ ions on the surface of ZnO: Mn NC which indicates the increase of intensity of EPR spectrum line (Fig. 1, a). The research of patterns by the method of vibratory magnetometry also showed the increase of their paramagnetic properties at heat treatment in the presence of PVA (Fig. 1, б). Thus, we showed the possibility of realization of surface modification of NC ZnO: Mn by heat treatment of dry salts in mixture with the admixture with PVA.

Magnetic Properties of New High Entropy $Fe_{25}B_{17.5}Co_{21.35}Nb_{3.65}Ni_{25}Si_{7.5}$ Metallic Glass

Kushnerov O.I., Bashev V.F.

Oles Honchar Dnipro National University, Dnipro, Ukraine, kushnrv@gmail.com

About 14 years ago, the first papers on the study of high-entropy alloys (HEAs) were published. The HEAs are composed of at least 5 major components with equiatomic or nearly equiatomic concentrations which are between 5 and 35 at. %. The HEAs are characterized by unique structures and a number of useful service characteristics, such as hardness, wear resistance, resistance to oxidation, corrosion, and ionizing radiation, and high thermal stability. Thus, the HE alloys show promise as materials for application in electronics, atomic power engineering, transportation equipment, space-rocket hardware, etc. In contrast to HEAs, metallic glasses (MGs), known as another type of advanced materials, usually contain more than two kinds of elements but only one, sometimes two principal constituents. Due to their considerably different characteristics in structure and composition rules, the HEAs and MGs have been studied independently until the HEAs with an amorphous structure, namely high entropy metallic glasses (HE-MGs) were successfully synthesized. The developed HE-MGs provide a new strategy to design and synthesis MGs. The HE-MGs possess excellent mechanical and physical properties inherited from the advantages of both HEAs and MGs and show great potential for practical applications. In particular, MGs usually possess excellent soft magnetic properties including low power loss and high saturation magnetization.

In this study, a new nanostructured $Fe_{25}B_{17.5}Co_{21.35}Nb_{3.65}Ni_{25}Si_{7.5}$ (at.%) HE-MG was synthesized by the means of splat-quenching (SQ) technique. The estimated cooling rate was ~10^6 K/s.

The coercive force (H_c) of the SQ films of investigated HE-MG alloy was measured with a B–H loop tracer and reaches a relatively low value of 40 A/m, which is much smaller than in the crystallized as-cast alloy. So in accordance with the measured values of H_c the SQ alloy exhibit a typical soft magnetic hysteresis characteristic. The origin of the lower H_c can be attributed to the low number density of the domain-wall pinning sites resulting from the high degree of amorphicity and structural homogeneity proceeding from the high glass forming ability. Such behavior is typical for alloys in the amorphous state. The $Fe_{25}B_{17.5}Co_{21.35}Nb_{3.65}Ni_{25}Si_{7.5}$ HE-MG exhibits also high saturation magnetization of 74 A·m^2/kg, measured by a vibrating sample magnetometer at room temperature. SQ films demonstrate high microhardness value of 8000 MPa indicating good mechanical properties of $Fe_{25}B_{17.5}Co_{21.35}Nb_{3.65}Ni_{25}Si_{7.5}$ HE-MG.

Stable Leadless Nanocomposite Material for Thick-Film Sensor Elements and Hybrid Integrated Circuits

Lepikh Ya.I., Lavrenova T.I.

Interdepartmental Scientific and Educational Physical-Technical Center of the MES and NAS of Ukraine at the Odessa I.I. Mechnikov National University, ndl_lepikh@onu.edu.ua

As it is known, the characteristics of the thick-film sensors and the film elements of hybrid integrated circuits (HIC) are determined by the composite material composition, structure and electrophysical parameters.

The functional basis of resistive pastes, which are widely used in thick-film technology, are usually ruthenium, silver and palladium oxide compounds. As a glass binding agent in the paste composition the special glass from the group (lead-boron-aluminum) - silicate glass includes. Such materials have a number of disadvantages, in particular, the presence of lead toxic compounds in the glass binding agent; low reproducibility and instability of electrophysical parameters.

The material developed by us contains the conducting phase on the basis of ruthenium, silver and palladium oxide compounds, glass-bonding agent from fusible glass with the main component of bismuth oxide instead of toxic lead. Alloying impurities are selected in such a way as to provide the necessary composite material physical and technical characteristics.

The advantages of the glass binder agent in the nanocomposite material are: a significant reduction in the temperature of the softening beginning (400 – 430 °C) and linear thermal expansion coefficient (LThEC) ($80 \cdot 10^{-7}$ – $95 \cdot 10^{-7}$ degree^{-1}); the glass specific surface resistance increase of ten times (10^{14} Ohm·m), which makes it possible to use it in the manufacture of thick-film resistors for operation in high-voltage equipment. Experimental studies have shown that glasses can crystallize in the process of heat treatment. The concentration of the α-SiO_2 crystalline phase under the influence of temperature increases, changing the material electrophysical parameters.

The presence of the α-SiO_2 crystalline phase in the glass in the initial state and the growth of its concentration after annealing leads to an increase in the specific surface resistance of resistive thick-film elements by 10%, which affects the scattering of their resistance values (reproducibility).

In addition, the presence of unburnt crystalline phase α-SiO_2 causes the surface roughness.

In the material for thick-film elements, the concentration of SiO_2 is reduced by about 4 times, which reduces the effect of α-SiO_2 on the element electrophysical properties: it increases the reproducibility of the resistance and reduces their surface roughness.

The proposed resistive material allows to obtain thick-film elements with a specific surface impedance of 0.5-10.0 Ohm / cm^2.

Surface-Modified Nanoadsorbent for the Removal of Heavy Metals and Halogen Ions from Aqueous Solution

Mironyuk I.[1], Tatarchuk T.[1], Vasylyeva H.[2], Gun'ko V.M.[3], Bezruka N.A.[4], Dmytrotsa T.V.[4]

[1]*Vasyl Stefanyk Precarpathian National University, Ivano-Frankivsk, Ukraine,* tatarchuk.tetyana@gmail.com
[2]*Uzhgorod National University, Uzhgorod, Ukraine*
[3]*Chuiko Institute of Surface Chemistry, Ukraine*
[4]*Ivano-Frankivsk National Medical University, Ivano-Frankivsk, Ukraine*

The adsorption processes are most commonly used to remove inorganic and organic pollutants from wastewater. However, there are no studies on adsorption of alkaline-earth cations onto partially modified hydrophobized/hydrophilic silica surfaces. It is known that silica is inert, non-toxic, and non-corrosive. It has stable thermal and chemical characteristics, and it is widely used as an adsorbent. In current research the study of effects of the nanosilica surface silylation degree (i.e., hydrophobization) on the adsorption of metal and halogen ions (Ba(II), Sr(II), Zn(II), Ca(II), Mg(II), Cl^-, Br^-, I^-) from aqueous solutions has been done.

It was shown, that the chemical modification of the surface of fumed silica by substitution of silanols on the TMS groups affects both the morphology of primary and secondary particles and the atomic structure of nanooxide. An increase in the degree of silylation from Θ_{TMS} = 0.272 to 0.483 results in an increase in mesopore volume more than twice and changes in the structural characteristics of the material such as an increase in the valence angle in the Si-O-Si bridges and a decrease in interatomic distances. The degree of nanosilica silylation by trimethylethoxysilane at Θ_{TMS}<0.5 does not result in complete hydrophobization of the surface; *i.e.*, these samples can be suspended in the aqueous media. However, the hydrophilicity coefficient decreases with increasing Θ_{TMS} value. A mosaic hydrophilic/hydrophobic surface of partially silylated nanosilica is characterized by increased adsorption capability with respect to both positive charged metal species (series Sr(II) < Mg(II) < Zn(II) < Ca(II) < Ba(II)) and halogen anions (series Br^- < I^- < Cl^-). The most effective organosilica at Θ_{TMS} = 0.483 adsorbs 1.8 mmol/g of Ba(II) from 0.01 M $BaCl_2$ solution that is three times higher than that for unmodified silica. Among anions, the adsorption of Cl^- is maximal (1.34 mmol/g of Cl^- from 0.01 M $CaCl_2$ solution) onto silylated nanosilica at Θ_{TMS} = 0.272 that is eight times greater than that for the unmodified nanosilica. An increased adsorption ability of partially silylated nanosilica in comparison to unmodified silica can be explained by nonuniformity of a modified silica surface resulting in enhanced clusterization of adsorbed water that leads to reduction of its activity as a solvent. Therefore, the desolvation energy decreases for adsorbed cations and anions having smaller solvated shells near the modified silica surface.

Adsorption of Ba(II) and Zn(II) cations by mesoporous TiO_2

Mironyuk I.[1], Vasylyeva H.[2], Tatarchuk T.[1], Mykytyn I.[1], Danyliuk N.[1]

[1]*Vasyl Stefanyk Precarpathian National University, Ivano-Frankivsk, Ukraine,*
tatarchuk.tetyana@gmail.com
[2]*Uzhgorod National University, Uzhgorod, Ukraine*

Adsorption technologies are widely used to extract heavy metals cations Pb(II), Cd(II), Ba(II), Zn(II), Hg(II), Sr(II), Cs(I) and anions AsO_4^{3-}, SeO_4^{2-}, F^- (which have cancer, mutagenic and teratogenic effects on human organism) from aqueous medium. Synthetic adsorbents such as activated carbon, metal oxides Fe_3O_4, CeO, ZnO, TiO_2, titanium or zirconium phosphates are typically used for adsorption of these ions. However, low adsorption capacity of known materials encourages invention of much more effective adsorbents.

In present investigations, we propose a new high effective adsorbent toward barium and zinc ions – mesoporous anatase modification TiO_2. For synthesis of porous anatase modification of TiO_2, the solution of titanium aquacomplex precursor $[Ti(OH_2)_6]^{3+}\cdot 3Cl^-$ and modifying reagent Na_2CO_3 (4 wt.%) were used. Such modification leds to formation of globular particles with diameter of 3 mm with chemosorbed carbonate groups ≡TiOCOOH during the liquid-phase synthesis. On the stage of gel formation and drying of the dispersion, a xerogel-like material with a homogeneous mesoporous structure is formed (size 2-4 nm). The volume of mesoporous adsorbent is 0.29 $cm^3\cdot g^{-1}$ and a specific surface area is 373 $m^2\cdot g^{-1}$. According to those characteristics, the modified sample exceeds the unmodified TiO_2 in 2.8 and 2.7 times respectively.

The developed mesoporous structure, large surface area and the ionogenic nature of chemosorbed groups provides its high selectivity for the adsorption binding of barium and zinc cations. Since carbonate groups shift the point of a zero charge pH_{pzc} from 5.35 to 3.36, the functionality of the sorbent expands, namely, it provides an effective adsorption of metals in the acid solutions. In electrolytic mediums, modified adsorbent shows higher adsorption capacity toward Ba(II) and Zn(II) cations, compared to unmodified adsorbent. In solutions with concentrations $BaCl_2$ and/or $ZnCl_2$ from 0.01 $mol\cdot L^{-1}$ to 0.1 $mol\cdot L^{-1}$ the adsorption of heavy metal cations by modified adsorbent in 2-2.7 times higher than adsorption by an unmodified adsorbent.

The experimental results for Ba(II) and Zn(II) adsorption by the modified TiO_2 fit well with Langmuir adsorption model. According to Langmuir model the maximum adsorption value of barium and zinc cations onto modified TiO_2 are 5.67 $mmol\cdot g^{-1}$ for Ba(II) and 1.96 $mmol\cdot g^{-1}$ for Zn(II) compared with 1.38 $mmol\cdot g^{-1}$ for Ba(II) and 1.43 $mmol\cdot g^{-1}$ for Zn(II) onto unmodified TiO_2.

The Influence of the Mechanical and Electric Fields on the Nucleation of the Nanometer Structure in Semiconductors under the Action of Laser Irradiation

Peleshchak R.M., Kuzyk O.V., Dan'kiv O.O. and Bryzhko V.S.

Drohobych Ivan Franko State Pedagogical University, Drohobych, Ukraine,
rpeleshchak@ukr.net

The elastic fields created by defects are the determining factor in the formation of the surface superlattice of adatoms [1]. The periodic deformation arising on the surface of semiconductor leads to the modulation of the bottom of the conduction band and, respectively, to the modulation of electronic density. The arising nonuniform electric field leads to the nonuniform displacement of the nodes of the crystal lattice and, respectively, to the change in the amplitude of the surface acoustic wave (SAW). Therefore, it can be expected that when placing a semiconductor in the external electric field, it is possible to change the conditions of the formation of laser-induced periodic surface nanostructures and predictably control their parameters due to the interaction of the electric field with nonuniform distributed on the surface of free current carriers.

The theory of nucleation of the surface superlattice of adatoms in GaAs semiconductor under the influence of laser irradiation at the action of electric field, directed perpendicular to the direction of propagation of the SAW, is developed. The proposed theory takes into account the interaction of adatoms and conduction electrons with self-consistent SAW. The semiconductor can be located both in the external electric field and internal, created, for example, by a hetero-borders. And depending on the direction of the electric field, it is possible to increase or decrease the deformation flows of adatoms.

The formation of the superlattice is possible if the average concentration of adatoms exceeds a certain critical value (or the temperature is less than a certain critical value). It is established that in GaAs semiconductor, an increase in the electric field strength, depending on the direction, leads to an increase or decrease of the critical temperature (the critical concentration of adatoms), at which the formation of self-organized nanostructure is possible. It is shown that the influence of the electric field is more significant in the highly doped semiconductors and also in semiconductors with a high value of the constant of hydrostatic deformation potential of the conduction band and electron mobility. GaAs is the most optimal for these parameters.

1. Peleshchak R.M., Kuzyk O.V., Dan'kiv O.O. The influence of ultrasound on formation of self-organized uniform nanoclusters. *Journal of nano- and electronic physics*. 2016. V.8, №2. P. 02014.

Equilibrium States in Nano-Scale Binary Metallic Materials and Equilibrium Curves in the Two-Phase Region of the Phase Diagram

Shirinyan A.S.[1], Bilogorodskyy Y.S.[2], Wilde G.[3] and Makara V.A.[1,4]

[1] *"Physical-chemical materials science" center of National Academy of Sciences of Ukraine, Kyiv, Ukraine, aramshirinyan@ukr.net; shirinyan@nas.gov.ua.*

[2] *Research and Education Institution "Cherkasy Regional Center of works with students", Cherkasy, Ukraine*

[3] *Institut für Materialphysik, Westfälische Wilhelms-Universität, Münster, Germany*

[4] *Department of Metals Physics, Faculty of Physics, Kyiv National University named after T. Shevchenko, Kyiv, Ukraine*

Surface and volume confinement effects need to be taken into account into the description of phase changes in nanoscale systems [1]. In our investigation a modified Gibbsian thermodynamics approach has been suggested to describe: i) the solidification of a nano-sized liquid alloy droplet, ii) melting of a nano-sized solid particle of a spherical shape and iii) the equilibrium states in the two-phase region of the temperature-composition phase diagram. Cu-Ni has been chosen as a model system.

This description shows for the first time the occurrence of melting and solidification loops at the size-dependent temperature-composition phase diagram for the isolated Cu-Ni nanosystem, showing two-phase equilibrium states for droplet / particle radii of 25nm, 40nm and 80nm, i.e. well within the size domain of nanoparticles that are used for applications in additive manufacturing [2]. Results lead to the new "melting loop" and "solidification loop" concepts concerning the phase diagram [3].

1. Shirinyan A. S., Wautelet M. Phase separation in nanoparticles *Nanotechnology*. 2004. **15**. P. 1720–1731.
2. Shirinyan A., Wilde G., Bilogorodskyy Y.S. Solidification loops in the phase diagram of nanoscale alloy particles: from a specific example towards a general vision. *Journal of Materials Science*. 2018. **53**. P. 2859–2879.
3. Shirinyan A. Two-phase equilibrium states in individual Cu-Ni nanoparticles: size, depletion and hysteresis effect. *Beilstein Journal of Nanotechnology*. 2015. **6**. P. 1811-1820.

Electronic Structure of Pr*M*O_3 (*M*=Co, Fe) Perovskites

Shved V.M., Hreb V.M., Turchak S.L., Vasylechko L.O.

Lviv Polytechnic National University, Lviv Ukraine, crystal-lov@polynet.lviv.ua

Rare earth (RE) cobaltites and ferrites are intensively studied strongly correlated materials. Series of the micro- and nanocrystalline powders of $PrCo_{1-x}Fe_xO_3$ ($0 \le x \le 0$) were obtained by solid state and wet chemistry routes [1, 2]. The lattice parameters and atomic positions in the "pure" $PrCoO_3$ and $PrFeO_3$ compounds obtained from X-ray synchrotron powder diffraction data [1] were used in electronic structure calculations of these materials. Different approximations of DFT, such as GGA+U and hybrid functional, were employed to take into account the Coulomb repulsion between highly localized *3d* or *4f* electrons. All calculations were performed using ABINIT software package.

Our calculations revealed that at low temperatures $PrCoO_3$ is a nonmagnetic insulator with the direct (Γ-Γ) band gap of 2.06 eV (see Figure). The Co^{3+} ions are in low spin (LS) configuration, which agree well with the literature. According to literature data, praseodymium orthoferrite $PrFeO_3$ exhibits the G-type antiferromagnetic ordering with magnetic moment of 4.14 μ_B per Fe^{3+} ion. Our GGA+U calculations show that $PrFeO_3$ is the antiferromagnetic insulator with indirect Y-Γ band gap of 1.35 eV. The magnetic moment of 4.14 μ_B per Fe^{3+} ion in our calculations was obtained applying the U values of 5.5 and 7 eV for Fe 3*d* and Pr 4*f* states, respectively. To the best of our knowledge, no electronic structure calculations for orthorhombic $PrFeO_3$ perovskite were reported in the literature so far.

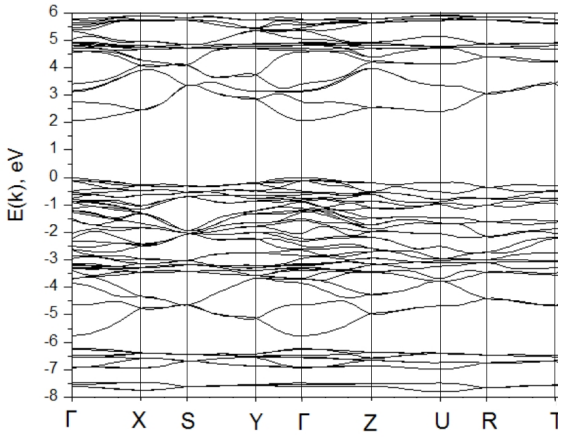

The calculated band structure of $PrCoO_3$

1. O.V. Kharko, L.O. Vasylechko. Structural behaviour of solid solutions in the $PrCoO_3$– $PrFeO_3$ system. *Visnyk of Lviv Polytechnic National University* 734 (2012) 119-126 (*in Ukrainian*).
2. O. Pekinchak, L. Vasylechko, I. Lutsyuk, Ya. Vakhula, Yu. Prots, W. Carrillo-Cabrera. Sol-gel prepared nanoparticles of mixed praseodymium cobaltites-ferrites. *Nanoscale Research Letters* (2016) 11:75 (6 pp).

Peculiarities of dark and illuminated current-voltage characteristics of nanocrystalline anatase and rutile TiO_2

Smertenko P.S.[1], Naumov V.V.[1], Kernazhitsky L.A.[2], Shymanovska V.V.[2], Gavrilko T.A.[2], Manuilov E.V.[2], Solntsev V.S.[1], Yukhymchuk V.O.[1]

[1]*Lashkaryov Institute of Semiconductor Physics, NAS of Ukraine, Kyiv, Ukraine,* petrosmertenko@gmail.com

[2]*Institute of Physics, NAS of Ukraine, Kyiv, Ukraine*

Titanium dioxide (TiO_2) is a well-known metal-oxide wide-gap *n*-type semiconductor material with unique electrophysical and optical properties, widely used in photonics, photosensors, and photovoltaics. But despite advances in applications, the mechanism of electrical conductivity in TiO_2 is still far from clarity. Here we report our first study of current-voltage characteristics (CVC) of nanocrystalline TiO_2 with different anatase (*A*) and rutile (*R*) structure.

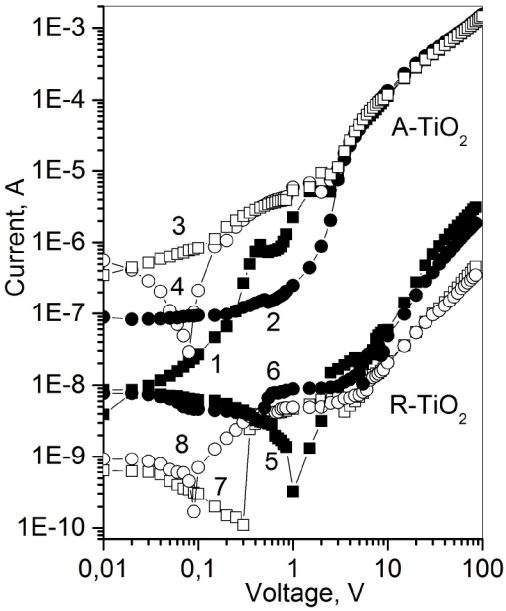

Fig. 1. Anatase and rutile TiO_2 current-voltage characteristics in the dark (1, 2, 5, 6) and light (3, 4, 7, 8) in the forward (1, 3, 5, 7) and reverse (2, 4, 6, 8) loading.

High-purity single-phase *A* and *R* TiO_2 was synthesized by thermal hydrolysis followed by calcination at 300ºC. The initial structural, morphological, compositional, and optical properties were studied by XRD, SEM, FTIR, UV-VIS, and PL methods [1]. According to the analysis, the TiO_2 particles had a well-crystallized structure (size of crystallites ~10-15 nm), and the surface density of the powder was ~240 m^2/g (anatase) and 95 m^2/g (rutile). The CVC were measured by an automated 14TKS-100 tester in a quasi-stationary mode (voltage range up to 100 V, measurement pulse ~90 ms, light power of illumination ~10 mW/cm^2) [2]. The samples were prepared in the form of a 100 μm thick powder layer between two ITO plates with ohmic contacts made using Ag paste. The experimental CVC in Fig. 1 show the following: (i) key features appear at low voltages (<3 V); (ii) at higher voltages (>3 V), the curves coincide; (iii) under illumination, anatase curves have a usual behavior, whereas rutile curves are unusual, and dark curves are below the illuminated ones; (iv) anatase and rutile curves differ by three orders of magnitude; (v) dark curves have a negative range. Note that Raman spectroscopy, carried out after electrical experiments, revealed the appearance of a secondary oxide phase in the form of thin films on ITO plates as a result of electrophotocatalytic effects. Research is in progress.

1. Kernazhitsky L. et al. *Ukr. J. Phys.* 2014. V. 59, No. 3. P. 246-253.
2. Gorbach T.Ya. et al. *Ukr. J. Phys.* 2014. V. 59, No. 6. P. 601-611.

Thermo- and Photoluminescence of Tl_4CdI_6 and Tl_4HgI_6 Nanocrystals Embedded in Natural Cavities

Solovyov M.V.[1], Bovgyra O.V.[1], Franiv I.A.[2], Futey O.V,[1], Solovyov V.V.

[1]*Lviv National Ivan Franko University of Lviv, Lviv, Ukraine, Solov_Nik@ukr.net*
[2]*National University "Lviv Polytechnic", Lviv, Ukraine*

At present, of a topical problem of semiconductor microelectronics is controlled change in the fundamental characteristics and spectral-kinetic parameters, particularly, such as the bandgap of a semiconductor, the energy position and half-width of exciton absorption and photoluminescence bands. etc. without changing the crystalline structure and chemical composition of a semiconductor.

It is known that suitable object for studying the above mentioned problem is that one in which the gradual reduction of its dimentionality and volume at transition from the block three-dimentional to quasi zero-dimentional crystal of a quatum-dot type is realized. Promising model objects of quasi zero-dimensional media whose properties are currently being studied actively are the periodic lattices of microcrystals of various semiconductor compounds synthesized in the cavities of various matrices as well as those grown by the epitaxial methods. The main scientific interest in such objects is concentrated around the questions of possibility of forming three-dimensional superlattice, the regularities of renormalization of the energy spectrum of charge carriers, general problems of the theory of electron energy specrum at the transformation of crystals from purely three-dimensional, block, single crystal to quasi three-, two- and zero-dimentional structures.

In this paper, we investigate the optical properties of Tl_4CdI_6 and Tl_4HgI_6 crystals synthesized in the structural matrices of natural zeolite (mordenite), beryl, alkaline borosilicate glass and porous silicon at changing the structure and parameters of the matrices and creating the conditions under which the predefined number of elementary cells is formed in the quantum dot.

On the basis of the obtained results one can propose the method of exciton spectroscopy as a way that practically allows to analyze the effective sizes of nano- and microcavities of porous materials with using the parameters of high-energy shift of the thermo- and photoluminescence spectrum of Tl_4CdI_6 and Tl_4HgI_6 crystals.

Synthesis and Growth of Tl_4CdI_6 and Tl_4HgI_6 Nanocrystals in Dielectric Matrices

Solovyov M.V.[1], Kashuba A.I.[1], Vasyliuk S.V.[2], Franiv A.I.[1], Franiv V.A.[1]

[1]*Lviv National Ivan Franko University of Lviv, Lviv, Ukraine, Solov_Nik@ukr.net*

[2]*National University "Lviv Polytechnic", Lviv, Ukraine*

Natural or synthetic zeolites can serve as model objects for synthesis and growth of nanocrystals of fixed dimensions. These minerals are formed by alternate substitution of tetrahedral sublattices of AlO_4 and SiO_4 compounds with the cavity structure in which alkaline cations and molecules of crystalline water are present. Channels existing in the structure of zeolites are formed by various combinations of bound rings of tetrahedra. Depending on the type of natural zeolite, the diameter of the inner cavity can vary within the range from 2,2 Å to 8 Å, and in synthetic zeolites - up to 13 Å. Without taking into account details of the synthesis process, we note that our choice was made on natural zeolite - mordenite. The chemical formula of the latter has the form $Na_2(AlSi_6O_{12})_2 \cdot 7H_2O$. The temperature of destruction of mordenite lattice is ~ 800°C, and the temperature of dewatering (water separation from the cavities) is 150 ÷ 250°C. In this respect, in the interval 200 <T <700°C, it was possible to obtain a stable dewatered matrix of nano-cavities with an effective diameter d≈7Å, in which the synthesis of nanocrystals of the studied objects was carried out. It turned out that the etched in a solution of hydrochloric acid alkaline borosilicate glass Na_2O-B_2O_3-SiO_2, or natural mineral "beryl" - $Al_2Be_3[Si_6O_{18}].H_2O$ can be considered as the the most suitable vitreous matrices In the process of etching by three molar solution of hydrochloric acid (at a temperature of 100-150 ° C), on the surface of the alkaline borosilicate glass, the cavities with an average size $a_i = 5 \div 7$ nm are formed. The structure of beryl is such that within the mineral there are filamentary channels with a diameter $a_i = 8 \div 12$ nm, filled with crystalline water. At a temperature of 150 ° C, by means of evacuation, the dehydration of mineral channels was carried out. In the cavities of matrices of alkali-borosilicate glass and beryl prepared by this technique the synthesis of nanocrystals was carried out at corresponding temperatures by the method of vacuum sublimation.

Thus, the samples of nanocrystals synthesized in various glass-like matrices with the required set of a_i / a_{ex} ratios were obtained which can be used for experimental verification of the effects of quantization of exciton states in Tl_4CdI_6 and Tl_4HgI_6 crystals.

Optical and Magneto-Optical Properties of Mn-Doped $A^{II}B^{VI}$ Quantum Dots

Stolyarchuk I. D., Serbin H.O., Stolyarchuk A.I.

Department of Physics, Drohobych Ivan Franko State Pedagogical University, Drohobych, Ukraine, istolyarchuk@ukr.net

Doping with magnetic impurities has led to formation of new class of materials, diluted magnetic semiconductors (DMSs) [1]. Among these materials the most studied are Mn-doped II-VI based DMSs type of (II-VI):Mn or ternary solid solutions type of $II_{1-x}Mn_xVI$. Dopant-carrier exchange interactions in the DMSs give rise to large Zeeman spin splittings of the excitonic or band states and related giant magneto-optical Faraday rotation. The usefulness of magnetic doping process for bulk semiconductors has influenced its application for case of nanostructured materials type of nanocrystals, nanoparticles or quantum dots [2,3].

Up to now, the mechanism that controls dopant incorporation into nanoparticle is not fully understood. The developed theoretical doping models were mainly applied to explain the experimental results on chemical colloidal nanocrystal-doping synthesis. In this paper, we compare structural, optical and magneto-optical properties of Mn-doped semiconductor CdS, CdTe, ZnO nanoparticles prepared by different physical and chemical methods. Among physical techniques we have chosen ball milling or mechanical synthesis, melting powder mixtures of semiconductor and glass components, and pulsed laser deposition technique using combined targets. Chemical methods are represented by the aqueous solution precipitation technique.

All the samples were characterized by X-ray diffraction (XRD), transmission electron microscopy (TEM), optical absorption, magnetophotoluminescence, and Faraday rotation spectroscopy.

In magnetic field up to 7 T shift of the photoluminescence structure towards long wavelength was observed due to the strong spin-exchange interaction between band carriers and magnetic ions. The linear magnetic field dependence of the Zeeman shifts and Faraday rotation for nanoparticles with low mangan content suggest of increase of the role pairs and antiferromagnetic interaction between Mn^{2+} ions.

1. Introduction to the Physics of Diluted Magnetic Semiconductors, J. A. Gaj, J. Kossut (Ed.),Springer, 2011, 491 p.
2. Hedin E.R., Joe Y.S. Spintronics in Nanoscale Devices // Pan Stanford Publishing: Singapore, 2013.
3. Awschalom D.D., Bassett L.C., Dzurak A.S., Hu E.L., Petta J.R. Quantum Spintronics: Engineering and Manipulating Atom-like Spins in Semiconductors // Science. – 2013. – 339. – p. 1174-1179

Interaction Aspects of Nanostructured TiO_2 Thin Films and Bovine Leucosis Proteins in Photoluminescence Based Immunosensor

Tereshchenko Alla[1], Smyntyna Valentyn[1], Bubniene Urte[2]

[1]*Odesa National I.I. Mechnikov University, Odesa, Ukraine,*
alla_teresc@onu.edu.ua, smyntyna@onu.edu.ua
[2]*Vilnius University, Vilnius, Lithuania, urte.bubniene@gmail.com*

In this research the main aspects of the interaction mechanism between nanostructured TiO_2 layer and *Bovine Leucosis virus* (BLV) proteins *gp*51, during the formation of photoluminescence-based immunosensor, have been investigated. BLV antigens *gp*51 was adsorbed on the surface of a nanostructured TiO_2 thin film, formed on glass substrates [**Ошибка! Закладка не определена.**]. A photoluminescence (PL) peak shift from 517 nm to 499 nm was observed after modification of the TiO_2 by adsorbed *gp*51 (*gp*51/TiO_2). Incubation of the *gp*51/TiO_2 in a solution containing anti-*gp*51 antibodies resulted in the formation of a new structure (anti-*gp*51/*gp*51/TiO_2) and the backward PL peak shift from 499 nm to 516 nm. The PL shifts are attributed to the variations in the self-trapped exciton energy level, which were induced by the changes of electrostatic interaction between positively charged atoms and groups provided by the adsorbed *gp*51 protein and negatively charged surface of TiO_2. The charge–charge-based interaction in the double charged layers *gp*51/TiO_2 can also be interpreted as a model based on 'imaginary capacitor', formed as a result of the electrostatic interaction between oppositely charged protein *gp*51 layer and the TiO_2 surface. The established interaction mechanism provides the general understanding of the interaction between TiO_2 and proteins that is a key aspect in the development of new PL-immunosensors and solving of many issues related to an improvement of performance of the PL-based immunosensors [2].

1. Tereshchenko A., Smyntyna V., Ramanavicius A. Interaction mechanism between TiO_2 nanostructures and bovine leukemia virus proteins in photoluminescence-based immunosensors, *RSC Advances*. 2018. V. 8. P. 37740-37748.
2. Tereshchenko A., Bechelany M., Viter R. [et.al.]. Optical biosensors based on ZnO nanostructures: advantages and perspectives. A review. *Sensors and Actuators B.* 2016. V. 229. P. 664–677.

Acknowledgement. This research was supported by Ukrainian-Lithuanian Research project "Application of hybrid nanostructures which are based on TiO_2 or ZnO and modified by biomolecules, in optoelectronic sensors" Lithuanian Research Council project No P-LU-18-53.

Multi-Phonon Processes as Mechanism of Formation of Resonant Energy Spectra in the Extractors of Quantum Cascade Detectors

Tkach M.V., Seti Ju.O., Voitsekhivska O.M., Gutiv V.V.

Chernivtsi National University, Chernivtsi, Ukraine, m.tkach@chnu.edu.ua

The detail analysis of experimental papers [1, 2], where the constructive characteristics of active regions and extractors of certain cascades of quantum cascade detectors (QCD) are presented, reveals the paradox situation. Its sense is the following: for the relaxation of electronic energy from the excited state of active region of the previous cascade into the ground state of active region of the next cascade, the extractor is constructed from such number of nano wells and barriers that provides the demanded potential profile for the creation of electron energy spectrum like “phonon ladder”. The distance between neighbour levels is equal to the energy of one phonon.

Recently the QCDs operating in near infrared range were fabricated [2] at the base of anisotropic structures, where the “phonon ladders” were torn. However, this fact did not prevent successful functioning of these unique devices. The theory describing the physical processes which provide the mechanism of electron energy relaxation in such detectors is still absent. In this paper we observe this mechanism as the interlevel radiationless electronic transitions accompanied by multi phonon processes due to the interlevel electron-phonon interaction.

Using the Hamiltonian of the system which takes into account both intralevel and interlevel interaction between quasiparticles and polarization phonons, the Feynman-Pines diagram technique is generalized and renormalized spectrum is obtained at cryogenic temperature. It is shown that in resonant structures, where quasiparticles have several levels, the energy spectrum containing the infinite number of quasi-equidistant groups of levels which are formed by main and bound (satellite) states is observed. Such spectrum is quite suitable for the compensation of absent main levels in torn “phonon ladder” and can completely ensure the successful operation of QCD extractors.

1. Reininger P. et al. Diagonal-transition quantum cascade detector. *Appl. Phys. Lett.* 2014. 105, 091108.
2. Sakr S. et al. GaN/AlGaN waveguide quantum cascade photodetectors at $\lambda \approx 1.55\,\mu m$ with enhanced responsivity and $\sim 40\,GHz$ frequency bandwidth. *Appl. Phys. Lett.* 2013. 101, 011135.

Manifestation of Spin-Orbit Interaction in Germanium Atoms Adsorbed on Si(001) (4×2) Surface

Tkachuk O.I., Terebinska M.I., Krivoruchko Ya.S., Lobanov V.V.

Chuiko Institute of Surface Chemistry of National Academy of Sciences of Ukraine, Kyiv, Ukraine, tkachuk_olya@bigmir.net

Until 1960s, experimental studies of the electronic structure of molecules have been mainly provided by such physical methods as the electron spectroscopy, the electron ionization or photoionization, and the inelastic electron scattering. Due to a number of reasons, until 1970s the energy of valence levels of organic molecules has been experimentally available only for a few of upper π-type molecular orbitals.

Development of the X-ray photoelectron spectroscopy (XPS) has provided an availability of the ionization energies due to valence core levels of such objects as molecules and adsorption complexes on solid surfaces. However, an adequate interpretation of complicated XPS spectra has required the development of the corresponding theoretical tools. Underlying physical effects that are responsible for the sophisticated structure of those spectra comprise spin-orbit splitting of the levels, their multiplet splitting , shake-up and shake-down of electrons from higher levels.

Among the listed effects, the spin-orbit (SO) interaction should be considered as the most important one, since the magnitude of the SO splitting provides valuable information on the structure of an object of study.

In this work we present the calculated density of one-electron states for the $Si_{96}H_{84}$•Ge_2 cluster that models a fragment of the relaxed Si(001)(4×2) surface with the >Ge=Ge< surface dimer situated over the set of >Si=Si< surface dimers.

All the calculations of the equilibrium geometry and electronic structure have been performed in the framework of the density functional theory (B3LYP, 6-31G**). The photoelectron spectrum has been constructed using the Gaussian line shape ($\sigma = 0.02$).

Simulated XPS spectrum of the $Si_{96}H_{84}$•Ge_2 cluster shows the bimodal distribution for the 2*s* and 3*s* lines that reflects the non-equivalency of germanium atoms within the >Ge=Ge< surface dimer on the relaxed Si(001)(4×2) surface. 2*p* and 3*p* core levels are spin-orbit doublets with the splitting of 0.24 and 0.75 eV, respectively. The latter have nearly equal intensity in a contradiction with the theoretical population arguments. However, such a situation can be explained by a re-distribution of the electron density between the adsorbed >Ge=Ge< dimer and its support, followed by the formation of so-called internal molecular orbitals that are responsible for the high binding energy of the Ge_2 admolecule.

Biopolimeric Nano Structural Compositions Based on Caramelized Honey

Tsap M. R., Kurta S.A., Khatsevich O.M.

Department of Chemistry Faculty of Natural Science,
Precarpathian National Vasyl Stefanyk University, kca2014@ukr.net

According to the World Health Organization, periodontitis is diagnosed in 90-95% of adult patients with such diseases as gingivitis and periodontitis. Periodontal diseases are caused by health disorders, human body infections, and the psycho-emotional stress of a person and result in a catastrophic loss of teeth. Periodontal diseases are a medical problem as well as a social problem. Thus, the solution to this problem is an actual task to date. The purpose of our work is the invention and research of the properties and efficiency of the chewing gum made of natural caramelized honey, wax, and bee-glue for gum and teeth protection and prevention of various diseases, especially periodontal. Our working hypothesis is that our chewing gum will prevent and treat dental diseases due to the high efficiency of nanoparticles of caramelized honey, wax, and bee-glue (in the prepared composition), by their mutual synergistic amplification of each other, as it happens in the bee hive in honeycomb, where all three of these products are present. For making chewing gum, we made a special low-temperature thermochemical caramelization of natural honey.

The biopolymer composition based on caramelized honey, is made as a chewing gum for the prevention and treatment of gums and teeth from various dental microbiological and bacterial diseases. The result is achieved by introducing into the biopolymer composition of nanostructures of caramelized natural bee honey. The aim of this work is to synthesize and investigate the caramelized honey nanostructures.

On the basis of the researches carried out in 2016-2018 by scientists of the department of chemistry the Faculty of Natural Sciences of the Vasyl Stefanyk Precarpathian National University in Ivano-Frankivsk, Ukraine, a specially developed biochemical technology of low temperature catalytic caramelization of honey was developed. Research was conducted on its biochemical properties. Gum tests, conducted in vivo, in vitro, showed high biological activity of caramelized honey in relation to a number of microbiological objects on periodontal tissues in the prophylaxis and treatment of gingivitis, periodontitis and periodontal disease.

We first investigated the reactions of caramelization of honey and other bee products to study the biochemical properties of the products obtained, showing the possibility of their transformation into nanostructural formations in the thermochemical treatment of honey in the presence of catalysts. The infrared spectra, the size of the nanoparticles in the caramelization honey are measured by the content of oxymethylfurfural and the diastase number, the caramelized

honey polysaccharide nanoparticles, which differs from those of normal natural honey (Fig. 1). The size of the honey polysaccharide nanoparticle after honey caramelization decreases by 4-6 times.

The technology of caramelizing honey and honey-related products through thermo-chemical treatment was proposed. Reactions honey caramelization and bioche-mical properties of received products were investigated. The possibility of transfor-ming honey into biologically active compounds after its thermochemical treatment was shown. It has been proven that caramelized honey nanoparticles are significantly different from nanoparticles of natural honey.

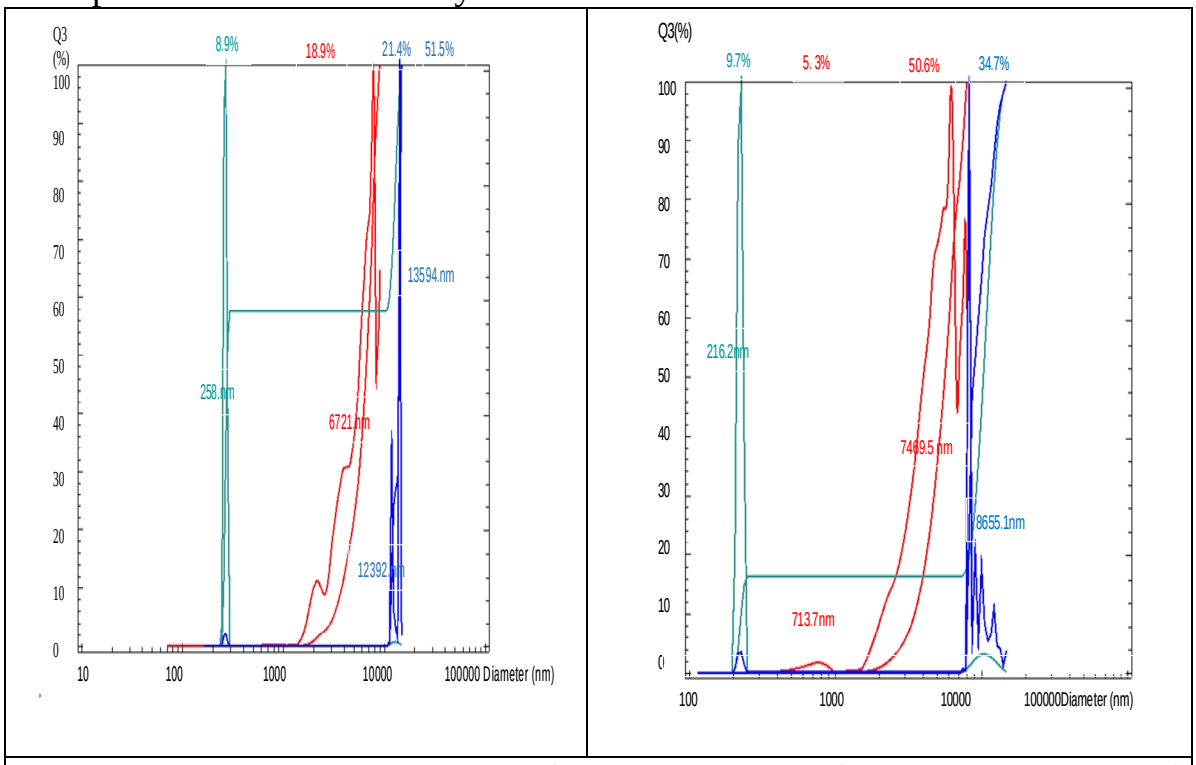

Fig. 1. Distribution by size of nanoparticles of macromolecules of polysaccharides of 1-natural bee-honey and 2-caramel-derived honey at dynamic and static conditions of measured diameter (nm). on NANO DS; CILAS.

1. https://zak.depo.ua/ukr/zak/frankivski-studenti-rozrobili-zhuyku-yaka-zahischaye-vid-parodontozu-video-20171122680399.
2. https://news.karpaty.rocks/ivano-frankivska-oblast/frankivski-studenti-rozrobili-zhuyku-yaka-zahishchaie-vid-parodontozu-video.
3. https://uain.press/science/ukrayinski-studenty-vynajshly-zhujku-yaka-zahyshhaye-vid-parodontozu-583539.
4. http://shablya.if.ua/prykarpattia/10991-frankivski-studenty-rozrobyly-zhuiku-iaka-zakhyshchaie-vid-parodontozu-video.html.
5. https://www.5.ua/nauka/smachne-likuvannia-studentka-z-ivanofrankivska-stvoryla-zhuiku-vid-parodontozu-161032.html.
6. https://youtu.be/CTTgraIXlkE.

Long-Wave Luminescence of Zinc Sulfide Group Nanocrystals

Vaksman Yu.F., Nitsuk Yu.A.

Odesa I.I. Mechnikov National University, Odesa, Ukraine, vaksman_yu@onu.edu.ua

Zinc sulfide group nanocrystals are widely used as effective phosphors in the visible spectrum. At present, a significant number of studies are aimed at studying the processes of absorption and luminescence in the region of fundamental absorption edge of semiconductor nanocrystals. At the same time, the features of the long-wavelength luminescence centers in nanocrystals are not well understood.

In the present work, the characteristics of the long-wavelength luminescence of CdS:Cu, ZnSe:Al, ZnS:Fe nanocrystals are investigated. Copper and aluminum impurities are known as an effective luminescence activators in zinc sulfide group compounds. Fe^{2+} ions are the centers of monomolecular luminescence in wide-gap II-VI crystals.

The studied nanocrystals were obtained by the colloidal method. As a source of cadmium and zinc ions, cadmium chloride and zinc chloride are used. Sulfur and selenium sources include sodium sulfide and sodium selenosulfate. Impurities Cu, Al, Fe were introduced from the corresponding chlorides in the synthesis process of nanocrystals. The synthesis of nanoparticles was carried out in a 5% solution of gelatin. Particle size was determined by the precursor concentrations. The average sizes of the obtained nanocrystals were 4–6 nm, which corresponds to the strong confinement mode.

In the investigated nanocrystals a low-energy shift of the absorption edge with increasing impurity concentration is observed. It is shown that this shift is due to the inter-impurity Coulomb interaction. In the luminescence spectrum, bands are observed whose energy position coincides with the data obtained for single crystals. The same coincidence of the composition of the emission spectra of nanocrystals and single crystals was observed in ZnSe:Al and ZnS:Fe.

The luminescence spectra of all the studied nanocrystals are characterized by the complex structure of the bands. The Gaussian components of the emission spectra of CdS:Cu, ZnSe:Al nanocrystals were decomposed. The longwave luminescence spectrum of ZnS:Fe consists of a series of lines in the visible and near infrared regions.

It has been shown that in the CdS:Cu, ZnSe:Al nanocrystals, the photoluminescence spectra are due to the presence of donor–acceptor pairs. The exciton luminescence band was also observed in CdS:Cu nanocrystals. This band was shifted along with the absorption edge of the semiconductor. In ZnS: Fe nanocrystals, the photoluminescence spectra in the visible and near infrared regions are due to transitions within the limits of Fe^{2+} ions.

A Novel Solid-Phase Extraction Method for Preconcentration Of Silver and Antimicrobial Properties of the Na-Clinoptilolite–Ag Composite

Vasylechko V.O.[1,2], Fedorenko V.O.[1], Gromyko O.M.[1], Gryshchouk G.V.[1], Kalychak Ya.M.[1], Tistechok S.I.[1], Us I.L.[1], Tupys A.M.[1,3]

[1] *Ivan Franko National University of Lviv, Lviv, Ukraine, vasylechko@ukr.net*
[2] *Lviv University of Trade and Economics, L'viv, Ukraine*
[3] *Lviv Polytechnic National University, Lviv, Ukraine*

Silver is used in modern nanotechnologies quite often. This metal belongs to the physiologically active components of mineral waters. During the analysis of waters and technological solutions the previous preconcentration, exclusion and/or separation of Ag trace amounts oftenly needs to be carried out. The regeneration of this precious metal from the exhausted technological solutions is essential too. The solution of these problems is to a large extent connected with the application of efficient selective sorbents of Ag. Intensive investigations of natural zeolites sorptive properties towards Ag(I) have been carried out for last years. It is known that the "Ag-zeolite" composite samples exhibit high antibacterial activity and even are used to dispose a bacteriological weapon. Sorptive properties of the Na-form of Transcarpathian clinoptilolite towards trace amounts of Ag(I) were studied under dynamic conditions using solid phase extraction method. The maximal sorption capacity of Na-clinoptilolite (NaC) was observed in weakly acidic solutions of Ag(I) at pH 6.0. The sorption capacity value of NaC towards Ag(I) under the optimal conditions is 7.46 mg/g. The efficient desorbents of Ag are solutions of $RbNO_3$, $CsNO_3$ and $NaNO_3$. It was established that (15–100)-fold excesses of common components of waters do not affect the sorption capacity of NaC towards Ag(I). The method of Ag(I) preconcentration in a solid phase extraction mode during the preparation of waters for analysis has been proposed.

The antibacterial properties of NaC and the composite of NaC with Ag against the gram-negative bacteria *Escherichia coli* ATCC 25922 and gram-positive bacteria *Staphylococcus aureus* ATCC 25923 were studied. The composite was poured into the water suspensions of bacteria cells with the concentration of 0.1; 0.5 and 1.0 μg/mL. NaC in the concentration of 1 μg/mL decreases the survival of *E. coli* only two times (to 54.4 % of cells). At lower concentrations NaC is less efficient. The NaC–Ag composite, in which the Ag fraction was equal to 2.9 mg per 1 g of a zeolite (NaC–Ag 2.9) and 7.4 mg per 1 g of a zeolite (NaC–Ag 7.4) proved to be more efficient regarding the decrease of these bacteria cells survival. The lowest level of survival – 5.6 % was observed during the application of 1.0 mg/mL NaC–Ag 7.4 composite. NaC exhibited the maximal antibacterial effect against *S. aureus* with the concentration 1.0 μg/mL (68.5 % survival). The composites NaC–Ag 2.9 and NaC–Ag 7.4 at different concentrations killed ~ half of *S. Aureus* cells. The data obtained indicate that the combination of Na-form of clinoptilolite with Ag enhances the antibacterial effect against *E. coli* much more than against *S. aureus*.

New $R_3Fe_5O_{12}$-Based Nanocrystalline Materials: Synthesis, Crystal Structure and Some Magnetic Properties

Vasylechko L.O.[1], Shved V.M.[1], Lutsiuk I.V.[1], Hreb V.M.[1], Tupys A.M.[1,2], Hurskyy S.T.[3], Syvorotka I.I.[3]

[1] *Lviv Polytechnic National University, Lviv Ukraine,*
crystal-lov@polynet.lviv.ua
[2] *Ivan Franko National University of Lviv, Lviv Ukraine*
[3] *SRC "Electron-Carat", Lviv, Ukraine*

Among the materials applied in electronics the rare earth (RE) garnet-structured ferrites $R_3Fe_5O_{12}$ play an important role. In particular, the $R_3Fe_5O_{12}$-based materials are used in microwave and magnetic recording devices. The properties of ferrogarnet materials can be effectively tuned in via a combination of RE elements in the garnet structure or substitution of Fe^{3+} ions both in octahedral and tetrahedral sites with nonmagnetic element, such as Al or Ga.

Series of the nanocrystalline garnet materials $R_{3-x}R`_xFe_5O_{12}$, $R_3Fe_{2.5}Al_{2.5}O_{12}$ and $R_3Fe_{2.5}Ga_{2.5}O_{12}$ ($R$, $R`$ = Pr, Nd, Sm, Eu, Gd, Tb, Dy, Ho, Er, Tm, Yb and Y) were prepared by low-temperature sol-gel citrate method using corresponding RE oxides, iron and aluminum nitrate nonahydrates $Fe(NO_3)_3 \cdot 9H_2O$ and $Al(NO_3)_3 \cdot 9H_2O$ and metallic gallium as initial reagents. It was established that formation of crystalline garnet-structured materials begins at 600 ^oC and completes at 700 – 1100 ^oC, depending on composition. Phase and structural characterization of the materials obtained was performed by means of the X-ray powder diffraction. Precise values of the lattice parameters, positional and displacement parameters of atoms and site occupancies were obtained by full profile Rietveld refinement by using WinCSD program package. The evaluation of microstructural parameters from angular dependence of the Bragg's maxima broadening shows that depending of the heat treatment temperature and composition, the average grain size of the $R_{3-x}R`_xFe_5O_{12}$ and microstresses values in the powders synthesized are in the limits of 25–150 nm and 0.11–0.25 %, respectively.

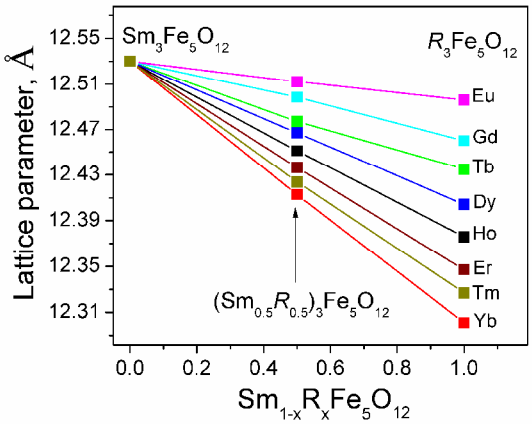

The values of structural parameters of new mixed $R_{3-x}R`_xFe_5O_{12}$ ferrogarnets obtained by us agree well with the literature data for the "pure" $R_3Fe_5O_{12}$ compounds, thus proving formation of continuous solid solution in the corresponding systems (see Figure as an example).

Impact of Shock-Vibration Treatment on the Electronic Structure of $SiO_2 + TiO_2$ and $SiO_2 + \alpha Fe_2O_3$ Mixtures and Charge Capacities of Lithium Power Sources with Cathodes on Their Basis

Yavorskyi Y.V.[a], Zaulychnyy Ya.V.[a], Dudka O.I.[a], Kononenko Ya.A.[a], Naumenko M.[a], Karpets M.V.[b]

[a] *Physical Engineering Faculty, National Technical University of Ukraine "Kyiv Polytechnical Institute", Kyiv Ukraine, yar-yra@ukr.net*
.[b] *Frantsevich Institute for Problems of Materials Science, Kyiv, Ukraine, mkarpets@ukr.net.*

Among the large number of unique properties of nanosized oxides, one should specifically mention their sorption and electrochemical properties, which are used to create the latest sorption materials and cathodes of lithium pwer sources (LPS). In this case, the content of sorbents and intercalated lithium ions depends primarily on their interaction with ions located on the defective surface of nanoparticles. The nature of such interaction is determined by the charge state of these anions and the energy distribution of valence electrons in them. One of the ways of increasing charges of near-surface anions of oxygen is to ensure their interaction with atoms of other substances in the presence of differences in chemical potentials. Therefore, different types of thermal and chemical processing are used for this purpose. In this case, thermal treatment often leads to the recrystallization of grains, and chemical processing changes their composition. At the same time, mechanical processing due to high local pressure can lead to the interaction of surface particle atoms (10 μm^2 pressure 12.6 GPa). Therefore, in order to combine the electronic properties of the materials was selected shpck vibration treatment in the Ardenne vibrating mill with an oscillation frequency of 50 Hz for 5 minutes.

In determining the impact of shock-vibration treatment on the distribution of valence electrons on the interphase boundaries of mixtures of $TiO_2 + SiO_2$, α-$Fe_2O_3 + SiO_2$ and charge capacities of LPS with cathodes on their basis, it was first established that: interatomic interaction on interphase contacts is the result of the overlapping of O*p*-orbitals, as a result of which the population of *p*-states of oxygen increases. At the same time, the settlement of the O*p*-binding states contributes to the increase of charge capacities of the LPS with the cathode basis of mixtures after mechanical treatment with subsequent cycling, whereas when the non-connecting high-energy O*p*-states are populated, charge capacities and recombination capacity of lithium ions increases, causing the formation of oxide passivation) of the film on the surface of the cathode material of the LPS, which prevents its subsequent cycling.

Composite Bi-Containing Electrode for Power Energy Devices

Zatovsky I.V.[1], Butenko D.S.[1], Klyui N.I.[1,2], Han W.[1,3]

[1]*College of Physics, Jilin University, Changchun, P.R. China,*
Zvigo@yandex.ru
[2]*V. Lashkaryov Institute of Semiconductor Physics, NAS of Ukraine, Kyiv, Ukraine*
[3]*International Center of Future Science, Jilin University, Changchun City, P. R. China*

Considerable proportion of energy collected from renewable sources, such as sunlight or wind, may be lost irreversibly due to unstable or unpredictable nature of its generation. There are two main ways to solve the problem: storing electric power in the rechargeable batteries and supercapacitors, or converting electric power to another form (as example, hydrogen). To solve these problems, new electrode materials for batteries and supercapacitors are design intensively.

It should be noted, $Bi^0 \leftrightarrow Bi^{3+}$ electrochemical junction corresponds to a rather high value of theoretical specific capacity. For a long time Bi_2O_3 was considered as an electrode material only occasionally due to its low electrical conductivity. However, in recent years this problem has solving through two strategies: creation of hybrid nanostructures of Bi_2O_3 with high-conductivity materials (e.g. carbon) or growing of thin films and nanostructures of bismuth compounds on the surface of current collector.

Herein, we reported of synthesis Bi-Bi_2O_3 nanomaterial by bismuth reduction in aqueous media and subsequent development of Bi-Bi_2O_3-C of composite electrodes with application to Ni foam. The electrochemical performance of the Bi-Bi_2O_3-C/NF electrode was investigated by cyclic voltammogram (CV), galvanostatic charge-discharge (GCD) and impedance spectroscopy in 6 M KOH electrolyte solution. Starting Bi-Bi_2O_3 material and Bi-Bi_2O_3-C/NF electrode before and after electrochemical tests was characterized using XRD, SEM, TEM, FTIR, Raman and XPS methods. The specific capacitance of the electrode material reaches 1188 $F \cdot g^{-1}$ (for areal capacitance 88 $F \cdot cm^{-2}$) at 5 $mA \cdot cm^{-1}$ and slightly decreases within the range of 5 to 20 $mA \cdot cm^{-1}$ (12% less). The cyclic life time of the Bi-Bi_2O_3-C/NF electrode is also measured and the capacitance only declines by 5 % after 200 cycles. According to calculations, the values of specific energy and specific power are in the ranges of 165-24 $Wh \cdot kg^{-1}$ and 34-679 $W \cdot kg^{-1}$, respectively (at current densities from 5 to 100 $mA \cdot cm^{-2}$), as shown in Fig. 1. The found electrochemical characteristics and calculations allow us to consider Bi-Bi_2O_3-C/NF a good candidate for the role of the electrode for supercapacitors and batteries.

Acknowledgements: Funding: This work was supported by the national long-term project [no. WQ20142200205] of “Thousand Talents Plan of Bureau of Foreign Experts Affairs” of People’s Republic of China.

ORAL REPORTS

Session 3
Physical-chemical properties of thin films

Evolution of a Solid-State Area on Au-Ni Phase Diagram at Nanoscale

Bogatyrenko S.[1], Kryshtal A.[2], Minenkov A.[1], Kruk A.[2]

[1] *Karazin Kharkiv National University, Kharkov, Ukraine, sib@univer.kharkov.ua*
[2]*AGH University of Science and Technology, International Centre of Electron Microscopy for Material Science and Faculty of Metals Engineering and Industrial Computer Science, Krakow, Poland*

Researches on the stability of nanoscaled binary alloys solid phases are still limited. Scarce literature data indicate that the mutual solubility of the components in the solid state increases with their characteristic size decrease. Unfortunately, the data obtained for nanosystems via direct experimental methods are scant and do not allow tracing the evolution of the entire solid-phase region on the phase diagram.

The present work is aimed to experimentally outline the solid-state miscibility gap on the phase diagram of nanosized Au-Ni system using advanced *in situ* transmission electron microscopy techniques. The nickel-gold islet films were formed by sequential condensation of components in a vacuum of $1x10^{-7}$ Torr. The total mass thickness of the films was 2 – 140 nm, which corresponded to the overall composition of 30 at.% Au–Ni. The homogeneous solid solution of this composition has the highest formation temperature, i.e. lays on a very top of the miscibility gap for bulk samples. In order to obtain a nickel nanostructure in a non-defective, quasi-equilibrium state, Ni was condensed on a carbon substrate at a temperature of 350°C at a rate of about 0.5 nm per second. Immediately after samples cooling down to room temperature, gold was condensed on the Ni islet film. The mass thickness was controlled by the quartz crystal microbalance (QCM) method.

Phase structure of the Au–Ni film was traced during *in situ* heating of the samples in a PEM-125K transmission electron microscope fitted with in-house heating holder in the 20–850 ºC range. Morphology, composition and distribution of chemical elements in Au–Ni islands were studied using a Cs-probe corrected FEI Titan G2 60–300 transmission electron microscope with ChemiSTEM technology at 300 kV. A MEMS-based Wildfire S3 heating holder from DENSsolutions was used for *in situ* heating. HAADF-STEM images from the sample were recorded in the 20–450 ºC range. The temperature measurement error did not exceed 5% according to the manufacturer specification. STEM-EDX elemental mapping was performed at 20 and 350ºC. The overall composition of the film was determined by quantification of EDX spectrum using Cliff–Lorimer standard-less method.

In summary, the formation of solid solutions in Au–Ni nanoparticles has been painstakingly investigated via cutting edge TEM techniques. The curve limiting the components solid-state miscibility gap was experimentally constructed in the whole concentration range at all temperatures for samples of various sizes. The miscibility gap shrinking on the phase diagram of Au-Ni nanoparticles has been witnessed.

This work was supported by the Ministry of Education and Science of Ukraine (0118U001772, 0118U002027) and by European Union's Horizon 2020 research and innovation program under grant agreement No. 823717_ESTEEM3.

Modelling Adsorption of H_2O and O_2 of Al Surface.

Chernikova O.M.[1], Ogorodnik Y.V.[2]

[1] *Kryviy Rih National University, Kryviy Rih, Boston,Ukraine, hmchernikova@gmail.com*
[2] *Radiation Monitoring Devices, Inc., Boston, USA*

The chemisorption and dissociation of O_2 and H_2O molecules are the major significance and fundamental steps for the oxidation of Al. The mechanisms of chemisorption for O_2 molecules and dissociation of Al surfaces have been study by using a large variety of experimental and theoretical techniques [1, 2].

We study the adsorption behavior of H_2O and O_2 on the Al surfaces and to assess the adsorption and diffusion of H along the Al. The main research methods are theoretical calculations based on the density of functional theory and the ″ab initio″ pseudopotential method. The work illustrates that the O atoms can stable adsorb on fcc sites of Al (100) surface of the adsorption of O_2 at three different initial adsorption sites (top, bridge and hollow site) and their adsorption energy referenced single O atom increases with the increasing O coverage. The migration of H atom is easier on surface than that in the interior and H atom must overcome a higher energy barrier to move from surface to subsurface.

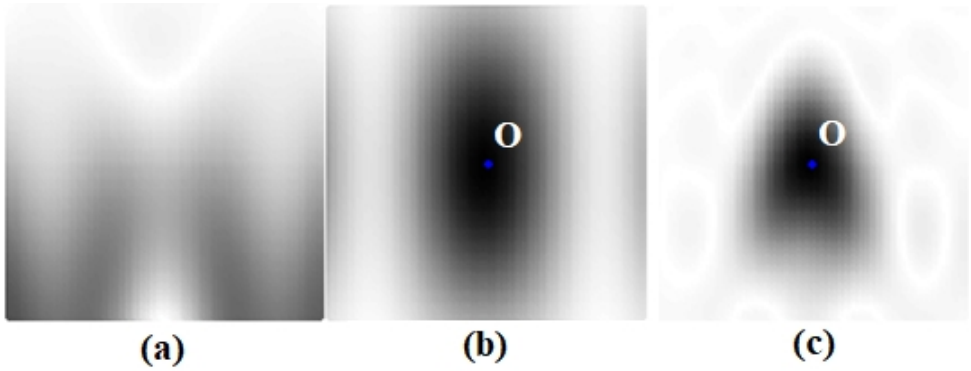

Fig.1 Intersections of spatial density distributions with valence electrons in plane (110). The film of Al with oxygen atoms and molecule of H_2O on surface: (a) film of Al; (b) film of Al with additional O atoms (fcc); (c) Al film with atoms of O (fcc) and molecule of H_2O.

1. Honkala K, Laasonen K. Oxygen molecule dissociation on the Al (111) surface. *Phys.Rev.Lett.* 2000. V. 84(4). P. 705-708.
2. Jörg Behler, Karsten Reuter, Matthias Scheffler. Nonadiabatic effects in the dissociation of oxygen molecules at the Al (111) surface. *Phys.Rev.Lett.* 2008. V 77, 115421.

Creation of Self-Organizing Nanoparticle Arrays by Thermal Dispergation of Continuous Films

Dukarov S.V., Petrushenko S.I., Churilov I.G., Orlov G.O., Sukhov V.N.

V.N. Karazin Kharkiv National University, Kharkiv,
petrushenko@univer.kharkov.ua

The study of the decay of continuous polycrystalline films into separate islands is of general scientific and applied importance. Thermal dispergation is a promising method for the creation of self-organizing functional nanoarrays.

Island Sn/C films, prepared in a vacuum of 10^{-6} Torr on fresh cleavages of KCl single crystals were chosen as the object under study. Tin was deposited by the method of thermal evaporation, and carbon by the way of sputtering from the electric arc. Two series of samples were obtained. In the first one of them, the films were condensed onto the substrate at room temperature, i.e. by the mechanism of vapor-crystal, and then heated them to the melting point of tin. In the second one, the substrate temperature was higher than the melting point of tin, i.e. the vapor-liquid condensation mechanism was realized. Then the films were cooled to the room temperature, removed from the vacuum chamber and examined using SEM methods. The asymmetric position of the tin evaporator in relation to the long substrate made it possible to obtain a series of samples, differing only in the layer thickness, within one vacuum cycle.

The coverage of the substrate by the film (k), for samples of mass thickness (t) less than 500 nm, which were obtained in the result of melting of solid layers, increases rapidly with the decrease of their thickness, growing from 0.13 (t = 500 nm) to 0.4 (t = 100 nm). At the same time, in films initially condensed into a liquid phase, value of k doesn`t depend on the thickness and is about 0.4. In films, which were obtained in a result of melting, a single maximum is observed on histograms of the particle size distribution. The most likely size and FWHM of distributions almost linearly depend on the sample thickness.

The comparison of the initial and final state of the film makes it possible to estimate the excess energy f, which releases during the melting process. For films with $t > 500$ nm, the f value doesn`t depend practically on thickness and is about 600 mJ/m^2. At the same time, for thinner films, it diminishes rapidly with thickness decreasing and at $t < 50$ nm, used phenomenological models lead to the negative value. This is apparently due to the fact, that such films initially form island structures and, therefore, do not possess excess energy.

Effect of Extraterrestrial Solar UV Radiation on Structure and Properties of ZnO Films Obtained by Wet Chemical Methods

Klochko N.P.[1], Khrypunova I.V.[1], Klepikova K.S.[1], Petrushenko S.I.[2], Kopach V.R.[1], Zhadan D.O.[1], Khrypunova A.L.[1], Dukarov S.V.[2], Lyubov V.M.[1], Kirichenko M.V.[1]

[1]*National Technical University "Kharkiv Polytechnic Institute", Kharkiv, Ukraine*
[2]*V.N. Karazin Kharkiv National University, Kharkiv, Ukraine,*
klochko.np16@gmail.com

Sunlight in space at the top of Earth's atmosphere, which is named as extraterrestrial solar radiation, contains of about 10% of ultraviolet light (UV) with a wide range of wavelengths (λ), mostly with λ = 100-399 nm, having total UV intensity of about 140 W/m^2. Solar long-wave (315–399 nm) ultraviolet A (UVA) is not absorbed by the ozone layer and arrives the Earth's surface, but short-wave (100-279 nm) ultraviolet C (UVC) is completely absorbed by the ozone layer and atmosphere. Influence of solar UV radiation on different materials is manifested in photochemical reactions which lead to the photodegradation. However, pure and doped wide band gap semiconductor zinc oxide films and nanostructures have to work under the influence of solar UV radiation, including in solar cells and other optoelectronic devices for space applications. In addition, ZnO nanostructures are commonly used in the reflective coatings for the external spacecraft surfaces.

The research of effect of UVA and UVC light on the nanostructured zinc oxide arrays, which were grown by pulsed electrodeposition, as well as on the ZnO and ZnO:In films produced by Successive Ionic Layer Adsorption and Reaction (SILAR) method confirmed their suitability as UVA-active photosensitive materials. Thereafter, we analyzed an influence of UVC on crystal structure, optical and electrical properties, namely on the thermal activation energy of electrical conduction, on the thermoelectric characteristics and on the photosensitivity range of the ZnO and ZnO:In films. As shown by the results of XRD, SEM, XRF and optical spectrophotometry investigations, the crystal structure, surface morphology, chemical composition and optical properties found no obvious significant destructive changes after UVC irradiation. However, we detected some irreversible changes in the nature of point defects under the influence of UVC, which affect the ZnO and ZnO:In resistivity, activation energy, photosensitivity and thermoelectrical properties. As was shown, the effect of the UVC irradiation can be explained as the halving of shallow donors when the zinc interstitials Zn_i, Zn_i^+ and Zn_i^{++} and indium interstitial In_i take the sites of oxygen vacancies V_O^+, thus creating zinc antisite and indium antisite, respectively.

Own Point Defects in Cadmium Telluride Thin Films

Mazur T.M.

Vasyl Stefanyk Precarpathian University, Ivano-Frankivsk, Ukraine,
tetyana.m.mazur@gmail.com

Cadmium telluride, due to a special complex of physico-chemical properties, is a promising material for use in solar-energy converters, X- and γ-radiation detectors, which function at room temperatures.

The defect formation in thin films of cadmium telluride during their growing from the vapor phase by the hot wall method at relatively low temperatures is considered in the paper.

The defective structure of the material was studied by simulation using a system of quasi-chemical reactions equations. The values of the equilibrium constants for quasichemical defect formation reactions in CdTe were calculated theoretically. Constants of $K_{Te2,V}$ and $K_{Cd,V}$ of formation of neutral defects $\frac{1}{2}Te_2 = Te_{Te}^0 + V_{Cd}^0$ and $Cd^V = Cd_{Cd}^0 + V_{Te}^0$ respectively calculated by the method of thermodynamic potentials; constants K_a, K_a', K_b, K_b' ionization reactions $V_{Te}^0 = V_{Te}^+ + e^-$ $V_{Te}^0 = V_{Te}^{2+} + 2e^-$ $V_{Cd}^0 = V_{Cd}^- + h^+$ $V_{Cd}^0 = V_{Cd}^{2-} + 2h^+$ and the Ki constant of the excitation of their own conductivity $"0" = e^- + h^-$, were calculated using the band theory of nondegenerate semiconductors.

The analytical expressions of the dependences of the concentration of free charge carriers and the prevailing own atomic defects from technological factors are obtained: temperature of the substrate Ts, temperature of the evaporation Te and partial vapor pressure of cadmium P_{Cd}.

$$n_H = n - K_i/n;\ \left[V_{Cd}^-\right] = \frac{K_b \cdot K_{Te_2,V} \cdot K_{CdTe} \cdot n}{K_i \cdot P_{Cd}};\ \left[V_{Cd}^{2-}\right] = \frac{K_b^{'} \cdot K_{Te_2,V} \cdot K_{CdTe} \cdot n^2}{K_i^{\,2} \cdot P_{Cd}};$$

$$p = K_i/n;\ \left[V_{Te}^{2+}\right] = \frac{K_a^{'} \cdot K_{Cd,V} \cdot P_{Cd}}{n^2};\quad \left[V_{Te}^{+}\right] = \frac{K_a \cdot K_{Cd,V} \cdot P_{Cd}}{n}.$$

It is shown that in CdTe films the concentration of free charge carriers is determined by vacancies of cadmium $\left[V_{Cd}^-\right]$, $\left[V_{Cd}^{2-}\right]$ and tellurium $\left[V_{Te}^+\right]$, $\left[V_{Te}^{2+}\right]$. The change in the partial vapor pressure of cadmium P_{Cd} at the constant substrate temperature Ts and evaporation temperature Te at low values of cadmium pressure (P_{Cd} <10^{-2}Pa) does not affect the concentration of free charge carriers and defects. The subsequent increase in P_{Cd} leads to a decrease in the concentration of cadmium vacancies $\left[V_{Cd}^-\right]$, $\left[V_{Cd}^{2-}\right]$ and an increase in the concentration of tellurium vacancies $\left[V_{Te}^+\right]$, $\left[V_{Te}^{2+}\right]$, which causes an increase in the concentration of electrons n.

Plasmon-Phonon Interaction in Undoped and Tb-Doped ZnO Films Studied by Means of Infrared Spectroscopy

Melnichuk O.[1], Venger Ye.[2], Melnichuk L.[1], Guillaume C.[3], Portier X.[3], Khomenkova L.[2,4], Korsunska N.[2]

[1]*Mykola Gogol State University of Nizhyn, Nizhyn, Ukraine*
[2]*V.Lashkaryov ISP of NAS of Ukraine, Kyiv, Ukraine*
[3]*CIMAP/ENSICAEN/Normandie Université/CEA/CNRS, Caen, France*
[4]*National University "Kyiv-Mohyla Academy", Kyiv, Ukraine,*
mov310310@gmail.com

The combination of unique optical, piezoelectric and mechanical properties of zinc oxide (ZnO) explains its wide applications. Nowadays, because of the high cost of ZnO single crystals, an increasing attention is paid to ZnO films. Due to high transparency, structural quality, as well as high chemical inertness and resistance to the ambient atmosphere, ZnO films become to be widely used in light emitting devices, biological sensors, acoustic devices, and many other functionalities.

The important parameters for such films are their conductivity, carrier concentration and mobility. However, in most cases the direct methods give controversial results for textured films. Therefore, the development of non-destructive methods for the monitoring of the parameters of such films is important.

Recently, we have shown the application of infrared (IR) spectroscopic methods for the determination of mentioned above parameters of ZnO films grown on dielectric substrates [1,2]. In this report, the results obtained for textured ZnO films grown on Si substrates by magnetron sputtering will be presented.

The films were grown by radio-frequency magnetron sputtering in Ar or Ar-O_2 plasma on Si substrates (p-type, B-doped, (100)-oriented, ρ=15 Ohm·cm). The undoped ZnO films were deposited from single ZnO target. For doped films, composed Tb-ZnO target was used allowed achieving of about 3 at.% of Tb content in the films. For all deposition runs, the substrate temperature and power density applied to the target were kept at 100°C and 1.9 W/cm^2, respectively. The films were submitted to various annealing treatments and investigated by means of spectroscopic ellipsometry, AFM, TEM and external IR reflection method.

It was observed that the shape of IR reflection spectra in ZnO «residual rays» range depends significantly on film thickness and on growth conditions. The position of IR reflection maximum was found to be consistent with the frequency of ZnO TO phonon, indicating a slight deviation of the growth direction of the ZnO film from perpendicularity to Si substrate, as well as the uniformity of the orientation of the ZnO columns. These results were supported by the microscopic studies.

The decrease of the intensity of the maximum reflection and its broadening was explained by the effect of the phonon- and plasma-related subsystems in ZnO «residual rays» range.

For the analysis of IR spectra, it was proposed a theoretical model considering the parameters of Si substrate and the phonon and plasmon-phonon interaction of the ZnO film with underlying substrate. Simulating experimental IR spectra, carrier concentration and mobility, as well as film conductivity were extracted. The method developed here can be applied for determination of the parameters of various textured films grown on semiconductor substrates.

[1] O. Melnichuk et al. Thin Solid Films, 2019, doi: 10.1016/j.tsf.2019.01.028.

[2] N. Korsunska et al., Mater. Sci.Semicond. Proc., 2019, accepted for publication.

Enhanced Solid-State Solubility of Ge in Nanosized Ag Films

Minenkov A.A.[1], Kryshtal A.P.[2], Bogatyrenko S.I.[1]

[1] *Karazin Kharkiv National University, Kharkiv, Ukraine,*
alexey.a.minenkov@univer.kharkov.ua
[2] *AGH University of Science and Technology, International Centre of Electron Microscopy for Material Science and Faculty of Metals Engineering and Industrial Computer Science, Krakow, Poland*

It is evident that understanding the nature of components interaction in binary nanosystems is vital for effective application of these objects. Unfortunately, fundamental insight into phase diagram evolution at the nanoscale (which commonly describes this interaction) is still insufficient.

In this work, we present the results of comprehensive experimental study of the effect of scale on solid-state solubility of components in nanosized films. Since the study of the mutual solubility of components at the nanoscale is a rather difficult task, it is advisable to use model systems with a simple type of interaction; and a eutectic Ag-Ge system is definitely one of those.

The layered film systems were formed at room temperature by sequential electron-beam evaporation of pure silver and germanium from independent sources at a pressure of 10^{-7} Torr. To trace the solid-state solubility enhancement, experiments were carried out for samples' series with Ag layer thickness of 50, 25 and 13 nm. The concentration of Ge in these samples was varied in 3–14 at.% range.

We have used two complementary experimental approaches as a basis for studying the solid-state solubility of Ge in nanosized Ag films. The first one is the method of electrical resistance measurement during samples' thermal cycling. This *in situ* method allows tracing the onset and terminal temperatures of a solid solution formation. The second one is an investigation of samples' structure (HEED) and morphology (BF) evolution during *in situ* TEM heating. These direct techniques helped us to interpret results obtained by the indirect resistance measurement method more clearly and, in the long run, served as evidence of the solid solution formation. In addition, The HAADF STEM and Elemental mapping of samples plain-views and cross-sections were painstakingly fulfilled to bring more light to the components interaction process.

In summary, values of the solid-state solubility of germanium in nanosized silver films have been quantitatively determined for the first time. Using our results on the eutectic temperature size dependence for the Ag - Ge system, the experimental data were extrapolated to the intersection with the solidus line. As a result, a significant increase of germanium terminal solubility in solid silver with characteristic size reduction, as well as the shifting of solubility curves to the region of lower temperatures, has been shown.

This work was supported by European Union's Horizon 2020 research and innovation program under grant agreement No. 823717_ESTEEM3 and by the Ministry of Education and Science of Ukraine (0118U001772, 0118U002027).

Temperature Dependencies of Surface Contribution on the Thermodynamic Properties of Lead Chalcogenide Films

Naidych B.[1], Nykyruy L.[1], Moiseenko M.[2], Turovska L.[2], Parashchuk T.[3]

[1]*Vasyl Stefanyk Precarpathian National University, Ivano-Frankivsk, Ukraine, e-mail: bvolochanska@i.ua*
[2]*Ivano-Frankivsk National Medical University, Ivano-Frankivsk, Ukraine*
[3]*The Institute of Advanced Manufacturing Technology, Krakow, Poland,*

Based on the analysis of the rock salt structure for modelling studies and electronic structure of cubic phase PbX (X=S, Se, Te) the cluster models have been built for calculation of the geometric and thermodynamic parameters. According to density functional theory (DFT) and using the hybrid valence base set B3LYP the temperature dependence of the energy ΔE and the enthalpy ΔH of formation, Gibbs free energy ΔG, entropy ΔS, specific heat at constant volume C_V and pressure C_P of the all surface atoms of lead chalcogenide films have been found. The analytical expressions of the temperature dependences of presented thermodynamic parameters, which was approximated from the quantum- chemical calculations data and with using mathematical package Maple 18 have been received.

Use of the computer quantum chemistry calculations caused by the possibility of investigations of short-range order of the atoms in real crystals and analysing of the properties caused by them. It is also important, that intensive research of atomic clusters as components of new nanostructured materials is caused by the perspective application in nanotechnology.

The first step for the quantum-chemical calculation of the cluster properties was the determination of the lowest energy configuration. All calculations started with SCF convergence and geometry optimization; after obtaining a stable minimum, the frequencies were calculated. The calculations were carried out using density functional theory, on the basis of the Stevens–Basch–Krauss–Jasien–Cundari (SBKJC) [1] parameterization. DFT calculations were performed by using Becke's three parameter hybrid method [2] with the Lee, Yang, and Parr (B3LYP) gradient corrected correlation functional [3] using the PCGamess program packages [4].

1. W.J. Stevens, H. Basch, M. Krauss, J. Chem. Phys. 81, 6026 (1984).
2. A.D. Becke, J. Chem. Phys. 98 №2, 1372 (1993).
3. Chengteh Lee, Weitao Yang, Robert G. Parr, Phys. Rev. B 37 № 2, 785 (1988).
4. Granovsky, PC GAMESS version 7.0, ⟨http://classic.chem.msu.su/gran/gamess/index.htmlJ ⟩.

Effect of Annealing on Thermally Evaporated CdTe Thin Films for Photovoltaic Absorber Application

Nykyruy L.[1], Yavorskyi R.[1], Wisz G.[2], Zapukhlyak Z.[1], Yavorskyi Ya.[1], Potera P.[2]

[1]*Vasyl Stefanyk Precarpathian University, Ivano-Frankivsk, Ukraine, roctyslaw@gmail.com*
[2]*Rzeszow University, Rzeszow, Poland*

Cadmium telluride (CdTe) has been recognized as a very promising material for thin film photovoltaic (PV) devices. CdTe is a II–VI semiconductor compound with a direct optical bandgap of ~ (1.45 – 1.5) eV that is nearly optimally matched to the solar spectrum for PV energy conversion. It has also a high absorption coefficient, >5 10^4/cm, which means that ~99% of photons with energy greater than the bandgap (E_g) can be absorbed within 2 μm thickness of CdTe film.

The CdTe thin films deposited on a cleaned glass substrates by Physical Vapor Deposition (PVD) technique. The substrate temperature T_s was 470 K, the evaporation temperature of the pre-synthesized compounds CdTe changed in range (790 – 850) K. The thickness of the thin films defined by deposition time τ = (160-570) sec and the deposition at 10^{-4} Pa vacuum.

The thickness of samples was analysis by profilometer Bruker Dektak XT. Optical transmission spectra were investigated by measuring transmittance, T at normal incidence and room temperature in the wavelength range of (190 – 3300) nm with 1 nm step using Agilent Technologies Cary Series UV-Vis-NIR Spectrophotometer before and after annealing. Optical spectra were determinate using the Swanepoel method [1]. The films were annealing in Oxygen atmosphere for 90 min at 720 K in Nabertherm LH04 furnace.

For analysis of optical spectra, the absorption coefficient has been calculated using the Envelope Method (EM) developed by Swanepoel. By the interference patterns can be calculated d, n, α, s, λ and T denote the thickness of films, refractive index, absorption coefficient, substrate refractive index, wavelength and transmission of the film, respectively.

Recrystallization of CdTe thin films strongly depends on the annealing process, altering many properties like crystallite size, intrinsic defects and stress, slightly shifting the optical absorption edge. Accordingly, it is important to understand the behavior of optical properties with annealing temperature as it is one of the most important tools for determining of the band structure of semiconductor. Heterojunction thin film solar cells with multilayer structure require precise annealing process to minimize the inter-diffusion layers beneath during the annealing process.

1. R. Swanepoel, Determination of surface roughness and optical constants of inhomogeneous amorphous silicon films, Journal of Physics E: Scientific Instruments. 17(10) (1984) 896-903.

Structure of Tin-Indium Alloys in Condensed Films

Petrushenko S.I., Dukarov S.V., Bloshenko Z.V., Bulgakova O.O., Sukhov V.N.

V.N. Karazin Kharkiv National University, Kharkiv, petrushenko@univer.kharkov.ua

The knowledge of phase diagram is necessary for predicting the behavior of alloys. The construction of phase diagrams usually requires obtaining the alloys of various concentrations, phase transitions in which can be recorded with the help of various techniques. At the same time, such a laborious approach, in which samples are obtained in different experimental cycles, loses its effectiveness during the study of thin films that are extremely sensitive to the preparation conditions. In this case, it is reasonable to use variations of the method of variable content and variable state, which allow to obtain a section of the phase diagram within a single experimental cycle. This work is devoted to the study of the phase state of In-Sn films obtained by this method.

The samples were obtained by consistent condensation of the components onto a glass substrate. Then, with the help of a heater, located on one edge of the substrate, the necessary temperature gradient was created along it. The mutual arrangement of the substrate, evaporators and screens provided the creation of the concentration gradient on the substrate in the interval of 0–100%, which is perpendicular to the temperature gradient. This method of samples formation allows, within a single cycle, to realize the entire phase diagram on the substrate and to visualize its main contours. Solidus is visually observed on the substrate, as well as lines dividing various crystalline phases, which exist in the solid state.

With the help of SEM studies, it was found that the visualization of the contours is due to the differences in the morphology of the areas. Thus, the visualization of the solidus line is due to the change of the light reflection from a practically mirror-like one, which is typical for solid-phase areas, to a diffuse one, which is observed in a dispergated film. The visualization of the contours in the solid-phase area is also due to the morphology of areas.

By the study of the through porosity, which was observed in continuous areas of the sample, the data about the effect of the concentration of components on the activation energy of diffusion processes that provide film dispergation were obtained. The concentration dependences of the substrate coverage by the film and the histogram of the distribution, which were obtained in the island areas of the sample, gave the information about the excess energy which was due to the defective nature of polycrystalline samples.

Electrical and Optical Properties of CdTe Films

Prokopiv V.V.

Vasyl Stefanyk Prearpathian National University, Ivano-Frankivsk, Ukraine, prkvv@i.ua

CdTe films are successfully used to create solar cells based on the heterostructures. Increasing the efficiency of such solar cells is directly related to improving the quality of the source materials as well as understanding their physical properties.

CdTe films have been obtained from a pre-synthesized material by vacuum-evaporation technique and physical vapour deposition on freshly prepared mica chips and polished glass.

The electrical parameters of CdTe films have been determined both in a constant electric field and by impedance spectroscopy method (Autolab PGSTAT 12/FRA-2 analyzer) in the frequency range of 0.01-100 kHz.

It has been found that up to 600 V the current-voltage characteristics of the films are linear, and the resistivity is 10^8-10^9 Ω·cm.

The frequency dependence of the conductivity of polycrystalline CdTe films indicates a variable-range hopping conductivity. An increase in conductivity with frequency also indicates the existence of localized states in CdTe thin films.

The photoelectric properties of CdTe films obtained on various substrates have been studied. The dependence of the photosensitivity on the structure of the films and the technological conditions of growing has been found. It has been determined that the photosensitivity of the films obtained on the polished glass substrates is significantly higher than those of the films on freshly prepared mica chips (111) and increases with decreasing film thickness. This is due to the fact that the specific contribution of the grain boundaries increases with decreasing crystallite size.

Since annealing is used to increase the efficiency of surface-barrier solar cells, the effect of thermal processing (at 700-1000 K) on the optical properties of cadmium telluride thin films has been studied. A comparison of the optical transmission and reflection spectra of the films before and after annealing has revealed the formation of a modified surface. The possibility of obtaining intense photoluminescence, which is formed by interband recombination and transitions due to size quantization of the energy of charge carriers, has been established.

ORAL REPORTS

Session 4
Thin film compounds for electronic devices, nanoelectronics

Polymer-Semiconductor Hybrid Systems for Organic Electronics

Aksimentyeva O.I.[1], Tsizh B.R.[2,3], Olenych I.B.[1]

[1]*Ivan Franko National University of Lviv, Lviv, Ukraine, aksimen@ukr.net*
[2]*Stepan Gzytsky Lviv National University of Veterinary Medicine and Biotechnologies, Ukraine,*
[3]*Kazimierz Wielki University in Bydgoszcz, Bydgoszcz, Poland*

The advantages of organic electronics such as ability to create ultra-thin and ultra-light devices on a flexible basis, compatible with inkjet and printing technologies, access to new markets and cheaper production have some disadvantages – insufficiently high-performance device derived, instability in normal conditions, etc. Improving performance of devices of organic electronics is possible due to the development of hybrid nanosystems with inorganic semiconductors. Hybrid composites based on semiconductor nanoparticles and polymer matrices have a potential application as materials for electrooptical, sensor devices and alternative energy sources. These composites may be fabricated by simple, safe and energy saved methods without vacuum technologies. Semiconductor nanocrystals embedded in polymer matrix and conducting polymers integrated with semiconductor mediums may significantly affect the electrical, electrooptical, luminescent properties of materials. In the present work the new progressive methods for fabrication of polymer-semiconductor nanomaterials have been used – encapsulation of inorganic particles with polymer shells, intercalation, layer-by-layer assembling, “in situ” and electropolymerization. Application of proposed nanosystems in hybrid solar cells, optical gas sensors, organic electrochromic displays and light emitting diodes are demonstrated [1,2]. The effect of the change in the intensity of light transmission of polymer films under the action of an external electric field is used to control the spectrum of photoluminescence of nanoporous silicon [3]. The interconnection of electrooptical and sensory characteristics with the composition and nature of components, their structure and film morphology was determined. The ways of increasing the characteristics of electrooptical devices based on conjugate polymers and semiconductor nanosystems are proposed.

1. Aksimentyeva O.I. et al. Electrooptic phenomena in conjugated polymeric systems. *Computational and Experimental Analysis of Functional Materials*: Toronto: Apple Academic Press. 2017. P. 91–150.

2. Tsizh B.R., Aksimentyeva O.I. Organic high-sensitive elements of gas sensors based on conducting polymers. *Mol. Cryst. Liq. Cryst.* 2016. Vol.639. P. 33–38.

3. Olenych I. B., Aksimentyeva O. I., Monastyrskii L. S. Electrochromic effect in photoluminescent porous silicon – polyaniline hybrid structures. *Journal of Applied Spectroscopy*. 2012. Vol. 79, № 3. P. 495–498.

Intercalation of Li Atoms in a SnS_2 Anode of Battery: *ab Initio* Calculation

Balabai R.M., Prikhozha Yu.O.

Kryvyi Rih State Pedagogical University, Kryvyi Rih, Ukraine,
balabai@i.ua, prihozhaya.yuliya93@gmail.com

Lithium-ion battery is one of the most promising power source candidates for large-scale energy storage systems such as battery packs in smart grids and electric vehicles [1]. Sn-based materials with layered crystalline, especially tin disulfide (SnS_2), attract a lot of interest as Li storage materials (battery electrode). Because the layered structure of battery electrode can to minimize the volume change during lithiation (delithiation) cycling and improve the Li mobility [2].

Applying the methods of the functional of electronic density and *ab initio* pseudopotential, we carried out computational experiments, using the author's software complex [3], on atomic models that correctly reproduced the 2-D layered structure of tin chalcogenides with intercalated Li atoms. We have obtained the spatial distributions of the density of valence electron, the energy barriers of migration of Li atoms in the interlayer of SnS_2. Such a transfer was investigated at various degrees of filling of the interlayers spatial of metal atoms. Fig. 1 shows properties of migration of Li atoms (indicated by the cursors in the fig. 1) at fullness of 25% interlayer space.

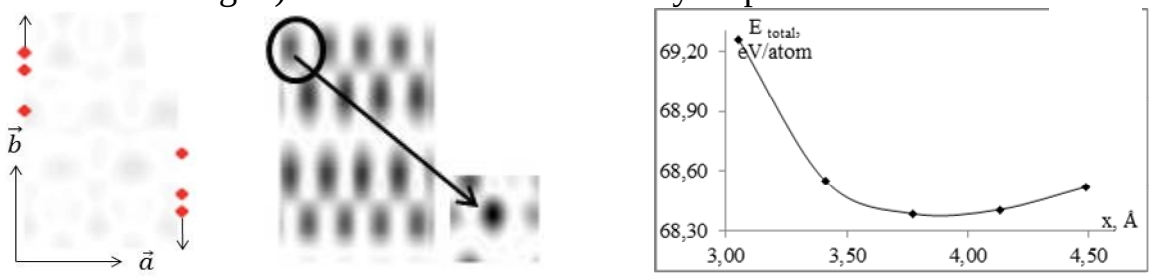

Fig. 1. The (100) section of the spatial distribution of valence electrons within the supercell at the *c/2* level. Shown here the direction of migration of Li atoms in the interlayer SnS_2 (a). The (110) section of the spatial distribution of valence electrons within the cell (b). The energy relief of migration of Li atoms in the SnS_2 interlayer (c)

[1] M. Thackeray, et. all. Electrical energy storage for transportation-approaching the limits of, and going beyond, lithium-ion batteries, Energy Environ. Sci. 5 (2012) 7854

[2] Wang, et. all. Single-Layered V 2 O 5 a Promising Cathode Material for Rechargeable Li and Mg Ion Batteries: an Ab Initio Study. Phys Chem. 2013, (22), 8705-8709.

[3] Ab initio calculation [Electronic resource]: Internet portal. Access mode: http://sites.google.com/a/kdpu.edu.ua/calculationphysics/.

Strategy of creating integrated lateral p-n junctions in two-dimensional phosphorene, using adsorbed molecules as dopant impurities

Balabai R. M., Solomenko A. G.

Kryvyi Rih St. Pedagogical Un., Kryvyi Rih, Ukraine, solomenko.anastasiia@gmail.com

The high carrier mobility and tunable and moderate direct bandgap of black phosphorus (BP, phosphorene) deliver great promise in electronic and optoelectronic applications. Phosphorene, as a phosphorus analogue of graphene, refers to the monolayered black phosphorus crystal [1]. As shown by the authors of studies [2] chemical doping of black phosphorene with benzyl viologen molecules modulates the electron density and allows acquiring a large built-in potential in BP plane, which is crucial for achieving high responsivity photodetectors and high quantum efficiency solarcells.

For extension of information about electronic properties of two-dimensional phosphorene with a surface molecules, the valence electron density spatial distribution, the densities of electron states, the band gaps, the core charges and the Coulomb potentials have been calculated in the framework of the electronic density functional and *ab initio* pseudopotential based on own program code. It was established that the lateral configuration on the basis of two-dimensional phosphorene with adsorbed molecules on its surface is characterized by the charge regions of different values (or/and signs), which are similar to the regions of ionized impurities of bulk p-n-junctions (Fig. 1). Areas with charges of different values create conditions for the appearance of potential jumps, which is the main characteristic of p-n junctions.

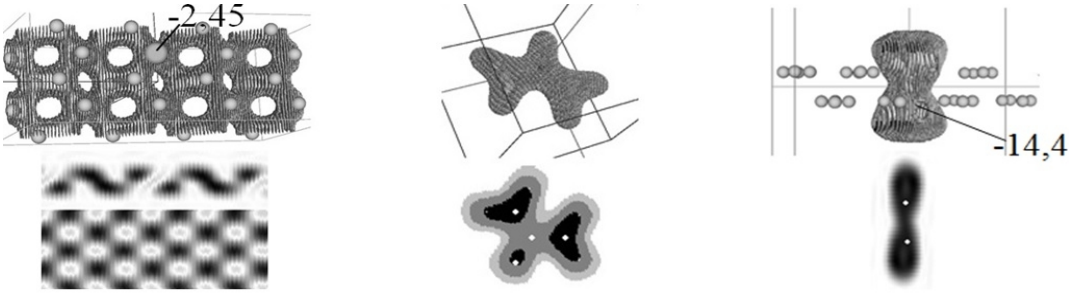

Fig. 1. Spatial distribution of valence electrons density and its cross-section in the monolayer of the black phosphorus crystal (left), in the flat urea molecule (center) and in the monolayer of BP with adsorbed urea molecules (right). The values of charges in the vicinity of phosphorus atoms are given.

1. Yi Y. et al. Two-dimensional black phosphorus: Synthesis, modification, properties, and applications. *Mater. Sci. Eng., R.* 2017. 120. P. 1-33.

2. Yu X. et al. Lateral black phosphorene p-n junctions formed via chemical doping for high performance near-infrared photodetector. *Nano Energy*. 2016. 25. P.34-41.

Development of Surface 2D Lasers Based on the Generation of e-h Exciton Liquid Layer (ZnO) at Non-Cryogenic Temperatures

Fedorenko L.L., Litovchenko V.G., Korbutyak D.V., Zagorodniy A.G.

V.E. Lashkaryov ISP NASU, Kyiv, Ukraine, leonfdrn@gmail.com

2D lasers formed on the basis of a surface two-dimensional electron-hole plasma determine a new direction in the creation of effective sources of radiation for modern electronics. The experimental data obtained earlier relate to materials with relatively low coupling excitons energy (GaAs, AlGaAs [1]), hence the low operating temperature (4÷10 K, or lower). But the requirements for modern electronics updates the functioning of such devices at room temperatures (300 ^{0}K and above). Naturally, materials with high electron-hole coupling energy are here promising, based on the ratio proposed by Keldysh [2]: $kT_{cr} \approx 0.1 \cdot E_{ex}$, where E_{ex} is the energy of the Wannier-Mott exciton. This semiconductors with strong ionic bond [1], in particular, ZnO (T_{cr} ~ 110 K), InSe (T_{cr} ~ 200 K) [3]. At present, encouraging results of lasing at room temperatures in thin layers of 3 D have been obtained in polycrystalline ZnO layers of the submicron scale thicknesses [1]. In this paper, the results of the possibility of lasing in thin ZnO layers close to the geometry 2D (quasi-2D) based on the structure of ZnO/SiO_2/Si are presented. The possibility of E_{ex} growth due to increasing of the condensation centers concentration n_{cond} (dusty plasma) was shown. Surface localization of the exciton plasma was carried out by the formation of condensation centers by the ZnO surface bombarding with argon ions of relatively low energies. Spectral and photoluminescence (PL) intensity from the pumping level of the structures are analyzed. The lower degree rise of the PL intensity from the pumping level of 2D structures as compared with the 3D case has been established.

1. I. Bercha, D. V. Korbutyak, Yu. B. Kryuchenko, V. G. Litovchenko, R. Baltrameyunas, E. Gerazimas. Optical gain in quantum superlattices. Solid State Physics. 1992, **34**, N6, pp.1696-1700 (in Russian).
2. L.V. Keldysh, A.P. Silin. Condensation of excitons in direct semiconductors. *Zhurnal Eksperim.Teor. Fiziki* **69** (3), p. 1053-1065 (1975) (in Russian).
3. V.G. Litovchenko, D.V.Korbutyak, Yu.V.Kryuchenko. Investigation of collective properties of excitons in polar semiconductors (ZnO). JETP, 1981, 6, pp. 1965-1977 (in Russian) .
4. N. Gruzintsev, V. T. Volkov, C. Barthou, and P. Benalloul. Spontaneous and Stimulated Emission from Magnetron-Deposited ZnO–SiO2–Si Thin-Film Nanocavities. Semiconductors, 36, No. 6, 2002, pp. 701–705.

A Correlation Between Network Properties of Polymer Matrix and Parameters of Amperometric Biosensor Based on Polymer Matrix

Kavetskyy T.[1,2], Kukhazh Y.[1], Zubrytska K.[1], Smutok O.[3], Demkiv O.[3], Gonchar M.[3], Šauša O.[4], Švajdlenková H.[5], Boev V.[6], Ilcheva V.[6], Petkova T.[6], Kasetaite S.[7], Ostrauskaite J.[7]

[1]*Drohobych Ivan Franko State Pedagogical University, 82100 Drohobych, Ukraine*
[2]*The John Paul II Catholic University of Lublin, Lublin, Poland, kavetskyy@yahoo.com*
[3]*Institute of Cell Biology, National Academy of Sciences of Ukraine, Lviv, Ukraine*
[4]*Institute of Physics, Slovak Academy of Sciences, Bratislava, Slovak Republic*
[5]*Polymer Institute, Slovak Academy of Sciences, Bratislava, Slovak Republic*
[6]*Institute of Electrochemistry and Energy Systems of BAS, Sofia, Bulgaria*
[7]*Kaunas University of Technology, Kaunas, Lithuania*

Technogenic pressure on the environment has significantly affected human health due to the pollution of water resources. The one of the most dangerous pollutants of wastewater are xenoestrogens. They arrive in the surface water with drains of oil, shale, forest-chemical, and cox-chemical industries as well as with drains of hydrolysis industry. For example, xenoestrogen Bisphenol A is a monomer that is used for the manufacture of polycarbonate plastic and epoxy resins, which are raw materials for the production of packaging materials for food and drinks. The development of new approaches for monitoring of these dangerous substances coming from the wastewater is a topical problem to improve human life first of all. To do that, the most promising in analytical biotechnology seems to be amperometric biosensors – bioanalytical devices that combine the best features of bioelements (selectivity) and physical transducers (high sensitivity and accuracy). The present work reviews the recent results obtained in the construction of laccase-based amperometric biosensors using ureasil and photocross-linked polymers as host or holding matrixes [1-5]. A correlation between network properties of polymer matrix and operational parameters of amperometric biosensor based on polymer matrix is reported.

1. T. Kavetskyy, O. Smutok, M. Gonchar, O. Demkiv, H. Klepach, Y. Kukhazh, O. Šauša, T. Petkova, V. Boev, V. Ilcheva, P. Petkov, A.L. Stepanov, J. Appl. Polym. Sci. **134** (2017) 45278(1-7).
2. T. Kavetskyy, O. Šauša, K. Čechová, H. Švajdlenková, I. Maťko, T. Petkova, V. Boev, V. Ilcheva, O. Smutok, Y. Kukhazh, M. Gonchar, Acta Phys. Pol., A **132** (2017) 1515-1518.
3. T.S. Kavetskyy, O. Smutok, M. Gonchar, O. Šauša, Y. Kukhazh, H. Švajdlenková, T. Petkova, V. Boev, V. Ilcheva, NATO Science for Peace and Security Series B: Physics and Biophysics (2018) 309-316.
4. T.S. Kavetskyy, H. Švajdlenková, Y. Kukhazh, O. Šauša, K. Čechová, I. Maťko, N. Hoivanovych, O. Dytso, T. Petkova, V. Boev, V. Ilcheva, NATO Science for Peace and Security Series B: Physics and Biophysics (2018) 333-338.
5. T. Kavetskyy, O. Smutok, O. Demkiv, S. Kasetaite, J. Ostrauskaite, H. Švajdlenková, O. Šauša, K. Zubrytska, N. Hoivanovych, M. Gonchar, Eur. Polym. J. **115** (2019) 391-398.

Structure and Optical Properties of CdTe and CdS Thin Films after Hard Ultraviolet Irradiation

Kopach G.I., Dobrozhan A.I., Khrypunov G.S., Mygushchenko R.P., Kropachek O.Y., Zaitsev R.V., Meriuts A.V.

National Technical University «Kharkiv Polytechnic Institute», Kharkiv, Ukraine, gkopach@ukr.net

Solar cells based on the CdS/CdTe heterosystem are considered to be promising for space use. Therefore the study of the hard ultraviolet influence on the structural and optical properties of CdS and CdTe thin films is relevant.

CdS and CdTe films were obtained on glass substrates by non-pulsed DC magnetron sputtering in accordance with [1]. The crystal structure of the films was investigated by using X-ray diffractometry, scanning electron microscope and optical spectroscopy. Cadmium sulfide and cadmium telluride films were irradiated by hard ultraviolet with the energy of quanta 10 eV for 10 hours.

After irradiation of the CdS film structural changes were detected. An increase of the integral intensity in the reflection of the hexagonal phase (002) at the angle of 11.99° was found. And the constant crystal lattice c, which was c = 6.78 (88) Å, was 1.03% different from the table value. The value of the integral width of the peak (002) decreases to 0.2 deg from 0.24 deg in the initial sample of the cadmium sulfide layer. The spectral dependence of the transmission coefficient did not change. The mean values of the refractive index n and band gap Eg for samples, irradiated by hard ultraviolet, are similar to the corresponding values of non-irradiated cadmium sulfide films.

After irradiation of the CdTe film it was found, that the intensity of the reflection peak (201) increased, while the intensity of all other peaks decreased. At the same time, the integral width of all peaks decreased. The calculated values of permanent crystalline lattice constant for CdTe were similar to these values in the initial state. As for CdS, the spectral dependence of the transmission coefficient of CdTe films has not changed. The mean values of n and Eg did not differ from these values before irradiation.

Thus, the optical characteristics of semiconductor films obtained by the non-pulsed DC magnetron sputtering method were insensitive to irradiation by hard ultraviolet. The crystalline structure of the CdS and CdTe films changes after irradiation. The lattice period for cadmium sulfide films increases, which may be due to the formation of point defects and defective complexes. The decrease of the peaks width on the X-ray diffraction patterns of CdS and CdTe layers is due to the increase of the coherent scattering regions in the process of near-surface layers partial recrystallization of the developed grain boundary surface of the films as a result of irradiation by the hard ultraviolet.

1. G.I. Kopach, R.P. Mygushchenko, G.S. Khrypunov, A.I. Dobrozhan, M.M. Harchenko, J. Nano-Electron. Phys. 9, (2017) 05035.

Application of a-SixC1-x:H Films for Improvement of Silicon-Based Devices Properties in UV-VIS-IR Spectral Range

Lukianov A.M.[1,2], Klyui N.I.[1,2], Lozinskii V.B.[2], Dusheiko M.G[2,3], Avksentyeva L.V.[2], Kasatkin V.P.[2], Slepkin O.P.[2]

[1]*College of Physics, Jilin University, Changchun People's Republic of China*
[2]*V. Lashkaryov Institute of Semiconductor Physics, NationalAcademy of Sciences of Ukraine, Kyiv, Ukraine*
[3]*National Technical University of Ukraine "Igor Sikorsky Kyiv Polytechnic Institute",*
lukianov@isp.kiev.ua

The carbon-rich a-SiC_{1-x}:H films were prepared by PECVD deposition from gas mixture of CH_4, SiH_4, H_2 and *Ar* on silicon substrates and silicon solar cells. The optical and electronic properties of the deposited films were analyzed from spectra of reflection and transmission in the UV-VIS-NIR and mid-IR wavelength ranges by spectrophotometry, laser ellipsometry and FTIR. The mechanical properties of the films were characterized by nanoindentation method and the Young modulus and nano-hardness measurements. The SEM and EDS analysis were used for estimation of films content.

As the result, the dependencies of optical bandgap, refractive index and extinction coefficient, hardness and Young modulus from deposition parameters were obtained. Increasing the RF power from 100 to 300 W increases silicon content from 20 to 28 at%, decreases optical bandgap values from 4.0 to 2.5 eV, whereas refractive index (at wavelength 632 nm) varied in the range 1.8-2.05. At the same time, Young modulus and nanohardness values decreased from 144 to 70 GPa and from 14.8 to 8.6 GPa, respectively. Such films were deposited onto silicon solar cells and silicon plates as antireflective and protective coatings for VIS and IR ranges. The reflection from silicon in the visible wavelength range decreased to 0.3% at wavelength 630 nm for the ARC film based on a-SiC_{1-x}:H film with thickness 80 nm. It allowed improving the silicon solar cell efficiency by 1.12. The transmission of the silicon plate (thickness 1 mm) in IR wavelength range was increased from 55% to 66 and 96% at wavelength 5.1 μm by deposition of front side and front+rear side ARCs, respectively, based on a-SiC_{1-x}:H films with thickness about 620 nm and refractive index 1.9 (at 632 nm). Thus, the studied films obtained by PECVD method are attractive material for application as protective coatings for optical and photoelectronic devices based on silicon and working in the wavelength range from UV to mid-IR (0.3-10 μm).

This work was supported by the national long-term project No WQ20142200205 of "Thousand Talents Plan of Bureau of Foreign Experts Affairs" of the People's Republic of China as well as by III-10-19 and III-4-19 scientific theme of NAS of Ukraine.

Glass Ceramics Complex Oxide Films for WLED and Silicon Solar Cells

Nedilko S.G.

Taras Shevchenko National University of Kyiv, Kyiv, Ukraine, snedilko@univ.kiev.ua

The development of scientific basis for creation of new micro/ nanostructured luminescent light transforming glass ceramic oxide composites for their application as coatings of white LEDs, solar cells etc. is important for solving a number of fundamental and applied problems in the field of light interactions with nanostructured broadband hybrid composites and optimizing their optical properties by formation of complex luminescent-active centers. The first of our task is to determine peculiarities of the physical processes of excitation, transfer and dissipation of energy and charge in the centers of luminescence in micro/nanostructured materials on the basis of oxide and carbon glass ceramic composites. At the same time, the second task of our work is to improve an efficiency and to modify characteristics of white light-emitting diodes and solar cells using luminescent transformers of light from one spectral range to other.

In order to create effective inorganic glass-ceramic composites, on the first stage of our work, the conditions of synthesis, structural, morphplogical and optical characteristics of some oxide compounds of borates, vanadates, lanthanum vanadates and molybdates, doped with bismuth and/or rare-earth ions (dysposium, erbium, europium, praseodymium, samarium) were observed and some of them were made and studied as crystalline component of glass ceramics composites. Besides, some glasses consisting of the chemical elements mentioned above and which can be suitable luminescent matrices for glass ceramics composites were also studied.

Modern equipments and technsique nad been applied for films and glass ceramic preparation and investigation. Thus, morphology of the films and their components surfaces, structure, chemical composition, thickness, optical transmittance and reflectivity, as well as luminescence properties were measured using SEM, AFM, optical microscopes and various spectrometers.

Taken results can be the basis for development and production of new effective luminescent materials useful not only for WLED and solar cell creation, but for some other applications too.

The work was supported by Ministry of Education and Science of Ukraine (Project 18BF051-01) and have been benefited from the access provided by EU-H2020 program under grant agreement No 654360 (Projects ID 532 and ID 663).

Obtaining and Luminescent Properties of Zinc Sulphoselenides Thin Films

Slyotov M.M., Slyotov O.M., Kushneryk L.Ya.

Yuriy Fedkovych Chernivtsi National University, Chernivtsi, Ukraine,
m.slyotov@chnu.edu.ua

Wideband heterolayers of II-VI compounds can be widely used in the manufacture of various types of light-emitting and photosensitive devices. The direct gap of the energy structure is an important condition for a high efficiency of generation-recombination processes. The wideband (the big band gap E_g) of ZnSe and ZnS predetermines the possibility of mastering of the little-used short-wave region of the optical range by instruments based on these materials. Therefore, the search and selection of technological processes for manufacturing both initial base materials and possible electronic devices, obtained on their basis, remain of particular importance.

The possibility of obtaining of thin films and heterolayers by isothermal annealing of basic II-VI crystals in a pairs of isovalent elements has been established. The optimal technological conditions of growing by isovalent substitution were determined and layers of α-ZnSe, α-ZnS and solid solutions α-$ZnSe_xS_{1-x}$ were obtained. Using this method, thin layers of stable hexagonal modification were obtained as opposite to the widely used materials of cubic structure. This showed a complex of studies of electrical, optical, luminescent and photoelectric properties. The most significant of them is the generation of intense radiation in the short-wave optical range $\Delta\lambda$ = 0.36-0.46 μm with a quantum efficiency η = 10-12% (for cubic structures η = 0.1-0.4%). It is formed in α-ZnSe and α-$ZnSe_xS_{1-x}$ due to the annihilation of bound excitons, and in the case of α-ZnS – due to recombination on donor-acceptor pairs. The conditions of α-ZnSe production were established and thin layers with violet ($\Delta\lambda$ = 0.41-0.47 μm), blue ($\Delta\lambda$ = 0.46-0.49 μm) and green ($\Delta\lambda$ = 0.49-0.55 μm) radiation were obtained. A weak temperature dependence of intensity was found at ΔT = 300-550 K and the repeatability of their characteristics and parameters, as well as high color saturation of 92.3%, 97.6% and 98%, respectively, of their maxima at λ_{m1} = 0.446 μm, λ_{m2} = 0.477 μm, λ_{m3} = 0.517 μm. The growth conditions of α-$ZnSe_xS_{1-x}$ with radiation that captures the ultraviolet region $\Delta\lambda$ = 0.35-0.41 μm and is characterized by efficiency η = 5.8% with a weak temperature dependence of its intensity are determined. The possibility of spectral region extending to the UV range up to $\lambda \approx 0.345$ μm by the formation of a nanostructured surface by special chemical etching is shown. Also, it is found the high radiation resistance of parameters and characteristics of thin heterolayers radiation to irradiation with a density of $D = 7.5 \cdot 10^{15}$ electron/cm^2 with an energy of ≈ 2 MeV and influence of high temperatures T up to 550 K.

Space-Charge-Limited Current in *A*-SiCN Layers

Sukach A.V., Tetyorkin V.V., Tkachuk A.I.[1], Ivaschenko V.I.[2], Porada O.K.[2], Kozak A.O.[2]

V. Lashkaryov Institute of Semiconductor Physics, NAS Ukraine, Kyiv, Ukraine
[1]V. Vynnychenko Central Ukrainian State Pedagogical University, Kropyvnytskyi, Ukraine, atkachuk08@meta.ua
[2]Institute for Problems of Materials Sciences NAS Ukraine, Kyiv, Ukraine

Amorphous SiCN compound is a promising material for different applications in micro- and optoelectronics, since combines semiconductor properties of silicon carbide and dielectric properties of its nitride. High chemical, radiation and mechanical stability over a wide temperature range makes it possible to use *a*-SiCN for manufacture semiconductor devices which can operate under critical conditions. As thin passivation and protective layers, *a*-SiCN may find application in technology of IR detectors based on narrow-gap A_3B_5 and A_2B_6 semiconductors.

The carrier transport mechanisms were investigated in *c*-Si/*a*-SiCN heterostructures produced by plasma chemical deposition method in the temperature range 196-353 K. The amorphous SiCN films with thickness 0.39 and 0.83 μm were deposited using the gas mixture containing the hexamethyldisilazane vapor, H_2 and N_2 in the high-frequency (40.68 MHz) capacity-coupled plasma system in which a negative bias was applied to the *p*-Si substrate. The unipolar space-charge-limited (SCL) current is shown to be dominant conduction mechanism in the forward-biased heterostructures. The SCL current is controlled by shallow and deep traps in thinner and thicker *a*-SiCN layers respectively. A model of exponential distribution of traps over a certain range in energy is proposed for explanation of experimental data. Basic electrical parameters of *a*-SiCN layers estimated from the SCL current measurements are as follows: the concentration of traps ~10^{16} cm^{-3}, the electron mobility 10^{-3}-10^{-2} $cm^2/V\,s$ and the specific conductivity 10^{-8} - 10^{-9} $\Omega^{-1}\cdot cm^{-1}$.

The reverse current at bias voltages U>0.6 V is determined by a potential barrier at the *c*-Si/*a*-SiCN interface. At temperatures higher 296 K the generation in the depletion region is dominant transport mechanism, whereas at temperatures lower 244 K the tunneling current prevails. The current at bias voltages U<0.1 V for all measuring temperatures is ohmic in nature as a result of high-resistance *a*-SiCN layers. Due to presence of a potential barrier at the *a*-SiCN/*c*-Si interface, which can block the injection of holes from the *p*-Si substrate, the double-injection SCL currents in the investigated structures were not observed. The heterostructures exhibited photovoltaic response in the spectral range of 0.4-1.2 μm with the peak wavelength at 0.7-0.74 μm. This means that the photosensitive region is mainly localized in *p*-Si.

ORAL REPORTS

Session 5
Functional crystalline materials: growth, physical properties and applications

Two- and Multi-Beam X-ray Diffraction Diffractometry of Si/SiGe Heterostructures

Borcha M.[1], Solodkiy M.[1], Fodchuk I.[1], Kladko V.[2], Liubchenko O.[2], Safriuk N.[2]

[1]*Yuriy Fedkovych Chernivtsi National University, Chernivtsi, Ukraine*
[2]*V. Ye. Lashkaryov Institute of Semiconductor Physics of NASU, Kyiv, Ukraine,*
(m_borcha@ukr.net)

The method of X-ray high-resolution two-beam diffractometry with multi-beam diffractometry gives promise of practical applications for study of nanostructures [1]. They have been used to analyse chemical composition and strains, mechanisms of growth, shape, processes of lateral and vertical ordering of self-induced quantum dots in Si/SiGe heterostructures. We also studied composition and distortions in near-surface layers (111) of InSb after implantation by Mg ions in two stages (E = 66 keV, D = 25 μC and E = 80 keV, D = 50 μC).

Experimental researches of Si/SiGe and InSb (Mg) heterostructures were carried out on the Philips X'Pert PRO diffractometer in different circuits of two-beam diffraction (symmetrical 333, quasi-forbidden 222, and asymmetric 331 reflections), and multi-beam diffraction (Renninger scan) of $CuK_{\alpha 1}$ radiation. Appropriate conditions of multi-beam diffraction are realized to implement the specific cases of multiple diffraction, in particular, coincidental coplanar three-beam diffraction [1]. Reflections 200 and 222 were chosen as primary reflections for Si/SiGe and InSb(Mg), respectively. The intensity distributions $I_h(\omega)$, $I_h(\omega\text{-}2\theta)$ and $I_h(\omega, \omega\text{-}2\theta)$) are analysed using the kinematical and dynamical theory of X-ray diffraction and numerical simulation [1].

Using data of two-beam diffractometry and the dynamics of single multibeam maxima on Renninger scans, the values and signs of strains (compression or tension) were determined as well the degree of tetragonal lattice distortions i.e. the relationship between $a_{\perp}$ and $a_{||}$ in each layer of Si/SiGe heterostructure. The relaxation degree in the buffer layer and the angular misorientation of the SiGe layers relative to the (001) Si surface are determined. It gives possibility to establish how the Ge component is included to lattice: substituting Si or generating interstitial point defects. Features of distortions and reconstructed 2-D strain profile in the near-surface layers of InSb were obtained at the each stage of ion implantation by Mg.

The complex application of two-beam and multi-beam diffractometry in a single gives additional possibilities in determining the values and 2-D and 3-D distribution of residual mismatch strains in the interface layers of Si/SiGe heterostructures, as well as the reconstruction of strain and Mg distribution profiles in the near-surface InSb layer.

1. Borcha M., Fodchuk I., Solodkyi M., Baidakova M. Structure diagnostics of heterostructures and multilayered system by X-ray multiple diffraction, *Journal of Applied Crystallography*. 2017. 50, №3. P. 722-726.

Influence of Hydrogen Passivation on the Intensity of Exciton Luminescence in Single $Cd_{1-X}Zn_XTe$ Crystals

Brytan V.B., Uhryn Y.O., Peleshchak R.M., Bechkhalo Kh.B.

Ivan Franko Drohobych State Pedagogical University, Drohobych Ukraine, vbrytan2@gmail.com

An important problem of modern optoelectronics is the fabrication of high-efficiency and cheap light-emitting devices with high quantum efficiency of photoluminescence (PL) in a wide spectral range intended for use in optical communication systems, high-energy radiation detectors, and others like that. To do this, it is necessary to investigate both the physical properties of materials used for the manufacture of devices, as well as the impact on these properties of various factors. Semiconductors A^2B^6, in particular, single crystals $Cd_{1-x}Zn_xTe$ are prospective materials for this purpose.

One of the key issues in the development of devices based on $Cd_{1-x}Zn_xTe$ is to determine the energy characteristics of impurities and defects. The presence of electrically active centers (EACs) in such single crystals leads to a violation of the symmetry of chemical bonds, that is to the formation of energy levels in the energy gap of the crystal, the position and structure of which determines the electrical properties of the material. Hydrogen passivation is one of the methods for increasing the quantum efficiency of photoluminescence (reducing the number of recombination centers), reducing the level of defect and improving the optical and electrical properties Such passivation is carried out by growing single crystals in an atmosphere of hydrogen or by treating the crystal in a gas discharge of the hydrogen atmosphere.

Treatment in the gas discharge of hydrogen passes the part of the electrically active centers, which manifests itself in the spectrum of the boundary PL [1]. The improvement of the structural quality of the near-surface layer of samples after their treatment in the hydrogen atmosphere is also confirmed by the presence in the exciton range of PL of hydrogenated samples of free excitons (FE) emission line and the greater clarity of the widths of bound excitons.

It has been experimentally established that after processing of monocrystalline samples $Cd_{1-x}Zn_xTe$ in the hydrogen atmosphere, the intensity of PL excitons bound by neutral acceptors increased by ~30%, while the intensity of PL excitons bound by donors decreased by ~ 15%. This is due to the passivation effect by atomic hydrogen of EAC, the mechanism of which is the electrostatic-deformation interaction of an acceptor with atomic hydrogen.

1. Hamann J. Hydrogen-related photoluminescence in CdTe / J. Hamann, D. Blaß, A. Burchard [et al.] // J. of Crystal Growth. 1998. V.184-185. P. 1147-1150.

Point Defects and Thermoelectric Properties of PbCdTe Solid Solutions

Horichok I.V.[1], Parashchuk T.O.[2], Wojciechowski K.T.[2,3], Shemerliuk Y.V.[1].

[1]*Vasyl Stefanyk Precarpathian National University, Shevchenko str., 57, Ivano-Frankivsk, Ukraine, HorichokIhor@gmail.com*
[2]*The Institute of Advanced Manufacturing Technology, Krakow, Poland,*
[3]*AGH University of Science and Technology, 30-059 Krakow, Poland*

One of the widely used thermoelement materials is a semiconductor Lead Telluride, that operating at 500-800 K temperature range. The main disadvantage of PbTe is the relatively low efficiency of devices based on it (≤ 10%). Among many possible attempts to solve low efficiency, is creating the solid solutions based on the PbTe, which can significantly improve the thermoelectric properties of the base compound.

In this work synthesis of $Pb_{0.9}Cd_{0.1}Te$:Pb (3 at.%) solid solutions along with phase composition investigations have been carried out. Measurements of the thermoelectric properties (Seebeck coefficient, electrical conductivity, thermal conductivity coefficient, and Hall effect) has been performed for samples obtained by sophistical powder metallurgy technology. The method of thermodynamic potentials has been applied for creating a model that allows explanation observed properties of the crystals defect subsystem.

The application of the sophistical powder metallurgy technology give us opportunity to obtain n-type thermoelectric material based on $Pb_{0.9}Cd_{0.1}Te$:Pb (3 at.%) solid solution with a dimensionless thermoelectric figure-of-merit $ZT \approx 1.4$, a promising candidate for application in the thermoelectric converters.

The concentration of free charge carriers in PbCdTe solid solutions significantly depends not only on the amount of cadmium impurities dissolved in the crystalline lattice, but also on the concentration of the over-stochiometric component in the base lead material.

The comparison of present results, literature experimental data as well as theoretical attempts give us opportunities to explain observed phenomena by the proposed defective subsystem model for the solid solution. Our model takes into account own point defects (lead and tellurium vacancies), neutral impurity atoms in cationic sublattice, as well as interstitial cadmium atoms in a neutral and single ionized state. In this case, the obtained experimentally values of the solubility were almost completely determined by the concentration of substitutional atoms. The measured Hall concentration of carriers has been well described by single-ionized interstitial cadmium atoms.

Acknowledgments: The work was partially supported by statute refunds N 11.11.160.438.

Exposure of Individual Bands of Emission in the Photoluminescence Spectra of ZnO:Mn Nanocrystals

Kovalenko A.V., Vorovskiy V.Yu., Khmelenko O.V., Vovk S.M., Plakhtii Ye.G.

Oles Honchar Dnipro National University, Dnipro, Ukraine,
kovalenko.dnu@gmail.com

We investigated an analysis of photoluminescence (PL) spectra of ZnO:Mn nanocrystals which have magnetic properties at a room temperature, obtained by the ultrasonic pyrolysis method [1]. In order to perform the analysis, the initial experimental photoluminescence spectra (Fig.1a) were smoothed by Tikhonov's method (Fig.1b) with the regularization parameter $a = 2.5 \cdot 10^7$. The regularization parameter was obtained by the method of mathematical modeling. The model of noise was set by the sum of noise which depends on a signal and thermal noise: $x_i = |g(x_i)|^{1/2} h_i + 15V_i$, where h_i and V_i are the values of gaussian random quantities with the zero mathematical expectation and unit variance.

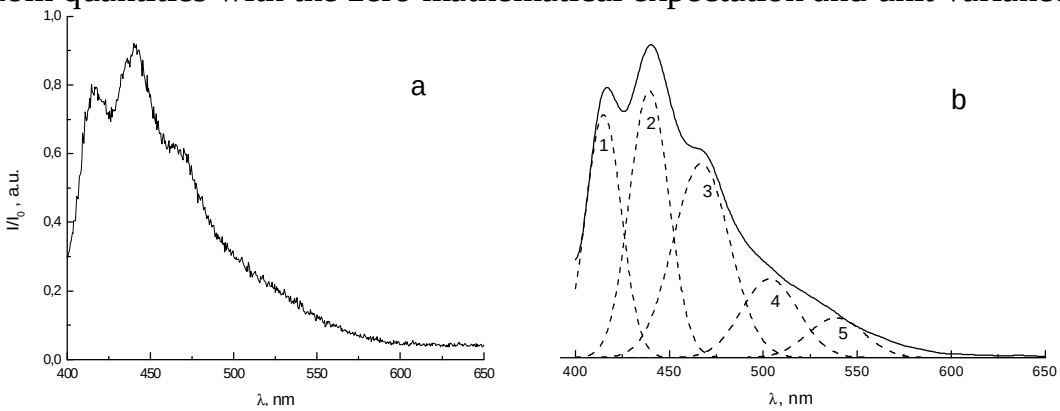

Fig.1. The experimental (a) and initial smoothed and expanded (b) into individual bands (1-5) photoluminescence spectra of ZnO:Mn nanocrystals.

We applied the method of derivative spectroscopy based on the 4^{th} – 6^{th} derivatives for decomposition into elementary bands [2]. After determination of elementary bands parameters – the maximum position of spectrum (λ_{max}) and its half-width ($\Delta\lambda$) – the clarification of parameters was made by the least square method with a limit of the square of norm. The conducted analysis allows to assert that there are at least 5 elementary bands with: 1- $\lambda_{max=}$415 nm, $\Delta\lambda$ =25 nm; 2- $\lambda_{max=}$440 nm, $\Delta\lambda$ =22 nm.; 3- $\lambda_{max=}$467 nm, $\Delta\lambda$ =35 nm; 4- $\lambda_{max=}$504 nm, $\Delta\lambda$ =35 nm; 5- $\lambda_{max=}$540 nm, $\Delta\lambda$ =35 nm. In the experimental photoluminescence spectrum of ZnO:Mn nanocrystals. The nature of centres responsible for exposure of individual bands of emission is discussed.

1. Bulaniy M.F., Vorovsky V.Yu., Kovalenko A.V., Khmelenko O.V. Journal of Nano- and Electronic Physics. 2016. Vol. 8, No. 2, pp. 2043(1-4).
2. Kovalenko A.V., Plakhtii Ye.G., Vovk S.M.. Ukrainian Journal of Physical Optics. 2018 v.19, N 3, pp.133-140.

Structural Changes in Ge-S-Ag Glasses Depending on Ag Concentration

Lishchynskyy I.M.[1], Kaban I.G.[2], Stronski A.V.[3], Voitkiv H.V.[1]

[1]*Vasyl Stefanyk Precarpathian National University, Ivano-Frankivsk, Ukraine,*
igor.lishchynskyy@gmail.com
[2]*Leibniz Institute for Solid State and Materials Research Dresden, Germany*
[3]*V.Lashkaryov Institute of semiconductor physics NAS Ukraine, Kyiv, Ukraine*

Chalcogenide glasses, which are basically semiconductors, become superionic conductors upon doping with metal species. Ge-S-Ag glasses are very attractive, e.g. for the conductive-bridge memories, due to significantly higher glass transition temperature and consequently better thermal stability compared to the Ge-Se based glasses. Also, Ge-S-Ag glasses are free of toxic elements.

In this contribution, we present analysis of the structural changes in rapidly quenched Ge-S-Ag glasses along $(GeS_2)_{100-x}Ag_x$, $(Ge_{42}S_{58})_{100-x}Ag_x$ and $(GeS_3)_{100-x}Ag_x$ lines, where x= 5, 10, 15, 20, and 25 at.%.

Figure 1 shows the concentration dependences of the height of the main three peaks of the structure factors for the $(GeS_3)_{100-x}Ag_x$ and $(Ge_{42}S_{58})_{100-x}Ag_x$ glasses measured by X-ray and neutron diffraction (XRD, ND). The intensity of the first sharp diffraction peak (FSDP) and of the second peak (Q_2) for $(GeS_3)_{100-x}Ag_x$ and $(Ge_{42}S_{58})_{100-x}Ag_x$ glasses decreases with increasing Ag concentration, while that of the first peak (Q_1) increases.

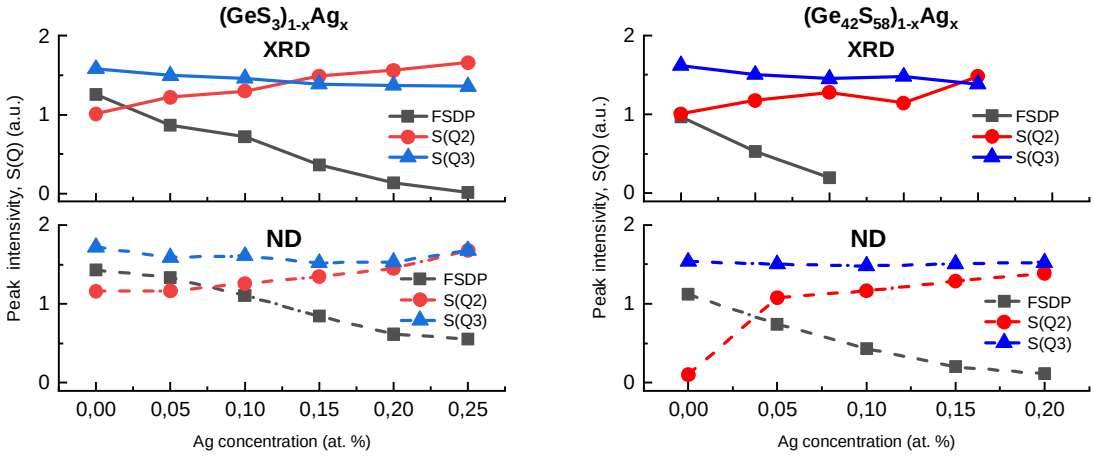

Fig. 1. Composition dependences of the peak intensities on the XRD and ND structure factors of Ge-S-Ag glasses.

The analysis of the peak positions reveals that for homogeneous $(Ge_{42}S_{58})_{100-x}Ag_x$ glasses the position Q_{FSDP} shifts practically linearly with Ag concentration, whereas that for the phase separated glasses $(GeS_3)_{100-x}Ag_x$ and $(GeS_2)_{100-x}Ag_x$ deviates from the linearity.

Electronic and Optical Properties of Tl_4HgI_6 and Tl_4HgBr_6

Luzhnyi I.[a], Khyzhun O.Y.[a], Bekenev V.L.[a], Lavrentyev A.A.[b], Gabrelian B.V.[b], Tuan V.Vu [c,d], Parasyuk O.V.[e]

[a] *Frantsevych Institute for Problems of Materials Science, NASU, Kyiv, Ukraine , Luzhnyi92ivan@gmail.com*

[b] *Don State Technical University, Rostov-on-Don, Russia*

[c] *Division of Computational Physics, Institute for Computational Science, Ton Duc Thang University, Ho Chi Minh City, Vietnam*

[d] *Faculty of Electrical & Electronics Engineering, Ton Duc Thang University, Ho Chi Minh City, Vietnam*

[e] *Department of Inorganic and Physical Chemistry, Lesya Ukrainka Eastern European National University, Lutsk, Ukraine*

Tl_4HgI_6 and Tl_4HgBr_6 belong to a broad class of ternary halogenides that are in the focus of experimental and theoretical research within the recent years [1,2]. The interest to these compounds is primarily due to their perspective applications as detectors of X ray and γ ray radiation as well as parametric generators for the mid-infrared spectral range. Moreover, the latter group of materials suffers from their mechanical brittleness and instability over time of some of their properties. That is why a search for new materials, which could be effective as detectors of ionizing radiation, continues. Tl_4HgI_6 and Tl_4HgBr_6 possess attractive physical properties [3]. In particular, high atomic numbers *Z* of the constituents (Tl: 81, Hg: 80, I: 53, and Br: 35) result in rather high material densities of 6.719 and 6.558 g/cm^3, respectively. With regard to their applications for optical parametric generators, the presence of heavy Tl and Hg atoms warrant material stability under intense laser irradiation. Importantly, I- and Br-bearing halogenides are transparent materials in the near infrared spectral range (1–2 μm), which is typically used for pumping, and in the mid infrared range (15–40 μm), where the optical parametric generators typically operate. Excellent radiation damage threshold in the picosecond regime and high optical nonlinearities make Tl_4HgI_6 and Tl_4HgBr_6 potential candidates for active elements of optical parametric generators. In the present report we present data of coupled experimental and theoretical studies of the electronic and optical properties of Tl_4HgI_6 and Tl_4HgBr_6 halides.

1. S. Wang, Z. Liu, J. A. Peters, M. Sebastian, S. L. Nguyen, C. D. Malliakas, C. C. Stoumpos, J. Im, B. W. Wessels, M. G. Kanatzidis, Cryst. Growth Des. 2014, 14, 2401.

2. A. A. Lavrentyev, B. V. Gabrelian, T. V. Vu, P. N. Shkumat, P. M. Fochuk, O. V. Parasyuk, I. V. Kityk, I. V. Luzhnyi, O. Y. Khyzhun, M. Piasecki, Inorg. Chem. 2016, 55, 10547.

3. O. V. Parasyuk, O. Y. Khyzhun, M. Piasecki, I. V. Kityk, G. Lakshminarayana, I. Luzhnyi, P. M. Fochuk, A. O. Fedorchuk, S. I. Levkovets, O. M. Yurchenko, L. V. Piskach, Mater. Chem. Phys. 2017, 187, 156.

4. V. O. Yukhymchuk, V. M. Dzhagan, N. V. Mazur, O. V. Parasyuk, O. Y. Khyzhun, I. V. Luzhnyi, A. M. Yaremko, M. Ya. Valakh, A. P. Litvinchuk, J Raman Spectrosc. 2018, 49,1840.

Ultradispersed $Y_3Al_5O_{12}:Ce^{3+}$ + Ln_2O_3 Phosphor with a High Luminescence Quantum Yield

Malashkevich G.E.[1], Khottchenkova T.G.[1], Shevchenko G.P.[2], Bokshyts Yu.V.[2], Tret'yak E.V.[2]

[1]*B.I. Stepanov Institute of Physics, NAS of Belarus, Minsk, Belarus*
[2]*Research Institute of Physicochemical Problems of BSU, Minsk, Belarus,*
g.malashkevich@ifanbel.bas-net.by

Ultradispersed phosphors are of interest to use in the systems of LED lighting, the high definition television, as different luminescent tags and to activation of the materials obtained without melting stage. Lack of such phosphors is a decrease in a luminescence quantum yield (η) at reduction of the area of coherent-scattering region that constrains the minimum value of grain.

In the present work we describe the ultradispersed phosphor obtained by the colloid-chemical method on the basis of $Y_3Al_5O_{12}$ (YAG) activated by Ce^{3+} ions with additives of La_2O_3 and Lu_2O_3 oxides, providing a high η value and significant red shift of the activator luminescence band.

The microphotograph and the diffractograms of such phosphor are shown in Fig. 1. As is seen, it represents spherical particles with an average diameter close to 500 nm, and there are reflexes inherent YAG (undesignated), Lu_2O_3 (designated by ▪) and $Y_4Al_2O_9$ (designated by ∗) in its diffractogram.

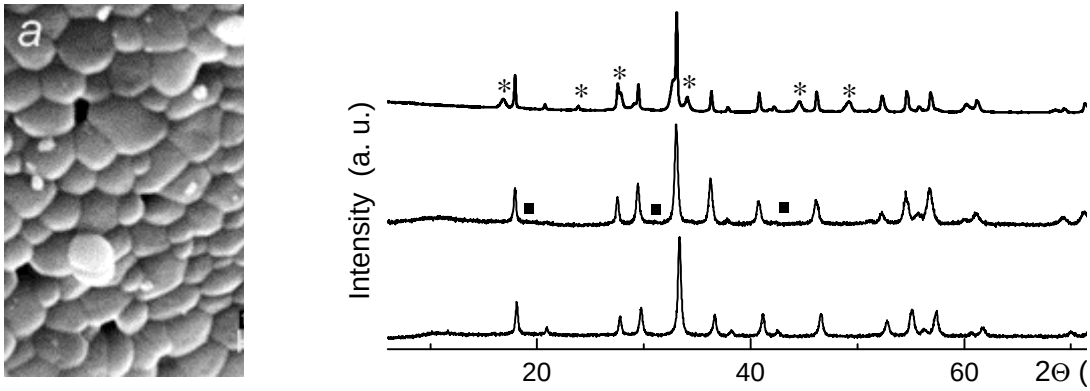

Fig. 1. Microphotograph (a) of YAG:Ce^{3+} + La_2O_3 and diffractograms (b) of YAG:Ce^{3+} (*1*), YAG:Ce^{3+} + Lu_2O_3 (*2*) and YAG:Ce^{3+} + La_2O_3 (*3*) phosphors (λ = 1.54050 Å).

The spectra of luminescence and its excitation of similar phosphors are presented in Fig. 2. Here curves *1* and *2* belong to the phosphor with additive Lu_2O_3, and curves *3* and *4* – with additive La_2O_3. It is seen that upon transition from the first phosphor to the second one takes place a significant broadening of the luminescence band and shift of its maximum from 560 nm to 590 nm. At the same time the luminescence excitation band broadens too. By variation of redox and temperature-time conditions of thermal treatment, we reached value of an

internal quantum yield of luminescence equal to 91% for the phosphor with additive La_2O_3 and to 85% with additive Lu_2O_3. It is established that further coarsening of individual grains of the phosphors slightly effects on increase in η while reduction of their size leads to fast decrease in η value.

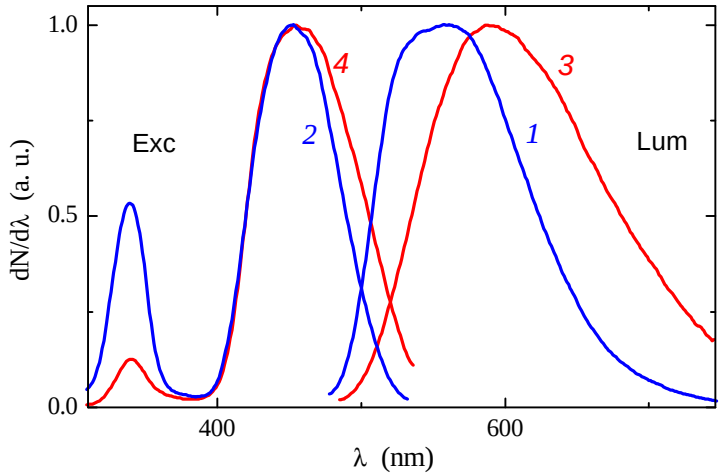

Fig. 2. Spectra of luminescence (*1*, *3*) and its excitation (*2*, *4*) of YAG:Ce^{3+} phosphor with additives of Lu_2O_3 (*1*, *2*) and La_2O_3 (*3*, *4*). λ_{exc} = 450 nm, λ_{rec} = 560 nm (*1*) 590 nm (*3*); $\Delta\lambda_{rec} = \Delta\lambda_{exc}$ = 2 nm.

For practical application of these phosphors, especially in the systems of LED lighting, an important indicator is a degree of stability of intensity and spectra of luminescence at increase of temperature of the phosphor. It was turned out that their luminescence spectrum practically does not depend on temperature in the range of 20–180 °C, and its intensity, as it is seen from Fig. 3, decreases approximately by 10% in the range.

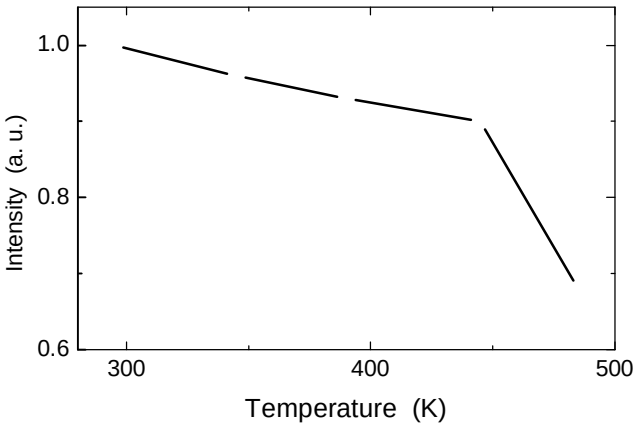

Fig. 3. Temperature dependence of luminescence intensity of

The "spectroscopic behavior" of these phosphors in a matrix of silica gel-glass, polymethyl methacrylate and ceramics with silica binding and some fields of application of the phosphors are considered.

This research has been partially supported by the Belarusian Republican Foundation for Basic Research (projects no. F18R-039 and no. X17D-012).

Synthesis and Properties of Heterophase Materials Based on Lead Telluride Doping with Antimony

Matkivskyi O.M.[1], Zapukhlyak.R I.[1], Horichok I.V.[1], Konevych O.P.[1], Khshanovska O.I.[1], Mateik H.D.[2]

[1]*Vasyl Stefanyk Precarpathian University, Ivano-Frankivsk, Ukraine*
[2]*Ivano-Frankivsk National Technical University of Oil and Gas Ivano-Frankivsk, Ukraine,*
o.matkivsky@opora.org.ua

Thermoelectric converters are one of the most reliable in exploitation types of alternative sources of electric energy. To their advantages also can be included a significant period of unattended exploitation, which may proceed decades of years. This determines the prospect of using thermoelectric generators for military technical needs and other systems in which the energetic autonomy is one of the main priorities.

From the point of view of improving the thermoelectric properties, the materials in which the additional phase is formed as a result of doping with an admixture in excess of the solubility limit proved to be more effective. In this paper, the influence of antimony on the complex physical and chemical properties of lead telluride – one of the materials used to create converters in the temperature range (500-800) K.

Based on the performed studies, it was found that in the case of a solid solution $Pb_{0.49}Sb_{0.01}Te$, the donor effect is significantly less pronounced than in the case of doping PbTe:Sb (1 at.%.Sb). Most likely, this is associated with the possibility of formation during doping, in addition to substitution defects of the donor type (Sb_{Pb}^{1+}) as well as interstitial donor defects Pb_i^{2+}. At the expense of higher in comparison with solids the carrier concentration of PbTe:Sb (1 at.%. Sb), the specific electrical conductivity and heat conductivity coefficient have high value for this material. An increase in the amount of impurity up to 8 atm.% leads to the allocation of an additional phase of pure antimony, which contributes to a significant decrease in the value of k. Size of the inclusion the Sb phase, determined using the Debye-Sherer formula, is 55 nm. This provides the obtaining material with a fairly high dimensional thermoelectric figure of merit: $ZT \approx 1.25$ at $500^{\circ}K$.

Acoustic-Induced Temperature Hysteresis of Electrical Conductivity in CdZnTe:Cl

Olikh Ya.M.[1], Tymochko M.D.[1], Olikh O.Ya.[2]

[1]*V.Ye. Lashkaryov Institute of Semiconductor Physics NAS of Ukraine, Kyiv, Ukraine, tymochko@ukr.net*

[2]*Faculty of Physics, Taras Shevchenko National University, Kyiv, Ukraine*

In low-resist crystals $Cd_{0.96}Zn_{0.04}Te$:Cl ($N_{Cl}\approx5\cdot10^{24}$ m^{-3}) the peculiarities of the ultrasound (US) influence on the temperature characteristics (77÷300) K of electrical conductivity σ(*T*) were revealed, which were determined not only by temperature but also the direction of its change. Thus σ(*T*) depends on the previous state of the sample – from the direction of temperature change, or in the process of heating or cooling (see Fig.). We observe the following: а) hysteresis σ(*T*) without of US does not appear (curves 1 and 2); б) the maximum acoustic-indused changes σ(*T*) are observed at temperatures (100÷200) K. In the process of the sample heating, after the pre-cooling, the value of the acoustic-indused changes σ(*T*) is ~2 times greater than for the cooling (curves 3 and 4). A separate comparison of the acoustic-indused electron concentration and their mobility magnitude, which are received from independent Hall measurements [1], have been led according to the measurements, curves 1-4. It allowed to establish that the determining contribution to the hysteresis effect σ(*T*) is acoustic-indused residual growth of the electron concentration.

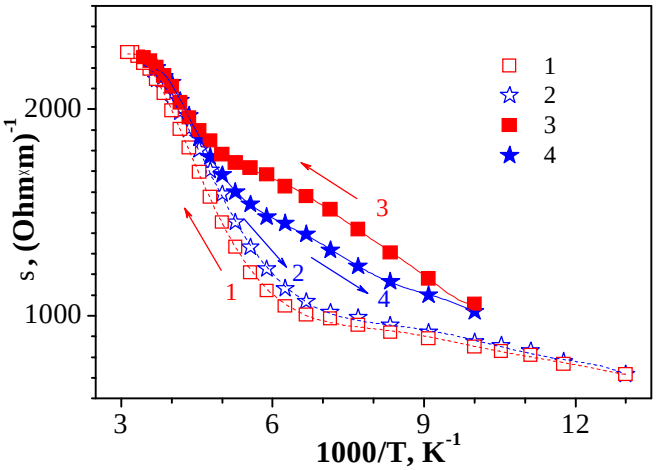

Fig. σ(T). Curves 1 і 2 with open symbols correspond to the initial sample; curves 3,4 with filled symbols – at US loading ($W_{US}\approx10^4$ $W\cdot m^{-2}$). Curves 1,3 obtained by cooling the sample; 2,4 – by heating it. The arrows indicate the direction of temperature change.

The explanation of the effect was carried out within the framework of the long-term relaxation processes mechanism σ(*t*), which can occur due to the release (capture) of donors from compound complexes in near-dislocation areas of vibrating dislocations [2]. The study of the effect allows us to obtain information about the defect structure of the material, and the nature of the acoustic-induced changes its macroscopic characteristics.

1. Olikh Ya.M., Tymochko M.D. Ukr. J. Phys. V. 61, No. 5. P. 381-392 (2016).
2. Olikh Ya.M., Tymochko M.D., Safriuk N.V., Ilashchuk M.I., Olikh O.Ya. Optoelectronics and Semiconductor Technique. V. 52. P.108-122 (2017).

Tenzoresistive Properties of Instrumental Film Systems Based on Py and Ag

Pazukha I.M., Pylypenko O.V.

Sumy State University, Sumy, Ukraine, pylypenko.o@gmail.com

Functional materials based on ferromagnetic and noble metals represent an independent interest in terms of their practical application. In this concern, the study of the effect of strain sensitivity in film such systems is an actual problem in terms of the study of physical processes in functional materials under the influence of external fields.

The paper presents the results of the tensoresistive studies of films based on permalloy $Fe_{20}Ni_{80}$ (Py) and Ag with a total thickness of 20 nm, formed in vacuum chamber with base pressure 10^{-4} Pa by the method of simultaneous condensation at a temperature 300 K. Tensoresistive studies were conducted with the help of deformation machine on the basis of a micro-screw (price of a section – 0.01 mm) using an automated complex. The thickness of the deposited metal was controlled "in situ" by the method of the quartz resonator. The concentration of components of the films was determined by using Scanning electron microscope equipped with an energy dispersive detector to perform the X-ray spectrometry Tescan VEGA3.

Series of deformation dependences for different concentrations of components show a different form. At a concentration of noble metal 75 at.%, the tendency to stabilize the tensoresistive properties is observed in the first deformation cycle. With a decrease in the concentration of Ag atoms up to 25 at.%, the extension of deformation loop is observed. On the deformation dependences of the differential strain coefficient $(g_l)_{dif}$, the maximum is observed. This maximum corresponds to the transition boundary elastic/plastic deformation. Moving of the boundary transition elastic/plastic deformation is associated with structural changes in the samples and depends on the concentration of components in the samples.

The analysis of the concentration dependence (Py + Ag)/S films, shows that the maximum value of the integral strain coefficient in the range of elastic and plastic deformation is observed at $c_{Ag} = 35$ at.%. The increase in the content of silver in nanostructural films up to 35 at.% results in a grow of $(g_l)_{int}$ from 2 to 82 units. A sufficiently large increase in the integral coefficient value is most likely due to changes occurring in the crystalline structure of the samples when the concentration of components in the film sample changes. Another reason of $(g_l)_{int}$ grows is probably associated with the changes in the grain boundary dispersion process that determines the absolute value of the strain coefficient.

This work was funded by the State Program of the Ministry of Education and Science of Ukraine (2019-2021).

Effect of Bi on Mechanical and Transport Properties of Antimony

Rogacheva E.I., Doroshenko A.N., Khramova T.I., Men'shov Yu.V.

National Technical University "KhPI", Kharkiv, Ukraine, rogachova.olena@gmail.com

Isovalent Bi and Sb semimetals crystallize in a rhombohedral layered structure and form a continuous series of $Bi_{1-x}Sb_x$ solid solutions. These solid solutions belong to the best thermoelectric (TE) materials used in refrigerating devices operating in the temperature range below ~ 150 K. Recently, interest in transport properties of $Bi_{1-x}Sb_x$ has grown sharply due to the experimental observation of the special properties characteristic of topological insulators in $Bi_{1-x}Sb_x$ crystals and thin films.

Earlier, anomalies in the dependences of mechanical and transport properties of $Bi_{1-x}Sb_x$ on composition at $x \sim 0.01$ (near pure Bi) were detected [1] and attributed to the manifestation of percolation effects, accompanying the transition from dilute to concentrated solid solutions. This was consistent with our assumption [2] that the presence of concentration-dependent anomalies of properties in the region of low impurity contents is of a general nature and is inherent in all solid solutions.

The goal of this work was to study the influence of Bi on both electronic and mechanical properties of Sb in the vicinity of pure Sb in order to identify the peculiarities of the transition from dilute to concentrated solid solutions.

The $Bi_{1-x}Sb_x$ samples with compositions in the range of $x = 0.975–1.0$ were prepared by fusing high-purity elements in evacuated quartz ampoules and subsequent annealing for 720 hours at $T = (725 \pm 5)$ K. The dependences of microhardness H, electrical conductivity s, Hall coefficient R_H, charge carrier mobility m_H, and Seebeck coefficient S on the composition of $Bi_{1-x}Sb_x$ solid solutions near pure Sb ($x = 1.0–0.975$) were measured. In the range of $x = 0.995–0.9875$, an anomalous decrease in H, R_H S and an increase in σ and μ_H with increasing Bi concentration were observed. For all the alloys, the dependences of H on the load P on the indenter were built, and it was established that near composition $x \sim 0.99$ the character of the $H(P)$ dependences changes.

The results obtained are interpreted on the basis of our assumptions about the presence of a percolation-type phase transition in any solid solution, i.e. transition from an impurity discontinuum to an impurity continuum, from dilute to concentrated solid solutions.

1. E. I. Rogacheva, A. A. Drozdova, and O. N. Nashchekina, Phys. Stat. Sol. A, 207, 344, (2010).
2. E.I. Rogacheva, Jpn.J.Appl. Phys, 32, Suppl. 32-3, 775 (1993).

Effect of Annealing on the Magnetoresistance of Bismuth Coatings

Shendyukov V.S., Perevoznikov S.S., Tsybulskaya L.S.

Research Institute for Physical Chemical Problems, Belarusian State University, Minsk, Belarus, Tsybul@bsu.by

Bismuth has some unique electrophysical properties. One of them is the effect of anomalous magnetoresistance, which was detected in a magnetic field. The crystal growth structure and the grain size have a significant effect on the magnetic properties of bismuth. Earlier [1] was shown that growth texture and grain size of the electrodeposited films can be varied by changing the regimes of synthesis and adding some organic substances.

In this work, we investigated the effect of annealing of bismuth crystalline films, which were prepared by electrochemical deposition from perchlorate electrolyte on their magnetoresistance value. The annealing was carried out at temperature of 267 ± 1 °C in an inert atmosphere of helium. The measurements of magnetoresistance were carried out using the installation of the Cryogen Free Measurement System. In the temperature range of 5 – 300 K in a magnetic field up to 8 T, perpendicular to the route of transmission of electric current through the sample. Fig 1 shows the dependences of the relative magnetoresistance of film samples before and after annealing.

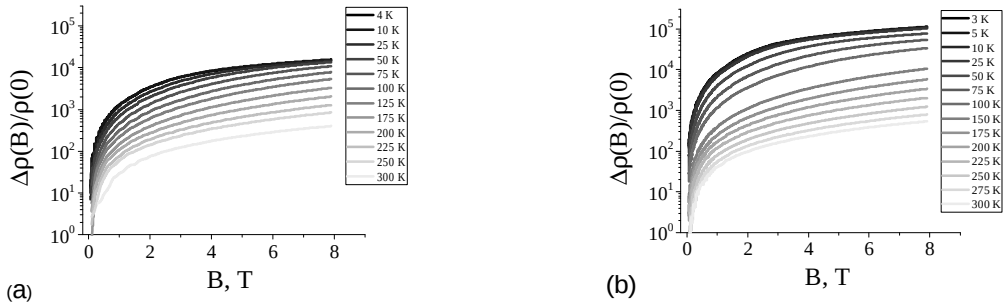

Fig. 1 Magnetoresistance of bismuth samples from perchlorate electrolyte (0,51 M $Bi(ClO_4)_3$ and 3 M $HClO_4$, t=23 ^oC, i_c=0,18 A/dm^2) before (a) and after (b) annealing

From Fig 1b it can be seen that annealing led to increasing of the relative samples magnetoresistance. At low temperatures (up to 50 K), the magnetoresistance of the annealed samples exceeds by one order of magnitude the magnetoresistance of the initial bismuth films. With an increase in the measurement temperature, the difference between the relative magnetoresistance of the annealed and initial samples decreases and at room temperature is 10-20 %.

1. Shendyukov V.S., Perevoznikov S.S., Tsybulskaya L.S., Poznyak S.K. Preparation of Textured Bismuth Films by Electrochemical Deposition // Physics and technology of thin films and nanosystems. XVI international conference. 15-20 may, 2017. Ivano-Frankivsk, Ukraine. – P. 52

Raman Spectroscopy and EXAFS Studies of Structural Peculiarities of As_2S_3-As_2Se_3 Chalcogenide Glasses

Stronski A.[1], Kavetskyy T.[2,3], Revutska L.[4], Kaban I.[5], Shportko K.[1], Baran J.[6], Trzebiatowska M.[6]

[1] *V.E. Lashkaryov Institute of Semiconductor Physics, National Academy of Sciences of Ukraine, Kyiv, Ukraine, alexander.stronski@gmail.com*
[2] *Drohobych Ivan Franko State Pedagogical University, Drohobych, Ukraine*
[3] *The John Paul II Catholic University of Lublin, Lublin, Poland*
[4] *National Technical University of Ukraine "Ihor Sikorsky Kyiv Polytechnic Institute", Kyiv, Ukraine, liubov.revutska@gmail.com*
[5] *IFW Dresden, Institute for Complex Materials, Dresden, Germany*
[6] *W. Trzebiatowski Institute of Low Temperatures and Structure Research, Polish Academy of Sciences, Wroclaw, Poland*

The chalcogenide glasses (CG) are attractive materials for new generation optoelectronics [1]. Studies of nanocomposite materials based on chalcogenide glasses have been actively conducted. The structural features of chalcogenide glasses and films are important in photoinduced processes. Accordingly, better understanding of the structural properties can help in the optimization of the sensitivity and relief formation processes of composite nanomultilayer structures based on As_2S_3-As_2Se_3 alloys, which are perspective for the direct recording of optical elements. Thus, the purpose of the present work is to find, complementary to the Raman data, a structural evidence for existence of mixed pyramidal units in the $As_{40}Se_xS_{60-x}$ glasses (x = 0, 10, 30, 60) using EXAFS technique.

The Raman data show that As_2S_3-As_2Se_3 glasses contain different structural units whose concentration changes along chosen compositional cross-section. The intensity of the bands corresponding to molecular fragments with Se-related and homopolar As–As bonds decreases with the growth of S content. The intensity of the bands corresponding to the presence of $AsS_{3/2}$ pyramidal units increases with higher S content.

The EXAFS measurements of both As and Se K-edges of As_2S_3-As_2Se_3 system provide an evidence for the isostructural substitution of chalcogen atoms in pyramidal structural units. Formation of mixed AsS_2Se and $AsSe_2S$ pyramids in the ternary glasses is suggested. No evidence for existence of heteronuclear Se–S bonding is found.

1. Stronski A.V., Achimova E., Paiuk O., Meshalkin A., Prisacar A., Triduh G., Oleksenko P.F., Lytvyn P., Direct Magnetic Relief Recording Using $As_{40}S_{60}$:Mn-Se Nanocomposite Multilayer Structures, *Nanoscale Res. Lett.* 12:286 (2017).

Thermally Stimulated Conductivity $AgCd_2GaS_4$ Crystals

Tretyak A.P., Bulatetska L.V., Bozhko V.V., Bulatetsky V.V.

Lesya Ukrainka Eastern European National University, Lutsk, Ukraine, fttkaf@gmail.com

The single crystals of $AgCd_2GaS_4$ crystallize in a rhombic structure with lattice parameters: a = 0.81459 nm; b = 0.68989 nm; c = 0.65932 nm and have an n-type conductivity [1]. According to the results of microprobe analysis, they are nonstoichiometric by several percent for cadmium, i.e. enriched with cadmium vacancies (VCd), and have an excess of Ag and Ga atoms [1].

A study of thermally stimulated conductivity was carried out to study the characteristics of the shallow donor centers of single crystals of $AgCd_2GaS_4$.

The donor centers at the bottom of the conduction band, having lost electrons in a compensated semiconductor, can play the role of traps for free charge carriers. Filling such centers with electrons can be accomplished by lighting the photosensitive semiconductor with light from the intrinsic absorption region at a low temperature, at which the probability of thermal excitation of electron from the trap to the zone is insignificant. Heating of the sample, that is activated this way, in the darkness will lead to the release of electrons from the traps and the appearance of peaks on the curve TSC.

In the work [2], studies of TSC in the temperature range T = (110-150) K revealed the existence of an impurity zone of sticking levels in the range of 0.07-0.18 eV. TSC studies were carried out at the temperature of liquid helium and above to identify shallow donor centers.

It was found from the results of the study, that the slope of the FSC initial section gradually increases from a value of 0.007 eV to 0.02 eV.

Taking into account that the electron traps are distributed in a certain energy range of quasicontinuos states, we used the decomposition of the diffuse peak of the SMT applying the «thermocleaning» method to estimate Et. As a result, it was possible to identify the levels with energies of 0.02 eV, 0.04 eV, and 0.1 eV. The role of shallow traps in single crystals of $AgCd_2GaS_4$ be played by inter-node atoms of Ag_i, Cd_i, Ga_i in different inter-nodal positions, as well as by sulfur vacancies (V_S).

1. Chykhriy S. Y., Parasyuk O. V., Halka V. O. Crystal structure of the new quaternary phase $AgCd_2GaS_4$ and phase diagram of the quasi-binary system $AgGaS_2$-CdS. *Journal of Alloys and Compounds*. 2000. Vol. 321, № 1–2. P. 189–195.
2. Халькогенідні почетверенні монокристалічні сполуки $AgCd_2GaS_4$ і їх фізичні властивості / В.В. Божко, Г.Є. Давидюк, Л.В. Булатецька, О.В. Парасюк. *УФЖ*. 2008. Т. 53, № 3. С. 257–261.

Hydrothermal Growth of ZnO Crystals Under Mild Conditions Utilizing Thermodynamics

Uhrin Robert

XLight Corporation, Mendham, NJ, USA, ruhrin@aol.com

ZnO is a II-VI semiconductor that crystallizes in the Wurtzite structure (hexagonal space group $P6_3mc$, a = 3.250 Å; c = 5.207 Å). It was originally considered for use as a substrate for CVD growth of Group III-nitride films, but its reducibility at high temperature (1100 °C) prevents its use as a substrate for CVD growth of the aforementioned films. The conventional hydrothermal growth of ZnO began in the 1960's, when large crystals were grown. However, the technique of using mild conditions (< 250 °C, subcritical pressures) for hydrothermal growth was developed during the 1990's at Rutgers University. This was accomplished solely by applying thermodynamic stability to selected conditions of temperature and composition. Preselected crystal growth conditions could then used to predict actual crystal growth results using a desktop computer and commercial software that resulted from the Rutgers research. This approach was utilized to grow the described ZnO crystals.

Several advantages result from using this technique. Film growth can be accomplished as well as bulk crystal growth. Lattice matching of a substrate to a desired compound can be achieved. Doping of ZnO using Mg (i. e.) can improve the temperature stability of ZnO. While it is normally a n-type semiconductor, p-type ZnO may be possible using mild conditions and pure chemicals. Phase-pure compounds of binary, ternary, and quaternary materials can be realized. This paper will discuss the conditions under which the thermodynamic approach was utilized to grow bulk ZnO crystals.

.

ORAL REPORTS

Session 6
Thin films technology for energy application

Mobile Combined Photovoltaic / Wind Power Station for Autonomous Power Supply of Electronic Equipment

Korkishko R.M., Litovchenko V.G., Kostylyov V.P.,
Chernenko V.V., Dvernikov B.F.

V. Lashkaryov Institute of Semiconductor Physics,National Academy of Sciences of Ukraine, Kyiv, Ukraine, romkin.ua@gmail.com

Solar photovoltaic power station, which operate on the principle of direct conversion of solar energy into electrical energy, are reliable, highly efficient, compact energy sources in the absence of stationary electrical networks.

Fig. 1. Mobile combined photovoltaic / wind power station

The analysis of proposals for mobile solar power station [1,2] has shown that their main disadvantage is a rather significant duration of charge (exceeding 10 hours) of low-power equipment, even at a high level of energy illumination, due to insufficient output power of solar panels. Such devices do not have an internal buffer accumulator that accumulates energy during the day. And then it allows to carry out power supply or charging low-power equipment at low light (at night). Also, the low reliability of the design, does not allow to effectively use them in the field.

The purpose of this work is to develop and manufacture a mobile combined photoelectric / wind power station (Fig. 1), which enables the power or charging of a wide range of low-power equipment (laptops, radio-stations, mobile phones, thermal imagers, tablets, GPS-navigators), under extreme conditions, even at low light levels, which is an advantage over a range of chargers offered on the market.

1. Литовченко В.Г. Сонячна енергетика: порядок денний для світу й України / В.Г. Литовченко, М.В. Стріха.- Київ: К.І.С.- 2014.- 40 с.
2. Оксанич А.П. Сучасні технології виробництва кремнію та кремнієвих фотоелектричних перетворювачів сонячної енергії / А.П. Оксанич, В.А. Тербан, С.О. Волохов, М.І. Клюй, В.А. Скришевський, В.П. Костильов, А.В. Макаров.- Кривий Ріг: Мінерал.- 2010. - 300.- 266 с.

Hybrid PEDOT:PSS/Si Solar Cells with Nanostructured Interface

Mamykin S.V., Lunko T.S., Kondratenko O.S., Kondratenko S.V.,
Mamontova I.B., Kotova N.V., Romanyuk V.R.

V.E. Lashkaryov Institute of Semiconductor Physics National Academy of Sciences of Ukraine
Kyiv, Ukraine, mamykin@isp.kiev.ua

PEDOT:PSS is one of the most promising organic materials for photovoltaics due to its high conductivity, thermal and chemical stability, transparency and simple deposition technology. Hybrid solar cells based on heterojunctions between PEDOT:PSS and texturated Si are being actively developed. Such solar cells achieve an efficiency of 8-11% [1,2] and up to 15% using the method of chemical etching initiated by metal particles (MACE) [3].

In this work we used spincoated PEDOT:PSS to prepare the heterojunctions on flat and microrelief Si surfaces of the quasigrating type and the so-called “black” silicon. Quasigrating surfaces were obtained by chemical etching of n-type (110) silicon wafers in 30% KOH for 60 min. Si nano-textured surfaces (“black” Si) were obtained by chemical etching initiated by metal nanoparticles (Au, Ag). The depth of the relief was varied by the etching time. The top contacts are made of silver by evaporation through the shadow mask. The back ohmic contacts were made by indium deposition. The light and dark current-voltage characteristics of the prepared solar cells and photocurrent spectra have been measured. As expected, texturization increases the energy conversion efficiency. Structures obtained using silver nanoparticles show better results compared with gold nanoparticles.

1. Jheng-Yuan Chen, Celal Con, Ming-Hung Yu, et al. Efficiency enhancement of PEDOT:PSS/Si hybrid solar cells by using nanostructured radial junction and antireflective surface. *ACS Appl. Mater. Interfaces*, 2013. V. 5, No. 15. P. 7552–7558.
2. Jeong S., Garnett E.C., Wang S., et al. Hybrid silicon nanocone-polymer solar cells. *Nano Lett.* 2012. V. 12, No. 6. P. 2971–2976.
3. Rongzong Shen, Ming Liu, Yurong Zhou, et al. PEDOT:PSS/SiNWs hybrid solar cells with an effective nanocrystalline silicon back surface field layer by low temperature catalytic diffusion. *Sol. RRL*. 2017. V. 1,No. 1. P. 1700133.

CNTs Growth on Reduced Iron

Sviatenko A.M., Khovavko A.I.[1], Filonenko D.S.[1], Strativnov E.V.[1], Barabash M.Yu.[2]

[1] *Gas Institute of National Academy of Sciences Kyiv, Ukraine, ahova2005@ukr.net*
[2] *Technical Centre NAS of Ukraine, Kyiv, Ukraine*

In the present work we continued our previous investigations to obtain CNTs by CVD method [1,2]. The analysis of the known technologies for CNTs producing by low-temperature synthesis is associated with the conversion of hydrocarbons at different temperatures and is ineffective in terms of the use of hydrocarbons. High-temperature processes of CNTs formation are energy-intensive and difficult to manage. We have proposed the basics of the technology of CNTs formation when freshly reduced iron is processed by converted natural gas.

The mechanism of CNTs growth on thin iron films is considered. The method of vacuum evaporation was used for the deposition of thin iron films with a thickness of ten till hundreds of nanometers. It provides films of a given composition with a controlled structure with minimal impurities. The deposition was performed using an upgraded vacuum universal post VUP-5M. The pressure of the residual gases in the chamber did not exceed ($10^{-2} \div 10^{-3}$ Pa). Samples in the form of thin layers (10 ÷ 100 nm) of iron on a substrate of glass-ceramic material (sitall) at room temperature were obtained by electron evaporation in vacuum, the intensity was E = 60 ÷ 80 V/cm^2. This method is characterized by special efficiency and good handling.

The mechanism of occurrence and growth of CNTs on iron catalyst under conditions of low-temperature disproportionation of carbon monoxide contained in products of air conversion of natural gas is considered. A highly dispersed structure of iron in the form of a chaotic accumulation of its particles of microscopic size is formed In terms of low-temperature reduction, the boundaries of contact of particles have the highest catalytic activity, where the nucleation of a new phase occurs in the form of ring-shaped cuffs due to emitted carbon while carbon monoxide decomposes. Fragmentation of the catalyst with separation of iron particles from the main mass occurs as the result of carbon subsequent crystallization. The outer diameter of nanotubes formed while growth of carbon cuffs is determined by the size of separated iron particles. The optimum temperature for CNTs formation from products of air conversion of natural gas is 600–650°C. It was suggested that the mechanism of carbon nanotube formation in considered conditions flows through the intermediate stage of oxidation-reduction of iron on the active centers of the catalyst.

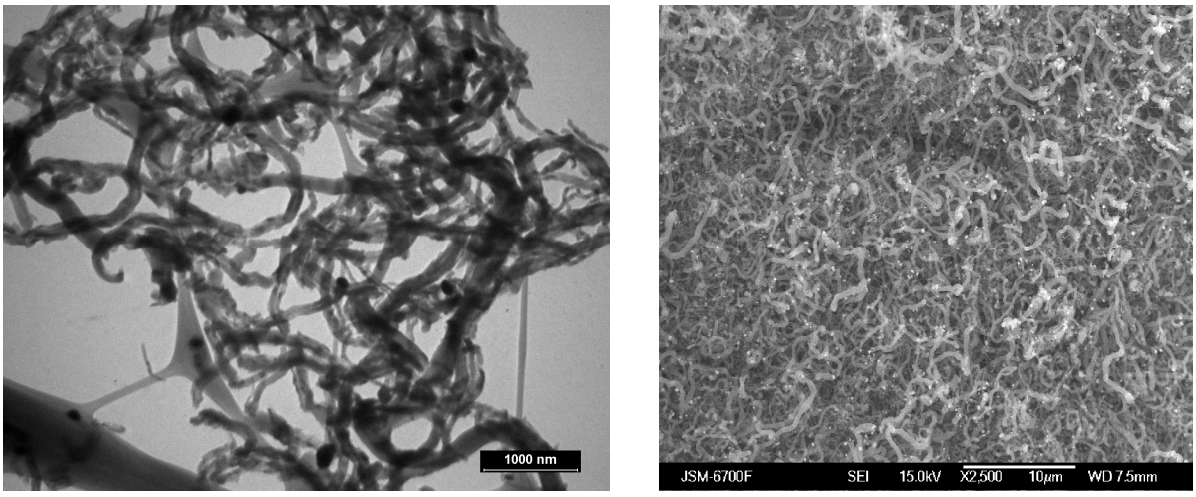

a *b*

Fig.1. Photo of CNTs: a) transmission microscopy (TEM) b) scanning microscopy (SEM) × 2500.

Fig. 1 shows the structure of obtained CNTs. Evidence for the hypothesis that the reaction mechanism of CO disproportionation proceeds through the intermediate stage of iron oxides formation is given. Also it is noticed the positive influence of hydrogen on CNTs formation, which is always present in a large quantity in a converted gas.

References

1. A. Khovavko, A. Sviatenko, V. Kotov, B. Bondarenko, A. Nebesniy, D. Filonenko. Technology of carbon nanotubes production in gas mixtures containing carbon monoxide. // Physica Status Solidi – 2013. – C 10, No. 7-8. – P. 1180-1182 (2013).
2. Carbon nanomaterial Formation on Fresh-Reduced Iron by Converted Natural Gas et al. Nanoscale Research Letters (2017) 12:107 DOI 10.1186/s11671-017-1882-6

Structural, Photoelectrical and Optical Properties of the Organic-Inorganic Perovskites Investigated by Noncontact Methods

Vlasiuk V.M.[1], Belous A.G.[2], Kobylianska S.D.[2], Kostylyov V.P.[1], Sachenko A.V.[1], Sokolovskyi I.O.[1], Torchyniuk P.V.[2], V'yunov O.I.[2]

[1]*V. Lashkaryov Institute of Semiconductor Physics, National Academy of Sciences of Ukraine, Kyiv, Ukraine.*
[2]*Vernadsky Institute of General and Inorganic Chemistry, National Academy of Sciences of Ukraine, Kiev, Ukraine, viktorvlasiuk@gmail.com*

In this report is presented the results of the investigation of the structural and physical properties of $CH_3NH_3PbI_{2.98}Cl_{0.02}$ perovskites. Peculiarities of the film synthesis and the method to determine unit cell parameters are described. Parameters are investigated by non-contact methods utilizing the spectral characteristics of the small-signal surface photovoltage and transmission spectra.

To obtain the $CH_3NH_3PbI_{2.98}Cl_{0.02}$ films, the input reagents PbI_2, CH_3NH_3I, and CH_3NH_3Cl were dissolved in dimethylformamide (DMF) in stoichiometric proportions and mixed for 1 hour at 70°C. The so obtained transparent solution was then deposited onto a pre-cleaned substrate by spin-coating at 1200 rotations per minute during 30 seconds. Glass or ITO-coated glass were used as substrates. Thermal treatment of the films was carried out on a pre-heated stove at 90°C for 30 minutes.

The spectral characteristics of low-signal surface photovoltage $V_{ph}(\lambda)$ ($V_{ph}<<kT/q$) were measured in the wavelength range $\Delta\lambda$ = 400-900 nm on the perovskite $CH_3NH_3PbI_{2.98}Cl_{0.02}$ films deposited on glass with an ITO layer. The measurements were performed at a constant flux of photons of monochromatic light and a constant irradiance. Surface photovoltage measurements were performed with a non-destructive method using a clamping ITO electrode.

Since the spectral dependences of the low-signal photovoltage, as well as the spectral dependences of the short-circuit current, are determined by the spectral dependences of the external quantum yield (EQE), the experimental value $V_{ph}(\lambda)$ near the absorption edge is described by the empiric formula $EQE(\lambda)=[1+(4\alpha(\lambda)n_r^2d/b)^{-1}]^{-1}$ where $\alpha(\lambda)$ is the light absorption coefficient, d is the perovskite film thickness, n_r is the refractive index of the film, $b > 1$.

Conclusions. Analysis of the spectral characteristics of the small-signal surface photovoltage and transmission spectra show the high (relative to the film thickness) minority charge carriers diffusion length. It is found that the film morphology represents a net of non-oriented needle-like structures with significant roughness and porosity. It leads to natural film profiling and therefore to the drastic increase of photons path in the structure. Such a situation is also typical for other perovskites, particularly for $FAPbI_3$ perovskites. Therefore the films are promising for the use in photoelectric.

Optimization Of the High Efficiency Silicon Solar Cells with Texturized Surface

Vlasiuk V. M.[1], Dvernikov B. F.[1], Evstigneev M.[2], Kostylyov V. P.[1], Sachenko A. V.[1], Serba O. A.[1], Sokolovskyi I. O.[1]

[1]*V. Lashkaryov Institute of Semiconductor Physics, National Academy of Sciences of Ukraine, Kyiv, Ukraine.*
[2]*Department of Physics and Physical Oceanography,Memorial University of Newfoundland, St. John's, NL, Canada, viktorvlasiuk@gmail.com*

The purpose of this report is (i) to analyse the experimental external quantum efficiency (*EQE*) curves in the high-efficiency textured silicon solar cells (SCs), (ii) to develop a model aimed at numerical determination of their characteristics depending on the base thickness and (iii) to optimize their.

Results. The experimental $EQE(\lambda)$ curves were analyzed for several high-efficiency p-n junction-based SCs, as well as for the HIT SCs. It is shown that all the samples studied are well described by the empirical formula $EQE(\lambda)=[1+(4\alpha(\lambda)n_r^2 d/b)^{-1}]^{-1}$, where $\alpha(\lambda)$ is light absorption coefficient, d is the base thickness, n_r is the refraction index, and b is an empirical non-dimensional coefficient above with the coefficient b in the range between 1.6 and 12. Based on the experimental $EQE(\lambda)$ results and this formula, the short-circuit current density J_{SC} is found as a function of the base thickness d for the samples investigated. A self-consistent approach is proposed to calculate the photoconversion efficiency in textured silicon SCs, which is valid under two conditions: (1) the base region minority carriers diffusion length L_d should be much larger than d, (2) surface recombination velocity S must be much smaller than D/d, where D is the minority carrier diffusion coefficient.

The $EQE(\lambda)$ curves and the b-values are used to find $J_{SC}(d)$, from which the open-circuit voltage V_{OC} and the illuminated current-voltage curve $J_L(V)$ are established. The photogenerated voltage and the corresponding current density at the maximal power are found by setting the derivative of the output power with respect to bias to zero, $d(J_L(V)V)/dV = 0$. Finally, the photoconversion η and the fill factor FF are determined from this condition. Surface recombination velocity S and the series resistance R_s are found from the comparison of V_{OC} and η with the experiment. The dependence of S on the level of doping is carefully analyzed and taken into account.

Conclusions. Thus it is established that the experimental *EQE* in textured silicon SCs near the absorption edge is well described by an empirical formula. With increasing degree of the SC light capture, the value of b tends to unity. The approach proposed in this contribution allows modeling the short-circuit current and photoconversion efficiency in textured silicon solar cells. The modeling results were used to optimize the parameters of these SC.

ORAL REPORTS

Session 7
Innovative methods for teaching

The Role of Foreign Trips of Scientists in the Development of Physics and Methods of Physics Teaching

Chumak Mykola

M.P. Dragomanov National Pedagogical University, Kyiv, Ukraine,
chumak.m.e@gmail.com

Mykhailo Petrovych Avenarius (1835–1895) – Doctor of Physics, Honored Ordinary Professor studied physics from Magnus in Berlin and Kirchhoff in Heidelberg. He taught experimental physics, meteorology, physical geography, special courses on the mechanical theory of heat (thermodynamics), the theory of electricity and magnetism and optics. He founded the first physics school in Ukraine. The lighting system improved by Avenarius was exhibited at Paris Electrotechnical Exhibition (1881), where it was awarded a silver medal. As a participant in the exhibition and congress of electricians, he was awarded the highest award of the French Republic — the Order of the Legion of Honour.

Heorhiy Heorhiyovych DeMetz (1861 - 1947) substantiated the conclusion about the complexity of the structure of solutions of high molecular organic compounds and about the presence of the structure in liquid colloidal solutions. He reported on his scientific achievements at the International Aeronautics Congress in 1909 in Nantes (France) and at the International Radiology and Electrical Engineering Congress in September 1910 in Brussels.

Pylchykov Mykola Dmytrovych (1857 — 1908). In 1888-1889, Mykola Dmytrovych went on a scientific trip abroad where he worked in laboratories of prominent French physicists such as Lipman, Cornus, Mascara. It was then that "student" Pylchykov drew attention of "his teachers" to the errors in the design of the seismograph in their magnetic observatory that had to be corrected.

In Paris he carried out a number of important studies in the field of electrochemistry, in particular, he developed an effective optical-galvanic tool for studying the electrolysis. He made presentations at the 2nd International Electricity Congress and the 1st International Meteorological Congress. He was elected member of the French Physical Society and the International Society of Electricians. In Paris, he began a major experimental research in the field of electrochemistry, which he managed to complete only a few years later.

After returning from a business trip, Pylchykov became a professor at Kharkiv University. He gives lectures for senior students in mathematical and experimental physics which were always accompanied by a demonstration of well-developed experiments.

Fedir Nykyforovych Shvedov (1840 - 1905), a scientist-physicist, a theorist and an experimenter. In 1865, he was sent abroad to broaden knowledge and was taught by Henry Gustav Magnus (Berlin). He is one of the founders of a new direction in dendrochronology. In particular, he studied the ratio of the thickness of annual tree rings as a record of droughts associated with eleven-

year solar cycles. In his paper "On Electrical Rays and the Laws of Their Distribution" (1873), he established an analogy between electric and light phenomena. He studied comet formation causes, comet shape, as well as the nature of northern lights. The scientist’s most important works are dedicated to the elastic-viscous flow of bodies. In the works published in 1889 - 1890, Shvedov laid the foundations for the study of the rheological properties of disperse systems and macromolecular compounds. For the first time in science, he discovered the elasticity of the form and the anomaly of viscosity of colloidal solutions, which consists in the fact that in the sphere of fluidity limit the effective viscosity drops sharply with the current voltage, therefore the voltage is not completely dissipated and the liquid retains residual deformation.

Purpose and Objectives of Ecological Education

Hladun Tetiana

M.P. Dragomanov National Pedagogical University, Kyiv, Ukraine, gladunt@ukr.net

The main objective of ecological education is the formation of the ecological culture of individuals and society as a whole, the formation of skills, fundamental ecological knowledge, ecological thinking and consciousness, which are based on handling nature as a universal and unique value. On the one hand, ecological education should be an independent element of the general education system, and on the other, it plays an integrating role in the education system. This goal is achieved gradually by solving educational and educational tasks and improving practical activities.

The most important tasks of ecological education include:

1. **Formation of ecological culture** of all population segments, which includes raising public awareness of modern ecological problems of the State and the world, awareness of their importance, relevance and universal nature (a link between local and regional and global problems); the revival of the best traditions of the Ukrainian people in handling the environment, teaching love for nature; formation of awareness of the hopelessness of the technocratic idea of development and of the need to replace it with an ecological one, which is based on the understanding of the unity of all animate and inanimate objects in the complex global system of harmonious coexistence and development; formation of an understanding of the need to coordinate the strategy of nature and human strategy on the basis of the idea of the universal character of connections in nature and self-restraint, eradication of the consumer attitude to nature; development of personal responsibility for the state of the environment at the local, regional, national and global levels; ability to predict personal activities and activities of other people and groups; development of skills to make responsible decisions on ecological problems, acquisition of standards of ecologically sound behavior; education of deep respect for one's own health and development of skills to maintain it.
2. **Training of ecological specialists** for various sectors of the national economy, including the educational sector — school teachers, university teachers; for state authorities on ecological protection and rational use of natural resources, as well as public ecological organizations.
3. **Improvement, harmonization and standardization of terminology in the field of ecological knowledge**. Ecological education is based on the principles of humanism, scientific approach, continuity, transversality and systematic approach. Ecological education is aimed at combining the rational and the emotional in man's relations with nature on the basis of principles of the good and beauty, reason and consciousness, patriotism and universalism, scientific knowledge and compliance with ecological laws.

Ecological education includes the following components: ecological knowledge - ecological thinking - ecological outlook - ecological ethics - ecological culture.

Each component corresponds to a certain level (degree) of ecological maturity: from elementary ecological knowledge and pre-school concepts to their profound understanding and practical implementation at higher levels. In abstract terms, the following generalized levels of ecological maturity can be singled out: initial (informative-preparatory), basic (basic-ideological), high, profile-professional (worldview-mature).

Software Systems for Studying and Modeling the Operation of Electronic Circuit Components and Boards

Kivgilo V.[1], Semikina T.V.[1,2]

[1]*National Technical University of Ukraine named I. Sikorsky "KPI",Kyiv, Ukraine,*
kivgilov1902@gmail.com
[2]*Institute of semiconductor physics named V.Lashkarev NANU, Kyiv, Ukraine,*
tanyasemikina@gmail.com

This paper is devoted to a review of existing software systems that can be used in the courses "Solid State Electronics", "Semiconductor Electronics", "Modeling Electronic Devices and Circuits", "Analog Circuit Engineering", etc. The following software packages are considered: "OrCAD, Altium Designer, Sprint - Layout, LTspice, Proteus, NI Multisim".

Using these programs allows to create circuit diagrams, printed circuit boards, and simulate the work of the assembled devices. Modeling in these programs is due to the libraries embedded in them. Libraries are based on mathematical models of various components (resistors, diodes, transistors, etc.). Programs calculate the physical quantities of the components of electronic circuits when specifying their parameters (for example, resistance, voltage, etc.). For example, the LTspice complex (also known as SwitcherCAD) is a universal environment for designing and creating electrical circuits with an integrated simulator of mixed simulation. LTspice is one of the simplest and multi-operation programs, which allows you to study the different characteristics of transistors diodes and other components and circuits built on them. The main advantages of the complex are the simplicity of the interface, a large list of electronic components. The program allows to quickly change the components and parameters of electronic circuits, test the performance of new options, find the best solutions.

The paper will present the main characteristics of the complexes, their differences from each other, advantages and disadvantages from the point of view of application in the educational process.

Application of the Project Method in the Educational Process of the Modern School

Shkurenko Olexandra

Kyiv Boris Hrinchenko University, Kyiv, Ukraine, aleksandritta7@gmail.com

The educational project is one of the personality-oriented technologies, a method of organizing students' independent activity, which is aimed at addressing the problem of an educational project, which integrates a problem approach, group methods, reflection, research, search and other techniques [6, P. 102].

During the Project term, the students' autonomy, active stance, initiative and enthusiasm are of paramount importance. Projects can be personal, group or collective.

The purpose of educational design is to enable the teacher to create such conditions during the educational process under which its result is personal experience of the student's project activities.

The ability to use the project technology is indicative of the teacher's high professional skill, his/ her innovative thinking, orientation towards the personal and professional development of the child in the learning process.

As a result of the project, we will obtain both the external result that can be seen, interpreted, applied in practice (presentations, posters, textbooks, memos, etc.) and the internal result, that is, experience including knowledge, skills, competences and values.

The systematic introduction of the project technology at school level (from the elementary level) leads students to gradually mathe ability to study independently, to think critically, but also as a method of organizing and planning his/her subsequent life. This helps train young people who are guided by democratic values in their activities, are inclined to engage in lifelong learning, can compete in the European and world educational space and labor market.

Project activity is a rather promising component of the educational process, as it creates proper conditions for students' creative self-development and self-realization, forms all necessary vital competencies, which at the Council of Europe were defined as the main ones in the XXI century, such as multicultural, linguistic, informational, political and social ones. Independent acquisition and systematization of knowledge, the ability to navigate the information space, to see the problem and make a decision have been made possible as a result of the application of the project method.

Using the project method allows students to acquire communication, theoretical and practical skills and to get an idea of different views of the problem. In so doing students learn how to use research methods to obtain information and to work on their own and in groups, to listen to the opinions of others and to develop productive way of thinking.

1. Pedagogical Technologies in Continuing Education / Edited by S.O.Sysoyeva - K., 2001. - 244 pp.

Possibilities of Mobile Technologies as a Means of Preparing Future Teachers

Stetsyk Sergii

M.P. Dragomanov National Pedagogical University, Kyiv, Ukraine, kmf_npu@ukr.net

The problem of training a teacher who is able to organize a successful student academic activity, the resulting in good knowledge of the subject is a the matter of the utmost urgency. Correctly oriented learning technologies are designed to help resolve this problem. One such technology is electronic learning based on mobile communications.

Platforms that implement mobile learning make it possible to centrally store and distribute access to learning material, include distance and mobile learning support systems and provide support for classroom learning (a mixed learning model).

G Suite is the basic platform for mixed and inverted learning that brings links to other online resources. Google Classroom is the open-access mixed-learning platform developed by Google for schools to simplify the creation, distribution and evaluation of tasks without the use of paper [1]. The platform connects to other G applications such as G. Documents, G. Tables, G. Presentations, G. Disk, G. Mail, G. Forms, G. Calendar, etc. and helps create and organize tasks, give grades, comment and organize effective communication with students in real time.

The platform's functionality is intuitive. The student has access only to their tasks, and the teacher sees the tasks of each student and can evaluate the work done, write comments and criticisms, or return a task for refinement. The service makes it possible to individualize the educational process by simplifying work while increasing the number of individual and group methods and forms of study.

One of the advantages of the technology is the use of mobile devices, which allows for organizing mobile learning. According to the face-to-face driver model, the proposed platform can be used as follows: classes are conducted in the classroom, and the classroom platform serves as an auxiliary tool that complements reality.

Using Classroom allows you to intensify the work of students who study on an individual schedule and is an effective tool for organizing and reporting of student independent work, allows one to abandon traditional lectures in favour of more effective learning. Combined learning allows students to develop students' professional competences and critical thinking skills.

1. Wikipedia - a free encyclopedia [Electronic resource]. - Access mode: https://en.wikipedia.org/wiki/Google_Classroom

The Role of Professionally-Oriented Disciplines in the Training of a Phtsics Teacher

Syrotyuk Volodymyr

M.P. Dragomanov National Pedagogical University, Kyiv, Ukraine, kmf_npu@ukr.net

An important reflection of the requirements of modern social globalization processes for the field of training specialists is the unification of educational systems and standards of education within, which leads to a mutual understanding and simplification of schemes of inclusion of persons in training and production both within the state borders and in international cooperation.

Since today the levels of the basic and complete higher education give educational qualifications, a professionally-oriented cycle of subjects must be present at each of these levels.

Joint professionally-oriented disciplines should be considered as special sections of fundamental disciplines (for example, natural sciences), although they have long been awarded the status of individual disciplines. However, their role in training specialists in the field of "Physics" is fundamental because these disciplines provide the immediate basis for studying professional disciplines both at the basic level and at the level of complete higher education. It is these disciplines that play an integrating role for the specialties that are part of a specific field of specialist training.

While at a higher educational institution, the future teacher of physics should deepen the knowledge and skills that they will need in their field of activity, mainly in the professional environment. In addition, they needs to develop their cultural level by studying philosophy, political science, economics, pedagogy, collective psychology, the foundations of management and to obtain profound legal knowledge. At the same time, at the higher educational and professional level (master's level) training in this area should become increasingly specialized.

Therefore, at M.P. Dragomanov National Pedagogical University the Faculty of Physics and Mathematics for Masters and the FKFn (1 year and 9 months of study) teach the discipline "Modern models of educational processes", which includes the following issues:

1. Modern problems of secondary education in Ukraine 2. Modern models of training organization. 3. Reforms in the education of Ukraine. 4. Impact of modern technologies on education (positive and negative). 5. Mankind's education needs in the future. 6. Disadvantages and advantages of online education. 7. Development of natural sciences at high school. 8. Teacher's overtime and extracurricular work. 9. Educational aspects in the teacher's work. 10. What should the school of the future look like?

It should be noted that society and the state require that after graduating from a pedagogical university the future teacher of physics to perform relevant professional tasks. Therefore, a higher educational institution should adjust a specialist's general cultural level to the requirements of society, who should be a leader in their professional environment today and in the future; to ensure the level of fundamental training of the future physics teacher to enable them to develop professionally in the process of professional activity, professional advanced training and lifelong re-training.

The Role of Psychological Science in the Formation of the Correct Perception of the Concepts of 'Radioactivity', 'Atomic Energy' or 'Radiochemistry'

[1]Tafiy D.P., [2]Vasylyev O.V., [3]Vasylyeva H.V.

[1]Uzhgorod National University, Chair of Psyhology, Ukraine, d.anielatafiy123@gmail.ru
[2]Uzhgorod National University, SEIT, Ukraine, nucleargoga@jmail.com
[3]Uzhgorod National University, Chair of theoretical physics, Department of physic of high energies, Uzhgorod, Ukraine, h.v.vasylyeva@hotmail.com

The variety of phobias, which arise due to insufficient information, formed in human minds. Fear of radiation can serve as a good example of such phenomena. Therefore, we face an important task that can be considered as the basis for the prevention of this fear.

The purpose of our work is to determine the role of psychological science in the formation of the correct perception of the concepts of 'radioactivity', 'atomic energy' or 'radiochemistry'. Another important task for us is to highlight and bring clarity to the problem of gender inequality during work in harmful conditions.

It is necessary, at least, to explain, what constitutes a terrible concept of 'radiation'. There are a few facts about radiation:

1. When humanity arose, the overall radioactive background was much higher.

2. An air travel between New York and Tokyo gives radiation dose equal eight Chest X-ray examination (50 μ Sv/each time or 400 μ Sv).

The same dose (50 μ Sv/per year) is standard dose of radiation around a nuclear power plant, which is working on light water reactor.

3. Chest CT scanning give 6900 50 μ Sv/each time [1].

Nobody is struggling against air transport or modern medical diagnostics.

4. However, in 1886 the nuclear magnetic resonance tomography was renamed in Magnetic resonance tomography due to fear of a word "nuclear", although this type of diagnosis has nothing to do with nuclear physic [1].

One of the tasks of psychology is the use of knowledge to improve the efficiency of various fields of practice. In order to reduce fear and increase the motivation of people working in the field of radioactivity, it is extremely necessary to provide a help of a practical psychologist. According to the point of practical psychology, working in dangerous conditions should be based on mutual respect, mutual assistance and strict fulfillment of their duty. Social and gender studies suggest that in this case gender inequality is not injustice. This is a necessity, which is in large measure provides the future of whole humanity. Therefore, the role of psychological science in the formation of the correct perception of the concepts of 'radioactivity', 'atomic energy' or 'radiochemistry' is indisputable.

1. William R. Hendee, E. Russel Ritenour "Medical Imaging Physics" 4th etdition / *A John Wiley &Sons inc. publication, New York*, 2002, 353p p.45-61

The Development of Children's Enthusiasm for Electronics by Applying Nanomaterials for Drones

Tkachuk R.Z.

Vasyl Stefanyk Precarpathian University, Ivano-Frankivsk, Ukraine, romvirtu@gmail.com

This article applies to the aircraft – a robotized quadcopter RS-17, which belongs to the class of professional prospecting and exploration devices. Such quadcopters are manufactured in Ukraine for the first time for the civilian needs of the rescue and medical service and for equipping the various types of troops of the Armed Forces. The aircraft will be useful for securing the safety of large warehouses, border guarding, monitoring of electrical grids, gas and oil pipelines, railways, forest plantations, for solving agrarian problems, for geodesy and high-rise construction. Due to his own imperceptibility, he is indispensable for journalistic needs.

The RS-17 device has a guaranteed range of 8.8 km and a duration of 38 minutes. The kit is equipped with a big 15'' display, making it easy to notice the small details of the surroundings. Important advantages over available on sale are the possibility of flights at temperatures from -20 ° C to +40 ° C and the presence of a night camera for observations in the dark. A high-performance image stabilization device and 10x optical zoom with 360 degree panoramic camera rotation considerably extend the viewing capability. The increased strength of the body thanks to the use of any nanomaterials such as carbon and kevlar to withstand shocks and vibrations. The cushioning chassis makes the landing soft. The on-board electromagnetic protection allows you to fly in conditions of significant radio interference. The device has successfully passed state tests and has a certificate of conformity[1]. Flights are carried out manually or according to a pre-programmed route map. RS-17 device was tested in August 2017, when it was found in a 15-minute breakdown of the Robinson R-22 business propeller in the Carpathians.

The complete set of the device includes an aircraft with batteries, four transmitting antennae, a ground station or a control panel and a monitor with video and telemetry receivers. The aircraft, ground station, remote control and monitor are powered by separate batteries.

We hope that the knowledge by application any materials such as karbon and kevlar in drones will be interesting for children and associated with learning a law of physic .

Reference

1. Certificate of type examination, registered at the Record of conformity assessment body under № UA1.TR.008000068-18, which is loaded at www.standart-service.com.ua.

The Development of Critical Thinking of Students at the Physics Lessons

Voitkiv H.V., Lishchynskyy I.M.

[1]*Vasyl Stefanyk Precarpathian University, Ivano-Frankivsk, Ukraine, h.voitkiv@gmail.com*

Critical thinking is a necessary skill of a modern person. In scientific literature, critical thinking is seen as the practical application of a scientific approach to solving life, professional and personal problems. Critical thinking is higher than science thinking. Critical thinking contributes to the formation of the ability of a person to realize his own position on a particular issue.

We represent critical thinking through **content** (this is a collection of information that children have acquired and which has become knowledge) and **instrumental** (the operations of analysis, synthesis, comparison, classification, compilation, systematization, which allow us to handle our perception, to transform it into knowledge, and also apply our knowledge in practice) components (fig.1).

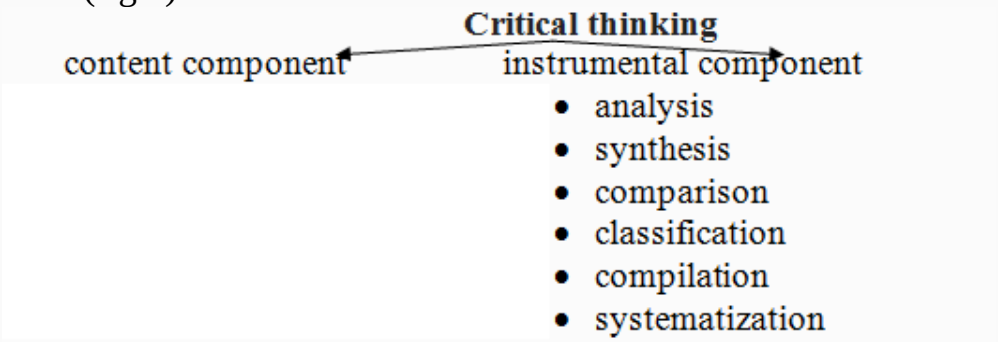

Fig.1. The strukture of critical thinking.

It is necessary to develop two components for the formation of critical thinking: **content** component – subject knowledge and **instrumental** – algorithms of action in one or another situation. Physics as a subject of study has great potential for the development of critical thinking. Material for the development of critical thinking is an active component of the content of physics education (demonstrations, laboratory works, projects), which allows training the instrumental component, that is, it teaches you to analyze, synthesize, compare, abstract, classify, synthesize and draw conclusions.

Some methodological techniques for the development of critical thinking are an algorithm for describing the phenomenon, problematic issues during demonstrations, etc. When working with the texts of the paragraphs we recommend using the methodological methods: "**Telegram of the text**", which helps to briefly pass the text of the paragraph; "**Reading in pairs**", which promotes the formation of skills for conducting an effective dialogue, tolerant advocacy of their own position; "**Reading with the marking of the text**", which allows to significantly increase the perception of information and improve its efficiency.

POSTER REPORTS
Session 1
Thin films technology (metals, semiconductors, dielectrics, conductive polymers) and their research methods

Electrodynamics of Metal-dielectric Layers

Barabash M.Yu., Vlaykov G.G., Litvin R.V., Martynchuk V.E.,
Kolesnichenko A.A., Rybov L.V.

Technical Centre NAS of Ukraine, Kiev, Ukraine 13, Pokrovskaya str., 04070
mbarabash@nasu.kiev.ua

Two-dimensional arrays (2D) of island-type gold nanoparticles located quasi-inhomogeneously on the surface of an ordered amorphous molecular semiconductor (AMS) are investigated. An ordered dielectric medium is a composite based on polyepoxypropylcarbazole (PEPC) with refractive index 1.55 and thickness 0.8-1.0 μm. The film surface was deformed in the electrographic process with the creation of an interferential pattern in multiple-beam holography. The spatial period was 500-1000 ln/mm. Gold nanoparticles were deposited by thermal spraying in vacuum on a modernized VUP-5M machine with layer thickness of 0.02-0.12 microns. The deposited gold nanoparticles layer has an island-type shape with a regular period that corresponds to the deformation period of the dielectric layer. The electrical conductivity of gold layers at a constant current was absent, which indicates that the concentration of metal nanoparticles is lower than the percolation threshold (p_c) (120 nm is close to the percolation threshold). This is a prerequisite for obtaining the unique optical properties in the visible and near infrared (IR) spectral regions due to the excitation of surface plasmon modes. A significant enhancement of electromagnetic fields (EF) is achieved in a wide spectral range for disordered metal-dielectric composites, and also at selected frequencies for periodic ordered nanostructures. At metal concentration below p_c, the composite is an insulator, but the presence of large metal clusters makes it possible to concentrate electromagnetic energy. The transition from the metallic state of the composite to the insulator state is a phase transition. Near p_c, an electric current flows through a random grid of conducting channels that permeate the entire system. The size of metal clusters increases while the concentration approaching to p_c from below. When the metal concentration decreases down to the percolation threshold, the percolation length increases, the macrogrid of the percolation channels becomes more rarefied, and the conductivity disappears. As a result, the effective dielectric constant ε diverges as p_c approaches from above and below. This state of the composite dielectric constant is determined by the existence of a multitude of conducting metallic clusters that stretch across the entire system. Each channel contributes to an abnormally high capacity, and all channels are connected in parallel. The size of the largest cluster is determined by the correlation length of the composite. The capacity C between clusters also increases with increasing of correlation length. This shows that high nonlinearity occurs in the response of a dielectric when the dielectric constant is high due to strong fields in thin dielectric barriers. Also, quantum mechanical tunneling through the barrier plays an important role near p_c [1]. In

such systems fluctuations of local electric fields can reach high values [2]. The spectral characteristics of such composites in the visible range of 400–900 nm are studied. The focus was on the absorption coefficient because the accumulation of electromagnetic energy (EM), which determines the existence of local EFs, depends on its magnitude. It was found that the absorption is maximal for gold film thicknesses of ~0.08 μm; for thinner and thicker films the absorption decreases. Large fluctuations of the local field exist near the percolation threshold.

1. Сарычев А.К., Шалаев В.М. Электродинамика метаматериалов / Пер. с англ. В.Г. Аракчеева, Ю.В. Владимировой. – М.: Научный мир, 2011. – 224 с.
2. S. Gresillon, L. Aigouy, A.C. Boccara, J.C. Rivoal, X. Quelin, X. Desmarest, P. Gadenne, V.A. Shubin, A.K. Sarychev, and V.M. Shalaev. *Phys.Rev.Lett.*, 82:4520, 1999.

Identification of Optical Resonances in Amorphous Carbon Films on a Glass Substrate

Barabash M.Yu., Vlaykov G.G., Litvin R.V., Kolesnichenko A.A., Martynchuk V.E., Ryabov L.V.

Technical Centre NAS of Ukraine, Kyiv, Ukraine, mbarabash@nasu.kiev.ua

The purpose of work is to study the amplification effect of combination scattering (CS) spectrum. The thermal spraying of amorphous carbon thin films at a glass substrate was carried out, followed by the depositing of ferro-metal-phthalocyanine (FePc) thin layer. The obtained metal films were used for improving the technique of surface-enhanced Raman spectroscopy (SERS). However, the mechanisms of the combination scattering signal amplification are not fully understood. Giant combination scattering occurs through molecules adsorption on an uneven metal surface, or plasmon nanostructures, and that allow the detection of single molecules presence.

There are two basic mechanisms that allow obtaining giant combinational scattering: an increase in the intensity of local electromagnetic fields around metal structures (electromagnetic mechanism), and the interaction between the sample and the substrate with the charge transfer between them. The second mechanism is usually difficult to detect and use, since it causes less impact than the electromagnetic mechanism, which allows to obtain a "pure" signal of combination scattering of the analyzed substance. The combination of such metal films with thin films of amorphous carbon (d <100 nm), which amplify the CS by the help of the second mechanism (phase with sp^2-hybridization) and have CS spectrum with wide peaks, can significantly enhance the CS spectrum and simultaneously increase the signal-to-noise ratio of the analyzed substance.

The research was carried out on ferro-phthalocyanine molecules (FePc), used as a "probe". Thin films of ferro-phthalocyanine have a complex absorption spectrum, which is characterized by surface plasmon resonance absorption in the spectral range from 300 to 700 nm (Fig. 1). The phthalocyanine films deposited on the carbon film surface strongly scatter the combinational radiation and have low background photoluminescence.

Three systems were studied: at first case thin films of (FePc) were deposited on glass substrates, at others thin films of copper, amorphous carbon and (FePc) were deposited in sequence on the substrates. CS signals of these three systems were compared with each other.

The technology of obtaining plasmon nanomaterial on the basis of amorphous carbon thin films with a layer of metal-phthalocyanine FePs as a probe of optical resonances is developed in this work. Changing the concentration of nanoclusters by using different conditions for the formation of amorphous carbon films leads to structural-phase transformations in these films and to a significant change in their physical properties. However, the conditions of native and metallic

nanoclusters formation in amorphous materials and their influence on the electronic properties of these materials are almost not studied.

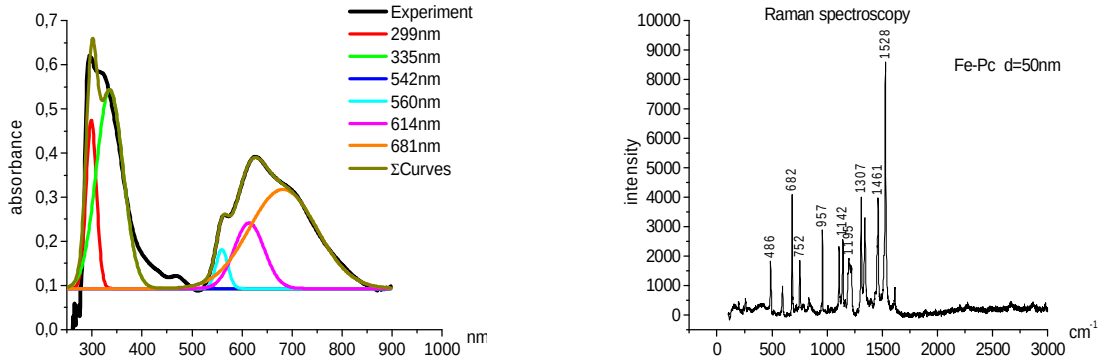

a *b*

Fig. 1. Optical spectrum of phthalocyanine (FePc) film on glass substrate: *a* – typical absorption spectrum of FePc film is shown. It is decomposed by "Origin" program to 6 bands that are typical for the system of π-connected bonds in the phthalocyanine molecule; *b* – typical combination scattering spectrum of FePc film. Spectrum characterizes the process of spraying phthalocyanine film.

In this regard, the development of nanomaterials with new properties on the basis of amorphous carbon media with varying the concentration of native and metallic nanoclusters and the study of their influence on the atomic structure and electronic properties are currently one of the most relevant and extremely important areas of research in the field of nanomaterials and nanotechnology. It is shown that the CS spectrum of carbon materials depends on the clusterization degree of the sp2 phase, the disorder in sp3 bonds, the presence of sp2 hexagonal rings or chains, and the ratio of sp3 phases. All these structure elements depend on number of competitive processes that determine the type of the spectrum of light combinational scattering.

The Influence of Receiving Conditions on the Structure and Morphology of the Surface of Thin Films b-Ga_2O_3 and $(Y_{0.06}Ga_{0.94})_2O_3$

Bordun O.M., Bordun B.O., Kukharskyy I.Yo., Medvid I.I.

Ivan Franko National University of L'viv,Ukraine,, Lviv, bordun@electronics.lnu.edu.ua

The thin films based on β-Ga_2O_3 are widely used as thin-film materials for field-effect transistors (FET), gas sensors and electrodes, which transparent in the UV region.

The thin films of β-Ga_2O_3 and $(Y_{0.06}Ga_{0.94})_2O_3$ were obtained by radio-frequency ion-plasmous sputtering. The thickness of thin films ranged between 0.2 μm and 1.0 μm. The heat treatment of thin films was performed after deposition in oxygen atmosphere or in argon atmosphere as well as in hydrogen atmosphere. The X-ray diffraction studies showed the presence of the polycrystalline structure of thin films that preferentially oriented in the planes (400), (002), (111) and (512). The investigation of surface morphology of thin films by the atomic-force microscopy showed that the least diameter of the grains on the surface of thin $(Y_{0.06}Ga_{0.94})_2O_3$ films without heat treatment is average equal to 16 nm and the average roughness of thin films is about 2 nm. The treatment of thin films of $(Y_{0.06}Ga_{0.94})_2O_3$ in argon atmosphere leads to the increase size of grains through the processes of growth and sintering, thus, the average diameter of grains is increased to 110 nm and the average roughness of thin films is about 12 nm.

Average grain diameters and surface roughness of thin films b–Ga_2O_3 and $(Y_{0.06}Ga_{0.94})_2O_3$

Films	Atmosphere of Heat Treatment	Average Grain Diameters D, nm	Surface Roughness of Films Z, nm
β–Ga_2O_3	without heat treatment	30	7
$(Y_{0.06}Ga_{0.94})_2O_3$	without heat treatment	16	2
β–Ga_2O_3	oxygen	45	15
$(Y_{0.06}Ga_{0.94})_2O_3$	oxygen	55	16
$(Y_{0.06}Ga_{0.94})_2O_3$	argon	110	12
$(Y_{0.06}Ga_{0.94})_2O_3$	hydrogen	75	7

The processes of sintering and growth of crystallites more considerably take placed in films $(Y_{0.06}Ga_{0.94})_2O_3$, regarding of films β-Ga_2O_3 was showed.

Development of Method of Layers Removing from the CdTe and $Zn_xCd_{1-x}Te$ Surfaces by the $K_2Cr_2O_7$ – HBr – Lactic Acid Etchants

Chayka M.V.[1,2], Tomashyk Z.F.[2], Tomashyk V.M.[2], Denysyuk R.O.[1], Malanych G.P.[2]

[1]*Zhytomyr Ivan Franko State University, Zhytomyr, Ukraine, laridae92@gmail.com*
[2]*V.E. Lashkaryov Institute for Semiconductor Physics NAS of Ukraine, Kyiv, Ukraine*

The purpose of this work is to develop the method of layers removing from the CdTe and $Zn_xCd_{1-x}Te$ surfaces by the $K_2Cr_2O_7$ – HBr – lactic acid (LA) etchants. Single crystals of CdTe and $Zn_{0,1}Cd_{0,9}Te$, which have been grown by Bridgman method, and $Zn_{0,04}Cd_{0,96}Te$ obtained from the gas phase were used for experiments. Preliminary surface treatment of semiconductors consisted of the following steps: ***grinding of the plates*** by abrasive powders M10-M1 (3-5 min) → ***mechanical polishing*** with diamond paste (3-5 min) → ***chemical etching to remove the damaged layer*** (80-100 μm) by the HNO_3 – HBr – $C_4H_6O_6$ etchants compositions → ***finishing chemical-dynamic polishing*** (CDP) by new slow etchants ($\mathbf{v_{pol}}$ = 0,1-3,8 μm/min).

Finishing step is the process of CDP using the method of disc rotating at T = 284 K and disk rotation speed $\gamma = 82$ min^{-1}. The etchants were prepared using 40 % HBr, 10,9 % $K_2Cr_2O_7$ and 80 % LA. A certain amount of viscosity modifier – LA ($C_3H_6O_3$) was added to the etchants for obtaining low rate of CDP of CdTe and $Zn_xCd_{1-x}Te$ supporting a polishing effect. This can partially regulate the interaction of HBr and $K_2Cr_2O_7$ with evolving of Br_2 and promotes the better dissolution of interaction products of etchant with crystals.

The dependence of the CDP rates of the CdTe and $Zn_xCd_{1-x}Te$ versus solutions concentration, mixing, temperature, nature of material has been established. As the Zn content in the $Zn_xCd_{1-x}Te$ solid solution increases, $\mathbf{v_{pol}}$ increases and the surface polishing quality improves. It is recommended to remove the layers from the surface with polishing using next solutions (vol. %):
CdTe – (20-46) $K_2Cr_2O_7$: (20-46) HBr : (7-60) LA; ($\mathbf{v_{pol}}$ =0,1-3 μm/min);
$Zn_{0,04}Cd_{0,96}Te$ – (20-24) $K_2Cr_2O_7$: (20-80) HBr : (0-60) LA; ($\mathbf{v_{pol}}$ =0,2-3,5 μm/min);
$Zn_{0,1}Cd_{0,9}Te$ – (20-39) $K_2Cr_2O_7$: (20-54) HBr : (22-60) LA; ($\mathbf{v_{pol}}$ =0,1-3,8 μm/min).

After CDP, the samples must be washed by the next technological scheme: ***30 s 0,1 M $Na_2S_2O_3$ + 1 min H_2O + 2 min H_2O + 1 min H_2O*** (at T = 294 K). Plates can be stored in DMF for several weeks. The results of metallographic and profilometric analysis of surfaces after finishing CDP showed that etched semiconductor surfaces are characterized by high quality ($\boldsymbol{R_z}$ <0,05 μm) and good luster. Optimized composition and technological modes of surface treatment can be used for controlled removal of layers, chemical treatment of films and finish polishing of the surface of CdTe and $Zn_xCd_{1-x}Te$.

Synthesis and Morphology of Films Incorporated by luminescent Ortovannadate Nanoparticles

Chukova O.V.[1], Kondratenko S.V.[1], Naumenko S.M.[1], Nedilko S.A.[1], Nedilko S.G.[1], Revo S.L.[1], Sheludko V.I.[2], Slipets A.A.[1], Voitenko T.A.[1]

[1] *Taras Shevchenko National University of Kyiv, Kyiv, Ukraine*
[2] *O. Dovzhenko Hlukhiv National Pedagogical University, Hlukhiv Sumy region, Ukraine,*
chukova@univ.kiev.ua

Composite thin films with oxide nanoparticles have recently attracted increased scientific interest in connection with their applications for optical materials science needs, in particular, these materials are now being developed to adapt incident sunlight to the spectral sensitivity of silicon solar cells and to convert the violet and blue colors of radiation of light emitting diodes in white light. During the last decade, many efforts have been made to synthesize and study the nanoparticles of oxides and composites on their basis. Our own studies have also shown that some of developed oxide compositions in the form of micro/nanoparticles are able to demonstrate promising optical and structural characteristics. In particular, we have developed vanadate nanoparticles with enchanced light harvesting from violet spectral range and intensive luminescence emission.

The next important task is to to save the obtained high optical characteristics of oxide nanoparticles under their incorporation into composite film coatings. The purpose of this work is to develop and investigate the model of a composite thin film with luminescent nanoparticles of vanadates of the $La_{1-x-y}Sm_xCa_yVO_4$ composition in different matrices. To obtain films with the necessary characteristics, we have developed various techniques for applying model films, and then the dependencies of the properties of the obtained samples on composition of the films and on conditions for their application are investigated. In this paper, the films were obtained in two different ways, namely, spin coating or chemical evaporation. As substrates, duplicate polished n-type Si (100) plates with a specific impedance of 4.5 Ω·cm and 500 μm thickness were used.

Morphology of the films was studied using optical, atomic force and scanning electron microscopy. It was shown that films obtained from the same compositions but under different procedures have different morphology. Influence of procedure type on structure and luminescence characteristics of films is discussed.

Effect of the Modified Silica on the Conductivity and Sensory Properties of Polyaniline Nanocomposites

Dzeryn M.R.[1], Tsizh B.R.[1,2], Horbenko Yu.Yu.[3], Aksimentyeva O.I.[3], Olenych I.B.[3], Bogatyrev V. M.[4]

[1]*Stepan Gzytsky Lviv National University of Veterinary Medicine and Biotechnologies,Lviv, Ukraine, marjawka232@ukr.net;*
[2]*Kazimierz Wielki University in Bydgoszcz, Bydgoszcz, 85-064, Poland*
[3]*Ivan Franko National University of Lviv, Lviv, Ukraine*
[4]*O. O. Chuiko Institute of Surface Chemistry NAS of Ukraine, Kyiv, Ukraine*

Semiconductor polymers with a system of conjugated electronic bonds are promising materials for electronic technology, since they exhibit interesting optical properties, the ability to convert light energy, have sensitivity to chemical and physical influences. The introduction of nanosized fillers into composites with conductive polymers allows them to control the characteristics of these polymers. Silica nanobeads – excellent platform for development of smart sensing systems for numerous applications in analytical chemistry, medical diagnostics and therapy, environmental and food analysis, security due to its unique set of remarkable properties, which include large ratio of surface area to volume, excellent chemical stability, low cost of synthesis, and low toxicity, especially convenient surface modification.

The choice of gases for studying the sensory properties of hybrid structures is caused by the importance of their control in the atmosphere of residential, office and industrial premises, food quality. As one of the main sources of air pollution, ammonia is released due to the decomposition of organic nitrogen-containing materials of animal and vegetable origin, from industrial effluents and motor vehicles. Due to the toxic properties of HCl in both gaseous and solution forms, there is a great need to detect and establish the concentration of particles. Currently available detection methods are long-lasting, complex and expensive, operate at high temperatures.

So, in this work, samples of nanostructured composites based on polyaniline with nanoparticles of silica modified by titanium and phosphorus compounds have been obtained both by the method of polymerization filling and electrochemical deposition on the optical transparent substrates. The influence of the content of organic-inorganic composites and the action of moisture on their specific conductivity, activation conductivity parameters for testing materials as possible stabilizers of polymer matrices used in resistive or optical gas sensors in real conditions of operation, that is, in an atmosphere with natural humidity have been shown.

Reconstruction of the Real Magnetic Structure by Simulations and Artificial Neural Network Processing of Multi-Pass Magnetic Force Microscopy Data

Efremov A.A., Lytvyn P.M., Prokopenko I.V.

V.E. Lashkaryov Institute of Semiconductor Physics NAS of Ukraine, Kyiv, Ukraine, plyt@isp.kiev.ua

The quantitative analysis of magnetic force microscopy (MFM) data is encountered with a number of intrinsic problems caused by the peculiarities of the method itself. It is known that profile (or map) of a force gradient measured at the surface scanning by a magnetic tip cannot provide distribution of a real magnetization of bulk or/and under-surface layer of a sample. MFM records some spatial characteristics of magnetic stray field over its surface only. For this reason, to perform quantitative measurements an additional a priori information is necessary about possible magnetic structure, properties of MFM tip and so on.

It would allow us to narrow the range of possible physical models suitable for the estimation of magnetic properties of a nanostructure and would make easier the individual nano-objects recognition. One of the ways to obtain such specifying information could be the multi-pass MFM diagnostics at different heights above the surface followed by an appropriate modeling. We have shown that different types of magnetic nano-objects, including those that have internal subdomains, demonstrate their own specific magnetic image transformation with the lift-height variation.

This feature was confirmed by a modeling with our original magnetic force microscope simulator. It allows us to calculate magnetic forces and their gradients during the interaction between a magnetic tip and a modeled sample. Two- and three-dimensional magnetic force images are generated here for an arbitrary magnetic structure with predetermined parameters. We also used these images for training of special neural networks (created both in MATLAB and C # in MS Visual Studio) for express analysis of the real MFM data.

In this case, the auxiliary neural network classifies magnetic objects according to their orientation along the surface. The main network with a good accuracy determines the desired value of their magnetization and individual geometrical dimensions of domains.

Some prospects for the multi-pass MFM application in quantitative and qualitative analysis of magnetic nanostructures as well as the tandem use of artificial intelligence approaches and usual equation-based computer simulations are further discussed in the report. The set of experimental MFM data is analyzed by the modeling and the neural networks processing.

Poling of Side-Chain Non-Linear Optical Thin Polymer Films During Their Solidification

Fedosov S.N.[1], Carr P.[2], Sergeeva A.E.[1]

[1]*Odessa National Academy of Food Technologies, Odessa, Ukraine, snfedosov@ukr.net*
[2]*University of Leeds, Leeds, UK*

Due to potential applications in telecommunication and photonic nano-micro devices, non-linear optical (NLO) polymers attracted growing interest of researchers during the past years. In order to activate the performance of a side-chain NLO polymer, it must be poled, i.e. subjected to a high DC field at the temperature exceeding the glass transition temperature T_g of the host polymer. However, some polymers start to decompose even before their T_g is reached. Thus, this phenomenon should be considered for selecting a poling procedure.

We developed a novel method for poling NLO polymers at temperatures much lower than their T_g in the solid state. High mobility of polymer matrix and chains necessary for alignment of dipoles was provided by the artificial lowering of the T_g. The samples were poled in a corona discharge while they were still in a viscous state, or even during their spinning from the corresponding solution. Thus, the solidification occurs in the electric field created by corona ions adsorbed on the surface of the forming film.

The method was tested at the copolymer of methylmetacrilate and 4-(methacryloyloxypropoxy)-4'-nitrostilbene having T_g about 70°C in the solid state. Cyclopentanone was used as a solvent. We modified a photoresist spin coater for our experiments by insulating the chuck, connecting the electrometer for measuring poling current, and placing a specially designed corona triode over the spin coater. Microscopic glass slides with evaporated Al electrodes were used as substrates. Films of the NLO polymer of about 20 μm thickness were spinned from the solution. Kinetics of the solidification at room temperature was measured by monitoring the electric conductivity and the weight of the samples. After the initial sharp decrease of both parameters due to evaporation of the solvent, the steady-state condition of the solidification has been reached in about 1 h. During all this time, a negative corona was applied. In some samples we observed remarkable decrease of the poling current in 50-60 min indicating probably that poling is completed. Quasi-static measurements of the pyroelectric coefficient and the thermally stimulated depolarization (TSD) current were performed in order to evaluate the poling efficiency.

It has been found that the position of the T_g peak at the TSD current curve depended on the storage time of the poled samples, gradually increasing from 54 to 68°C. Relatively high values of the pyrocoefficient of about 2 C/m^2K were observed clearly indicating that the side-chain dipoles were properly aligned. The method can be recommended for poling other NLO polymers with high T_g.

Dielectric Relaxation in Polystyrene Thin Films Doped with DR1 Guest Molecules

Fedosov S.N.[1], Giacometti J.A.[2], and Sergeeva A. E.[1]

[1]*Odessa National Academy of Food Technologies, Odessa, Ukraine, snfedosov@ukr.net*
[2]*Instituto de Física de São Carlos, Universidade de São Paulo, Brazil*

The information on the chromophore dynamic and stability of the poled order in nonlinear optical polymers can be obtained by studying dielectric relaxation processes. In this work, the dielectric properties of the guest-host PS/DR1 system has been studied by the AC dielectric spectroscopy method at frequencies from 1 Hz to 0.5 MHz and by the thermally stimulated depolarization (TSD) current method in the range from -160 to 0^{o}C.

There were four peaks on TSD curves at -15, -30, -61 and -129 ^{o}C. The peak at the lowest temperature was attributed to the γ-relaxation, while the peak at -15 ^{o}C was probably caused by the space charge accumulated due to interfacial and/or electrode processes. The origin of other two peaks was not clear, but they were probably related to β-processes. Real and imaginary parts of the dielectric constant ε in the frequency domain have been measured at constant temperatures from 30 to 130 ^{o}C. The α-relaxation was seen as well defined loss peaks at T higher than glass transition temperature T_g. Increase of the ε with decreasing frequency at sub-T_g temperatures can be attributed either to the conductivity effect, or be considered as the high frequency part of the α-peaks positioned out of the employed frequency range.

The empirical Havriliak-Negami's model has been applied for fitting the experimental data. It has been found that the experimental curve approached the Debye curve (with increase of temperature) only from the low frequency side. The dielectric strength in doped PS appeared to be much higher than that in pure polymer indicating that the high dipole moment of the chromophore molecules affects the dielectric constant of the system only at low frequencies.

We performed Hamon's transformation of the isothermal (absorption) currents at different temperatures from 20 to 125 ^{o}C in order to obtain the frequency dependence of the dielectric constant in this range. It has been found that the temperature dependence of the characteristic peak frequencies at sub-T_g temperatures was close to the Arrenius formula with the activation energy of 0.52 eV, while the Williams–Landel–Ferry model was more suitable above T_g.

Our results were in good agreement with the reported data on the same system obtained by the more complicated measurements of the second harmonic generation signal. Thus, the combination of three methods allowed us to study dielectric properties of the system in wide range of temperatures and frequencies.

Electrodeposition of Molybdenum Carbide onto the Surface of Silicon Carbide and Boron Carbide Disperse Materials from Ionic Melts

Gab A.I.[1], Kublanovsky V.S.[2], Pleshkun A.G.[1], Malyshev V.V.[1,2]

[1]*University "Ukraine", Kyiv, Ukraine, lina_gab@ukr.net*
[2]*Institute of General and Inorganic Chemistry, Kyiv, Ukraine, viktor.malyshev.igic@gmail.com*

Electrochemical studies showed that the grains of diamond, boron nitride, and silicon and boron carbides in contact with the melt can be used as a cathode material for the high-temperature electrochemical synthesis (HTES) of molybdenum carbide. To electrochemically coat the semiconductors (SC) grains, they were held in the melts of the following compositions: Na_2WO_4 - 5 mol % of MoO_3-10 mol % of Li_2CO_3 or KCl-NaCl (1:1) -5 mol % of Na_2MoO_4-7.5 mol % of Na_2CO_3 at 1073-1173 K and the cathode current densities 10-100 $A \cdot m^{-2}$. Under such conditions the SC surfaces become conducting and play the role of an active support for the HTES of molybdenum carbide. The obtaining of Mo_2C coating consists of the co-precipitation of molybdenum and carbon with the simultaneous reduction of the molybdate and carbonate ions, which are present in the melts and have close discharge potentials. Superficially the coating presented a light green thin-crystal compact precipitate. Its continuity is pronounced on chips. The intense lines of molybdenum carbide were present in the X-ray diffraction patterns of the surface layer of coated grains. The rate of coating SC grains with Mo_2C substantially depends on both the electrolysis temperature and the cathode current density.

Mo_2C coatings were deposited on the silicon carbide grains with the 400/320 granularity and the boron carbide grains with the 160/125 granularity at 1173 K and cathode current densities 50-200 $A \cdot m^{-2}$ within 15-90 min. We established that the coating degree substantially depends on the cathode current density and the electrolysis duration: the deposition rate increases, as these parameters increase.

The grains of boron and silicon carbides were tested for breaking in accordance with the State Standard 9206-81 on a DA-2 installation. The capillarity characterizing the wettability of abrasives was determined by the lift of water level in glass tubes filled with the starting and coated grains. Upon coating with molybdenum carbide, the coefficient of the breaking load of the grains of boron and silicon carbides was 1.5-2.5; the capillarity of the grains of silicon and boron carbides increased by the factors of 3.4-4.0 and 2.3-2.5, respectively.

Electroplating of the grains of dielectrics and semiconductors with molybdenum carbide favors the increase in their breaking load and wettability and in the efficiency of tools.

Electrooptical Transitions in Thin Films of Conjugated Polymers Doped with Graphene Oxide

Horbenko Yu. Yu., Konopelnyk O. I., Mykhalec A. V., Matkivska H. M.

Ivan Franko National University of Lviv, Lviv, Ukraine, y_bilka@ukr.net

The interest in the research and development of organic macromolecules and polymeric compounds for industrial application has continuously grown in the last years. Conjugated polymers are expected to find widespread application in thin film transistors, displays (OLED), optical shutters (smart windows, mirrors, sunglasses), smart papers, controllable light-reflective or transmissive display devices for optical information and storage [1,2]. The demand for polymer based electrochromic material is increasing due to not only the advantages of conjugated polymers such as high color versatility, large optical contrasts, excellent switching reproducibility, ease of manipulation of its properties through structural modifications, facile preparation and low cost, but also their potential applications in flexible devices [3]. Moreover, many polymers can exhibit more than two red/ox states and generate multiple colour.

Graphene and its derivatives, graphene oxide (GO) and reduced graphene oxide have huge potential for applications owing to their 2D structure, large specific surface area, high electrical and thermal conductivity, optical transparency, and mechanical strength combined with inherent flexibility. In view of these advantages, incorporation of GO in electrochromic polymer matrices can lead to new nanocomposites with enhanced structural and functional properties due to synergistic effects.

So, in this work, the influence of an electric field on optical properties and morphology of poly-*o*-anisidine and poly-3,4-ethylenedioxythiophene thin films obtained on the surface of semi-conducting SnO_2 electrode by the method of electrochemical polymerization and doped with graphene oxide have been studied. Both optical absorption and the color of obtained material can be controlled, that indicates the ability of these films to electrochromic transitions.

1. Abidin T., Zhang Q., Wang K-L., Liaw D-J. Recent advances in electrochromic polymers. *Polymer*. 2014. 55. 5293-5304.
2. Wang H., Barrett M., Duane B., et al. Materials and processing of polymer-based electrochromic devices. *Mater. Sci. Eng. B*. 2018. 228. 167-174.
3. Аксіментьєва О., Конопельник О., Оленич І., Польовий Д., Горбенко Ю., Михалець А. Фізико-хімія електрооптичних явищ у спряжених полімерних системах. // VI Український з'їзд з електрохімії: Збірник наукових праць, Ч. 1. Львів, Україна, 4–7 червня 2018. 112-114.

Photoconductivity Relaxation in the Macroporous Silicon in the Ultraviolet Range of the Optical Spectrum

Karas' M.I., Karachevtseva L.A., Onyshchenko V.F.

Lashkryov Institute of Semiconductor Physics NAS of Ukraine, Kyiv, Ukraine,
nikar@isp.kiev.ua

Porous silicon attracts the attention of researchers in connection with the potential for creating sources of visible radiation, as well as use as photodetectors. Its photoelectric properties are an effective tool for studying electronic processes in the surface layers of semiconductors.

The "slow" relaxation of negative photoconductivity in the structures of macroporous silicon in the ultraviolet wavelength range of 360 - 410 nm was studied. Two relaxation times have been established, arising due to slow surface states localized at the Si / SiO_2 interface and in the SiO_2 dioxide layer, equal to 2 s and 300 s, respectively. The starting material was single crystal n-Si with a resistivity of 4.5 Ohm. Macropores with a depth of 80 μm and a diameter of 4 μm were formed by electrochemical etching in hydrofluoric acid solution. The thickness of the structure of the macroporous silicon was 520 microns.

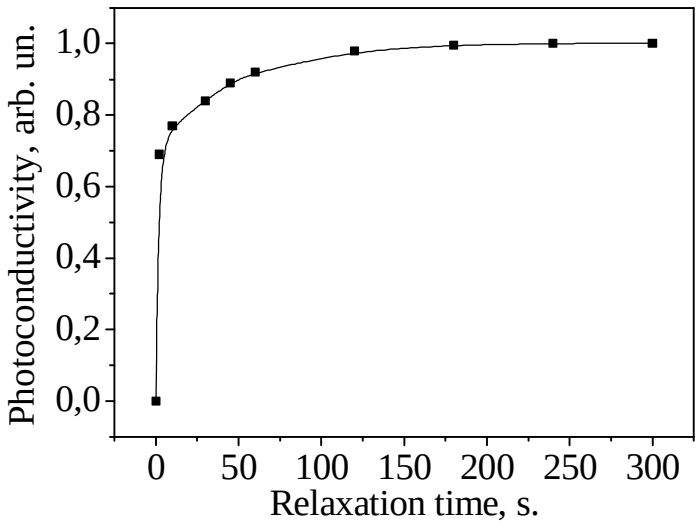

Fig. Dependence of negative photoconductivity on relaxation time

From a comparison of the experimental data obtained with the literature data [1], it follows that the slow relaxation of photoconductivity in the macroporous silicon structures in the ultraviolet range of the optical spectrum is due to "slow"states that are localized in a layer in SiO_2 (relaxation time 300 s) and "slow" states that are localized within 1 nm from the silicon surface (relaxation time 2 s) in the transition SiO_x layer. Approximately 80% of the photoconductivity is due to "slow" states at the Si / SiO_2 interface.

1. Белоус А.И. Космическая электроника. В 2-х книгах. Книга 2, С.724 / Белоус А.И., Солодуха В.А., Шведов С.В.–М.:Техносфера, 2015.–488 с.

The Optical Features of $Zn_{1-x}Mn_xTe$ Thin Film

Klymov O.V.[1], Kurbatov D.I.[1], Kudiy D.A.[2]

[1] *Sumy State University, Sumy, Ukraine, dkurbatov@sumdu.edu.ua*
[2] *National Technical Universit Kharkivsky Polytechnic Institute, Kharkiv, Ukraine, kudiy@ukr.net*

In recent years the interest of scientists in the field of materials science to obtain and research new film materials for optoelectronics, solar power and spintronics has increased significantly. These materials include chalcogenide compound group A_2B_6, and semimagnetic solid solutions based on them, such as $Zn_{1-x}Mn_xTe$ [1]. Features of this material allow to use it as window layers in solar cells. Nevertheless, the optical properties of this compound have not insufficiently studied yet.

Thin films of compounds $Zn_{1-x}Mn_xTe$ were taken by evaporation method in a quasi-closed volume vacuum system VUP-5M [2] on the glass substrates under the following conditions: 1) temperature of the evaporator was T_e = 1073 K; 2) substrate temperature was changed in the range T_s = (623-923) K. Evaporation time was t = 4 minutes. Evaporation of semiconductor purity powder $Zn_{1-x}Mn_xTe$ containing 5% manganese was carried. Those films had a polycrystalline structure stable cubic modification with thickness l ~ (0,85-1,69) mkm. The optical properties were analyzed using a spectrophotometer SF – 2000. Measurement of spectral transmittance was made in a range of filming 190-1100 nm. The spectral range for measuring reflectance was 400-800 nm.

The experiment showed that at wavelengths ranging from 540 nm transmittance is increasing to 47-75%, whereas with increasing substrate temperature its value is falling. The value of the absorption coefficient does not exceed 0.2%. In this case, observed an increase in the parameter of coefficient with increasing temperature. Band gap of the material was calculated, it was about 2,24 eV for the researched films $Zn_{1-x}Mn_xTe$. It was established physical and technological modes of obtaining films of high optical quality.

1. W.M. Chen, I.A. Buyanova, Handbook of Spintronic Semiconductors, Singapore, Pan Stanford Publishing, 2010, P. 400.
2. V.V. Kosyak, A.S. Opanasyuk, Study of the structural and photo-luminescence properties of CdTe polycrystalline films deposited by close-spaced vacuum sublimation. *Journal of Crystal Growth*, 2010, Vol 312, p. 1726-1730

Formation of Multicomponent Metal Coatings on Inner Surfaces of Low Diameter Pipes

Kosminska Yu.O., Kornyushchenko G.S., Natalych V.V., Perekrestov V.I.

Sumy State University, Sumy, Ukraine, y.kosminska@phe.sumdu.edu.ua

Operational properties of low diameter pipes for various applications can be improved by deposition of protective coatings. Recent progress in fabrication of protective coatings is related to investigations of multicomponent high entropy alloys and thin layers on their basis. Here the problem consists in obtaining uniform characteristics of the coatings over the pipe surface while keeping their protective properties as high as possible, as well as keeping the deposition process reproducible, controllable, universal and relatively simple. This requires developing of new deposition techniques and materials.

In this work we deposited Ti–Cr–Fe–Co–*X* coatings, where *X* being changeable, by means of a specially developed ion-plasma sputterer. The developed sputterer is a variant of a dc magnetron sputterer but is notable for its rod-like target, magnet system inside an anode assembly and hollow cylindrical cathode. The created configuration had perpendicular intersection region of electric and magnetic fields situated around the rod, good enough ventilation by argon, and stable discharge. The rod could be made of either longitudinal sections or multiple disks of different chemical elements. The rod length was increased to 140 mm, argon pressure was 3 Pa, the discharge power was 800 W.

We studied structural and morphological characteristics and elemental composition of the coatings depending on the technological parameters. Main finding was that in absence of carbon highly porous layers are formed that is caused by proximity to thermodynamical equilibrium between the sputtered phase and the deposit. To enhance functionality of the layers by decreasing the porosity, we deposited and studied Ti–Cr–Fe–Zr–Cu–C, Ti–Cr–Fe–Co–Ni–C, and Ti–C–Ni–Cr–C layers additionally. It was found that addition of carbon influenced the structure formation sufficiently. Thus, the obtained layers were pore-free and possessed the microhardness of 17–27 GPa for the carbon concentration up to 37–43 at. %.

The mathematical model of mass transfer of sputtered substance was also developed for the two configurations of the rod-like target [1]. The model considers radial and axial distribution of sputtered fluxes and allows estimating elemental composition distribution along the inner surface of a cylindrical substrate holder.

1. Yu. O. Kosminska, V. I. Perekrestov, G. S. Kornyushchenko. Calculation of elemental composition distribution of multicomponent metallic coatings deposited onto inner surfaces of low diameter pipes // *Metallofizika i Noveishie Tekhnologii*. 2019. V. 41, No. 3 (to be published).

Influence of Cooling Regimes on the Crystallization Kinetics of Metal Alloys

Kosynska O.L., Sheveleva K.Yu.

Dniprovsk State Technical University, Kam'yanske,Ukraine, krao@ua.fm

By methods of mathematical modeling investigated the cooling regimes and crystallization kinetics of thin $Fe_{80}B_{20}$ melt layers in contact with the massive copper semi-infinite substrate, and $Cu_{47}Ni_8Ti_{34}Zr_{11}$ alloy, which is solidified in a copper mold with a wall thickness of 15 mm.

To study the effect of the cooling regime on the melts crystallization kinetics, the modeling results obtained in the form of time dependences of the melt temperature $T(t)$ and the crystallized volume fraction $x(t)$. According to obtained results, it was found that, when changing the thickness of the molten layer l, solidification of the melt can be carried out in three cooling modes, which ensure the formation of three types of structure: amorphous, amorphous-crystalline and completely crystalline. For $Fe_{80}B_{20}$, a completely crystalline structure is fixed in layers with a thickness of more than 34.9 μm, complete amorphization is observed in layers $l < 34$ μm and amorphous-crystalline structures are obtained at $34\ \mu m \leq l \leq 34.9\ \mu m$. For the $Cu_{47}Ni_8Ti_{34}Zr_{11}$ alloy, the complete crystallization of the melted layer is observed at $l > 1043$ μm, the complete amorphization of the alloy is fixed in layers with $l < 850$ μm, and the amorphous-crystalline structure can be obtained in the thickness range $850\ \mu m \leq l \leq 1043\ \mu m$.

In order to find out the conditions for non-crystalline solidification of investigated alloys in calculations, it was determining the critical thickness l_c and the critical cooling rate u_c, in which the crystalline volume fraction decreases to insignificantly small values ($x \leq 10^{-6}$), lying behind the sensitivity limits of modern methods of structural analysis. It is shown that the largest tendency to amorphization has $Cu_{47}Ni_8Ti_{34}Zr_{11}$ alloy, which can be obtained in a fully amorphous state in sections 450 μm and $u_c=1{,}4\cdot10^3$ K/s, full amorphization of $Fe_{80}B_{20}$ alloy achieved with more extreme cooling at $l_c=10$ μm and $u_c=10^7$ K/s. The results show a satisfactory agreement with known experimental data [1, 2], which evidences to the correctness of the developed mathematical models.

1. Tkatch V.I., Denisenko S.N., Selyakov B.I. Computer simulation of $Fe_{80}B_{20}$ alloy solidification in the melt spinning process. *Acta Metallurg. Mater.* 1995. Vol. 43, No 6. P. 2485-2491.
2. Bossuyt S. Microstructure and crystallization behavior in bulk glass forming. – Pasadena: California, 2001. 85p.

Optimization of Growing Process of the Thin-Film Structures ZnS by Method of Gas-Dynamic Flow of Vapor

Lopyanko M.A.

Vasyl Stefanyk Precarpathian National University, Ivano-Frankivsk, Ukraine,
lopyanko@gmail.com

In this work is research basic parameters of the deposition process ZnS by gas-dynamic flow of vapor. The dependence of parameters of the deposited material from technological conditions and made optimization for nanostructures and films. Described opportunities for effective recruitment of technological parameters for materials with predictable properties [1-3].

The growth of coefficient values of condensation α and bringing them closer to 1 indicates on the prevalence of the condensation process of reevaporation material particles from the walls surfaces in the high range of values ξ (Fig. 1). This process also illustrates that when ξ ≈ 0,6 curve of condensation velocity exposed fracture. The dependence of the calculated values of the resulting condensation velocity ω * from dimensionless coordinate ξ indicates that when ξ ≈ 0,35 received film have the largest thickness. Evaluation of the reevaporation material makes it possible to specify a region with a structural perfect material which is before the maximum of resulting condensation velocity. Further reduction of the relative density ρ/ρ_1 and increasing degree of vapor phase supersaturation with increasing ξ can be explained by increasing the mean free path of molecules (Fig. 2).

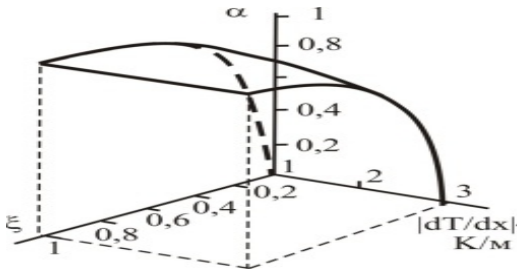

Fig. 1. The dependence of the calculated values of the condensation coefficient α from temperature gradient dTc/dx and dimensionless coordinates ξ (Ts = 923 K, L = 0,08 m, d = 0,05 m).

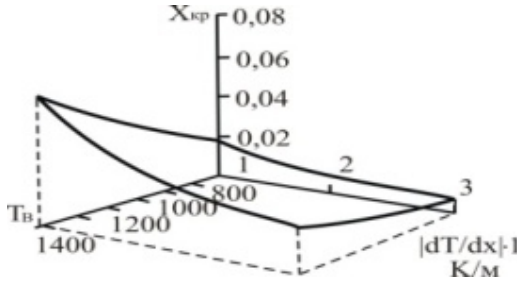

Fig. 2. The dependence of the calculated values of the critical cross section $x_{кр}$ from substrate temperature Ts and temperature gradient dTc/dx (L = 0,08 m, d = 0,05 m).

1.C. Ricolleau, L. Audinet, M. Gandais, T. Gacoin, J.P. Boilot. 3D morphology of II-VI semiconductor nanocrystals grown in inverted micelles // *Journal of Crystal Growth*, 203, pp. 486-499 1999.

2.Андриевский Р.А. Наноматериалы: концепция и современные проблемы // Рос.хим.ж., XLVI(5), сс. 50-56 2002.

3.W.T. Tsang, in: R.K. Willardson, A.C. Beer (Eds.) // Semiconductors and Semimetals, Academic Press, New York, 24, pp. 397 1990

Structure and Conditions for Forming Nanocrystallites of GaSb in Thin Films GaSb-Ge System

Lutsyk N.Yu, Mykolaychuk O.G.

Ivan Franko National University of L'viv, Physical Faculty,Chair of Physics of Metals,
nyuluts@i.ua

Structure, substructure, concentration areas of existence of metastable solid solutions and an amorphous state and kinetics of structural transformations depending on technological conditions of evaporation of thin films of system GaSb-Ge were studied by methods of electronography (EG-100) and transmission electron microscopy (UEMB-100K). Using a method of the flesh evaporation in vacuum, the films have been prepared, from previously synthesized powder GaSb-Ge, with the thickness approximately 50 nm. Glass, ceramic and spallings NaCl monocrystals were served as substrates. Equilibrium of system GaSb-Ge in a massive state is featured by the diagram of the eutectic type, and mutual solubility of components on the molar composition does not exceed 1 %. The composition of films is more convenient to represent using the formula $(GaSb)_{1-x}(Ge_2)_x$ because in the investigated system solid thin-film solutions are formed by substitution.

The temperature of a substrate supported in a precipitation process of films has dominant effect on structure formation of explored films. Films of all explored compositions, precipitated on substrates at room temperature, were amorphous. The linear relation of the proximate interatomic distance (from 2.72A for a-GaSb to 2.45 A for a-Ge) in amorphous films from composition is observed. The linear relation of the proximate interatomic distance in coordinate Ge_2 specifies random distribution of atoms with forming "alloyed" structure such as a solid solution of substitution. In amorphous films GaSb threefold coordination in distribution of the proximate atoms is observed. The magnification of concentration Ge gives in conversion of allocation of the proximate atoms. At concentrations Ge_2 about 20 % transferring from threefold coordination to tetrahedral is observed.

Amorphous films at heat crystallized, but phases of a solid solution it is not observed. Initial crystallization phases are crystal grains GaSb. The growth of crystallite sizes of GaSb takes place with the temperature increase. A speed of continuous heating has essential influence on the density and sizes of crystallites of GaSb formed in the amorphous semiconductor matrix based on Ge. With an increase of temperature of a substrate there is a forming the nonuniform amorphous films. Areas of initial ordering on a basis GaSb are observed. Forming of areas of initial ordering on basis GaSb proves to be true their etching in bromine - methanol etching agent with its heightened reactivity to connections Ga-Sb.

Effect of Heat Treatment on Structure and Properties of Chemically Precipitated Coatings $Ni_{88}P_{12}$

Lysenko A.B., Kalinina T.V., Zagorulko I.V., Kugai N.A.

Dniprovsk State Technical University, Kamyanske, Ukraine, Zagorylko@ukr.net

X-ray phase, resistometric and durometric analyzes have been used to investigate the heat changes in the structure and properties of nickel-phosphorus coatings obtained by non-electrolysis. The investigated precipitates were deposited on the copper substrates from aqueous solutions containing nickel sulphate, sodium hypophosphite and stabilizing additives. The phosphorus concentration in the deposited layers was estimated using an empirical dependence on the pH value of the working solution, built by summarizing the literature data, and selectively controlled by chemical analysis.

It is shown that freshly-deposited coatings with a content of 12 at.% P gives the diffraction patterns with three damped diffuse maximums, similar to the diffractograms of amorphous metal-metalloid alloys obtained by quenching from a liquid state. In the process of subsequent isochronal (15 min) vacuum annealing, the amorphous structure of the coatings is stable up to 250 °C. Exceeding of this temperature limit value causes the crystallization of amorphous precipitates. At the early stage of transformation, in the structure of the coatings a metastable crystalline phase is formed, the diffraction signs of which are revealed in the samples annealed at 260 – 350 °C. With a further increase of the annealing temperature, the metastable phase decomposes into an equilibrium mixture of Ni and Ni_3P compound. The processes of formation and decomposition of the metastable phase are reflected in the temperature dependences of the electrical resistivity $\rho(T)$: in the range of 250 – 260 °C a jump-like increase in ρ values is recorded and borders with the area of its intensive fall at $T > 280$ °C. According to the results of X-ray phase analysis, the growth of the electrical resistivity caused by the formation of a metastable phase in the amorphous layers, and its subsequent sharp decrease is caused by the decomposition of this phase and the contemporaneous crystallization of the amorphous coating sites as a mixture of equilibrium phases, which terminated at 450 – 500 °C.

Structural transformations during heating of the investigated precipitations are accompanied by a general decrease of resistivity in 3 – 4 times, a change in the sign of its temperature coefficient from negative to positive, and an increase in microhardness to values of ~ 11 – 12 GPa, which persist to 580 – 600 °C.

Effective Methods of Mechanical and Chemical Treatments of PbTe and $Pb_{1-x}Sn_xTe$ Crystals Surfaces

Malanych G.P., Tomashyk V.M.

V. Lashkaryov Institute of Semiconductor Physics of NAS of Ukraine, Kyiv, Ukraine, galya.malanich@gmail.com

The main purpose of this work was to investigate the process of chemical treatment of the PbTe and $Pb_{1-x}Sn_xTe$ crystals surfaces by bromine emerging solutions and to establish the surface state after chemical etching using atomic force microscopy. The concentration regions of polishing solutions have been found for various types of PbTe and $Pb_{1-x}Sn_xTe$ surface treatment: (1) to remove the damaged layer, (2) to control the etching rate, (3) to obtain the samples of a given thickness.

Microstructure of the treated surfaces after various stages of the mechanical and chemical treatments was studied using table scanning microscope JEOL JCM-5000 NeoScope. Morphological study of the polished surface of PbTe was spent on scanning probe microscope NanoScope IIIa Dimension 3000TM (Digital Instruments, USA).

The processes of chemical-mechanical polishing and chemical-dynamic polishing lead to improve the surface quality of the PbTe and $Pb_{1-x}Sn_xTe$ crystals surfaces. The high quality of the wafers surface after the chemical polishing process was confirmed by atomic force microscopy (Fig.1).

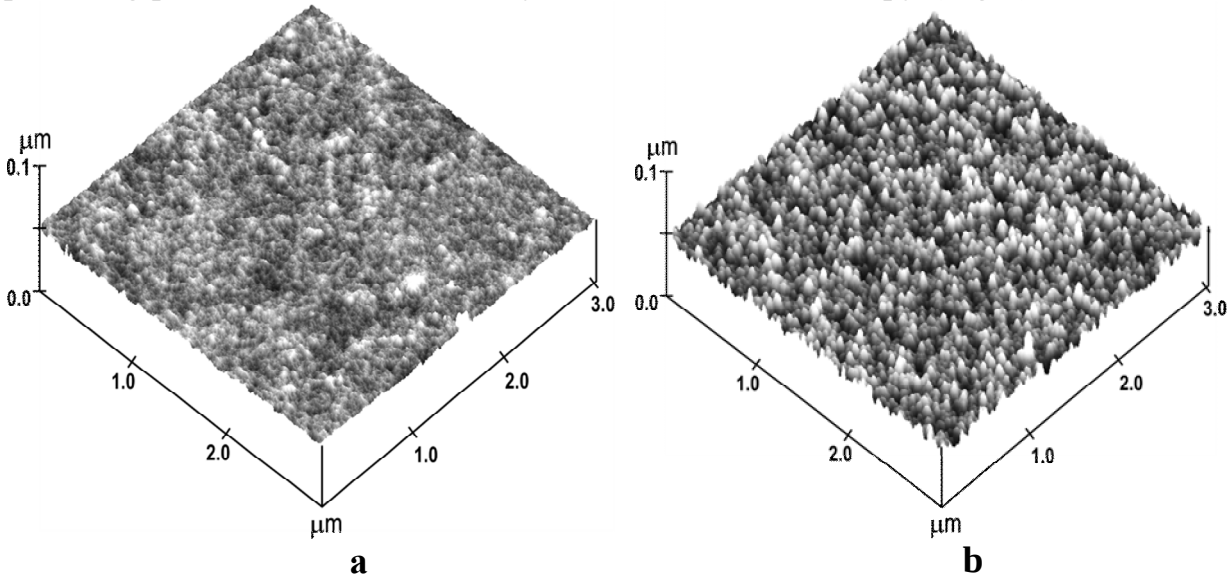

Fig.1. The surface morphology of the PbTe crystals after, a – chemical-mechanical polishing and b – chemical-dynamic polishing.

Practical Atomic Force Spectroscopy Assisted by Artificial Neural Networks

Malyuta S.V.[1,2], Lytvyn P.M.[1], Lytvyn O.S.[1,3], Efremov A.A.[1], Prokopenko I.V.[1]

[1]*V.E. Lashkaryov Institute of Semiconductor Physics NAS Ukraine, Kyiv, Ukraine*
[2]*National Technical University of Ukraine «Igor Sikorsky Kyiv Polytechnic Institute», Kyiv, Ukraine*
[3]*Borys Grinchenko Kyiv University, Kyiv, Ukraine,* plyt@isp.kiev.ua

Methods of atomic force spectroscopy of tip-surface interactions have been widely used in material science and biomedical researches. However, there is a significant gap between their use in academic research and the practical implementation, for example, to control of high-tech processes in production or medical clinical diagnostics. One of the reasons is the need for staff with the appropriate level of professional knowledge, which would ensure competent in the analysis and the interpretation of results. In the context of the development of modern information technologies, it is reasonable to involve expert systems based on artificial intelligence to the analysis and classification of large amount of nano-diagnostics data.

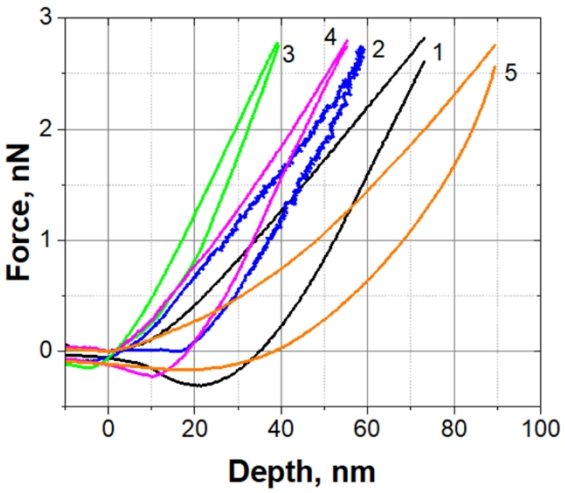

Fig.1 Fragment of the input data for artificial neural network processing (one experimental set contains about a thousand of curves): blood cells nanoindentation curves, obtained by atomic force spectroscopy; 1 - control sample, 2-5 - blood samples after the action of various drugs.

The authors used fitting and classification artificial neural networks to create a prototype of the expert system for processing of force spectroscopy raw data in the nanomechanical diagnostics of 2D materials and biological samples. The development makes it possible to simplify their practical implementation by replacing the physical models of analysis by deep-learning and decision-making algorithms, which in the future can completely automate diagnostics of this kind.

A prototype of expert system has been tested at the studies of the erythrocyte's cells walls rigidity in the problem of blood circulation control for patients with the type II diabetes (Fig. 1) and studying the mechanical and lyophilic properties of thin carbon films as well as flakes of graphene oxide.

Analysis of Methods of Obtaining CdTe Layers with Preper-Defective Hole Conductivity

Mazur T.M.[1,3], Makhniy V.P.[2], Berezovsky M.M.[2], Kinzerska O.V.[2]

[1] *Vasil Stefanik Precarpathian National University., Ivano-Frankivsk, Ukraine,* tetyana.m.mazur@gmail.com

[2] *Yuri Fedkovich Chernivtsi National University, Chernivtsi, Ukraine*

[3]*Ivano-Frankivsk National Technical University of Oil and Gas, Ivano-Frankivsk, Ukraine*

One of the serious problems arising in the development of barrier detectors based on crystalline cadmium telluride is the difficulty of obtaining layers with high hole conductivity. This is due to the high ionization energy and low solubility of acceptor impurities even at high T, as well as an intensification in self-compensation processes with increasing temperature. An alternative way to solve this problem may be the use of technologies that can provide the preferential generation of small (20-40 meV) own point defects (OPD) of the acceptor type with cadmium telluride. In this paper, relatively simple methods are discussed, with the help of which layers with proper-defective hole conductivity in a number of II-VI compounds have already been obtained.

The first of these is based on the introduction of a certain type of isovalent impurity (IVI) into a crystal, which itself does not create levels in the forbidden zone and stimulates the generation of OPD of the acceptor type. At the same time, their concentration can be quite ligh, the solubility of the IVI is very high even at low (100-500ºC) temperatures. The second approach means using low-temperature annealing of CdTe substrates in activated tellurium pairs, under which quasi-epitaxial growth of layers with an excess concentration of small acceptors – cadmium V_{Cd} and interstitial tellurium – occurs Te_i. Since the dissociation energy of the molecule Te_2 is ~2.7 eV, it is easy to activate it activation by irradiating with a mercury or halogen lamps or a semiconductor source with a corresponding energy of light quanta. Another way is to change the stoichiometric composition of thin surface layers in favor of acceptor OPD, which is based on the difference in the solubilities of the components of the binary compound AB. Thus, in particular, the films of some metals of group I of the Periodic Table dissolve component A well and practically do not dissolve chalcogen B. At the same time, the solubility of the metal itself in compound AB under certain conditions is much less than the solubility of atoms A and B. And finally, let`s note that the efficiency of STD generation processes for all considered-above methods discussed above can be improved by previous loosening the surface of the substrates, for example, bombarded with inert gas ions.

Surface Patterning of Amorphous Chalcogenide Layers by Light- and Ion-Beams

Molnar S.[1*], Bohdan R.[1], Nagy Gy.[2], Rajta I.[2], Makauz I.[3], Shipljak M.[3], Pinzenik V.[3], Kokenyesi S.[1]

[1]*Institute of Physics, University of Debrecen, Debrecen, Hungary,*
[2]*Institute of Nuclear Research, Hungarian Academy of Sciences,Debrecen, Hungary*
[3]*Uzhgorod National University, Uzhgorod, Ukraine*

As(Ge)-S(Se) based layers made of proper chalcogenide glasses have been used for surface geometrical relief recording by laser beams as well as by 2 MeV energy H^{+1} and He^{+1} ion-beams. The formation of giant (height modulation from nanometers up to micrometers) geometrical reliefs and elements (dots, lines and diffractive elements), applicable in the 0.6 – 10 micrometer spectral range have been investigated. Efficiency of surface patterning was compared in few selected compositions of chalcogenide glasses but varying the type, energy of ion beam, intensity of green (532 nm) and red (632 nm) laser beams, as well as temperature and conductivity of substrate. It was shown that basically the same structural and volume transformations occur during different irradiations, excitation and energy transfer in the recording material, except of additional input of light-polarization effects in the case of polarized laser beam recording.

The results showed on the applicability of high energy ion beams for fabrication, direct lithography and prototyping of planar optical elements on the surface of amorphous chalcogenide layers.

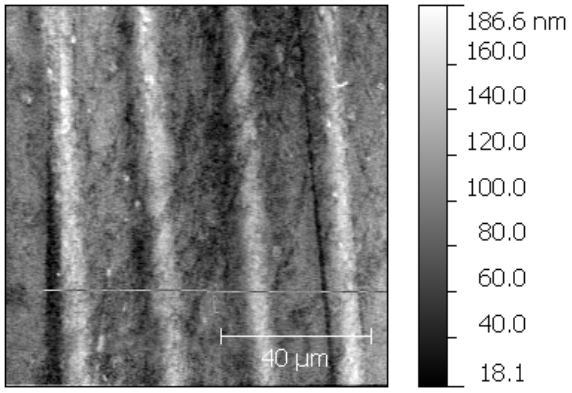

Figure presents an example of the ion-beam recorded relief structure on $As_{20}Se_{80}$ layer.

The authors acknowledge the financial support of the GINOP-2.3.2-15-2016-00041 project.

Reconstitution of Strain Distribution from X-Ray Moiré Images by Characteristics of the Fourier Energy Spectrum

Novikov S., Balovsyak S., Yaremchuk I., Romankevich V.

Yuriy Fedkovych Chernivtsi National University, Chernivtsi, Ukraine, ifodchuk@ukr.net

Deformations are reason of phase difference between X-rays diffracted in the analyser of X-ray LLL-interferometer. The interpretation of resultant moiré image is ambiguous problem due to necessity to separate the contribution of strain fields from single defects and their complexes.

In this work, the specified strain field is composed of concentrated forces definitely distributed on the analyzer exit surface accordingly to the loading magnitudes. Moiré images are calculated on the basis of the relations presented in the work [1]. It is shown that the method of the Fourier power spectral density gives the possibility to reproduce not only a magnitude but also spatial distribution of sources of residual strains from the analysis of experimental moiré images.

The analysis of parameters of calculated moiré images f with the same sum of linear loads F_{LT} and different their spatial distribution is carried out. The image f treatment by a two-dimensional direct discrete fast Fourier transform is executed. As the parameters of moiré images the values of the radial distributions P_R for the energy spectrums P_S are used, as well as their mean spatial frequencies v_{CR} [2]. This allows us to find the normalized areas of ranges of the P_R distribution and the corresponding spatial distribution of loads F_{LE}, on the basis of which inverse problem is solved. There are the resulted examples of moiré image reconstruction on Fig.1: the distribution of single sources of the residual strains F_{LE} and their total value F_{SE} were determined from the theoretical (Fig. 1a) and experimental (Fig. 1c) moiré images.

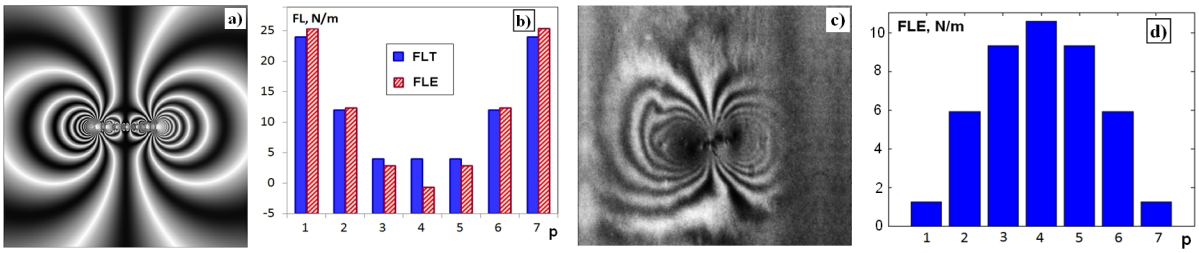

Fig. 1 a) calculated moiré image with parabolic load distribution F_{LT} (sum of F_{LT} is 84 N/m); b) the distribution of loads F_{LE} (F_{SE} = 85.9 N/m) reproduced from the analysis (Fig. 1a); c) experimental moiré image; d) the load distribution F_{LE} (F_{SE} = 43.6 N/m) reproduced from the analysis (Fig. 1c); p is the number of concentrated force

1. Fodchuk I.M., Raransky V.D. Moiré images simulation of strains in x-ray interferometry *J. Phys. D: Applied Physics.*,**36**, A55 (2003)
2. Gonzalez.R., Woods R., Eddins L. Digital Image Processing using MATLAB. – Prentice Hall, 2004. – 609 p.

Structural, Optical and Electrical Properties of Iron-Doped Indium Saving Indium-Tin Oxide Thin Films Sputtered on Preheated Substrates

Ohtsuka M.[1], Sergiienko R.[2], Petrovska S.[3], Ilkiv B.[3], Nakamura T.[1]

[1]*Institute of Multidisciplinary Research for Advanced Materials (IMRAM), Tohoku University, Sendai Japan*
[2]*National Academy of Science of Ukraine, Physico-Technological Institute of Metals and Alloys, Kyiv, Ukraine*
[3]*National Academy of Science of Ukraine, Frantsevich Institute for Problems of Materials Science, Kyiv, Ukraine, sw.piotrowska@gmail.com*

Iron-doped indium tin oxide (ITO) thin films with reduced to 50 mass% indium oxide content were prepared by co-sputtering of ITO and Fe_2O_3 targets in mixed argon-oxygen atmosphere onto glass substrates preheated at 523 K (ITO50:Fe_2O_3). The influence of working gas flow rate and heat treatment temperature on the electrical, optical, structural, and morphological properties of the films was characterized by means of four point probe, Ultraviolet-Visible (UV–Vis) spectroscopy, X-ray diffraction (XRD) and atomic force microscopy.

Doping of ITO films by iron using Fe_2O_3 target resulted in increasing transmittance of films as compared to undoped ITO50 thin films. ITO50:Fe_2O_3 thin films even at oxygen flow rate $Q(O_2)$ = 0.1-0.2 sccm satisfied the required condition of $\tau > 85$ % in the visible region of the spectrum.

Iron doping hindered the crystallisation of indium saving ITO thin films. ITO50:Fe_2O_3 films heat treated at temperatures 723 K showed an improvement of the crystallinity. The main peaks of the measured XRD pattern can be assigned to $In_4Sn_3O_{12}$.

The volume resistivity of as-deposited ITO50:Fe_2O_3 thin films sputtered on preheated substrates (down to 1240 μΩcm) was significantly decreased in comparison with that (25400 μΩcm) of ITO50:Fe_2O_3 thin films deposited on unheated substrates.

The best obtained values of volume resistivity 992 μΩcm and transmittance of 93.4 % at a light wavelength of 550 nm were derived after heat treatment at 523 K and at $Q(Ar)/Q(O_2)$=50/0.2 sccm for the ITO50:Fe_2O_3 thin films sputtered on preheated substrates. Further increase of heat treatment temperature conduces to increase of volume resistivity. The electron mobility and carrier concentration of ITO50:Fe_2O_3 thin films sputtered under optimum conditions were 36 cm^2/Vs and $1.93 \cdot 10^{20}$ cm^{-3}, respectively.

Structure and Analysis of Element Composition of MgO Films

Ostafiychuk B.K., Poplavskyi I.O.

Vasyl Stefanyk Precarpathian National University,
Ivano-Frankivsk, 76018, Ukraine, omeliantru@gmail.com

The problem of the dependence of properties of films on the structure and elemental composition of the surface, which are determined by technological conditions, has an important place in the physics of oxide films.

The necessity for films of different thickness (from nanosized to micron) requires the use of certain technologies, including powder coating methods.

The structure and elemental composition of MgO films obtained by different methods were investigated in the paper. Methods for high-frequency ion-plasma spraying and electrophoresis were used to deposit MgO films.

The MgO films were applied on polycrystalline molybdenum substrates and to chip of NaCl (100) single crystal. The structure of the films was investigated by electron microscopy. The calculation of electronograms was made using gold as a benchmark. The films of a polycrystalline structure were obtained by the method of high-frequency ion-plasma sputtering in an argon medium. Films, deposited in a medium of a mixture of argon and 15% oxygen at a temperature of the substrate 400K, have a texture. The structure of MgO films obtained by electrophoresis depends on the composition of the suspension, the conditions of deposition and dehydration of the films. When using a polymer suspension and the same particle size (less than 0.01 μm), we obtained porous films of a fibrous structure.

By AES method we studied the change of the stoichiometry of the surface of thin films and crystals of compounds after their contact with the air. The Auger-spectra of the surfaces were recorded in the mode of differentiation of the energy spectra of emitted electrons *(dN(E)/dE)* upon the energy of exciting electrons of 3 keV. The density of the electron beam can be varied in the range 5–10 A /m^2. Auger-spectra in the differential form *dN(E)/dE* were registered at the modulation amplitudes U_m = 2V for Auger-peaks Mg (32 eV), C (270 eV), O (32 eV), Mg (1172 eV). Under such conditions of registration, the differential spectra of the Auger-electrons of a chemical element are proportional to the currents of their Auger-electrons.

By the method of AES we studied the cleavage surfaces, which were derived in air from the crystals MgO (100) and MgO films obtained by high-frequency ion-plasma sputtering, as well as films which were deposited by the electrophoresis method.

The violations of the stoichiometric composition to the side of the excess Mg, as well as the phase of hydroxide Mg $(OH)_2$, were revealed. In films deposited in medium of a mixture of argon and 15% oxygen, the violation of stoichiometry was not detected.

Novel Methods of Titanium Blackening

Perevoznikov S.S., Shendyukov V.S., Tsybulskaya L.S., Poznyak S.K., Maltanova A.M.

Research Institute for Physical Chemical Problems of the Belarusian State University, Minsk, Belarus, PerevoznikovS@yandex.ru

Titanium is a widely used material in optical equipment production for spacecraft industry due to its low density, sufficient mechanical and excellent anticorrosive properties and similarity of thermal expansion coefficients of titanium and optical glasses. To reduce stray light and increase the resolution of equipment, the internal surface of titanium optical components must have a low reflectivity. Current methods of titanium blackening are complicated and the coatings formed are not durable at elevated temperature and humidity [1].

In the present work we developed two different methods of titanium blackening. The first one is based on the chemical processes and includes two steps: chemical polishing pre-treatment followed by chemical etching in ethylene glycol – water mixture containing HF and $ZnCl_2$. After following treatment in nitric acid solution, titanium surface turns black. SEM inspection revealed the formation of array of needles (Ø ~ 100 nm) on the etched surface that act as an effective light absorbing system (Fig.1*a*). Appearance of the black surface from matt to specular can be changed by varying the parameters of the etching process. The lowest reflectivity for such samples was found to be 1-2%. Unfortunately, they are not wear resistant and can be damaged by touching.

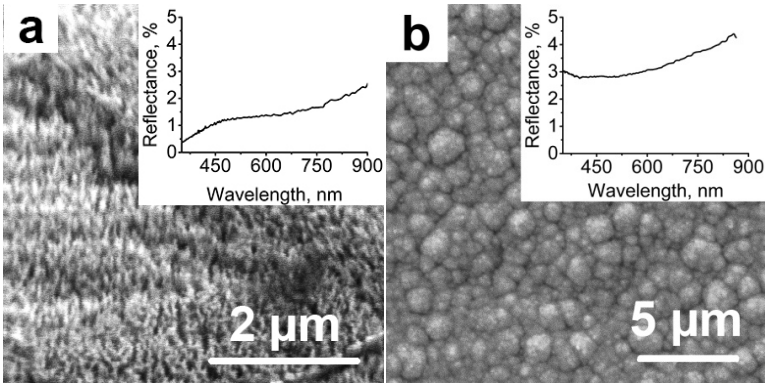

Fig. 1. SEM images of black surfaces obtained by chemical (*a*) and electrochemical (*b*) methods and their reflection spectra (on inserts)

The second method of titanium blackening is based on cathodic deposition of "black nickel" coating and includes the following steps: a) chemical matting pre-treatment, b) specific hydride treatment, c) electrodeposition of a matt nickel underlayer (4-6 μm) and d) electrodeposition of a thin layer (1-2 μm) of "black nickel" at a linear rise of cathodic current density. Such sequence of the procedures provides an excellent adhesion of the black coating to titanium substrate. The deposited "black nickel" coating has a complex composition (Ni, Zn, O, S), globular structure (Fig.1*b*) and the reflectance ranging from 3 to 4% in the visible region of spectrum.

Both types of the coatings have been proved to be stable at 35 °C and 98% relative humidity for 15 days, as well as under vacuum conditions.

1. Kuhn, A.T., 2005. The blackening of titanium. Metal Finishing 103, 41–45.

Stability of Structure and Magnetic Properties of Gd-Fe Films

Prysyazhnyuk V.I., Mykolaychuk O.G.

Faculty of Physics, Ivan Franko National University of Lviv, Lviv, Ukraine, prysjan@i.ua

Thin films of Gd-Fe compounds were obtained by means of a thermal vacuum evaporation of polycrystal mix material of a corresponding composition. The films with by thickness of 50-60 nanometers were evaporated on splitting of NaCl, then NaCl dissolved in water. The part of films was picked up at once on copper electron diffraction grids. The second series of films transplanted on copper grids, prestressly coated thin collodion supports and in such way was maintained 3-6 years. Then recurring researches were carried out. The temperature of substrates had two values 300 and 500 K. For structural investigation the electron microscope UEMV-100K and high-temperature attachment PRON-2 were used. Angle dependence of atomic factors of electron scattering was considered by atoms of gadolinium and iron. All measurements were repeated in 3-6 years after the first stage of measurings.

Electron diffraction examinations of structure of films of Gd-Fe system specify that the given films are condensed in amorphous-crystalline state. Structure formation essentially depends on requirements of condensation of films. Substrate rise in temperature leads to magnification of a polycrystalline phase.

It is known that the given compounds belong to the class soft magnetic material. We had been spent measurings of some magnetic performances of films and massive samples of Gd-Fe system. Hysteresis curves and numerical values of a coercive force are gained for massive and thin films samples. For this samples the Curie temperature also is determined. Influence of formation of a polycrystalline phase on absolute value of a coercive force is studied. Temperature dependences of magnetic saturation and curve magnetisations for films and compounds of Gd-Fe system are gained [1].

By us it is explored structure and magnetic properties of Gd-Fe films in the range of 3-6 years. It is revealed high temporary durability of physical performances of Gd-Fe films and lack of an oxidizing.

1. *В.Присяжнюк О.Миколайчук* Структурні перетворення та магнітні властивості аморфних плівок системи Gd-Fe // Вісник Львівського університету. Серія фізична. – 2016. – Вип.51. – С. 44-51.

Structural Changes in $As_{40-x}Sb_xS_{60}$ Films under Laser Irradiation

Rubish V.M.[1], Yasinko T.I.[1], Pop M.M.[1,2], Mykaylo O.A.[1], Makar L.I.[1], Kryuchyn A.A.[1], Kostyukevich S.O.[3], Veres M.[4], Holomb R.M.[4], Himics L.[4]

[1]*Institute for Information Recording, NAS of Ukraine, Uzhhorod, Ukraine,* center.uzh@gmail.com

[2]*Uzhhorod National University, Uzhhorod, Ukraine*

[3]*V. Lashkaryov Institute of Semiconductor Physics, NAS of Ukraine, Kyiv, Ukraine*

[4] *Wigner Research Centre for Physics, Hungarian Academy of Sciences, Budapest, Hungary*

Earlier [1], we investigated the optical transmission spectra of $As_{40-x}Sb_xS_{60}$ amorphous films with low Sb content and their changes at annealing and under laser illumination. It was established that the laser illumination and annealing of films induce the absorption edge shift into the long-wave spectral region (the pseudoforbidden gap width of films decreases whereas the refractive index increases). We have assumed that these changes are caused by the photo- and thermostructural transformations in amorphous matrix. However, the amorphous films of the As-Sb-S system with low antimony content were not studied in this regard.

In the present report, the result of Raman studies of $As_{40-x}Sb_xS_{60}$ ($0 \le x \le 12$) amorphous films and their changes under laser unfocused illumination (λ=530 nm, P=100 mW) are reported. Amorphous films (1 μm) were obtained by vacuum evaporation of the glasses of corresponding compositions from quasiclosed effusion cells onto cold silica substrates. The Raman spectra of as-prepared and illuminated films were measured at room temperature using Renishaw system 1000 Raman spectrometer. The exposure of the films was carried out during 1-5 min.

It was established that all studied $As_{40-x}Sb_xS_{60}$ amorphous films have a nanoheterogenous structure. Their structural network is constructed mainly of trigonal AsS_3 and SbS_3 pyramids linked through a common two-fold coordinated atoms of sulphur and contains also a considerable number of structural groups with homopolar bonds As-As and S-S (As_4S_4, As_4S_3, S_n). The concentration of such groups depends on the chemical composition. No molecular fragments with antimony-antimony bonds in the structure of $As_{40-x}Sb_xS_{60}$ films were detected. The illumination of amorphous films leads to the breaking and switching of As-As and S-S bonds in structural fragments As_4S_4, As_4S_3, S_n type with the formation of structural groups AsS_3.

The mechanism of photostructural transformations tacking place in $As_{40-x}Sb_xS_{60}$ amorphous films under laser illumination is discussed.

1. Rubish V.M., Pop M.M., Mykaylo O.A. et. al. Laser-induced changes in the optical characteristics of amorphous films of the As-Sb-S system // Scientific Herald of Uzhhorod University Physics series. 2017. No.42. P. 14-26.

Surface Morphology of Thin Films

Saliy Ya.P.

Vasyl Stefanyk Precarpathian University, Ivano-Frankivsk, Ukraine,
saliyyaroslav@gmail.com

Undoubtedly, thermal evaporation is considered as an attractive method of fabricating high quality thin films. Morphological properties of thin films are strongly dependent upon the fabrication techniques. These properties were usually investigated by Atomic Force Microscope.

The symmetry and periodicity of surface structures of the original image allow establishing by two-dimensional Fourier transforms and auto-correlation function. The Fourier spectrum is ideally suited for detecting periodic or quasiperiodic of the two-dimensional structures in the image. Textures easily differ in the spectrum in the form of impulses with high intensity.

The Fourier coefficients S (k, l), forming the two-dimensional frequency spectrum of the image s (n, m), were determined by the direct Fourier transform formula:

$$S(k,l) = \sum\sum s(n,m)\exp(-j2\pi(kn+lm)/N),$$

N is the number of image points.

A two-dimensional auto-correlation function C (k, l) was calculated by the formula

$$C(k,l) = \left(\sum\sum s(n,m)\cdot s(k+n,l+m)\right)^{1/2} N.$$

The 2D- and 3D- auto-correlation images as well as Fourier transforms were obtained in the graphical programs Microsoft.

Cadmium Telluride thin films grown on glass and (100) Silicon substrates have been analyzed by AFM.

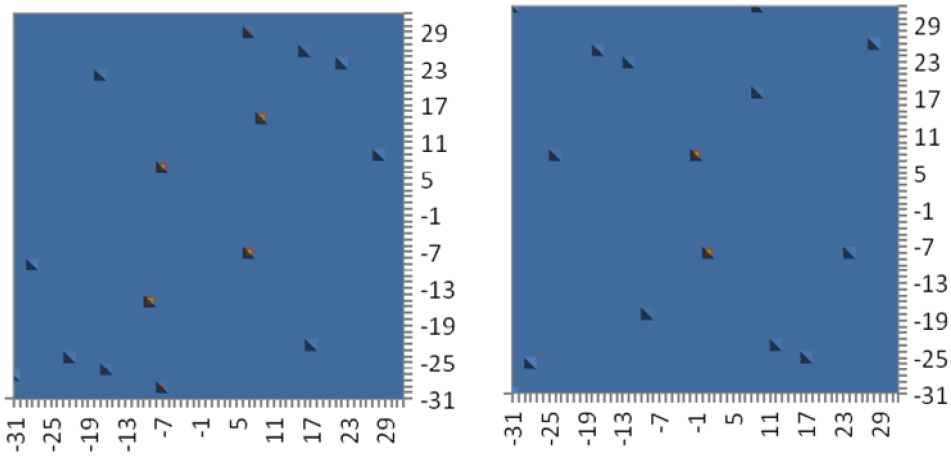

In the figure on the example of the two samples, modules of two-dimensional Fourier amplitudes of images are represented, which is 2 times higher than the eight nearest adjacent values.

Optical and Electrical Properties of CdTe Polycrystalline Films Obtained by Quasi-Closed Sublimation Method

Semikina T.V.[1,2], Mamykin S.V.[1], Shmyrieva L.N.[2]

[1]*Institute of semiconductor physics named V.Lashkarev NANU, Kyiv, Ukraine,* tanyasemikina@gmail.com
[2]*National Technical University of Ukraine named I.Sikorsky "KPI", Kyiv, Ukraine*

The paper discusses the results of studying the electrical and optical properties of CdTe films obtained by thermal deposition in a quasi-closed space. In the process of film deposition the technological parameters (temperature of the shoots, temperature of the quartz glass, weight of the initial powder and time of its heating) changed. The crystal structure of the resulting layers depends on the temperature of the substrate, its crystalline structure, the temperature gradient of the source-substrate and the vapor saturation of the deposited material. The influence of technological regimes on the properties of CdTe was studied with the aim of obtaining CdTe of p-type conductivity with a carrier concentration of 10^{15} cm^{-3} and more. The CdTe layers were deposited on optical glasses (pure and coated with ZnO film), pyroceram substrates (pure and coated with molybdenum), as well as on CdS layers of different thickness. The resistivity of the films was measured using the 4-probe method on the CHE660E potentiostat. The optical transmission and reflection spectra of the films under study were measured on an installation consisting of an IKS-12 monochromator, a CDSH-100 lamp, and a FD-24K silicon photodetector. Characteristics were measured at angles of incidence of polarized light of 15 °, 45 °, 60 ° and 75 ° with respect to the normal in the spectral range of 0.45 - 1.1 μm. The dependences of the optical constants (reflection coefficient and absorption coefficient) on the wavelength were taken into account. The calculations were performed under the assumption of a single-layer model. The study of the electrical and optical characteristics of the CdTe layers obtained by the quasi-closed volume method showed that polycrystalline films have a carrier concentration of 10^{8} - 10^{11} cm^{-3} and a specific resistance of 10^{3} - 10^{6} Ω ·m. The optical band gap E_{opt} for direct transitions depended slightly on technological factors and amounted to 1.56 eV. The paper discusses ways to increase the conductivity of CdTe layers.

Magnetoresistive Properties of Ferromagnetic-Insulator Nanocomposites at the Percolation Boundary

Shchotkin V.V., Pazukha I.M.

Department of Electronics, General and Applied Physics, Sumy State University, Sumy, Ukraine, v.shchotkin@aph.sumdu.edu.ua

The steady interest in nanostructures that has arisen recently is due to the possibility of significant modification and a fundamental change in the qualities of known materials during the transition to the nanocrystalline state. A distinctive feature of low-dimensional systems is that their properties are determined not only by the properties of the elements that make up their composition but, to a greater extent, by the surface of the section and the size of the volumes that form a similar structure.

According to the results of the research, negative giant magnetoresistance (GMR) is realized when specimens have been obtained by the method of dc magnetron sputtering. Along with the negative GMR, positive magnetoresistance can also occur. As a rule, positive magnetoresistance was observed beyond the percolation boundary, but a certain orientation of the magnetic field and current had to be maintained. Such positive MR has an anisotropic structure – electric transfer is performed on metal clusters and occurs in nanocomposites based on magnetic particles (Ni, Ni_xFe_{1-x}) embedded in insulator matrix SiO_2. However, investigations of Fe-SiO_2, Co-SiO_2, Fe-Al_2O_3 nanocomposites have shown that near the percolation boundary it was also possible to observe isotropic positive MR. On the other hand, superparamagnetic granules can occur, which need a very large magnetic field to change the magnetization vector. For $Co_x(Al_2O_n)_{100-x}$ nanocomposites, it was shown that negative GMR reached a value of 6.5% with a field applied at 10kOe. The percolation boundary was observed at x = 54-67%, where positive MR also occurred at 1.5% in fields – 10kOe. The existence of positive magnetoresistance is explained by the simultaneous presence of composites of clusters and isolated nanogranules, in which different values of magnetic anisotropy are observed.

Hence, an analysis of the literature devoted to the study of ferromagnetic-insulator nanocomposites reveals that their magnetoresistive properties strongly depend on components and their concentration. Percolation parameters are non-universal, sensitive to the ferromagnetic particles distribution and must be determined for each case. Therefore, the main goal of our investigations is to investigate the concentration effects on the magnetoresistive properties of nanocomposites based on Co and SiO prepared by co-evaporation technique.

This work was funded by the State Program of the Ministry of Education and Science of Ukraine.

Electrochemical Production of Silicon from Chloride-Fluoride Melts

Shumakova N.I.[1], Protsenko Z.M.[2]

[1]*Sumy State University, Sumy, Ukraine*
[2]*SMS State Pedagogical University named after A.S. Makarenko, Sumy, Ukraine,*
nshumakova@ukr.net

Electrolysis of ion melts is the least studied and rather essential part of electrochemical production. He represents the greatest interest in obtaining metals and nonmetals that can not be isolated from aqueous solutions of electrolytes (alkali and alkaline earth metals, boron, aluminum, silicon, titanium, zirconium, etc.), alloys and compounds (borides, silicides, aluminides), diffusion coatings and powdered products. One of the promising methods for the production of silicon and its borides is the electrolysis of salt melts.

The purpose of the work was to study the process of formation of a powdery sediment based on Si without impurities B on thesubstrate of steel. The interconnection between the parameters of the electrolysis process, the dispersion of the powdered product and the elemental and phase composition of the precipitate are established. On the basis of experimental data, it was established that in the electrolysis of a melt KCl - KBF_4 - K_2SiF_6 - SiO_2 at cathode current density up to $(1\text{-}3)\cdot10^2$ A/m^2 and voltage up to 2.0-2.4 V, coatings of a small thickness are formed on the substrate with a relatively low adhesion, and with an increase in the current density up to $(7\text{-}17)\cdot10^2$ A/m^2 - porous powdered sediments that are easily removed mechanically.

The method of separation and purification of the resulting powdered product, which consists in the use of hot distilled water and vacuum-thermal distillation, is developed. X-ray diffraction analysis (Siemens D 5000 diffractometer) was used to determine the phase composition of the electrolysis product. The elemental and granulometric composition of the powdered sediment was established using the electronic microscope REMMA-102-02. The granulometric composition of the powdered precipitate depends on the electrolysis conditions and averaged 1-10 μm. The phase and elemental composition of the sediment depends on both the electrolysis current density and the composition of the electrolyte and temperature.

It was established that the phase composition of the product of the electrolysis product obtained from the melt KCl - KBF_4 - K_2SiF_6 - SiO_2 at a current density of $17\cdot10^2$ A/m^2, voltage of 2,4-2,8 V and temperature 815 K corresponds to silicon. Formation of silicides Ferum occurs only on the substrate of steel, in the powdered product, silicides are not found.

Morphology and Properties of $Cd_{1-x}Mn_xTe$ and CdSb Thin Films Obtained by RF-Cathode Sputtering

Strebezhev V.M., Kleto G.I., Fochuk P.M., Yuriychuk I.M., Pylypko V.G., Strebezhev V.V.

Yuriy Fedkovych Chernivtsi National University, Chernivtsi, Ukraine,
v.strebezhev@chnu.edu.ua

In order to obtain $Cd_{1-x}Mn_xTe$ and CdSb thin films we use RF-cathode sputtering in an Ar atmosphere. This method is less sensitive to the difference of the partial pressures of the components and ensures a stoichiometric composition the films. In this case, the morphology and structure of the film are determined not only by the RF power regime, but also by the crystallographic parameters of the selected substrate. Solid polycrystalline $Cd_{1-x}Mn_xTe$ (x=0.05-0.35) films were obtained by deposition on glass and $Cd_{1-x}Hg_xTe$ substrates (Fig. 1, a, b; Franck-van der Merwe growth mode).

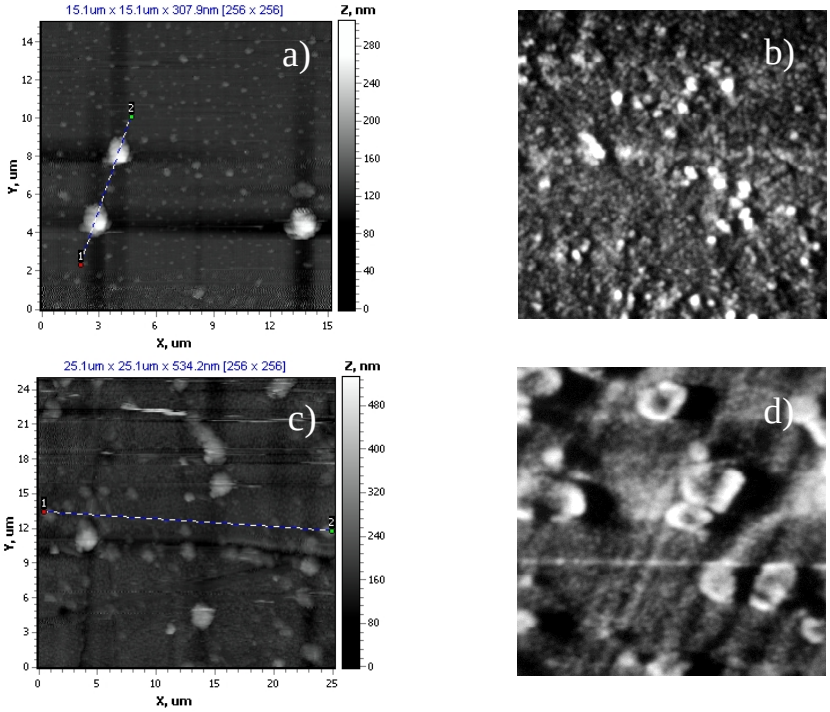

Fig. 1. Morphology of the continuous (a, b) and island (c, d) $Cd_{1-x}Mn_xTe$ films: a), c) – study in AFM; b), d) – study in SEM.

The systems of $Cd_{0.9}Mn_{0.1}Te$ and $Cd_{0.75}Mn_{0.25}Te$ islands were obtained at the deposition on the substrates of the layered In_4Se_3 crystals (Fig. 1, c, d; Volmer-Weber growth mode). Continuous CdSb films were grown at the deposition on the substrates of In_4Se_3crystals. In the case of the deposition on In_4Te_3 crystal chips – a system of islands was obtained. Electrophysical properties of the obtained films depending on the morphology and structure were studied, their application in micro- and nanotechnology is discussed.

Photoluminescence features of the CdZnTe thin films irradiated by fast neutrons

Strilchuk O., Rashkovetskyi L., Maslov V., Plyatsko S., Lyapina A., Gromovyi Yu.

Lashkaryov Institute of Semiconductor Physics, NAS of Ukraine, Kyiv, Ukraine,
strilchuk@isp.kiev.ua

We present a study of the effects of fast neutron irradiation with fluence of 10^{13} N/cm^2 on low temperature (T = 77 K) photoluminescence (PL) of $Cd_{0.95}Zn_{0.05}Te$ thin films. This films were grown on CdTe(111) substrates by the methods of liquid phase epitaxy. The thickness of pointed films was about 10 μm.

The photoluminescence spectrum of $Cd_{0.95}Zn_{0.05}Te$ thin films at T = 77 K consists of an bound exciton emission band caused by the recombination of free excitons bound on neutral donors D^0X [1] with a peak position $h\nu_m$ = 1.6392 eV and a half-width w = 8.7 meV, and wide emission band associated with the donor-acceptor recombination of shallow donors – A centers [2]. This band is a superposition of two emission bands: D_1 with a peak position $h\nu_m \approx 1.53$ eV and D_2 with a peak position $h\nu_m \approx 1.45$ eV.

At irradiation with fast neutrons the narrowing of the exciton band (up to w = 7.6 eV) was observed. The peak position of the bands did not change, there was a slight decrease in the PL intensity of the excitonic and D_1 bands and a significant decrease in the PL intensity of the D_2 band. In our opinion such changes in the PL spectra of irradiated specimens caused by the respective centers (donors) concentration decrease due to their interaction with radiation-induced defects or complexes formed by them.

It is known that irradiation with fast neutrons leads to the creation of displacement defects in a lattice of bulk material CdZnTe [3], in particular, the formation of Cd-vacancies. Obviously this is true for CdZnTe thin films. Consequently, the fast neutron irradiation of CdZnTe thin films leads to decrease in the concentration of donors (responsible for the high-energy part of the exciton spectrum and the D_2 band) due to their interaction with radiation – induced Cd-vacancies or created by these defects complexes.

1. Glinchuk K.D., Maslov V.P., Strilchuk O.M., Lyapina A.B. *Semiconductor Physics, Quantum electronics and Optoelectronics*.2017.V.20(3).P. 305-313.
2. Schieber M., Schlesinger T.E., James R.B., Hermon H., Yoon H., Goorsky M. *Journal of Crystal Growth*. 2002. V. 237–239**.** P. 2082–2090.
3. Eisen Y., Shor A. *IEEE Transactions on Nuclear Science*. 2009. V. 56(4). P.1700 – 1705.

Comparative Study of Electrical Conductance Dependence on Temperature for RNi_5 (R=Ce, La) Thin Films

Todoran, R.D.[1], Todoran D.C. [1], Szakacs Zs.L. [1]

[1]*Technical University of Cluj Napoca, North University Center of Baia Mare, Baia Mare, Maramures, Romania, todoran_radu@yahoo.com*

This work presents a comparative study of the temperature and thickness dependent electrical conductivity of six different pulsed laser deposited $LaNi_5$, respectively $CeNi_5$ nanoscale films. Electrical conductivity was measured using the classical four-probe method [1]. All the measurements were made at temperatures ranging from 80K to room temperature. The chosen deposited film thicknesses are representative for three different conduction regimes. The lowest thickness films of 68nm for $LaNi_5$ and 45nm for $CeNi_5$ display a semiconductor-like increasing conductivity with temperature, up to around 270K. Electrical conductivity has an approximately constant value over a large temperature domain up to around 270K for film thicknesses of 110nm, in the case of both semi-metallic alloys. The thickest studied films, of 180nm for $LaNi_5$ and 220nm for $CeNi_5$, display a metallic conductivity, which decreases with temperature over the whole temperature domain. This decreasing metallic conductivity behaviour is also recovered by the other four studied thinner films over an approximate temperature value of 270K.

The different conduction regimes can be explained by the film deposition patterns. For the thinner films one has the case of insular depositions. Increasing temperature activates the surface state electrons, which can tunnel to the nearest isles, for lower temperatures. At higher temperatures they gain enough thermal energy to hop between the isles. The thickest films exhibit a metallic behaviour because almost all inter-insular gaps disappear now, and the deposited films behave like the bulk compound. For the middle thickness films, the two different conduction mechanism, the decreasing-type metallic one and the activated-type semiconductor one, seems to compensate each other's effect, so that, electrical conductivity is almost constant on a temperature domain of 200K.

Studying these behaviours on a Richardson plot can lead to the identification of the involved energy band gaps [2,3].

1. Valdes, L.B. Resistivity measurements on germanium for transistors. *Proc. Inst. Rad. Eng.* 1954. V. 42, No 2. P. 420–427.
2. Todoran, R., Todoran, D., Racolta, D., Szakacs, Zs. Electrical and Optical Properties of $CeNi_5$ Nanoscale Films, *Nanoscale Res. Lett.* 2016. V. 11, No 253. P. 1-10.
3. Todoran, D., Todoran, R., Szakacs, Zs., Anitas E. Electrical Conductivity and Optical Properties of Pulsed Laser Deposited $LaNi_5$ Nanoscale Films, *Materials* 2018. V. 11, No 1475. P. 1-19.

Theoretical Fundamentals and Electrolysis Conditions Influence on Tungsten Thin Films Electrodeposition from Halide-Oxide and Oxide Melts

Uskova, N.N.[1], Shakhnin, D.B.[2], Pasishnyk O.V.[2], Malyshev, V.V.[1,2]

[1]*Institute of General and Inorganic Chemistry, Kyiv, Ukraine,* *viktor.malyshev.igic@gmail.com*

[2]*University "Ukraine", Kyiv, Ukraine,* *viktor.malyshev.igic@gmail.com*

The tungsten coatings were deposited from KCl-NaCl-Na_2WO_4-$NaPO_3$ or Na_2WO_4-$NaPO_3$ systems electrochemically. The effect of Na_2WO_4 and $NaPO_3$ concentrations, temperature, cathodic current density, and electrolysis duration changes on the deposits composition and structure was investigated, and the optimal conditions for reversive current mode were found for deposition.

The tungsten coatings from the KCl-NaCl-Na_2WO_4-$NaPO_3$ melts were deposited when the concentration conditions met the following conditions: $0.02<[PO_3^-]/[WO_4^{2-}]<0.18$.

Continuous tungsten coatings were obtained from halide-oxide electrolytes at 973-1073 K and cathodic current density up to 25 A/dm^2, and from oxide electrolytes – at 1023-1123 K and cathodic current density up to 40 A/dm^2.

The effect of the cathodic current density, as well as of the electrolysis duration and the reversive deposition mode usage, was studies in KCl-NaCl-2.5 mol.% Na_2WO_4-0.35 mol.% $NaPO_3$ and Na_2WO_4-5 mol.% $NaPO_3$ melts. Continuous, adherent, and nonporous coatings were obtained at 923-1173 K with current densities 1-15 and 3-25 A/dm^2, respectively.

Coatings grains size showed a minimum between current densities 2.5 and 25 A/dm^2. Tungsten deposition rate for studied current densities was 5-15 μm/h for halide-oxide electrolytes and 20-45 μm/h for oxide electrolytes. Tungsten deposition current efficiency was up to 60% and 95 %, respectively, dropping with electrolysis duration increase.

Continuous and adherent tungsten coatings were obtained from halide-oxide electrolytes on nickel, copper, graphite, tungsten, and molybdenum. From oxide melts, such coatings were obtained also on different steels and copper- and nickel-plated titanium.

Profilometric study shows that, as the deposit thickness increases, its single-phase fine-crystalline structure transforms into a coarser one. We tried to prevent the formation of a coarse-grained structure by applying reversive electrolysis mode. The cathodic to anodic periods duration ratio was varied from 15 up to 50 with the anodic period duration from 0.5 to 3.0 s and the anodic current density varying from 20 up to 50 A/dm^2. The following conditions were optimal for Na_2WO_4-5 mol.% $NaPO_3$ electrolyte at 1173 K: i_c = 15 A/dm^2, i_a = 30 A/dm^2,τ_c = 25 s, τ_a = 1.5 s. In this case, smooth coatings up to 0.5 mm thick were obtained at the cathode.

The Influence of Silver on the Molybdenum Carbide Thin Films Electrodeposition from Tungstate-Molybdate Melts

Uskova, N.N.[1], Shakhnin, D.B.[2], Rybalchenko D.S.[2], Malyshev, V.V.[1,2]

[1]*Institute of General and Inorganic Chemistry, Kyiv, Ukraine,* viktor.malyshev.igic@gmail.com

[2]*University "Ukraine", Kyiv, Ukraine,* viktor.malyshev.igic@gmail.com

The effect of silver on the electrochemical deposition of Mo_2C coatings was studied earlier in a Na_2WO_4-Na_2MoO_4-5 mol % MoO_3-10 mol % Li_2CO_3 melt. Nickel plates (10 x 20 x 1 mm) were used as the cathodes. Electrochemical deposition of Mo_2C was performed at 1073 -1223 K and cathodic current density of (2-50) x 10^2 A/m^2. The deposit was subjected to X-ray analysis and profilometric analysis. The thickness of the coatings were measured by a high-speed indicator 2IGM.

Small additions of Ag_2MoO_4 (10^{-3} – 10^{-2} mol %) to the previously studied electrolyte result in significantly decreasing the roughness of the electroplate (the profile amplitude becomes lower than 1 μm instead of 2-3 μm) and increasing its maximum thickness to 150 um. However, when Ag_2MoO_4 content exceeds 10^{-2} mol %, the deposit becomes spongy and their adhesion to the substrate worsens.

At 1073 K and Ag_2MoO_4 content 10^{-3} – 10^{-2} mol % the spongy deposits Mo_2C-Ag are formed. In a temperature range of 1073 to 1123 K thin (up to 10 μm) deposits are obtained, while above 1223 K they are again non-adhered and spongy. The optimum is a range from 1123 to 1173 K.

When cathodic current density is lower than 5 A/dm^2, the metallic silver is mainly deposited, within the range 5-15 A/dm^2 it is a Mo_2C-Ag coating with proper adhesion, and at a higher current density the dendrites rapidly begin to grow.

The co-deposited silver increases the free corrosion potential of Mo_2C by 0.7 - 0.8 V, i.e. from -1.05 ± 0.05 to-0.35 ± 0.05 V.

Weight loss of the samples with a Mo_2C-Ag electroplate after a 34-day test in the Na_2S_3 melt at 623 K is 3.5 ± 0.5 g/m^2, which is comparable to the losses of the diffusionally chromized Steel 45. This testifies the applicability of the electroplating for corrosion protection of containers for sodium-sulphur chemical cells.

Electrochemical behaviour of silver in tungstate-molybdate melts was studied. The electrodeposition of silver proceeds according to the single-electron reversible mechanism and is diffusionally controlled. The effect of silver on the electroplating with molybdenum carbide was also studied. Conditions for proper electroplating were experimentally determined. The electroplates may be recommended for pilot corrosion protection of containers for sodium-sulphur chemical cells.

POSTER REPORTS
Session 2
Nanotechnologies and nanomaterials, quantum-size structures

Spectral and Luminescent Properties Of Sb-Containing Sol-Gel Silica Glasses Co-Doped with Al and B

Akinshau K.A.

B.I. Stepanov Institute of Physics, NASB, Minsk, Belarus, akinshau@ifanbel.basnet.by

The main aim of the work was to synthesize Sb^{3+}-doped sol-gel silica glasses and to study its structure and spectral and luminescent properties.

Silica glasses of the following systems Sb_2O_3-SiO_2, Sb_2O_3-B_2O_3-SiO_2, Sb_2O_3-Al_2O_3-SiO_2 were synthesized. The modified sol-gel technique followed by the heat treatment at different temperatures were used for glass synthesizing. Studying of the spectral and luminescent properties of the samples was carried out on the DRON 3.0 diffractometer, the LEO 1420 SEM-microscope, the Cary-500 spectrophotometer and the SDL-1 spectrofluorometer.

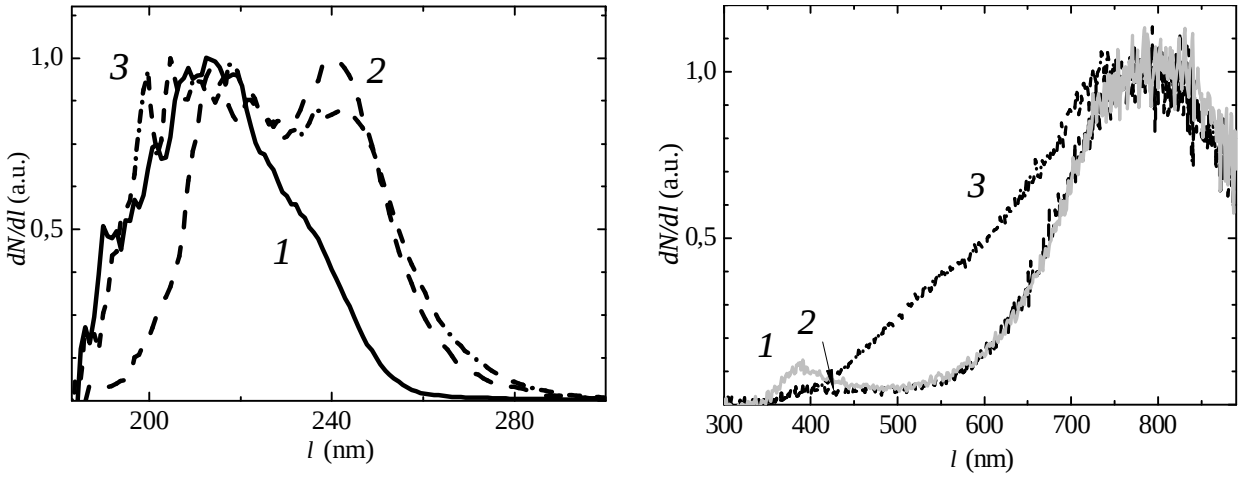

Figure 1 – Excitation (a) and luminescence (b) spectra of sol-gel silica glasses of the systems Sb_2O_3–SiO_2 (1), Sb_2O_3–B_2O_3–SiO_2 (2), Sb_2O_3–Al_2O_3–SiO_2 (3). λ_{exc} = 270 nm, λ_{reg} = 750 nm.

The X-ray structural analysis of the glasses showed the samples haven't any nanostructured centers until the ≤ 4 mass % of the doping compounds summary concentration. The absorption spectra of the samples are transparent in the visible range and the near UV and the near IR. The UV absorption bands of the Sb- and the Sb–B-containing silica glasses are almost equal and they are characterized with the high steep long-wave edge, but the similar steepness of the Sb-Al-containing silica glass absorption band is less. The luminescence spectra of the glasses have a complex structure: the Sb- and Sb–B-containing glasses have wide and intensive bands at 790 nm and slight and relatively narrow bands with the maximum about 390 nm (Fig. 1b, 1st & 2nd curves). The additional wide band of the medium intensity at 550 nm appears in the luminescence spectrum of the Sb–Al-containing glass (Fig. 1b, 3rd curve). The excitation luminescence spectra (Fig. 1a) of all the silica glasses have the weakly-resolved structural bands at the near vacuum and solar-blind UV.

Intramolecular Structure and Conductive Characteristics of Polyethylene Composites with Multi-Wall Carbon Nanotubes and Dyes

Alieksandrov M.A., Pinchuk-Rugal T.M., Dmytrenko O.P., Kulish M.P., Poprugko V.M.

Taras Shevchenko Kyiv National University, Kyiv, Ukraine, mmarafon@gmail.com

Polyethylene (PE) due to its satisfactory mechanical properties, high plasticity, relatively low cost, is used in many technological processes. In order to improve its characteristics, composites with many wall carbon nanotubes MWCNT) are manufactured, which, due to their exceptional characteristics, such as geometrical sizes, conductive and mechanical properties, are widely used as fillers for the creation of polymeric composites. In addition, as filler is still used squarine dyes (DBSQ). When added to the polymer of dye as a filler, the electrical conductivity of the polymers increases, because of the increase in the efficiency of the thermopole generation of charge carriers in the volume of the polymer.

The intramolecular structure and conductive characteristics of nanocomposites PE - MWCNT and PE - MWCNT - DBSQ have been studied. It is shown that for nanocomposites PE - MWCNT and PE - MWCNT - DBSQ there is a change in the intramolecular structure, and the reorganization of the polyene sequences, which manifests itself in the displacement of the vibrational modes ν(C-C), ν (C = O), ν (CH_2) in the Raman spectrum and the emergence of new emission centers in the PL spectra. It is established that in the nanocomposite PE - MWCNT the electrical conductivity is improved by Ϭ 10 cm / cm, while in the nanocomposite PE - MWCNT - DBSQ there is a slight decrease by Ϭ ≈ 1 cm / cm, which is related to the aggregation of MWCNT and DBSQ.

The Influence of Magnetic Oxygen Vacancies on Resonant Phenomena in Co/Al_2O_3 Nanocomposite Films

Baibara A.E.[1], Bugaiova M.E.[1], Lashkarev G. V.[1], Radchenko M.V.[1], Stelmakh Y.A.[2], Krushynskaya L.A.[2], Knoff W.[3], Story T.[3], Dmitriev A.I.[1]

[1] *I.M. Frantsevich Institute for Problems of Material Science, National Academy of Sciences of Ukraine, Kyiv, Ukraine, gvl35@gmail.com*

[2] *E.O. Paton Electric Welding Institute, National Academy of Sciences of Ukraine, Kyiv, Ukraine*

[3] *Institute of Physics, Polish Academy of Sciences, Warsaw,Poland*

Air-bearing (oxidation) of films of ferromagnetic nanocomposite Co/Al_2O_3 without special protection results in a significant change in their magnetic properties. The anomalous low-temperature damping of superparamagnetic (SPMR) and ferromagnetic (FMR) resonances in nanocomposite (NC) films are observed [1]. The low temperature damping of the giant thermoelectric power (GTEP) have also been observed [2].The observable was analyzed taking into account the complicated structure of Co shell. The possible sources of perturbations are an ensemble of magnetic oxygen vacancies on the interface $CoO\text{-}Al_2O_3$. The interface of Co nanoparticles (NP's) forms an antiferromagnet CoO in the oxygen-containing matrices. Pair interaction of the two doubly charged identical surface defects (oxygen vacancies) has an magnetic state with the maximal exchange energy at the definite distance between the defects ($5 \div 25$ nm) [3]. Thus, the ferromagnetic resonance for Co / Al_2O_3 (43.2 at.% Co), which disappeared at oxidation at $T < 120$ K, after oxidation, was observed over a wide temperature range of $300 \div 3$ K. This is possible in the case of saturation of the film with oxygen (oxidation), which leads to filling the magnetic vacancies of oxygen, one of the causative factors affecting the ferromagnetic resonance. The latter confirms the existence of magnetic vacancies of oxygen in the interface layer of cobalt nanoparticles and the important role of interfaces in the formation of the properties of ferromagnetic nanocomposites.

Therefore nontrivial damping in SPR, FMR and GTEP in magnetic nanocomposites of Co/Al_2O_3 films probably is due to the conflict between ferromagnetic Co NP's and magnetic state in NP's shells.

1. Dmitriev A., Lashkarev G., Radchenko M. et al. *44th International School and Conference on the Physics of Semiconductors, 2015 June 20-25, Jaszowiec, Poland*, 2015, P. 219.

2. Lashkarev G, Radchenko M., Dmitriev A. et al. *Phys. Stat. Sol. (b)*, vol. 254, 2017, P.1700153.

3. Morozovska A., Eliseev E., Glinchuk M. et al. *Phys. B.* 2011 Apr. 15; 406(9): P.1673-1688.

Synthesis and Optical Properties of Quantum Dots ZnSe:C

Bardashevska[1] S.D., Budzulyak[1] I.M., Budzulyak[2] S. I., Rachiy[1] B.I., Yablon[1] L.S., Morushko[1] O.V.

[1]*Vasyl Stefanyk Precarpathian National University, Ivano-Frankivsk, Ukraine, ivan-budzulyak@ukr.net*

[2]*V.E. Lashkaryov Institute of Semiconductor Physics NAS of Ukraine Kyiv, Ukraine*

For the implementation of semiconductor quantum dots with high quantum efficiency, several methods have been developed that allow them to be obtained in corresponding matrices. The promising material of the matrix is nanoporous carbon, which can be controlled to obtain the required pore size.

To obtain ZnSe:C quantum dots, 0.8 g of gelatin, 0.8 g of carbon and 50 ml of distilled water were used, the resulting mixture was heated to 200 °C and kept for 3 hours, followed by natural cooling to room temperature. Subsequently, ZnSe were added, carefully stirred, heated to 200 °C and held for 2.5 hours.

PL spectra measured at different excitation wave-lengths at room temperature (T=300 K) and low excitation density. At the excitation with λ = 466 nm a single intense PL band is observed, centered at λ = 643 nm (1.928 eV), that has near –Gaussian line shape. Taking into account that the energy band gap of bulk ZnSe at room temperature is of 2.7 eV (459 nm) the PL emission is spectrally shifted to red side by 0.772 eV. In order to get more information about the origin of 643 nm emission the PL excitation spectrum has been recorded at the l =643 nm, at room temperature. At 466 nm there is a strong resonance. The latter implies that the 466 nm transition mainly contributes the emission at 643 nm. While this resonance is observed very close the ZnSe band edge one can attribute it to the exciton transition. However the exciton binding energy in ZnSe is ~ 14 meV and at room temperature the excitons will be dissociated. On the other hand we do not see any near band emission. Therefore, the peak near the band edge in the excitation spectrum can be assigned to the highest transfer efficiency of photogenerated carriers at the correlated sub-band states (about 34 meV below the conduction band of ZnSe) to the deep center states.

Modeling of Photon Crystals of Microwave Range Using Interference Matrixes

Bilozeretseva V.[1], Diakonenko N.[1], Ovcharenko O.[2]

[1] *National Technical University "Kharkiv Polytechnic Institute", Kharkiv, Ukraine, dnina490@gmail.com*

[2] *V.N. Karazin Kharkiv National University, Kharkiv, Ukraine, apomira20b@gmail.com*

The ability to control the properties of photonic crystals by changing the parameters of the layers allows you to create unique optoelectronic devices. In this connection, the actual problem of modern optics is the study of defect modes arising due to the violation of periodicity in photonic crystals. The results of theoretical and experimental studies in artificial media (metamaterials) are known today. The spectral characteristics of an anisotropic wire metamaterial with a spatial defect in the microwave range were analyzed in [1]. An analysis of the dependences of the positions of transmission peaks in the frequency range 22-40 GHz, corresponding to the occurrence of defect modes, from the thickness of the defect layer, demonstrated a good agreement with the experimental results. The calculation was careered out for a defect layer with a thickness of d= 9 mm. It is shown that with an increase in the thickness of the defective layer, the peaks of the defective modes shift to low frequencies.

There is a well-developed theory of interference of multilayer coatings, which describes the behavior of forbidden and allowed zones (areas of high reflection and high transmittance) [2]. The calculation programs make it possible to obtain the given optical characteristics (reflection, transmission, etc.) for any multilayer coatings using the matrix method.

In this work, we simulated the transmission spectra of photonic crystals given in [1]. An interference mirror with quarter-wave optical thicknesses of alternating layers with normal incidence of light is taken as a basis. A system with a defective layer is a conventional interference filter with a half-wave separation layer. The results obtained are in good agreement with those given in [1].

Literature.

1. Ивженко И., Юдина Д. И., Тарапов С. И. // Радіофізика та електроніка. -2017.- Т.22. № 2.-с.11-16.
2. Macleod H. A. Thin-Film Optical Filters. Bristol: Adam Hilger Ltd., 332p (1986).

Impedance Studies of Lithium Superionic Conductors at Different Temperatures

Boichuk A.M., Gasyuk I.M., Boichuk T.Ya, Chervinko D.V., Grabko T.V.

Vasyl Stefanyk Precarpathian University, Ivano-Frankivsk, Ukraine, andboi8891@gmail.com

Lithium superionic conductors (LISICON) are used often as solid-state electrolites for lithium power sources. This allows to obtain reliable batteries without liquid electrolyte, which often leads to degradation of parameters of such power supplies. The conductivity of LISICON - materials is important - the amount of conductivity influence on the specific capacity of batteries on their basis. In addition, important is understanding of conduction mechanisms. In this work, impedance studies of nanosized powders Li_4SiO_4 were committed at different temperatures.

For synthesis, lithium oxide (Li_2O) and silicon dioxide (SiO_2), the masses of which were calculated in a stoichiometric ratio, are used. Silicon dioxide was added to a solution of lithium oxide in distilled water. After that, citric acid was added to reach the desired pH level (8). Obtined gel was dried and burned for 4 hours at 800C. The results of the x-ray analysis indicate the formation of the phase of lithiated silicon oxide (94% by mass). Impedance studies were performed on spectrometer AUTOLAB in frequency range 0.01-100000 Hz.

Impedance spectra at different temperatures are shown in figure 1.

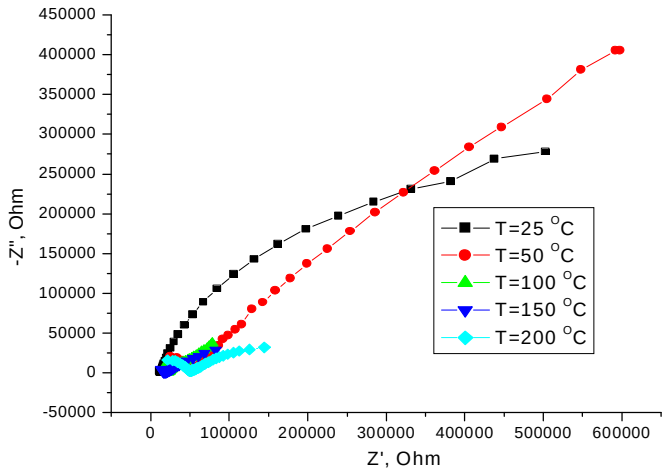

Figure 1. Impedance spectra of LISICON at different temperatures

At the whiskers of the temperature, the spectra have a branch inclined at an angle of 45 degrees. This indicates that there is a stable ionic strength. It is realized by the migration of lithium at crystalline positions at low frequencies. These materials can be used smoothly as solid electrolytes for power sources and capacitors.

Synthesis, Structural and Morphological Properties of $Ni(Oh)_2$ / Reduced Graphene Oxide Composite Materials

Boichuk V.M, Bandura Kh.V., Kotsyubynsky V.O., Yaremiy I.P., Hodlevska M.A.

Vasyl Stefanyk Precarpathian National University, Ivano-Frankivsk, Ukraine,
kotsuybynsky@gmail.com

Hybrid supercapacitors successfully combine different mechanism of energy storage (fast Faradaic reactions and the electric double layer formation). Among the perspective materials for redox electrode (RuO_2, MnO_2, MoO_3) $Ni(OH)_2$ has high theoretical capacitance, but low electrical conductivity restricts its efficiency. The formation of $Ni(OH)_2$ / reduced graphene oxide (rGO) composite materials allows improving the material's capabilities.

Ultrafine β-$Ni(OH)_2$ was synthesized by hydrothermal route with the presence of PEG 6000 as a surfactant. Graphene oxide was synthesized by Hammers method. The reduction of graphene oxide (GO) was carried out under the hydrothermal conditions using hydrazine hydrate. β-$Ni(OH)_2$ /rGO composite materials (CM) were prepared by ultrasound treatment at different mass ratio of the components. The broadening of (001) diffraction peak is an evidence of dominant particle growth (average size of about15 nm) along the [100] and [110] directions that caused plate-like morphology (confirmed by SEM). The preferred orientation degree of β-$Ni(OH)_2$ crystallites was calculated by analysis of intensity ratio between (001) and (101) reflexes for CM with different rGO contents. The increasing of intensity ratio between (001) and (101) with the increasing of rGO contents was observed that corresponds to increasing of the preferred growth degree. It can be assumed that ultrasonic dispersion leads to the rGO fragments insertion into the interplanar spaces of β-$Ni(OH)_2$ that is in good agreement with SEM data. Specific surface areas (SSA) for pure rGO and β-$Ni(OH)_2$ sample were of about 402 and 20 m^2g^{-1}, respectively. The linear increasing of SSA at graphene content increasing was observed. The electrical conductivity mechanisms for $Ni(OH)_2$ / rGO CM was analyzed by impedance spectroscopy in the temperature range of 25-200°C. The obtained results open the possibility of $Ni(OH)_2$ / rGO properties flexible control.

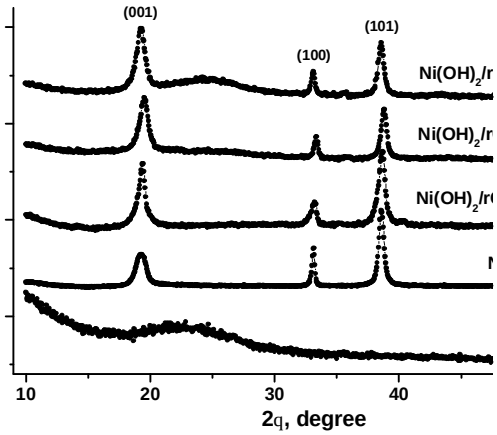

Fig.1. XRD patterns of $Ni(OH)_2$ / rGO CM

Ionic Strength-Responsive Bioarhitectures: Analysis within the Model of Variative Refraction

Boltovets P.M., Snopok B.A.

V.Ye. Lashkaryov Institute of Semiconductor Physics NASU, Kyiv, Ukraine,
paraskeva2013@gmail.com

Stimuli-responsive materials get a lot of interest during last years due to their ability to tune their structure and functional properties in response to the external stimuli. Special attention should be paid to bioarchitectures which can be applied in biosensing, medicine, environmental monitoring, bioelectronics. However for the analysis and prediction of the behavior of such a system adequate methods are needed. The model of variative refraction earlier proposed by us can be useful for the analysis of such complex systems. Indeed, the response of surface plasmon resonance (SPR) transducer depends not only on the thickness of the layer, but also on the change in the refractive index within the layer itself. Thus, variations in the density of the molecular layer can also affect the response value by changing the refractive index inside the layer. To identify possible changes in interfacial organization, the immobilization of trypsin molecules on polymer brushes has been investigated. It was shown that in this case the SPR response specific for the trypsin fixed on the brush decreases with increasing the concentration of NaCl in the solution. Analysis based on the variative refraction approach indicates the decreasing of the thickness of the molecular layer. At the same time, the refractive index demonstrates relatively constant value up to the concentration of NaCl above 0.1 M. The obtained results indicate that at small levels of ionic strength the redistribution of flexible fragments of brushes with immobilized trypsin molecules change their spatial distribution by moving closely to the surface without essential changes of their density.

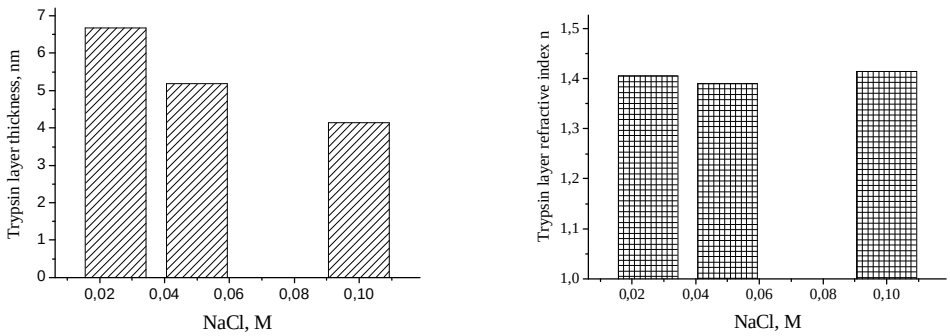

Fig.1.Dependance of the thickness of the trypsin layer and its refractive index on the NaCl concentration in the solution

This research was partly funded by the NATO Science for Peace and Security Programme under the Grant G5140 and Projects of the National Academy of Sciences of Ukraine. The authors wish to thank Dr E.Brynda (IMC ASCR) for polymer brushes samples.

Theoretical and Experimental Studies of Cr(Vi)-Containing Molecular Anions Adsorption on the Surface of Carbon Nanostructures

Borysiuk V., Nedilko S., Hizhnyi Yu.

Taras Shevchenko National University of Kyiv, Kyiv, Ukraine, borysyukviktor@gmail.com

Molecular anions of hexavalent metals like Cr(VI) are harmful and widely-spread industrial pollutants, and their removal is an urgent technological problem. One of the most promising methods of removal of such toxic compounds is grounded on their adsorption on artificial adsorbents. At present, carbon nano-structured materials are intensively studied as adsorbents for efficient removal and storage of various toxic pollutants, including molecular complexes of hexavalent metals. Theoretical modeling of molecular adsorption on the CNTs and graphene surfaces is a powerful tool that allows prediction of some important properties of materials perspective for removal and storage of Cr(VI)-containing oxyanions.

In this work we present results of the electronic structure calculations and related analysis for adsorption of CrO_4^{2-}, $Cr_2O_7^{2-}$ and $HCrO_4^{-}$ oxyanions on several types of CNT surfaces (undoped, B- and N-doped CNT(3,3), CNT(5,5) and grapheme sheets). Graphene sheets were considered as a model approximation for high-diameter CNTs. Geometry-optimized calculations of the electronic structures were carried out at the density functional theory (DFT) level within molecular cluster approach using Gaussian 09 software package [1]. Relaxed geometries, binding energies between the adsorbates and the nanotubes, charge states of the adsorbates were calculated and analyzed.

The calculation results are analysed together with experimental spectra of optical absorption and luminescence. As absorption, as well as the luminescence spectra of the systems containing carbon nanostructures measured before and after adsorption of chromate anions reveal substantial difference that confirms the principal possibility of the optical monitoring the CrO_4^{2-} anion adsorption on carbon nanostructures. The calculation and experimental results were discussed in view of potential application of the CNT-based materials as efficient adsorbents of Cr(VI)-containing molecular anions.

1. Frisch M.J., Trucks G.W., Schlegel H.B., et al. // Gaussian 09 (Gaussian, Inc., Wallingford, CT, 2009).

Metal Nanoparticles –Semiconductor Nanocrystals Composites

Budzulyak S.I., Kapush O.A, Korbutyak D.V., Ermakov V.M.,
Kosinov O.H., Kulchytskiy B.N., Gatilov S.E.

V.Ye. Laskaryov Institute of Semiconductor Physics of NAS of Ukraine,
Kyiv, Ukraine, buser@ukr.net

The size and shape controlled metal nanoclusters has drawn a considerable research interest due to their tremendous applications in optics, biology, catalysis and biomedicine. Metal nanoparticles (NPs) – semiconductor nanocrystals (NCs) composite materials remain a frontier area of research for the development of optoelectronic, photovoltaic and light harvesting devices because they are promising materials for photon harvesting.

Colloidal synthesis was carried out by the use of ions of cadmium precipitated by ions of tellurium under an argon atmosphere in a three-necked flask equipped an electromagnetic mixer, thermometer, partitions and valves. Deionized water has been used as the solvent. For stabilization of CdTe NCs surface during the synthesis tioglycol acid were used. Au NPs with different sizes was also formed by the method of colloidal synthesis.

Thiol-stabilized CdTe NCs and Au NPs from aqueous synthesis act as building blocks for the hybrid material. In this paper, the Au NPs/CdTe NCs nanocomposite films were fabricated using a layer-by-layer self-assembly technique. The obtained structures were characterized by means of absorption spectroscopy and photoluminescence (PL) spectroscopy.

PL spectra showed that Au NPs incorporation resulted in an increase of PL intensity compared with that of the samples without Au NPs. PL enhancement of Au NPs/CdTe NCs nanocomposite films can be controlled by tuning the thickness of spacer layer between the metal nanoparticles and semiconductor NCs. The influence of the spacer layer thickness on the variations of PL intensity of NCs was analyzed. In addition, the effect of the size of Au NPs on the plasmonic interaction was studied. Optical absorption spectra exhibited the incorporation of Au NPs boosted the absorption of Au NPs/CdTe NCs nanocomposite films. Some possible mechanisms by which localized surface plasmon fields can enhance nonradiative relaxation processes of any quantized electronic excitations are proposed.

The diffusion layer formation at the aluminum surface in the nonequilibrium conditions of electrolyte plasma

Fedorenkova L.I.

Oles Honchar Dnipro National University, Dnipro, Ukraine, Luba.Fed@gmail.com

The diffusion layer formation on aluminum and its alloys in nonequilibrium conditions of electrolyte plasma was investigated. The treatment of aluminum and its alloys in electrolytic plasma was carried out in the laboratory conditions in the electrolysis regime: U=30-80V, j=0,3–1,8A/sm^2, t=10-30min. The electrolyte was an aqueous solution with boron carbide powder. The anode was an electrode made of stainless steel; cathodes were samples from aluminum and its alloys. The samples treated in electrolyte plasma were analyzed by X-ray diffraction, metallographic, and spectral analysis.

Metallographic analysis of the aluminum and its alloys surface treated in electrolyte plasma, showed the diffusion layer of 30 to 80 μm in thickness and with microhardness, changing in depth from 10 GPa to 4 GPa, depending on the saturation regime and aluminum alloy composition was formed.

X-ray structural analysis showed that the following compounds: α-AlB_{10}, α-AlB_{12}, γ-AlB_{12}, α, β-AlB_3H_{12}, $NaAlH_4$ and AlH_3 hydrides formed in the nanostructures of the layer distributed mainly along grain boundaries, phases, microdefects.The size of the nanostructures is estimated by the method of Selyakov-Sherer. For technically pure aluminum, depending on the electrolysis regime, the nanostructures dimension is from 6 nm to 22 nm, and for the annealed specimens at 473 K is 45 nm and 88 nm. It is established that with increasing current density, the size of nanostructures decreases. A characteristic feature of the aluminum hydrides formation in nonequilibrium conditions of electrolyte plasma is to obtain of almost all polymorphic modifications $(AlH_3)_n$ and AlB_3H_{12}.

Diffusion in the electrolyte plasma is carried out in a hydrogen environment, where the hydrogen atoms have the highest energy and are one of the main forces that activate the diffusion process, affecting the structure, composition and micromechanical characteristics of the diffusion layer. The diffusion process into metals under electrolyte plasma conditions is characterized by high heating and cooling rates. Rate of boron penetration into the metal is, approximately, 20 μ/min. In the process of diffusion boron on the one hand hinders the hydrogenation of aluminum and unlike hydrogen, forms with aluminum atoms more stable bonds, and on the other hand promotes hydrogen retention even with an increase in temperature up to the melting point of aluminum.

Treatment aluminum alloys can be used at a temperature above the maximum operating temperature of the working parts of aluminum, and as a conductor with hole conductivity. In addition, it is possible to use in the nuclear industry due to the large neutron absorption radius of boron.

Quantumchemical Calculation of ^{29}Si NMR Spectrum of Silicic Acid Molecules $[HOSiO_{1.5}]_n$

Filonenko O., Kuts V., Lobanov V.

A.A. Chuiko Institute of Surface Chemistry of National Academy of Sciences, Kyiv, Ukraine, filonenko_ov@ukr.net

There are many synthesized silica structures nowadays, such as silica films, nanotubes, nanospheres, nanoparticles of amorphous silica. However some physical and chemical aspects of silica nanoparticles formation have not been fully explained yet.

Most of silica materials are received by using sol-gel and hydrothermal method of synthesis. Experiment shows at the initial stages of synthesis in solution during the first hours of sol-gel synthesis different oligomers are forming. The formed oligomers are: dimers, linear trimers and tetramers, cyclic trimers and tetramers, prismatic hexamers, cubic octamer and other oligomers with more elaborated structure.

A powerful tool to identify species present in silicic acid solutions is a nuclear magnetic resonance spectroscopy of ^{29}Si (NMR) which allows making conclusions about polymer structure in solutions without changing its state.

In this paper we have been calculated ^{29}Si NMR spectra of fullerene-like molecule $[HOSiO_{1,5}]_{20}$. We consider we can prove the possibility of formation of fullerene-like structures in solution during synthesis of silicon dioxide based systems by researching the influence of polysilicic acid degree of condensation N (N = 2, 4, 8, 10, 20) on calculated ^{29}Si NMR spectra.

^{29}Si NMR spectra was calculated according to Gaussian 09 (D. 01) program using density functional theory (the functional B3LYP, basis set 6-311+G (2d, p) and GIAO (Gauge invariant atomic orbitals) method for the optimized structures related to DFT approach (B3LYP/6-31G(d, p)/PCM without symmetry restrictions). ^{29}Si chemical shifts were calculated according to TMS.

Comparing of ^{29}Si NMR spectra of different silicic acids (n = 1, 2, 4, 8, 10, 20) proves the signals of all the frame-like structure molecules are belong to the one range of the spectrum (δ = - 98 – - 113 ppm). We can clearly see the positions of the lines which make isolated silanol groups (δ = - 106 – - 113 ppm) and hydrogen bound silanol groups (δ = -98 – -107 ppm). $[HOSiO_{1,5}]_{20}$ fullerene-like molecule gives an intensive signal in the range of – 102 – -105 ppm. The results we have received from analysis of ^{29}Si NMR spectra for silicic acids (n = 1, 2, 4) and the frame-like structure silicic acids (n = 8, 10, 20) could be helpful in assigning signals of unknown silica structures in ^{29}Si NMR spectra.

Formation of Indium Nanowires on (100) Surface of In_4Se_3 Layered Crystal

Galiy P.V.[1], Nenchuk T.M.[1], Mazur P. [2], Poplavskyy O.P.[3]

[1] *Electronics and Computer Technology Department, Ivan Franko Lviv National University, Lviv, Ukraine, galiy@electronics.lnu.edu.ua*

[2] *Institute of Experimental Physics, University of Wroclaw, Wroclaw, Poland*

[3] *Vasyl Stefanyk Precarpatian National University, Ivano-Frankivsk, Ukraine*

Nanofabrication of metal nanowires (NW's) on flat or textured substrate surfaces, which uses the phenomenon of self-organization of such structures under the influence of surface relief, is now an important area of research.

We report on obtaining the array of NW's with controlled transverse cross section due to the thermal activation of the surface migration of indium atoms, which are deposited as a result of the thermal evaporation of indium in an ultrahigh vacuum on the cleavage (100) surface of In_4Se_3 crystal with a characteristic furrowed structure, which acts as a natural high resolution template. The orientation effect of the In_4Se_3 (100) surface furrowed structure on the formation of indium nanostructures was reported in [1]. It has been found that elongated indium nanostructures are formed in the direction of furrows on the surface (100) of the In_4Se_3 crystal, that is, in the direction of ***c*** axis.

The morphologies of the surfaces - initial, after indium deposition onto the surface and after thermal annealing at 500 K were investigated by scanning tunneling microscopy (STM). The degree of surface metallization was analyzed using scanning tunneling spectroscopy (STS). The STM/STS data were obtained using the Omicron NanoTechnology STM / AFM System at ultrahigh vacuum of 10^{-10} Torr. STM images were acquired in constant current mode. The STS data were obtained in the mode of current imaging tunneling spectroscopy (CITS). The NW's ordering on the surface was analyzed by computer processing of output images in the WSxM application using a 2D fast Fourier transform.

Obtained result is based on the effect of self-organization according to the vapor phase - solid phase - solid phase technology. That is, the formation of ordered nano structures occurs as a result of the solid state dewetting process. In addition to the furrowed structure of In_4Se_3 (100) surface, the factor affecting the formation of 1D metallic structures is the presence of the, so-called, natural wetting layer on the surface, or In^+ atoms from the structure of the In_4Se_3 crystal.

1. Galiy P.V., Mazur P., Ciszewski A., Nenchuk T.M., Yarovets' I.R., Dveriy O.R. Structural aspect of formation of a nanosystem of In/In_4Se_3 (100). *Metallofiz. Noveishie Tekhnol*. 2018. V. 40, №10. P.1349-1358.

Spectra of Porous *p*-Si (100) in the Near Infrared Range

Gentsar P.O.[1], Vuichyk M.V.[1], Isaev M.V.[2], Lischuk P.O.[2]

[1]*V.Ye. Lashkarev Institute of Semiconductor Physics of NAS of Ukraine, 03028, Kyiv, pr. Nauki 41, tel .: 38-044-525-84-37, Ukraine, rastneg@isp.kiev.ua*
[2]*Taras Shevchenko National University of Kyiv, Volodymyrska ave, 64, 01601, Kyiv, Ukraine*

Most of the properties of materials that consist of grains of micrometers (nanometers) sizes strongly depend on their specific surface. An effective method of increasing the specific surface of the sample is to reduce the size of its grains. Another method of increasing the specific surface *S* is to make small volumes in the bulk material.

In this paper we present the results of investigations of optical reflection spectra and transmission spectra of porous silicon *p*-Si (100) with pore sizes of 5 μm and 50 μm with porosity of 45%, 55% and 65%, as well as silicon wires with lengths 5.5 μm, 20 μm and 50 μm and 60% porosity of nanowires l_{NW} in 200 ÷ 1800 nm spectral range.

Samples of porous *p*-Si with different porosity were made by electrochemical etching of the surface of Si plates in a solution of concentrated hydrofluoric acid (49% HF in water) and pure ethanol. In the work, the porosity (45%, 55% and 65%) and the thickness of the porous layer (5 microns, 50 microns) of specimens varied by applying to the plate controlled by the magnitude of the current density and the duration of etching. Silicon nanowires by liquid chemical etching (MAWCE) were grown. The etching time ranged from 10 to 60 minutes to obtain a layer with different lengths of nanowires.

In the high-energy region of the optical reflection spectra of porous silicon at a pore size of 5 μm two peaks of monocrystalline *p*-Si (100) were seen. In the low-energy region of the reflection spectrum of porous *p*-Si (100) an interference pattern is observed.

The reflection and transmission spectra of porous Si with a pore size of 50 μm and porosities of 45% and 55% are similar to monocrystalline *p*-Si(100). At a porosity of 65% in the low-energy region of the spectrum two peaks appeared with energies of 1.025 eV and 1.07 eV respectively.

In the optical reflection spectra of silicon nanowires in the wavelength range λ = 0.2 - 1.8 μm are found three peaks corresponding to the energies of 0.862 eV; 1.046 eV and 1.198 eV respectively. As the length of the silicon nanowires increases, also the reflection coefficient *R* increases.

According to experimental data and calculations the energy spectra of investigated structures strongly depend on their specific surface. The possibility of controlling the energy spectrum by manage the technology of fabricating structures is analyzed.

Oriented Organic Films on Aligned Polymer Surfaces

[a] Grytsenko K., [a] Lytvyn P., [b] Navozenko O., [c] Kryuchyn A., [d] Ksianzou V., [d]Schrader S.

[a]*Institute of Semiconductor Physics, NASU, Kyiv, Ukraine*
[b]*T. Shevchenko Kyiv State University, Kyiv, Ukraine*
[c]*Institute for Information Recording Problems, NASU, Kyiv, Ukraine, kryuchyn@ipri.kiev.ua*
[d]*University of Applied Sciences Wildau, Germany*

The aligning polytetrafluoroethylene **(**PTFE) layer can be produced by hot friction transfer (FT) of bulk PTFE. The method, which allows to produce aligning PTFE layer at room temperature of substrate, consists of the two stages: 1 - heating of the bulk PTFE in vacuum with activation of the emitted gas with cloud of electrons (EVD); 2 - consequent unidirectional rubbing of the grown layer with a cloth at room temperature, which produces aligned relief on the surface and unidirectional aligning of the PTFE macromolecules as well. Recently was found, that optimal orienting layer thickness is 50 nm with grooves width 40 nm and the height about 10 nm. Another type of the aligning surface is stamped polycarbonate plate (PC) - bare substrate of DVD disc, which has aligned surface profile (grooves of 110 nm in depth and period of 7400 nm) and DVD disk with pits. The Pc plates were made by the injection molding, therefore, no orientation of polymer chains on the surface was expected.

Pentacene (PN) and squaraine (Sq) compounds were deposited on the PTFE and PC surfaces by deposition in vacuum. PN and Sq deposits revealed dichroic ratio up to 4 (Fig.1). The FT PTFE, EVD PTFE and PC surfaces showed different orienting actions for organic materials deposited on them. AFM images of the Sq films, deposited in one run on FT- and EVD- PTFE layers, revealed some features (Fig.2). The comparatively large round (diameter 100 nm, 15 nm high) separated Sq nano-aggregates were grown on the FT-PTFE ridges. Twice smaller nano-aggregates were grown between the ridges. Joined Sq nano-aggregates, grown on the rubbed EVD-PTFE, had the morphology of the nano-aggregates on the surface close to isotropic. The EVD layer led to formation of trice more uniform Sq film with smaller nano-aggregates (diameter 30 nm). The more uniform film on EVD-PTFE shows, that interaction between Sq molecules and EVD-PTFE is stronger, than between Sq and FT-PTFE**.**

Sq film grown on aligned PC surface showed small dichroic ratio but with absorption band at 760 nm, prevailed for parallel polarization of light in respect to the groove direction. This is feature of the J-aggregates. The needle-like nano-aggregates were positioned across the substrate grooves and ledges. From optical spectra it is seen, that Sq molecules inside J-aggregates preferably oriented along grooves, while macroscopically the nano-aggregates oriented across the grooves. So the molecular orientation was the same as on aligning PTFE layers, but another kind of nano-aggregates was grown.

Recently three aligning mechanisms have been considered: geometrical matching, topographic adaptation, molecular interactions. Seems, all the mechanisms are taking place with different contributions in dependence on the

properties of the condensing molecules, the properties of the orienting surface, the deposition conditions and the deposit thickness. Correct model should take into account the wide range of the surface characteristics: geometrical parameters of grooves and their not ideally flat distribution, defects density and morphology, etc.

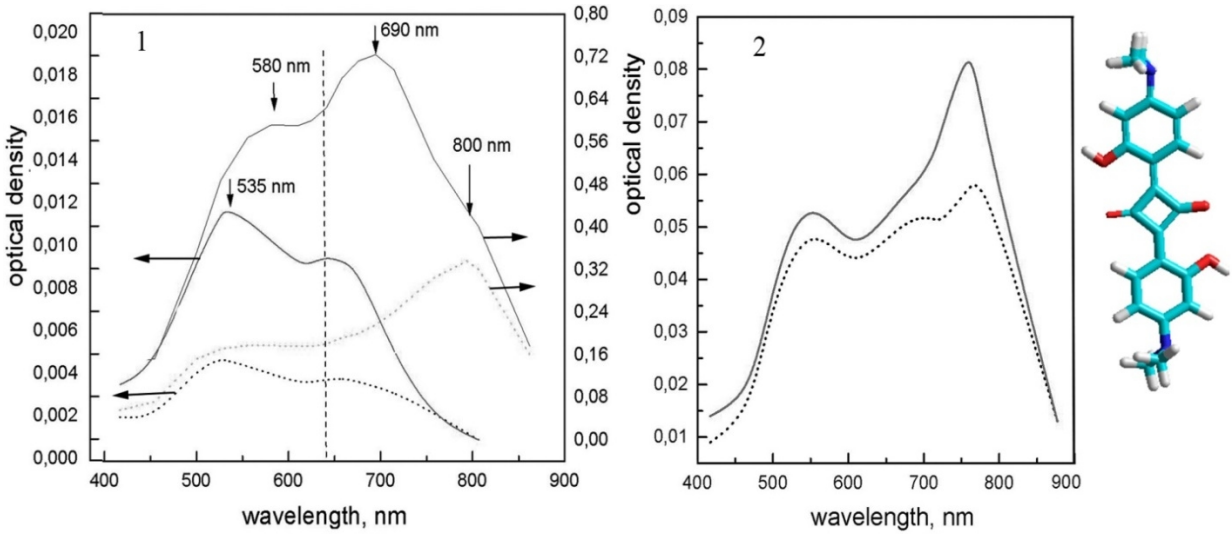

Fig.1. Polarized optical absorption spectra of the Sq deposits on the substrates: 1 – rubbed EVD PTFE, 2 – microgrooved PC surface; continuous line - electric vector of light was parallel to rubbing direction and direction of grooves, dotted line – electric vector of light was perpendicular to direction of rubbing and grooves; left side - the structure of Sq molecule.

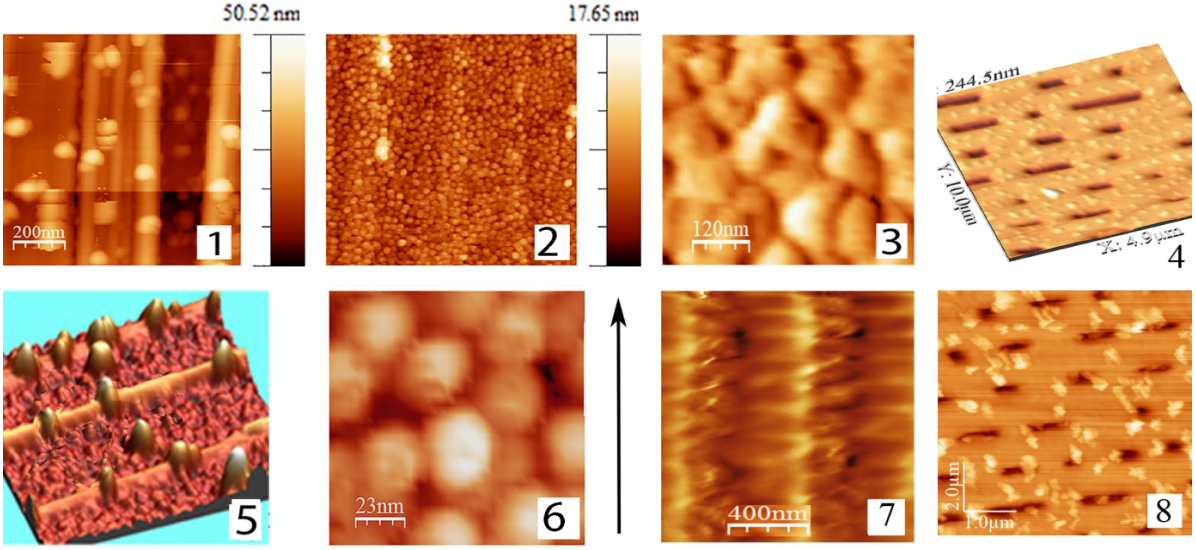

Fig.2 Images of Sq and PN films grown at deposition rate 1 nm/s on: 1 – Sq on FT PTFE, 2 – Sq on rubbed EVD PTFE, all Sq "films" were 5 nm thick; 3 – dicroic PN film, 4 - 3D image of Sq on DVD; 5 – 3D image of 1, 6 - increased magnification of 2, 7 –Sq on DVD surface; 8 –thick Sq film on DVD; arrow shows aligning direction of substarte 1,2,3,6,7 surfaces.

Conclusions: Self-assembled nano-structured oriented organic films were produced on different aligning polymer surfaces.

Kinetics Formation of InAs Quantum Dots in GaAs – QD InAs - GaAs Heteronanowhisker Structure by CVD – Method

Guba S., Galan I. , Kost Ya.

Lviv Polytechnic National University, Lviv, Ukraine, gubask@polynet.lviv.ua

Heterostructures with spatial restrictions of charge carriers in all three directions (quantum dots) realize the limiting case of dimensional quantization in semiconductors, when the modification of electronic properties of a material is most pronounced. All the most important for application characteristics of the material, for example, the time of radiative recombination, the coefficients of Auger-recombination, etc., appear to be fundamentally dependent on the geometric size and shape of the quantum dot.

A qualitative breakthrough in this area is associated with the use of the effects of self-organization of semiconductor nanostructures in heteroepitaxial semiconductor systems with the formation of quantum dots. Thus, $In_{1-x}Ga_xAs/InAs/GaAs$ heteronanostructures were constructed with quantum dots of InAs of high crystalline perfection, high quantum yield of radiative recombination, and high homogeneity in size (about 10%) in semiconductor injection lasers.

To date, a number of technologies and methods have been developed that effectively function and provide nanostructured materials for laser use. This is, first of all, molecular-beam and MOCVD epitaxy. Here we focus on low-temperature vapor-transport chloride-hydride epitaxy (CVD-method) as a means of forming semiconductor quantum-sized structures. Interesting properties are possessed by heteronanowhiskers with quantum dots growing in an array. It is heterogeneous, which makes it impossible to establish the dependence of the properties of QD on its size and shape. To establish this dependence, the task was to investigate the formation of InAs quantum dots in the structure of the GaAs - InAs - GaAs heteronanowhisker by the low temperature CVD method.

The purpose of this work was to develop model representations of the formation of a single InAs quantum dot in the structure of the GaAs-InAs-GaAs heteronanowhisker by a low-temperature CVD method based on work [1]. The formation of a heteronanowhisker in a flow-through multichannel reactor was considered. It was assumed that the Au droplet serves as a surface activator applied to the GaAs substrate in the form of a circle of radius r_{Au} and a thickness h. During investigation of the growth of the GaAs nanowhisker structure, the dependence of the growth rate $\boldsymbol{V_L}$ of the structure of the GaAs nanowhisker on the radius of the golden droplet r_n was established. From it can be seen that with increasing radius of the droplet, the growth rate of the GaAs nanowhisker structure increases.

1. С.К. Губа // Журнал Нано – та електронної фізики –2017. – Т.9, № 3.– С. 03026 -1 –03026-6

Effective nanostructured SERS substrates are made by photolithography

Hreshchuk O.M., Yukhymchuk V.O., Valakh M.Ya., Dzhagan V.M., Danko V.A., Lytvyn P.M.

V. Lashkaryov Institute of Semiconductor Physics, National Academy of Sciences of Ukraine, Kyiv, Ukraine, Hreshchuk@gmail.com

Surface-enhanced Raman spectroscopy (SERS) extends the possibilities of "conventional" Raman spectroscopy by the possibility of studying of trace amount of substances up to one molecule. SERS method due to its advantages have found a lot of applications in various scientific fields such as biomedical, environmental safety, chemistry, biology, etc. In terms of commercialization of SERS substrates, the "price / quality" aspect should be taken into account, in which the substrate produced by photolithography method has several advantages compared to resource-cost electron beam lithography. Namely, the high reproducibility of samples, the orderliness of nanostructures, the cost of production, the possibility of controlling the size and shape of nanostructures and the type of metal.

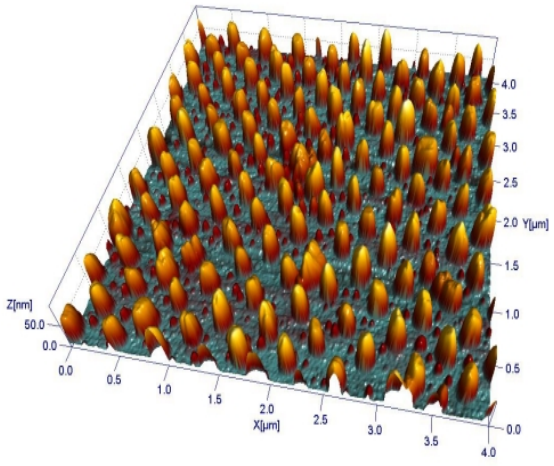

Fig. 1. AFM image of SERS substrate obtained by photolithography and annealed at 350°C.

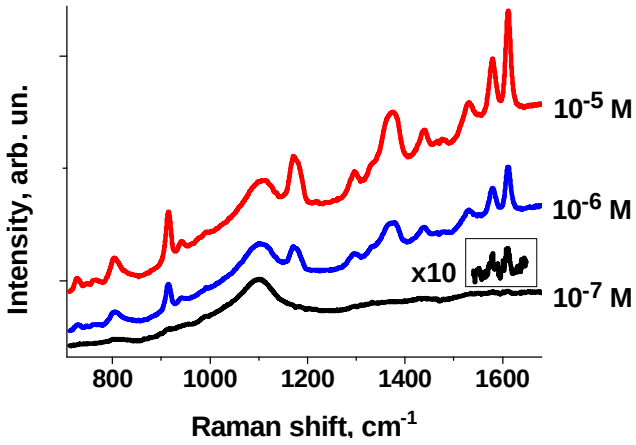

Fig. 2. Raman spectra of crystal violet molecules deposited on a SERS substrate, at different concentrations.

SERS substrates based on ordered arrays of nanoislands with an average height of 55 nm, and lateral dimensions of ~ 180 nm (Fig. 1) have been developed. Figure 2 shows the Raman spectra of crystal violet (CV) molecules with different concentrations deposited on nanostructured SERS substrates. It can be seen from the figure that for this type of substrate, it is possible to register the SERS signal from the CV molecules at a concentration of 10^{-7} M. The developed substrates have plasmon absorption with a maximum at 600 nm.

Electrochemical Properties of Nitrogen-Doped Porous Carbon

Kachmar A.I., Boichuk V.M., Budzulyak I.M., Kotsyubynsky V.O., Rachiy B.I., Yablon L.S.

Vasyl Stefanyk Precarpathian National University, Ivano-Frankivsk, Ukraine,
andrij.nj@gmail.com

Nitrogen-doped porous carbon nanomaterials have a various technological application, cathode catalyst for fuel cells with excellent oxygen reduction electrocatalytic activity. At the same time N-doped activated carbons have a good prospects for application in supercapacitor. The combination two ways of charge storage (the electric double-layer capacity with pseudocapacy) mechanisms to obtain a low-cost materials with high specific capacitance at high charge-discharge rates.

The microporous carbon was obtained on the base of plant feedstock using carbonization and chemical activation with sodium hydroxide [1]. The obtained powders were mixed with HNO_3 as nitrogen source with the continuous stirring at 50 °C under N_2 flow.

It was determined that both activation agent concentration and carbonization temperature effect on the porous structure and electrochemical performance of obtained carbons. The highest value of specific surface area (582 m^2g^{-1}) at simultaneous maximal relative contents of micropores (up to 95% of total area) observed for sample obtained at 900^{o}C after one activation procedure at m(NaOH):m(C)=1:1. The highest capacity value (calculated both from galvanostatic charge-discharge and voltammetry cycling) was observed for the samples with the low relative contribution of the double layer capacity that indicates the pseudocapacitance presence. It was found the increasing of m(NaOH):m(C) weight ratio at synthesis causes the increasing of redox capacitance contribution for once activated samples. The repeating of activation procedure results the decrease of diffusion controlled capacitance caused by the nitrogen-contained groups on the surface of carbon particles. The highest values of specific capacity for carbons obtained at 600ºC and 900ºC are about 100 and 120 F/g, respectively. The variation of activation agent concentration and the number of activation procedures allow controlling specific surface area and micropores relative content and predicting the contributions of double layer capacity and diffusion-controlled redox capacity to the total capacity of microporous carbon.

1. Ostafiychuk B.K., Budzulyak I.M., Kachmar A.I., at all. Effect of Thermochemical Modification of Activated Carbon Materials on Specific Capacity of Electrochemical Capacitors. *Nanosistemi, Nanomateriali, Nanotehnologii.* 2018. V.16, №2. p. 303-312.

Formation of Gold Islands on Oxidized Silicon Substrate

Kalashnyk Yu.Yu., Klimovskaya A.I., Oberemok O.C., Pedchenko Yu.M., Lytvyn P.M.

Lashkaryovs Institute of Semiconductor Physics, National Academy of Sciences, Kyiv, Ukraine, yu.kalashnik@gmail.com

Gold is used as a metal catalyst for growth of silicon nanowires (SiNWs) on a silicon substrate using CVD technology. The formation of gold islands (growth seeds) is an important technological step. The properties of gold islands (morphology, size distribution, density) determine parameters of the grown SiNWs. In this paper, we investigated how the preliminary treatment of the surface of substrate influences the characteristics of the formed islands. The formation process includes the following steps:

1. Chemical cleaning of the silicon surface in acetone vapors.
2. Deposition a thin gold film of 3 and 5 nm-thick on the substrate.
3. Following annealing of the substrate to form gold islands.

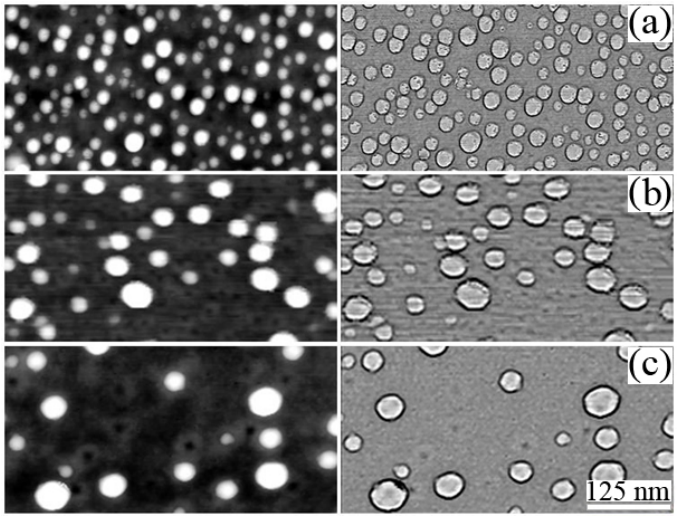

AFM image of 3 nm-thick gold film surfaces deposited onto silicon substrates after annealing:
(a) – 900 °C, 15 sec;
(b) – 1000 °C, 20 sec;
(c) – 1050 °C, 20 sec.
On the left, the maps of heights are shown. On the right are the same maps with distinguished grain boundaries.

To anneal the substrate we used illumination by linear halogen lamps (RTA) at different duration and at different temperature regimes. Theese techniques allowed varying the size and density of the islands. So, we have a possibility to control size and density of silicon nanowires, which are grown by metal-catalysed chemical deposition from the gas phase.

Photoconductivity of macroporous and monocrystalline silicon in conditions of strong surface light absorption

Karas' M.I., Karachevtseva L.A., Onyshchenko V.F.

Lashkryov Institute of Semiconductor Physics NAS of Ukraine, Kyiv, Ukraine,
nikar@isp.kiev.ua

The surface photoconductivity in macroporous and monocrystalline silicon has been studied at absorption coefficient in the range of 200–10^4cm^{-1}. Positive and negative photoconductivity was observed [1]. "Slow" negative photoconductivity is due to capture of the main charge carriers at "slow" surface levels and the appearance of an inversion layer upon illumination. The concentration of "slow" surface levels causing "slow" surface photoconductivity in macroporous and monocrystalline silicon has been calculated.

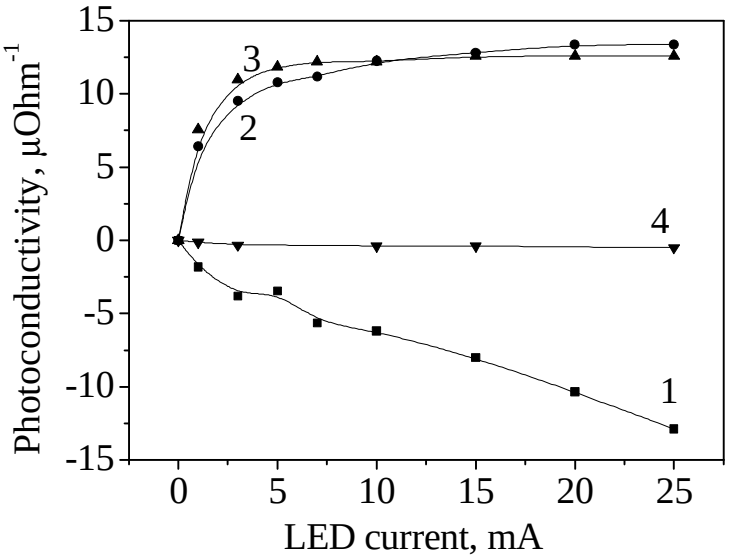

Fig. Lux-ampere dependences of the photoconductivity of the periodic structure of macroporous silicon (1-3) and monocrystalline silicon (4) at different wavelengths of illumination: 1, 4 - 0.52 μm, 2 - 0.62 μm, 3 - 0.93 μm.

On the basis of the measured negative photoconductivity, the photoconductivity of the inversion layer was calculated, and the concentration values of the "slow" surface levels were obtained from it both in the macroporous silicon structure ($N_{mpSi} > 10^{13}$ cm^{-2}) and in single-crystal silicon ($N_{Si} < 10^{13}$ cm^{-2}). It is shown that the ratio of negative photoconductivity values in the macroporous silicon and in monocrystalline silicon almost coincides with the ratio of the illuminated areas of the macroporous silicon and monocrystalline silicon (27 and 25, respectively), which confirms the purely surface nature of negative photoconductivity under conditions of strong surface light absorption.

1. Konin K.P., Goltvyansky Yu.V., Karachevtseva L.A., Karas M.I., Morozovs'ka D.V. Photoconductivity of Macroporous and Nonporous Silicon with Ultra thin Oxide Layers. *J. Electronic Mat.* 2018. V. 47, P. 5105-5108.

Perovskite-Type Material of $LaFeO_3$ for Solar Cells Applications

Kolkovska H.M., Mokhnatskyi M.L., Yaremiy I.P., Kolkovskyi P.I.

Vasyl Stefanyk Precarpathian University, Ivano-Frankivsk, Ukraine,
galyna.godovska@gmail.com

In recent years, the problem of obtaining new and more effective solar cells have attracted considerable attention. Perovskite-based solar cell manufacturing technology has received particular attention.

The selection of the conditions for the interaction of the dye and $LaFeO_3$ film on the glass surface is a key factor in testing $LaFeO_3$ nanopowder as the electrode material of the solar cell. SnO_2: F coated glass was pre-treated in a solution of hydrochloric acid for 60 minutes. Subsequently, a colloidal paste was prepared, which was deposited on a glass / SnO_2: F substrate. After drying in air, in order to create an ohmic contact with lanthanum orthoferrite / SnO_2: F film, the deposited film was annealed at 200 °C. Anthocyanin dye, electrolyte and incandescent lamp were used to increase the absorption spectrum, LiI, I_2, $LiBF_4$ (0.5: 0.05: 1 mol / l) in γ-butyrylactones and to simulate solar radiation, respectively.

The voltage-current characteristic of a sample based on a $LaFeO_3$ dye-sensitized solar cell is presented in Fig. 1, a

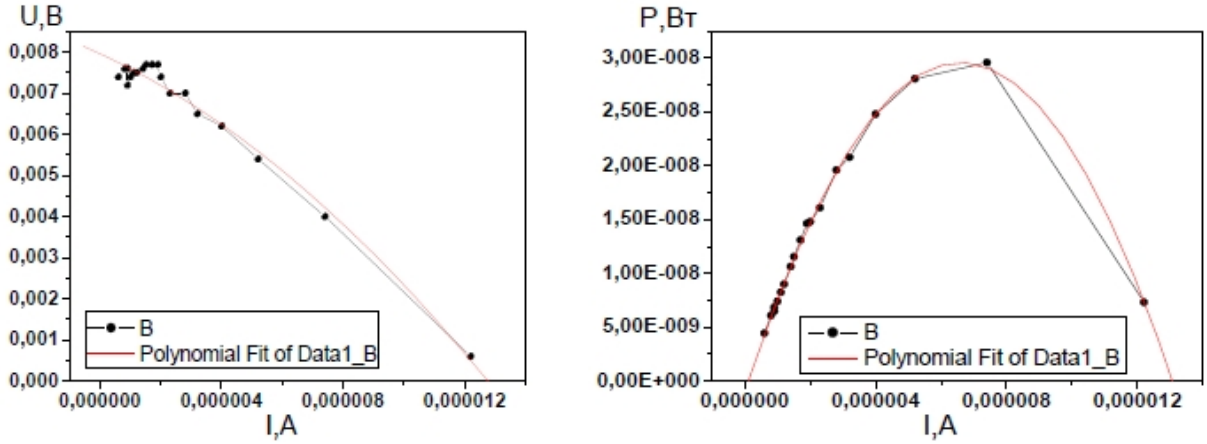

a) b)

Fig. 1. The energy characteristics of a solar cell, based on $LaFeO_3$: current-voltage characteristic (a) and the dependence of power on current strength (b).

To determine the numerical characteristics of the design of the solar cell, the dependence of power on current strength was built (Fig. 1, b). The EMF value of the solar cell and its internal resistance was obtained on the basis of approximation of the experimental point by a parabolic function which for the applied experimental conditions are: $\xi = 0.01$ V, $r = 700$ Ω.

Influence of metal-dispersed filler on the relaxation component of visco-elastic modules and internal friction of polyvinyl chloride based composites

Kolupaev B.S., Levchuk V.V., Lyashuk T.G.

Rivne state university of humanities, Rivne, Ukraine, Levchuk_VV@ukr.net

The processes of mechanical relaxation in polyvinyl chloride (PVC) based systems containing nano-dispersed copper powders as a filler have been investigated by the pulsed method with a pass signal along with a rotating plate method at a frequency (ω) of 0,4 MHz in the temperature range (T) 298 - 353 K. (Cu), nichrome (NiCr), graphite (C) obtained by physico-chemical (ph/ch) and electric exploded conductor (EVP) method. The volumetric content (φ) of the ingredients was $0 \div 5.0$ vol. % in T-r mode. Investigation of dynamic mechanical characteristics of PVC systems was carried out under volumetric deformation (K), deformation of shear (G) and stretching (compression) (E) of composites characterized by internal friction.

It is established that the curves of the modulus magnitude modifications (E, G, K) are of a step-by-step nature. Extrapolation from 533 K to lower temperatures indicates relaxation. In this case, the action of the filler decreases in the series: C, NiCr, Cu (ph/ch) and Cu (EVP) at φ = *const*.

It is shown that the relaxation component of internal friction is the sum of the maxima of β- and α-relaxation, and their positions on the temperature scale, exactly as the width and height, depend on the type, content of the nanodispersed metal in PVC.

The relaxation component of changes in the magnitude of moduli and decrement in the investigated region T is described by the relaxation spectrum of the species

$$H(t) = (a r N_0 / 2p M_0)(z_0 kT/6)^{1/2} t^{-1/2} \qquad (1)$$

It is shown that for the systems of PVC + NiCr the tangent of the tilt angle of the graph of the dependence of lg H on lg τ approaches the theoretical value - 1/2. According to (1) for the region $H \sim \tau^{1/2}$, the value (ζ) of the monomer coefficient of friction, the average molecular weight of the structures between the nodes of the PVC mesh network, the active center of the surface of Cu (ph/ch), their resonant frequency and the quasi-elastic force coefficient are calculated. The results of studies have shown that the introduction into PVC $2 \cdot 10^{-4} \div 1{,}5 \cdot 10^{-2}$ vol. % of the above nanodispersed ingredients most effectively affects the change in the relaxation characteristics of the composites.

Background component of internal friction in PVC filled with nanodispersed metal

Kolupaev B.B.,[1] Maksymtsev Yu.R.[2] Sidletsky V.O.[2]

[1] *Institute of cybernetics of the Rivne International university of economics and humanities named after Academician Stepan Demianchuk Rivne, Ukraine,*
[2] *Rivne state university of humanities, Rivne, Ukraine, vsidletsky70@gmail.com*

The high-temperature (298 K ≤ T ≤ (Tg + 10) K) internal friction background in nanostructured composites formed on the basis of polyvinyl chloride (PVC) filled with nano-dispersed powder of copper (Cu) and nichrome (NiCr) obtained by an electrical explosion of the conductor (EVP) and/or physico-chemical (ph/ch) method. It is established that with contents (φ) Cu ph/ch over $6 \cdot 10^{-4}$ vol. % of PVC passes to the state of the boundary layer, and the amount of free volume, which is statistically distributed between the structural elements, providing their mobility under the action of external fields, lies in the range of 2-6%.

The study of the background component of internal friction was carried out at a frequency (ω) of 0.4 MHz at 0 ≤ φ ≤ 5,0 vol.%, and it was established that this dependence on the return temperature in semi-logarithmic coordinates is characterized by the presence of points of deviation from the linearity. This indicates a change in the texture of nanocomposites, the boundaries of phase distribution, the number of kinetic elements of PVC and their mobility.

As a result of the change in T, φ, type of nanodispersed metal, the action of the y / field, information is obtained about the degree (α, β) and the relaxation time (τ) of the energy dissipation process and the equation of the curvature of the internal friction of the form

$$\Delta = \frac{b(a)}{wt + (wt)^{-1}}, \qquad (1)$$

at $t = t_0 \exp(W/kT)$; $\tau_0 - const$; W – activation energy

It is shown that the presence of energy and entropy bonds at the interface between phases is the polymer-active centers of the surface of nanodispersed metal, which causes saturation of the background component of internal friction. It has been established that the plane regions on the curves of the first background effect at T≤T (β) differ in magnitude from the curves of the temperature dependence of the background on the second interval T (α), due to the change in the length of the structural elements of the composite. They are minimal for PVC + Cu systems (ph/ch). It is concluded that with the help of nanodisperse Cu, NiCr it is possible to direct the value of the background component of internal friction of PVC systems as one of the characteristics of areas of practical use of a composite under the influence of external u/s and T fields.

Reversible Laser Assisted Structural Modification of the Surface of As Rich As-Se Nanolayers

Kondrat O.[1], Holomb R.[1,2], Mitsa V.[1], Veres M.[2], Csik A.[3], Takáts V.[3], Tsud N.[4], Vondráček M.[5], Matolin V.[4] and Prince K.C.[6]

[1] *Uzhhorod National University, 88000 Uzhhorod, Ukraine, oleksandr.kondrat@uzhnu.edu.ua*
[2]*Wigner Research Centre for Physics, Hungarian Academy of Sciences, Budapest, Hungary*
[3]*Institute for Nuclear Research, Hungarian Academy of Sciences, Debrecen, Hungary*
[4]*Charles University, Faculty of Mathematics and Physics, Department of Surface and Plasma Science, Prague, Czech Republic*
[5]*Institute of Physics, Academy of Science of the Czech Republic, Prague, Czech Republic*
[6] *Elettra-Sincrotrone Trieste S.C.p.A., in Area Science Park, St., Basovizza (Trieste), Italy*

Stoichiometric $As_{40}Se_{60}$ has an interesting feature of having a composition exactly at the floppy-to-rigid transition. Evaporated films are characterized by a large degree of structural disorder depending on the deposition method and conditions. Less literature information is available for non-stoichiometric As-Se materials, especially in their thin film form. However, it is expected that the magnitude of induced structural changes will be higher for As enriched As-Se films due to initially higher concentration of photosensitive homopolar As-As bonds.

The $As_{56}Se_{64}$ nanolayers were prepared *in-situ* in preparation chamber of Materials Science Beamline (MSB, Elettra–Sincrotrone Trieste) by thermal evaporation of bulk glass powder at the temperature of 220 °C and deposition onto a silicon substrate. The atomic composition, local structure, and their characteristics, as well as reversible structural changes of *in-situ* fabricated As-rich $As_{56}Se_{44}$ nanolayers during thermal annealing and laser illumination by monochromatic coherent light with over band-gap photon energy were examined by synchrotron radiation photoelectron spectroscopy. It was established that the structure of as-deposited $As_{56}Se_{44}$nanolayers is enriched by As occurring mainly due to dominance of As-$SeAs_2$ s.u. *In situ* thermal annealing rearranges the structure of As-Se films and leads to the formation As-Se_3 and As-Se_2As s.u. following by dissociation of As-$SeAs_2$ s.u. The *in situ* over band-gap laser illumination increases the contribution of As-Se_2As s.u. in the structure of As-Se nanolayers. The "thermal annealing" - "laser illumination" of As-Se nanolayers performed in cycle mode reveals the reversibility of the structural changes. These facts together indicate the possibility of post fabrication modification of the structure and properties of As-Se nanolayers, expanding the functionality of these materials for wide range of modern applications such as photonics, non-linear optics, information recording, ultrafast information processing *etc.*

Transport and Magnetic Phenomena in Nano-Conductors with Weak Shielding of Field

Kopeliovich A.I., Petrenko L.G.

National Technical University "Kharkiv Polytechnic Institute", Kharkiv, Ukraine,
linagpetrenko@gmail.com

The paper considers the possibility of the existence of nanoscale conductors, whose properties differ significantly from those known due to the anomalously weak Coulomb fields created by the current carriers in these conductors. In fig. 1 shows a thin conductor in the alternating field of the condenser.

We have shown that when performing inequality

$$e^2 \Pi \ell n \frac{L}{d} \ll \varepsilon ,$$

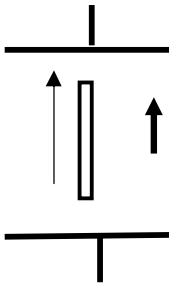

where e - the carrier charge, Π - the density of carrier states per unit of energy and unit of conductor length, L and d - the length and smallest size of the conductor, respectively; ε - the dielectric constant created by the bound carriers, the electric field of non-equilibrium carriers can be neglected. This inequality is quite rigid. Its implementation is facilitated by a small effective mass of carriers, a high value of ε (in some semiconductors it reaches several hundred), a high temperature exceeding the Fermi energy of carriers.

It is shown that the transport properties of such conductors are characterized by resonances of the frequency dependence of the conductivity of the type of resonances of a sound wave in the resonator.

Observation of these properties is facilitated if the conductor is polarized along its spin; in this case, in an external magnetic field, it becomes a magnetic quadrupole and its response to an external electric field is reflected in the magnetic field created by it. In fig. Figure 2 shows the frequency dependence of the quadrupole moment of the conductor; the first two resonances of the current-carrier density waves are visible.

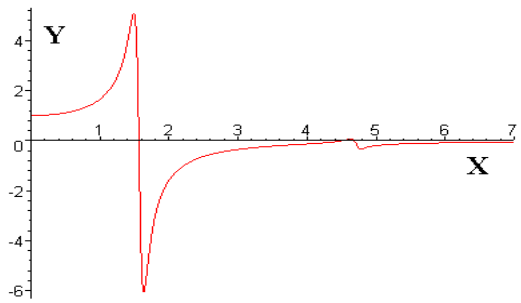

Electrospin effect was found in the considered type conductors. It is shown that the applied electric field changes the magnetic field around the considered conductor-magnetic to a much greater extent than in the case of magnetic conductors, well shielding the external field.

1. Kopeliovich A.I., Petrenko L.G. Transport-spin phenomena in nanowires with a large radius of shielding. "Low Temperature Physics", 2017. V.43, №2. P. 253-258.

Formation Peculiarities of Fractal Percolation ZnO/NiO Nanosystems

Kornyushchenko A.S., Perekrestov V.I., Kosminska Y.O.

Sumy State University, Laboratory of Vacuum Nanotechnologies, 2, Rimsky-Korsakov Str, Sumy, Ukraine, a.kornyushchenko@mss.sumdu.edu.ua

Zinc oxide and nickel oxide possess a number of unique physical properties determining a wide range of their practical applications, among them gas sensor applications and as electrodes of electrochemical batteries. ZnO/NiO fractal percolation nanosystems have been sensitized using a newly developed three-step technology. During the first stage, ionically sputtered Zn vapors have been deposited under near-equilibrium condensation conditions (Fig. 1a). This technology, which is based on the self-organization of stationary small supersaturations, allows obtaining zinc nanosystems with reproducible structural and morphological characteristics. The diameter of individual zinc nanowires varied between 50 to 140nm. In the second stage, Zn layers have been oxidized in air atmosphere at 350 C. The diameter of individual ZnO nanowires varies between 80 to 100 nm, which is comparable with two values of the Debye screening length (Fig. 1b).

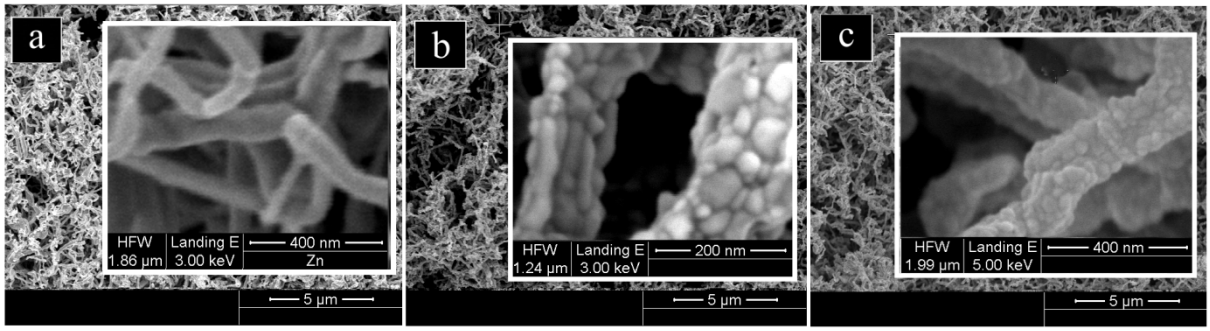

Figure 1 – Scanning electron microscopy investigations of Zn nanosystems (a), ZnO nanosystems (b) and ZnO/NiO (c).

Consequently, during oxygen chemisorption on thin sections of ZnO nanosystems, the current flow channels close, and conversely, chemisorption of reducing gases can open current flow channels, which is the defining characteristic of fractal-percolation systems. During the final stage, a NiO layer has been deposited onto the ZnO surface using reactive magnetron sputtering. The results of X-ray investigations of the ZnO/NiO fractal percolation nanosystems indicate the presence of only one HCP lattice whose lattice parameters coincide with the lattice parameters of ZnO. Diffraction peaks indicating the presence of NiO have not been detected. On the other hand, results of energy-dispersive X-ray elemental analysis evidence the presence of zinc, nickel and oxygen with sufficiently high concentrations that allow the oxides formation.

Optical Properties of Au-Containing Glasses Co-Doped with Eu and Er

Kouhar V.[1], Akinshau K.[1], Stepko A.[2], Shakhgildyan G.[2], Lotarev S.[2]

[1]*B.I. Stepanov Institute of Physics, NAS of Belarus, Minsk, Belarus*
[2]*Mendeleev University of Chemical Technology of Russia, Moscow, Russia,*
v.kouhar@ifanbel.bas-net.by

Nowadays, one of the important challenges in optical material science is the development of efficient luminescent optical media based on oxide glasses containing rare-earth ions (REI) for the high power laser applications. In this regard, studies related to the phenomenon of enhancement of REI luminescence intensity in the vicinity of noble metal nanoparticles in REI-doped glasses are of particular interest. In this work, we investigate the influence of gold nanoparticles on the optical properties of Au-Eu and Au-Er co-doped silica and phosphate glasses.

It is shown, that $(Au^0)_n$ nanoparticles in synthesized glasses can be identified according to their extinction due to the surface plasmon resonance (SPR) band on the luminescence spectra, but can't be identified with XRD method. The performed analysis shows that luminescence intensity of REI in co-doped glasses depends on the size of gold nanoparticles which have been precipitated during heat treatment of glass. We observe nearly double increase of the integral luminesce intensity at early stages of heat treatment while no SPR of $(Au^0)_n$ could be detected. A decrease of luminescence intensity have been observed with further increase of heat treatment temperature and of the gold nanoparticle size as a consequence. Calculation of average Au-Eu distance in the studied glass samples shows that it changes from 0.8 to 4 nm, while calculated gold nanoparticle size shows growth up to 8 nm. Thus, we assume that generation of small non-plasmonic gold nanoparticles with sizes less than 2 nm must increase luminesce intensity of REI due to effective energy transfer between nanoparticle and REI. At the same time, generation of plasmonic nanoparticles with sizes over 2–3 nm leads to a decrease of REI luminesce intensity due to internal optical filter effect which is induced by the local surface plasmon absorption band of gold nanoparticles. Additional doping of Eu-containing silica glass with Al results in significant change of the luminescence spectrum, driven by the formation of complex Al-Eu-centres, which affect the shape of SPR-band.

Some applications of such glasses are discussed.

This work was partly supported by the Belarusian and Russian Foundation for Basic Research (grants no. F17RM-005 and no. 17-53-04123, respectively) and SPNI "Photonics, opto- and microelectronics 1.2.03".

Synthesis of Ni@Ag bimetallic nanostructures as the fillers for electroconductive composites

Kytsya A.R., Bazylyak L.I., Pobigun-Halaiska O.I.

Department of Physical Chemistry of Fossil Fuels
of the Institute of Physical–Organic Chemistry and Coal Chemistry
named after L. M. Lytvynenko of the National Academy of Sciences of Ukraine,
Lviv, Ukraine, andriy_kytsya@yahoo.com

Nickel nanoparticles (NiNPs) are interesting material for different applications, for example as filler for microwave absorbing composites [1], magneto-separable carrier for catalysts [2], etc. In recent work [3] we have announced the possibility of using of nickel nano- and submicron particles as self-assembled fillers for electroconductive composites that characterized by low percolation threshold. At the same time NiNPs can be used as precursor for synthesis of bi- and polymetallic nanostructures that will combine and supplement the properties of both of metals. That is why herein we report the test of bimetallic Ni@Ag nanopowder as electroconductive filler for polymer composites.

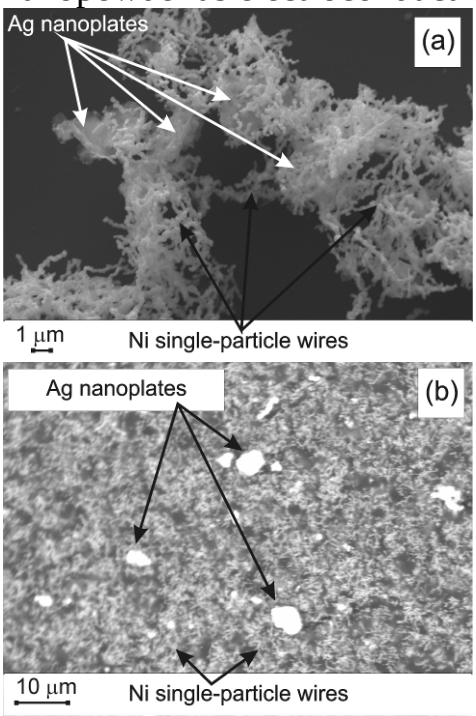

Ni@Ag have been synthesized via cementation of Ag^+ on NiNPs (synthesized as it was reported in [3]) at the starting concentrations of $[Ag^+]$ = 0.0025…0.01 mol/L, [NiNPs] = 4 g/L. Using scanning electron microscopy it was found that Ag was crystalized as thin nanoplates intercalated into the single-particle nanowires that formed by NiNPs (Fig. a). Then 0.15 g of obtained Ni@Ag was mixed with 0.3 g of methacrylic copolymer that soluted in 1mL of buthylacetate and sonificated. Obtained mixture was plated on glass and dried at 120 °C. It was found that self-assembling of Ni@Ag is retained in obtained composite (Fig. b) and specific resistance of composite is equal to 80 Ω·m.

1. Srivastava R. K., et al. Ni filled flexible multi-walled carbon nanotube-polystyrene composite films as efficient microwave absorbers. *Appl. Phys. Lett.* 2011. V. 99. P. 113116.
2. Opeida I. A., Kytsya A. R., Bazylyak L. I., Pobigun-Halaiska O. I. Magnetically separable nanocatalyst Ag@Ni for the liquid-phase oxidation of cumene. *Theor. Exp. Chem.* 2018. V. 54, No. 4. P. 242-246.
3. Kytsya A., Bazylyak L., Pobigun O. Nickel submicron particles as fillers for electroconductive polymer composites. *Visnyk Lviv Univ. Ser. Chem.* 2017. Is. 58, Pt. 2. P. 442-449.

Magnetooptical Kerr and Faraday Effects in Multilayer Co/Cu(111) Nanofilms

Lukienko I.M.[1], Stetsenko O.M.[2], Kharchenko M.F.[1]

[1] *B.Verkin Institute for Low Temperature Physics and Engineering of the National Academy of Sciences of Ukraine, Kharkiv, Ukraine*
[2] *National Technical University "Kharkiv Polytechnical Institute", Kharkiv, Ukraine,*
lukijenko@ilt.kharkov.ua

In the work we notify about study of magnetooptical Kerr and Faraday effects in $[Co(0.8nm)/Cu(111)]_{20}$ GMR (Giant Magneto Resistance) nanofilms. The films were obtained by the magnetron sputtering and were different from each other with Cu layer thickness from 0.8 to 2 nm.

Dependences of the Faraday and longitudinal Kerr rotation angles of the films on magnetic field strength were analyzed with taking into account presence of superparamagnetic (SPM) clusters from Co atoms in the films. As results, we obtained distributions for magnetic moments of the SPM clusters f(μ) and strength of antiferromagnetic (AFM) exchange coupling between Co layers for all films. It was determined that sizes of the SPM clusters, their total volume and magnetization were reduced in the films with the AFM bounded Co layers. It is concluded that these features of the cluster structure are created during precipitation of Co atoms on surfaces of Cu layers, in volume of wich the redistribution of electron density takes place is due to the electron-quantum size effect.

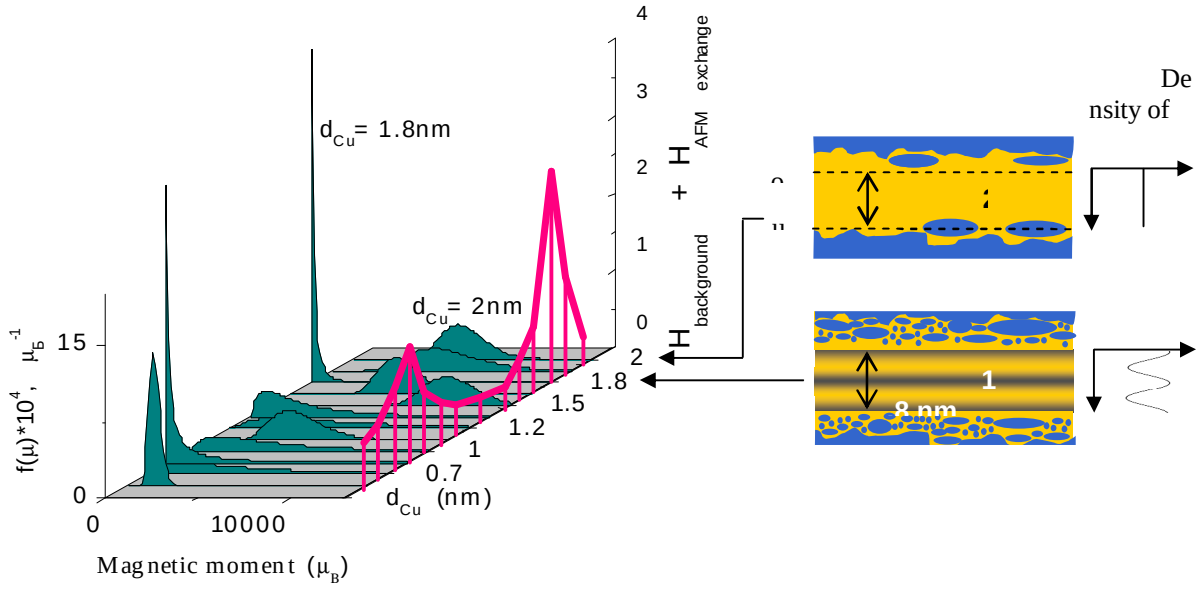

Fig. Log-normal distributions for magnetic moments of the SPM clusters (left scale) and strength of AFM exchange coupling (right scale). Electron density redistribution in the Cu layers of the films without and with AFM exchange bounds are shown schematically in the upper and bottom pictures on the right, respectively.

Band Structure of the Strained Germanium Nanofilm

Luniov S.V., Koval Yu.V.

Lutsk National Technical University, Lutsk, Ukraine, luniovser@ukr.net

Recently, heterostructures have been widely used in microelectronic devices, both with strained borders, and without them. Semiconductor germanium nanofilms are of interest in connection with their compatibility with silicon technologies and new possibilities of their practical application in field transistors, infrared detectors, solar cells, photodiodes, memory systems, lasers. The presence of various impurities and fields of internal mechanical strains in nanocrystalline Ge and SiGe films grown on a silicon substrate significantly influences on the transport of current carriers, the electrical and optical properties of such films. During the synthesis of such nanostructures, controlled and uncontrolled impurities are introduced, the energy levels of which can be subjected the displacement during the deformation and significantly affect the physical properties of the obtained nanostructures.

Therefore, interesting and relevant from both scientific and practical points of view is the study of the influence of internal deformation fields on the band structure of the germanium nanofilm, doped with shallow and deep donor impurities.

The effect of internal mechanical strains on the ionization energy of donor impurities in a germanium nanofilm, grown on the $Ge_{(x)}Si_{(1-x)}$ substrate with crystallographic orientation (001), was investigated by us. The data on the energy positions of various minima of the conduction band and the valence band branches of the strained germanium nanofilm, the components E_1 and E_2 of the splitted level of the impurity, the effective mass tensor for L_1 and Δ_1 minima were taken into account for such calculations. Calculations for impurities with the ionization energies of $E_r^0 = 50$ meV, $E_r^0 = 100$ meV and $E_r^0 = 200$ meV for germanium nanofilm by the thickness d=12 nm have been conducted. As calculations show, the increasing of the Si content in the substrate leads to a growth of ionization energy of the doping impurity. This is due to the radical deforming reconstruction of the structure of the conduction band of the nanofilm at the expense of the internal mechanical strains. The presence of such strains leads to the inversion of the type (L_1-Δ_1) of absolute minimum of the conduction band of the nanofilm. The obtained results can be used in designing and modelling on the basis of a strained germanium nanofilm, which is doped with various donor impurities, of electronic devices and sensors of modern nanoelectronics. A purposeful change of the component composition of the substrate and the predicted a choice of the type of doping impurities with some value of the ionization energy will allow controlling the electrical and optical properties of the germanium nanofilms.

Influence of substrate material on properties fullerite films

Martynenko I. M., Odnodvorets L.V., Shumakova N.I.

Sumy State University, Sumy, Ukraine, nshumakova@ukr.net

The unique electronic, physico-chemical, mechanical, electrical and optical properties of fullerenes in a condensed state indicate the prospects of using these materials in many branches of nanoelectronics [1]. The purpose of this work is to conduct a study of the structural-phase state and electrophysical properties of thin fullerite films obtained on substrates of Cu or Ni films of different thicknesses.

Condensation of fullerenes was carried out by the thermal method: fullerene-containing soot was added to the crucible, a pad carrier with fixed Ni or Cu films was placed over it and the crucible was heated in the temperature range T = 600-700°C for 40 minutes in high vacuum (10^{-4} Pa). After that, the temperature was raised to 800-900°C and the fullerenes were deposited for 40 minutes.A microscope TEM-125 K was used to analyze the crystalline structure of thin films. The study of the structure-phase state shows that in the C_{60} /Cu/S (S - substrate) films, an increase in the lattice parameter (a = 3,657 Å (as-deposition), a = 3,695 Å (after annealing) for films thickness d = 30 nm is compared with a film Cu (a = 3,608 Å). Ni films do not contain extraneous atoms, but they have a fcc phase with a parameter as in bulk samples.

After the fullerene C_{60} deposition and thermal cycling cycles, we observe phase changes: the formation of a phase corresponding to a certain modification of carbon with interplanar distances d_{hkl} = 2,799 and 2,444 Å in the sample C_{60}(69)/Ni (15)/S and d_{hkl} = 2,868 and 2,507 Å in C_{60}(69)/Ni(33)/S (in brackets - the thickness in Å).

The conclude about the fullerite layer role of the two-layered films C_{60}/Cu/S conductivity allows you to make the dependence of the resistance versus thickness and the value resistivity. The fullerite layer role can manifested in reducing the resistivity in the transition to the parallel connection of the two films and the possible injection of free electrons from the fullerite layer into the Cu film.

The dependence of the resistance for system C_{60}(69)/Ni(15)/S is semiconductor character. This can be explained by the fact that the Ni film has an islet character, which causes the thermosactivated injection of electrons from the Ni islands in the continuous fullerite film crystallites.

1. Наноматеріали і нанотехнології в електроніці: підручник / І.Ю. Проценко, Н.І. Шумакова.− Суми: Сумський державний університет, 2017.−151 с.

Two-Dimensional Magnetoexcitons With Linear Dispersion Law Interacting with Quantum Point Vortices

Moskalenko S.A., Moskalenko V.A., Podlesny I.V., Zubac I.A.

Institute of Applied Physics, Chișinău, Republic of Moldova, exciton@phys.asm.md

1. The theory of the two-dimensional (2D) magnetoexcitons was completed taking into account the electron-hole (*e-h*) Coulomb exchange interaction in addition to the direct one. The exchange *e-h* Coulomb scattering takes place with the annihilation and the creation of the *e-h* pairs with the resultant electronic charges equal to zero. They have dipole-dipole interaction, when the interband dipole moments r_{c-v} are different from zero. It happens when the crystals have the dipole active optical quantum transitions. We have considered the semiconductor layers of the type *GaAs* with *s*-type conductions band and *p*-type valence band with magnetoexcitons formed by electrons with spin projections $s_z^e = \pm 1/2$ and by heavy holes with full angular momentum projections $j_z^h = \pm 3/2$. The Lorentz force in the Landau gauge description determines the positions of the Landau quantization oscillations of the electrons and holes and their distances in the frame of the magnetoexcitons. Their relative and center of mass motions are interconnected. In difference on the direct Coulomb *e-h* interaction, which gives rise to the quadratic dispersion law $\mathbf{h}^2k^2/2M(B)$ with magnetic mass $M(B)$ depending on the magnetic field strength B, the exchange *e-h* Coulomb interaction gives rise to linear dispersion law known as Dirac cone $\mathbf{h}\mathrm{v}_g k$ with group velocity v_g depending on the interband dipole moment in the way: $\mathrm{v}_g \approx \left| r_{c-v}/l_0 \right|^2 \approx B$, where l_0 is the magnetic length.

2. The thermodynamic properties of the ideal 2D Bose gas with linear dispersion law were discussed in the Ref [1]. The critical temperature of the Bose-Einstein condensation (BEC) of the 2D magnetoexcitons is different from zero even at the infinite homogeneous surface area and following [1] is proportional to the group velocity: $T_c : \mathrm{v}_g : B$. In the case of the magnetoexcitons it increases with the increasing magnetic field strength *B*.

3. It was shown that the Chern-Simons (*C-S*) gauge field created by the quantum point vortices in the conditions of the fractional quantum Hall effects (*FQHEs*) leads to the formation of the composite electrons and holes with equal integer numbers of the attached to each particle quantum point vortices. The coherent superposition of the velocities of these vortices leads to the formation of the *C-S* vector potential, which depends on the difference between the density operators $\hat{r}_e$ of the electrons and $\hat{r}_h$ of the holes. The *C-S* vector potential generates the effective magnetic field acting on the particles in addition to the external magnetic field. In the mean field approximation, when the average densities of electrons and of the holes coincide the effective *C-S* magnetic and electric fields vanish and the Landau quantization of the composite particles with the bare electron and hole effective masses take place only under the influence of the external magnetic field [2].

1. Moskalenko, S.A. and Snoke, D.W. *Bose-Einstein condensation of excitons and biexcitons and coherent nonlinear optics with excitons* (2000), Cambridge University Press, p.189.
2. Moskalenko, S.A. Moskalenko, V.A. *Mold. J. Phys. Sci.* **17**(1-2), (2018).

Low-Temperature Rf Plasma Monolayer Doping of Si Nanowires

Nazarov A.N.[1], Okholin P.N.[1], Gomeniuk Yu.V.[1], Stepanov V.G.[1], Glotov V.I.[2], Nazarova T.M.[3], Duffy R.[4]

[1] *Lashkarov Institute of Semiconductor Physics NASU, Kyiv, Ukraine,* nazarov@lab15.kiev.ua
[2] *Institute of Microdevices NAS of Ukraine, Kyiv, Ukraine*
[3] *National Technical University of Ukraine "Igor Sikorsky KPI", Kyiv, Ukraine*
[4] *Tyndall National Institute, University College Cork, Cork, Ireland*

Monolayer doping (MLD) is novel alternative to conventional doping technique, such as ion beam implantation and plasma doping. Ion implantation is industrial standard technology which includes the crystal damage introduced by ion bombardment and lack of dopant conformality. Plasma doping has the advantage of generating more conformal doping profiles than ion implantation, but it causes damage to the target as ions strike. In MLD organic molecules are covalently bonded to the semiconductor surface at relatively low processing temperatures. Then a thermal treatment is applied to diffuse dopant atoms into the semiconductor. Usually, for silicon nanowires (NWs) a rapid thermal annealing is used at temperature about 1000 °C for 5 s [1]. In this work in order to decrease the processing thermal budget a combination of MLD technology with low-temperature RF hydrogen plasma treatment technique is studied.

The Si nanowires were fabricated from silicon film of SOI wafer (thickness of the Si film was 30 nm). To study MLD the NWs were treated by allyldiphenylphosphine (ADP), which provides P as the dopant molecule, and coated by SiO_2 layer. In our samples metal electrodes were formed before of the SiO_2 coating. In order to perform a doping of the NWs RF plasma treatment in forming gas ($90\%N_2+10\%H_2$) was used. Power of the RF plasma treatment was changed from 0.5 to 2.0 W/cm^2; additional temperature heating was 150°C; time of the treatment was 15 min. To extract electrical parameters of the NWs Isd-Vbg characteristics of pseudo-transistor were used.

After RF plasma treatment with increasing of plasma power we observed: increase of saturation current in factor of about $1x10^4$; decrease of negative charge in the buried dielectric; decrease of subthreshold slope. The first effect is associated with decrease of contact resistance and increase of dopant concentration in the NWs. The last effect is connected with decrease of interface states concentration. Using regimes of RF plasma treatment allow us to decrease of resistivity, ρ, of the NWs up to 10^3 Ohm×cm that corresponds to doping of our NW is about 5×10^{14} cm^{-3}. The nature of the doping is discussed.

1. Duffy R., Ricchio A., Murphy R. et al. Diagnosis of phosphorus monolayer doping in silicon based on nanowire electrical characterisation. *Journal of Applied Physics.* 2018. V.123, P.125701.

EPR of Cu-doped Y- stabilized ZrO_2 nanopowders

Nosenko V.V., Korsunska N.E., Baran N.P., Vorona I.P., Khomenkova L.Yu.

[1] *V. Lashkaryov Institute of Semiconductor Physics, Natl. Acad. of Sci. of Ukraine, Kyiv, Ukraine, vvnosenko@ukr.net*

ZrO_2 is a widely used material due to its versatile properties, such as high chemical inertness, photochemical stability, good wear resistance, and wide band gap. Addition of yttrium oxide makes the cubic crystalline structure of zirconium dioxide stable at room temperature. Dopping of Y-stabilised ZrO_2 with Cu is a very effective method to vary the structure and phase composition of ZrO_2 and, thereby its properties. However, the effect of copper impurities on the structural characteristics of the composites was previously studied in powders that do not contain yttrium. Therefore, we carried out the EPR investigation of Cu-doped Y- stabilized ZrO_2 nanopowders prepared by coprecipitation method and calcined at different temperatures.

Depending on calcination temperature (Tc), two types of EPR spectra are observed in our samples. The first type of spectra is observed at Tc = 500–900°C, it was shown that these spectra are composed at least of three signals. The first component exhibits the characteristic copper hyperfine splitting and can be described by the following spin-Hamiltonian parameters $g_\perp = 2.072$, $g_\parallel = 2.32$, $A_\perp \sim 0$G, $A_\parallel \sim 150$G. Two others components are single unstructured lines with g~2.15 and g~2.20, respectively. Because these signals are absent in Cu-free samples, one can assume that they are also caused by Cu-related centers. In the case of the latter two components the absence of Cu-related hyperfine structure can be explained by the exchange interaction between copper ions. Upon T_c increase, the intensities of all signals of the spectrum of the first type decrease monotonically.

The spectrum of the second type is observed in the samples calcined at higher temperatures (800–1,000◦C) when the contribution of the spectrum of the first type decreases. This signal was ascribed to the substitutional Cu^{2+}_{Zr} ions in monoclinic ZrO_2 structure. We take in account that Cu has two stable isotopes, ^{63}Cu and ^{65}Cu. For ^{63}Cu we used the following spin-Hamiltonian parameters: $g_x=2.002$, $g_y=2.027$, $g_z=2.168$, $A_{xx}=35\ 10^{-4}cm^{-1}$, $A_{xy}= 0cm^{-1}$, $A_{xz}=10\ 10^{-4}cm^{-1}$, $A_{yy}=33\ 10^{-4}cm^{-1}$, $A_{yz}=5\ 10^{-4}cm^{-1}$, $A_{zz}=186\ 10^{-4}cm^{-1}$. The contributions of ^{63}Cu and ^{65}Cu correspond to their abundance.

We conclude that at calcination temperature (500–900°C) the EPR signal is caused by Cu-related complexes on the surface of ZrO_2 crystallites. At 800–1000 °C we observed Cu ions that are located in the regular positions of crystalline lattice. The contribution of the latter signal correlated with contents of monoclinic phase.

Scattering Mechanisms in Crystals PbS p-Type Conductivity

Nyzhnykevych V.V. Luchytskyi R.M.

Ivano-Frankivsk National University of Oil and Gas, Ivano-Ivankivsk, Ukraine,
galuschak@nung.edu.ua

The theoretical analysis of scattering mechanisms of carriers by thermal vibrations of crystal lattice is done. The calculation provided of the mobility of carriers in a wide temperature (77 – 300 K) and concentration (10^{16} – 10^{20} sm^{-3}) bands in view of interacting conduction of holes of deformation potential acoustic and optical phonons and polarization potential of optical phonons.

Kinetic parameters of semiconductor materials are largely determined by the scattering mechanisms of carriers. Scattering mechanisms of carriers in lead chalcogenides have been studied repeatedly by different authors. But despite this, at present there is no consensus on the concentration and temperature limits the dominance of certain types of scattering. In this paper, based on comparison of theoretical calculations with the experimental Hall mobility data of specified concentration and temperature limits the use of approximate models of the band structure and the prevailing scattering mechanisms of charge carriers in lead selenide crystals p-type conductivity.

The dominant scattering mechanisms of carriers in hole lead selenide crystals are the scattering of short-range potential vacancies for the concentrations of $l0^{19}$ – 10^{20} sm^{-3} and the lattice thermal vibrations.

Scattering of phonons gives a correct picture of the quality necessary to characterize transport phenomena. The role of polar optical phonon significant at temperatures of 77 and 300 K for concentrations of 10^{17} – 10^{18} sm^{-3}. When increasing the concentration scattering on optical phonons is reduced due to screening.

At high concentrations (higher 10^{19} sm^{-3}) scattering on optical phonons is manifested through their deformation potential, whose influence on the total scattering at certain concentrations is very essential at room temperature. Scattering of carriers by acoustic phonons significant for all temperatures in the considering the whole studied concentration range. For temperature 77 K influence on the total scattering dominates deformation potential scattering on optical phonons.

1. Ravich Yu.L., Efimova B.A., Tamarchnko V.I. Scattering of current carriers and transport phenomena in lead chalkogenides. I. Theory // Phys. Stat. Sol. – 1971. – Vol.43, № 1. – P. 11-33.
2. Freik D.M., Nykyruy L.I., Ruvinsky M.A., Shperun V.M., Nyzhnykevych V.V. Scattering of charge carriers in lead chalcogenides crystals n-type // Physics and Chemistry of Solids. – 2001. – Vol.2, № 4. – P. 681-685.

Model Description of Short Range Order in Liquid Intermetallics

Oliinyk Z.M., Korolyshyn A.V., Mudry S.I.

Faculty of Physics, Ivan Franko National University of Lviv
Lviv, Ukraine, andrykorol@gmail.com

Interest to intermetallics is motivated by their wide application in various areas of industry that requires fundamental studies of structure and physical-chemical properties. Crystalline structure of binary and ternary intermetallic compounds is detailed studied, whereas available literature data on structure in liquid state are scarce. Numerous results on physical properties measurements shown that in liquid atomic distribution in liquid intermetallics deviates from random atomic distribution. Available data on structure investigation by means of diffraction methods confirm this fact. Considering such experimental results in many works it was concluded that liquid intermetallic compounds reveal not only topological short range order but also chemical ordering.

In order to describe chemical ordering in liquid intermetallics model of associated solution is currently used. This model is commonly used for interpretation of thermodynamic data, especially integral enthalpy of mixing and thermodynamic activity. Liquid compound is considered as mixture of clusters of different composition, which coexist with matrix, consisting of randomly distributed constituent atoms.

Unfortunately there are only available publications, where authors attempt to use the model of associated solutions to describe the results of diffraction studies. In this work we present the results on X-ray diffraction investigation of molten intermetallic compounds, existing in phase diagram of Ni-Si binary system. We have obtained structure factors, from which the pair correlation functions have been calculated. Model structure factor for intermetallic was calculated with taking into account the thermodynamic data and crystalline structure of this intermetallic phase.

Concentration Dependence of Mechanical Characteristics of Carbon Nanotubes and Polyethylene, Radiation Cross-Linked Hydrogels, Expanded Polystyrene

Onanko A.P., Kulish M.P., Dmitrenko O.P., Pinchuk-Rugal T.M., Aleksandrov M.A., Busko T.O., Pavlenko O.L., Charny D.V., Onanko Y.A., Kurochka L.I.

Taras Shevchenko Kyiv National University, Kyiv, Ukraine, onanko@univ.kiev.ua

Introduction. The anharmonic effects are studied on measuring of elastic characteristics descriptions of crystals, because elastic constants C_{ijkl} is determined through the second derived quantity from energy of co-operation between the atoms of crystalline grate F on deformation ε $C_{ijkl} = \partial^2 F/\partial\varepsilon^2$.

Experiment and results. For measuring diagram σ – ε the machine "ALA-TOO" (IMASH-20-75) was used [1]. The quasilongitudinal US velocity $V_{\parallel}$ = 9 m/sec, elastic module $E = \rho \cdot V_{\parallel}^2$ = 82,70 KPa; "fast" quasitransversal US velocity $V_{\perp}$ = 5 m/sec, shear module $G = \rho \cdot V_{\perp}^2$ = 25,53 KPa of radiation cross-linked hydrogels (CLHG) + 10% $(C_2H_4O)_n$ were determined from the oscillograms.

The Puasson coefficient μ is equal to ratio of relative transversal compression to relative longitudinal lengthening and equal [1]:

$$m = \frac{e_{\perp}}{e_{\parallel}} = \frac{1}{2}\left[1 + \frac{1}{1 - \left(\frac{V_{\parallel}}{V_{\perp}}\right)^2}\right]. \quad (1)$$

Concentration dependence of static elastic module E, strength limit at compression σ_{st}, elastic limit σ_E radiation cross-linked hydrogel + % $(C_2H_4O)_n$ are represented on fig. 1 in consequence of the formation of the polyvinyl alcohol molecules nanoclusters.

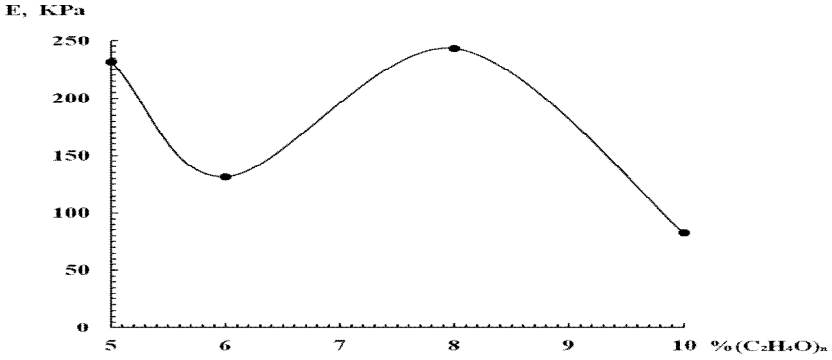

Fig. 1. Concentration dependence of static elastic module E radiation cross-linked hydrogel + % $(C_2H_4O)_n$.

1. Onanko Y.A., Vyzhva S.A., Onanko A.P., Kulish N.P. Automated system of treatment of ultrasound longitudinal and transversal velocities measuring. *Metalphysics and new technology*. 2011. V. 33, № 13. P. 529-533.

Mechanical Characteristics of Carbon Nanotubes and Polyethylene, Radiation Cross-Linked Hydrogels, Expanded Polystyrene

Onanko A.P., Kulish M.P., Dmitrenko O.P., Pinchuk-Rugal T.M., Aleksandrov M.A., Busko T.O., Pavlenko O.L., Charny D.V., Onanko Y.A., Rozhkovskiy O.M.

Taras Shevchenko Kyiv National University, Kyiv, Ukraine, onanko@univ.kiev.ua

Introduction. The values of static module E, elastic limit σ_E, effective fluidity limit σ_{fl}, strength limit at compression σ_{st} of the radiation cross-linked hydrogels are determined by the formation of the polyvinyl alcohol molecules nanoclusters.

Experiment and results. The thermal capacity – parameter of the thermodynamic system equilibrial state in Debye model. Therefore waves, that elementary oscillators excite, can't carry the energy. There are stand waves. One oscillator produce 3 waves: 1 longitudinal and 2 transversal. Debye temperature θ_D was determined after the formula [1]:

$$q_D = \frac{h}{k_B} \cdot \left(\frac{9N_A r}{4pA} \right)^{1/3} \cdot \left(\frac{1}{V_{II}^{\ 3}} + \frac{2}{V_{\perp}^{\ 3}} \right)^{1/3}. \quad (1)$$

The quasilongitudinal ultrasonic (US) velocity $V_{\parallel}$ = 504 m/sec, dynamical elastic module $E = \rho V_{\parallel}^2$ = 15,24 MPa, "fast" quasitransversal US velocity $V_{\perp 1}$ = 280 m/sec, shear module $G = \rho V_{\perp 1}^2$ = 4,704 MPa, Puasson coefficient μ = 0,3532, specific density ρ = 60 kg/m^3 of expanded polystyrene are determined from the oscilloscopegramma on fig. 1.

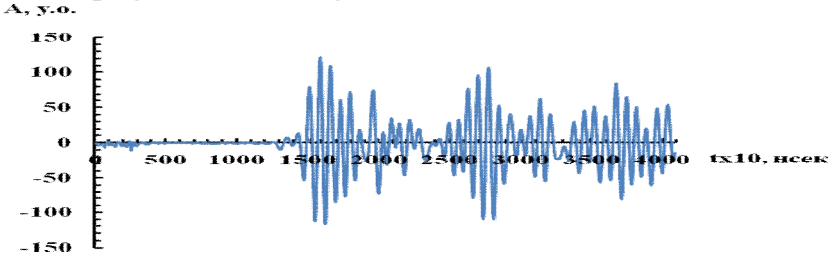

Fig. 1. Oscilloscopegramma of impulses with "fast" quasitransversal polarization $V_{\perp 1}$ in expanded polystyrene.

Conclusions

1. The optimum concentration C = 5% of polyvinyl spirit $(C_2H_4O)_n$ radiation sutured hydrogel with the maximal absolute values of the static module E at compression, at extension; elastic limit σ_E; effective fluidity limit σ_{fl}; strength limit at compression σ_{st} in consequence of the formation of the polyvinyl spirit molecules nanoclusters.

1. Onanko A.P., Lyashenko O.V., Onanko Y.A. Acoustic attenuation in silicon and silicon oxide. *J. Acoust. Soc. Am.* 2008. V. 123, № 5, Pt. 2. P. 3701.

Sol-Gel Synthesis of Nanostructured Nickel-Cadmium Ferrites and Their Optical, Electrical and Magnetic Properties

Ostafiychuk B.K., Bushkova V.S., Yaremiy I.P.

Department of Metallophysics and New Technologies, Vasyl Stefanyk Precarpathian National University, Ivano-Frankivsk, Ukraine, bushkovavira@gmail.com

Nickel ferrite $NiFe_2O_4$ in pure and substituted form constitutes technologically important material, which have been studied in many experimental and theoretical works [1]. The cadmium ferrite $CdFe_2O_4$ is well known as one type of the geometrically frustrated systems. The substitution of Cd^{2+} in ferrite is well-known to enhance the magnetic properties like saturation magnetization. The crystallographic, electrical, and magnetic properties of ferrites depend strongly on the method of preparation [2], chemical composition, synthesis parameter, type, and amount of dopant.

The nanopowders of nickel-cadmium ferrites were prepared by the technology sol-gel with participation of auto-combustion. After annealing at a temperature of 900 °C, the monophase powders were received. The average size of particles was found to be in the range 40 – 60 nm. It was shown that the lattice parameter increases with increasing content of Cd^{2+} ions. It was found that the optical band gap increases with increasing concentration of cadmium ions in the ferrite structure and it is in the range of 1.91 to 2.56 eV. It was shown that with increasing temperature increases conductivity of nickel-cadmium ferrites. It was detected that the activation energy of dc-conductivity at high temperatures increases significantly. This is due to a change in mechanism of conductivity in the range of temperature 67 – 88 °C for samples containing Cd^{2+} ions.

The magnetic structure was found to be ferrimagnetic for all samples. The increase of Cd^{2+} ions yields the increase of specific saturation magnetization, magnetic moment, initial permeability, and coercivity up to $x = 0.3$ then decreases thereafter. The Neel's two sub-lattice model can be applied to the samples up to $x = 0.3$. The composition dependence of the specific saturation magnetization and magnetic moment with $0.4 \leq x \leq 0.6$ were explained on the basis of the existence of Yafet–Kittel angles on the octahedral site spins. It was found that Curie temperature decreases from 558 °C to 424 °C with increasing of Cd^{2+} ions.

1. A. Sutka, R. Parna, G. Mezinskis, V. Kisand, *Sens. Actuator B-Chem.* **192**, 173 (2014).
2. Vira S. Bushkova, Ivan P. Yaremiy, *J. Magn. Magn. Mater*. **461**, 37 (2018).

Holographic Gratings Recording in Yb Doped As_2S_3–Se Nanomultilayer Structures

Paiuk O.[1], Meshalkin A.[2], Stronski A.[1], Achimova E.[2], Abashkin V.[2], Prisacar A.[2], Triduh G.[2], Korchovyi A.[1], Kidalov V.[3]

[1]*V. Lashkaryov Institute of Semiconductor Physics, NAS of Ukraine, Kyiv, Ukraine,* paiuk@ua.fm
[2]*Institute of Applied Physics, Chisinau, Moldova;*
[3]*Berdiansk State Pedagogical University, Berdiansk, Ukraine*

Properties and direct one-step relief formation of optical elements using amorphous chalcogenide nanomultilayer structure As_2S_3:Yb–Se were studied in present work.

Amorphous As_2S_3:Yb–Se nanomultilayer structures were prepared by cyclic thermal vacuum deposition from two isolated boats with As_2S_3:Yb and Se chalcogenides on constantly rotated glass substrate at room temperature in one vacuum deposition cycle with chalcogenide thickness of 13 nm and Se –10 nm. The total number of nanolayers was 200. Optical transmission was measured in 200-900 nm optical range in order to determine the refractive index, thickness and optical band-gap energy of As_2S_3:Yb and Se layers and As_2S_3:Yb–Se nanomultilayers.

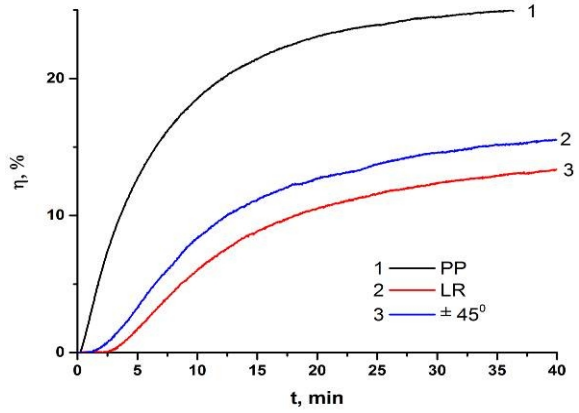

Fig. 1. Dependence of diffraction efficiency kinetics on polarization of recording beams

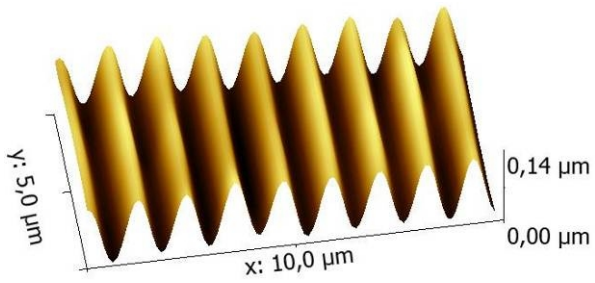

Fig. 2. Surface of diffraction grating recorded in As_2S_3:Yb–Se multilayers

Diffraction gratings were recorded by two laser beams using different polarizations of light (λ=532nm and I= 3057 mW/cm^2) with synchronous diffraction efficiency measurement at 650 nm wavelength.

As one can be seen from Fig. 1, the process of surface relief formation depended on the polarization of recording light beams. Diffraction efficiency of recorded gratings was ~ 25% in absolute value. Morphology and surface relief of the obtained gratings were studied by AFM microscopy (Fig 2). Due to the changes in transmission, reflection, and in thickness under the influence of laser irradiation, As_2S_3:Yb–Se nanomultilayer structures may be used for effective amplitude-phase optical information recording and for the production of surface-relief optical elements.

Electron structure and optical properties of conjugated systems with fullerenes

Pavlenko O.L. [1], Busko T.O. [1], Lesiuk A.I. [1], Nikolayenko T.Yu. [1], Pundyk I.P. [1], Dmytrenko O.P. [1], Kachkovsky O.D. [2]

[1] *Faculty of Physics, Taras Shevchenko National University of Kyiv, Kyiv, Ukraine,* olpavl57@gmail.com

[2] *Institute of Bioorganic Chemistry and Petrochemistry, NAS of Ukraine, Kyiv, Ukraine*

It is known that carbon atoms in the conjugated systems have sp^2 - hybridization forming 3 carbon–carbonσ-bonds while the residual $2p_z$ electrons can generate the collective systems of π-electrons. Such systems form not only one-dimensional π-molecules but also the branched π-electron systems. According to the Daehne's triad theory, the conjugated systems are divided on cyclic molecules (or aromatics) and linear molecules (neutral polyenes and ionicpolymethine dyes as well as their derivatives including the donor-acceptor conjugated molecules).Structural organization is important in considering of interaction between the dyes and carbon nanostructures, especially with fullerenes, antitumor agents. The aggregation points in particular on the important influence of the solutions on the spectral properties of the linear conjugated systems.

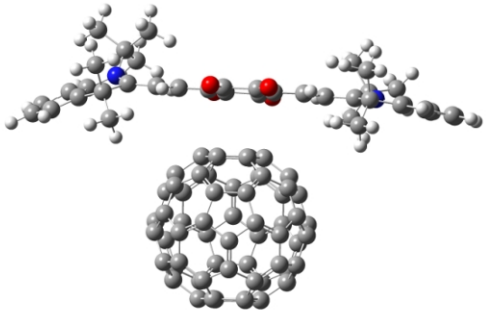

Fig.1. Optimized geometry of C_{60}-dye system.

The high mobility of the collective π-electron shell in the linear conjugated molecules (and their ions) is confirmed by their spectral propreties. This electron mobility depends on the type of the conjugated system, chain length, symmetry, molecular constitution of the terminal groups, as well as the electron shell (neutral or charge system). Besides, different molecular types show the different sensitivity to the solvent polarity.

Surface Stabilization of the MnS Nanoparticles

Pylypko V.G. and Shcherbak L.P.

Yuriy Fedkovych Chernivtsi National University,
Chernivtsi, Ukraine, v.pylypko@chnu.edu.ua

Manganese sulfide MnS is a wide band-gap magnetic semiconductor with a bulk band edge ~3,1 eV and band edge about 400 nm. Described in many papers nanosized MnS show the absorption band-edge (λ_{max}) ranged 278÷488 nm depending on the wet-synthesis thermodynamic conditions and capping agents' nature [1]. According to various investigations MnS nanoparticles (NPs) had attracted interest for the potential applications in the field of short wavelength optoelectronics, as photoluminescent component, photocatalists, or contrast agent for magnetic resonance imaging *etc*.

The aim of the paper is to compare stabilizing effect of L-cysteine and citrate-ions to MnS nanoparticles synthesized with equal precursors content and coordination number for the ligands (c.n=2).

Manganese chloride $MnCl_2 \cdot 4H_2O$, Trisodium citrate $C_6H_5Na_3O_7 \cdot 2H_2O$, L-cysteine and Sodium sulfide $Na_2S \cdot 9H_2O$ of high chemical grade were used for the synthesis. Initial prepared the Mn-citrate and Mn-L-cysteine complexes aqua solutions were mixed simultaneously with the Na_2S solution with the [cation]: [anion]: [stabilizer] ratio equal to 1:1:2. Influence of the precursors' concentration and the synthesis temperature were studied.

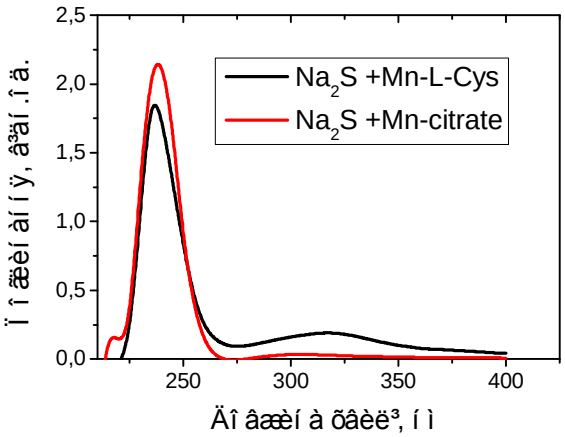

Fig. 1. Absorbance spectra of the MnS/L-cys and MnS/citrate NPs colloidal solutions 1 hour after the synthesis.

It was obtained that typical for the MnS colloidal solutions pink-like hue appeared faster in the case of the system with L-cysteine than with the citrate-iones though the absorbance spectra of both solutions at one hour after synthesis almost coincide (Fig.1). However the MnS/L-cysteine NPs were less stable and precipitated during one day while MnS/citrate NPs demonstrated slight growth (λ_{max} shifted from 260 to 262 nm). Weaker bonding of the L-cysteine to the MnS NPs surface in comparison with the citrate ions was observed also after boiling of the solutions during 1 hour that had resulted in a white powder appearance in the MnS/L-cys NPs' solution.

Reference

1. Ferretti, A. M., Mondini, S., & Ponti, A. (2016). *Manganese Sulfide (MnS) Nanocrystals: Synthesis, Properties, and Applications. Advances in Colloid Science.*doi:10.5772/65092

Electrode Material for Supercapacitors Based on Thermally Exfoliated Graphite

Rachiy B.I.[1], Revo S.L.[2], Budzulyak I.M.[1], Lisovsky R.P.[1], Musiy R.Y.[3]

[1]*Vasyl Stefanyk Precarpathian National University, Ivano-Frankivsk, Ukraine*
[2]*Taras Shevchenko National University of Kyiv, Kyiv, Ukraine*
[3]*Department of Physical Chemistry of Fossil Fuels InPOCC, National Academy of Sciences of Ukraine, Lviv, Ukraine, bogdan_rachiy@ukr.net*

The main criteria for choice of active material of electrodes supercapacitor (SC) are a large specific surface area, desire pore size distribution, a high electrical conductivity to provide large values of specific power and chemical resistance to electrolyte. A promising material for use as electrodes in the SC is a nanoporous activated carbon with a highly developed surface (> 1000 m^2/g). However its electrical conductivity is small and depends on the conductivity of the material particles, their contact, porosity and chemical composition. To overcome this problem, a composite material nanoporous carbon (NC) - thermally exfoliated graphite (TEG) was developed. Composite material (CM) was manufactured by mechanical mixing of NC and TEG. Depending on the content of the TEG (5÷30%), a series of CMs is obtained.

The specific energy characteristics of the SCs, formed on the basis of CM, were determined by the galvanostatic method at charge/discharge currents of 10÷100 mA. For all CMs, the voltage dependence of the SC from time, at different discharge currents is linear, indicating the dominance of the charge accumulation process in the double electric layer. The increase of the discharge current reduces the duration of charge/discharge cycle, and also leads to an increase in voltage drop during discharge.

For all systems, the specific capacity decreases linearly with increasing discharge current (Fig. 1). For a CM15, the increase of current from 10 to 100 mA leads to a 20% capacity reduc-tion. The optimal concentration ratio of components (NC:TEG = 85:15) were obtained for preparing of CM with high electrical conductivity (≈ 240 S/m) and a developed specific surface area (≈ 700 m^2/g), which provides the maximum specific electrical capacity of CM 150-165 F/g in 30 % KOH electrolyte.

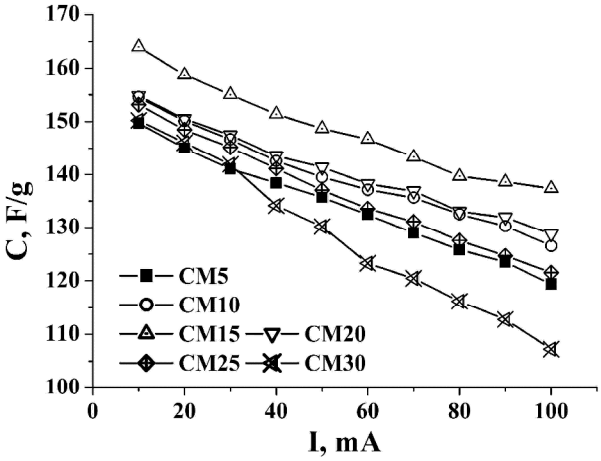

Fig.1. Dependence of the specific capacitance of the CM from the discharge current SC

Features of the Heat Conductivity of Penton Filled by MWCNT

Rokytska H.V., Stoliarova S.S., Rokytskyi M.O., Shut M.I.

National Pedagogical Dragomanov University, Kyiv, Ukraine, galinadarla@gmail.com

Purpose of this work is ascertainment of multi-walled carbon nanotubes influence on heat conductivity of polymer composite materials based on highly stable and chemically resistant high-molecular polyether – penton.

As fillers were used acid cleaned from mineral impurities multi-walled carbon nanotubes 10 ÷ 40 nm in diameter, with specific surface about 200 ÷ 400 m^2/g and with specific electrical resistance about 0,05 ÷ 0,1 ohm·cm.

Penton - multi-walled carbon nanotubes system specimens were prepared at following thermo-baro-time (T-p-t) condition: heating rate 3,5 K/min, aging at 483 K pending 15 min under pressure of 20 MPa, cooling from melt with 0,5 K/min rate. Investigations of polymer nanocomposites heat conductivity temperature dependences were conducted by the dynamic λ-calorimeter that was the modernized thermal conductivity meter "*ИТ-l-400*" in 293 - 443 K temperature rate for different disperse fillers volume content ($0 \leq \varphi \leq 2$ %).

The analysis of experimental data shows that the breakdown in the intensity of the change in the heat conductivity of pure penton and composites, observed at temperatures above 360 K, occurs because the polymer matrix at these temperatures completely shifts from the glassy to the highly elastic state. A further sharp increase in the thermal conductivity of composites occurs due to a violation of the measurement regime as a result of the processes of pre-melting of the polymer matrix, changes in its viscosity and thickness of the samples under the influence of temperature. With an increase in the concentration of carbon nanotubes, this effect is observed at higher temperatures due to the being of such concentrations of the polymer component in the state of the wall layer with more perfect structure, the formation of a rigid framework of the particles of the filler and a small total deformation of the composites.

With low content of dispersed filler, the thermal conductivity of polymer composite materials is low and close to the thermal conductivity of the polymer and is ensured by the implementation of the phonon mechanism in the crystalline and amorphous regions of the penton, as well as by the conductivity of kinetic units in the amorphous regions of the polymer by the diffusion mechanism. With an increasing in the concentration of MWCNT ($\varphi \geq 0.37$ vol. %), an increase in the thermal conductivity is observed, apparently due to the formation of the interphase transition layer around the filler particles with more densive and ordered structure, which in turn has a higher thermal conductivity. With further increase in the content of MWCNT in composites, their thermal conductivity is practically unchanged, which indicates the transition of the entire volume of penton to the state of the wall layer.

Acoustic Properties of Polymer Nanocomposite System Polychlortrifluoroethylene – Tin Dioxide

Rokytskyi M.O., Sichkar T.G., Shut A.M., Tulzhenkova O.S., Shut M.I.

National Pedagogical Dragomanov University, Kyiv, Ukraine, maksal@bigmir.net

Polymer oxide nanocomposites are characterized by high levels of protective and absorption properties, and excellent electrophysical and thermophysical properties and compares favorably with classic materials by low filler content. In this respect, it is interesting from a scientific and practical point of view to conduct experimental studies of the structural features, as well as the mechanical properties of such composite materials. Purpose of this work is investigation of the acoustic properties of polychlorotrifluoroethylene (PCTFE) polymer nanocomposite system - tin dioxide (SnO_2).

Polymer nanocomposites PCTFE - SnO_2 obtained by hot pressing. The density and total moisture of received composites are investigated experimentally with using hydrostatic weighing method. The propagation velocity, the absorption coefficient, the complex modulus of elasticity, the tangent of the angle of mechanical losses, and the jump in the absorption of ultrasound as the frequency changes were determined by ultrasonic method. The investigations of the acoustic properties of nanocomposites were carried out by pulsed phase method at room temperature in the frequency range of 5 - 10 MHz.An ultrasound speed meter and ultrasound transducer “УС-12-ИМ”, an ultrasound emitter and a receiver with buffer rods were used for the implementation of the pulsed phase method.

The results of ultrasound studies show the main factors affecting the structure of the system: the achievement and development of the percolation threshold (~ 3 vol. %); change in the properties of the surface layer of the polymer matrix under the action of the filler and the change in the porosity of the system. The result of this cumulative effect is the existence of two characterized zones of concentration: from 0 to 10 vol. % and from 10 to 20 vol. %. In the first zone, the most influential are the achievement of the threshold of percolation and the change in the structure of the surface layer of the polymer matrix. In the second zone, it appears that the influence of various factors is offset, which illustrated by the concentration dependencies of the modules. This leads to virtually unchanged physical and mechanical characteristics, although the introduction of a more elastic and dense filler in a less elastic matrix should lead to significant changes in these characteristics, especially with constant porosity.

Thus, low porosity and high levels of mechanical characteristics characterize the obtained polymer oxide nanocomposites. This allows to operate the system of composites PCTFE - SnO_2 for large loads in difficult weather conditions and in the presence of aggressive environments.

Resonant Tunneling Through Graphene-Based Double-Barrier Structure

Sakhnyuk V.E., Zamurujeva O.V., Fedosov S.A., Dmytruk O.V.

Lesya Ukrainka Eastern European National University, Lutsk, Ukraine, sve2008@ukr.net

For the electrons that are incident on the potential barrier in graphene, there are the following values of the angles of incidence, for which the coefficient of passage is equal to one. For electrons with the normal incidence barrier is completely transparent regardless of its height and width. Such an effect for relativistic electrons has long been known as the "Klein's paradox" [1, 2] and is associated with the preservation of pseudopsin.

We investigated the symmetric double-barrier structure of rectangular shape determined by the function

$$V(x) = \begin{cases} 0, & x < -a - d, \\ V_0, & -a - d < x < -a, \\ 0, & -a < x < a, \\ V_0, & a < x < a + d, \\ 0, & x > a + d. \end{cases} \quad (1)$$

A massless two-dimensional Dirac equation with potential (1) was solved to analyze the tunneling of electrons through such a potential barrier.

The main results of the study:

1) A new formula for the dependence of the coefficient of transparency of a symmetric double-potential rectangular barrier on its parameters and on the angle of incidence of electrons has been obtained;

2) Conditions which must satisfy the angles with 100 % probability of tunneling of electrons through the barrier have been found;

3) Angles of incidence at which the probability of a tunneling is equal to one have been found from the analysis of the conditions of resonance tunneling for certain values of the barrier parameters. It is shown that with the decrease in the barrier height, the number of resonance angles increases, and the maxima become more acute.

1. Klein O. *Die reflexion von elektronen an einem potentialsprung nach der relativistischen dynamik von Dirac. Z. Phys.* 1929. Vol.53. P. 157-165.
2. Katsnelson M.I., Novoselov K.S., Geim A.K. *Chiral tunnelling and the Klein paradox in grapheme. Nat. Phys.* 2006. Vol.2. P. 620-625.

Nanocrystalline Thermoelectric Materials Based on Pb (Sn)-Ag-Te Compounds

Semko T.O.[1], Ogorodnik Y.V.[2], Halushchak M.O.[3], Mudryj S.I.[4]

[1]*Vasyl Stefanyk Precarpathian National University, Ivano-Frankivsk, Ukraine, t.semko@i.ua*
[2]*Radiation Monitoring Devices, Inc., Boston, USA*
[3]*Ivano Frankivsk National Technical University of Oil and Gas, Ivano-Frankivsk, 76000, Ukraine*
[4]*Ivan Franko National University of Lviv, Lviv, Ukraine*

For active elements of thermoelectric converters in temperature range (500-850) K widely used the lead telluride, due to the uniqueness of its physical and chemical properties, as well as the relatively simple technology of obtaining qualitative crystals. One of the most important problems of thermoelectric converters, and not only on the basis of PbTe, is their relatively low efficiency (6 - 9) %. One of the ways to solve it is to modify the properties of the material by doping, creating solid solutions and nanocrystalline materials.

In the work investigated the thermoelectric properties of materials of $Pb_{14}Sn_4Ag_2Te_{20}$ and $Pb_{16}Sn_2Ag_2Te_{20}$ for the first time, the influence of technological factors on obtaining experimental samples on microstructure and temperature dependences of the coefficient of thermoelectric power, specific electrical conductivity and thermal conductivity coefficient have been established. It is shown that for optimization of PbTe thermoelectric parameters, the formation of solid solutions of $Pb_{1-x}Ag_xTe$ is more promising than that of PbTe:Ag doping, in which the acceptor activity of argentum atoms is poorly expressed as a result of the manifestation of amphoteric properties. The main factor which results in the production of materials of the Pb-Sn-Ag-Te system with low thermal conductivity (≈ 0.002 W/(cm C)) is that sample contain two-phases: in addition to the main phase of the structural type NaCl, exist the additional phase of $Ag_{10.6}Te_7$ whitch fixed by X-ray.

In order to explain the complex of experimental data obtained, we propose models that take into account the formation of a surface layer with properties different from those of a voluminous material. In particular, for the purpose of explaining the temperature dependences of specific conductivity, a modified electrical model is presented which takes into account the differences in the specific resistance of the grain boundaries along and across the compression axis.

The Theory of Electron States on the Dynamically Deformed Adsorbed Surface of Semiconductor With a Zinc Blende Structure

Seneta M.Ya.[1,2], Slyusarchuk Yu.M.[2], Gal' Yu.M.[1], Peleshchak R.M.[1], Chopyk P.Ya.[1]

[1]*Drohobych Ivan Franko State Pedagogical University, Drohobych, Ukraine*
[2]*Lviv Polytechnic National University, Lviv, Ukraine, marsen18@i.ua*

The creation of a new class of gas sensors, biosensors, quantum-sized heterolazers and signal processing systems requires the researches of the mechanisms of electron states excitation on the adsorbed rough surface of semiconductors in the presence of an acoustic quasi-Rayleigh wave propagating along the surface.

The self-consistent interaction between the surface elastic acoustic wave and adsorbed atoms leads to the dynamic deformation of the adsorbed surface. As a result of this process there are the renormalization of the acoustic quasi-Rayleigh wave spectrum and the phonon mode width, and the appearance of localized electron states near the roughness on the surface. The surface roughness are created by a dynamic deformation and adsorbed atoms with concentration N_{0d}. The interaction between a surface acoustic wave and adsorbed atoms is carried due to the deformation potential.

The purpose of this work is the investigation of the influence of the adsorbed atoms concentration on the electron characteristics of the monocrystal surface (the dispersion law of electron states; the electron concentration; the density of electron states) on a dynamically deformed adsorbed surface of semiconductors with a Zinc blende structure.

The electron spectrum on the rough adsorbed surface of the semiconductor is founded from the non-stationary Schrödinger equation:

$$i\mathbf{h}\frac{\partial y(x,z,t)}{\partial t}=\frac{-\mathbf{h}^2}{2m^*}\left(\frac{\partial^2 y}{\partial x^2}+\frac{\partial^2 y}{\partial z^2}\right)+V_0 e^{-k_l(N_{od})z}\cos(qx-w'(q,N_{od})t)y(x,z,t), \quad (1)$$

where m^* is the effective electron mass; V_0 is the amplitude of the deformation potential created by the surface acoustic wave and adsorbed atoms; q is the module of wave vector of quasi-Rayleigh wave; $w'(q,N_{0d})$ is the dispersion law of quasi-Rayleigh wave; $k_l^2(N_{0d})=q^2-w^2(N_{0d})/c_l^2$; c_l is the longitudinal sound velocity.

The solution of equation (1) is obtained as a sum of space-time harmonics

$$y(x,z,t)=\sum_{n=-\infty}^{\infty} y_n(z)e^{iF_n(x,t)}, \quad (2)$$

where $F_n(x,t)=(k_x+nq)x-(w_e+nw'(q,N_{0d}))t$ is the phase of the electron wave; $\mathbf{h}w_e=E$ – the electron energy; $\mathbf{h}k_x$ is its impulse.

Determination of Optimal Conditions for the Deposition of Gold Nanofilms on a Silicon by Galvanic Replacement Method

Shepida M.V., Nichkalo S.I.

Lviv Polytechnic National University,Lviv, Ukraine, maryana_shepida@ukr.net

Nanoparticles and nanofilms of gold are widely used in the field of biomedicine as biosensors, biomarkers, as well as for the formation of silicon nanostructures of different morphologies (nanopores, nanowires, nanopillars etc.) [1, 2]. The deposition method and the control of morphology of deposited gold nanoparticles and nanofilms are known to be urgent tasks. Thus, widely studied physico-chemical methods of deposition are carried out mainly in aqueous solutions, in which, besides the main process of metal reduction, there are side processes, in particular the separation of hydrogen in the cathode regions and the decomposition of the substrate on which the particles or films are deposited. This issue complicates the controlled formation of metal nanoparticles, which is a necessary condition for surface modification. In contrast, utilizing the galvanic repalcement in the medium of organic aprotic solvents (dimethyl sulfoxide, DMSO) can prevent the occurrence of these disadvantages, as it was shown previously in [2]. Therefore, the aim of this work is to study the formation conditions of gold nanofilms by galvanic replacement method in a DMSO solvent, and their subsequent use for the fabrication of silicon nanostructures by means of metal-assisted chemical etching method.

The experimental results showed that the main factors influencing the geometry of gold nanoparticles, which determine the morphology of the resulting film, are the composition of a solution, the temperature and duration of the process. It was found out that from complex ions $[AuCl_4]^-$ ($K_H = 1\times10^{-19}$), the high stability of which causes a significant cathode polarization, the deposition of nanoparticles with an average diameter of 100 nm occurs. It was shown that the non-aqueous medium contributes to the formation of spherical gold nanoparticles and the 2D surface of silicon is filled up by them. It has been established that with an increase in the duration of galvanic replacement process from 30 to 240 s, a tendency exists for the agglomeration of gold nanoparticles into a porous film.

1. A. Lahiri and S.-I. Kobayshi, “Electroless deposition of gold on silicon and its potential applications: review”, *Surface Engineering*, vol. 32, pp. 321–337, 2016.
2. O. Kuntyi, M. Shepida, L. Sus, G. Zozulya, S. Korniy, “Modification of silicon surface with silver, gold and palladium nanostructures via galvanic substitution in DMSO and DMF solutions”, *Chemistry & Chemical Technology*, vol.12, pp. 305–309, 2018.

Phase Transitions in a Model of BEDT-TTF Compound Electron Subsystem

Skorenkyy Yu.

Ternopil Ivan Puluj National Technical University, Ternopil, Ukraine,
skorenkyy@tntu.edu.ua

In recent years experimental studies of low-dimensional materials and theoretical investigations of quasi-2D conductor models have been intensified. Bis(ethylenedithio)tetrathiafulvalene (BEDT-TTF) molecule is a basis for large variety of cation-radical salts [G13] having rich phase diagram with pressure, temperature, anion doping-driven transitions. Organic molecular crystals with formula $(BEDT\text{-}TTF)_2X$ are composed of dimerised BEDT-TTF molecules and conducting anion planes. Such structure causes strongly anisotropic electrical properties and peculiar phase transitions. For example, two-dimensional metal $(BEDT\text{-}TTF)_3(HSO_4)_2$ undergoes the metal-insulator transition at 126 K. At the transition point structural changes were observed therefore it can be classified as the Mott transition caused by anisotropic thermal contraction of the lattice. Temperature decrease gives rise to antiferromagnetic fluctuations and the external pressure transition to superconducting state occurs. Electron localization effects are crucial for narrow energy bands of these materials.

We generalize the approach of works [3,4] on two-dimensional conductors with strong electron correlations, using the configurational representation of the model Hamiltonian which allows us obtaining of the Green function analytically and calculation of the energy spectrum. Effective Hamiltonian [13] of the model takes into account the strong intra-site Coulomb, intersite exchange interaction of electrons and correlated hopping of electrons both along the chain and in transversal direction. With rise of intraatomic Coulomb repulsion U in the energy spectrum a gap opens and the transition to antiferromagnetic state is realized. The pressure application is shown to eliminate dimerization, kinetic energy increases and Fermi surface symmetry brokes down. At the external pressure and decreasing temperature the transition from insulator to metallic phase occurs due to reduction of electron correlation.

1. Lebed, A.G. (Ed.) *Physics of Organic Superconductors and Conductors. Vol. 110*, Springer: Heidelberg, 357 p., 2008.
2. Skorenkyy Yu., Didukh L., Kramar O., Dovhopyaty Yu. Mott transition, ferromagnetism and conductivity in the generalized Hubbard model. *Acta Physica Polonica A.* 2007, V.111, P.635-644.
3. Skorenkyy Yu., Kramar O. Antiferromagnetic ordering and pseudogap in a model of quasi-1D organic superconductor electronic subsystem. *Mol. Cryst. Liq. Cryst.* 2016, V.639, P.24-32.

Spatial Structure of the Adsorption Complex of Water Molecules on TiO_2 Films

Smirnova O.V., Grebenyuk A.G., Lobanov V.V.

Chuiko Institute of Surface Chemistry of National Academy of Sciences of Ukraine, Kyiv, Ukraine, osmirnova@isc.gov.ua

The atomic and electronic properties of pure and nitrogen-doped TiO_2 clusters of different composition (14 or 21 Ti atoms, stoichiometric and having oxygen vacancies) were analyzed earlier in [1]. In this work, we studied the equilibrium structure (Fig. 1) and the IR absorption spectra of model titanium dioxide clusters of composition $Ti_{21}H_2O_{42}$ with different types of adsorption complexes of a water molecule. According to experimental data (IR spectroscopy), it is possible to determine the types of different structural OH groups on the titanium dioxide surface, which differ in the pK_a value. Fragments of the surface, similar to the structure of metatitanic acid (H_2TiO_3), form a region of Bronsted acids, and titanium hydroxides ($TiO(OH)_2$, $Ti(OH)_4$) form Bronsted bases. Hydrated forms of TiO_2 correspond to pK_a values close to 7. The considered structures are studied by DFT method (B3LYP/3-21G**). The calculations were performed using the PC software package GAMESS (FireFly version 8.1.0, A.Granovsky). The Lewis and Brønsted sites of adsorption of water molecule were studied with a model TiO_2 cluster of composition $Ti_{21}H_2O_{42}$ (Fig. 1) and several proposed options for adsorption of a water molecule were considered. Adsorption occurs with the formation of a coordination bond between the titanium atom of the anatase surface and the oxygen atom of the water molecule. In the second case, it was assumed that due to adsorption of water a hydrogen bond is formed between the oxygen atom of the anatase surface and the hydrogen atom of the water molecule. It turned out that the optimization of the geometry leads to the transition to the first adsorption variant, that is, a coordination bond is formed between the atoms of titanium and oxygen. Water adsorption energy is 74.7 kJ/mol. The possibility of proton transfer through the hydrogen bond, leading to the dissociation of the adsorbed water molecule on the anatase surface with the formation of two types of Ti-OH groups, was also studied. The resulting structure is energetically more beneficial than the previous one: the effect is 18 kJ/mol. Thus, the adsorption of water on the surface of anatase predominantly occurs by proton transfer through the dissociative mechanism.

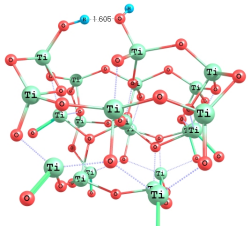

Fig. 1. The structure of the adsorption complex of a water molecule on the anatase surface

1. *Smirnova O., Grebenyuk A., Linnik O., and Lobanov V.* Quantum Chemical Study of Water Molecule Adsorption on the Nitrogen-Doped Titania Thin Films // Nanophysics, Nanomaterials, Interface Studies, and Applications: Selected Proc. 4th Int. Conf. Nanotechnology and Nanomaterials (NANO2016, Aug. 24-27, 2016, Lviv, Ukraine). - Springer, 2017. - P.603-609.

Influence of Technology on the Formation Of Luminescence Centers in QDs CdS

Smyntyna V.A., Skobeeva V.M., Verheles K.A., Malushin N.V.

Odessa National University named after I.I. Mechnikov Odessa, Ukraine,
v_skobeeva@ukr.net

From the point of view quantum dots (QD) of A_2B_6 compounds application, their luminescent properties cause the greatest interest. The high quantum yield of luminescence and the stability of luminescence open up the prospect for using semiconductor QDs in practical applications such as phosphors, LEDs, and also as fluorescent markers for biochemical and biomedical applications.

The research of CdS QDs the luminescence is devoted a large number of papers, but the question of the nature of the luminescence centers and the conditions for their formation in the synthesis process is still relevant. This is due to the use of different technologies, different synthesis conditions. Colloid-chemical synthesis of nanoparticles is influenced by a large number of factors. In addition to the nature and concentration of precursors and stabilizers, synthesis temperature, the acidity of the dispersion medium pH turned out to be an important factor in controlling the optical characteristics of the obtained NPs. In this work, we studied the effect of acid - alkaline balance on the formation of defects in CdS QDs, which are centers of luminescence.

The cadmium sulfide nanocrystals under study were chemically prepared from solutions of cadmium and sulfur salts in an aqueous solution of gelatin. The pH values of the solutions were changed by adding a solution of alkali or hydrochloric acid to a water solution of gelatin with cadmium nitrate to obtain the required pH values (2 ÷ 10).

In this work it was shown that to understand the mechanism of defects formation in CdS nanocrystals (NCs), when they are synthesized in salts aqueous solutions, one should take into account the result of the hydrolysis process and the dependence of its products on the pH of the solution. It was found that before the value of pH≤8 the concentration cadmium ions in the solution is dominant. With further increase in pH the concentration of sulfur ions increases and the concentration of cadmium ions decreases. Analysis of the CdS NCs absorption and luminescence spectra has allowed us to propose the nature of the centers responsible for the emission. It was established that the nature of the band with $\lambda = 470 \div 498$ nm is associated with cadmium interstitial. The luminescence in the region of $\lambda = 630$ nm may be due to an associative defect associated with cadmium and sulfur vacancies, and the nature of the long wavelength band ($\lambda = 720$ nm) with sulfur vacancies.

Electroluminescence from n-ZnO Microdisks/p-GaN Heterostructure

Turko B.I.[1], Nikolenko A.S.[2], Sadovyi B.S.[1, 3], Toporovska L.R.[1], Rudko M.S.[1], Kapustianyk V.B.[1], Strelchuk V.V.[2], Panasyuk M.R.[1], Serkiz R.Y.[1]

[1]*Ivan Franko National University of Lviv, Lviv, Ukraine, tyrko_borys@ukr.net*
[2]*V.E. Lashkaryov Institute of Semiconductor Physics NAS of Ukraine, Kyiv, Ukraine*
[3]*Institute of High Pressure Physics PAS, Warsaw, Poland*

Nowadays, in the world of cutting edge technologies it is very important to invent highly efficient and low-cost ways of designing of the light emitting diode (LED) consuming as minimum energy as possible. For the last years such a wide band gap semiconductor as zinc oxide have been substantially drawing an attention as a superior material for optoelectronic applications over GaN [1]. ZnO and GaN are related semiconductor materials having the same crystalline structure (wurtsite) and close values of the lattice parameters (lattice mismatch is only about 1.8 %). It is possible to further reduce the tension between the heterolayers and increase the probability of radiative recombination of charge carriers using, for example, ZnO micro-/nanostructures instead of the film in the heterostructure.

The LED structure based on *p*-GaN film/*n*-ZnO microdisks quasiarray heterojunction was fabricated. It is shown that the epitaxial quality of *p*-GaN films upon growth from the vapor phase can lead to growth of the hexagonal microdisk ZnO rather than the vertical nanorods. The density of the microdisks changed across the substrate surface. ZnO hexagonal microdisks are characterized by the average height of about 5 μm with diameters ranging from 25 μm up to 60 μm. The turn-on voltage of the heterojunction of ZnO/GaN (disks/film) is around 3 V. The diode-ideality factor was estimated to be of around 30. The large values of the ideality factors indicate a high density of trap states and also may be connected with the quality of the contacts to the *p*-*n* junction. The electroluminescence (EL) spectrum acquired from the *p*-GaN film/*n*-ZnO microdisks junction exhibited the bands with maxima at 366, 394 and 495 nm. On the basis of the data of X-ray diffraction, electrical and optical studies these peaks were associated with GaN near-band-edge (NBE) emission, ZnO NBE emission, and emission from the defect levels in ZnO, respectively. The EL emission of *p*-GaN film/ZnO microdisks quasiarray heterojunction LED structure possesses the following CIE color coordinates: x=0.36, y=0.38. It means that the cold white light with an equivalent temperature T = 4500 K is emitted.

1. ZnO as Multifunctional Material for Nanoelectronics / Kapustianyk V., Turko B. – Beau Bassin : Scholars' Press, 2018. – 84 p.

Quantum Dots Grown by Femtosecond Laser Ablation

Tur Y.[1], Virt I.S.[1,2]

[1]*Drogobych State Pedagogical University, Drogobych, Ukraine, tur2014@meta.ua*
[2]*University of Rzeszow, Rzeszow, Poland*

Lead telluride (PbTe) is an important group IV-VI semiconductor with a narrow fundamental band gap Eo ˜ 0.3 eV at room temperature. Extensive research has been done in the last two decades on PbTe thin films, mainly due to the technological importance for use in a variety of optoelectronic devices like infrared detectors and tunable midinfrared quantum well diode lasers. PbTe thin films have been deposited using techniques such as hot-wall epitaxy, magnetron sputtering, thermal evaporation, electrodeposition , molecular beam epitaxy and pulsed laser deposition More recently, PbTe grown in form of Quantum Dots is been studied because of its interesting non linear optical properties. The fact that PbTe present quantum confinements effects in the region used for optical communications transforms this material in an excellent candidate for developing all-optical switching devices.

Pulsed laser deposition (PLD) is a thin film growth method which has generated a lot of interest in the past few years as one of the simplest and most versatile technique for the deposition of a wide variety of materials. PLD enables easy stoichiometric transfer from the target to the deposit in a convenient gas atmosphere, becoming a powerful technique for fabricating high-quality films of high-Tc superconductor oxides and a number of others, such as piezoelectrics and ferroelectrics. More recently, this technique was used to deposit polycrystalline and epitaxially oriented films of PbTe on KCl(100) and BaF_2(111) substrates. The major disadvantage of PLD has been the deposition of particulates or droplets (splashing) on the film surface during the deposition process. The splashing formation is a great drawback for applications related to the fabrication of nanostructured materials. Obviously, the arrival of micron or submicron sized particulates at the substrate is detrimental to the properties of an optical device based on nanoparticles. With the rapid development experienced in the generation of ultra short laser pulses, new possibilities were opened for the PLD technique by using femtosecond lasers as ablation source. It is commonly believed that when the temporal length of the laser pulse became shorter than the several picoseconds required to couple the electronic energy to the lattice of the material, thermal effects could not play a significant role. Since the pulsewidth is too short for thermal effects to take place, the material is direct vaporized away from the surface. Nevertheless, more recently other processes have been suggested to occur during the interaction of material with ultra-short laser pulses.

1. S. Krishna, A. Sharma, N. Aggarwal, S. Husale. Ultrafast photoresponse and enhanced photoresponsivity of Indium Nitride based broad band photodetector //Solar Energy Materials and Solar Cells. – 2017. – V.173. – P.376–383

Structure and properties of composite nickel coatings obtained by pulsed current

Tytarenko V.V., Zabludovsky V.A., Shtapenko E. Ph.

Dnipropetrovsk National University of Railway Transport named after Academician V. Lazaryan, Dnipro, Ukraine, dudkina2@ukr.net

Application of electrolysis in its non-steady mode represents one of the methods for improvement of composite electrolytic coatings (CEC) functional properties. With continuous growth of interest to nanocomposite electrolytic materials reinforced with CNS not too many research and consequent technical applications are conducted and realized in this field.

It was find out that composite nickel coatings deposited with use of pulse current were characterized with the more uniform and higher UDD particles distribution density across a coating. Analysis of nickel coatings microphotographs discovered that dimensions of coating grains vary of DC-deposited pure nickel crystalline grains from 100 nm (Fig. 1a) to 65 nm for pulse current-deposited composite nickel coatings (Fig. 1c).

Formation of more fine-crystalline CEC and change of growth structure in cross section from columnar structure to microlayer structure in conditions of pulse deposition mode (Fig. 2) governed increase of mechanical and resistance properties of carbon-containing nickel coatings (coating microhardness increase by 75 – 77%, wearing and porosity decrease in 3 and 2.4 times respectively) (Table 1).

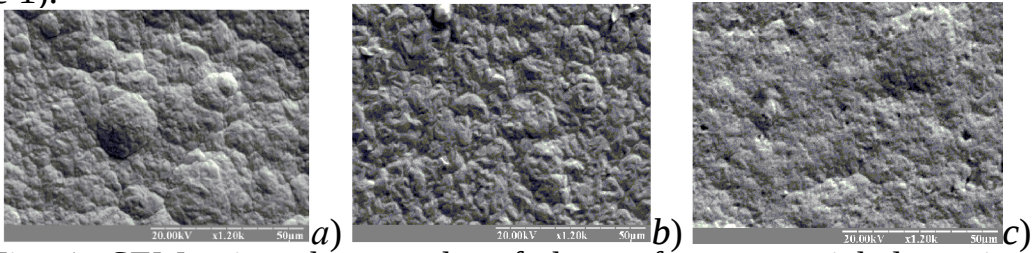

a) *b*) *c*)

Fig. 1. SEM microphotographs of the surface: a – nickel coating (DC, j=100 A/m^2), b – composite nickel coating (DC, j=100 A/m^2), c – composite nickel coating (PC, j_{av}=100 A/m^2, f=50 Hz, Q=50)

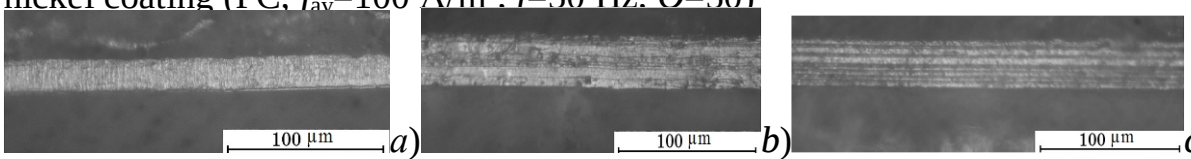

a) *b*) *c*)

Fig. 2. Structure of composite electrolytic nickel coatings in cross section: *a* – nickel coating (DC, j=100 A/m^2), *b* – composite nickel coating (DC, j=100 A/m^2), *c* – composite nickel coating (PC, j_{av}=100 A/m^2, f=50 Hz, Q=50)

Table 1 Deposition modes effect on mechanical and resistance properties of nickel and carbon-containing nickel coatings

Deposition mode				H_μ, MPa	Average wear, mg/hour	Average corrosion penetration, mm/year	Number of pores per 1 cm^2
	j, A/m^2	f, Hz	Q				
DC	100	-	-	1,800	1.8	0.011…0.014	24
Pulse current		50	50	3,200	0.6	0.005…0.010	10

Surface Structural Properties of Chemically Modified Carbon

Vashchynskyi V.M.

Separate Structural Department Technology College of Lviv Polytechnic National University, Lviv, Ukraine, v.vashchynskyi@gmail.com

One of the ways of improving the existing and creating new electrochemical technologies is the development of new electrode materials which have relatively high electrical conductivity, large specific surface area and low chemical activity of surface. Temperature and technological peculiarities of carbonization and activation processes are important factors because of formation of a porous carbon structure, and at the almost identical chemical composition of carbonaceous raw materials, the results can differ significantly in structural and texture parameters.

The aim of work is to investigate the influence of the conditions of obtaining and modifying porous carbon material (PCM) on the porous structure characteristics. PCM obtained from raw materials of vegetable origin by its carbonization and activation with potassium hydroxide was used as carbon material. The raw materials were dry apricot pits, crushed to a fraction of 0,25-1 mm and were carbonized at 300 ºC. Obtained carbon was activated with potassium hydroxide in different proportions. Samples were numbered according to carbonization temperature and percentage of chemical activator. C43 is a material carbonized at 400 ºC and mixed with potassium hydroxide at the ratio of 1:3.

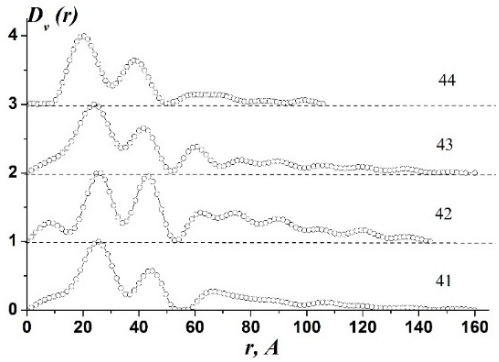

Fig. 1 Volume distribution functions of pores

Fig. 1 shows volume distribution functions, which express the dependence of relative pore volume on their radii. To calculate the functions of the pore radii distribution, the correction for height and width of the detector receiving slit was made to the scattering intensity curves. As can be seen, the main contribution to the porous volume formation of is made by pores with a radius of 50 Å. (Table 1). The samples for which KOH/precursor ratio is 1:1–1:3 display a significant number of micropores with radii of 8-10 Å, while they are practically absent in C44 sample. Calculations has exposed that the materials are characterized by a microporous structure and the main contribution is pores with a radius of 8-10 Å. The presence of mesoscopic pores with a radius of ~ 25 Å should be noted, which is especially manifested in samples C41-C43. The porous structure of C44 is formed by pores with a radius of ~ 20 Å.

Table 1. Parameters of the porous structure

Sample	ρ, g/cm^3	W	S, m^2/g	$R_{im.}$, Å	R_c, Å
C41	0.76	0.60	786	10.2 ± 1.6	21.5 ± 1.6
C42	0.44	0.77	830	8.3 ± 1.5	19.5 ± 1.5
C43	0.51	0.73	1255	9.4 ± 1.6	21.5 ± 1.6
C44	0.33	0.83	1005	20.2 ± 1.3	24.4 ± 1.3

Comparative Study of the Luminescent Properties of Chemically Synthesized Carbon Nanodots Dispersed in Oligomeric Silsesquioxane Polymer and Carbon Nanoagregates Pyrolitically Synthesized and Dispersed in Fumed Silica Nanopowder

Vasin A.V.[a,b], Virnyi D.[a], Isaieva O.F.[a], Kysil D.V.[a], Rudko G.Yu.[a], Kalytchuk S.[a], Piryatinski Yu.P.[c], Sevostianov S.V.[d], Tertykh V.A.[d], Nazarov A.N.[a,b], Lysenko V.S.[a]

[a]*Lashkaryov Institute of Semiconductor Physics of the NAS of Ukraine, Kyiv, Ukraine, av966@yahoo.com*
[b] *National Technical University of Ukraine "Igor Sikorsky KPI", Kyiv, Ukraine*
[c]*Institute of Surface Chemistry of the NAS of Ukraine, Kyiv, Ukraine*
[d]*Chemistry, Faculty of Science, Palacký University Olomouc, Olomouc, Czech Republic*
*****Institute of Physics of the NAS of Ukraine, Kyiv, Ukraine*

Two kinds of luminescent nanocomposites have been synthesized and studied. (1) The N,S-co-doped CDs were synthesized by typical “wet chemistry” procedure using citric acid and L-cysteine as carbon precursors through a previously reported one-step hydrothermal treatment [1]. Synthesized N,S-co-doped carbon nanodots were mixed with aqueous solutions of octa(tetramethylammonium)-functionalized polyhedral oligomeric silsesquioxane as a matrix followed by drying procedure. (2) Another silica/carbon nanocomposite has been synthesized by chemo-thermal treatment of fumed silica with phenyltrimethoxisilane followed by thermal pyrolysis at 600 ^{o}C in inert atmosphere [2].

Comparative study of chemically synthesized carbon nanodots dispersed in oligomeric silsesquioxane polymer and carbon nanoagregates pyrolitically synthesized and dispersed in fumed silica nanopowder have been performed using steady state photoluminescence emission/excitation spectroscopy, time resolved photoluminescence spectroscopy and optical absorption spectroscopy. While PL in colloidal CDs is widely reported and discussed in scientific community, the PL properties of solid state CDs based nanocomposites is not well studied. Present researches are focused on comparative examination of optical properties of two kinds of nanocomposites for clarification of light absorption and emission mechanisms in their correlation with nano/subnanoscale structure. Special focus is targeted on the analysis of optical absorption and photoluminescence excitation of the CDs based nanocomposites.

1. Y. Q. Dong, H. C. Pang, H. B. Yang, C. X. Guo, J. W. Shao, Y. W. Chi, C. M. Li and T. Yu, Angew. Chem., Int. Ed., 2013, 52, 7800–7804.
2. A.V. Vasin, D.V. Kysil, L. Lajaunie, G.Yu. Rudko, V.S. Lysenko, S.V. Sevostianov, V.A. Tertykh, Yu. P. Piryatinski, M. Cannas, L. Vaccaro, R. Arenal, A.N. Nazarov, Multiband Light Emission and Nanoscale Chemical Analyses of Carbonized Fumed Silica, Jour. Appl. Phys. **124**, 105108 (12 pages) (2018).

Simulation of Particles Scattering on Nanostructures with the Potential of an Arbitrary Form Using the Method of Analytical Transfer-Matrix

Voznyak O.M., Voznyak O.O.

Vasyl Stefanyk Precarpathian National University
Ukraine, Ivano-Frankivsk,
Department of physic and chemistry solids, voznyakorest@gmail.com

At the present stage of microelectronics development heterostructures with nanometer sizes are used and they are functioning exclusively on quantum phenomena. In the case of nanoscale region the particle can transmitted through by tunneling, and resonance tunneling can take place at such process. As known, the resonant tunneling and negative differential conductivity through a two-barrier quantum structure or quantum dot are caused by the emergence of a resonant level due to spatial quantization.

The particle passing simulation is implemented either by using of potential profiles in the form of rectangular potential wells or barriers, or by use of quasi-classical approximation for more realistic potentials. The popular methods related with the use of numerical implementations, which are based on the breakdown of barriers or wells of arbitrary shape into narrow rectangular potential layers. The number of these layers chosen by large one for increasing the accuracy, which leads to accumulation of calculation errors and consequently does not give the necessary precision. At the same time, potentials of arbitrary form are important for modeling the behavior of electrons in quantum dots. In particular, the using of Gaussian potentials is relevant.

In recent years, the new method has been proposed to devoid this imperfection and it is based on analytical approach to the theory of transfer-matrix. In this case, instead of multiplying a large number of distribution matrices, the problem is reduced to the solution of transcendental equations, which ensures the high accuracy of the resulting solution. Within the framework of this approach, it was possible to obtain general expressions for the coefficients of reflection and transmission for quantum well and barrier in a closed and clear form. The calculation procedure implement using the modified Pőschl-Teller potential, Wood-Saxons potential and Gaussian potentials.

It is shown that taking into account the summarized total phase shifts, as a result of the passing of the classical turning points and boundaries of the segments with homogeneous potential energy layers on which the potential of the arbitrary form is broken we can receive the exact results, provided that their number is approaching infinity.

POSTER REPORTS
Session 3
Physical-chemical properties of thin films

Accelerated studies of multilayer polymer film materials for electronic devices

Domantsevich N.I.[1], Yatsyshyn B.P.[2]

[1]*Lviv Trade and Economic University, Ukraine, Lviv, nina.domantzevich@gmail.com*
[2]*National University "Lviv Polytechnic", Ukraine, Lviv, bogdan.yatsyshyn7@gmail.com*

To safeguard the materials used for packaging and storage of electronic devices and equipment are additional requirements nominated, which combine functions of conservation and packaging in a single technological process. The multilayer polymer films based on polyolefin are used for this purpose [1]. The film of polyethylene, which modified by a volatile corrosion inhibitor, as the inner layer is used in this case. The outer layers may be such materials as polypropylene, polystyrene or polyethylene terephthalate.

The multilayer films with inside layer on the basis of high-pressure polyethylene (GOST 16337) with additions of inhibitors and plasticizers as objects for researches were selected. The microstructure of the surface of polymer films by electron microscopes "Tesla-250" and EVO 40XVP was investigated. A method of accelerated research on durability in liquid aggressive environment to determine the reliability of the coatings was used. The lifecycle of the coating according to these researches was determined. The measurement scheme and the aggressive environment were selected according to GOST 9.083.

It was established that two-layer films whose composition included modifying components showed significantly more intense dynamics in changing of electrical resistance, compared with similar samples without additions. Initial growth of the electrical resistance during 25-27 days was associated with a degradation of the film structure and with formation of new defects under the influence of aggressive environment. Subsequently, there was a slight increase of resistivity value, and on the 40th day of research - a marked decrease in electrical resistance, which was associated with the loss of barrier properties of the coating.

The lifecycle of multi-layer coatings were determined by extrapolating experiments data. The protective resource of multilayer polymer films without inhibitors in warehouse conditions was predicted near 11 years and 8 years – for coatings with inhibitors.

Domantsevych N., Yatsyshyn B. Application of multilayer polymer films for packaging microelectronic devices and equipment. *Commodity Science in Research and Practice: Innovation in Product Development and Packaging.* Cracow, 2014. P. 121-128.

Conductive Characteristics of Thin-Film Composite Materials with Mineral Fillers

Domantsevich N.I.[1], Yatsyshyn B.P.[2]

[1]*Lviv Trade and Economic University, Ukraine, Lviv, nina.domantzevich@gmail.com*
[2]*National University "Lviv Polytechnic", Ukraine, Lviv, bogdan.yatsyshyn7@gmail.com*

The usage of polymer film materials for electronic equipment is mainly due to the need for its minimization and the need for reliable barrier materials. Characteristics and properties of polymeric materials should correspond to certain parameters of electronic products and provide the total time of job of devices. The main of the polymeric materials used for such applications is polyethylene, the composition of which is modified depending on the requirements and terms of operation. The purpose of the research was to study the changes in the electrical conductivity of polyethylene films when they are filled with inorganic non-conductive addition.

The object of research is the low density polyethylene (65-80 wt. %), for which granulate (LDPE 15803-020) was used. As an addition the mineral filler "Credolene" (up to 30 wt. %) was used. The charge composition was injected up to 1 weight. % of the application for the slip based on oleamide for ensures the technical parameters of production.

The research has found that the addition of mineral filler up to 20 wt. % slightly increases the crystallinity and leads to an increase in surface resistivity. The value of the surface resistivity is stabilized at $\rho_s \approx 5 \cdot 10^{11}$ Ω·m with the next increase of the mineral addition. The surface resistivity even somewhat decreases in the subsequent increasing of filler's amount.

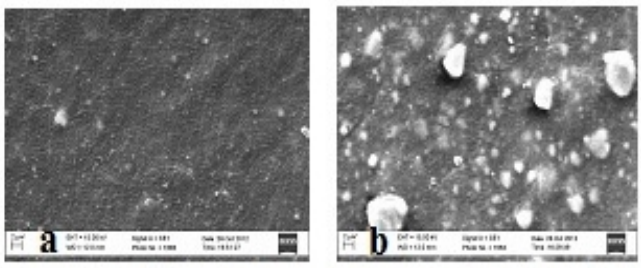

Fig. 1. Morphology of the surface of the polyethylene film which contain 16,6 wt. % (a) and 28 wt. % (b) mineral filler. X 2000.

The volume resistivity of polyethylene films that did not contain filler has a value two orders higher in comparison with the surface resistivity $\rho_v = 4 \cdot 10^{13}$ Ω·m. The volume resistivity slightly increases to $\rho_v \approx 10^{14}$ Ω·m in additions of the filler.

The structure of the surface of all samples were approximately smooth and with a small number of defects as cracks and pores. The surface by an uneven distribution of the filler was characterized as wavy, which corresponded to fibres packaging.

Structure and Thermal Stresses of TiN Films Produced by Magnetron Method

Dranenko A.S., Koshelev M.V.

Frantsevich Institute for Problems of Materials Science of NASU, Kyiv, Ukraine,
silica-lum@ukr.net

Titanium nitride combines high hardness, conductivity, chemical resistance and heat résistance making it a unique material for improving the wear resistance and hardness of product and creating golden film coatings on decorative articles, such as glasses and watches. It is also used in structural engineering, dentistry and Schottky contacts for *n*-Si and *n*-GaAs in microelectronics, as well as diffusion barriers in multilayer systems for semiconductors.

Thin (~100nm) TiN films were prepared by magnetron method sputtering of titanium nitride target produced by powder metallurgy method, in argon at substrate temperature T_s of 470 K. The substrates were single-crystalline silicon wafers <111> and pyroceram. The samples were annealed in a pressure $7 \cdot 10^{-3}$ Pa and a temperature of 973 to 1273 K, for 1 h in an oven with oil-free evacuation. The deposited and annealed films were examined using an EMR-100 electron diffractometer. The calculated interplanar spacing was compared with reference value.

The resulting electron diffraction pattern as arc-shaped reflection indicate that the films have a texture polycrystalline structure with the <111> orientation axis, the textured orientation being stubble. Despite the similarity of electrons, the electron diffraction patterns differ by width resistive intensity. Since the film changes in structure from columnar to nanosized granular during annealing at 973 K, the reflection with decreases with lower imperfection of in lattice. Different coefficients of thermal expansion of the film and substrate induce thermal stresses during annealing at 1273 K in the film, increasing the width of reflection. When the films are deposited onto a pyroceram substrate, the number of reflection decreases and the intensity of scattered electrons increases in the central part of the electron diffraction patterns. Therefore, the film has an amorphous-crystalline structure.

Thermal stresses arising from the difference in coefficient of thermal expansion of the film and substrate can be expressed as follows:

$$s(T) = (E(a_f - a_x)/(1-m) - \Delta T,$$

were α_f, E and μ are the coefficient of thermal expansion, Young`s modulus, and Poisson`s ratio of the film; ΔT – is the difference in temperature of film deposition and annealing and temperature at which the stresses are determined. The constants used in the calculation were: $\alpha_f = 10.3 \cdot 10^{-6} \text{deg}^{-1}$, E = 440 GPa, μ = 0.25 and $\alpha_x = 4.15 \cdot 10^{-6}$ deg^{-1} (for silicon).The calculated thermal stresses are as follows: 0,65 GPa after deposition of the film and 2.45 and 3.53 GPa after annealing at 973 and 1273 K.

Supercooling of the Fusible Component in Ag/Bi/Ag and Ag/Pb/Ag Layered Film Structures

Dukarov S.V., Petrushenko S.I., Nevgasimov O.O., Kravtsov P.O., Sukhov V.N.

V.N. Karazin Kharkiv National University, Kharkiv, Ukraine,
petrushenko@univer.kharkov.ua

The study of the crystallization of metastable melts is necessary both for advancement in the technology field and for fundamental physics. Such studies, in particular, are in demand in solving problems, which are related to the transportation and storage of the thermal energy, the development of innovative sensors, actuation devices and methods for recording the information. At the same time, the study of the crystallization of supercooled liquids allows to obtain the information about the energy particularities of the interfaces.

This work is devoted to the determination of the crystallization temperature of bismuth or lead layers, which are located between silver films. The samples were obtained by vacuum condensation of components, which was performed by the method of the thermal evaporation from independent sources. The registration of the melting and crystallization temperature of the fusible component was carried out with the use of two complementary methods: by measuring the electrical resistance of films and electron diffraction, which were performed directly during heating and cooling of the sample. In the first case, phase transitions were recorded by jumps in electrical resistance, and in the second case, by the appearance and the disappearance of reflections from the crystallographic planes of the fusible component.

It was established that, as in previously studied Bi-Cu and Bi-Mo contact pairs, for Bi-Ag samples, which were obtained by the condensation of components onto a substrate at the room temperature, the avalanche-like crystallization that occurs at a temperature of about 200°C is typical. In film systems in which bismuth was deposited through the liquid phase, the diffuse crystallization, which starts under deeper supercoolings and ends at 115°C, was observed. According to the SEM studies differences in temperatures and crystallization natures are due to the morphology of the samples. However, the crystallization of lead is always diffusive and ends at the temperature of 265°C.

All in all, samples studied in this work confirm the previously established trend, according to which Bi provides the greatest jumps of resistance during phase transitions in comparison to other metals. Besides, lead provides the rapid decay of initially continuous layer of silver into individual islands.

Photosensitivity of Polycrystalline Films of Cadmium Telluride

Dzundza B.S.[1], Prokopiv V.V.[1], Mazur T.M.[1], Turovska L.V.[2], Yavorskyi Ya.S.[1]

[1]*Vasyl Stefanyk Precarpathian National University, Ivano-Frankivsk, Ukraine, kbgd@pu.if.ua*
[2]*Ivano-Frankivsk National Medical University, Ivano-Frankivsk, Ukraine*

In recent years, scientific research has increasingly focused on renewable energy sources, in particular solar energy. Promising solar cells are second-generation photovoltaic cells, where cadmium telluride thin-film materials are commonly used. In addition, II-VI compounds are relevant due to the prospect of their use to create ionizing radiation detectors and as IR filters.

CdTe films were obtained from a pre-synthesized material by vacuum-evaporation technique and physical vapour deposition on freshly prepared mica chips and polished glass. The photoelectric properties of CdTe semiconductor films obtained on various substrates have been investigated using the developed automated device. The dependence of the photosensitivity on the structure of the films and the technological conditions of growing has been determined.

The photosensitivity is defined as $S = (\sigma_L - \sigma_D)/\sigma_D$, where σ_D is dark conductivity, σ_L is conductivity under illumination. Photosensitivity largely depends on structural defects that can act as trapping or recombination centres. In CdTe polycrystalline films, photoconductivity is mainly determined by processes at the grain boundaries. Based on the results of AFM studies (Fig. 1, a), the average crystallite size has been determined, and the photosensitivity of the films of various thickness and structural perfection is shown in Fig. 1, b.

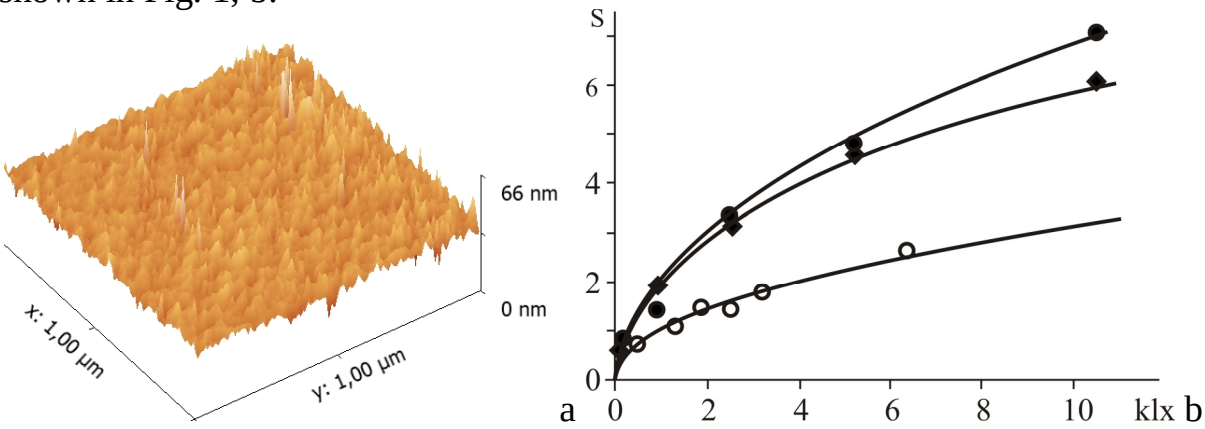

Fig. 1. AFM image of the surface of a CdTe film with a thickness of 300 nm on the polished glass substrate (a) and photosensitivity of films on mica (○) and polished glass (●, ♦); thickness is 200 nm (●), 320 nm (♦), 540 nm (○); the average grain size is 25 nm (●), 30 nm (♦), 90 nm (○) (b).

It can be seen that the photosensitivity of the films obtained on the polished glass substrates is significantly higher than those of the films on freshly prepared mica chips (111) and increases with decreasing film thickness. This is due to the fact that the specific contribution of the grain boundaries increases with decreasing crystallite size.

Physico-Chemical Properties of Thin Films of Molybdenum, Tungsten and their Carbides Deposited from Ionic Melts

Gab A.I.[1], Uskova N.N.[2], Rozhalovets K.S.[1], Malyshev V.V.[1,2]

[1]*University "Ukraine", Kyiv, Ukraine, lina_gab@ukr.net*
[2]*Institute of General and Inorganic Chemistry, Kyiv, Ukraine, viktor.malyshev.igic@gmail.com*

The aim of this study was to investigate the physicochemical properties of galvanic coatings of molybde num, tungsten, and carbides thereof.

Scanning images of the coating surface confirm the deposit columnar structure. Coatings were obtained with concentrations of metal impurities including Al, Cr, Ni, Si, Fe of about 2×10^{-2} - 6×10^{-3} wt % according to the data of X ray spectral microanalysis.

Microhardness is 2.16-2.26 GPa (molybdenum), 4.02-4.22 GPa (tungsten), 28.44-30.40 GPa (W_2C). Layers adherent to the support are notice ably hardened, which points to mutual diffusion of the coating elements into the support. This is also confirmed by the data of X ray spectral microanalysis pointing to the presence of a diffusion region at the depth of up to 5-10 μm.

A detailed test of wear resistance was carried out for samples of Steel 45 with different coatings. In the case of application of coatings, wear resistance was enhanced by 9-11 times for zirconium diboride, by 7-9 times for tungsten carbide, by 4–7 times for molybdenum carbide, by 3-5 times for tungsten, and by 1.5-3 times for molybdenum.

Tests of the abrasive resistance of Steel 45 samples with various coatings were carried out in the medium of electrocorundum, the μm fraction, at the load of 44.1×0.55 N. The abrasive resistance of samples increases four to ninefold as a result of application of coatings of tungsten and molybdenum carbides.

Due to the problem of noble metal replacement in titanium doping by cheaper metals, electrochemical and corrosion behavior of titanium with a galvanic tungsten coating is studied. Application of tungsten coatings on nitrided titanium was carried out from a halide-oxide electrolyte. Thus, coatings with the thickness of 30-50 μm were obtained on the titanium surface. Corrosion tests were carried out in 15% H_2SO_4 solution at 100°C. Here with, variation of the potential and corrosion rate was registered. The corrosion potential of titanium after coating by tungsten increases from – 0.63 to 0.37-0.39 V and passes into the passive-active region of titanium. Here, it practically reaches the corrosion potential of tungsten. The calculated average corrosion rate of tungsten coated titanium samples was 0.01-0.04 g/(m_2/h). The above coating, while passivating titanium, causes a 500 to 2000 fold decrease in its corrosion rate in 15% H_2SO_4 at 100 °C.

The prospects of application of galvanic coatings of molybdenum, tungsten, and carbides thereof for enhancement of surface hardness, wear and abrasive resistance, and corrosion stability of various structural materials are shown.

Influence of Vacuum Annealing on the Dispersion of Thin Double Nickel-Silver Films Deposited onto Oxide Ceramic Materials

Gab I.I.[1], Stetsyuk T.V.[1], Kostyuk B.D.[1], Shakhnin D.B.[2]

[1]*Frantsevich Institute for Materials Science Problems of NAS of Ukraine, Kyiv, Ukraine, gab@ipms.kiev.ua*
[2]*University "Ukraine", Kyiv, Ukraine*

In modern technology there is a need for the production of permanent vacuum-tight precision ceramic joints with an ultra-thin seam. Such joints can be made by brazing or pressure welding of metallized ceramic parts. This purpose can be achieved by application onto ceramic surfaces of double metal films, one part of which is 100 – 200 nm thickness and consists of an adhesion-active metal (e.g. Ti, Cr etc.), and the other layer is slightly thicker (1 – 3 microns) and serves as a solder (e.g. Cu, Ag etc.) ensuring joining of metallized ceramic materials during brazing or pressure welding with a fine brazed seam (2 – 4 microns thickness).

In this work, specimens were used made of alumina and dioxide-zirconium ceramics and metallized with a 150 nm nickel nanofilm and then atop, by a 1,5 – micron silver film serving as a soldering metal for ceramic samples joining. Silver was chosen as a solder in view of the fact that it is able to wet nickel well, and also it does not interact with nickel forming new phases.

Since, during the joining process, the samples can be heated to a temperature up to 1000 °C or even more, it would be well to study the behavior of such double films during annealing. In this work, we have studied the behavior of the double nickel-silver film deposited onto the ceramic samples mentioned above during their annealing in a vacuum at temperatures up to 1000 °C with different exposition time at each temperature (from 5 up to 20 minutes). It was found that the initial solid films on both oxide ceramics samples undergo only a slight change during their annealing up to 900 °C. However, after the annealing at 950 °C, and even more at 1000 °C, these films begin to disperse rather quickly to separate drops covering almost 70% of the alumina oxide ceramics sample surface and about 50% of the zirconium dioxide sample surface.

According to our study results, kinetic curves of the investigated thin double metallic films decomposition have been built, using which one can determine the basic process parameters (temperature and exposition time at this temperature) for brazing or pressure welding of ceramic materials.

Conductivity of CdTe Polycrystalline Films

Gasyuk I.M.[1], Kostyuk O.B.[1,2], Pysklynetsj U.M.[2], Yurchyshyn L.D.[1], Potyak V.Yu.[1], Katanova L.O.[1]

[1]*Vasyl Stefanyk Precarpathian National University, Ivano-Frankivsk, Ukraine*
[2]*Ivano-Frankivsk National Medical University, Ivano-Frankivsk, Ukraine,*
oksanakostuk@gmail.com

The electrical parameters of polycrystalline films depend both on the properties of the grain volume and on the properties of the grain boundaries. In the work, measurements of the frequency dependence of the impedance for the CdTe film on the mica-muscovite substrate were performed. For the separation of the contribution in the volume of grains and at their boundaries, an equivalent scheme was chosen that includes two serial connected circuits with parallel capacitors and resistance.

In Fig. 1 the frequency dependence of the real component of the impedance Z 'for the CdTe film is given at T = 293K. A good coincidence over the whole frequency range means that the proposed electrical circuit properly describes the properties of the films. Parameters used to calculate: R_G=106.7 Ω, R_{GB}=4024 Ω was obtained using the ZView2 program. That is, the resistance of grain boundaries is an order of magnitude higher than grain resistance. The high resistance of the grain boundaries is due to the presence of a large number of defects in them in comparison with the volume of grain. Grain boundaries show the effect of capturing most of the charge carriers (holes). The potential barrier on the grain boundaries provides high resistance in the transfer of carriers from grain to grain. Consequently, for polycrystalline CdTe films, charge transfer is determined mainly by the grain boundaries. With the increase in the frequency of the electric field, the transport of charge carriers to the new position of equilibrium is complicated, which leads to an increase in the contribution to dielectric system losses and to the growth of conductivity.

An increase of conductivity with frequency also indicates the existence of localized states in thin CdTe films. The possibility of the existence of such states is confirmed by the fact that the film under investigation is a polycrystal, where the transfer of charge carriers is limited by the presence of potential barriers on the grain boundaries, as well as by their own defects directly in the crystallites.

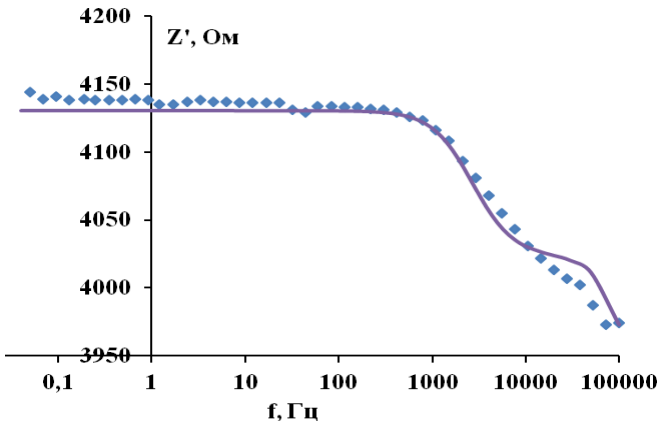

Fig. 1. Frequency dependence of the real component of the impedance Z ' for the film CdTe at T = 293 K. Points – experiment, lines – calculation

Defect Structure And Magnetic Properties of YLaFeO Epitaxial Films under Influence of Different Growth Conditions

Gutsuliak I.[1], Fodchuk I.[1], Dovganyuk V.[1], Kotsyubynskiy A.[1], Kuzmin A.[1], Sumariuk O.[1], Lytvyn P.[2], Kladko V.[2], Gudymenko O.[2], Syvorotka I.[3]

[1]*Yuriy Fedkovych Chernivtsi National University, Chernivtsi, Ukraine, ifodchuk@ukr.net*
[2]*V. Ye. Lashkaryov Institute of Semiconductor Physics of NASU, Kyiv, Ukraine*
[3]*Scientific Research Company "Carat", Lviv, Ukraine*

We studied a set of $Y_{2.95}La_{0.05}Fe_5O_{12}$ (YIG) epitaxial films with 6.4 μm, 55.1 μm, 70.7 μm and 94.4 μm thicknesses. The influence of the defect structure model on formation of distribution of X-rays intensity in reciprocal space and microstructure of magnetic domains was investigated. Films were analysed by AFM and high-resolution X-ray diffractometry. RSMs and rocking curves were analysed to determine the dominant types of microdefects and their parameters. The propriety of chosen defect structure model is confirmed by RSM simulation based on Krivoglaz kinematic theory of X-ray diffraction combined with Monte Carlo method [1]. YIG magnetic characteristics were studied by MFM, the width of feromagnetic resonance FMR line, amplitudes and fluctuations of the MFM signal in the magnetic field were also determined and analyzed. YIG epitaxial films have microblock structure, what explains structure of magnetic stripes and the presence of extended defects such as column boundaries. Domain structure of films with thicknesses in the order of several micrometers is significantly influenced by transition layer between film and substrate [2].

We chose the model of microdefect structure that is presented by columns and the set of edge and screw dislocations with $\{11\bar{2}\}$ sliding planes. Burgers vectors of dislocation are $\vec{b}_e = a[\bar{1}10]$ and $\vec{b}_s = a[111]/2$. This model is confirmed by the correlation between experimental RSMs and calculated ones with Monte Carlo method, as well as by the analysis of the rocking curves. Mostly edge dislocations form the diffraction pattern. Dislocation density, depending on the sample, lie within the range of ~10^5-10^8 cm^{-2}. The most perfect sample with t=55.1 μm has the lowest dislocation density, ordered magnetic domain structure and the smallest width of the FMR line ΔH=0.7 Oe compared with other films. Microdefect model confirms significant influence of transition layer with column microstructure, as well as film growth temperature and rate.

1. Barchuk M., Holy V., Miljevic B., Krause B., Baumbach T. et al. X-ray diffuse scattering from threading dislocations in epitaxial GaN layers. *J. Appl. Phys.* 2010. V. 108. P. 043521.
2. Fodchuk I., Gutsuliak I., Dovganiuk V., Kotsyubynskiy A., Pietsch U. et al. Magnetic and structural changes in the near-surface epitaxial $Y_{2.95}La_{0.05}Fe_5O_{12}$ films after high-dose ion implantation. *Appl. Opt.* 2016. V. 55. P. B144.

Size Effects in Properties of Thin-Films Lead of Chalcogenides

Klanichka Y.V., Klanichka V.M.

Vasyl Stefanyk Precarpathian National University, Ivano-Frankivsk, Ukraine,
yuriy.klanichka@gmail.com

For all investigated films, the dimensional effect in electrical resistance or electrical conductivity is characteristic. In the first case, there is a growth of the specific resistance with a decrease in thickness (growth 1 / d), and in the second one - a decrease in the specific conductivity. The latter points to the fact that the interphase boundaries of "film - substrate", "film - free surface" and intercrystalline boundaries affect the transport processes. This is due to the change in the mean free path of charge carriers. Attention is drawn to the relation between the mean effective lengths of the free path of charge carriers l_0 for films obtained under different technological conditions. Thus, in particular for monocrystalline films, it is two orders of magnitude larger than for polycrystalline fine-dispersed films. This makes it possible to assert that the intercrystal boundaries are effective scattering sites for charge carriers, while the average external free path length is proportional to the size of the crystallites (D). For monocrystalline films, l_0 in order of magnitude exceeds its thickness (d) for 300 K.

The effective mean free path of charge carriers also depends on temperature. Both for monocrystalline and polycrystalline films, l_0 increases with decreasing temperature. Its especially significant increase is typical for a structurally perfect condensate deposited under equilibrium conditions on chips of single crystals of KCl. So, if for 300 K, l_0 = 2.73 μm, then for 77 K it is one and a half orders larger and is l_0 = 43.3 μm. For polycrystalline films, scattering is still dominant on the boundaries of crystallites.

For monocrystals with increasing temperature resistance for films of different thickness has a metallic nature of change - it grows, then for polycrystals characterized is semiconductor - conductivity increases, resistance decreases.

In PbTe single crystals from almost 4 K to the beginning of the impurity conductivity (450 K), the Hall coefficient does not change, which indicates the constant value of the concentration of carriers. This is due to the fact that both donor and acceptor energy levels are in the conduction band and the valence band, respectively, and therefore do not freeze. In the experimental case, the observed growth of the specific resistance with the temperature in monocrystalline films, is related mainly to the scattering of carriers by the oscillations of the crystalline lattice.

The activation character of conductivity for polycrystalline films can be related to energy barriers on intergranular boundaries.

The determined values $\lg \rho(\sigma)$ of the activation energy from the temperature dependences $\lg \rho\ (\sigma) \sim T^{-1}$ for polycrystalline films of different thickness are from 0.08 to 0.11 eV. Energy barriers in polycrystalline films may be due, in particular, to the acceptor influence of atmospheric oxygen.

]Barrier Effects in Properties of Thin-Films Lead of halcogenides

Klanichka Y.V., Klanichka V.M.

Vasyl Stefanyk Precarpathian National University, Ivano-Frankivsk, Ukraine,
yuriy.klanichka@gmail.com

To study the effect of potential barriers on charge transfer, measurements of the coefficient of thermo-electric, transverse and longitudinal magnetoresistance, as well as the analysis of the temperature dependence of the Hall mobility were carried out.

Anisotropy of the magnetoresistance

In polycrystalline PbSe films, the longitudinal magnetoresistance should be changed $\Delta\rho_{\parallel}/\rho_0$, while the transverse $\Delta\rho_{\perp}/\rho_0$ will remain almost unchanged. This is due to the fact that the latter is determined mainly by the properties of the internal volume of crystallites. As a result, anisotropy of the magnetoresistance coefficient, characterized by the ratio $k = \Delta\rho_{\parallel} / \Delta\rho_{\perp}$, will exceed one [1].

Coefficient of thermo-e.m.f.

The experimental dependence of the ratio of coefficients of thermo-e.m.f, poly- and monocrystalline films $\gamma = \frac{\alpha_n}{\alpha_m}$ obtained. At the same Hall concentration of carriers α in polycrystalline films is higher. Since the band structure of the films does not depend on the degree of their crystalline perfection, we can assume that the observed features in thermoelectric energy are related to the difference in the mechanisms of scattering of charge carriers.

Drift barrier and carrier mobility

For PbSe polycrystalline films, the drift barrier, determined from inclination of dependence $\lg(\mu_H T^{1/2} = f(T^{-1}))$ in the low temperature area, is (0,02 ... 0,04) eV.

The presence of a drift barrier in polycrystalline films of PbSe also causes a change in the Hall mobility and the nature of its temperature dependence.

Oxygen and transport processes

With increasing annealing temperature in interval $300 \le T_0 \le 500\,K$, the multiplicity of relative conductivity (RC) σ_0/σ_m (σ_0 is conductivity for the given temperature T_0; σ_m is dark conductivity) increases, in particular for layers of n-type conductivity, the mobility of charge carriers decreases μ_H. At T_0> 500K in samples of n-type, the concentration of electrons decreases; a type of conductivity is inversed. Multiplicity of RC, having reached the maximum, begins to decrease sharply, and μ_H in films increases.

It can be assumed that the atmospheric oxygen admixture near the intergranular boundaries in polycrystalline films leads to a decrease in the potential barriers for p-PbSe holes and their increase for electrons in n-PbSe.

1. Bytensky L.I., Gudkin TS, Kaz'min S.A. Anisotropy of magnetoresistance in PbSe films with potential barriers // Physics and technology of semiconductors. 13 (2), pp. 300-304 (1979).

Radiation Spectrum of System of Electrons Moving in Spiral in Transparent Medium

Konstantinovich I.A.[1,2], Konstantinovich A.V.[1]

[1]*Chernivtsi National University, Chernivtsi, Ukraine, aconst@ukr.net*
[2]*Institute of Thermoelectrics, National Academy of Sciences and Ministry of Education and Science of Ukraine, Chernivtsi, Ukraine, dj_kneo@ukr.net*

The time-averaged radiation power $\overline{P}^{rad}$ of system of electrons moving one by one along a spiral in transparent medium can be calculated by the instrumentality of spectral distribution $W(\omega)$ [1]

$$\overline{P}^{rad} = \int_0^\infty W(\omega) d\omega,$$

$$W(\omega) = \frac{2e^2}{\pi c^2} \int_0^\infty dx \mu(\omega) S_N(\omega)\, \omega \frac{\sin\left\{\frac{n(\omega)}{c}\omega\eta(x)\right\}}{\eta(x)} \cos\omega x \left[V_\perp^2 \cos(\omega_0 x) + V_\parallel^2 - \frac{c^2}{n^2(\omega)}\right],$$

where $\eta(x) = \sqrt{V_\parallel^2 x^2 + 4\frac{V_\perp^2}{\omega_0^2}\sin^2\left(\frac{\omega_0}{2}x\right)}$, ω is the cyclic frequency, $r_0 = V_\perp \omega_0^{-1}$, $\omega_0 = ec^2 B^{ext} \tilde{E}^{-1}$, $\tilde{E} = c\sqrt{p^2 + m_0^2 c^2}$, the magnetic induction vector $\vec{B}^{ext} \| 0Z$, $V_\perp$ and $V_\parallel$ are the components of the velocity, $\vec{p}$ and $\tilde{E}$ are the momentum and energy of the electron, e and m_0 are its charge and rest mass, respectively, Δt_l is the time shift of the l^{th} electron, c is the velocity of light in vacuum.

In the case of system of electrons moving one by one along a spiral the coherence factor $S_N(\omega)$ takes the form:

$$S_N(\omega) = \sum_{l,j=1}^{N} \cos\left\{\omega\left(\Delta t_l - \Delta t_j\right)\right\}.$$

For small time shifts between the electrons for the system of two, three, and four electrons in the frequency range of $0 - 50w_0$ we have found the existence of the coherent radiation $S_N(w) = N^2$ so far as the dimension of this system is smaller in comparison to the radiation wavelength. The oscillations in the spectral distribution of radiation power of the one, two, three, and four electrons are founded and studied for the case when the transversal component of velocity is bigger than the light phase velocity ($V_\perp > c/n(\omega)$) in the medium. The obtained results are in good agreement to those obtained in [1].

1. A.V. Konstantinovich, Radiation spectra of relativistic and non-relativistic electrons and their sequence in vacuum and transparent medium, These on search of a scientific degree of doctor of physical and mathematical sciences, Cernivtsi National University, Ukraine, 330p., 2012.

Mathematical Methods of Optimization Processes Growing of Nanostructures $A^{II}B^{VI}$ and $A^{IV}B^{VI}$ from the Vapor Phase

Lopyanko M.A.

Vasyl Stefanyk Precarpathian National University, Ivano-Frankivsk, Ukraine,
lopyanko@gmail.com

In this paper, using the method of mathematical planning of multifactor experiments received the dependence of the electrical properties of thin layers and nanostructures of PbTe from technological factors of growing from vapor phase by the method of hot wall.

As substrate used fresh chips (111) of crystal BaF_2. To describe the dependence of the electrical parameters of thin layers from technology factors were constructed global polynomial models in 3-factor hyperspace using mathematical modeling. For factors which vary (k=3) were selected substrate temperature (T_S), evaporator temperature (T_V) and chamber walls temperature (T_C) technologically acceptable change range of which are respectively:

$$473\ К \le T_S \le 623\ К,\ 758\ К \le T_V \le 878\ К,\ 833\ К \le T_C \le 983\ К.$$

Optimization parameters are: charge carrier mobility (μ), concentration (n), Seebeck coefficient (α), conductivity (σ), thermoelectric power ($\alpha^2\sigma$), and value:

$Z=\mu/\mu_{max} +(n/n_{min})^{-1} + (\alpha^2\sigma)/(\alpha^2\sigma)_{max}$,

which is a complex optimization parameter.

The data presented in the table.

Table

Parameters	Regression equation	Values of factors
Charge carrier mobility μ′	$3.89-0.20x_1-0.12x_2+0.22x_1x_2-0.36x_1x_3+0.23x_2x_3-0.76x_1^2-0.31x_2^2-0.44x_3^2$	$x_1=\frac{(T_{II}-548)K}{45K}$ $x_2=\frac{(T_B-818)K}{35K}$ $x_3=\frac{(T_C-908)K}{45K}$
Concentration n′	$1.07-0.15x_1-0.31x_2-0.44x_3+0.15x_1x_2+0.23x_1x_3+0.35x_2x_3-0.06x_1^2+0.19x_3^2$	
Seebeck coefficient α′	$2.51-0.44x_1x_3-0.31x_3^2$	
Conductivity σ′	$2.97-0.35x_1+0.18x_2+0.50x_3+0.16x_1x_3+0.77x_2x_3+0.31x_2^2+0.24x_3^2$	
Thermoelectric power $(\lambda^2\sigma)'$	$1.90-0.26x_1-0.59x_1x_3+0.43x_2x_3-0.28x_3^2$	
Z	$2.53-0.35x_1x_3-0.30x_1^2-0.23x_2^2-0.38x_3^2$	

1. Хартман К., Лецкий Э., Шефер В. Планирование эксперимента в исследовании технологических процессов. – М.: Мир, 1977. – 246 с.

Peculiarities of dislocations behavior in quasi isotropic 2D layers in the process of thermocycling

Lysiuk OV, Kurek I.G., Oliynich-Lysyuk A.V., Raransky M.D.

Yuriy Fedkovych Chernivtsi National University, Chernivtsi, Ukraine, lusiuknomer@ukr.net

The widespread use of sandwich structures in modern electronics requires prediction of the behavior of their characteristics (electronic, mechanical, etc.) under exploitation, especially during rigid thermocycling. It is known that deformation in such structures proceeds mainly due to the formation and sliding of dislocations. Their properties (fields of stress, displacement, energy, width of the band gap near the defect, etc.) depend on the value and sign of the Poisson coefficients (ν), which vary with the temperature, from one layer to another. In addition, in small-scale objects, the coefficients ν influence the surface energy of deformation of micro contacts and films [1]. Failure to consider these dependencies in predicting the properties of sandwich structures leads to a deterioration in the predictions of their reliability and the appearance of a significant number of failures in the operation of the devices in the process of operation. Therefore, in this study, the behavior of stress fields (s) and displacements (U) around dislocations in non-auxetic and auxetic 2D-quasi isotropic layers with a change in magnitude and sign ν at different temperatures are analyzed.

Briefly, the main results of research can be reduced to the following:

• The value of s near dislocations in 2D layers in a non-auxetic state is almost an order of magnitude higher than in auxetic.

• Characteristic values of Poisson's coefficients (0.9, 0.5, 0.3, -0.9) are revealed, in which the distribution of displacement fields around dislocations becomes fundamentally different (Fig. 1).

• Changes in the energy of dislocations interaction with force fields at these U (x, y) lead to different behavior of defects under the same mechanical stresses.

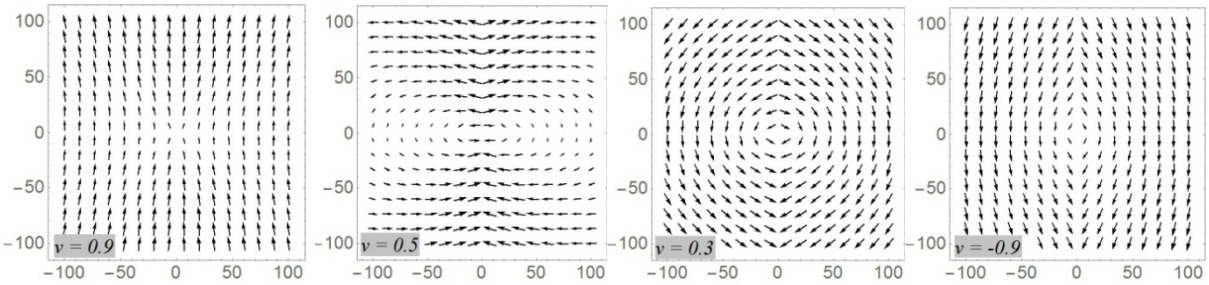

Fig. 1. Vector fields of displacements around edge dislocations in 2D layers of non-auxetic (ν> 0) and auxetic (ν <0).

1. Cheng X., Liu C., Silberschmidt V. V. Computational Materials Science. 2012. **52** (1). P. 274-281.

Optical Properties of Isovalent-Substituted β-CdS Heterolayers

Makhniy V.P.[1], Melnyk V.V.[1], Berezovska N.I.[2], Dmytruk I.N.[2], Slyotov M.M.[1]

[1] *Yuriy Fedkovych Chernivtsi National University, Chernivtsi, Ukraine,*
VPMakhniy@gmail.com
[2]*T.G. Shevchenko Kyiv National University, Kyiv, Ukraine*

It is well known that bulk crystals of wide-gap II – VI compounds (with the exception of ZnS) have only one time-stable modification - cubic (β) or hexagonal (α). Thus, in particular, cadmium sulfide which is widely used in optoelectronics crystallizes into a hexagonal structure with a band gap of E_g≈ 2.5 eV at 300 K. Meanwhile, the transition to β-CdS, which has E_g≈2.9 eV, can significantly expand the spectral range, as well as to increase the temperature and radiation resistance of the parameters of the devices based on them.

In this work, we studied the main optical properties of cadmium sulfide layers, obtained for the first time by the isovalent substitution method on β-ZnS single crystal substrates. The formation of the β-CdS layer is confirmed by the presence of two peaks in the differential reflection R'_ω spectrum which are characteristic for cubic structures, curve 1 in the figure. The first of them at ħω≈2.9 eV corresponds to E_g of cubic CdS, and the second is shifted to the high-energy region by the amount of spin-orbit splitting Δ_{so}≈0.3 eV. Additional evidence for the formation of the β-CdS layer is also the appearance in the luminescence spectrum of N_ω (curve 2) of two bands with maxima near 2.9 and 2.7 eV, which is noticeably larger than E_g of hexagonal CdS. It has been established that an increase in the synthesis temperature in the range of 850–1000°C (1000–1300 K) leads to a weakening of the low- and high-energy emission bands. The mechanisms of radiative transitions and the nature of the recombination centers are discussed.

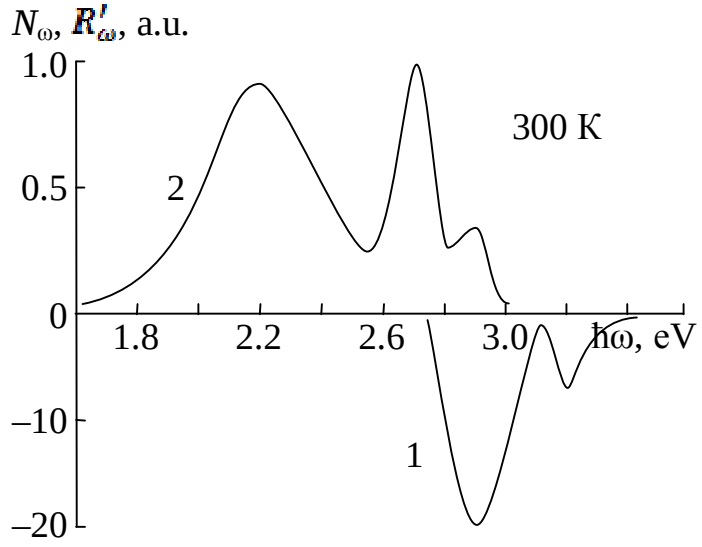

Formation and Modeling Nanosized Levels of the Self-Organized Structures in the Non-Crystalline Materials of Systems As(Ge)-S(Se), Ge-As-Te

Mar'yan Mykhaylo, Yurkovych Nataliya

Uzhhorod National University, Uzhhorod, Ukraine, mykhaylo.maryan@uzhnu.edu.ua

The dynamic stability of crystalline and non-crystalline solids, taking into account hetero phase fluctuations and soft atomic configurations as the systems of open exchange of mass, energy and information are investigated. Method of Green's functions, the principle of Prigogine's subordination of the modes, and the hierarchy of the time scale development of Bogolyubov's instability are applicated. A three-dimensional bifurcation diagram that takes into account the existence of crystalline, liquid and non-crystalline states are constructed. The levels of ordering self-organized structures of non-crystalline materials on spatial and temporal scales, their stability and comparison with empirical dependencies for the systems As(Ge)-S(Se) are considered.

The fractality of the formation of non-crystalline state and application of neural networks are founded [1, 2]. Classes of ordering and hyper sensibility of self-organized structures, prognostication and recommendations for their practical application are identificated.

The studies of the influence of laser irradiation in the visible and infrared region of the spectrum on the structural-sensitive properties of thin-film layers of the non-crystalline materials of systems As(Ge)-S(Se) and Ge-As-Te(Se) are presented. The formation of self-organized structures, the parameters of which can be controlled by the technological conditions of synthesis (sedimentation rate, synthesis temperature, bio-exchange with environment) and type of electromagnetic radiation are founded. The levels of ordering (scales of spatial and spatial-temporal ordering, time intervals of instabilities) and their application in sensor systems, forecasting of structural sensitive parameters of materials and synergetic approach to their formation are considered [2].

1. Yurkovych, N., Mar'yan, M., & Seben, V. (2018). Synergetics of the instability and randomness in the formation of gradient modified semiconductor structures. *Semiconductor physics, quantum electronics and optoelectronics*, 21 (4), 365-373.
2. Mar'yan, M. & Yurkovych, N. (2019). *Self-organized structures in non-crystalline solids and other systems: Methods, concepts and applications to the information technology*. – Lambert Academic Publishing. 133 P.

Resonant Phenomena at III-V Thin Films Processing in Electromagnetic and Magnetic Fields

Milenin G.V.[1], Red'ko R.A.[1,2]

[1]*V. Lashkaryov Institute of Semiconductor Physics, National Academy of Sciences of Ukraine, Kyiv, Ukraine, redko.rom@gmail.com*

[2]*State University of Telecommunications, 7, Solomenska street, 03680 Kyiv, Ukraine*

The influence of both weak magnetic fields (it means that for such fields the relationship $m_B B \ll kT$, where m_B is the Bohr magneton, B is the magnetic field induction, k is the Boltzmann constant, T is the absolute temperature, could be applied) and non-thermal effect of electromagnetic radiation of the microwave range on the state of defects in diamagnetic (semiconductor) crystals refer to the number of experimentally confirmed phenomena. At the same time, this fact is nontrivial, since the energies of interaction of particles and defects in crystals with such fields are negligible as compared to the energy barriers that they need to overcome in their movement. Considering that such a small effect leads to a significant physically observable response, it is quite reasonable to assume that these fields either act on the spin of the particles or cause resonant phenomena in the system of crystal defects

Possible mechanisms of transformation of defects in *n*-GaAs and *n*-GaN epitaxial films under action of electromagnetic radiation in the microwave range and pulsed magnetic field have been analyzed. Electrical-resonance effects under non-thermal action of electromagnetic fields (2.45 GHz) have been considered, namely: resonant detachment of dislocations and destruction of impurity complexes in semiconductor crystals, electrical-resonance transformation of defects in semiconductor crystals under action of weak pulsed magnetic fields (60 mT); magnetic-resonance effects on defects in semiconductor crystals under action of weak magnetic electromagnetic fields.

Electrically charged dislocations fixed at the ends have their own (main) angular frequency of oscillations ω_1 equal to:

$$\omega_1 = \frac{\pi}{L}\left(\frac{G}{\rho_V}\right)^{1/2}, \qquad (1)$$

where G is the Poisson module, ρ_V is the bulk density of the material, L is the dislocation length.

Ion-plasma oscillations of singly charged tellurium ions with an angular frequency ω_p are observed in the bulk of doped semiconductors outside the near-surface area of the space charge region:

$$\omega_2 = \left(\frac{e^2 N}{\varepsilon\varepsilon_0 M}\right)^{1/2}, \qquad (2)$$

where N is the concentration of impurity ions; e – elementary electric charge (charge of electron); ε_0 – dielectric permittivity of semiconductor; ε – electric constant; M is the mass of impurity ion.

Resonant phenomena of various natures occur, which in generally, do not require high energies, and have been realized when the oscillation frequencies of the system and the external action are coincide.

The Passing Current Mechanisms and Photosensitivity of the Oxide/$Cd_{0,96}Zn_{0,04}Te$ Surface-Barrier Structures

Novosad O.V., Bozhko V.V.

Lesya Ukrainka Eastern European National University, Lutsk, Ukraine, ovosa@ukr.net

CdTe is recognized as one of the most promising materials for the production of low-cost large-area solar cells [1]. In this work photosensitive structure of $Cd_{0,96}Zn_{0,04}Te$ single crystals with p-type conductivity has been fabrication. The stationary current-voltage characteristics and the photosensitivity processes of these surface-barrier structures are studied.

The measurements were carried out using the specimens fabricated in the form of plates 3×3×1 mm^3 in size. Photosensitive surface-barrier structures were produced by heat-treatment of monocrystalline p-$Cd_{0,96}Zn_{0,04}Te$ plates in the air at temperature near 570 °C for t≈40 min. Just as in article [1].Then the crystals cooled down to room temperature at a rate of 200-300 K/min. As a result, on the $Cd_{0,96}Zn_{0,04}Te$ plates homogeneously colored layers of blue were formed. After heat treatment the formed layers were removed from all sides except one.

The forward portion of current-voltage characteristic in the structures subjected to bias voltages U>2 V are typically described by the relation

$$I = \frac{(U - U_0)}{R_0},$$

where the cutoff voltage U_0≈1,2 V and the residual resistance $R_0 \approx 4 \cdot 10^5$ ohm at T=300 K. The forward current-voltage characteristic follow, at U<1,2 V, the exponential law typical of a photodiode [2]

$$I = I_0\left[\exp\left(\frac{eU}{nkT}\right) - 1\right].$$

The reverse current of oxide-$Cd_{0,96}Zn_{0,04}Te$ surface-barrier structures without illumination is described by the power law [2]

$$I \sim U^m$$

with the m≈2,6 exponent. The forward-to-reverse current ratio for a voltage close to the cutoff voltage (U_0) was 20.

When illuminated using integral light of halogen lamp, photovoltaic effect was observed. On the spectrum of photovoltage, there is one with a narrow peak width at half height of 120 meV. The energy position of the maximum the photovoltage was equal to hυ≈1,54 eV.

1. G. A. Il'chuk, V. I. Ivanov-Omskii, V. Yu. Rud' [et al.]. Fabrication and photoelectric properties of oxide/CdTe structures. *Semiconductors.*2000. V.34, №9, pp 1058–1061.
2. Sze S. M. Physics of Semiconductor Devices (Wiley, New York, 1969; Mir, Moscow, 1973).

One-Phonon Raman Spectra of Graphite Thin Films Prepared by the Electron-Beam Evaporation Technique

Orletskyi I.G., Ilashchuk M.I., Brus V.V., Maryanchuk P.D., Parfenyuk O.A., Grushka O. G.

Chernivtsi National University,Chernivtsi, Ukraine, i.orletskyi@chnu.edu.ua

Thin graphite carbon films were prepared by electron-beam evaporation technique using of pure polycrystalline graphite. Graphite evaporation lasted 1.5 minutes at an average deposition rate of 0.27 nm/s on pre-purified quartz glass substrates heated to a temperature of 723 K.

The determined thickness of the graphite films was 30 nm. Under excitation of unpolarized light with a wavelength of 514.5 nm, one-phonon Raman spectra in the frequency range 1000-2000 cm^{-1}, corresponding to the fluctuations of carbon sp^2-bonds, were obtained using the Jobin Yvon t64000 spectrometer.

In the experimental Raman spectra of carbon films obtained, there were two distinct bands at frequencies 1596 and 1355 cm^{-1}, which corresponded to known bands G and D inherent in graphite structures with oscillating sp^2-bonds. A detailed analysis of experimental spectra by means of computer decomposition into Gaussian components shown that in addition to the main bands G and D, there was a band B with a maximum at 1510 cm^{-1}, the intensity of which was much smaller. The observed displacement of the maximum of the main band G (which corresponded to a frequency of 1581 cm^{-1} in monocrystalline graphite), in the region of higher frequencies close to 1596 cm^{-1} indicated the nanocrystalline structure of the films obtained. The evaluation of the sizes of nanocrystallites was carried out on the basis of an empirical correlation between their size and the ratio of the intensities of bands *G* and *D*, $I_D/I_G = 44/L_a$ [1]. The value of I_D/I_G was determined using the height of the peaks of the corresponding Gaussian (absolute maxima). The size of the clusters, calculated according to indicated above formula, was $L_a \approx 4.8$ nm. As result of the Gaussian decomposition of the Raman spectrum, the dedicated band B with a maximum at 1510 cm^{-1} was due to the displacement of the main band G into the range of lower frequencies in the transition from nanocrystalline graphite to amorphous graphite. Band B indicated the presence of graphitized carbon amorphous phase in the studied carbon films. Determined from the peak height of the corresponding Gaussians ratio of $I_D/I_B \approx 2.4$ corresponded to the transition region from amorphous to nano-crystalline carbon.

Since the intensity of the band G with a maximum of 1596 cm^{-1} substantially exceeded the intensity of the band B, the produced films of graphitized carbon can be considered as nanocrystalline carbon structures with the inclusion of the amorphous phase.

1. F. Tuinstra, J. L. Koenig. Raman Spectrum of Graphite // J. Chem. Phys. 53, (1970) 1126 – 1130.

Defect Formation in the Tin Telluride Thin Films at their Growth from a Vapour Phase

Prokopiv V.V.[1], Turovska L.V.[2], Nykyruy L.I.[1], Dzundza B.S.[1]

[1]*Vasyl Stefanyk Prearpathian National University, Ivano-Frankivsk, Ukraine, prkvv@i.ua*
[2]*Ivano-Frankivsk National Medical University, Ivano-Frankivsk, Ukraine*

The main factor determining the performance of the device structures is defect subsystem of crystal structure of the base material, which in turn is determined by technological factors of growing process.

The thin films have been grown from the vapour phase by the hot-wall epitaxy method on monocrystalline BaF_2 (111) substrates. The defect subsystem of the material has been studied using modelling method via quasichemical reactions. The values of the equilibrium constants for quasichemical reactions of defect formation in SnTe have been calculated theoretically. The constant $K_{Te_2,V}$ of the reaction of formation of neutral defects $\frac{1}{2}Te_2^V = V_{Sn}^0 + Te_{Te}^0$ has been found by the method of thermodynamic potentials; constants K_a, K_a' for reactions of ionization of formed defects $V_{Sn}^0 = V_{Sn}^- + h^+$, $V_{Sn}^0 = V_{Sn}^{2-} + 2h^+$ and the constant K_i for the reaction of excitation of intrinsic conductivity $"0" = e^- + h^+$ have been calculated using the band theory of non-degenerate semiconductors.

Analytical expressions for determination of Hall concentration p_H, concentrations of electrons n and singly and doubly charged tin vacancies $[V_{Sn}^-]$, $[V_{Sn}^{2-}]$ have been obtained: $p_H = p - K_i / p$; $n = K_i / p$; $[V_{Sn}^-] = K_a K_{Te_2,V} P_{Te_2}^{1/2} \cdot p^{-1}$; $[V_{Sn}^{2-}] = K_a' K_{Te_2,V} P_{Te_2}^{1/2} \cdot p^{-2}$. The hole concentration p is defined by the cubic equation: $p^3 - \left(K_a K_{Te_2,V} P_{Te_2}^{1/2} + K_i\right)p - 2K_a' K_{Te_2,V} P_{Te_2}^{1/2} = 0.$

Based on the obtained ratios, the dependences of the concentrations of charge carriers and point defects in tin telluride thin films on substrate temperature T_S, evaporation temperature T_E and partial vapour pressure of tellurium P_{Te_2} have been calculated. It has been shown that in SnTe films, concentration of charge carriers is determined by singly charged tin vacancies.

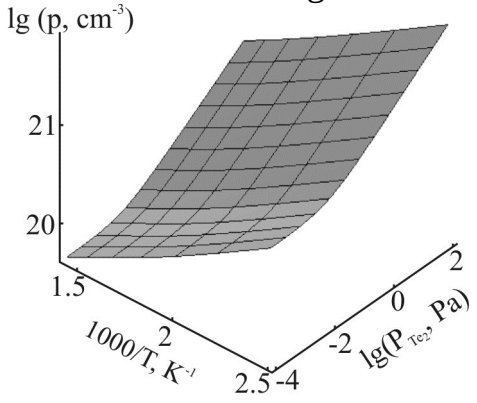

3d-Diagram of the dependence of hole concentration in tin telluride films on partial vapour pressure of tellurium P_{Te_2} of additional source and the substrate temperature T_S at evaporation temperature T_E = 800 K

Thermoplastic Properties of Quasi-Isotropic Indium Layers

Raransky M.D., Tashchuk R.Yu., Kurek I.G., Oliynich-Lysyuk A.V.

Yuriy Fedkovych Chernivtsi National University, Chernivtsi, Ukraine,
romatastshcuk@gmail.com

Indium is widely used in electronics as a contact material (for flip-chips, hybrid pixel detectors, etc.). It is capable of self-alignment and compensation of thermomechanical stresses that arise due to the difference in the coefficients of thermal expansion (αij) [1]. However, when cycling in the conditions of a sharp change in temperature (0 - 300 K), problems arise in the reliability of the operation of such contacts, which are connected with the ignored thermal voltages, which leads to failure in their work.

Monocrystalline In is an axial auxetic, the values of the components of the Poisson coefficients tensor (n_{ij}) vary from 0.9 to -0.7. However, polycrystalline indium is not an auxetic in the entire temperature region. At the same time, the transition to 2*D* layers can increase the role of individual grains in the layer and increase the anisotropy of its mechanical properties. This assertion requires further study; therefore we have studied the influence of the magnitude of the thermomechanical stresses determined by α_{ij} (T) and the coefficients n_{ij} (T) of indium, in the process of rigid thermocycling, on the nature of its deformation, e_{ij}, elastic moduli, etc.

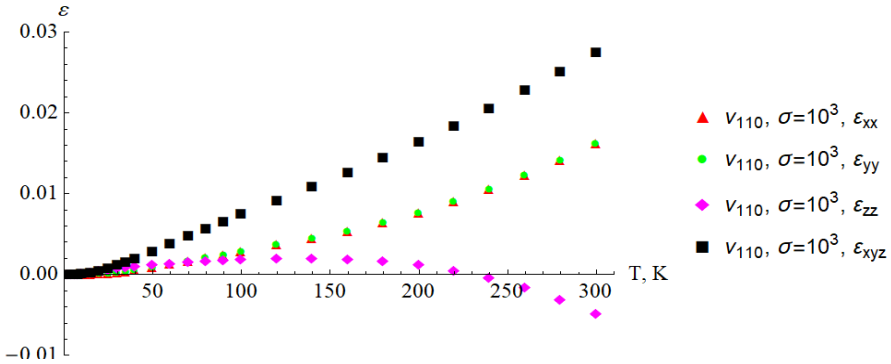

Fig.1 Dependence e_{ij} in 2*D*-quasi isotropic layers In from temperature.

It was found that in the direction perpendicular to the plane of the layer, with the temperature increase, the components of the deformation tensor ε_{zz} change their sign from negative to positive and again to negative for all investigated *s* from 1 kPa to 10 MPa for all n_{ij} except n_{101} (Fig. 1), which may cause the contacts to fail during thermocycling.

1. Cheng X., Liu C. and Silberschmidt V.V. Mechanical response of In micro-joints to low temperature cycling. In: Electronic Components and Technology Conference (ECTC 2009), San Diego, CA, 26-29 May, p. 1792 - 1795.

Calculation of optimal temperature and concentration conditions of CdTe epilayers growth from non-stoichiometric melt

Rashkovetskyi L.V.*, Beketov G.V.*, Plyatsko S.V.*, Gromovoj Y.S.*, Moskvin P.P.**

** Institute of Semiconductor Physics NAS Ukraine, Kyiv, Ukraine, rashlv@ukr.net*
*** Zhytomyr State Technological University Zhytomyr, Ukraine*

We present results of a numerical solution for the reverse Stefan problem which describes epitaxial growth of CdTe on the CdTe substrates with a constant growth rate. The liquid phase was a non-stoichiometric Cd/Te melt in which the liquid-solid interface advances with a constant velocity. The computational model was built under the following simplifying assumptions: diffusion in the solid phase and convection in the liquid phase could be neglected; the Cd diffusion coefficient in the liquid phase was assumed to be constant; no volume nucleation and crystal growth in the liquid phase did occur.

Expressions used to determine Cd concentration X at the interphase boundary and the absolute temperature T at a given time were as follows:

$$X = \left[0.5 \cdot V \cdot \Delta r / (D - b)\right] / \left[a \cdot V \cdot \Delta r / (D - 1)\right]$$

$$T = \left\{\Delta S_{CdTe} \cdot T_{CdTe} + 0.5 \cdot g\left[1 - X(1 - X)\right]\right\} \Big/ \left[R \cdot \ln X / (1 - X) + \Delta S_{CdTe}\right]$$

where V=Const is the interphase boundary velocity, Δr is the distance traveled by the boundary for a certain interval of time, D is a discrete analogue of the Stefan's condition, ΔS_{CdTe} is the CdTe melting entropy, α, β are the sweep optimization parameters, g is the interaction parameter, and X is the Cd concentration.

The families of plots were build which correspond to three levels of initial Cd concentration in liquid phase (x = 0.6, 0.7, 0.8) at different crystallization rates ($V=1.0 \cdot 10^{-5} - 1.0 \cdot 10^{-6}$ cm·c$^{-1.}$). It has been shown that the increase in the Cd concentration in the growth melt results in essential reducing the temperature of the epitaxy, thus lowering the concentration of the growth defects. Enlargement of the liquid phase volume (thickness) from 1 to 3 mm leads to narrowing the temperature variation range for plot families corresponding to a constant X value. At low growth rates, the diffusion Cd transport to the interphase boundary is becoming a rate limiting step. At high growth rates, the constant crystallization velocity, V=Const, is provided mainly by decreasing the temperature.

The presented calculations can be generalized on more complicated cases of liquid phase epitaxy of multi-component compounds, such as CdZnTe, CdHgTe, A_3B_5, and A_4B_6, as well as on the growth of monocrystals, thus providing means for not only for the temperature control of crystal growth, but also for the composition of the epilayers.

Physical Properties and Structure of Vapor-Quenched (Fe, Ni, Co)-C Films

Ryabtsev S.I., Bashev V.F., Kushnerov O.I., Kutseva N.A.

Oles Honchar Dnipro National University, Dnipro, Ukraine,
siryabts@gmail.com

The work is devoted to the investigation of the features of the formation and thermal stability of high carbon films of Co – C, Fe – C, Ni – C systems, which state diagrams have much in common with each other. The relationship between the formation conditions and the physical properties of the amorphous and microcrystalline phases in high-carbon films of the C- (Fe, Ni, Co) systems is analyzed. Received experimental evidence that with increasing carbon content in the heat-treated films C-Fe (> 50 at. % C) obtained by the modified method of the three-electrode ion-plasma sputtering (MIPS) it is possible of major expansion of electrical denominations due to forming metastable phases. The conditions for the production and heat treatment of C-Fe films, which allow to obtain a significant (up to 0.5-1 kOhm/square) expansion of electrical resistivity and precision values of the temperature coefficient of electrical resistivity ($\sim 10^{-6}$ K^{-1}) are established.

Established that ion-plasma sputtering alloys Co-C in wide concentration range (5...52% C) leads to the formation of non-equilibrium states: supersaturated solid solution of carbon in β-Co, metastable carbides of Co_3C, Co_2C and phases without a distant crystalline order. Conception of diagrams of metastable equilibrium got subsequent development in the case of supercooling from the vaporous state considering a greater degree of supercooling liquid that exists briefly if deposition is carried out on the mechanism of vapor - liquid - solid state. Disintegration of nonequilibrium structures, that takes place in several stages, is accompanied by stabilization of high temperature fcc - modification of β-Co.

It is shown that ion-plasma sputtering of alloys of Ni-C extends the spectrum of the metastable states as compared to quenching from a liquid state. The intervals of concentration of carbon are first certain, when in the alloys of Ni-C at ion-plasma sputtering are formed: supersaturated solid solution, amorphous phase, nanocrystalline phase and metastable carbide of Ni_3C. The technology of modernized triode ion-plasma spraying of high-carbon films Ni-(7 ... 61.4) at. % C allows us to recommend the latter for practical use in microelectronics devices as corrosion-resistant high-resistance thin-film resistors.

Effect of Air Atmosphere on the Electrophysical Properties of Thin Nanocrystalline Silicon Carbide Films

Semenov A.V.[1], Kozlovskyi A.A.[2], Skorik S.N.[3], Lubov D.V.[4]

[1]*National Technical University "Kharkiv Polytechnic Institute", Kharkiv, Ukraine, savladi@ukr.net*

[2] *Institute for Single Crystals NAS of Ukraine, Kharkiv, Ukraine, khirnyi@isc.kharkov.ua*

[3]*Institute for Single Crystals NAS of Ukraine, Kharkiv, Ukraine stiksskits@gmail.com*

[4]*National Technical University "Kharkiv Polytechnic Institute", Kharkiv, Ukraine, welax94@gmail.com*

There is the great problem of search for new functional semiconductor materials for the creation of highly sensitive gas sensors that slightly change their properties over time under severe external influences. One of the promising materials with chemical inertness, resistance to radiation impacts and time stability of properties are materials based on SiC [1]. The purpose of this paper was to investigate the dependence of electrical conductivity of thin nanocrystalline SiC films with different polytype structure on the air atmosphere. The nanocrystalline thin SiC films were obtained by method of direct ion deposition on sapphire [2]. Measurements were performed on two series of nc-SiC films with different structure: one series contained mainly 3C-SiC polytype nanocrystals and were denoted as monopolytypic, the second series were a nanoheterostructures based on a mixture of 3C-SiC and 21R-SiC nanocrystals. It is shown that the initial films of MP-nc-SiC had greater resistance than heteropolype ones, and both series showed no reaction to changes in atmospheric pressure. Gas sensitivity of the films appeared after annealing in vacuum at temperatures above 500 K. Measurements of the gas sensitivity of the films to the air atmosphere at a temperature of 700 K showed that the resistance increased for 12 times (S=91.6%) for the monopolytype film, while the heteropolytype film showed an increase of resistance for almost 16 times (S=93.7%).

Thus, the values of air sensitivity of thin nc-SiC films were measured for the first time. The obtained results allowed to speak about the prospects of development of highly sensitive gas sensors on thin films of nanocrystalline SiC.

1. C.A. Zorman, R.J. Parro, Micro- and nanomechanical structures for silicon carbide MEMS and NEMS, *Phys. Status Solidi*, B 245 (2008) 1404-1424.
2. A.V. Semenov, V.M. Puzikov, M.V. Dobrotvorskaya, A.G. Fedorov, A.V. Lopin, Nanocrystalliine SiC films prepared by direct deposition of carbon and silicon ions, *Thin Solid Films*, 516 (2008) 2899-2905.

Relaxation Processes in Thin Films of PVDF-$BaTiO_3$ Composites

Sergeeva A.E. and Fedosov S.N.

Odessa National Academy of Food Technologies, Odessa, Ukraine, aeserg@ukr.net

Polymer-ferroelectric composites have advantage over ferroceramics due to their better mechanical properties. In this work, the PVDF-$BaTiO_3$ composites were subjected to thermally stimulated polarization (TSP) and depolarization (TSD) for obtaining information on electric relaxation in the composites.

The samples of 300 μm thickness were prepared by hot pressing of PVDF powder mixed with 10 μm $BaTiO_3$ particles. After the TSP, the samples were subjected to the TSD in a short-circuit mode. The samples annealed at 140 °C were also studied by the relaxation map analysis (RMA) method at the SOLQMAT 91000 Spectrometer. The fractional analysis of the relaxation processes was also performed by the method of thermal windowing. The activation energies of the relaxation processes were calculated.

During the TSP experiments, the linearity of the log*G*-(l/*T*) curves was distorted at 70-80 °C and the abrupt decrease in the apparent conductivity (*G*) was observed. The divergence between the direct and the reversed *G(T)* curves indicated that the change in conductivity was irreversible and related to the polarization buildup.

The fractures at the reversed curves corresponded to 120°C, being actually the Curie point of $BaTiO_3$. The activation energy of the conductivity in the paraelectrlc phase (0.53 eV) was much smaller than in the ferroelectric phase (0.98 eV). The phase transition was also seen at the TSD curve as a splash of current during heating and cooling.

The TSP during poling was essential, because the polarization was not formed at room temperature even under high fields of the order of 20 MV/m. Moreover, the I(V) characteristic at 20 °C was super-linear and typical for the space charge limited currents.

The similarity in the TSP curves of the PVDF-$BaTiO_3$ and PVDF has been found indicating that the mechanism of correlation between the polarization buildup and the decrease of conductivity is the same in both cases. The charge carriers were probably trapped at the boundaries of the polarized particles compensating the depolarizing field and providing for the lasting stability of the polarization.

The activation energy *Q* slightly decreased in the range of 20-80 °C from 1.17 eV to 1.09 eV. Then *Q* increased abruptly reaching the highest values of 1.23-1.55 eV at 105-110 °C. The magnitude of the energy correlated with the content of the ceramics filler being 1.23 eV at 40%, 1.40 eV at 50% and l.55 eV at 70% of $BaTiO_3$ in the composite. Moreover, the temperature of the peak was very close to the Curie point of $BaTiO_3$, proving that the relaxation behavior of the composite near this temperature is governed by ceramics.

Similarity of electrical relaxation in PVDF-$BaTiO_3$ composites and PVDF can lead to the development of a generalized model capable to interpret and even predict the electrical properties of the polymer-ceramics ferroelectric composites.

Pyroelectricity and Residual Polarization in PVDF Thin Films with Nano-Scale Structure

Sergeeva A. E. and Fedosov S.N.

Odessa National Academy of Food Technologies, Odessa, Ukraine, aeserg@ukr.net

Ferroelectric polymers having a nano crystalline structure were considered during the last years as new candidates for replacing inorganic materials in pyroelectric sensors due to their good mechanical properties, reasonably sufficient performance and easy fabrication. Polyvinylidene fluoride (PVDF), being a typical ferroelectric polymer, has prospects of widespread application in pyroelectric sensors. In this work, the relationship between pyroelectricity in PVDF films and residual polarization was investigated.

Polymer chains of PVDF are arranged in such a way that a semi-crystalline structure is formed consisting of nanosized crystallites and amorphous phase. The preferential orientation of the dipoles occurs only after poling, i.e. application of an external strong DC electric field. Short-circuited poled films possess the residual polarization P_r, presence of which and its dependence on temperature leads to appearance of pyroelectricity in PVDF.

Experiments were performed on 12.5 μm-thick biaxially stretched PVDF films with Au electrodes deposited by cathode sputtering. Initial poling and switching of polarization were performed by a step-wise application of DC high voltage. The pyroelectric dynamic coefficient was measured by the thermal pulse method developed by Collins. A heat pulse of 50 μs duration was generated by the Metz 45 CT-3 flash unit and absorbed by the metal electrode deposited on the sample surface. The heat flowing along the thickness direction created a temperature distribution $T(x,t)$ and caused appearance of the pyroelectric current recorded by Tektronix TDS 510A broadband oscilloscope.

Five series of experiments were performed, in which the polarization reversal was accomplished at different duration (from 10 μs to 100 s) of the applied voltage in the range from 0.5 kV to 2.5 kV

The one-dimensional (in the direction of thickness) homogeneous differential equation of the second order in partial derivatives has been solved for the case of the thermal pulse excitation.

Comparison of the switched polarization and the pyroelectric signal at the identical switching conditions has shown the absolute similarity of the corresponding experimental curves. This indicated that there was a direct proportionality between the residual ferroelectric polarization and the pyroelectric coefficient. On the basis of the obtained results, it was proposed to employ the measurement of the pyroelectricity by the simple Collins method to estimate the polarization state of PVDF films used for the manufacturing of sensors and actuators.

Structural Transformations and Optical Properties of Electon-Irradiated Glasses and Thin-Films of the As-S-Se System

Shpak I., Kunak S., Shpak O., Studenyak I.

Uzhhorod National University, Uzhgorod, Ukraine, shpak.univ@gmail.com

Glassy chalcogenides of arsenium are characterized by high transparency in a near and middle infrared and belong to a class of materials which are used as active or passive elements in optical engineering]. Experimental studies of the influence of radiation load (gamma radiation, X-radiation or electron radiation) enable to determine the character and change of physical properties of these materials, boundary doses of radiation, to learn the nature and mechanisms of radiational defect – formation, reveal conditions of renewing the initial parameters.

Gody et al. [1] were the first to determine experimentally the proportionality $E_g^*(T,X)$ and *(T,X)* for a- Si:H. By using the Tauc's concept of "freezed" phonons he spread the idea of the equivalency of the effect of a structural *Ws* and thermal *Wt* of disorder onto the band width E_g^* and got a linear relation between E_g^* and *W*:

$$E_g^*(T,X) = E_g^*(0,0) + D\cdot\langle W^2\rangle_0 - \frac{D}{K}W(T,X),$$

where *D* is a deformation potential, $\langle W^2\rangle_0$ – mean-square shift due to zero oscillations. According to this model the optical pseudogap E_g^*(T,X) is determined by the degree of disordering of a glass lattice which is described by $\langle W^2\rangle_S$ parameter, ie. By changing it by sources of different nature it is possible to influence the E_g^* value indirectly. Let us analyse our experimental results in the frameworks of this model. In the correlation between E_g^* and W for glassy $As_2S_3(Se_3)$ in dependence of the nature of disorder due to various external factors. This correlation shows that the optical pseudogap E_g^* and – this being more important – the slope of an exponential portion of the edge are changing in dependence of the disorder degree. A linear relation between E_g^* and W for chalcogenide glasses $As_2S_3(Se_3)$ is fulfilled practically in the whole range of the values of W energies which was studied up to this time. Thus it can be stated that in this case for these materials the contribution of the structural ("intrinsic" and induced) and the thermal contributions into a change of disorder potential is adequate, and the change of the slope probably reflects the change of the distribution of the states in the tails of zones.

Conclusions

Dose dependences of energy parameters of the intrinsic absorption edge testify to an electron-induced creation of new defects which change the disorder potential. A characteristic energy of the exponential absorption tail W(T,X) shows not only the temperature but also the structural disordering of other kinds:

a) intrinsic structural disorder of an "ideal" glass;

b) induced structural disorder due to external factors (of radiation or technological nature).

1. Gody G.D., Tiedje T., Abeles B., Brooks B., Goldstain Y. Phys. Rev. Letters **47** (1981) 1480.

Electrophysical Properties of Thin Film Systems Based on Permalloy and Silver Prepared by Co-evaporation Technique

Shuliarenko D.O., Romas′ O.V., Pazukha I.M.

Sumy State University, Sumy, Ukraine, denisshuliarenko@gmail.com

Resistivity is a basic parameter that influences on electronic, deformation magnetic and other physical properties of thin film materials. At the same time, the detail experimental investigation of electrophysical properties (resistivity and temperature coefficient of resistance (TCR)) of thin film based on permalloy $Ni_{80}Fe_{20}$ (Py) in a wide concentration range does not was performed. Therefore, the mean goal of our work is an investigation of concentration effect on electrophysical properties of such nanosized structures prepared by the method of electron-beam co-evaporation. The condensation was realized on the series of a glass-ceramic substrate in the vacuum chamber with base pressure 10^{-4} Pa. The substrates were situated in a row that allows to realize thin film structures in a wide concentration range in one technological cycle. The condensation rate was 0,1 nm/s. The total thickness that was controlled by the method of «*in situ*» quarts resonator was 55 nm. The heat treatment of the samples in the temperature range 300-520 K was conducted in a vacuum chamber in the automatic regime that allows to control the speed of samples heating, record and experimental data processing. The temperature dependences of resistivity $\rho(T)$ was created based on experimental data. The value of TCR was calculated according to the equation $\beta = (1/\rho(300)(\Delta\rho/\Delta T)$, where $\rho(300)$ is the initial value of resistivity, $\Delta T = 5$ K.

Comparison analysis of experimental results of investigation $\rho(T)$ and $\beta(T)$ dependences for nanosized thin film samples based on $Ni_{80}Fe_{20}$ and Ag showed that: (i) the character of temperature dependences of resistivity and TKO is typical for the components of the system, wherein ρ have an order of 10^{-7} Ohm·m, and $\beta - 10^{-3}$ K^{-1}; (ii) at the concentration dependence of resistivity the maximum value of $\rho = 3.5 \cdot 10^{-7}$ Ohm·m at the concentration of Ag atoms $c_{Ag} = 48$ at. % is observed. This can be described with the change of type and concentration of structural defects (the gradual transition from defects of the vacancy type at $c_{Ag} = 50$ at.% to the appearance of packaging defects), and with the change of mean value of grain size; (iii) at the dependences β as a function of c_{Ag} the minimum value of $\beta = 1.8 \cdot 10^{3}$ K^{-1} at $c_{Ag} = 48$ at. % is observed; (iv) the temperature of healing defects is in the range from 450 to 520 K for concentration interval $c_{Ag} = 20$-85 at.%.

This work was funded by the State Program of the Ministry of Education and Science of Ukraine.

Approbation of the Semiphenomenological Model for Magnetoresistance of Films Based on Magnetic and Noble Metals

Shumakova M.O., Odnodvorets L.V., Protsenko S.I., Rylova A.K.

Sumy State University, Sumy, Ukraine, larysa.odnodvorets@gmail.com

At the study of magnetoresistive effect it is necessary to take into account dependence on the magnitude of the magnetic field the mean free path (λ_0), but the specular parameter (p), transmission parameters at the grain boundary (r) and interfaces (Q_{ij}) of electrons. The purpose of this work was to approbation of the semiphenomenological model for magnetoresistance (MR) on the example of two-component films based on Fe or Co and Ag or Au.

We have proposed a model, which takes into account the indirect influence of an external magnetic field not only λ_0, but p, r and Q_{ij}. This is precisely the new idea that will more accurately describe the physical processes in multilayers that lead to changing the settings electron transport and, consequently, the MR magnitude. Mathematical relationships of the model are described in [1].

The quantitative characteristics of the action magnetic induction (B) may be appropriate magnetic coefficients:

$$b_B^K = \frac{\partial \ln R}{\partial B},\ \beta_{0i}^K = -\frac{\partial \ln \lambda_{0i}}{\partial B},\ \beta_{pi}^K = -\frac{\partial \ln p_i}{\partial B},\ \beta_{ri}^K = -\frac{\partial \ln r_i}{\partial B} \text{ та } \beta_{Qij} = -\frac{\partial \ln Q_{ij}}{\partial B},$$

where index «K» corresponds to three field orientations relative to the electric current.

To determine parameters is necessary to obtain two groups of values l_0, p, r and Q_{ij} at two values of the magnetic field B_1 and B_2 (can be taken $B_1 = 0$ and $B_2 \neq 0$):

$$b_p^K = -\frac{1}{p(B_1)}\frac{p(B_2)-p(B_1)}{(B_2-B_1)},\ b_r^K = -\frac{1}{r(B_1)}\frac{r(B_2)-r(B_1)}{(B_2-B_1)},$$

$$\frac{\Delta \ln k}{\Delta \ln p} = -\frac{p(B_1)}{p(B_2)-p(B_1)}\frac{d/l_0(B_2)-d/l_0(B_1)}{d/l_0(B_1)},\ \frac{\Delta \ln m}{\Delta \ln r} = -\frac{r(B_1)}{r(B_2)-r(B_1)}\frac{L/l_0(B_2)-L/l_0(B_1)}{L/l_0(B_1)}.$$

The experimental dependences of temperature coefficient of resistance versus thickness for one-layer films at the B_1 and B_2 were used.

This work was supported by the Ministry of Education and Science of Ukraine.

1. Protsenko I.Yu., Odnodvorets L.V., Protsenko S.I., Shumakova M.O. The contribution to the scattering of electrons in the magnetoresistance of multilayers of nonmagnetic metals. *Problems of atomic science and technology*. 2016. № 1. P. 121-123.

Temperature Acceleration of Photoinduced Mass Transport in Amorphous Chalcogenides

Trunov M.L., Tarnaj A.A., Rubish V.M., Pisak R.P., Kyrylenko V.K., Horvat Yu.A., Durkot M.O.

Institute for Information Recording, NAS of Ukraine, Uzhhorod, Ukraine,
center.uzh@gmail.com

The present report is devoted to investigation of the influence of temperature on the photoinduced mass transport (PhMT) and formation of surface relief gratings (SRG) under holographic exposure by band-gap light in amorphous films of germanium, arsenic and antimony selenides.

Thin (~0.8 μm) Ge_xSe_{100-x}, As_xSe_{100-x} and Sb_xSe_{100-x} ($0 \le x \le 25$) amorphous films were obtained by vacuum evaporation of the glasses of corresponding compositions from quasi-closed effusion cells onto glass substrates at ambient temperature. All films after deposition were annealed near the glass-formation temperatures of appropriate bulk glasses during 1 h. The SRGs were then generated by a strongly absorbed linearly polarized solid-state lasers with wavelength λ=660 mW (*P*=25 mW) and λ=532 nm (*P*=18 mW) using holographic technique. Diffraction efficiently (η) of the recorded gratings was measured by spectrophotometer Optic Ocean using a violet laser (λ=404 nm, *P*=10 μW).

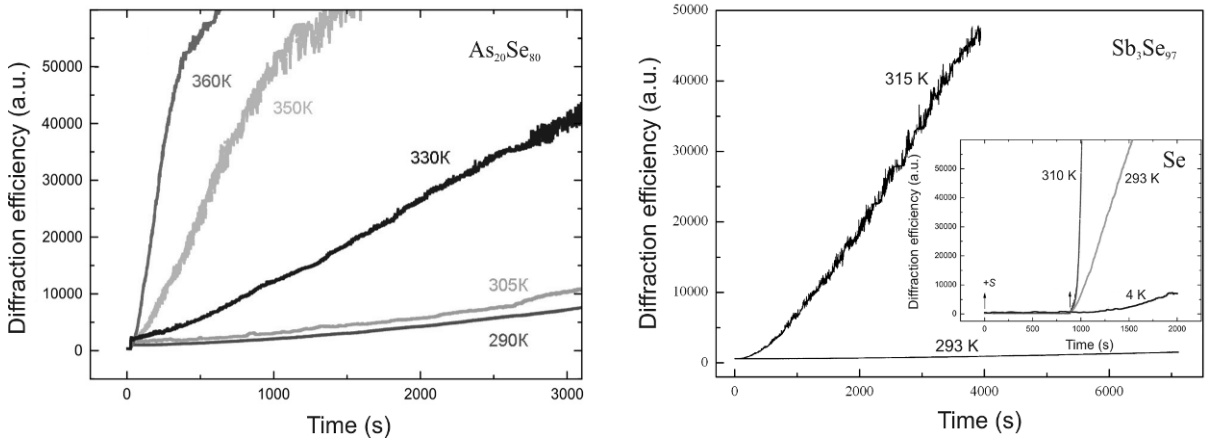

Fig. 1. Diffraction efficiency variation during the formation of SRGg in chalcogenide films at various temperatures

It was established that the efficiency of PhMT and their direction, the rate of SRG formation depends on the composition of chalcogenide films, polarization (*p* or *s*) and power of the laser irradiation.

It was detected, that the rate of photoinduced mass transport in chalcogenide films increases essentially with the temperature of recording (Fig.1) and reaches the maximum near T_g. This phenomenon is promising for practical use in integrated optics and photonics, holography and lithography.

The Investigation of Crystal Structure of Ni–B Coatings

Tsybulskaya L.S., Perevoznikov S.S., Shendyukov V.S.

Research Institute for Physical Chemical Problems of the Belarusian State University, Leningradskaya str., 14, Minsk, Belarus,220006, tsybul@bsu.by

Electrodeposited Ni–B coatings is perspective material due to their low contact electrical resistance, enhanced corrosion and wear resistance [1]. But structure of these coatings still remains the subject of discussions. XRD investigation of Ni–B coatings revealed that inclusion of boron in the Ni matrix led to the broadening of nickel X-ray peaks and eventually even to the halo-peak that indicates amorphous structure (fig. 1). This broadening may be due to decreasing of coating grain size also as increasing of defects amount. To estimate the contribution of these two components the dependence of broadening of peaks from the same crystallographic plane but different order on 2θ has been investigated. This dependence was shown to be proportional to sec2θ. That indicates the decreasing of grain size during increasing boron content in coatings. The lattice parameter *a* was calculated through the measured value of peak (220) position and was about 3,524 Å for Ni coating and 3,508 Å for Ni–B coating with 4 at. % of boron. The lattice parameter decreasing may be concern with formation of solid substitution solution of nickel by boron atoms which have smaller size. However the value of lattice parameter under the assumption of all boron atoms to be in the position of substitution was calculated to be 3,493 Å. Such difference can be explained by segregation of the part of boron atoms at the grain boundaries. To confirm this assumption the atomic probe tomography investigation of nickel–boron coating with 4 at. % of boron has been performed (fig 2). At the depth profile can be seen the increasing of boron content at the distances of about 15 – 25 nm which corresponds to grain size of these coatings. In this way Ni–B coatings contain boron atoms which substitutes Ni atoms in its crystal lattice and which segregates at the grain boundaries.

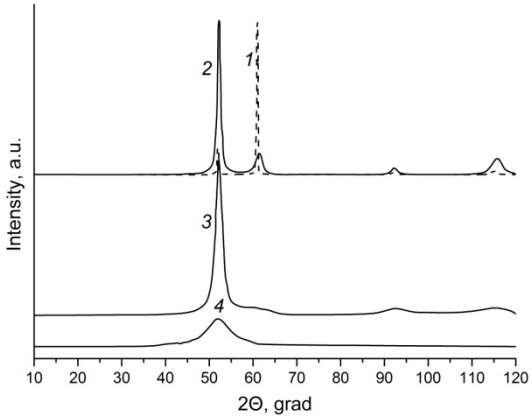

Fig. 1 XRD of nickel (*1*) and nickel–boron coatings with boron content (at. %): 4 – *2*, 8 – *3*, 20 – *4*

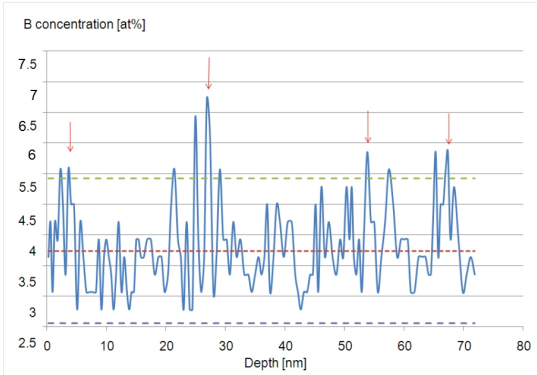

Fig. 2 The depth profile of B distribution

Electrodeposited Ni–B alloy coatings: Structure, corrosion resistance and mechanical properties / Y.N. Bekish [et al.] // Electrochimica Acta. – 2010. – Vol. 55, № 7. – P. 2223-2231.

Charge Carriers Study and Thermoelectric Properties of PbTe:Bi Thin Films

Tsymbaliuk T.[1], Nykyruy L.[1], Zapukhlyak R.[1], Dzumedzey R.[1], Mazur M.[2], Pavlyuk M.[1]

[1]*Vasyl Stefanyk Precarpathian University, Ivano-Frankivsk, Ukraine,*
tetyanatsymbaliuk@gmail.com
[2]*Ivano-Frankivsk National Technical University of Oil and Gas, Ivano-Frankivsk, Ukraine*

The thin films have an interest to researchers because it is possibility of significant improvement of certain properties, in particular, thermoelectric properties, and possible to create thermoelectric micro-modules on the basis of thin films, that will be practical using for miniature devices [1].

PbTe:Bi alloyed films were deposition on chips (0001) mica-muscovite and ceramic substrates (named as sital) by open vacuum evaporation method.

The choice of the type of substrate material and the temperature modes of the deposition changed the structure of the film surface and, accordingly, the values of thermoelectric parameters of the initial material. In particular, the selection of experimental modes allows manipulating of the both the size and grains of films and the thickness of the film, and different structure of substrates can contribute to the implementation of various scattering mechanisms. The consideration of the surface scattering, as well as size-related effects, can have a significant effect on the finite material properties [2].

It is shown that the effects of grain boundaries scattering are dominant for all films (Mayadas and Shatzkes theory) [3]. The surface effects (Fuchs and Sondheimer theory) are only significant for thin films [4], the thickness of which is commensurate with the mean of free path.

It was shown, for PbTe:Bi, the surface of the film substantially affects on transport phenomena for thicknesses ~ 100 nm. The obtained results allow setting the technological regimes for optimization of the material parameters in order to obtain the maximum values of thermoelectric figure of merit ZT.

1. Bulman G., Barletta P., Lewis J., Baldasaro N., Manno M., Bar-Cohen A., & Yang B. Superlattice-based thin-film thermoelectric modules with high cooling fluxes. Nature communications, 7, 2016, 10302.
2. Panchenko O.A., Sologub S.V. Dimensional phenomena and surface scattering of current carriers in metals (review), Physics and Chemistry of Solid State, 4(1), 2003, 7-42.
3. Mayadas A. F. and Shatzkes M.; Electrical-Resistivity Model for Polycrystalline Films: the Case of Arbitrary Re6ection at External Surfaces. Phys. Rev. B, 1, 1970, 1382.
4. Sondheimer E. H.; The mean free path of electrons in metals. Adv. Phys. 1, 1952, 1.

Modification of Optoelectronic Properties of ZnO Thin Films Using Methane as Reactive Gas During RF-Magnetron Deposition

Vasin A.V.[a,b], Rusavsky A.V.[a], Gomeniuk Yu.V.[a], Slobodyan A.M.[b], Kysil D.V.[a], Yatskiv R.[c], Kostylyov V.P.[a], Vlasyuk V.M.[a], Stepanov V.G.[a], Borschagovsky E.G.[a], Nazarov A.N.[a,b]

[a] *Lashkaryov Institute of Semiconductor Physics NAS of Ukraine, Kyiv, Ukraine*
[b] *National Technical University of Ukraine "Igor Sikorsky KPI", Kyiv, Ukraine*
[c] *Institute of Photonics and Electronics CAS, Praha 8 - Kobylisy, Czech Republi,*
av966@yahoo.com

ZnO thin films were deposited on silicon and other ceramic substrates at 200 ^{o}C by RF-magnetron sputtering of ZnO microcrystalline powder target with 160 mm diameter. It was demonstrated that “densified” ZnO powder with grain size of about 5 microns can be effectively used as inexpensive sputtering target instead of hot-pressed ceramics. It is demonstrated that morphology and electronic properties of the films (optical absorption, photoluminescence, resistivity) can be managed by introducing of methane during the deposition process. Adding of methane to argon results in enhancement of ZnO crystalinity, high energy shift of excitonic ultraviolet photoluminescence band as well as optical absorption edge, strong reduction of yellow-green emission band and decreases drastically sheet resistance of ZnO layers. The effect of CH_4 addition into working gas on optical, electrical and photovoltaic properties of the obtained ZnO thin films and n-Si/n^+-ZnO heterojunction have been studied. Structural and optical properties of the ZnO films were analyzed by SEM/EDS, FTIR, Raman scattering, photoluminescence cpectroscopy and ellipsometry. It was demonstrated that CH_4 incorporation results in drastic change of charge transport mechanism in ZnO films: sheet resistance in ZnO films decreased four orders of magnitude (90-230 Ω/sq depending on doping) and appeared to be independent on the temperature in range of 150-300 K while undoped ZnO films exhibited classical semiconductor temperature behavior i.e. exponential increase with temperature (with sheet resistance at room temperature about $1.4x10^6$ Ω/sq). It was shown that carbon is not incorporated into synthesized ZnO film, and observed phenomena are similar to ones in hydrogenated ZnO film.. The illumination results in the increase of the current by a factor of 3-5 at room temperature and by several orders of magnitude at 180 K. The possible mechanisms responsible for the effects of strong doping and structure enhancement from methane as reactive gas will be discussed.

Kinetic Processes in Films of Metal Oxides

Vilinskaya L.N., Burlak G.M.

Odessa State Academy of Civil Engineering and Architecture, Odessa, Ukraine, demiga89@gmail.com

It is known that the interaction of metal oxide films with water vapor leads to the accumulation of light sum, the excitation of exoelectron emission and the formation of EMF. One of the most promising materials for the creation of nonporous oxide layer is aluminum and tantalum. The appearance of EMF was observed in the structures $Al - Al_2O_3 - SnO_2$ and $Ta - Ta_2O_3 - SnO_2$ during their interaction with water vapor and ammonia. Such structures are created by electrochemical oxidant of aluminum foil in water solution of sorrel acid with the following deposit SnO_2 layer on oxide film by pyrolysis method. In order to clarify the mechanism of EMF occurrence, the kinetics of the rise and fall of EMF in films of aluminum oxide and tantalum was studied.

The study of the kinetics was carried out according to a scheme in which a key, an oscilloscope, and a load resistance were connected in parallel to the sample. When the key is closed, the potential difference at the terminals of the sample is zero, and when the key is opened in the presence of water vapor or ammonia, an increase in the EMF to a certain stationary value was observed. The time constant of the EMF increase process, depending on the conditions of the experiment, varied. Measurements showed that at relatively low densities of water vapor, less than $7 g/m^3$ at room temperature, the aluminum electrode acquires a positive potential and the time constant of the EMF rise process is 0.02-0.2 s, and with increasing water vapor density a negative potential occurs aluminum electrode and the time constant is 0.01-0.1 s. It is established that with an increase in vapor density, the value of load resistance and film thickness, the value of the time constant increases. The kinetics of the decay EMF is studied. The time constant of the decay process does not depend on the density of water vapor or ammonia in the surrounding atmosphere and decreases with increasing temperature.

It is shown that the kinetics of EMF is determined by the kinetics of adsorption-desorption processes occurring on the film surface with a sharp change in the density of water vapor in the surrounding atmosphere, as well as the kinetics of electronic and ionic processes occurring directly in the volume of the film at a constant density of water vapor. The kinetics caused by the adsorption-desorption processes occurring on the film surface occurs by the Langmuir mechanism. An analytical expression is obtained for the time constant of the EMF increase process, from which it follows that the time constant of the growth process is determined mainly by diffusion processes occurring in the oxide film.

Simulation of Ion Implantation and Diffusion Processes in Garnets

Yaremiy S.I.[1], Povkh M.M.[2], Burdiak V.R.[2], Ovcharyk R.Ya.[2], Vovk T.M.[2]

[1]*Ivano-Frankivsk National Medical University Ivano-Frankivsk, Ukraine,*
yaremiyip@gmail.com
[2]*Vasyl Stefanyk Precarpathian National University, Ivano-Frankivsk, Ukraine*

For the study of diffusion processes in ion-implanted ferrite-garnet films, simulation of ionic implantation and diffusion processes was carried out.

Simulation of the ion implantation process in iron-yttrium garnets, gallium gadolinium garnets and substituted ferrite garnets was made using the SRIM program. Implants were He^+, B^+, N^+, F^+, Si^+ and As^+ ions. Distribution profiles of ion-implants, profiles displaced ion of the matrix and energy loss parameters are obtained. To perform statistical processing of simulation results, a spatial program was developed. This program made it possible to determine the number of displaced atoms in radiation clusters and the volume of clusters. The dependence of these parameters on the mass of the ion implant is established.

The distributions obtained during the simulation of the ion implantation process were used as start approximations for the simulation of further diffusion processes. Diffusion was considered from two approaches:

- the continual approach considers the diffusing substance and the substance in which the diffusion proceeds as a continuous medium. In this approach, differential equations were solved using the finite difference method;
- the atomistic approach takes into account the fact that the diffusing substance and the substance in which the diffusion proceeds consist of atoms. In this approach diffusion by the method of Monte-Carlo was modeled.

Both approaches led to the same result: when aging at room temperatures, the maximum deformation decreases, and the gradient of the distribution profile of radiation defects decreases, especially from the side of the surface.

The obtained results are consistent with the data of X-ray two-crystal diffractometry of implanted ferrite-garnet films.

For a more detailed description of the diffusion processes that occur during the aging of the ion-implanted layer, it is also necessary to take into account the possibility of annihilating Frenkel's pairs when meeting interstitial atoms with vacancies, and the possibility of joining defects to clusters or dislocation loops.

Aging Processes in Films of Iron-Yttrium Garnet Implanted by He^+, B^+ and F^+ Ions

Yaremiy I.P.[1], Yaremiy S.I.[2], Povkh M.M.[1], Fedoriv V.D.[1], Pashkovska R.I.[1]

[1]*Vasyl Stefanyk Precarpathian National University, Ivano-Frankivsk, Ukraine,*
yaremiyip@gmail.com
[2]*Ivano-Frankivsk National Medical University Ivano-Frankivsk, Ukraine*

Epitaxial films of iron-yttrium garnet (YIG), irradiated by He^+, B^+ and F^+ ions with energies of 80-100 keV, were used to study the processes of low-temperature relaxation (aging) of the implanted layer.

X-ray structural investigations were carried out using two-crystal diffractometry using $CuK\alpha_1$ radiation. From the experimentally obtained rocking curves, strain profiles $Dd/d(z)$ and defect parameters were calculated. These calculations were made by simulating X-ray diffraction in a nonideal crystal by means of the statistical dynamical theory of scattering of X-rays.

The peculiarities of natural aging at room temperatures of ferrite garnet films implanted with He^+, B^+ and F^+ ions were established.

With the He^+ implantation, the process of rebuilding the structure of the near-surface disturbed layer can be divided into two stages over time (for doses $\leq \leq 6\cdot10^{15}$ cm^{-2}): the first stage - up to 38 months, the second stage - after 38 months. At $D = 1\cdot10^{16}$ cm^{-2}, the first stage of aging lasts more than 50 months. At the first stage of aging at room temperature there is an increase in maximum deformation, and in the second stage – a decrease in the magnitude of the maximum deformation.

At implantation of ions B^+ on the rocking curves, obtained with an interval of 15 years, there is a decrease in the maximum deformation. It is possible that for some time the deformation increased as in the case of implantation with He^+ ions, but we did not fix this due to the too long time interval between X-ray studies.

At implantation with F^+ ions, a decrease in the maximum deformation in the case of monotonically descending profiles (at doses $\leq 2\cdot10^{13}$ cm^{-2}) and its increase in the case of nonmonotonic profiles (at higher doses of implantation) is observed.

The mechanism of diffusion in the ion-implanted layer is proposed, which determines the behavior of the distribution of deformation in the near-surface layer over time.

Effect of Annealing on the Magnetic Properties of $Y_3Fe_5O_{12}$ and $Y_{2,95}La_{0,05}Fe_{4,7}Ga_{0,3}O_{12}$ Garnet Films

Yushchuk S.I., Yuryev S.O.

Lviv Polytechnic National University, Lviv, Ukraine, s.o.yuryev@gmail.com

We have studied the effect of high-temperature (1273-1673 K) and low-temperature (523-873 K) annealing in air, O_2, and N_2 on the saturation magnetization ($4\pi M_s$) and ferromagnetic resonance linewidth (ΔH) of $Y_3Fe_5O_{12}$, and $Y_{2,95}La_{0,05}Fe_{4,7}Ga_{0,3}O_{12}$ garnet ferrite films. Films of 5-15 μm in thickness were grown on (111)- oriented gadolinium gallium garnet ($Gd_3Ga_50_{12}$) substrates through isothermal dipping of rotating substrates in a supersaturated high- temperature solution of ferrite-forming oxides in a $PbO-B_2O_3$ solvent.

It is established that the annealing of La,Ga:YIG films at temperatures 1273-1673 K in air leads to a decrease of the parameter $4\pi M_s$ and increasing ΔH. This trend increases with increasing temperature and time of annealing. The decrease of magnetization saturation apparently is related to the diffusion of ions Ga^{3+} from the transition layer of film-substrate and incorporation into the tetrahedral sites of the garnet structure. Due to the formation of Fe^{2+} and Fe^{4+} ions and diffusion across the film thickness of Gd^{3+} ions from the transition layer of film-substrate is an increase in ΔH parameter.

During high-temperature annealing of YIG films the parameter ΔH is grows and the saturation magnetization decreases slightly compared to the La,Ga:YIG. After of low temperature annealing of the $Y_3Fe_5O_{12}$ films in the temperature interval from 523 to 873 K in different gas environment, their magnetization is almost constant. It is explained by that at the low temperature annealing there is not migration of Gd^{3+} and Ga^{3+} ions in the crystalline lattice.

The low temperature annealing of $Y_3Fe_5O_{12}$ films in the N_2 atmosphere sharply increases a value of ΔH because nitrogen gas is reductant and increases the concentrations of Fe^{2+} ions in films. Isothermal holding of $Y_3Fe_5O_{12}$ films for 20 h at T=723 K in a stream of dry oxygen minimizes the number of Fe^{2+} iron and partly removes mechanical stress, which leads to decrease of the ΔH parameter at 18-25 %.

After annealing of $Y_3Fe_5O_{12}$ films at T=723 K in the stream of oxygen their spectra of magnetostatic waves represent single lines compared to the spectra of unannealed films, where there is a series of additional highs.

The annealed films were subjected to environmental tests: epitaxial ferrite structures were held for 312 h at T= 313 K in air of 95% relative humidity.

Electrosynthesis of nanostructured hard and corrosion resistant thin coatings with CoW, CoRe and CoWRe superalloys

Yapontseva Yu.S., Maltseva T.V., Kublanovsky V.S.

V.I. Vernadsky Institute of General and Inorganic Chemistry NASU, Kyiv, Ukraine,
kublan@ukr.net

The superalloys of refractory metals (W, Mo and Re) with metals of the iron subgroup have a wide range of valuable physicochemical properties, such as high corrosion resistance, hardness, abrasion and wear resistance, heat resistance, magnetic and electro-catalytic properties, and are also considered as the main alternative to electrolytic chromium [1].

Thin electrolytic coatings with CoW, CoRe and CoWRe alloys were obtained from a polyligand citrate-pyrophosphate electrolyte of the following composition, mol L^{-1}: $CoSO_4 \cdot 7H_2O$ - 0.1; $Na_2WO_4 \cdot 2H_2O$ - 0.2; $KReO_4$ - 0.01, 0.03 and 0.05; $Na_3C_6H_5O_7 \cdot 5.5H_2O$ - 0.2; $K_4P_2O_7$ - 0.2; $Na_2SO_4 \cdot 10H_2O$ - 0.3 at pH 9.0, 50 ° C and a deposition current density of 10 mA cm^{-2} on the surface of the copper substrate. The study of the corrosion properties of coatings with a thickness of 5 μm was carried out in 1.0 mol L^{-1} KOH at a temperature of 25 °C using the methods of impedance spectroscopy and voltammetry.

The Table presents the Vickers micro hardness (HV), corrosion resistance (R, R_p) determined by the methods of impedance and voltammetry, respectively.

Physical and chemical properties of electrolytic coatings with superalloys

	CoW	CoWRe			CoRe
		$[ReO_4]^-$ 0.01	0.03	0.05	
HV	493	504	636	644	841
[W], at.%	24.0	6.26	5.93	9.31	-
[Re], at.%	-	17.67	22.54	26.53	13.47
R, kOhm cm^{-2}	18.8	14.0	13.6	15.72	12.2
R_p, kOhm cm^{-2}	6.9	24.4	32.0	36.0	19.6

Experimental data allow us to conclude that the coatings obtained have a high microhardness, the value of which depends on the alloy composition. An increase in the amount of rhenium in the coating leads to an increase in its hardness. The highest corrosion resistance of ternary alloys in an alkaline medium corresponds to the highest total concentration of refractory metals.

1. Yu.S. Yapontseva, V.S. Kublanovsky, O.A. Vyshnevskyi. Electrodeposition of CoMoRe alloys from a citrate electrolyte. *Journal of Alloys and Compounds*. 2018. v. 766. p. 894-901.

Electrical Breakdown of Thin of Polytetrafluoroethylene Films Deposited by Vacuum Evaporation

Zadorozhny V.G., Polischuk S.G.

Odessa National Academy of Food Technologies, Odessa, Ukraine, aurora14@ukr.net

We investigated dependence of the electrical strength of thin polytetrafluoroethylene (PTFE) films on the current density and energy of electrons bombarding the substrate. The films have been obtained by vacuum evaporation of PTFE powder (FT-4 brand) with initiating the secondary polymerization on the substrate by electrons. The results are presented in Fig.1.

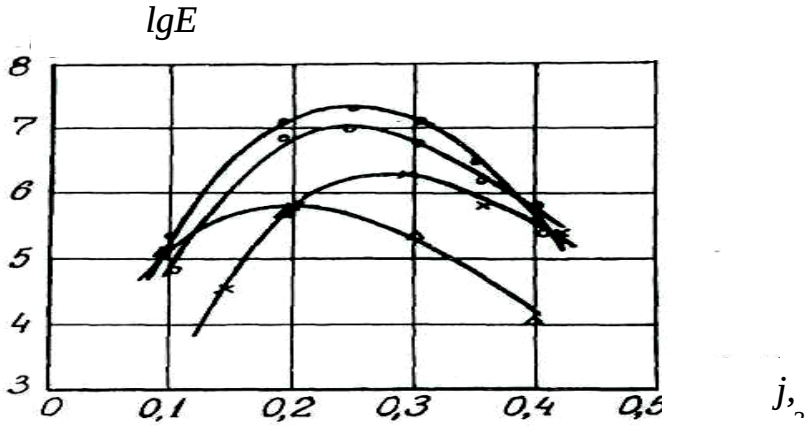

Fig.1. Dependence of electrical breakdown strength E_s of FT-4 thin films on the current density of electrons j at various electron energies: x – 100 eV; • – 400 eV; o – 400 eV + annealing; Δ – 700 eV.

As it follows from the Fig. 1, the films deposited in the best mode (j=0.25 mA cm^{-2}, E=400 eV) have the highest electrical breakdown strength. It has been found that in this mode, the obtained films had the highest molecular weight and the smallest number of pores per unit surface area. In other modes (j <0.15 mA cm^{-2}, j> 0.35 mA cm^{-2}; E <100 eV; E> 600 eV), the electrical breakdown strength of the films decreased and the breakdown strength was only equal to E_s=10^4-10^5 V/m.

While assessing the effect of the molecular weight on the dielectric strength of the polymer film, the possibility of structural changes in samples with changing the molecular weight must be also considered.

We have found that with decrease of the films thickness, the electrical breakdown strength also decreases. This feature can be associated with increase in the number of pores. After the heat treatment of the thin films in vacuum at the pressure of 10^{-3} Pa at the temperature of 250–350 °C during 1.5–2.5 hours, the electrical breakdown strength slightly increases in the films obtained under the best conditions. This is probably caused by the formation of voids at the places where evaporation of low molecular weight fractions occurs.

POSTER REPORTS
Session 4
Thin film compounds for electronic devices, nanoelectronics

Formation of Ordered Magnetic Nanoparticles Arrays Using Various Obtaining Techniques

Bezdidko O.V., Cheshko I.V., Kostiuk D.M., Protsenko S.I.

Sumy State University, Sumy, Ukraine, bezdidko.o@gmail.com

Magnetic nanoparticles (NP) are most widely used and are usually found in organic or polymeric matrices. Separately, it is worth highlighting the methods of applying nanoparticles to substrates of different types, which is an important stage in the technology of manufacturing functional elements of different nature. Nanoparticles of metal oxides (Fe_3O_4, $NiFe_2O_4$ and $CoFe_2O_4$) were obtained by the method of chemical synthesis by the authors of work [1] and used unchanged. As a method of application, the modified Langmuir - Blodgett technique, the method of simply dripping the solution of NP to the substrate surface and the method of spin coating were used. These methods obtained monolayers from nanoparticles for further introduction into the conducting matrix, and subsequent use in instrumental structures of the spin-valve type.

To study the structure of the obtained layers with NPs, we used the methods of transmission and scanning electron microscopy, as well as atomic force microscopy. The formation of a conductive matrix on top of the NP array occurred by the thermal evaporation of Cu or Ag in the vacuum chamber at a residual atmosphere pressure of 10^{-3}–10^{-4} Pa.Without annealing, the size of the nanoparticles is too small, and they are in a superparamagnetic state. The results for flow annealing temperatures were discussed in paper [2], in which it was shown that the magnetoresistance begins to manifest itself from 600 K and reaches its maximum at 1100K. Directly heat treatment leads to the enlargement of NP, which provides for an increase in the amount of magnetic material in a separate particle and, as a consequence, an increase in their magnetic moment. NPs increase in size by almost 3-4 times (from 10 nm to 40nm).

It is shown that the Langmuir – Blodgett method makes it possible to obtain the most qualitative homogeneous single and multilayers over a relatively large area of the substrate. However, it is complicated and low-productive. On the other hand, the dripping method allows to obtain single and multilayers with satisfactory parameters controlling only the concentration of nanoparticles in the final solution. Spin coating also showed the impossibility of forming uniform layers of nanoparticles, since even at low concentrations of nanoparticles, the formation of clusters of different sizes is observed. Maximum value of magnetoresistance in the conducting matrix Ag reached: Fe_3O_4 – 6%, $NiFe_2O_4$ – 10%, $CoFe_2O_4$ – 12%.

This work was done within the state project № 0117U003925 with the financial support of MES of Ukraine

1. J. Ivanco, S. Luby, M. Jergel, et al., Sensor Lett. 11 No 12, 2322 (2013)
2. S.A. Nepijko, H. J. Elmers, G. Schönhense, M. H. Demydenko, S.I. Protsenko, D. M. Kostyuk, Applied Physics A 112(2), 463 (2012)

Structures Based on Metal Nanolayers for Radiation-Resistant Hall Sensors

Bolshakova I., Vasyliev O., Guba S., Kost Ya., Radishevskyi M.

Lviv Polytechnic National University Lviv, Ukraine, gubask@polynet.ua

In modern accelerators of elementary particles (nuclear colliders, medical cyclotrons), in nuclear and thermonuclear reactors, the use of radiation-resistant, high-temperature magnetic field sensors is relevant. Radiation-resistant semiconductor Hall sensors are widely used to control the magnetic field [1]. However, their application is limited by a certain range of temperatures (2 – 500 K) and radiation loads (neutron fluences up to 10^{17} n/cm^2). In the case of application in more intense temperature and radiation fields, Hall sensors based on Al_2O_3 / Ti / Au / Al_2O_3 thin-film structures is an alternative to semiconductor Hall sensors. The maximum temperature of such a structure is limited by the diffusion of Ti from the Ti adhesion sublayer (5 nm) to the active layer of gold (35 nm), which changes the surface resistance and affects the current sensitivity of the Hall sensors. In order to reduce the influence of titanium diffusion, the influence of the Pt barrier layer (6 nm) on the high-temperature sensitivity of Hall sensors is investigated in this work.

In this paper, the stability of the electrophysical parameters of the Al_2O_3 / Ti / Pt / Au / Al_2O_3 structure in the temperature range from 300 to 573 K for neutron fluences up to 10^{19} n/cm^2 has been experimentally proved [1].

1. N. Kargin, I. Bolshakova, M. Pmlavin, Ya.Kost, T. Kuceh, S. Kulikov, F. Shurygin, M. Strikhanov, I. Vasil'vsrii, A. Vasyliev Metal Hall Sensors of DEMO Scale // Nucler Fusion. – 2016. – P. PDP-18-1– PDP-18-7

Reliability Improvement for Integrated Thin Film Bar Graph Display Devices

Bushma A.V.[1], Turukalo A.V.[2]

[1]*Borys Grinchenko Kyiv University, Ukraine, o.bushma@kubg.edu.ua,*
[2]*NUBiP of Ukraine, Kyiv, Ukraine, tyrykalo@gmail.com*

Thin film bar graph display devices are widespread in a variety of responsible industrial systems, including built-in ones. Therefore their reliability and accuracy are the most important characteristics.

This work is dedicated to a creation of the reliable integrated bar graph display device (DD) based on a microprocessor controlled thin film scale.

The information model (IM) and its software realization determine all the main technical parameters of integrated DD. Such devices implementing a bicyclic IM at the information field of a matrix of light-emitting elements have one of the best complexes of technical parameters [1]. So we form the ν-th symbol at m×m matrix from the dynamic set $\mathbf{A}_\nu$ of elements a_{xy} as

$$A_\nu^D = \left\{ \mathop{\mathbf{U}}_{y=1}^{\nu-m\,\nu^*} \left[\mathop{\mathbf{U}}_{x=1}^{\nu^*+1} a_{xy} \Big|_{t=t_1} \right] \right\} \mathbf{U} \left\{ \mathop{\mathbf{U}}_{y=\nu-m\nu^*+1}^{m} \left[\mathop{\mathbf{U}}_{x=1}^{\nu^*} a_{xy} \Big|_{t=t_2} \right] \right\},$$

where $n^* = E\left(\frac{\nu}{m}\right)$, E(z) – Entier of z.

The main part of realization of the DD is software algorithm for microcontroller, which is presented at the figure. The DD receives the data to be displayed (1). After that the data processing divides into 2 directions (2): corresponding to the first t_1 (Y) and the second t_2 (N) cycles. Blocks 3, 8 switch off and 7, 12 ones switch on the scale excitation. Further we form the excitation signals at the x-lines (4, 5 and 9, 10) and at y-lines (6 and 11) of the matrix. Block 13 changes the synthesized image only after the procedure is completed. At the end we change the number of next cycle (14). The data image is synthesized by interrupt system in two cycles with a frequency above 50 Hz.

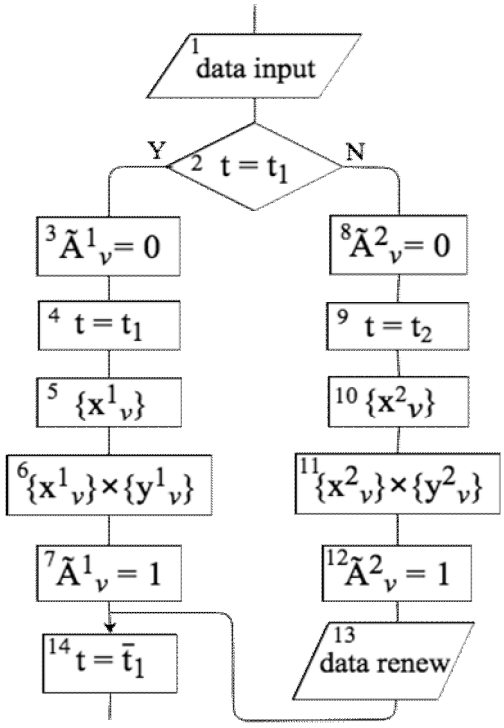

1. Bushma A. V. Matrix models of bar graph data display for bicyclic excitation of the optoelectronic scale // Semiconductor physics, quantum electronics and optoelectronics. 2008. V.11, N2. – P. 188-195.

Resistance Switching in Ni-NiO_x-Si Structures

Ievtukh V.A.[1], Rusavsky A.V.[1], Khyzhun O.Yu.[2], Nazarov A.N.[1]

[1] *Lashkaryov Institute of Semiconductor Physics NAS of Ukraine, Kyiv Ukraine*
[2] *Frantsevych Institute for Problems of Materials Science NAS of Ukraine, Kyiv, Ukraine, nazarov@lab15.kiev.ua*

Binary transition metal oxides like NiO, TiO_2, and ZnO are very attractive for their employment in the field of resistive switching due to low deposition temperature and compatibility with complementary metal-oxide semiconductor (CMOS) technology. It should be noted that different resistive switching behaviors, such as unipolar, bipolar and threshold resistive switching, have been found in metal/NiO/metal structures [1]. In the same time the metal/NiO/Si structure was not sufficiently studied for resistance memory application while it is a most suitable structure for CMOS technology.

In this work we study formation of the threshold resistance memory effect in Ni/NiO_X/n-Si structures there the NiO_X film was synthesized by reactive RF magnetron sputtering of Ni target in O_2+Ar gas mixture. Concentration of O_2 in the gas mixture was changed from 6% to 20%. Chemical composition of the deposited NiO_X film was determined by XPS technique. Electrical properties were studied by I-V and C-V characteristics.

It was shown that increase of oxygen concentration in the gas mixture resulted in increase of Ni^{3+} concentration, reduction of dielectric constant of fabrication film and hysteresis formation in the high-frequency C-V characteristic. In the same time threshold resistance switching was observed in NiO_X film fabricated with low oxygen concentration. Study of C-V characteristics changing during the threshold resistance switching formation shows considerable increase of dielectric constant after implementation of high current condition. Nature of threshold resistance switching is discussed.

1. Yuan X.-C., Tang J.-L., Zeng H.-Z., Wei X.-H. Abnormal coexistence of unipolar, bipolar, and threshold resistive switching in an Al/NiO/ITO structure. *Nanoscale Research Letters*. 2014, V.9. P. 268-1-5.

Excess minority carrier concentration in macroporous silicon with various arrangements of macropores

Karachevtseva L.A., Onyshchenko V.F., Karas' M.I.

V. Lashkaryov Institute of Semiconductor Physics NAS of Ukraine, Kyiv, Ukraine,
onyshchenkovf@isp.kiev.ua

Macroporous silicon structures with a periodic arrangement of macropores in the form of a quadrangular and triangular lattice with a volume fraction of macropores of 0.2 [1] are investigated. When the distance between the edges of macropores greater than 5 microns the dependence shown in Figure decreases, because the increasing a role played by the bulk lifetime of excess minority carriers. The concentration of excess minority carriers does not depend on the placement of macropores, if the distance between the edges of macropores equal to the diffusion length. When the distances between the edges of macropores less than 0.1 μm the difference in relative equilibrium concentration decreases and comes nearer to 0.01. At this distance, the main role is played by the surface recombination velocity at the surface macropores and not placing macropores.

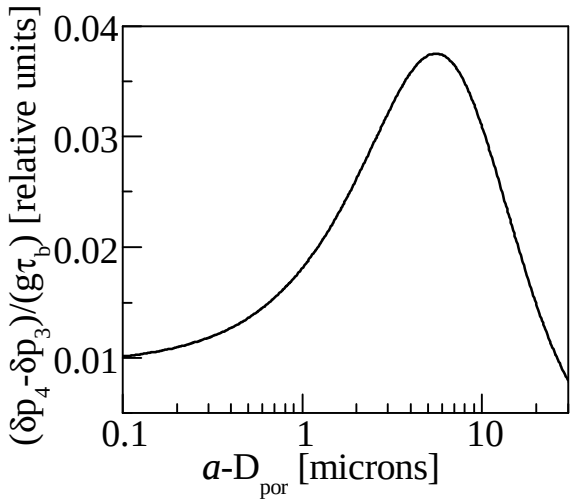

Fig. The concentration ratio of excess minority carriers in macroporous silicon with periodically arranged macropores in the form of quadrangular Δp_4 and triangular Δp_3 lattice depending on the distance between the edges of pores.

It was found that the difference between the relative concentration of excess minority carriers in macroporous silicon structures with a periodic arrangement of macropores in the form of a quadrangular and triangular lattice depends on the distance between the edges of macropores and has a maximum at 5 microns. The concentration of excess minority carriers does not depend on the placement of macropores, if the distance between the edges of macropores is greater than the diffusion length and less than 0.1 microns.

1. Karachevtseva L.A., Onyshchenko V.F. Relaxation of excess minority carrier distribution in macroporous silicon. *Chemistry, Physics and Technology of Surface*. 2018. V. 9, N 2. – P. 158-166.

Influence of Electromagnetic Impulses on the Electric Processes in the Telluride Cadmium Film Layers

Khrypunov M.G., Rezinkin O.L., Nikitin V., Drozdov A.N., Meriuts A.V., Khrypunova A.L., Kudii D.A.

National Technical University "Kharkiv Polytechnic Institute", Kharkiv, Ukraine
lauman@ukr.net ; klochko.np16@gmail.com

Under actual operating conditions of electronic equipment, various types of electrical overloads can occur in its circuits. The most dangerous are overvoltage caused by electromagnetic impulses. This determines the relevance of the development of instrument structures for active protection. Such structures include transient voltage stressor diodes (TVS –diodes), which have a pronounced nonlinear current-voltage characteristic (CVC), which limits the voltage surge to safe. One of the main advantages of TVS-diodes is high speed (no more than 5 ns).

In this paper, we consider the possibility of using device structures with a nonlinear CVC based on CdTe film layers as impulse overvoltage protection devices. Cadmium telluride film layers with a thickness of 5–7 μm were formed on molybdenum foil, by thermal vacuum evaporation from a graphite crucible. The fabricated film samples were exposed to voltage impulses (U_{max}) of 23V, 46V, 76 V in frequency (10 Hz) mode and single impulse mode.

It was established experimentally that the volt-time characteristic of the instrument structures with the base layer of cadmium telluride has four distinct time intervals: I interval corresponds to the time of voltage rise on the sample, II - time of rapid decrease, III - time of slow voltage decrease, IV - asymptotic decrease period (50 ns after operation) to some residual voltage (U_{fin}). It was found that the manufactured protection elements are triggered at voltages at the level of 1/3 of the applied impulse value. The timing of the operation depends on the magnitude of the electrical voltage of the applied impulse. With an increase in the applied overvoltage impulse, the time of rapid decline decreases and the relaxation time increases. When exposed to voltage impulses 46V, the average rise time of the voltage to the maximum (I-segment) on the sample is 2.6 ns and is determined by the steepness of the «load» impulse. The average time for the rapid voltage decreases (II section) to a value of 0.25 U_{max} is 2.7 ns. The average relaxation time (III segment) to $2U_{fin}$ is 7.2 ns. The residual voltage after 50 ns after operation is U_{fin} = 1.5 V for all samples.

Thus, experimental studies of fabricated device structures based on film layers of cadmium telluride showed that when exposed to electromagnetic impulses, they limit the voltage in the circuit due to the recovered sharp decrease in the electrical resistance of the operating layer. At the same time, in comparison with industrial samples of TVS – diodes, fabricated structures based on film layers of cadmium telluride have a simpler cost-effective design and have almost the same speed.

Layouts Design Features of Matrix Elements with “Kink-Effect” Control for Microsystems-on-Chip

Kogut I.T., Dovhyi V.V., Benko T.H.

Vasyl Stefanyk Precarpathian University
Ivano-Frankivsk, Ukraine, igorkohut2202@gmail.com

In this paper the results of the layouts design optimized cell for matrix use in microsystems-on-chip are presented. A layouts feature of the matrix elements are additional contacts to the sub-channel areas of the SOI MOS-transistors for the "kink-effect" control and the use of a controlled bipolar effect for expanding the functionality of circuits and the creation of new circuit design solutions [1] (Fig. 1).

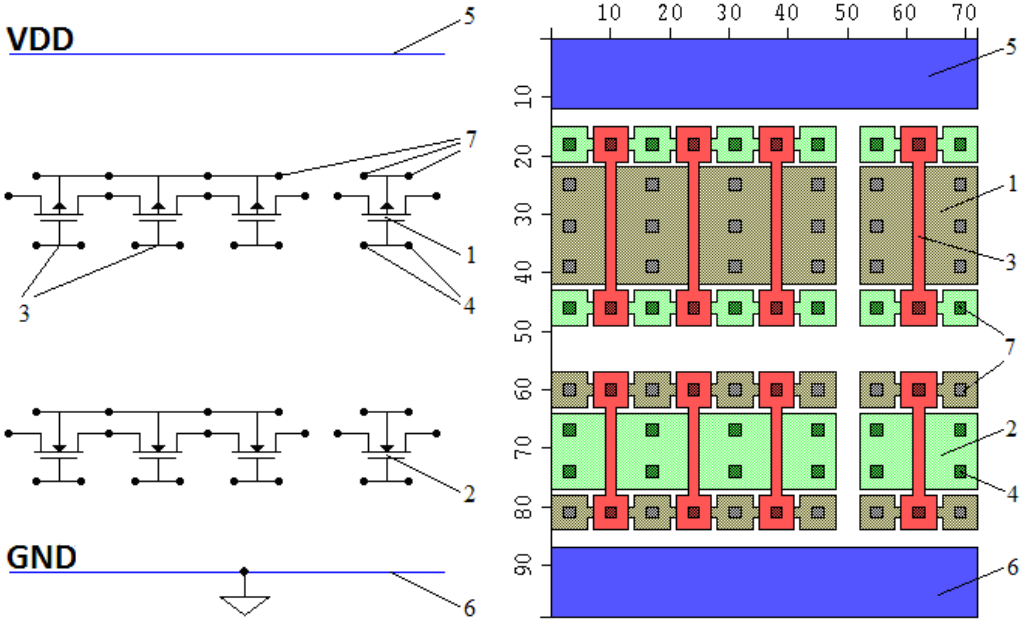

a) b)

Fig. 1. Electrical circuit (a) and layouts (b) of a matrix cell with contacts to subchannel areas for the dual control in the SOI MOS-transistors: 1, 2 - source/drain areas of the p- and n-type; 3 - polysilicon gates; 4 - contacts; 5, 6 - power and ground lines; 7 - contacts to subchannel areas of SOI MOS-transistors

The proposed matrix cell with CMOS SOI-structures and gate arrays based on it have improved frequency and electrical characteristics, high density of elements on the chip, high coefficient of transistors usage and improved commutation capabilities.

1. Druzhinin A. Electrical and layouts simulation of analytical microsystem-on-chip elements for high frequence and low temperature applications / A. Druzhinin, Y. Khoverko, V. Dovhij, I. Kogut, V. Holota // UkrMiCo’2016. – Kyiv, 2016. – P. 29-32.

The Simulation of Integrated Capasitive SOI Elements for Sensor Microsystem-on-Chip

Kogut I.T., Holota V.I., Gryga V.M., Benko T.H.

Vasyl Stefanyk Precarpathian University
Ivano-Frankivsk, Ukraine, igorkohut2202@gmail.com

The important components of the microsystems-on-chip (MSoC) sensory or analytic types are integral sensor capacitive element (SE). Such SEs can be used in studies as external influences, for example, deformations, changes in pressure, temperature, humidity, and the construction of capacitive type SEs required in the research of new structural materials for monolithic integration in MsoC, as well as biomedical research with the registration of quantities or types of biomolecules charges, effects of light, etc. In this case, CEs should have high sensitivity to very small capacitance changes.

To register changes in capacities under the influence of external factors, a scheme of the SE was developed based on the integral SOI CMOS transistor and capacitive structures (Fig. 1.). Their simulation was carried out to evaluate the sensitivity parameters and change the parameters of the response signals.

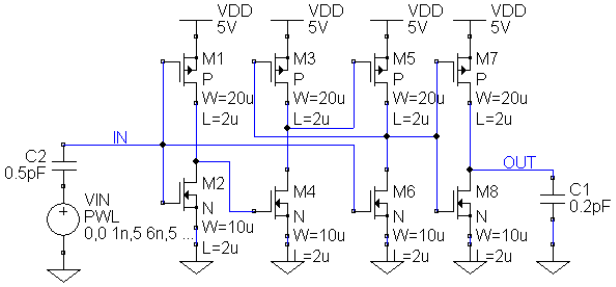

Fig.1 Functional scheme of registration of small capacity changes registration in MSoC with the SOI structure (one channel).

By the integral structure, sensitive capacitive SEs (C2) are in fact an extended gate of the input transistors M1 and M2 and can be made on the basis of thin films, in particular, polysilicon on insulator, monocrystalline silicon films, monocrystalline silicon films with SOI structures, films of metal-insulator-polysilicon, the SOI MOS-transistor structures in which capicitors are formed between the gate of the transistor and the connected areas of the source and drain or gate and the conducting channel of the transistor and other types.

Depending on the purpose of the topology of capacitive CEs, they can be formed with standard flat surfaces or in the form of combing capacitors with the formation of sensitive capacities on their vertical walls, moving beams, etc. For different intervals of measured capacitance values, it is expedient to have multichannel circuits that differ in the topological sizes of the channels of the input transistors and, accordingly, the initial capacity of the extended electrode.

Capacitive SEs on the basis of such films can be formed as elements of MSoC, in particular on the surface of a special technological area covered with silicon oxide or integrated on the surface of the membrane or made as moving beams. For the schemes of initial processing of information, their implementation in the matrix part of the MSoC on the base cells is optimal.

Microsystem-on-Chip SOI Elements Based on Control Integrated Generators

Kogut I.T.[1], Kotyk M.V.[1], Dolishnyak O.I.[2]

[1] *Vasyl Stefanyk Precarpathian University*
[2] *Ivano-Frankivsk National Medical University, Ivano-Frankivsk, Ukraine,*
igorkohut2202@gmail.com

Important elements of signal transmission paths in microsystems-on-chip (MSoC) are monolithically-integrated signal generators (SG). The schemes of the integrated SG were proposed, in which as the frequency-setting elements CMOS transistors with the corresponding inclusion were used. The electrical scheme of such generator with a controlling n-channel transistor is shown in Fig. 1,a. During the simulation geometric dimensions of the transistor M13 were changed: the channel width from 12 to 96 μm and the length of the channel was constant - 2 μm. Such generator can be used as an element of MSoC for the construction of electronic biomedical devices for non-invasive measurements of blood glucose levels [1]. The results of simulations of the generator with different sizes of the control n-channel transistor are shown in Fig. 1, b, c.

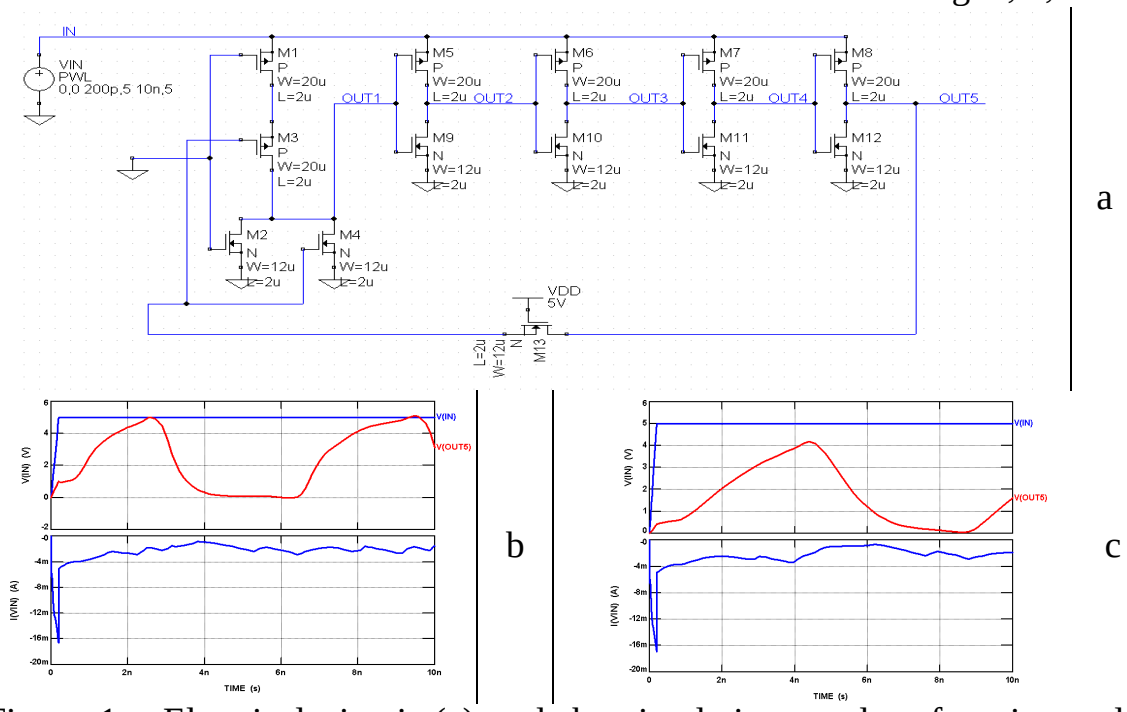

Figure 1 - Electrical circuit (a) and the simulation results of an integral generator with different sizes of the control n-channel transistor (b)W=12u, L=2u, (c) W=96u, L=2u

Simulation results of the generator using the control n-channel SOI MOS transistor is found that dimensions increase the ratio of the W/L transistor pulse amplitude decreases, and with the decrease - respectively, increases.

1. Simulation of system-on-chip elements with the SOI-structures for non-invasive blood glucose meters / M. Kotyk, I. Kogut, V. Holota, V. Dovhyi // Information Technology in Selected Areas of Management, Wydawnictwa AGH, Krakow 2018, p.81-88.

Effects of Weak Localization and Spin-Orbital Interaction in Films Based on PbSnAgTe Compounds

Kostyuk O.B. [1], Dzundza B.S. [1], Yavorskyi Ya.S. [1], Makovyshyn V.I. [2]

[1]*Vasyl Stefanyk Precarpathian National University, Ivano-Frankivsk, Ukraine,*
oksanakostuk@gmail.com
[2]*Ivano-Frankivsk National Medical University, Ivano-Frankivsk, Ukraine*

Semiconductor materials are often used to study ballistic effects, due to high dielectric permeability and low effective mass. In particular, for PbTe $\varepsilon = 1350$ at 4.2 K and $m^* = 0.024m_0$, which results in effective shielding from ionized impurities and defects. Therefore, there is the prospect of using PbTe in a new industry - spintronics, for example, as a spin filter.

In this paper, the experimental dependences of the magnetoresistance of PbSnAgTe films on the composition in a magnetic field perpendicular to the surface of the film are obtained. Their explanations are analyzed based on the theory of quantum corrections to conductivity. It should be noted that doping by Sn in the investigated compositions significantly changes the electrical properties, as well as the type of conductivity.

The dependences of the magnetoresistance of PbSnAgTe films in magnetic field perpendicular to the surface of the film are explained in the framework of the theory of weak localization, taking into account the mechanism of spin-orbit scattering. The curves of the magnetic-field conductivity or resistance dependence allow to determine the peculiarities of the transport of carriers in a magnetic field and to obtain information about the presence of spin-orbit interaction. Observed quantum interference effects in PbSnAgTe films can be explained by spin-orbital interaction in scattering on impurities, on the surface of the films and at grain boundaries. It is shown that for polycrystalline films on mica-muscovite substrates, the time of spin-orbital interaction depends on the composition and may change the sign of the magnetoresistance.

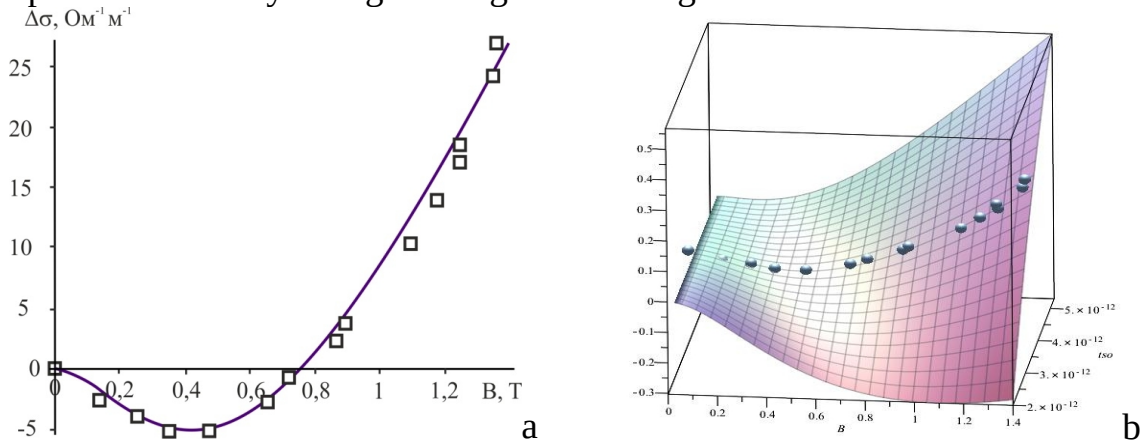

Figure 1. The dependence of the specific magnetic conductivity (a) and the theoretical 3d surface (b) for the film $Pb_{14}Sn_4Ag_2Te_{20}$ (d=54 nm, T=300 K).

Electronic Structure of ZnO Thin Films Doped with Group III Elements

Kovalenko M.V., Bovgyra O.V., Franiv A.V., Dzikovskyi V.Ye.

Faculty of Physics, Ivan Franko National University of Lviv, Lviv, Ukraine, mariya.kovalenko@lnu.edu.ua

There exists a great interest in zinc oxide (ZnO) materials because of their usefulness in a wide range of high technology applications, low cost, resource availability, non-toxicity and very high thermal/chemical stability. ZnO-based materials have considerable potential in transparent conductive oxides (TCOs) due to their wide band gap (3.37 eV) and transparency under visible light. A number of typical dopant elements such as F, B, Al, Ga, In and Sn have been used so far to produce conducting ZnO films.

In the present work, we tried to clarify the behaviors of dopant III group elements by the electronic structure calculations of the doped ZnO thin films by various concentrations of dopant atoms. This study performed the first principle calculations using pseudopotential method, within density functional theory (DFT). For more accurately description of the electronic structures, we adopted the DFT + U_d + U_p method. To calculate various concentrations of doped atoms, we considered 2×2×2 and 3×3×2 supercells in which one Zn atom is substituted with one dopant atom, corresponding to doping levels of 6 and 3%, respectively. We adopted boron (B), aluminum (Al), gallium (Ga), indium (In), yttrium (Y), scandium (Sc), and lanthanum (La) as substitution elements to Zn. Electron-ion interactions were modeled using ultrasoft pseudopotentials in the Vanderbilt form. The wave functions of the valence electrons were expanded through a plane wave basis-set and accurate Brillouin zone integration was performed via careful sampling of k points chosen according to the Monkhorst-Pack scheme. The energy cutoff of plane wave functions was set at 400 eV.

The calculated fundamental band gap and the lattice parameters of pure ZnO are close to the experimental ones and in a good agreement with other theoretical calculations. The calculated results show that calculated results show that the lattice parameters increase with the increase of dopant concentration. We found that the optical band gap of all III elements-doped ZnO thin films increase with an increase in dopant content, which leads to a blue shift of the optical edge absorption. The Fermi level of doping ZnO thin films shifts upward into conduction band, showing the properties of n-type semiconductor. The results are helpful to gain a systematic understanding of structure, and electronic properties of doped ZnO thin films with group III elements.

Magnetic Anisotropy Control Via Oxygen Plasma Irradiation and Magnetization Dynamics in Pt/Cofeb/Mgo System

Lytvynenko Ya.M.

Sumy State University, Sumy, Ukraine, y.lytvynenko@ssu.edu.ua

Current induced spin-orbit torques (SOTs) [1-3] in trilayer heterostructures, where ultrathin ferromagnetic layer (FM) is placed between a heavy metal (HM) with high spin-orbit coupling, such as Ta, W, Pd or Pt, [2,3] and a metal oxide have received considerable research interest for local electrical manipulation of the magnetization in metallic ferromagnets that have potential applications in spintronic devices with ultra-low energy consumption, high speed and almost unlimited endurance [1-4]. Thus, understanding the underlying physics of spin-orbit driven phenomena as well as different ways of anisotropy tuning in HM/FM/Oxide structures is essential in developing new generation memory and logic devices.

In this study, we examine SOT generated in a perpendicularly magnetized (PMA) Pt(2) / CoFeB(0 - 2) / MgO(2) trilayers with as-deposited and over oxidized in Oxygen plasma MgO layer with following UV-lithography patterning into Hall bar structures (where the numbers in parentheses are the thicknesses in nanometers). As it is well-known that the PMA originates from the Fe-O hybridization between ferromagnetic CoFeB and insulator MgO layers the oxidation process of top layer allows to control the Oxygen content at the CoFeB/ MgO interface and therefore tune magnetic anisotropy. Further we will discuss an experimentally study of the SOT-induced effective field dependence on varying PMA performed by harmonic Hall technique [5].

1. Brataas A. Current-induced torques in magnetic materials / A. Brataas, A. D. Kent, H. Ohno // Nature Materials. -2012. – V.11. -P.372-381.
2. Kim J. Layer thickness dependence of the current-induced effective field vector in Ta/CoFeB/MgO / J. Kim, J. Sinha, M. Hayashi et al. // Nature Materials. – 2013. – Vol.12. – P. 240-245.
3. Miron I. M. Perpendicular switching of a single ferromagnetic layer induced by in-plane current injection / I.M. Miron, K. Garello, G. Gaudin et al. // Nature. – 2011. – Vol. 476. – P.189-194.
4. Tacchi S. Interfacial Dzyaloshinskii-Moriya interaction in Pt/CoFeB films: effect of the heavy-metal thickness / S. Tacchi, R.E. Troncoso, M.Gubbiotti et al. // Physical Review Letters. – 2017. – Vol.118. – P.147201(1-6).
5. Hayashi M. Quantitative characterization of the spin-orbit torque using harmonic Hall voltage measurements / M. Hayashi, J. Kim, M.Yamanouchi, H. Ohno // Physical Review B. – 2014. – Vol. 89. – P. 144425(1-15).

Optical and Photovoltaic Properties of Nanocomposite Based on Porous Silicon

Mamykin S.V., Kotova N.V., Barlas T.R., Kondratenko O.S., Mamontova I.B., Romanyuk V.R., Smertenko P.S., Roshchina N.M.

V.E. Lashkaryov Institute of Semiconductor Physics National Academy of Sciences of Ukraine Kyiv, Ukraine, mamykin@isp.kiev.ua

The method of porous silicon formation (Si) based on metal-assisted catalyzed etching (MACE) was proposed for photovoltaic and optoelectronic applications [1]. MACE fabricated Si nanorelief provide improved antireflection functionality due to multiple reflection, light trapping and effective absorption of light incident on the surface with vertical pores compared to the traditional technique of surface texturisation [2] and can be the basis for organic/inorganic nanocomposites for the photovoltaic applications. The regular texturisation of pyramidal type on Si and heterojunction organic (clonidine)/Si demonstrates the energy conversion efficiency 8% due to incorporation of the functional groups of heteroatom aromatic drugs into the Si patterned [3]. Therefore there is an interest to increase the conversion efficiency by new type of texturisation and metal plasmon-active nanoparticles incorporated into the nanocomposite on the basis porous Si and clonidine.

Nanocomposites based on nanostructured (“black”) silicon, clonidine and Au nanoparticles have been made. Solar cells were fabricated on the basis of such nanocomposites. Polished *n*-type Si (100) with 0.5-2.4 Ohm·cm resistivity has been used as substrate. The optical properties of the nanocomposite modelled very well in the frame of effective medium approximation theory. The reflection spectra of light confirmed the excitation of the plasmon mode in nanocomposites with Au nanoparticles. Current-voltage characteristics in the dark and under AM0 illumination have been measured. Compared to the flat polished Si with clonidine the addition of Au nanoparticles increases photocurrent in 5.5 times. Joint effect of Au nanoparticles and “black” Si increases the photocurrent about 8 times.

1. Le Gall S., Lachaume R., Torralba E., et al. Advances in silicon surface texturization by metal assisted chemical etching for photovoltaic applications. *IEEE 44th Photovoltaic Specialists Conference (PVSC)*. 2017, Washington, USA. (http://www.ieee-pvsc.org/PVSC44/. hal-01579151).
2. Toor F., Miller J.B., Davidson L.M. Metal assisted catalyzed etched (MACE) black Si: optics and device physics. *Nanoscale*. 2016. V. **8**. P. 15448-15466.
3. Gorbach T.Ya., Smertenko P., Venger E. Investigation of photovoltaic and optical properties of self-organized organic-inorganic hybrids using aromatic drugs and patterned silicon. *Ukrainian Physical Journal*. 2014. V. 59, No. 6. P. 601-611.

Effect of porous layer thickness on photoconductivity relaxation time in macroporous silicon

Onyshchenko V.F., Karachevtseva L.A., Karas' M.I.

V. Lashkaryov Institute of Semiconductor Physics NAS of Ukraine, Kyiv, Ukraine,
onyshchenkovf@isp.kiev.ua

Macroporous silicon has found application in sensors, receivers, integrated microchips and solar cells. One of the main characteristics of a photodetector is the effective lifetime of minority charge carriers and photoconductivity [1].

The photoconductivity relaxation time in macroporous silicon with and without the substrate was found from the diffusion equation of minority charge carriers. The solution of the diffusion equation written for a macroporous layer and a single-crystal substrate is complemented by boundary conditions on the surfaces of the sample of macroporous silicon and on the boundary between the macroporous layer and the single-crystal substrate.

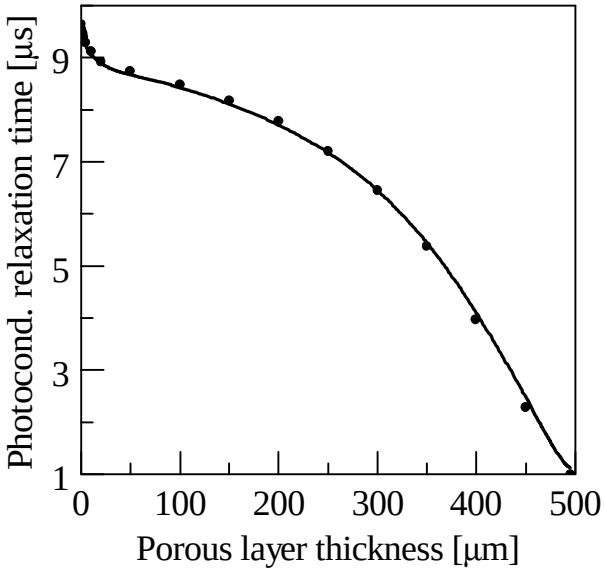

Fig. The dependence of photoconductivity relaxation time in macroporous silicon on porous layer thickness is shown as a solid line. Circles show numerical calculations of photoconductivity relaxation time.

The relaxation of photoconductivity is determined by the recombination of excess charge carriers on the pore surface and is limited by the diffusion of charge carriers from the substrate into the recombination surfaces. The photoconductivity relaxation time in macroporous silicon depends on such values as: volume lifetime of minority charge carriers, charge carrier diffusion coefficient, substrate thickness, average macropore diameter, average distance between macropore centers, surface recombination rate

1. Karachevtseva L.A., Onyshchenko V.F. Relaxation of excess minority carrier distribution in macroporous silicon. *Chemistry, Physics and Technology of Surface*. 2018. V. 9, N 2. – P. 158-166.

Photosensitive Heterojunction Prepared by Spray-Pyrolysis *n*-SnS_2 Thin Films

Orletskyi I.G., Kuryshchuk S.I., Maryanchuk P.D.

Chernivtsi National University,Chernivtsi, Ukraine, i.orletskyi@chnu.edu.ua

Indium selenide has the band gap width E_g = 1.2 eV, which is close to the optimum values for the photoelectric conversion of solar energy on earth. The crystal structure InSe is characterized by a weak Van der Waals bond between layers. It allows to receive substrates for heterostructures without operations of cutting of ingots, mechanical and chemical processing of a surface. When using indium selenide as a base material, photosensitive structures are formed on the basis of heterojunctions [1].

The photosensitive heterojunctions of *n*-SnS_2/*p*-InSe are prepared by the method of spray-pyrolysis of SnS_2 thin films [2] on heated surfaces of *p*-InSe plates. The electrical properties of the heterostructures are determined by the energy barrier $q\varphi_k$ = 0.61 eV (at T = 293 K) for the charge carriers in the conduction band at the edge of the heterojunction. Due to the difference in the electron affinity SnS_2 and InSe materials, the total barrier height is greater than the contact potential difference by 0.3 eV.

At direct bias up to 0.15 V, the current through the heterojunction proceeds as a result of recombination in the contact area from the side of *p*-InSe. At direct voltages V > 0.15 B, the mechanism of the current is the tunneling of electrons in the valence band of *p*-InSe from the traps at the boundary of the heterojunction. The reverse current is formed by the tunneling of electrons from the energy levels in the space charge region of the band gap *p*-InSe.

The spectrum of quantum efficiency of *n*-SnS_2/*p*-InSe heterostructures covers the energy range 1.2 - 3.1 eV. The long-wave edge of photosensitivity is observed at a quantum energy of 1.2 eV and is due to the edge of fundamental absorption in *p*-InSe. At a radiation energy of ~ 2.8 eV, the photoelectricity of nonequilibrium charge carriers is concentrated in a SnS_2 film. For irradiation of quantum energies $h\nu$ > 2.8 eV, the region of generation of electron-hole pairs approaches the frontal surface of SnS_2. Heterostructures *n*-SnS_2/*p*-InSe are perspective as photodetectors of radiation energy, subject to improvement by reducing the successive resistance.

1. I.G. Orletsky, M.I. Ilashchuk, V.V. Brus, P.D. Marianchuk, M.M. Solovan, Z.D. Kovalyuk, Electrical and Photoelectric Properties of the TiN/p-InSe Heterojunction, Semiconductors. 50 (2016) 334–338.
2. I.G. Orletskii, P.D. Maryanchuk, E.V. Maistruk, M.N. Solovan, D.P. Koziarskyi, V.V. Brus, Modification of the properties of tin sulfide films grown by spray pyrolysis, Inorganic Materials. 52 (2016) 851–857.

High Resolution Registered Media

Stetsun A.I.

Frantsevich Institute for Problems of Materials Science of NASU,
3 Krzhyzhanovsky Str., Kyiv, 03680, Ukraine, stetsun387@gmail.com

Important aspect of modern optics and solid state physics is construction of new sorts recording media with high resolution.

The heterostructures based on mixed ion-electron (hole) conductor can be used as a registered media for optical information recording [1, 2]. Such heterostructures are formed by two films or few films deposited on each other upper glass substrate. Main film is film of solid electrolyte with mixed ion-electron (hole) conductivity. The film of other material should provide photo e. m. f. generation at contact with film of solid electrolyte during illumination. Therefore these other films may be by photovoltaic materials, usual semiconductors, dielectrics, metals. When the heterostructures is illuminated by light then photo e. m. f. generates. The electric field appears in the heterostructure. This electric field forces of ions to move at interface of materials which are formed the heterojunction. Opposite direction moving ions to free surface of solid electrolyte film is possible, too. Owing to such action of electric field of photo e. m. f. the distribution of ions at thickness of solid electrolyte layer is changed. Thus photo-stimulated ion transfer takes place. If ions have come to interface or free surface then ions may be deposited as clusters. The size of such clusters may be from few tens of microns to one atom. This depends from concentration of ions in solid electrolyte and thickness of the film. Such physical phenomena can be used for optical information recording. Minimal size of photodeposited structure equal one atom or one ion. This just determine the resolving ability of such registered media.

1. A.I. Stetsun, 2002, Patent of Ukraine №73537.
2. A.I. Stetsun, Photodeposition of silver at the interface of heterojunction based on a solid electrolyte: the case of CdSe-As_2Se_3:Ag_x (x=0.9-2.4)//Semiconductors.-2003.-Vol. 37, №10.-p.1169-1176.

Investigation of the Interface of the $Y_3Fe_5O_{12}/Gd_3Ga_5O_{12}$ Structure, Obtained by the Liquid Phase Epitaxy

Sugak D.[1,2], Syvorotka I.I.[1,2], Yakhnevych U.[1*], Zhydachevskyy Ya.[1,3], Pieniążek A.[3], Włodarczyk D.[3], Buryy O.[1], Ubizskii S.[1], Suchocki A.[3,4]

[1] *Lviv Polytechnic National University, Lviv, Ukraine*
[2] *Scientific Research Company "Electron-Carat", Lviv, Ukraine*
[3] *Institute of Physics PAS, Warsaw, Poland*
[4] *Institute of Physics, Kazimierz Wielki University, Bydgoszcz, Poland*
[*] *Corresponding author: yakhnevych.u@gmail.com*

The liquid-phase epitaxy of single crystalline layers with the garnet structure is one of the most widely used technologies for obtaining functional materials of spin-wave- and magneto-electronics, integrated and magneto-optics, scintillation techniques, etc. The presence of defects in the epitaxial layers is often a determining factor in their ability to provide a necessary functionality. In particular, structural defects lead to unwanted dissipation of the energy of electromagnetic waves in layers based on $Y_3Fe_5O_{12}$ (YIG) grown on a $Gd_3Ga_5O_{12}$ substrate (GGG). One of the main sources and outlets of defects (point, linear, volume) is the interface between the functional epitaxial layer and its substrate.

The purpose of this work was to study the properties changes of YIG/GGG epitaxial structure by probing the interface area in its cross section. Because of the thickness of the standard substrate is 0.5 mm and the net thickness of the structure does not exceed usually 1 mm, to perform our study a layer of YIG of 160 μm thickness was grown on the 7 mm GGG thick substrate and a plate of 1 mm thickness was cut from it in the perpendicular to the grown layer direction. The surfaces of the plate were polished. Then the study of changes in properties in the interface from the substrate to the epitaxial layer was carried out using micro Raman spectroscopy (changes in the structure), electron probe micro-analysis (changes in the chemical composition) and optical spectrophotometry (changes in absorption spectra). The observed interface thickness was different in different methods, which may be due to variation of their sensitivity and space resolution. In particular, according to the results of optical studies, the value of absorption induced by iron ions varies from the maximum value in the epitaxial layer to the minimum in the substrate at a distance of about 20 microns, whereas this distance is about 10 microns from the data of the electron probe micro-analysis. The nature of the observed properties changes in the interface area of the YIG/GGG structure is discussed.

Acknowledgements: the work was supported by the Ministry of Education and Science of Ukraine (project DB/Mezha no. 0118U000273) and by the Polish National Science Center (project 2015/17/B/ST5/01658).

Electrical and Luminescence Properties of Ultraviolet LEDs 365 – 400 nm

Veleschuk V.P.[1], Vlasenko A.I.[1], Vlasenko Z.K.[1], Shynkarenko V.V.[1], Kudryk Ya.Ya.[1], Borshch V.V.[2], Borshch O.B.[2], Shefer A.V.[2], Kisselyuk M.P.[3]

[1]*V.E. Lashkaryov Institute of Semiconductor Physics of the NAS of Ukraine, Kyiv,* *vvvit@ukr.net*

[2]*Poltava National Technical Yuri Kondratyuk University, Poltava*

[3]*Podilsky Special Educational-Rehabilitation Socio-Economic College Kamianets-Podilskyi.*

Unlike ordinary LEDs of the visible radiation, ultraviolet (UV) InGaN/AlGaN/GaN LEDs at wavelength λ from 365 to 400 nm have a wide range of applications: in industry, medicine, biology, science, etc., and are replacing the UV sources – lamps. The main problem of UV LEDs 365 – 400 nm are decrease the intensity of radiation and operation time at the transition to the shorter- wavelength area – from 400 to 365 nm. Also are undesirable tunneling effects and yellow electroluminescence (EL) from defects [1].

The industrial InGaN/AlGaN/GaN UV LEDs on the Al_2O_3 and Si substrate are investigated. Nominal current I = 350..500 mA, electric power P_{el} = 1..2 W, area of structure 1143x1143 μm^2. The change of λ is achieved by changing the Indium content in the $In_xGa_{1-x}N$ quantum well.

It is established that with increase the quantum well bandgap of UV LED (λ from 400 to 365 nm), the relative and absolute contribution of the parasitic visible (yellow) EL and the current of non-radiation recombination increases.

The analysis of the Capacitance-Voltage characteristics of UV LEDs 365, 375, 385, 390, 395, and 400 nm showed that the active area of such industrial LEDs contains one quantum well. The relationship between the Capacitance-Voltage and the EL intensity of UV band was not detected, capacitance has a significant spread.

Current-voltage characteristic with negative differential resistance region of UV LEDs was observed at liquid nitrogen temperature. The *S*-shaped curves were obtained due to the transition from single injection (electrons) to double (electrons and holes) injection.

Acknowledgements – This work was supported by the State Fund for Fundamental Researches of Ukraine.

1. V.P. Veleschuk, A.I. Vlasenko, Z.K. Vlasenko, D.N. Khmil' etc. Visible Luminescence of the InGaN/GaN Ultraviolet Light-emitting Diodes 365 nm // Journal of Nano- and Electronic Physics (2017) **9**, № 5, 05031(5). DOI: 10.21272/jnep.9(5).05031.

CdTe Thin Films as Passivation to CdHgTe Photodiodes

Vuichyk M.V., Svezhentsova K.V., Tsybrii Z.F.

V.Ye. Lashkarev Institute of Semiconductor Physics of NAS of Ukraine, Kyiv, vuychik@isp.kiev.ua

Due to the narrow bandgap of CdHgTe, the device characteristics are largely influenced by the properties of the semiconductor surface and interfaces. Therefore, it is very important to create correct protective passivation layer for obtaining high-quality photodiodes based on CdHgTe. The requirements for passivation layers are predefined by design of the device. Fixed charges in the passivation layer can cause accumulation, depletion or inversion of CdHgTe and as a result increase surface leakage currents such as tunnelling, generation-recombination and other mechanisms. The main demand for the passivation is minimization of these surface leakage currents to achieve good photodiode performance. In our case, CdTe semiconductor films with nearly lattice matched parameters to CdHgTe (within 0.3%), high resistivity, chemical and thermal stability, enlightenment properties [1-2] were chosen as passivation for photodetectors based on CdHgTe. CdTe films were grown by the "hot wall" epitaxy method.

It is important to choose optimal thickness of the passivation layer. The thickness of deposited films was determined by the time of precipitation (up to 120 min), and controlled by 3D interference profilometer “Micron-alpha”. The morphology of the obtained structures was studied with using atomic force microscopy.

The main task of our research was to improve the existing parameters of a growth of thin passivation films. To solve this problem, the influence of temperature and time of growth on the formation of CdTe thin films on CdHgTe surface are studied. The task is complicated by the requirement of low-temperature growing of CdTe film because at high temperature growth in CdHgTe epitaxial layers there are irreversible structural transformations that lead to the destruction of ternary solid solution, primarily due to the escape of mercury atoms from the crystal lattice.

Thus, optimal temperature ranges and time of growth of CdTe passivation layers with a thickness of 600 nm were chosen for which the time degradation of electrical parameters of CdHgTe based infrared photodiodes has not been observed.

1. Tsybrii Z.F., Vuichyk M.V., Sizov F.F. Protective and enlightening properties of cadmium telluride thin layers grown by the method of "hot wall" epitaxy// Novi tekhnolohii. – 2008. – T.**20**, №2. – P. 21-24. (in ukr.)
2. Permikina E.V., Kashuba A.S. Characteristics of a CdTe Passivating Coating Applied to an HgCdTe Epitaxial Layer // Uspekhi prikladnoi fiziki. – 2016. – T.**4**, № 5. – P. 493-499. (in rus.)

POSTER REPORTS

Session 5
Functional crystalline materials: growth, physical properties and applications

SiGe epitaxial films with dislocations for the switchable memory: the accurate first-principle calculations

Balabai R.M., Zalevskyi D.V.

Kryvyi Rih State Pedagogical University, Kryvyi Rih, Ukraine, balabai@i.ua, denys.zalevski@gmail.com

The authors are demonstrated [1] analog resistive switching devices that possess desired characteristics for neuromorphic computing networks with minimal performance variations using a single-crystalline SiGe layer epitaxially grown on Si as a switching medium. Such epitaxial random access memories utilize threading dislocations in SiGe to confine metal filaments in a defined, one-dimensional channel. The [1] authors emphasized also that such confinement results in drastically enhanced switching uniformity and long retention/high endurance with a high analog on/off ratio, thus justifying the suitability of epiRAM for transistor-free neuromorphic computing arrays.

For extension of information about switching properties of the SiGe epitaxial films with dislocations with Ag doping regions (see Fig. 1) these objects are calculated with such methods as electron density functional and first-principles pseudopotential based on own program code [2]. The atomic basis of supercell that models a single-crystalline SiGe layer epitaxially grown on Si with the Ag filled dislocations contains 192 atoms (162 atoms of Si, 14 atoms of Ge and 16 atoms of Ag).

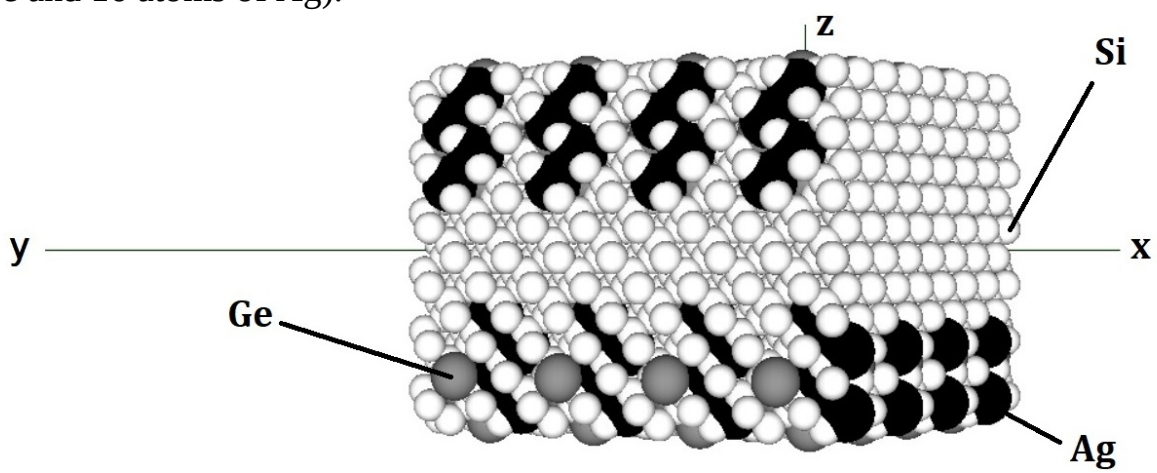

Fig.1. Fragment of an epiRAM device: a single-crystalline SiGe layer epitaxially grown on Si with the Ag filled dislocations (several supercells shown)

1. Shinhyun Choi et al. SiGe epitaxial memory for neuromorphic computing with reproducible high performance based on engineered dislocations // Nature Materials. – 2018. – V.17. – P. 335-340.
2. Ab initio calculation [E-resource] – Mode access to the resource: http://sites.google.com/a/kdpu.edu.ua/calculationphysics.

Determination of the Magnitude of Local Deformations in Synthesized Diamonds from the Data of Electron Backscatter Diffraction

Balovsyak S.[1], Borcha M.[1], Solodkyi M.[1], Kuzmin A.[1], Kazemirskyi T.[1], Tkach V.[2]

[1] *Yuriy Fedkovych Chernivtsi National University, Chernivtsi, Ukraine*
[2] *V. Bakyl Institute for Superhard Materials of NASU, Kyiv, Ukraine, ifodchuk@ukr.net)*

The great interest to synthesized diamond crystals is caused by unique outstanding physical and chemical properties. Therefore it is important to know the distribution of inhomogeneities and strains in this samples.

Experimental studies of the deformation state of synthesized diamonds were performed using a scanning electron microscope Zeiss EVO-50 with CCD detector. In this investigation, the analysis of the energy spectrum of Kikuchi band images, which is calculated on the basis of a two-dimensional Fourier transform, is proposed for determination of local deformations of crystals [1]. This technique allowed us to determine the anisotropy of magnitude and direction of local deformations in selected areas of synthesized diamond (fig. 1a). The lateral distribution of the deformations for investigated diamond crystal is calculated by approximation of obtained values of ε_S deformations (fig.1b).

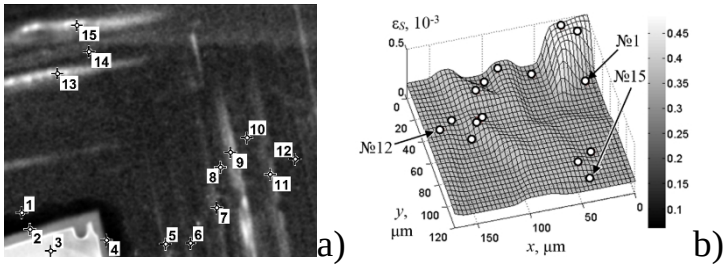

a) b)

Fig. 1. The topography image (a) and lateral distribution (b) of ε_S deformations in local areas №1-№15 of synthesized diamond crystal.

The analysis of distribution features of local deformations in marked crystal areas (fig.1a) gives not only a qualitative presentation of anisotropy nature, but also shows the nature of the heterogeneity of crystal growth conditions and the distribution of doping impurities. The expressiveness of this approach and its integral nature substantially complement existing methods for determining deformations from Kikuchi's images.

1. Borcha M., Solodkyi M., Balovsyak S., Fodchuk I., Kuzmin A., Tkach V., Yuschenko K., Zviagintseva A. Determination of local strains in a neighborhood of cracks in a welded seam of Ni-Cr-Fe according to the power Fourier spectrum of Kikuchi patterns. *Physics and chemistry of solid state*. 2018. V. 19, No 4. P. 307-312.

Crystalline Structure and Magnetoresistance Properties of High-Entropy Film Alloys

Bereznyak Yu., Ilin S., Poduremne D., Protsenko I., Shabelnyk Yu.

Sumy State University, Sumy, Ukraine, shabelnyk@gmail.com

A new class of materials such as high-entropy alloys (HEA), proposed in the work [1], demonstrate the unique physical-mechanical and magnetic properties in a bulk state. At meantime, the study of the physical properties of the HEA films has only been initiated [2]. We have investigated the electrophysical properties of non-equiatomic HEA films based on Fe, Co, Ni, Cr, Cu or Al, which were formed by simultaneous or layer condensation of separate metals. The component concentration was calculated based on the final thickness value of the separate component layers and clarified by the energy-dispersion analysis method.

The phase state and crystalline structure were investigated by electron diffraction and electron microscope methods.

The samples of a total thickness $d \cong$ 30-80 nm were obtained in a vacuum 10^{-4} Pa with subsequent annealing up to 600 K. HEA samples have fcc lattice (a = 0.3604 nm) with traces of bcc phase in both cases – after condensation and annealed; the parameter of lattice is closed to the a-Fe or bcc Cr, or to the a-Fe(Cr) solid solution.

The value of magnetoresistance (*MR*) is calculated on the basis of field dependence $R(B)$ and based on ratio $MR = (R(B) - R(0))/R(0)$. An appropriate computerized complex is used for the $R(T)$, $R(B)$ and *MR* measuring.

The *MR* research was performed in CIP geometry (current $\boldsymbol{j}$ in the film plane) in the three magnetic field orientations: longitudinal (||), transverse (+) and perpendicular (⊥) at a current intensity from 0.5 to 1 mA. The effect of annealing to 800 K leads to some increase of the MR amplitude, while the MR amplitude does not change. The relatively small size of the amplitude (maximum is 0.15 %) is explained by small thickness (40 nm) and very small working current value. The nature of the *MR* dependence on the magnetic field indicates the existing of anisotropic magnetoresistance. When NiAl ferromagnetic nanoparticles forme in HEA films, the $R(B)$ dependence has giant magnetoresistance characteristics with an amplitude value of 0.3%. Realization of GMR occurs as a result of spin-dependent scattering of electrons by on NiAl particles.

The work has been performed under the financial support of the Ministry of Education and Science of Ukraine (state registration number0118U003580).

1. J.-W. Yeh, S.-K. Chen, S.-J. Lin, J.-Y. Gan, T.-S. Chin, T.-T. Shun, C.-H. Tsau, S.-Y. Chang, Adv. Eng. Mater. **6**, 299 (2004).
2. S.I. Vorobiov, D.M. Kondrakhova, S.A. Nepijko, D.V. Poduremne, N.I. Shumakova, I.Yu. Protsenko, J. Nano- Electron. Phys. **8**, 03026 (2016).

The Effect of Sintering Conditions on Red Emission of Mn^{4+} Activated Mg_2TiO_4 Phosphors

Borkovska L.[1], Vorona I.[1], Khomenkova L.[1], Stara T.[1], Gudymenko O.[1], Rudko V.[1], Michailovska K.[1], Kladko V.[1], Labbe C.[2]

[1]*V. Lashkaryov Institute of Semiconductor Physics of the NAS of Ukraine, Kyiv, Ukraine, l_borkovska@ukr.net*

[2]*CIMAP, Normandie Univ, ENSICAEN, UNICAEN, CEA, CNRS, Caen, France*

Recently, Mn^{4+} activated materials have been attracted much attention as a cost-effective alternative to commercial red phosphors based on Eu^{2+} doped nitrides. They show broad excitation band in the blue-green spectral region and narrow emission band in the red that meet the spectral requirements for an ideal red-emitting phosphor to be applied in blue-chip excited white LEDs. Magnesium orthotitanate, Mg_2TiO_4, is considered as a proper matrix for Mn^{4+} ions. It can be easy obtained by traditional solid-state reaction route. Here, we present the results of study of the effect of sintering conditions on Mn^{4+} red emission in Mg_2TiO_4 phosphors. The latter were produced by sintering at 800-1200 °C in the air of MgO and TiO_2 powders weighted in a stoichiometric ratio. The content of Mn impurity varied in the range of 0.0001-1.0% of Ti site atoms.

Two magnesium titanate crystal phases, that were cubic Mg_2TiO_4 and rhombohedral $MgTiO_3$, were formed under annealing. The X-ray diffraction showed that formation of Mg_2TiO_4 crystal phase sets in at about 1000 °C and its concentration increased with the increase of the annealing temperature. In turn, the $MgTiO_3$ phase appeared at all temperatures due to thermal decomposition of Mg_2TiO_4. Quick cooling of the phosphors from the annealing temperature resulted in smaller concentration of $MgTiO_3$ phase in the final product.

Each of titanate phases demonstrated photoluminescence (PL) band due to spin forbidden $^2E \rightarrow {}^4A_2$ transitions of the Mn^{4+} ion substituted Ti^{4+} in the host. The band was peaked at about 659 nm in Mg_2TiO_4 and at 701 nm in $MgTiO_3$. The largest intensity of Mn^{4+} PL was found for Mn concentration of about 0.1 %. The relaxation of Mn^{4+} PL in Mg_2TiO_4 phase showed bi exponential decay with relaxation times varied in the ranges of 50-90 and 360-500 μs, the larger was Mn content, the faster was PL relaxation.

The X-band electron paramagnetic resonance (EPR) spectra of the annealed phosphors revealed several EPR sextets ascribed to Mn^{2+} ions in MgO, $MgTiO_3$ and Mg_2TiO_4 phases. The increasing of Mn doping level resulted in the increase of Mn^{2+} content in all phases. No EPR signal of Mn^{4+} ions was found. The phosphors subjected to quick cooling showed smaller intensity of Mn^{4+} red emission, but larger EPR signal of Mn^{2+} ions in Mg_2TiO_4 phase. The effect of thermal decomposition of Mg_2TiO_4 on the intensity of Mn^{4+} emission is discussed.

Calculation of the Stress-Strain State of the Container of a Six-Punch HPD

Bovsunivskiy O.V., Polotnyak S.B., Lysakovskii V.V., Lyeshchuk O.O.

V. M. Bakul Institute for Superhard Materials, National Academy of Sciences of Ukraine, Kyiv, Ukraine, olesbov@gmail.com

Chinese six- hammer cubic high-pressure devices (HPD) are widely used for the growth of structurally perfect monocrystals of diamonds. These presses are capable to build quasi-hydrostatic pressures in the range of 6 - 8 GPa, temperatures up to 1900^{o}C in sufficiently large growth volumes and to maintain such parameters for a long time; due to the such characteristics they should be used in materials science.

The material of the container for compression of the high pressure chamber and the lateral support of the working surface of the hammer in such HPD are pyrophyllite, for the use of which an important condition is the study of the compression mechanism.

Experimental studies of pressure distribution in a pyrophylitic container of cubic AVT showed that at P = 5 GPa in its central part, the pressure gradient along the axis of symmetry of the cube is on average 0.05 GPa/mm, and the pressure distribution is heterogeneous, resulting in a complex stress-strain state.

The method of mathematical modeling has calculated the stress-strain state of the cell of the selected configuration of a six- hammer apparatus with a diameter of the plunger 560 mm. The geometry of the working surface of the hammer has two pairs of bevels to the pyramidal pushing area: the first - with the angle α_1 = 41,5 ° and the second - at an angle α_2 = 46 °; the horizontal square of the punch is 44 × 44 mm^2.

The following properties of materials were used for calculations: hard-alloyed hammer (alloy ВК-6) - Poisson's coefficient ν = 0,21, Young's modulus E = 605 GPa; pyrophyllite - Young's modulus E1 = 30 GPa and E2 = 2.82 GPa, Poisson's coefficient ν1 = ν2 = 0.12, yield strength of 560 MPa and 100 MPa for the container and compression gasket, respectively. With such properties pressure in the pyrophyllite cube when the volume of the cavity of high pressure is reduced by 21.08% from the initial one reaches 4.93 GPa and the length of the gasket compression at this pressure takes the value of 13.8 mm.

It was established that the most unstable zone in the pyrophyllite cube is in the place of the formation of a gasket on the junction of three hammer; this zone is the most deformed in the entire cube.

On the basis of comparison of the obtained data with the results of published works, it was concluded that they coincide.

Theoretical Analysis of Experimental Thermoelectric Characteristics of Silicon-Based Whiskers

Budzhak Ya.S., Druzhinin A.A., Nichkalo S.I.

Lviv Polytechnic National University,Lviv, Ukraine, druzh@polynet.lviv.ua

In references [1-3], data on the Seebeck coefficient in silicon-based whiskers with a microscopic thickness d in which spatial quantization can be observed, is given. However, the data analysis of these works using a theoretical method described in [4] showed that there is no spatial quantization of the charge carriers' spectrum in the samples under study. Therefore, according to [4], the Seebeck coefficient α can be defined as:

$$a(m^{\bullet},T)=\left(\frac{k}{ze}\right)\left(\frac{\int_0^{\infty}x^{(r+2)}\left(-\frac{df_0}{dx}\right)dx}{\int_0^{\infty}x^{(r+1)}\left(-\frac{df_0}{dx}\right)dx}-m^{\bullet}\right)=\left(\frac{k}{ze}\right)\left(\frac{F_{(r+2)}(m^{\bullet})}{F_{(r+1)}(m^{\bullet})}-m^{\bullet}\right) \qquad (1)$$

where μ^* – the normalized chemical potential of charge carriers of a sample under study, $F_{(r+1)}(\mu^*)$ $F_{(r+2)}(\mu^*)$ – the Fermi integrals described in detail in [4], and the parameter r characterizes the mechanism of charge carrier scattering by defects of the crystal lattice. This parameter r=0 for scattering by acoustic phonons, r=1 for scattering by optical phonons, and r=2 for scattering by ionized defects of the crystal lattice.

The statistical calculations of whiskers' characteristics taken from [1-3] showed that the Seebeck coefficient, eq. (1), describes the experimental data of the studied samples adecuately only if r=0 or r=1. That is, in the studied whisker samples, depending on the conditions of experimental measurements the charge carrier scattering by acoustic or optical phonons is observed.

1. Druzhinin A.A., Ostrovskii I.P., Liakh-Kaguy N.S. Thermoelectric properties of SiGe whiskers. *Information and Telecommunication Sciences*. 2016. Vol. 7, No 2. P. 20-27.
2. Druzhinin A., Ostrovskii I., Kogut Iu., Nichkalo S., Shkumbatyuk T. Si and Si-Ge wires for thermoelectrics. *Physica Status Solidi C.* 2011. Vol. 8, No 3. P. 867-870.
3. Dolgolenko A.P., Druzhinin A.A., Karpenko A.Ya., Nichkalo S.I., Ostrovsky I.P., Litovchenko P.G., Litovchenko A.P. Seebeck's effect in p-SiGe whisker samples. *Semiconductor Physics, Quantum Electronics & Optoelectronics*. 2011. Vol. 14 (4). P. 456-460.
4. Буджак Я.С., Дружинін А.О., Вацлавський Т. Сучасні статистичні методи досліджень властивостей кристалів як матеріалів мікро– та наносистемної техніки. Львів. Видавництво Львівської політехніки. 2018. С. 230.

Growing of Large Single Diamond Crystals

Burchenia A.V., Lysakovskii V. V., Zanevskii O. O., Ivakhnenko S.O.

Institute for Superhard Materials, National Academy of Sciences of Ukraine, Kyiv, Ukraine,
Burchenia@bigmir.net

Diamond has been widely used in various fields such as industry, scientific research, national defense and medical treatment because it has numerous outstanding properties such as high thermal conductivity, highest hardness, wide wave band for light transmission, semiconductor properties. An increase in the size of diamond crystals make the application potential of diamonds more extensive. However, diamond are now extremely limited in application, because natural diamond are limited, especially the large natural single diamond crystals. Therefore, growing of synthetic diamond single crystals is an alternative to natural diamonds.

We report our applications for 6 – anvil high pressure apparatus model CS VII with working volume about 180 cm^3, in which large diamond crystals were grown under pressure of 6±0.5 MPa, temperature of 1380-1400 and temperature gradient of 5-7 /mm. Growing cell present as cube with dimensions of 58x58x58 mm. To initiate growth of diamond single crystals in growth cell 1 seed crystals was planted with sizes of 50x50x50 μm. Duration of the growing cycle was 180 hours. Obtaining of diamond single crystals was carried out in Fe–Al–C, Fe – Al – B – C and Fe–Ni–C growing systems.

As a result of the experiments was received single type IIa and Ib single diamond crystals with weight of 10.5 ct (type Ib), 8.7 ct (type IIa) and 9.3 ct (type IIb). Middle weight growth rate was: type Ib diamond single crystal 10,2 mg/h, type IIa – 8,45 mg/h, type IIb – 9,03 mg/h . Linear growth rate was: type Ib - 20 μm/h {100} and 30 μm/h {111}, type IIa – 16,5 μm/h {100} and 24,8 μm/h {111}, type IIb – 17,7 μm/h {100} and 26,5 μm/h {111}.

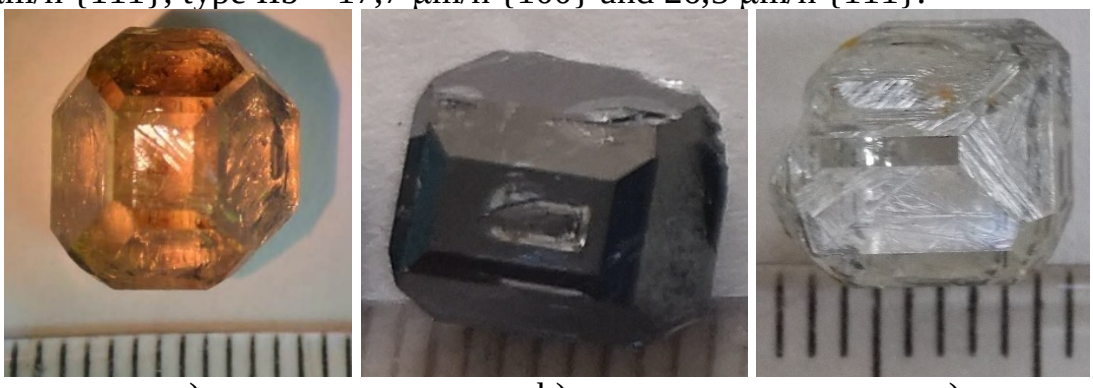

a) b) c)

Fig. 1. Samples of single diamond crystals: a) type Ib; b) type IIb; c) type IIa

Presented report showed possibility of using 6 – anvil high pressure apparatus with working volume about 180 cm^3 for high quality synthetic diamond crystal growing with weight 10 ct and more.

Crystal Structure, Electronic and Luminescence Properties of Undoped and Pr^{3+}- Doped $SrLa_4Ti_5O_{17}$ Powders

Chornii, V.P.[1,2], Nedilko, S.G.[1], Titov, Yu.O.[1], Boyko, V.V.[2], Chumak, V.V.[3], Sheludko, V.I. [4]

[1]*Taras Shevchenko National University of Kyiv, Kyiv, Ukraine*
[2]*National University of Life and Environmental Sciences of Ukraine, vchornii@gmail.com*
[3]*Zhytomyr Ivan Franko State University, Zhytomyr, Ukraine*
[4]*O. Dovzhenko Hlukhiv National Pedagogical University, Hlukhiv, Ukraine*

Compounds with perovskite-like structure those belong to $A_nB_nO_{3n+2}$ family (A = Ca, Sr, Pb, La ÷ Sm; B = Ti, Nb, Ta, Fe, Sc; n = 2 ÷ 6 is a number of BO_6 octahedra) possess important properties, in particular, they can be ferro- and piezoelectric, electrets, materials with optical nonlinearity etc. In the same time compounds of the $A_nB_nO_{3n+2}$ family were not studied before as optical materials. Although, one could expect a manifestation of luminescent properties from them, as the composition of such compounds with layered structures is similar to the composition of the perovskite structure of alkaline earth titanates $A^{II}TiO_3$ (A^{II} = Mg, Ca, Sr, Ba). In this work luminescence properties of the five-layered titanates $A^{II}Ln_4Ti_5O_{17}$ (A^{II} = Ca, Sr; Ln = La, Pr, Nd) are analyzed together with the results of electronic band structure calculations.

Synthesis of the powder samples was performed by heat treatment (T = 1670 K, t = 2 h) of co-precipitated hydroxycarbonates batch. The phase composition of prepared samples was determined by X-ray diffraction and IR spectroscopy methods. The VUV-excited PL properties were studied on SUPERLUMI station at HASYLAB (DESY), Hamburg, Germany in 3.7 – 25 eV region of excitation energies. The PL characteristics in visible spectral region were measured using diode-pumped laser (λ_{em} = 473 nm) and Xenon lamp as excitation light sources. Electronic band structure calculations were performed by full-potential linearized augmented planewave (FP-LAPW) method implemented in Wien2k package.

The wide-band complex spectra of intrinsic luminescence of the undoped $SrLa_4Ti_5O_{17}$ compounds were found in range 350 – 1100 nm under excitation in the 50 – 334 nm range. The possible origins of the luminescence are associated with peculiarities of the of the layered perovskite-like $SrLa_4Ti_5O_{17}$ lattice. Electronic band structure calculations showed that valence and conduction band edges are formed mainly by electronic states of oxygen and titanium respectively. So, three luminescence components of the intrinsic luminescence peaked near ~ 530, ~ 830, and ~ 1100 nm have been attributed to the radiation decay of excitons localized on three types of $(TiO_6)^{8-}$ molecular groups in the $SrLa_4Ti_5O_{17}$ crystal lattice. The luminescent features related with *4f→4f* and *4f5d→4f* radiation transitions in the Pr^{3+} ions were found in addition to mentioned intrinsic emission for the case of Pr^{3+} - doped $SrLa_4Ti_5O_{17}$ compound.

Composition Dependence of the Direct and Indirect Bandgap for $TlInX_2$–$D^{IV}X_2$ (D^{IV} – Si, Ge, Sn; X – S, Se)

Danylchuk S.P.[1], Fedosov S.A.[1], Sakhnyuk V.E.[1], Zakharchuk D.A.[2]

[1]*Lesya Ukrainka Eastern European National University, Lutsk, Ukraine, Fedosov.Serhiy@gmail.com*

[2]*Lutsk National Technical University, Lutsk, Ukraine, dima.zakharchuk@gmail.com*

Optical measurement constitutes the most-important means of determining the band structures of semiconductors. Photon-induced electronic transitions can occur between different bands, which lead to the determination of the energy bandgap, or within a single band such as the free-carrier absorption. Optical measurements can also be used to study lattice vibrations (phonons).

A photon may be absorbed by the excitation of an electron from a filled state in the valence band to an empty state in the conduction band. This process is the main process in a photodetector or solar cell.

Either for photon absorption, the conventional theory for optical transitions between the valence and conduction bands of direct-bandgap materials is based on the so-called $\vec{k}$-selection rule. The allowed transitions are then between initial and final states of the same wave vector – direct or vertical transitions (in $E-\vec{k}$ space). When the conduction-band minima are not at the same value of $\vec{k}$ as the valence band, assistance of a phonon is necessary to conserve crystal momentum – indirect transition.

We are investigated the energy gap for $Tl_{1-x}In_{1-x}(Si,Ge,Sn)_xSe_2$, $Tl_{1-x}In_{1-x}Sn_xS_2$ as a function of the mole fraction x. For $x=0$, the energy gap is direct. For $x \geq 0.1$, the energy gap is indirect and increasing

from E_g	at x	to E_g	at x	for
1.53	0.1	1.73	0.2	$Tl_{1-x}In_{1-x}Si_xSe_2$
1.56	0.1	1.58	0.2	$Tl_{1-x}In_{1-x}Ge_xSe_2$
1.42	0.1	1.64	0.25	$Tl_{1-x}In_{1-x}Sn_xSe_2$
1.34	0.1	1.91	0.5	$Tl_{1-x}In_{1-x}Sn_xS_2$

For direct-bandgap semiconductors, such as $TlInSe_2$ and $TlInS_2$ ($x=0$), the momentum is conserved and interband transitions may occur with high probability. The photon energy is then approximately equal to the bandgap energy of the semiconductor. The absorption transition mechanism is predominant in directbandgap materials. However, for $Tl_{1-x}In_{1-x}(Si,Ge,Sn)_xSe_2$, $Tl_{1-x}In_{1-x}Sn_xS_2$ with $x \geq 0.1$ that are indirect-bandgap semiconductors, the probability for interband transitions is extremely small, since phonons or other scattering agents must participate in the process in order to conserve momentum. Therefore, for indirect-bandgap semiconductors, special type of generation centers are incorporated to enhance the absorption transition.

Structurating in Concrete Composites of High Density and Density, Modified Complex of Transformed Additives

Fodchuk I., Sumaryuk O., Romankevych V., Roman Y. Myhailovich V.

Yuriy Fedkovych Chernivtsi National University, Chernivtsi, Ukraine, ifodchuk@ukr.net

In the work, the peculiarities of the formation of the microstructure of concrete fractures with and without the addition of ultrafine modifiers were investigated using the methods of scanning electron microscopy and X-ray diffractometry. The effect of the phase composition of the compounds formed on the nature of crack opening in the process of composite failure is analyzed.

Two experimental formulations of the concrete mixture were used: №.1 (initial) and №.2 (modified) with a complex of finely dispersed modifiers based on nanosilica and metakaolin.

The analysis of the features of the microstructure of concrete chips was carried out using a Hitachi SU 70 scanning electron microscope using a CCD detector. Elemental analysis of objects was carried out on the basis of energy dispersive X-ray spectroscopy (EDC) data. According to the EDC analysis, the fracture of concrete composite №.1 passes mainly through areas where there are high concentrations of calcite. So, the higher the dispersion of the phase components of calcite, the higher the concentration of aluminum atoms in them and the lower the silicon, which is the supposed reason for the decrease in the strength of the composite at the micro level. In a series of samples of 120 MPa strength (composition №.2), in the process of hydration of clinker minerals, a number of chemically active substances are formed during the hardening of concrete. First of all, it is calcium oxide hydrate, calcium silicate hydrate and such structural gel models as genite and tobermorite.

The higher the dispersion of the phase components of calcite, the higher the concentration of aluminum atoms in them and the lower the silicon, which is the supposed reason for the decrease in the strength of the composite at the micro level. Calcium hydrosilicate is the main binding agent in the cement matrix and is responsible for the strength and density of the structure. The C-S-H compound is formed as a result of the chemical interaction of the phases of Portland cement β-C2S, C3S and water. Calcium hydrosilicate (C-S-H) is a hydration product and forms approximately 60% of the phases of a concrete composite. The molar ratio of CaO to SiO2 in C-S-H is one of the main reasons for determining and controlling properties of the calcium hydrosilicate system.

1. Sumaryuk A.V., Romankevych V.F., Roman Yu.T., Fodchuk I.M., Tkach V.M. Concrete composites of high structural strength and density, modified by a complex of fine additives based on nanosilica and metakaolin. *Nanosystems, nanomaterials, nanotechnologies*. 2018. T.16, №1. C.117–128.

Influence of Gamma-Irradiation on Structural Disturbances in Cadmium Antimonide Crystals

Fedosov S.A.[1], Koval Yu.V.[2], Zakharchuk D.A.[2], Yashchynskiy L.V.[2]

[1]*Lesya Ukrainka Eastern European National University, Lutsk, Ukraine, Fedosov.Serhiy@gmail.com*

[2]*Lutsk National Technical University, Lutsk, Ukraine, dima.zakharchuk@gmail.com*

The CdSb semiconductor compounds occupy a special place among the semiconductors of group II-V, due to the peculiarities of changing the electrophysical parameters under the influence of high-energy radiation.

At irradiation of CdSb in the crystal lattice radiation defects are introduced as donor and acceptor types, and the effectiveness of their effect on the properties of this semiconductor depends on the level of doping and the type of conductivity of the source material. The rate of removal of current carriers is significantly dependent on the concentration of donors and acceptors in crystals, which is the result of the participation of impurity atoms in the formation of corresponding radiation defects with deep levels.

The appearance of radiation violations in CdSb changes its electrical properties. However, this change does not increase proportionally to the integral dose, as expected, but in a complex way. The irradiation of a specially undoped *p*-CdSb gamma-quantum ^{60}Co at $\Phi = 0 \div 1.9 \times 10^{16}$ cm^{-2} leads to an increase in the conductivity of the crystal, and with a subsequent increase in the irradiation dose of $\Phi > 1.9 \times 10^{16}$ cm^{-2} to its reduction below the original value. The complex character of the dependence $s = f(\Phi)$ was also observed in cadmium antimonide crystals, doped with an indium of *n*-CdSb<In>, when they are irradiated with gamma-quantum ^{60}Co.

It has been established that at irradiation of *n*-CdSb<In> there is removal of electrons from the conduction band due to the formation of radiation defects with a deep level in the bandgap of the crystal. There is practically no change in concentration from the radiation dose at room temperature. However, for $T = 77$ K, with an increase in the dose of radiation, the change in the concentration of carriers of the current has a more pronounced character.

The detected changes in the electrophysical parameters after the gamma-irradiation ^{60}Co for *n*-CdSb<In> crystals can be explained by the predominant generation of radiation defects of the acceptor type, whose levels are located in the lower half of the bandgap. For *p*-CdSb crystals, these changes are due to the introduction of more radiation defects of donor type compared to the number of radiation acceptors and the displacement of the Fermi level under the influence of radiation into the region of permitted energies.

Obtaining, Structure and Properties of Glasses and Composites in As_2S_3-Sb_2S_3-SbI_3 System

Gasinets S.M.[1], Guranich P.P.[2], Hreshchuk O.M.[3], Makar L.I.[1], Mykaylo O.A.[1], Rizak I.M.[1], Rubish V.M.[1], Solomon V.M.[4], Yasinko T.I.[1], Yukhymchuk V.O.[2], Yurkin I.M[2]

[1]*Institute for Information Recording, NAS of Ukraine, Uzhhorod, Ukraine,* center.uzh@gmail.com
[2]*Uzhhorod National University, Uzhhorod, Ukraine*
[3]*V. Lashkaryov Institute of Semiconductor Physics, NAS of Ukraine, Kyiv, Ukraine*
[4] *Institute of Electronic Physics, NAS of Ukraine, Uzhhorod, Ukraine*

In this report we present the technology of obtaining and results of investigations by DTA, X-ray diffraction, Raman and dielectric spectroscopy methods of glasses and composites in As_2S_3-Sb_2S_3-SbI_3 (A-B-C) system.

$(A)_{45}(B)_{27.5}(C)_{27.5}$, $(A)_{40}(B)_{30}(C)_{30}$, $(A)_{35}(B)_{32.5}(C)_{32.5}$, $(A)_{30}(B)_{35}(C)_{35}$ glasses were prepared by vacuum melting method. During synthesis we applied the stepwise increase in temperature. The melts were periodically mixed. The melts were homogenized at 820-850 K for 24-36 h. Cooling of the melts was carried out into cold (273 K) water.

It has been established that the crystallization of As_2S_3-Sb_2S_3-SbI_3 glasses takes place in several stages and is accompanied by anomalies on the temperature dependences of dielectric parameters. These studies have shown that DTA curves of these glasses, recorded at q=6 K/min, revealed two exothermic effects. Temperatures maxima of these effects (T_{cM1} and T_{cM2}) are determined. The first effect is less pronounced due to the nucleus formation and the SbSI nanocrystals formation in glassy matrix. DTA curves of glasses recorded at q=3 K/min, have demonstrated three exothermic effects. On DTA curves of glasses recorded at q=9 K/min, occured the only intensive effect at high temperatures. Nanoheterogenous structure of glasses established. Their matrix is formed by only binary structural units (As(Sb)S_3, As(Sb)I_3) and contains small amount groups with homopolar bonds (S_n).

The analysis of X-ray diffraction patterns and Raman spectra showed that the structure of the phase that arises in the glass matrix at low temperature annealing (355-450 K) corresponds to the structure of the crystalline antimony sulfoiodide. The formation of ternary chain groups $SbS_{2/2}I$ occurs as a result of the glass structural relaxation during its softening, which is accompanied by breaking and switching of homopolar (S-S) and heteropolar (As(Sb)-S and As(Sb)-I) chemical bonds in the binary groups that form the structural network of glasses. This process is accompanied by the diffusion of atoms in distances of interatomic order. The influence of annealing conditions on the structure and dielectric properties of glasses and composities is discussed.

Mechanisms of Laser-Stimulated Surface Treatment of Semiconductors

Gentsar P.O., Vlasenko O.I., Levytskyi S.M.

V.Ye. Lashkarev Institute of Semiconductor Physics of NAS of Ukraine, Kyiv, rastneg@isp.kiev.ua

In this paper, in order to find out the mechanisms of impact of pulsed laser irradiation on thin sub surface layers of semiconductors the reflection spectra of n-Si(100), n-GaAs(100), p-CdTe(111) and solid solutions $Ge_{1-x}Si_x$ (x = 0.85); $Cd_{1-x}Zn_xTe$ (x = 0.1) in the range of 0.2 ÷ 1.8 μm before and after laser irradiation at the length of the light (electromagnetic) wave λ = 532 nm with different energy densities E are measured.

It should be noted that for full information on the influence of pulsed laser irradiation on the optical properties of the investigated semiconductors, in addition to the reflectance spectra R, the transmission spectra T were measured and the absorption spectra $D = 1 - (R + T)$ from the length of the light (electromagnetic) wave λ were constructed.

The mechanisms of nonthermal nature of impulse laser radiation on semiconductor materials include the following: ionization mechanism; mechanism of radiationless recombination; the mechanism of radiative recombination; shock wave mechanism (structural gettering).

Methods of laser gettering allow avoiding additional defects of the crystal and creating the necessary configuration of the deformation field (local areas) [1-3].

It is concluded that the main mechanism of impulse laser irradiation influence on the optical properties of thin near-surface layers of the investigated crystals is structural gettering, namely absorption due to the presence of semiconductor regions having a defective structure and possessing the ability to actively absorb point defects and bind impurities. In silicon, the role of a getter is performed by the surface layers of SiO_x, SiO_2, Si_3N_4, $SiO_{2-x}P$, SiC and others, in germanium – GeO_2 or GeO, in gallium arsenide - Ga_2O_3, As_2O_5, and others.

1. Zuev V.A., Litovchenko V.G., Popov V.G. Laser Processing of Thin Surface Layers of Semiconductors // Quantum Electronics. - 1982. - T.**23**. - P. 33-43. (in rus.)
2. V.P. Weiko, M.N. Libenson, G.G. Chervyakov, E.B. Yakovlev. Interaction of laser radiation with matter - Moscow: Fizmatlit. - 2008 - 312 p. (in rus.)
3. U. Dyuli. Laser technology and material analysis - M .: Mir. - 1986 - 504 p. (in rus.)

Photoluminescence Features of Er-Doped Chalcogenide Glasses and Crystals

Halyan V.V.[1], Ivashchenko I.A.[2], Kevshyn A.H.[1], Tretyak A.P.[1]

[1]*Department of Experimental Physics and Technologies for Information Measuring, L. Ukrainka Eastern European National University, Lutsk, Ukraine, halyanv@ukr.net*
[2]*Department of Inorganic and Physical Chemistry, L. Ukrainka Eastern European National University, Lutsk, Ukraine*

Special attention is devoted to the research of the luminescence properties of chalcogenide crystals and glasses due to practical application in optoelectronic technology. Their unique properties create advantages over other light-emitting materials and cause considerable interest both from the fundamental and the applied point of view. The chalcogenide materials combine high transparency in the visible, near-infrared, and medium-infrared spectral regions. By selecting the optimal component composition, it is possible to obtain wide areas of glass formation and to introduce relatively high concentration of rare earth metals (RE). Additionally, chalcogenides are characterized by high refractive index, good nonlinear optical properties, resistance to aggressive media, and easy manufacture technology.

Elementary high-purity substances were used for the synthesis of samples: Ag (99.99 wt.% of the principal), Ga, In, Ge (99.999 wt.% purity), La, Er (99.9 wt.%), and S (99.997 wt.%). The elements for single crystal growth were further purified by double vacuum distillation. The weight of the starting components for the glasses was 3 g; the batches for the synthesis of single crystals were 10 g.

The glasses La_2S_3-Er_2S_3-Ga_2S_3 and $Ag_{0.05}Ga_{0.05}Ge_{0.95}S_2$-$Er_2S_3$ with different erbium content were synthesized. A single crystals of $(Ga_{54.59}In_{44.66}Er_{0.75})_2S_{300}$, $(Ga_{69.75}La_{29.75}Er_{0.5})_2S_{300}$, $(Ga_{69.5}La_{29.5}Er)_2S_{300}$ composition was grown by solution-melt method. The photoluminescence spectra in the visible and near infrared range for these glasses and crystals were investigated.

The principal mechanisms of the occurrence of PL due to the transitions in the 4f-shell of erbium ions are presented on the basis of sulfide glasses and single crystals [1]. The appearance of many emission bands in chalcogenide glasses (unlike single crystals) is due to the fact that in an amorphous medium, erbium ions may occupy several different positions in the glass-forming matrix. The change of the excitation wavelength leads to a change in the mechanism for the excited states in Er^{3+} ions and the emergence of some radiation bands and the extinction of others.

1. Volodymyr V. Halyan, Inna A. Ivashchenko. Mechanism of photoluminescence in erbium-doped chalcogenide // Luminescence. Edited by S.L. Pyshkin / Intechopen, 2018. – P. 1-22. DOI: 10.5772/intechopen.81445.

Optical and Non-Linear Optical Properties of the Solid Solutions $AgGaGe_{3(1-x)}Si_{3x}Se_8$

Hmaruk G. P.[1], Myronchuk G.L.[1], Koval Y.V.[2]

[1]*Lesya Ukrainka Eastern European National University, Lutsk, Ukraine,* gladchukgalyna@gmail.com

[2]*Lutsk National Technical University, Lutsk, Ukraine,* y.koval@lntu.edu.ua

Single crystals and polycrystalline metal mixed due to wide window of transparency up to several micrometers are used as active part of many optical devices operating in IR spectral range [1]. The unique crystal structure of the chalcogenide compounds give opportunity partial or complete substitution of cation or anion groups, and finally resulting significantlyimprove desired properties of pure compounds The significant field of applications metal chalcogenide compounds is nonlinear optics in infrared spectral range [1–3]. In particular, an effective method of searching for new materials is a changing the chemical composition: systematic substitution of one type of ion by another isovalent ion, possess differ ion radius.

The main goal of the present work is to explore linear and second order non-linear optical features $AgGaGe_{3(1-x)}Si_{3x}Se_8$ compounds. We will study the corresponding features at different temperatures for the fundamental absorption The FTIR and Raman spectra were studied. The second harmonic generation (SHG) was carried out versus the angle for samples with different composition for different light polarization and was spectrally separated using the interferometric filters.

We investigated the effect of the component composition on optical and non-linear optical properties of the crystals of the solid solutions $AgGaGe_{3(1-x)}Si_{3x}Se_8$ with x = 0.05, 0.1, 0.2, 0.3. It was shown that the band gap energy at 300K varies only slightly from 2.1 to 2.07 eV. Simultaneously, Urbach's energy is enhanced from 54 to 73 meV which indicates higher degree of structure defects for larger x values. The magnitudes of Urbach's energy remain stable for all studied temperatures which confirms the principal contribution of the static defect disorder into the formation of this energy. Characteristic IR transmission and absorption maxima are preserved for all crystals, with more pronounced peaks at higher x values. The presented SHG dependences demonstrate significantincrease of non-linear optical properties with x; however, after crossing a critical value of x = 0.20 the SHG intensity decreases.

1. Fei Liang, Lei Kang, Zheshuai Lin, Yicheng Wu, *Cryst. Growth Des.* 17 (2017) 2254–2289.
2. In Chung, Mercouri G. Kanatzidis, *Chem. Mater.* 26 (2014) 849–869.
3. W. Kuznik, P. Rakus, K. Ozga, O.V. Parasyuk, A.O. Fedorchuk, L.V. Piskach, A. Krymus, I.V. Kityk, *Eur. Phys. J. Appl. Phys.* 70 (2015) 30501.

New Iodine-based Etchant for $Zn_xCd_{1-x}Te$ Single Crystals

Ivanits'ka V.G., Tkachuk L. M., Fochuk P.M.

[1]*Yuriy Fed'kovych Chernivtsi National University, Chernivtsi, Ukraine,*
v.ivanitska@chnu.edu.ua

Semiconductor surface condition can be a determining factor in the device quality, created on its basis. It is known that bromine alcohol (methanol, ethanol) solutions in the range of 0.5-15.0 vol. % Br_2 are effective etchants for CdTe and $Zn_xCd_{1-x}Te$ surface. However, due to the reason of bromine volatility and toxicity, it would be great to create more stable and less toxic etchants. Iodine-based etchants are not widely used, however, our previous study [1] indicated satisfactory characteristics of CdTe and $Zn_xCd_{1-x}Te$ surface, treated in Iodine-based solution.

In present report a kinetics and mechanism of $Zn_xCd_{1-x}Te$ dissolution in I_2 – dimethyl sulfoxide etching solutions are discussed. Dimethyl sulfoxide (DMSO, $(CH_3)_2SO$) is an important bipolar aprotic solvent which can be used for dissolving both organic and also inorganic substances. $Zn_xCd_{1-x}Te$ samples with the surface orientations (111)A, (111)B and (110) were selected for study. The research was conducted with the help of rotating disc polishing setup which guaranteed reproducible etching environment. The dependences of etching rate on etchant composition, temperature, and rotation speed were measured. The rate of etching was determined by decreasing the thickness of the samples, using a clock-indicator. The surface roughness after etching was measured by interferometer surface profiler (Zygo).

Investigation was carried out using solutions, containing 0,5-15 mass.% I_2 in DMSO. It was found that the increasing of iodine concentration in etching solutions resulted in the increasing of $Zn_xCd_{1-x}Te$ dissolution rate (v) from 0,4 to 6,5 μm/min. The difference between dissolution rates of different oriented $Zn_xCd_{1-x}Te$ surfaces was insignificant. The dependences of the dissolution rate on the disk rotation speed and temperature were obtained and rate-controlling stages of etching processes have been determined. The value of apparent activation energy (E_a) was calculated from temperature dependences and it didn't exceed 20 kJ/mol. This fact indicated, that the diffusion was the most slowly stage of the chemical interaction, i.e. total velocity of reaction was limited by the diffusion processes. The diffusion limitation had positive influence on polishing properties of the developed solutions. High quality of etched $Zn_xCd_{1-x}Te$ surfaces was confirmed by the results of microstructure and profilography analyses.

Reference

1. P. Moravec, V.G. Ivanits'ka, V.M. Tomashik, K. Masek, J. Franc, Z.F. Tomashik, R. Grill, R. Fesh, P. Hoschl Chemical polishing of CdTe and Cd(Zn)Te surfaces in iodine-based solutions // E-MRS 2013 Fall Meeting (Warsaw, September 16-21, 2013). - 2013. Program book. – P.241.

Bridgman growth and characterization of $CsPbBr_3$ single-crystals

Kanak A.I.[1], Levchuk I.V.[2], Mykhailovych V.V.,[1] Fochuk P.M.[1]

[1]*Yuriy Fedkovych Chernivtsi National University, Chernivtsi, Ukraine*
[2]*Institute of materials for Electronics and Energy Technology, Friedrich-Alexander-universitat Erlangen-Nurnberg, Erlangen, Germany, andriy.kanak@gmail.com*

All-Inorganic Perovskite $CsPbBr_3$ it's a very promising material for several application in a wide range of electronic devices such as high-energy radiation detectors, solar cells [1,2], etc. This material has higher stability compared to hybrid perovskite materials which provide the possibility of wider application including long term working devices.

Bulk $CsPbBr_3$ single-crystal can be obtained by several ways including solution-growth method [1] and Bridgman method by growing from the melt [2].

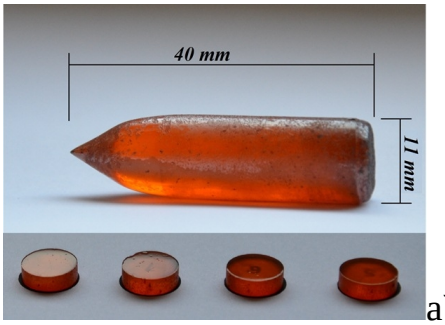

a)

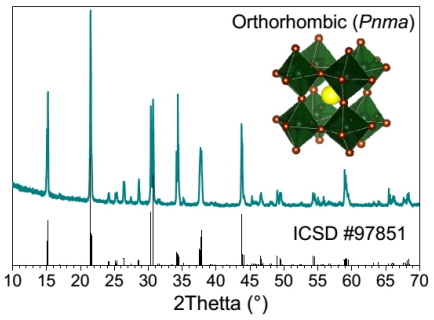

b)

Fig. 1. a)Photographs of the obtained $CsPbBr_3$ single-crystal; b) The XRD patterns of the $CsPbBr_3$ crystals

The aim of our study was to determine the optimal synthesis parameters and growth conditions for $CsPbBr_3$ perovskite single-crystals and to investigate their physical properties.

Several single-crystals of $CsPbBr_3$ were grown (Fig. 1) by Bridgman technique. The optimal conditions for the growing process were determined by the method of differential-thermal analysis (DTA). Structure of grown perovskite ingots was confirmed by XRD analysis (Fig. 1. b). Electrical and optical properties of the obtained material were investigated. Resistivity and width of the bandgap of $CsPbBr_3$ crystals were about ~ 4×10^9 Om×cm and 2.24 eV respectirvely.

1. Solution-Grown $CsPbBr_3$Perovskite Single Crystals for Photon Detection / Dmitry N. Dirin, Ihor Cherniukh, Sergii Yakunin et al. // Chem. Mater.2016. Vol. 28. P. 8470−8474.
2. Ultralarge All-Inorganic Perovskite Bulk Single Crystal for High-Performance Visible–Infrared Dual-Modal Photodetectors / Jizhong Song, Qingzhi Cui, Jianhai Li et al. // Adv. Optical Mater. 2017, 1700157.

The Quaternary Sulfide as a Novel Nonlinear Optical Material

Kevshyn A., Melnychuk K., Shugorin O., Shugorin P.

Lesya Ukrainka Eastern European National University, 13 Voli Ave., Lutsk, Ukraine,
fttkaf@gmail.com

$PbGa_2GeS_6$ crystal is transparent in the wide spectral range varying from 0.3 up to 15 μm. The measured mid- and IR-transmittance of a $PbGa_2GeS_6$ polycrystal sample shown in [1] confirms its high transparency in CO_2 laser operating range (covering its SHG and THG) which gives opportunity to consider $PbGa_2GeS_6$ as promising material for application in optoelectronic devices. As the reference for NLO measurements, we have taken a -BiB_3O_6 crystallites derived as reported elsewhere [2].

Following Fig. 1, one can clearly see that the SHG is maximal for the $PbGa_2GeS_6$ crystal studied in this work. Using as a reference the a -BiB_3O_6 crystallites, it was established that the optical susceptibility was equal to about 2.9 p.m./V at 1064nm. At the same time, for the $PbGa_2GeS_6$ compounds, this efficiency is at least one order less. The $PbGa_2$ GeS_6 sulfide has the same order of the THG efficiency as that of $PbGa_2GeS_6$. However, it is sufficient to use the $PbGa_2GeSe_6$ compound for simultaneous second and third harmonic generations and, contrary to a -BiB_3O_6 [2], it may be applied in the spectral range up to 10 μm. The principal influence on the observed nonlinear optical effects play huge anharmonic phonons for the lead chalcogenide crystals described by third rank polar tensors.

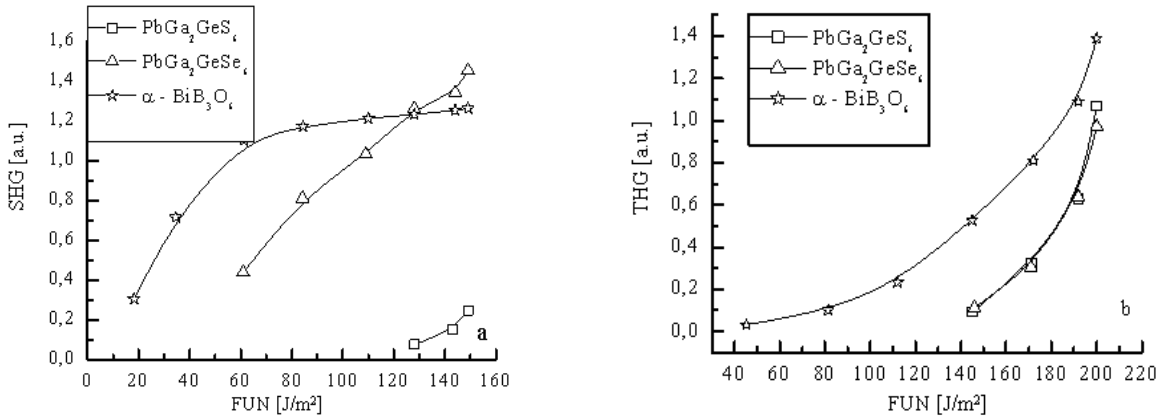

Fig.1. Dependence of the (a) SHG and (b) THG efficiencies versus the fundamental laser energy density

1. $PbGa_2GeS_6$ crystal as a novel nonlinear optical material: Band structure aspects / A.O. Fedorchuka, O.V. Parasyuk, O. Cherniushok, B.Andriyevsky, G.L.Myronchuk, O.Y.Khyzhun, G.Lakshminarayana, J.Jedryka, I.V.Kityk, A.M.ElNaggar, A.A.Albassam, M.Piaseck // *Journal of Alloys and Compounds.* 2018. V. – 740. P. 294-304.
2. Efficient third harmonic generation of microjoule picosecond pulses at 355 nm in BiB_3O_6 / M. Ghotbi, Z. Sun, A. Majchrowski, E. Michalski, I. V. Kityk, M. Ebrahim-Zadeh // *Appl. Phys. Lett.* 2006. Vol – 89. P. 173124.

Semiconductor Diamonds Crystallization in Fe-Co-Mg-C System

Kovalenko T. V., Lysakovskyi V. V., Ivakhnenko S. O.

Institute for Superhard Materials NAS of Ukraine, Kyiv, Ukraine,
tetiana.v.kovalenko@gmail.com

Diamond crystals properties – their structural perfection, thermal conductivity, electrical conductivity are determined by the presence and distribution of impurities in diamond, primarily nitrogen and boron. It is known that the doping growth systems with boron leads to crystallization type IIb diamonds with semiconductor properties. Boron forms in the diamond lattice an acceptor state (Ea=0.37 eV) provide to *p*-type conductivity. Diamonds containing uncompensated boron acceptors are rare in nature and typically has an uncompensated boron concentrations of $5 \cdot 10^{16}$ cm^{-3}.

To produce semiconducting diamond at high pressure and high temperature Fe-Al-C or Co-Fe-Ti/Al-C systems with the addition of boron or boron-containing components are usually used. Boron concentrations high as $>10^{20}$ cm^{-3} are reported for diamonds grown in these systems.

It was early reported by us [1] that diamond with semiconductor properties can be obtained without adding of boron or boron-containing compounds to growth system. It is shown that in the Mg–C system the boron content in grown crystals increases from $3.4 \cdot 10^{17}$ cm^{-3} to $1.1 \cdot 10^{18}$ cm^{-3}, and depending from the growing temperature from 1770 to 2000 °C. It is established that boron content in crystals grown in the Fe–Mg–C system with magnesium content of 30, 50, 70 at. %, increases in the range $(0.68–1.34) \cdot 10^{17}$ $cm^{-3} \rightarrow (1.23–2.10) \cdot 10^{17}$ $cm^{-3} \rightarrow (1.75–2.86) \cdot 10^{17}$ cm^{-3}, respectively.

However, the crystal growth process in these systems occurs at extremely high parameters; therefore, an actual task is to search for new growth systems and reduce the growth parameters.

This paper reported the semiconductor diamonds growth in Fe-Co-Mg-C systems without adding of boron or boron-containing components.

The experiments were carried out at high pressure and high temperature in large volume cubic high pressure apparatus $6 \times 2.8 \cdot 10^4$MN. A cubic container with dimensions of 58x58x58 mm was used. The growing process was carried out by the temperature gradient method under pressure of 6.0-6.5 GPa and a temperature of 1420-1500 °C.

It was established that adding of 10 wt. % Mg leads to the capture of boron impurities by grown crystal. Boron content in grown crystals increase up to $1.4 \cdot 10^{16}$ cm^{-3}.

1. Kovalenko T. V., Ivakhnenko S. O, Lysakovskyi V. V. Semiconductor Diamond Crystallization in Magnesium–Based Systems // Materials XVI International Conference On Physics And Technology Of Thin Films And Nanosystems, May 15-20, 2017, Ivano-Frankivsk, Ukraine. – P. 160.

Effective Masses of Current Carriers in the Doubly Degenerated Conduction Band: Interplay of DOS Peculiarities and Magnetization

Kramar O., Skorenkyy Yu., Dovhopyaty Yu.

Ternopil Ivan Puluj National Technical University, Ternopil, Ukraine,
skorenkyy@tntu.edu.ua

Strongly correlated electronic subsystem of functional crystalline materials with degenerate energy band may have unusual properties which can be controlled by various factors, including chemical composition and lattice symmetry as well as the external field application and heating. Transition elements compounds with double orbital degeneracy of energy levels can be appropriately modeled within the generalizations of Hubbard model [1-3], with taking into account the correlated hopping of electrons and peculiarities of electronic density of states (DOS). In this research, the effective masses of current carriers have been calculated for such a system at condition of less then quarter-filled band for different bare DOS forms and within the external magnetic field.

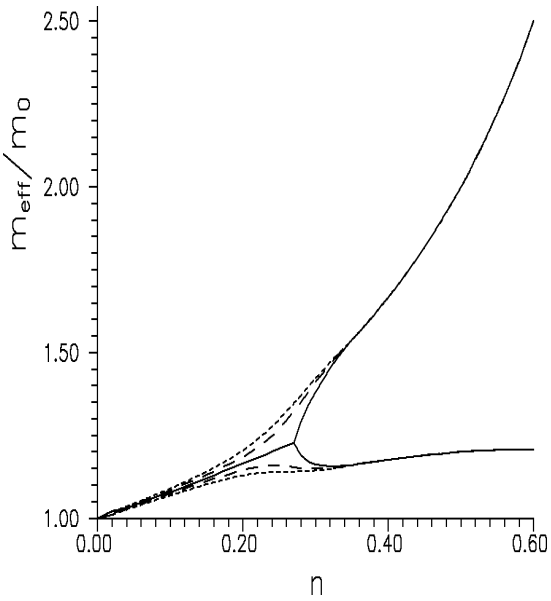

Concentration dependences of effective masses without (solid line) or with (dashed lines) magnetic field at semielliptic model DOS.

For various DOS forms, it has been found that in the concentration dependence of effective masses physically different regimes (of weak and strong magnetic field) can be realized. In a weak field, despite of the spin splitting occurrence due to translational mechanism of ferromagnetic order stabilization, a sharp change of the effective mass splitting exist for arbitrary electron concentrations, which can be utilized for tuning of the spin polarization by the external field. When the magnetic field is comparatively strong, the correlation band narrowing factor controls the critical concentration for the conduction type change. The DOS form governs the concentration dependence of transport characteristics, therefore the use of a realistic DOS for modeling of a spontaneous or magnetic field-induced ferromagnetic order is of great importance.

1. L. Didukh et al. *Phys. Rev. B* **64** 144428 (2001).
2. L. Didukh, O. Kramar. *Condens. Matter Phys.* **8** 547 (2005).
3 L. Didukh, O. Kramar and Yu. Skorenkyy. *Physica B: Condensed Matter* **359-361** 681 (2005).

Obtaining PbSe Crystals with Predicted Properties of Two Temperature Annealing Techniques

Prokopiv V.V. (Jr)[1], Lysak A.V.[1], Pylypiv V.M.[1], Mezhylovska L.Y.[1], Biletsky Y.S.[2], Cherkach K.P.[1]

[1]*Vasyl Stefanyk Prearpathian National University, Ivano-Frankivsk, Ukraine, alla.lysak@pu.if.ua*
[2]*Ivano-Frankivsk National Technical University of Oil and Gas, Ivano-Frankivsk, Ukraine*

The degree of practical use selenide of lead in microelectronics is largely determined by possibilities of deriving of crystals with beforehand specific performances. Therefore actual is crystallochemical modelling of a two-temperature annealing of crystals PbSe, that allows to find analytical dependence of concentration of defects and carriers of a charge from technology factors.

Defect formation in crystals PbSe for want of their two-temperature annealing it is possible to describe by a system of the equations

$$Pb_{Pb} = Pb_i + V_{Pb} \qquad K_F = [Pb_i][V_{Pb}] \qquad (1)$$

$$\tfrac{1}{2}Se_2^V = Se_{Se} + V_{Pb} \qquad K_{Se_2,V} = [V_{Pb}]pP_{Se_2}^{-1/2} \qquad (2)$$

$$Pb_i = Pb_i^+ + e^- \qquad K_a = [Pb_i^+]n[Pb_i]^{-1} \qquad (3)$$

$$V_{Pb} = V_{Pb}^- + h^+ \qquad K_b = [V_{Pb}^-]p[V_{Pb}]^{-1} \qquad (4)$$

$$0 = e^- + h^+ \qquad K_i = np \qquad (5)$$

$$n + [V_{Pb}^-] = p + [Pb_i^+] \qquad (6)$$

The joint solution of a set of equations I-VI enables to determine concentration of vacancies $[V_{Pb}^-]$, interstitial atoms of lead $[Pb_i^+]$, and also concentration of carriers of a charge through constants of an equilibrium and partial pressure of chalcogen P_{Se_2}. The expression for concentration of carriers of a charge will look like:

$$n^2(T, P_{Se_2}) = [K_i + K_a K_F K_{Se_2,V}^{-1} P_{Se_2}^{-1/2}][1 + K_b K_{Se_2,V} P_{Se_2}^{1/2} \cdot K_i^{-1}]^{-1} \qquad (7)$$

Temperature T* thermodynamic n-p-junction can be found from a condition, that n=p:

$$T^* = (2 \cdot \Delta H_{Se_2} - \Delta H_F)/(k \cdot \ln((K_{Se_2}^0)^2 \cdot P_{Se_2}/K_F^0)). \qquad (8)$$

The obtained analytical expressions well describe of experimental dependence of concentration of carriers of a charge and temperature thermodynamic n-p- junction for want of annealing of crystals PbSe in a pair chalcogen from technology factors: temperatures of an annealing and partial pressure of chalcogen.

Constructed because of conducted accounts space n-P-T-phase diagram and them n-P and P-T of a projection enable to place conditions of shaping of a material n- and p-type conductivity from specific concentration of carriers of a charge.

The Direct and Indirect Absorbtion Spectra of $TlGaSe_2$–Zn(Cd, Hg)Se Crystals

Makhnovets H.V., Myronchuk G.L., Korovytskyy A.M., Kot Y.O.

Department of Information Systems in Physics and Mathematics of
Lesya Ukrainka Eastern European National University
Lutsk, Ukraine, annamakhnovets@gmail.com

Due to the considerable structural anisotropy, the layered crystals possess unique physical properties promising for a number of applications in optoelectronics [1]. The purpose of the presented work is to study the optical properties of $TlGaSe_2$–Zn(Cd, Hg)Se crystals, namely, the direct and indirect band gap.

Optical measurements in the temperature range 100–300 K and spectral range 400–1100 nm were undertaken to obtain the information on the change of the band gap energy with temperature [1]. Typical absorption spectra are shown in Fig. 1, for some crystals. The analysis of experimental data shows that the absorption coefficient is proportional to $(hn - E_g)^p$ with $p = 1/2$ and $p = 2$. Linear dependences for relationships $(\alpha hn)^{1/2}$ vs. hn and $(\alpha hn)^2$ vs. hn allows us to settle the type, i.e. indirect and direct permitted transitions in the studied crystals. The band gap energy was estimated extrapolating the straight lines to $(\alpha hn)^{1/2} = 0$ and $(\alpha hn)^2 = 0$.

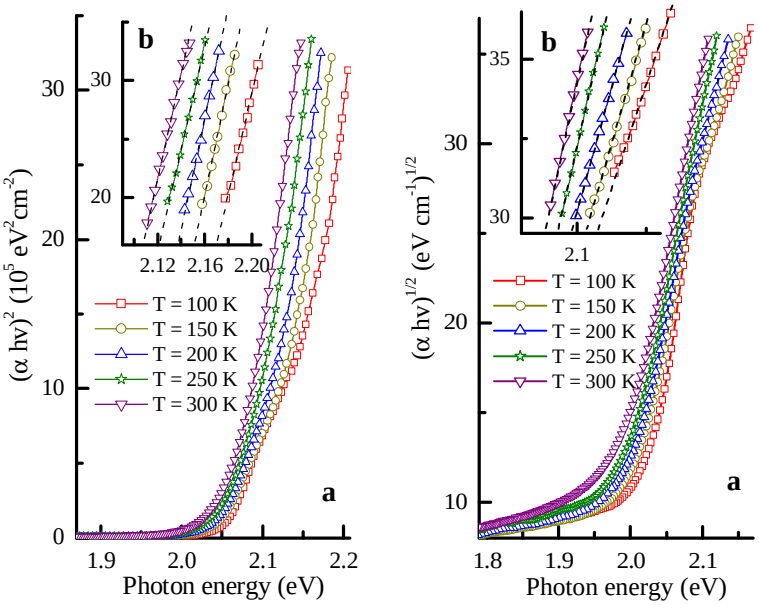

Fig. 1. The direct and indirect absorption spectra versus photon energy for 98 mol%$TlGaSe_2$-2 mol%ZnSe, samples

1. Phase diagram and specific band gap features of novel $TlGaSe_2$: Zn^{+2}(Cd^{+2}, Hg^{+2}) crystals / G. Makhnovets, Ph.D.; Galyna Myronchuk, Ph.D.; L. Piskach, Ph.D.; Oleg Parasyuk, Professor; Iwan Kityk // Journal: Journal of Alloys and Compounds, Volume 768, 2018, Pages 667-675.

Local Electron Interaction with Crystal Defects in $CdSe_xTe_{1-x}$(x=0.25) Solid Solution: ab Initio Calculation

Malyk O.P., Syrotyuk S.V.

Lviv Polytechnic National University Semiconductor Electronics Department, Lviv, Ukraine, omalyk@ukr.net

At present, the main method for increasing the efficiency of solar cells based on cadmium telluride is the using an additional absorbent layer created on the base of triple compounds of cadmium chalcogenides, in particular $CdSe_xTe_{1-x}$, as an absorbent layer. Therefore, the study of the quality of these absorbing layers is an actual application problem.

In the present paper, the estimation of the quality of the absorbing layer is carried out by analyzing of its kinetic properties. The description of the transport phenomena is carried out by combining two approaches: 1 – using of wave function and self-consistent potential which were determined from the first principles on the base of projector augmented waves (PAW), as implemented in the ABINIT code [1]; 2 – using the short-range principle to consider the charge carrier interaction with different types of crystal defects [2-5].

The PAW basis functions have been generated by means of the AtomPAW [6] code for the following valence states: $\{5s^25p^04d^{10}\}$ for Cd, $\{4s^25s^24p^25p^4\}$ for Te and $\{4s^24p^4\}$ for Se, respectively.

On the base of obtained wave function and self-consistent potential for for solid solution $CdSe_xTe_{1-x}$ (x=0.25) in the framework of short-range scattering models the calculation of transition probabilities for electron interaction with polar and nonpolar optical phonons, piezoelectric, acoustic phonons, static starin center, neutral and ionized impurities are presented. The transition matrix elements were obtained by integration over the unit cell. The conductivity tensor components were obtained from the exact solution of the stationary Boltzmann equation [7]. For crystals with impurity concentration $7\times10^{14} \div 1\times10^{19}$ cm^{-3} the temperature dependences of electron mobility and Hall factor in the range 15 ÷ 1200 K are calculated. The influence of different scattering mechanisms on the charge carrier mobility is considered. The theoretical curves obtained in the short-range approach differ qualitative and quantitative from those obtained within the long-range models in relaxation time approximation.

1. X. Gonze et al. *Computer Phys. Comm.* 2016. v. 205. pp. 106-131.
2. O.P. Malyk, *Mater. Sci. Eng. B*. 2006. v. 129. pp. 161-171.
3. O.P. Malyk, *Phys.Status Solidi C.* 2009. v. 6. pp. S86-S89.
4. O.P. Malyk, S.V. Syrotyuk. *Comput. Mater. Sci.* 2017. V. 139. p. 387–394.
5. O.P. Malyk, S.V. Syrotyuk. *J. Electron. Mater.* 2018. V.47. pp 4212–4218.
6. A.R. Tackett et al. *Comput. Phys. Commun.* 2001. V.135. p. 348–376.
7. O.P. Malyk. *J. Alloys Compd*. 2004. v. 371 pp. 146-149.

The Effect of Al^{3+} on the Structural and Adsorption Properties of Magnesium Ferrite-Aluminates

Myslin M.V., Tatarchuk T.R., Mironyuk I.F., Hreida N.V.

Vasyl Stefanyk Precarpathian National University,
Ivano-Frankivsk, Ukraine, marjanysik@gmail.com

Nowadays, the problem of environment pollution by dyes have attracted a lot of attention. The presence of even very low concentrations of dyes in water reduces the penetration of light through the water surface. This prevents the photosynthesis of aquatic plants, leads to a decrease in the level of oxygen in water, which, in turn, can lead to the death of aquatic flora and fauna. Many of these dyes are carcinogenic, mutagenic, as well as toxic to microorganisms, fish and humans. Therefore, the removal of dyes from wastewater before discharging them into the environment is an ecologically important task. Nano-sized spinel magnetic particles with large surface area are effective adsorbents, and their unique advantage is the easy separation under the action of an external magnetic field.

In this study, were synthesized new magnetically controlled magnesium-containing adsorbents with spinel structure. To improve the adsorption properties of magnesium ferrite, an admixture of aluminum was added. Magnesium-containing ferrite-aluminates with the general formula $MgAl_xFe_{2-x}O_4$ (where x = 0, 0.4, 1.0, 1.2 and 1.4) were synthesized by autocombustion sol-gel method using a new combined fuel – the mixture of alanine and urea. The samples were annealing at 400°C for 2 hours. The spinel structure of samples was confirmed by X-ray analysis. The average crystallite size calculated from XRD by Scherrer formula is found to be in the range 14 – 27 nm. With increasing Al^{3+} content, the lattice parameter decreases from 8,377 to 8,125 Å as a result of the smaller ionic radius of Al^{3+}. The system was also investigated using SEM, EDX, FTIR, BET and VSM. Adsorption properties of magnesium aluminate-ferrites were investigated on a model solution of one of the pollutants – methyl orange dye. In order to get adsorption equilibrium isotherms, the series of standard dye solutions was prepared with initial concentration 10 – 1500 mg/L.

The adsorption equilibrium data were fitted using Freundlich and Langmuir models. The Langmuir adsorption isotherm model fitted better because most closely matches with the experimental data. The maximum theoretical adsorption capacities of magnesium aluminate-ferrite, obtained from Langmuir model, were 23 mg/g and 400 mg/g for $MgFe_2O_4$ and $MgAl_{1.2}Fe_{0.8}O_4$ respectively (R^2 = 0.988 – 0.999). One of the main characteristics of the Langmuir isotherm is the adsorption coefficient R_L, which indicate the type of isotherm. R_L = 0.001 – 0.08 L/mg, since $0 < R_L < 1$ – this means that the surface of samples promotes the absorption of methyl orange in the conditions of this

study. The Freundlich model implies the non-uniform distribution of a heterogeneous surface and multilayer adsorption adsorbate on the surface. Freundlich constants K_F and 1/n depend on adsorption capacity and intensity of adsorption. It was found that K_F = 1.6 – 40 (mg/g)/(mg/L)^n, and 1/n = 0.31 – 0.54 (R^2 = 0.82 – 0.93).

The kinetics of the methyl orange adsorption process was investigated on the most active sample – $MgAl_{1.2}Fe_{0.8}O_4$. The equilibrium time of the adsorption process is reached in 180 min; the removal of the dye is about 100 %, and the maximum adsorption capacity is 50 mg/g. The adsorption data was also fitted to the pseudo-first-order and pseudo-second-order kinetic models. The pseudo-second order rate constant h was calculated: $h = k_2 q_e^2$ = 0.585 mg/(g·min). The adsorption of methyl orange on the surface of $MgAl_{1.2}Fe_{0.8}O_4$ passes according to the pseudo-second order model, which is in the good agreement with results reported in literature

Low-Temperature Plasticity of Uniaxially Deformed Silicon and Germanium Crystals

Panasjuk L.I.[1], Koval Yu.V.[1], Yashchynskyy L.V.[1], Zakharchuk D.A.[1], Misjuk S.Ya.[1], Fedosov S.A.[2]

[1]*Lutsk National Technical University, Lutsk, Ukraine, fnfizmat@lntu.edu.ua*
[2]*Lesya Ukrainka Eastern European National University, Lutsk, Ukraine, ftt@univer.lutsk.ua*

On the basis of analysis of results of studying the tensoresistive (TR) effects of germanium and silicon monocrystals, in conditions of high uniaxial pressures, we have got results that demonstrate the deviation of TR effects from their typical dependence on the elastic deformation area. Obtained results confirm the presence of low-temperature plasticity (LTP) at temperatures above T = 78 K in Ge and Si crystals the main characteristic of which is covalent type of interatomic bond.

Each sample of germanium and silicon, influenced by strong uniaxial pressure, possesses the low-temperature plasticity peculiarities which depend on the previous background of the sample. First of all, we can observe certain dispersion ΔX for Ge and Si at which manifestations of LTP begin to take place. In addition, a little bit smaller dispersions are distinctive for the same germanium and silicon crystals.

However, we have observed general manifestations of LTP which are determined by its mechanisms. Firstly, it is confirmed by experiments, that LTP occurs at pressures much lower than theoretical strength of Ge and Si crystals. Secondly, all the manifestations of plasticity are observed at higher pressures with the decrease of temperature. Thirdly, it was shown that micro-plasticity of investigated crystals takes place at relatively low uniaxial pressures. Then, with the growth of X (to 1.5–2 GPa) the distribution of dislocations in the whole volume of Si crystals occurs at T = 300 K as well as at T = 78 K in Ge crystals.

This fact affirms our conclusions. It means that under proper conditions of the experiment at relatively low pressures each sample passes the stage of plasticity with the corresponding changes in the lattice at the surface of the crystal. In the area of strong uniaxial pressures we determined the presence of evidence of the LTP mechanism which is directly related to the interface model of this phenomenon in crystals with a covalent type of interatomic bond.

Also all metallographic experiments have confirmed that a strong uniaxial deformation at LTP leads to the generation of the dislocation cluster in the area of the interfacial boundaries of the crystals. Effects of LTP in germanium crystals are the most noticeable with inclusion of Sb impurity. A cluster of dislocations, which later form “dislocation cracks” leading to the fracture of the crystal, is created around these impurities. Thus, under uniaxial pressures, much lower than the theoretical strength of crystals, there is a change in the strength of semiconductor monocrystals due to the plastic deformation.

The Electrochemical Processes at the Phase Boundary *p*-GaAs Electrode-HF Water Solution

Pashchenko G.A., Trishchuk L.I.

V.Ye. Lashkaryov Institute of Semiconductor Physics, NAS of Ukraine, Kyiv, Ukraine,
trishchukli@ukr.net

Interest to mechanism of electrochemical processes at the interface semiconductor–electrolyte in relation of perspectives for using semiconductor electrodes in many topical areas of up-to-date technique and semiconductor electrodes are also used to determine a number of parameters inherent to the electrode material.

Investigated in this work have been polarization curves typical for the interface *p*-GaAs–HF water solution with the concentration of HF between 1 and 10 mass %. The shape of polarization curves corresponds to the state when exchange reactions at the above boundary take place mainly via the valence band with participation of holes. The absence of rectifying effect signs in polarization curves for the case of cathode bias is likely indicative of the fact that some part of voltage drops inside the Helmholtz layer, *i.e.*, the electrode potential j is distributed between the Helmholtz layer and space charge region (SCR) of semiconductor. Although, as a rule, in semiconductors (Si, Ge) the dominant part of electrode potential is concentrated in SCR for both states.

In our case, the potential was considered as a sum of overpotentials in the Helmholtz layer and SCR of semiconductor:

$j_a = (a\ h + h_1) = (RT/nF)\cdot\ln(i_a/i_p^0) = A_a + B_a\cdot\lg i_a$, where $A_a = -(0.0592/n)\cdot\lg i_p^0$,

$B_a = (0.0592/n)$.

$j_k = b\ h = (RT/nF)\cdot\ln(i_k/i_p^0) = A_k + B_k\cdot\lg i_k$, where $A_a = -(0.0592/n)\cdot\lg i_p^0$,

$B_a = (0.0592/n)$.

Here, n – number of electrons taking part in a single act discharge – ionization, i_p^0 – exchange current.

Received equation enables to determine the charge carrier transfer coefficients for cathode $b = 0.3$ and for anode $a = 0.7$ shifts, respectively. This relationship between b and a values is responsible for asymmetry of anodic and cathodic branches in the polarization curves. The exchange current for anode shift increased with the growth of the electrolyte concentration from 10^{-6} A/cm^2 up to $7\cdot10^{-6}$ A/cm^2 is related with the limiting diffusion current of solution particles, since it depends on the concentration of reducing and oxidizing particles near the surface. Determined also have been the ranges of current density ($2.4\cdot10^{-4}$ A/cm^2 - $3\cdot10^{-4}$ A/cm^2) where transfer of current carriers takes place through the boundary *p*-GaAs–HF water solution (electrochemical stage).

The slope of straight line j =f(Lgi) $B = 0.11$ V - 0.1 V. The graphically obtained *B*-values have intermediate magnitude, which confirmes our assumption that the potential is redistributed between SCR of semiconductor and the Helmholtz layer in the studied system *p*-GaAs–HF water solution.

Electron Mobility in CdSe Crystal

Petrus R.[1], Kashuba A.[1,2], Semkiv I.[1], Honchar F.[1]

[1]*Lviv Polytechnic National University, Faculty of Physics, Lviv, Ukraine,*
AndriyKashuba07@gmail.com
[2]*Ivan Franko National University of Lviv, Faculty of Electronics and Computer Technologies, Lviv, Ukraine*

Cadmium selenide (CdSe) is a promising semiconductor material for optoelectronic devices due to the room temperature band gap value (~ 1.8 eV) which are in the visible spectrum of radiation. It was established that CdSe crystals crystallize in the space group *P*63*mc* [1].

Information about effective electron mass (m*) for a material are very important. This value determines the dynamics of electron conductivity in it and therefore is significant for the corresponding practical applications. The effective electron mass m* is usually defined by the following relation from the band structure calculations [2]:

$$\frac{1}{m^*} \propto \frac{d^2E(k)}{dk^2}$$

$E(k)$ is the dependence of the band energy E on the electron wave vector k. The electron mobility μ is associated with m*:

$$m \propto \frac{t_i}{m^*}$$

where τ_i is the relaxation time, which is inversely proportional to the ionized impurity concentration n_i,

$$t_i \propto \frac{T^{3/2}}{n_i}$$

Here T is the thermodynamic temperature.

The theoretical calculations band structure was made using the electron density functional theory (DFT). For ionic potentials, the ultrasoft Vanderbilt pseudopotentials were used [3]. To describe the exchange correlation energy of the electron subsystem, the GGA functional with the PBE parameterization [4] was used.

1. Xu Yong-Nian, Ching W.Y. Electronic, optical, and structural properties of some wurtzite crystals. *Phys. Rev. B.* 1993. Vol. 48, № 7. P. 4335-4351.
2. Kohn W., Sham L.J. Self-Consistent Equations Including Exchange and Correlation Effects. Phys. Rev. A. 1965. Vol. 140, № 4A. P. A1133-A1138.
3. Hasan M.Z., Hossain M.M., Islam M.S., Parvin F., Islam A.K.M.A. Elastic, thermodynamic, electronic and optical properties of U_2Ti. *Computat. Mater. Sci.* 2012. Vol. 63, № 1. P. 256-260.
4. Sun Jian, Wang Hui-Tian. *Ab initio* investigations of optical properties of the high-pressure phases of ZnO Phys. Rev. B. 2005. Vol. 71, № 12. P. 125132.

Estimation of the size of Si clusters in the Al-Si melts according to the structure of rapidly cooled metal films

Prigunova A.G.

Physical and Technological Institute of Metals and Alloys of NASU, Kyiv, Ukraine,
adel_nayka@ukr.net

Aluminum-silicon melts have a micro-inhomogeneous structure. In a disordered zone representing microregions with a statistical distribution of Al and Si atoms, clusters of Si atoms are distributed - in hypoeutectic and eutectic melts and according to the AlxSi intermetallic type, where x = 3 ... 5, and Si - in hypereutectic melts [1]. The cluster size in the melt is determined by the structural factor. In the presence of atoms of several kinds, this is an integral quantity. The task is complicated if the alloy components in the solid state have a different type of bond: metallic in aluminum, covalent in silicon. The size of Si clusters in Al-Si melts was determined by the structure of films obtained by high-speed cooling from a liquid state (Vc. > 105 - 106 °C/s), followed by electron microscopic examination of films without additional thinning (Fig.1).

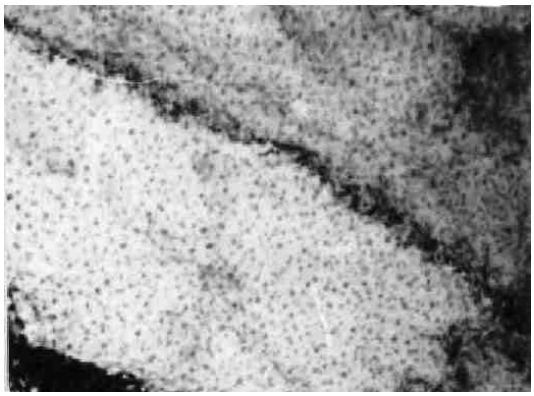

a

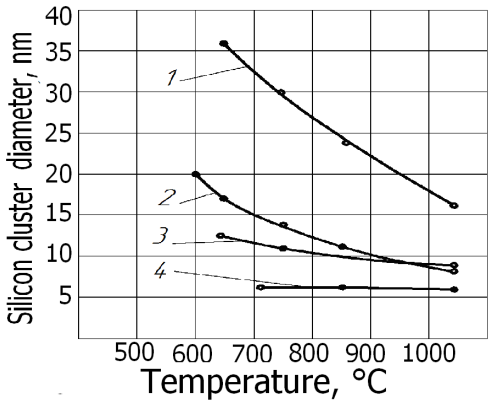

b

Fig.1 The structure of the film, representing the "frozen" melt Al - 6.5 % Si (a), and (b) the dependence of the size of the Si clusters on the melt temperature:
1 – Al - 6.5 % Si; 2 – Al - 12.5 % Si; 3 – Al - 15.5 % Si; 4 – Al - 16.5 % Si

With increasing temperature and Si concentration up to 16.5%, the size of silicon clusters in Al-Si melts decreases.

1. Study of the structure of liquid aluminum – silicon alloys / A.G. Prigunova, V.I. Mazur, Yu.N. Taran et al. // Metallophysics. – 1988. – Vol. 5: Part 1.–№ 1, p. 88 –94; Part 2. – № 3, p. 54–57, (in Russian).

Relative grain-boundary energy in undoped silicon films

Rodionova T.V.

Taras Shevchenko National University of Kyiv, Kyiv, Ukraine, rodtv@univ.kiev.ua

Since silicon films are widely used in microelectronics and solar energy, the issues of stability and reliability of elements containing silicon films are topical. The stability of the elements, in turn, is determined by the stability of the films structure, in particular, the grain-boundary structure [1].

In this work the relative grain-boundary energy of undoped silicon films depending on film thickness and structure types was determined by the method of grain boundary grooves with the use of atomic force microscopy (AFM).

Silicon films were prepared by low-pressure chemical vapor deposition. Films were deposited on thermally oxidized (100 nm oxide thickness) (100)Si wafers. The film thickness was ranged from 10 to 2200 nm. Depending on formation conditions, films had different structures: equiaxial, dendritic or fibrous. The equiaxial and fibrous structure was observed in films deposited at 630^0C. At film thickness < 70 nm -equiaxial, at thickness > 70 nm - fibrous. Dendritic structure was observed in films deposited in amorphous phase (the deposition temperature 560^0C) and annealed at temperature $\leq 1000^0$C [2]. The measurement of grain boundaries dihedral angles were performed by AFM.

Analysis of the data showed that the largest dihedral angle (178^0) and the lowest relative grain-boundary energy (0,02) are observed for undoped silicon films with a dendritic structure. The next with increasing relative grain-boundary energy (0,5) is equiaxed films. The smallest values of dihedral angles (141^0) and the largest values of the relative grain boundary energy (0,66 – 1,18, depending on the film thickness) are characteristic of films with fibrous structure. At thicknesses of 85 nm, a sharp increasing of relative grain boundary energy (1,62) is observed. This behavior correlates with changing of film structure from equiaxial to fibrous (at thickness $\geq$ 70 nm) and appearance of preferred orientation [110] [4]. The high relative energy of the grain boundaries in the fibrous silicon films is due to the presence of a large number of grain boundaries consisting of dislocations. Dislocations have a strong field of elastic stresses, which makes a significant contribution to the increase in grain-boundary energy.

1. Mukhopadhyay S. et al. Nanocrystalline silicon: A material for thin film solar cells with better stability. *Thin Solid Films.* 2008. V. 516, Issue 20, P. 6824-6828.
2. Nakhodkin N.G., Rodionova T.V. Formation of different types of polysilicon film structures and their grain growth under annealing. *Phys. Status Solidi A.* 1991. V. 123, № 2. P. 431-439.

Structural, Energy State and Electrokinetic Investigations of the $Zr_{1-x}V_xNiSn$ Semiconductive Thermoelectric Material

Romaka L.P.[1], Romaka V.A.[2], Stadnyk Yu.V.[1], Romaka V.V.[2,3], Horyn A.M.[1], Krayovskyy V.Ya.[2]

[1]*Ivan Franko National University of Lviv, Lviv, Ukraine,*
lyubov.romaka@gmail.com
[2]*National University "Lvivska Politechnika", Lviv, Ukraine*
[3]*Institute for Solid State Research, IFW-Dresden, Dresden, Germany*

Thermoelectric materials based on half-Heusler phases TiNiSn, ZrNiSn and HfNiSn are characterized by high efficiency of the conversion of thermal energy into electric [1]. However, the wide application of these materials is limited by uncontrolled changes in the crystal and electronic structures due to doping, which changes their properties. The crystal and electronic structure, electrokinetic and energy state characteristics of semiconductive $Zr_{1-x}V_xNiSn$ solid solution were studied to solve this problem.

The calculation of the density of electronic states (DOS) for all variants such as the distribution of atoms in the unit cell, and occupancy of all crystallographic sites by their own and/or other atoms, as well as presence of vacancies, was carried out. The optimal distribution of atoms in $Zr_{1-x}V_xNiSn$ structure was found, at which the motion rate of Fermi level ε_F calculated from DOS coincides with determined from the temperature dependences of $\ln\rho(1/T)$.

It was found that doping of ZrNiSn half-Heusler phase by V ($3d^34s^2$) atoms due to substitution of Zr ($4d^25s^2$) atoms in position 4*a* is accompanied by simultaneous occupation of Ni ($3d^84s^2$) atoms by V atoms in 4*c* position. As a result, in $Zr_{1-x}V_xNiSn$ semiconductive material the structural defects of donor nature (V atom has a greater number of *d*-electrons than Zr) and of acceptor nature (there is more 3*d*-electrons in Ni atoms than in V) are generated simultaneously. In this case, in the band gap of $Zr_{1-x}V_xNiSn$ the energy states of the impurity donor ε_D^2 and acceptor ε_A^1 levels (donor-acceptor pairs) appear, which determine the mechanisms of conduction in the semiconductor.

The simultaneous generation of donor-acceptor pairs provides the principle of electroneutrality and stability of the structure of $Zr_{1-x}V_xNiSn$ thermoelectric material and is a guarantee of the reproducibility of their characteristics.

1. V.A. Romaka, V.V. Romaka, Yu.V. Stadnyk. *Intermetallic semiconductors: properties and applications* // Lvivska politekhnika, Lviv, 2011, 488 p.

Migration of Sulfur to Surface of GaAs Stimulated by Vacancies

Saliy Ya.P.

Vasyl Stefanyk PreCarpathian National University, Ivano-Frankivsk, Ukraine,
saiyyroslav@gmail.com

It has been shown theoretically that intense migration of sulfur to GaAs surface is associated with vacancies. They formed near the surface of the semiconductor crystal when a dielectric film is deposited by a plasma-chemical method. To describe the migration of implanted impurities a model is used which takes into account the interaction of the impurity with these vacancies. Theoretical concentration profiles of electron are adequate experimental ones.

For the fabrication of optically active electronic devices as well as for ultrafast and radiation-resistant devices gallium arsenide (GaAs) is the material of choice. The diffusion behavior of impurities and native point defects in the material often determines the electrical properties of the final device. Diffusion processes therefore have to be studied carefully.

As is known, the electrical properties of the transition of the dielectric and semiconductor are determined by the crystalline and physical structure of the boundary of their separation.

In this paper we studied the stimulated by vacancies displacement of the impurity S in GaAs to the interface with a SiO_2 film deposited by the plasma-chemical method. To do this, we use a model of the interaction of impurities with vacancies formed at the settling of the film.

We assume that the electron concentration is associated with the ionized admixture S. To describe the migration processes and the interaction of impurities and vacancies, the equation are used:

$$\frac{1}{F}\frac{\partial C}{\partial t} = V(x,t)\frac{\partial^2 C}{\partial x^2} - C(x,t)\frac{\partial^2 V}{\partial x^2}, \qquad \frac{\partial V}{\partial t} = D_V\frac{\partial^2 V}{\partial x^2}.$$

The first equation takes into account that the impurity diffusion occurs with the displacement of vacancies, the flow of which is directed oppositely to the flow of atoms. The second equation is ordinary diffusion equation.

The solution of the system of differential equations is carried out in Excel. There was obtained a good agreement between calculated dependences and the experimental ones. The approximation parameters are obtained from the simultaneous fitting of the three experimental dependencies.

Conclusions

With the annealing of GaAs implanted with sulfur at temperatures around 800^0C, the migration of impurities through vacancies occurs intensively on the surface of the semiconductor if the dielectric is settled by a plasma-chemical method at a temperature of 400^0C. The model used by us adequately describes the experimental dependencies.

Influence of the Conditions of Heat Treatment and Thickness of the Layers on the Magnetoresistive Properties of Three-layer Films Based on $Fe_{80}Co_{20}$ Alloy and Cu

Saltykov D.I., Poduremne D.V., Shkurdoda Yu.O., Protsenko S.I.

Sumy State University, Sumy, Ukraine, dmytros94@gmail.com

Three-layer films, which consists of FeCo alloy layers, separated by a Cu layer were obtained by the method of layer-by-layer condensation. Measurement of the magnetoresistance (MR) and heat treatment of the films were carried out in a special device under ultrahigh oil-free vacuum ($10^{-6} \div 10^{-7}$) Pa in the magnetic field with induction to B = 0.2 T (special device). The films were heat treatment at the temperatures of 400, 550 and 700 K for 15 minutes then cooling. The magnetoresistance of the samples depends on both the heat treatment and the thickness of the layers. For as-deposited and annealed at temperatures of 400 and 550 K samples with d_{Cu} = 5-15 nm and d_{Cu} = 30-40 nm, an isotropic character of magnetoresistance is observed. Annealing at a temperature of 400 K leads to an increase in the amplitude of the isotropic MR in 2-3 times, and at a temperature of 550 K – 8-10 times. For all investigated three-layer films with d_{Cu} = 5-15 nm and d_F = 30-40 nm after annealing at a temperature of 700 K, an irreversible transition from the isotropic nature of magnetoresistance to anisotropic is fixed. The reason for changing the character of the magnetoresistance in this case is a breaking of the structural integrity of the copper layer. For all investigated samples, both as-deposited and annealed at different temperatures, only an increase in the magnitude of the isotropic magnetoresistance in 1.2-2 times at the temperature decreases in the whole temperature interval are fixed. As-deposited films with relatively thin magnetic layers (d_F = 10-20 nm, d_{Cu} = 5-15 nm) have anisotropic character of the magnetoresistance. After annealing at a temperature of 550 K, an isotropic magnetoresistance is observed, which is probably due to the formation of a granular alloy on the basis of Cu and $Fe_{80}Co_{20}$ ferromagnetic alloy. An increase in the annealing temperature to 700 K does not result to the appearance of anisotropic magnetoresistance, as was observed for films with relatively thick magnetic layers. It is fixed only a decrease in the isotropic magnetoresistance in 2-3 times. Besides, significant difference between the values obtained in the longitudinal and transverse measurement geometries is observed. This difference is due to the influence of anisotropic magnetoresistance of ferromagnetic layers. Reduction the temperature of the measurement to 120 K does not significantly affect on the form of field dependencies, whereas the value of isotropic MR grows in 1.2 - 1.8 times.

The work been performed under the financial support of the Ministry of Education and Science of Ukraine (state registration number №0118U003580 (2018-2020) and state program 2019-2021).

Optical and Electronic Characteristics of the CdMnTe solid Solution

Semkiv I.V.[1], Ilchuk H.A.[1], Petrus R.Yu.[1], Kashuba A.I.[1,2], Zmiiovska E.O.[1]

[1]*Lviv Polytechnic National University, Lviv, Ukraine*
[2] *Ivan Franko National University of Lviv, Lviv, Ukraine,*
Semkiv.Igor.5@gmail.com

Crystal solid solutions $Cd_{1-x}Mn_xTe$ were synthesized using the Bridgman vertical method in a quartz ampoule with a tapered bottom. The objects for investigation were thin plates (up to 100 microns) of a solid solution with the composition of $x = 0.12$ and 0.3.

The composition and crystal structure were measured using the X-ray diffraction method.

The study of the fundamental optical absorption edge was carried out using a spectrophotometer AvaSpec-2048 (AVANTES). Obtained spectral dependencies were plotted in coordinates $(\alpha hn)^{2/n}–hn$, where $n = 1$ for direct-gap semiconductors. On the graphs, there are linear regions that were approximated by a straight line to the intersection with the horizontal axis (energy or wavelength). This allowed obtained the value of the optical band gap of the solid solution. For a solid solution $Cd_{0.88}Mn_{0.12}Te$, the obtained value is $E_g = 1.664$ eV, and for $Cd_{0.7}Mn_{0.3}Te$ – $E_g = 1.989$ eV.

The electronic characteristics, namely the band structure, were calculated within the framework of the density functional theory (DFT). To describe the exchange-correlation properties of crystals, the generalized gradient approximation (GGA) was used (in the parametrization of Perdew, Burke and Ernzerhof (PBE)). The electron energy is determined from the Kohn–Sham equations, and for the ionic potentials description, the Vanderbilt Ultra-Soft Pseudopotential are used.

The calculations of the band structure were conducted for $Cd_{1-x}Mn_xTe$ solid solutions with the compositions x = 0.125, 0.375, 0.5. The results showed that the smallest energy intervals in the band gap are in the center of the Brillouin zone (point Γ). This once again confirms that CdMnTe is characterized by a direct band gap. The values of the bandgap width are $E_g = 1.66$ eB for x = 0.125, $E_g = 1.94$ eV for x = 0.375, $E_g = 2.1$ eV for x = 0.5.

We can see that theoretical calculations of the band gap are in good agreement with experimentally determined on the basis of optical absorption spectra. This allows us to use the obtained data to describe the nature of the change of the band gap width from the CdMnTe solid solution composition.

Modeling of Point Defects Structure in Mn-Doped CdTe Crystals

Solodin S.V., Fochuk P.M., Panchuk O.E.

Chernivtsi National University, Chernivtsi, Ukraine, fochukp@gmail.com

Up to now a clear understanding the nature of donor which defines electrical parameters of CdTe:Mn crystals is still missing. Nominally Mn atom, replacing atom Cd in the CdTe lattice, potentially forms electrically neutral atomic point defect Mn_{Cd} and should not reveal any electrical activity because it possesses two 4s-electrons only in the outer shell. However in some cases it is not true. Therefore, in this work a study of CdTe:Mn electrical properties using high temperature Hall effect measurements was performed.

Mn-doped CdTe crystals, with the 1×10^{17}-10^{19} at/cm^3 dopant concentration in the melt, were grown by the vertical Bridgman method. High-temperature Hall effect measurements were carried out on samples (12×2×1.5 mm^3) with six welded contacts.

For all measured crystals was obtained a higher free electron density comparatively undoped CdTe: increase of the lg[e$^-$] value varied around ~0.4 (Fig.1). These experimental data were used for a computer simulation applied Kroeger's quasi-chemical approach. Between the possibilities of whether predominantly Mn-single donors or Mn-containing associates occurrence the second possibility was confirmed. The ionization energy of Mn donor atoms was estimated to be ~ 0.1 eV.

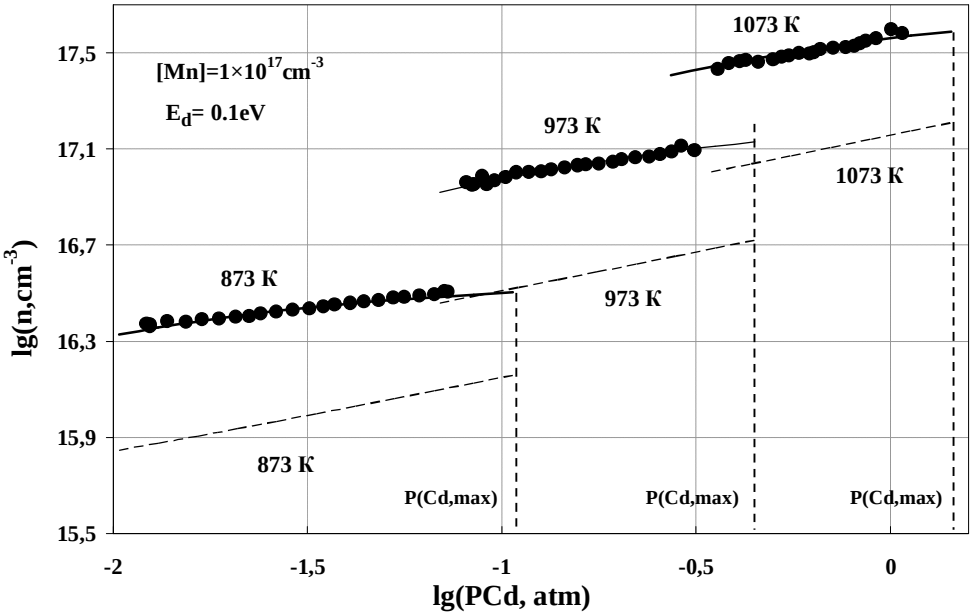

Fig.1. The modelled lg[e$^-$] versus lgP(Cd) isotherms at 873-1073 K assuming both single Mn donors and Mn associates occurrence

Distribution of Local Deformation in Germanium Plates Defined by the Power Fourier Spectrum of Kikuchi Patterns

Solodkyi M.[1], Balovsyak S.[1], Borcha M.[1], Fodchuk I.[1], Kuzmin A.[1], Tkach V.[2]

[1] *Yuriy Fedkovych Chernivtsi National University, Chernivtsi, Ukraine*
[2] *V. Bakyl Institute for Superhard Materials of NASU, Kyiv, Ukraine, ifodchuk@ukr.net*

A new approach of local strain determination in separate local areas (grains) of polycrystalline germanium is proposed. A discrete two-dimensional Fourier transform and the power Fourier spectrum are used to analyze the shape and area changes of the intensity profile of the Kikuchi bands. This significantly increased the informative and unambiguous interpretation of changes in the geometry (profile shape) of the Kikuchi bands.

A set of Ge plates of different degrees of perfection was studied using the methods of high-resolution X-ray diffraction and electron backscatter diffraction (the Kikuchi method), which is realized with a Philips X'Pert PRO diffractometer and Zeiss EVO-50 scanning electron microscope using a CCD detector, respectively. The values of strains in single crystalline grains and on the boundaries between them were determined. The obtained cathodoluminescence images and X-ray diffractometry demonstrate structural inhomogeneity and imperfection of the sample. Kikuchi patterns from different areas of the sample revealed different intensity distributions on Kikuchi bands. To determine the strain values the Fourier analysis of the Kikuchi patterns is carried out. Energy spectra of images were calculated using a fast two-dimensional discrete Fourier transformation [1].

The relationship between periods of energy spectra and strain values was established using radial intensity distributions on Kikuchi pattern. Due to locality of method, we studied the strain changes from one sample area to another. It should be noted that using artificial neural networks for analysing the energy spectrum of experimental image is promising for constructing strain map of polycrystalline plates.

Different approaches to the analysis of Ge gave possibility to determine the components of the strain tensor and their averaged values in single crystalline grains. The magnitude of local strains increases in direction to the grain boundary.

1. Borcha M., Balovsyak S., Fodchuk I., Khomenko V., Kroitor O. Tkach M., Local strains in diamond crystals determined by Fourier-transformation of Kikuchi patterns, *Journal of Superhard Materials*. 2013. 35, №5. P. 284-291.

Physical and Mechanical Properties of Structurally Perfect Diamond Single Crystals

Suprun O. M., Lysakovskyi V. V., Zanevskii O. O.

Institute for Superhard Materials, National Academy of Sciences of Ukraine, Kiev, Ukraine, alona.suprun@gmail.com

Diamond single crystals are widely used in electronics and semiconductor technology as heat sinks, optical windows, plates for initiating CVD deposition. It is necessary to know the values of microhardness, yield strengths, strain hardening of single crystal samples to providing the required properties of diamond single crystals for their further industrial using. Knowledge of parameters that show above is needed to provide the required properties and becomes especially important due to the opportunities for obtaining diamond semi conduction crystals and the use of diamond single crystals of a controlled defect-impurity composition in computer technologies.

The microhardness of the diamond type Ib, IIa and IIb single crystals during high-temperature indentation (900 – 950 °C) was studied. On the basis of the physical-mathematical model of the "penetrating core" equations, the physical-mechanical characteristics of the diamond have been calculated taking into account the presence of elastic-plastic deformation in both the sample and indenter.

On the basis of the proposed model, an approximate estimate of the average deformations in the region of the contact between sample and indent was carried out. The relative sizes of the elastic-plastic zones in the indenter and the sample were determined, which are 0,93 – 1,05 μm and 1,14 – 1,35 μm, respectively. The microhardness of structurally perfect type IIa diamond single crystals (79,36 ± 2,5 GPa) in 1,5 times higher the microhardness of single type Ib crystals (47,46 ± 7 GPa) and IIb (50,9 ± 2,5 GPa).

Diamond characterized by significant deformation strengthening and low mobility of dislocation under high temperatures. The deformation strengthening of diamond is due to the high shear modulus and the low mobility of dislocations, which leads to a very low value of the average value of the dislocation range. The magnitudes of microhardness and yield strength of diamonds for various types depend on the degree of deformation and increase with decreasing angles at the top part of the indenter. The ratio of the microhardness value to the value of the yield strength for diamond single crystals of all types at a temperature of 900 – 950 °C is approximately equal to 1.

Luminescent Properties and Electronic Structure of Pr^{3+} and Eu^{3+} - Doped $BiPO_4$ Nanocrystals

Terebilenko, K.V.[1], Nedilko, S.G.[1], Slobodyanik, M.S.[1],
Chornii, V.P.[1,2], Boyko, V.V.[2],

[1] *Taras Shevchenko National University of Kyiv, Kyiv, Ukraine, kterebilenko@gmail.com*
[2]*National University of Life and Environmental Sciences of Ukraine, Kyiv, Ukraine*

An affordable and clean energy is one of the key goals claimed by United Nations Organization to maintain future sustainable development. In this light significant attention has been paid to ensuring technological innovations in modern energy services. One of the targets being intensively studied is search for luminescent materials with intense red light for white LEDs. In this work, the luminescence properties of polycrystalline $BiPO_4$ doped with Eu^{3+} and Pr^{3+} ions and composites based on it are studied. The choice of the host - bismuth orthophosphate - is related to the simplicity of doping by rare earth element ions (RE) and the presence of three structural polymorphs (different site environments for RE ions). In addition, $BiPO_4$ as a representative of phosphates family is characterized by good physical and chemical properties, while europium and praseodymium ions within close structurally hosts have intense luminescence in the orange-red spectral region.

Finely grinded polycrystalline samples of europium and praseodymium ions doped bismuth orthophosphate are obtained by solid state synthesis. The structural features of the samples were studied by powder X-ray powder difraction using the SHIMADZU XRD-6000 diffractometer. The luminescence characteristics were obtained using a double monochromator DFS-12. A diode pumped laser (λ_{exc} = 473 nm) was used as a source of photoluminescence excitation. The photoluminescence excitation spectra were recorded using a DXeL-1000 Xenon lamp and a DMR-4 prism monochromator. Electronic band structures of both perfect and with defect $BiPO_4$ crystals were calculated by the FLAPW method realized in Wien2k package [1].

It has been established that polycrystalline samples of $BiPO_4$ doped with Eu^{3+} and Pr^{3+} ions reveal intense red luminescence in the case of excitation at 473 nm and room temperature. All observed lines are associated with characteristic *f-f* transitions in the rare-earth ions while the luminescence of the host was not observed. Analysis of the luminescence properties of the doped $BiPO_4$ compounds suggests that the investigated materials are promising red phosphors for LED and some other applications.

1 P. Blaha, K. Schwarz, G. Madsen, et al., WIEN2k, An Augmented Plane Wave + Local Orbitals Program for Calculating Crystal Properties, *ISBN 3-9501031-1-2*, Wien, Austria, 2001.

Study of the Thermal Processes During Cathode-Arc Deposition Using the Truncated Cone Emitter Model

Titov I.N.[1], Nedolya A.V.[2]

[1]*UAD-Systems, Zaporizhzhya, Ukraine, titovigorn@gmail.com*
[2]*Zaporizhzhya National University, Zaporizhzhya, Ukraine*

The vacuum-arc method is widely used for deposition of pure metals to the shaped surfaces. However, the deposition process is accompanied by the droplet appearance, which leads to the non-uniform metal film formation [1, 2].It is difficult to choose the technological parameters of the deposition due to the fleeting processes. Therefore, the model creation is an actual task that adequately describes of the thermal parameters at the heating the emitter. We propose a model that takes into account the cone-shaped emitter. The model includes the thermal conductivity equation for the truncated cone emitter presented in a cylindrical coordinate system, where the temperature does not depend on the polar angle φ, because of the axial symmetry:

$$\rho C_0 (1+\alpha T)\frac{\partial T}{\partial t} = \lambda_0 \left(\mathbf{e}_r \frac{\partial}{\partial r} + \mathbf{e}_z \frac{\partial}{\partial z} \right)(1-\beta T)\left(\mathbf{e}_r \frac{\partial T}{\partial r} + \mathbf{e}_z \frac{\partial T}{\partial z} \right) - j_e \frac{C_e}{e}\frac{\partial T}{\partial z} + j_e \chi , \quad (1)$$

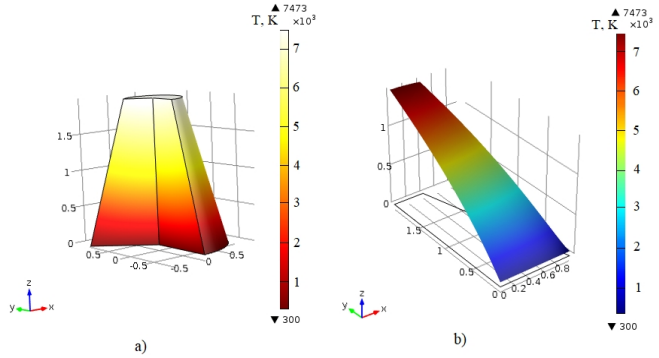

Fig. 1. Temperature distribution in the cone-shaped tungsten emitter (a) and its spatial distribution (b).

where $\mathbf{e}_r$ and $\mathbf{e}_z$ are the basis vectors of the cylindrical coordinate system, j_e – the electron current density from the cathode, ρ is the density of the emitter material, C_e – the electronic heat capacity, χ – the resistivity. The temperature distribution on a cone-shaped tungsten emitter was calculated using the mathematical model containing corresponding initial and boundary conditions, some of which were solved analytically (Fig. 1).

The model takes into account the temperature dependence of the heat conductivity and heat capacity coefficients and allows us to determine the technological parameters for the effective deposition of metals to the substrate using the vacuum arc.

1. Anders A. Some applications of cathodic arc coatings. In: Cathodic arcs. Springer series on atomic, optical, and plasma physics. 2008. V. 50. Springer: New York, USA. P. 1 - 42.
2. Takikawa H., Tanoue H. Review of cathodic arc deposition for preparing droplet-free thin films. IEEE Transaction on Plasma Science, 2007. V. 35, 4. P. 992-999.

Defect subsystem of $Pb_{1-x}Ag_xTe$ solid solutions

Turovska L.V.

Ivano-Frankivsk National Medical University, Ivano-Frankivsk, Ukraine, tlv87@i.ua

Nowadays, the issue of improving the efficiency of converting heat into electricity is highly important due to the problem of environmental pollution. So, lead telluride is promising thermoelectric material as its basic parameters can be changed effectively by doping and forming solid solutions. It is worth paying attention to silver, which has a number of advantages among other acceptor impurities, the behaviour of which is studied insufficiently in comparison with donor impurities.

In this paper, the analysis of possible mechanisms of formation of $Pb_{1-x}Ag_xTe$ solid solutions based on lead telluride has been presented.

For an explanation of the acceptor effect of silver dopant, we have offered the crystalloquasichemical formulas for n- and p-$Pb_{1-x}Ag_xTe$, taking into account the disordering in the cation sublattice:

$$V_{Pb}^{2-}V_{Te}^{2+} + Ag^0 + Te^0 \rightarrow \left[Ag_{1-z}^{-}Ag_z^0\right]_{Pb} Te_{Te}^0 + (1-z)h^+,$$

where z is coefficient of disproportionation of dopant charge state.

As $Pb_{1-x}Ag_xTe$ solid solutions are substitutional solutions according to the results of X-ray analysis, we have established that the main point defects in $Pb_{1-x}Ag_xTe$ are silver ions in cationic sublattice: Ag_{Pb}^{-} and Ag_{Pb}^{0}, whose concentrations increase with the content of AgTe, and, moreover, if in n-$Pb_{1-x}Ag_xTe$ tellurium vacancies V_{Te}^{2+} are dominant intrinsic defects, then in p-$Pb_{1-x}Ag_xTe$ cation vacancies V_{Pb}^{2-} dominate, which concentrations vary slightly with increase of the dopant content.

The proposed model satisfactorily explains the experimental data. We can assume that low effectiveness of the doping impurity is caused by the fact that most silver atoms are in an electroneutral state in a lattice ($z > 0.9$). Conditions of realization of n-p-conductivity change in n-$Pb_{1-x}Ag_xTe$ have been determined.

The analytical expressions for the concentrations of point defects and Hall concentration of current carriers in n- and p-$Pb_{1-x}Ag_xTe$ solid solutions have been derived, and their dependences on composition and dopant charge state have been calculated.

Thermoelectric Properties of $PbSe_{1-x}Te_x$ Solid Solutions

Vodoriz O.S., Tavrina T.V., Rogachova O.I.

National Technical University "KhPI", Kharkiv, Ukraine,
vodorez@kpi.kharkov.ua

The important characteristic of a thermoelectric (TE) material is the TE figure of merit $Z = \frac{S^2 s}{l}$ (S is the Seebeck coefficient, σ is the electrical conductivity, $S^2\sigma$ is the TE power and λ is the thermal conductivity). Increase in Z is achieved by creating of solid solutions with subsequent doping to obtain optimal charge carrier concentration. Isovalent and isostructural PbSe-PbTe solid solutions are among the promising TE materials. In [1] we reported about the nonmonotonic character of properties' dependences (microhardness, Seebeck coefficient, Hall coefficient, electrical conductivity, Hall mobility of charge carriers, thermal conductivity) of $PbTe_{1-x}Se_x$ (x = 0 – 0.05) solid solutions for both cast and pressed samples. The existence of anomalies was explained in the framework of percolation theory [2].

In this work a study of the TE properties (S, σ, λ, $S^2\sigma$ and Z) in the pressed samples of undoped solid solutions $PbSe_{1-x}Te_x$ (x = 0 – 0.045) at room temperature was conducted.

The samples for studies were prepared by hot pressing of cast samples (temperature 670 K, pressure 400 MPa) with subsequent annealing (temperature 720 K, duration 260 hours). All the samples were of *p*-type conductivity.

The Seebeck coefficient S was measured by compensation method in relation to copper electrodes; the electrical conductivity σ measurements were carried out by a four-probe method; the thermal conductivity λ was measured by dynamic calorimeter method. Relative mean-square fluctuation for all samples did not exceed 3 %, 7 % and 5 % for S, σ and λ, consequently.

It was established that all dependences of properties (S, σ, λ, $S^2\sigma$ and Z) on the composition of solid solutions have a nonmonotonic character. Anomalous growth in TE parameters in the vicinity x = 0.01 and x = 0.02 was found and associated with the interaction processes in the defect subsystem of the crystal under the transition from dilute to concentrated solid solutions.

The nonmonotonic character of concentration dependences should be taken into account under the subsequent doping of solid solutions for improving their TE properties.

1. Rogacheva E.I., Vodorez O.S. Peculiarities of the concentration dependences of structural and thermoelectric properties in solid solutions PbTe-PbSe. J. *Thermoelectricity*., 2013. V. 2. P. 61 – 73.
2. Stauffer D. and Aharony A. Introduction to Percolation Theory. Washington, DC: Taylor&Francis, 1992.

Influence of $Cd_{1-x}Mn_xTe$:In Crystals Purification by Te Zone on Electro-physical and Optical Properties

Zakharuk Z.I, Dremlyuzhenko S.G., Kolisnik M.G., Rarenko A.I., Fochuk P.M.

Yuriy Fedkovych Chernivtsi National University, Chernivtsi, Ukraine,
microel-dpt@chnu.edu.ua

At present, it is actual to obtain the perfect $Cd_{1-x}Mn_xTe$ single crystals, which are used as a material for fabrication of gamma-radiation detectors. In connection with this, it is interesting to study the growth process features of photosensitive high-ohmic $Cd_{1-x}Mn_xTe$ crystals suitable for the creation of these devices and investigation of their optical and electro-physical characteristics. High resistivity in these crystals can be achieved by doping with In impurity in small concentrations.

To conduct experiments the In-doped $Cd_{1-x}Mn_xTe$ (x=0,05; 0,1) crystals with the concentration of 3.5×10^{17} cm^{-3} were grown by Bridgman method. From the beginning, middle and end of the grown ingots, the pieces were cut off to carry out the control electro-physical and optical measurements, and the rest were loaded again into ampoule, in which at the bottom 5÷10 grams of Te was placed. Then ampoule with the material was inserted into the set-up for purification by a travelling heater method (THM). The process was carried out at a Te zone temperature of 1020K with the rotation of the ampoule around the axis at an angle to the horizon for melt mixing. After purification, the ingot end enriched by impurities was taken out, the ingot top was moved down and the crystal was grown again by Bridgman method.

Temperature dependence investigations of specific electro-conductivity, Hall constant, charge carrier mobility and optical transmission showed that after the first growing by Bridgman method, crystals was low-ohmic (n-type) and heterogeneous. The influence of In impurity along the ingots was consistent with the segregation coefficient, which has a value considerably smaller than unit. Hall mobility of equilibrium electrons was limited by the drift barriers and localized spatial-charge regions. The optical transmission in the IR region decreased from 60% at a wavelength of 2 μm to 20% at a wavelength of 20 μm.

In $Cd_{1-x}Mn_xTe$ crystals (x = 0.05; 0.1) previously purified by Te zone, the doping by In impurity in low concentrations is accompanied by the introduction of deep compensated donors, which provide a low concentration of equilibrium current carriers. The material resistance increases to a value of $1,5\div2,8\times10^{10}$ Ω·cm, the charge carriers mobility becomes equal to 235 $cm^2/V\cdot s$, and the optical transmission was stable in all long-wavelength region of the spectrum. It is possible to assert that the preliminary purification of the ingot by Te zone using the THM contributes to a significant improvement of electric characteristics. Influence of drift barriers on the electrons' mobility is reduced.

Spectral Dependence of the Absorption Coefficient $Tl_2S–Ga_2S_3–GeS_2$

Zamurueva O.V., Kityk I.V., Piskach L. V., Tsisar O.V., Piaseski M.

Lesya Ukrainka Eastern European National University,
Lutsk, Ukraine,
Zamurueva.o@gmail.com

Bandgap width E_g was estimated from the spectral distribution of the absorption coefficient at the fundamental absorption edge (for $\alpha \approx 550$ cm^{-1}) [1].

The increase of E_g with the concentration of Tl_2S and Ga_2S_3 (modifiers) is related to the distortion of the glass-forming matrix due to the introduction of Tl^+ and Ga^{3+} ions, which have larger radii compared to germanium [1].

The site disorder of atomic positions in non-crystalline materials results in the formation of tails of the density of states at the edge of the permitted energy bands which leads to exponential dependence of the absorption coefficient. This exponential dependence of α(hν) is observed from the high-energy part of the spectrum indicating the adherence to Urbach's rule that describes the edge of the fundamental absorption band in disordered systems [2].

Characteristic energy $\Delta = d(h\nu)/d(\ln\alpha)$ which defines a degree of the absorption edge tailing was determined from the energy dependence of the absorption coefficient and Urbach's rule. The parameter Δ lies for all samples in the range of 0.10–0.20 eV which is consistent with the data of [2] which state that the slope of Urbach's edge $\Delta = 0.05–0.25$ eV for a variety of vitreous systems.

In our case, the value of Δ depends on the composition of glassy alloys. Increasing concentration of Tl_2S and Ga_2S_3 (modifiers) results in an increase of the steepness of the absorption edge (lower tailing) which can be interpreted as a decrease in value of the random potential relief for electrons in the tails of the density of states adjacent to the band edges.

1. Photothermal poling of glass complexes $Ag_2S–Ga_2S_3 – P_2S_5$. / O.V. Parasyuk, A.H. Reshak, T.L. Klymuk, I.I. Mazurets, O.V., Zamuruyeva, G.L. Myronchuk, J. Owsik // *Opt. Commun.* 2013. Vol – 307. P.1–4.
2. $Tl_2S–Ga_2S_3 – GeS_2$ glasses for optically operated laser third harmonic generation / O. V. Tsisar, L. V. Piskach, O. V. Parasyuk, L. P. Marushko, D. Olekseyuk, O. V. Zamuruyeva, P. Czaja, P. Karasiński, A. M. El‑Naggar, A. A. Albassam, G. Lakshminarayana // *J Mater Sci: Mater Electron.* 2017. 28:19003–19009 DOI 10.1007 / s10854-017-7854-x.

Effect of B_2O_3 Additive to the Systems GeO_2-Ge (GeO), ZnO-Ge on the Properties of Obtained Thin-Film Coatings

Zinchenko V.F.[1], Magunov I.R.[1], Volchak G.V.[1], Mozkova O.V.[2]

[1]*A.V.Bogatsky Physico-Chemical Institute of NAS of Ukraine, Odessa, Ukraine, vfzinchenko@ukr.net*
[2]*State Enterprise for Special Instrument Making "Arsenal", Kyiv, Ukraine, borisgor@i.com.ua*

Boron oxide, B_2O_3 possesses the very wide area of existence in the liquid state - from 450°C (melting temperature) to 2200°C (boiling temperature). It stipulates its application as a gumboil and vitrificator. On the other hand, systems GeO_2 - Ge and ZnO - Ge are actively studied with the purpose of receipt of thin-film coatings of the visible and, mainly, IR spectrum ranges.

The aim of the actual work is a study of effect of addition of B_2O_3 on properties of the indicated systems and thin-film coatings obtained from them.

As a source of B_2O_3 for convenience ortho-boric acid was used that, unlike B_2O_3, is non-hygroscopic and is well exposed to treatment (grinding, pressing). Addition was calculated on the ratio B_2O_3: MO_x (M - GeO_2, ZnO) =1:1. Annealing of butch was carried out in the interval of temperatures up to 900°C with the purpose of complete removing of water up to beginning of GeO evaporation, appearing through CVD mechanism.

Because of X-ray amorphous character of the resulting composites the interaction between their components is studied by the methods of IR spectroscopy of transmission and electronic spectroscopy of diffuse reflectance. In the first of the systems there is superposition of peaks of IR spectrums of B_2O_3 and GeO_2 that specifies on introducing B_2O_3 in the GeO_2 structure with formation of the mixed borato-germanate glasses. It is caused by the closeness of acid-basic properties of components and their general propensity to vitrification. Opposite, in the second system there is a dramatic change of character of an IR spectrum that is explained by the expressed acid-basic interaction between ZnO and B_2O_3.

The test carried out by the method of thermal evaporation in the vacuum of composites of the systems showed a negative effect of B_2O_3 addition on character of evaporation (instability of process, burning out of vaporizer) and produced coatings (insufficient thickness, low operational parameters). The reason there is weakening of interaction of MO_x with Ge because of vitrification or binding in durable compounds (in case of ZnO). Such behavior differs essentially from influence of addition of B_2O_3 on GeO, introduction of which improves the manufacturability of process of evaporation of GeO and operational properties of the obtained coatings.

POSTER REPORTS

Session 6
Thin films technology for energy application

Uv-Initiated Formation of Thin Films on the Basis of Interpenetrating Polymer Networks for Solar Cells Coatings

Iarova N., Samoilenko T., Brovko O., Horbatenko O.

Institute of Macromolecular Chemistry of the National Academy of Science of Ukraine
Kyiv, Ukraine, ynv25@ukr.net

It is difficult to overestimate the benefits of cost-effective, environmental-friendly solar energy in our modern technogenically polluted world with ever-increasing needs and, at the same time, limited resources. Therefore, the simplification and cheapening of the solar cells production, which would provide their more widespread application, is a current important task for scientists. It is known that one of the elements of the solar collector is a transparent protective coating. Such a coating is typically comprised from glass, which makes it both heavy and fragile. A promising alternative to glass plates is polymer films, among which the most attention is paid to polycarbonate ones. However, due to their not very high optical transparency (up to 85%), thin films on the basis of simultaneous photocured epoxy-acrylate interpenetrating polymeric networks (IPNs) with an optical transparency of about 92% may be proposed for such purposes. In addition, they reveal other essential technological and operational advantages. Despite the known fact of difficult formation of thin acrylate-containing films by free radical polymerization due to its inhibition by the air oxygen, introducing an epoxy component, which serves as a barrier for oxygen diffusion to the reactive system, it is possible to obtain completely cured films with good physical and chemical characteristics without the need to create laminates or inert atmospheres. The presence of an acrylate, in turn, contributes to a more complete polymerization of the epoxide.

It was found that for the formation of coatings the use of epoxy-acrylate IPNs with the following mass ratios of components is preferred: UP-650T/UP-650D/TEGDM=25/25/50 (where UP-650T – 1-(2’,3'-epoxypropoxymethyl)-1-(2",3"-epoxypropoxymethyl)-3,4-epoxycyclohexane, cycloaliphatic-aliphatic triepoxide, UP-650D-1-(2',3'-epoxy-propoxymethyl)-1-(2",3"-epoxypropoxy-methyl)-cyclohex-3-ene, aliphatic diepoxide, and TEGDM - triethylene glycol dimethacrylate). Introducing of aliphatic and cycloaliphatic epoxides in the composition of the epoxy-acrylate IPNs, it is succeeded to combine the high hardness provided by UP-650T with high impact resistance provided by the UP-650D, which is especially important in terms of protective coatings formation.

Other advantages are attributed to simple and energy-saving essence of photocuring technology. The use of UV-light to initiate the polymerization processes instead of high temperatures allows not only to significantly shorten the preparation time, but also to reduce the energy costs necessary for the formation of films. Moreover, the use of solar radiation makes it even free of charge. In addition, polymerization in natural conditions provides the opportunity to form and repair protective coatings directly at the place of operation.

Some Features of Electronic Structure of Tetracene - Silicon Claster with Halogens

Smertenko P.S.[1], Roshchina N.M.[1], Solntsev V.S.[1], Katashinski A.S.[2], Barsukov V.Z.[2]

[1]*V.Lashkaryov Institute of Semiconductor Physics, NAS of Ukraine, Kyiv, Ukraine,* petrosmertenko@gmail.com

[2]*Kyiv National University of Technologies and Design, Kyiv, Ukraine*

For understanding of interaction between tetracene and silicon substrate some items were considered: (i) the theoretical study of interaction between tetracene and silicon substrate by quantum chemistry approach; (ii) the elucidton of the chalcogenide role in formation of effectiveness of tetracene-silicon hybrids for solar cells; (iii) calculation of electron density distribution and structural parameters. Silicon and tetracene with substitution of H atoms by Cl, F i Br atoms was under consideration. Quantum chemical calculation of electronic structure and their parameters of molecular clusters and complexes were made on the base of Hartree-Fock-Roothaan self-consistent field formalism [1] with the use of valence split basic 3-21G(d,p) set [2]. The calculation was made with full optimization of all structural parameters. The surface of crystalline silicon was modeled by molecular cluster $Si_{59}H_{54}$. For calculation the Firefly Programmed, version 8.2 was used [3]. The accuracy of structural parameters optimization was determined by maximum value of 10^{-5} Hartree-Fock derivatives of energy in Dekart coordinates. The equilibrium lengths of created the R(Si-C) intercenter adsorbtion bonds are close to sum of covalent radii of Si and C atoms. The calculation results show that the substitution of H atoms in tetracene for chalcogene atoms the R(Si-C) adsorption bonds length is increased and the corresponding p (Si-C) bonds are decreased. This evidences the subsiding of bond energy between cluster surface and corresponded adsorption substance. The forbidden zone width of silicon calculated is about 1,12 eV; at the same time the forbidden zone width in complexes is decreased on average up to 0.33 eV. The hybridization of electron envelope of C atoms, which created the bonds with Si atoms, s from sp^2 - to sp^3 - hybridization.

1. Butyrskaya E.V. Computer Chemistry: Theory Basis and work with Gaussian and GaussView Programmes [“Library for students”]. Moscow. Solon-Press, 2011. – 224 p.
2. Davidson E. R., Feller D. Basis set selection for molecular calculations. *Chem. Rev*. **86**,(4) 681–696 (1986).
3. M. W. Schmidt, K. K. Baldridge, J. A. Boatz [et al.]. General atomic and molecular electronic structure system. *J. Comput. Chem*. **14**, (11) 1347–1363 (1993).

Laser Synthesis of Silicon and Metal Oxide Nanostructures for Thin Film Fabrication

Shustava Elizaveta[1], Kiris Vasilii[1], Tarasenko Nikolai[1], Nevar Alena[1], Butsen Andrei[2], Zhavrid Kate[2], Mazgel Yulia[2]

[1]B. I. Stepanov Institute of Physics, National Academy of Sciences of Belarus, Minsk, Belarus
[2] Belarusian State Technological University, Minsk, Belarus, a.butsen@gmail.com

The materials for the new generation of photovoltaic cells are required to be effective, stable, environmentally friendly, energy-efficient and low-cost. The most promising materials are semiconductor nanomaterials, in particular, metal oxides and silicon quantum dots [1]. They are of particular interest for photovoltaic due to their optical and electronic properties, attributed due to surface and quantum-size effects. For instance, copper oxide (CuO) is a p-type semiconductor with a bandgap of 1.5 eV, that is close to the ideal bandgap of 1.4 eV, which is necessary in solar cells to ensure effective absorption of radiation from the solar spectrum. ZnO nanoparticles as the active layer of a solar cell can convert up to 40 % of the incident photons at a wavelength of 500 nm.

In this paper, copper and zinc oxides nanoparticles (NPs) were synthesized by pulsed laser ablation in liquids (distilled water and ethanol) using radiation of Nd:YAG laser operating at fundamental frequency. With applying of absorption spectroscopy, transmission and scanning electron microscopy, optical and structural-morphological properties of the formed particles were studied. Detailed physical and chemical characterization of the produced NPs confirmed the characteristic crystal structure and chemical composition of NPs with broadening of the bandgap induced by the quantum confinement. The possibility of film layers creating by depositing and assembling colloidal particles in organized structures on the surface of an indium-tin oxide (ITO) substrate was demonstrated. For thin film production, spin-coating and blade-coating methods were used. The perspectives of application of produced structures photovoltaic cells are discussed.

1. M. Rokhmat, Wibowo E., et.al. Performance Improvement of TiO_2/CuO Solar Cell by Growing Copper Particle Using Fix Current Electroplating Method. Procedia Engineering. 2017. V.170.P.72-77.

$PbTe/Bi_2Te_3$ thin films grown by PLD method

Virt I.S. [1,2], Tur Yu.[1], Dziedzic A.[2], Cieniek B.[2], Żak D.[2], Lopatynskyi I.Ye.[3], Frugynskyi M. S.[3]

[1]*Drogobych State Pedagogical University, Drogobych, Ukraine, isvirt@email.ua*
[2]*University of Rzeszow, Rzeszow, Poland,*
[3]*National University "Lviv Polytechnic", Lviv, Ukraine*

To form thermoelectric converters with high figure of merit in low and medium temperature ranges and infrared receivers of wide range, semiconductor compounds based on lead chalcogenides (IV-VI). Using solid solutions based on PbTe as thermoelectric converters requires dopants which can increase its thermoelectric efficiency. The present work studies effects of doping thin films in the range of solid solutions on temperature dependence of electrical conductivity and thermoelectric power in the temperature range of 300 – 480 K.

The morphology and compositional analysis of PbTe and Bi_2Te_3 were examined using a scanning electron microscope (Qunta FEG). The structural analysis of the films was carried out by Bruker D8 diffractometer. Very sharp peaks are present, with the highest maximum intensity corresponding of the face-centered cubic PbTe to the (200) plane. The crystallite sizes “D” of both PbTe and Bi_2Te_3 prepared films were determined according is the full width at half maximum “FWHM” of the XRD peak. The dislocation density is a measure of angular lattice misalignment of crystallites and onsequently gives us information about the local density of the accumulated dislocations and the strain “ε”. SEM micrograph of PbTe shows micro-flowers are clearly seen and their formation from cubes is observed; furthermore, dendrites are observed. We have investigated Raman spectra from the thin films and discuss the causes leading to the frequency shift of the Raman modes.

The data obtained show that for all the compounds under study an increase in temperature leads to an increase in the thermoelectric power coefficient. Using the obtained experimental values of the specific electrical conductivity and thermoelectric power for all the compounds under study, we calculated the specific thermoelectric energy (thermoelectric power factor). We attribute this remarkably decreased value to the well-preserved nanoscale grain boundaries which enhance the phonon-phonon scattering, resulting in values ZT.

1. Zhoua C., Dunc C., Wang K., Zhang X., Shi Z., Liu G., Hewitt C.A., Qiao G., Carroll D.L. General method of synthesis ultrathin ternary metal chalcogenide nanowires for potential thermoelectric applications. *Nano Energy*. 2016. V.30, N12. P. 709–716.
2. A. Azab, Azza A. Ward, G. M. Mahmoud Eman M. El-Hanafy, H. El-Zahed, and F. S. Terra Structural and dielectric properties of prepared PbS and PbTe nanomaterials *Journal of Semiconductors*. 2018. Vol. 39, No. 12. P. 123006-2 –123006-8.

TiO_2/Cu_2O Heterojunctions for Photovoltaic Cells Application Produced by Reactive Magnetron Sputtering

Wisz G.[1], Sawicka-Chudy P.[1], Yavorskyi R.[2], Potera P.[1], Bester M.[1], Głowa Ł.[1]

[1]*Faculty of Mathematics and Natural Sciences, Rzeszow University, Rzeszow, Poland, gwisz@ur.edu.pl*

[2]*Vasyl Stefanyk Precarpathian University, Ivano-Frankivsk, Ukraine*

In this work, heterojunctions of TiO_2/Cu_2O structures were obtained in a two-step process with a direct current magnetron sputtering method. Can be studied the morphological properties and composition of the thin films by scanning electron microscopy. Optical properties and energy bands at the heterojunction were recorded using a spectrophotometer. Additionally, the current–voltage characteristics examined in both total darkness and under illumination were performed. The possible cause of the lack of a photovoltaic effect was indicated.

Optically Transparent Protective Coatings on the Basis of Ti-Containing Epoxyurethane Oligomers

Yashchenko L.M.[1], Vorontsova L.O.[1], Alekseeva T.T.[1], Tsebrienko T.V.[1], Steblenko L.P.[2], Kuryliuk A.M.[2], Iarova N.V.[1], Brovko O.O.[1]

[1] *Institute of Macromolecular Chemistry of NAS of Ukraine, Kyiv, Ukraine, ynv25@ukr.net*
[2] *Faculty of Physics, Taras Shevchenko National University of Kyiv, Kyiv, Ukraine*

Nowadays scientists are intensively exploring the possibility of hybrid organic-inorganic materials to be applied in various fields as protective, thermoregulating, and optically transparent coatings. In particular, such coatings allow to significantly prolong the service life and to increase efficiency semiconductor solar cells (SCs).

In this research titanium-containing epoxyurethane oligomers were obtained *in situ* via sol-gel synthesis in a polyoxypropylene glycol medium. Polymer films of anhydride curing were obtained on the basis of them. By means IR-spectroscopy method it was shown that in the synthesis of prepolymers $(-TiO_2-)_n$ acts as a catalyst of urethane formation. The introduction of small additives of TiO_2 was established to improve the properties of the films significantly. Namely, it leads to the increase in hydrophobicity, the reduction of water absorption, the raise of hardness from 2H to 5H per pencil scale, and the enhance of adhesion to the aluminum surface. For Ti-containing epoxyurethanes (iEU), a significant raise in the value of the light transmission coefficient is observed (from 59% to 88%). At the same time, its spectral dependence shifts to the short-wave region, which correlates with the spectral sensitivity of silicon SCs. It was revealed that the application of such a coating to the surface of the silicon plates of solar quality (s-Si) prolongs the lifetime of charge carriers both on the surface - from 5 μs to 25 μs – and in the near-surface area - from 100 μs to 400 μs. Probably, the presence of a hybrid iEU coating contributes to a decrease in the number of surface electron states, potentially acting as recombination centers of charge carriers, that indicates its protective function and may enhance the efficiency of s-Si based solar cells.

Thus, having such characteristics, Ti-containing epoxyurethane formulations are promising materials for application as optically transparent protective coatings for silicon photovoltaic converters.

CdS as a Window Layer for Photovoltaic Application of II Generation

Yavorskyi R.S.

Vasyl Stefanyk Precarpathian University, Ivano-Frankivsk, Ukraine, roctyslaw@gmail.com

The second generation of solar cells managed to reduce the material cost by eliminating the use of silicon wafer and replacing it with thin-film technology. This technology is based on amorphous silicon, CIGS, CdTe etc. where the typical efficiency is around 30%. The energy consumption associated with the production of these solar cells is quite high due to the use of vacuum processes and high temperature treatments.

However, conversion efficiencies of homojunction CdTe solar cells have not been encouraging results. Thus, heterojunction cell structure with wide band-gap n-type semiconductor (commonly CdS) and p-CdTe are widely used. From optoelectronic and chemical properties, CdS is the best suited n-type hetero-junction partner to CdTe for high-efficiency and low-cost cells. The maximum theoretical efficiency for its band gap (1.45 eV) and a standard solar spectrum is about 29%.

CdS has high optical energy gap of 2.4 eV therefore the energetic short-wavelength photons can pass to the absorber with minimum absorption loss. The structural, electrical and optical properties of CdS can influence the characteristics of CdS/CdTe interface and consequently the performance of the device.

The performance of CdTe solar cells is strongly limited by the band gap and the thickness of the window layer. Increasing the energy gap of CdS allows large numbers of photons to pass to the absorber layer, consequently the short-circuit current increases. In this aspect, several methods have been studied to increase the energy gap of CdS thin films; such as doping with oxygen, alloying with a semiconductor with a wider energy gap, or carrying out an annealing treatment. On the other hand, decreasing the thickness of CdS layer leads directly to increase the performance of CdTe solar cells through decreasing the absorption losses that take place in window layer as well as higher short-circuit current might be achieved. Moreover, reducing the thickness of CdS increases the possibility of diffusion of CdS to CdTe during the solar cell fabrication process. Such diffusion between window layer and absorber layer can reduce the strain arising from lattice mismatch and thus causes a reduction of defects in the interface. But it is difficult to obtain uniform and pinhole free CdS layers thinner than 50 nm. It was reported that reducing the CdS thickness usually severely reduces the open circuit voltage and fill factor of the cell because thin CdS layer suffers from pinholes and shorts among grain boundaries.

Evaluation of thin film CdS/CdTe solar cells: SCAPS thickness simulation and analysis

Zapukhlyak Z.R.

Vasyl Stefanyk Precarpathian University, Ivano-Frankivsk, Ukraine,
zhanna.zapukhlyak@gmail.com

The PVSCs as one of renewable energy sources have been largely studied nowadays. The main aim of PV manufacturers must be price reducing and efficiency increasing of the solar cells. One of the promising thin film semiconductor materials for photovoltaic energy conversion and producing large area solar cells at low cost has been considered polycrystalline cadmium telluride (CdTe) with module efficiency 18.6% at the moment.

CdTe and CdS/CdTe thin films were obtained by thermal evaporation method with different thicknesses d = (0,01–12) μm on glass substrates. The deposition temperature was T_s = (300-570) K, the evaporation temperature changed within T_v = (600–1370) K. The thicknesses of the films were set by deposition time variation τ = (30–180) sec. CdS deposited on CdTe makes a very promising heterostructure for thin film photovoltaics. The theoretical efficiency of CdS/CdTe solar cell is predicted to be up to 28–30% because of it's appropriate band gap and high absorption coefficient for solar radiation.

The optical properties were analysed by Swanepoel method, using transmission spectra. Optical transmission spectra was investigated by measuring transmittance at normal incidence in the range of 190 – 3300 nm wavelength using Agilent Technologies Cary Series UV-Vis-NIR Spectrophotometer.

Currently numerical simulation have a great importance for understanding physical properties and design of solar cells. Therefore, advanced simulations were performed in electrical solar cell simulator SCAPS-1D to analyze numerically the performances of the proposed CdS/CdTe thin film heterostructures. Quantum efficiency (QE) is one of the most important parameter in solar cell domain.

According provided analysis the cell efficiency increases when the absorbing layer is thinner. The decrease of CdS absorber layer thickness leads to an increase in the quantum efficiency too, it maximizes to 17.46%. This affects also short circuit current Jsc and fill factor FF and finally the conversion efficiency. The QE for most real SCs is reduced because of the effects of recombination. The structure with highest quantum efficciency is CdS/CdTe with layers thicknesses (1 nm/3 μm) respectively.

This study is of great interest and has shown that CdS/CdTe heterojunctions have the prospect of using as photovoltaic light converters due to their high absorption capacity.

POSTER REPORTS

Session 7
Innovative methods for teaching

Interactive Technologies Using in the Chemical Disciplines Teaching

Dmytriv A.M.

Ivano-Frankivsk National Medical University, Ivano-Frankivsk, Ukraine,
dmytriv-ang@bigmir.net

A significant increase of the amount of information, that becomes nowadays, the present new requirements for the knowledge that higher education graduates have to possess, and hence to teaching technologies. Educational process should be directed to "A person who is able to solve various tasks and is guided in the information space" today.

The teaching aim of chemical discipline at the pharmaceutical faculty is formation scientific worldview in the students, develop their modern forms of theoretical thinking, and the ability to analyse phenomena, the formation of abilities and skills for the chemical laws application and processes in future practice, the competent use of chemical substances and materials in the pharmaceutical industry.

Therefore, the use of information and communication technology in education opens new perspectives and opportunities for learning of the material and further refines their professional skills and knowledge. Almost every class or lecture, to interest students in learning new material, taking into account their level of knowledge, autonomy and activity, the teacher can choose the method of interactive teaching.

Currently, computer technology is effectively used in the study of chemical disciplines, in particular for the simulation of chemical phenomena and processes, the control and processing of chemical experiment data, the organization of laboratory work, and the control of students' knowledge. In each practical class, certain programs can be used based on the objectives of the class, where the functions of the teacher and the computer may be different. The experience of using computer technologies in chemistry practical classes at higher educational institutions shows that their systematic use at the stage of studying the material, and at the stage of operational control over the acquisition of knowledge, is important for obtaining a high educational effect.

Consequently, the most effective ways to increase the efficiency and quality of training specialists in modern conditions, is to build a learning process based on interactive technologies with the use of problem learning. The teacher must find motivation for the student and build his activity so that the student has desire to learn and discover a new one.

Interactive Modelling for Remote Execution of Laboratory-Based Works

Forostyana N.P., Romanenko R.P., Kryvoruchko M.Y.

Kyiv National University of Trade and Economics, Kyiv, Ukraine, Romanco@ukr.net

The basic ways of developing interactive models of physical experiments and the method of applying the *Multimedia Laboratory ITM* software package and *Multi-Purpose Measuring Computer Device* for recording an experiment at laboratory classes and reproduction of experimental procedure during remote execution of laboratory-based work are offered.

Realization of remote execution of laboratory-based works has several perspective approaches. One of them is creation of a multimedia experimental procedure project. By now, the teachers of the Department of Engineering and Technical Disciplines (KNUTE) have been working with equipment and software of the *ITM* firm, the domestic producer of training equipment, for more than 10 years.

The *Multimedia Lab ITM* program allows to create a multimedia experimental procedure project (consisting of a task text file, description, a protocol pattern, video with explanation of essence of an experiment, a group of files with experimental procedure data), with further reproduction on any computer. All experimental procedure data are fixed by real digital sensors of the measurement module without the possibility of their change or correction, which, on the one hand, does not allow a student to falsify the result data, and on the other, the data contain real measurement uncertainties that would be available during a real experiment.

The sensor control settings allow to regulate frequency of data acquisition depending on an experiment. For the training software version, the highest frequency is 50,000 Hz, for the scientific one – 10,000 Hz, the lowest frequency for both program versions is 1.7×10^{-4} Hz. High frequency is required for electrical phenomena and fixation of instantaneous processes, for example, the maximum value of force while breaking a skin of berries by a penetrometer. However, high measurement frequency evokes difficulties during data array processing.

For further use of the multimedia project as a standalone electronic learning tool, it is saved in the *Experiments* directory. Review of a recorded experiment or its demonstration in a classroom does not require connection of the device so the saved experiment can be used for remote data processing and remote execution of a laboratory-based work.

Features of the Google Classroom Learning Management System

Garpul O.Z.

[2]*Vasyl Stefanyk Precarpathian University, Ivano-Frankivsk, Ukraine, ogarpul@gmail.com*

The development of the information society (IS) makes it necessary to use information and communication technologies (ICTs) in the management of the quality of education. The virtual classroom is not a distance education in the traditional sense of the word, it is an online learning environment, an on-the-spot learning that is implemented through modern Internet technologies and web applications. Worthy of note is the Google-based service developed by Google Apps for Education - the Google Classroom Learning Management System (LMS), the Google Docs, Google Drive and Gmail tool that's easy to use and helps teachers create and organize tasks, present ratings, comment and organize effective communication with students in real time. For effective work with students of the specialty "Physics. Secondary education "on the subject" Informatics and programming" was created a virtual class, through which the organization of the educational process (Figure 1).

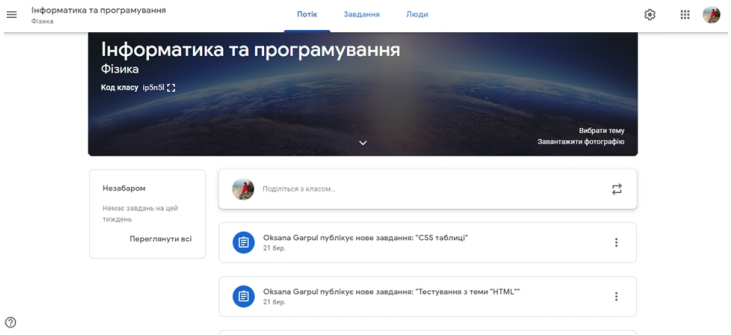

Fig.1 Screenshot of the virtual class page for students of the specialty "Physics. Secondary education "on the subject" Informatics and programming

With the Google Classroom, students can store their work files and perform tasks in Google Drive. Teachers have the ability to create and collect tasks online, view these tasks, and provide results of checking for each student, make announcements, ask questions and leave comments for students real-time. It allows to establish permanent communication with students not only at classes, but also during extracurricular time. Google Classes automatically creates folders for Drive for each task and student, on the task page students can always find out what work they need to do. On the basis of experience, we can conclude that the organization in the virtual classroom training contributes to enhancing motivation for learning and better study material.

1. Kalinina LM, Noskov MV Google's Teaching Services. First steps for a beginner: A tutorial. - Lviv, ZUCTS, 2013. - 182 p.
2. Google "Class" [Electronic resource]. - Access mode: https://classroom.google.com.

Educational Process in the System of Postgraduate Education Using Differentiation

Hotsuliak K.

Vasyl Stefanyk Precarpathian National University, Ivano-Frankivsk, Ukraine, Kate81@i.ua

The article describes the pedagogical conditions of teacher training in the system of postgraduate education, analyzes the significance and necessity of using differentiated learning in elementary school.

Among such pedagogical conditions it is defined: activation of the motivation of the elementary school teacher for the effective use of differentiated training of junior pupils; improvement of the content component of the postgraduate pedagogical process in order to expand the scientific representations of the teacher on differentiated training of junior pupils; use of training technologies for the implementation of differentiated learning in elementary school.

Consider the implementation of certain pedagogical conditions.

The first pedagogical condition - activization of the motivation of the elementary school teacher to the effective use of differentiated education of junior schoolchildren - envisaged the following tasks: the study of the theoretical basis of the very concept of "motivation", theories of motivation, functions of motivation.

The second pedagogical condition - the improvement of the content component of the postgraduate pedagogical process with the aim of expanding the scientific representations of the teacher about differentiated learning of junior schoolchildren - was implemented through the introduction of the content of the postgraduate pedagogical process of the author's special course "The Variance of Forms of Educational Work with Primary School Students."

The third pedagogical condition involved the use of training technologies for the implementation of differentiated learning in elementary school. Possible variants of their integration into the educational process of universities, the use of various training centers and similar organizations.

There is no doubt that the use of training technology is focused on the development of critical thinking, the search for answers to problematic professional situations, the creation of a relaxed communication between the teacher-trainer and the academic group.

1. Amonashvili Sh. A. To give the child a spark of knowledge, the Master must absorb the Sea of Light / Sh. A. Amonashvili. - Donetsk: [b. in.], 2009. - 84 p.
2. Babansky Yu.K. Optimization of the learning process: the generaladical aspect / Yu. K. Babansky. - M.: Pedagogics, 1977. - 250 s.
3. Baranova N.P. Trainings for Teachers of Pedagogical Excellence / N.P. Baranova. - X .: View. Group "Basis", 2009. - 159 p.

Method of Determination of Risk Caused by Industrial Danger

Koshel V.I., Poplavskyi O.P., Dzundza B.S.,
Saviuk H.P., Matkivskiy O.M., Poplavskyi I.O.

Vasyl Stefanyk Precarpathian National University, Ivano-Frankivsk, Ukraine, kbgd@pu.if.ua

One of the most man-made threats to the population and the environment are high-risk objects. Accidents on these objects, including fires, explosions, leakage of dangerous substances, can lead not only to the loss of people with potent poisonous substances, but also to the negative impact on the environment, the destruction of houses and buildings. The integral indicator of the level of technogenic safety in the region is determined by: the average individual risk of death in the result of an emergency situation for the population of the region; material damage to the region as a result of an emergency; saturation of the territory of the region where an emergency occurred.

In the field of technogenic safety, the functional structure includes: a system of monitoring, risk analysis and emergency forecasting as a basis for the reduction of the risk of emergencies; the system of prevention of emergency situations and mechanisms of state regulation of risks; liquidation system of the emergency. Quantitative assessment of technogenic risks creates a favorable basis for the classification of all economic objects by the degree of danger and makes it possible to apply to them the legal norms and state mechanisms of administrative and economic influence in order to ensure an acceptable level of risk.

It is expedient to analyze the risk of technological objects at the stage of designing an object or introducing new technologies according to the scheme:

- identification of hazards, possible accidents and scenarios for their development;
- analysis of the technological specificity of the object;
- quantitative estimation of frequency of accidents;
- selection of methods and models for studying the degree of danger and quantitative assessment of the level of risk using models;
- to develop possible scenarios for the development of accidents, taking into account the conditions of their occurrence, and to calculate the probable areas of influence of the impressive factors under different scenarios of the development of accidents;
- to evaluate possible negative consequences of accidents;
- development of risk management methodology.

Quantitative analysis of man-made risk should be conducted using statistical methods, probabilistic methods, expert methods and methods using index estimates.

Augmented Reality as a Tool for Improving Effectiveness of Natural Sciences Study

Midak L.Ia., Kuzyshyn O.V., Kravets I.V., Buzhdyhan Kh.V., Lutsyshyn V.M.

Vasyl Stefanyk Precarpathian University, Ivano-Frankivsk, Ukraine,
khrystja.buzhdyhan@gmail.com

It is a common knowledge that visualization of the study material makes its perception and digestion easier [1, 2]. A properly selected demonstration material helps understand various physical processes and phenomena, the structure of chemical compounds as well as mechanisms of their interference in a better way. These days, usual 2D-images of the traditional handbooks, textbooks and monographs do not give the full image about special structure of molecules, mechanisms of chemical reactionpaths, etc. In this way, for an effective study of natural sciences it is more than reasonable to use different demonstrations, which are impossible without implementation of Augmented Reality realization apps. Augmented Reality (AR) gives an opportunity to visualize the object (atoms and molecules, their interference, device circuits, technological processes, etc.) as much, as possible, which means to convert 2D images into 3D, as well as “make it alive”. While studying paragraphs of nuclear physics, the pupils view types of nuclear decay, nuclear chain reaction, structure of nuclear weapons, operating principles of a nuclearpower station and other subjects, an important element of which are not only a properly selected illustration of one or another concept, but also the demonstration of the very process (nuclear fission, operating mechanism of a nuclear warhead, operation of a NPS). A mobile application with Augmented Reality was created for such kind of illustrations. Augmented Reality markers were created on the platform “Vuforia”, 3D-objects were modelled in 3DMax, augmented reality objects were performed with a multi-platform tool for development of two- and three-dimensional applications “Unity 3D”.

Utilization of augmented reality objects gives the tutor an opportunity to explain a big amount of theory quickly and understandably, and for the students to digest it effectively, updated their creative thinking and boosts motivation for study.

1. Donets I.M. Vykorystannia informatsiino-komunikatsiinykh tekhnolohii ta Internet-resursiv dlia pidvyshchennia yakosti khimichnoi osvity v shkoli [The Application of information and communication technologies and Internet resources for improving the quality of chemical education at school]. virtkafedra.ucoz.ua. Retrieved from: virtkafedra.ucoz.ua/el_gurnal/pages/vyp14/Donec.pdf [in Ukrainian].
2. Cherniavska T.M. Vykorystannia IKT ta mozhlyvostei Internet na urokakh khimii [The Application of ICT and Internet facilities in chemistry classes]. (n.d.) teacher.ed-sp.net. Retrieved from: http://teacher.ed-sp.net/index.php?option= com_content&view= article&id= 120%3A2013-05-22-06-31-14&Itemid=25 [in Ukrainian].

Use of Technology of Organization of Project Activity in the Professional Training of Masters

Pletenytska L.S.

Vasyl Stefanyk Precarpathian National University, Ivano-Frankivsk, Ukraine,
ulja-cool@ukr.net

A significant trend in the training of masters in pedagogy is the unity and diversity of educational space. The future of the world is the project-advanced training; therefore, the implementation of this social task is to create a model of competence-oriented education. The project method is a leading means of transforming education of learning into education of life, mastering practical skills of planning their own activities, skills of choosing means and ways of its implementation, formation and actualization of life experience. The typical features of the project method are the possibility of creating such a learning environment in which the teacher trains, directs, investigates and strengthens relevant levels of understanding, as well as the fact that the form of control of professional knowledge, skills and abilities is a real product: tests, multilevel exercises, competence-oriented tasks, integrated tasks, lesson notes. At the same time, the masters form personal and professional qualities, which include the ability to work in a team (group long-term projects), take responsibility for the chosen decision (individual, short-term projects), analyze the results of colleagues' activities and feel like a member of the teaching staff.

Each pedagogical technology has its own specifics, advantages and certain difficulties of use. The features of the project activity determine planning of activity over a long period of time (classes, semester, course), the creation of a plan, a summary of the results of each phase; a combination of individual and collective activities on modeling and approbation of projects, use of a system of methods, directing the activities of future teachers to produce a practically significant product for teachers (collections of integrated essays on mathematics, copyright projects for the formation of mathematical competences for primary education).

Project planning includes familiarization with the relevance of the topic, justification of the ways of solving the problem, determination of criteria for evaluating activities. In the process of project implementation, masters need to identify sources of information and ways to collect them, independent scientific or research activities, distribution of responsibilities between participants during collective and group projects (teacher, vice principal, principal), making an educational product. The project summary involves design of the results, preparation for the presentation, defense, assessment of the activity, conclusions (score for the topic, examination). Formation of professional competence of teachers-masters in the process of teaching the mathematical disciplines with the help of the project activity induces systematic cognition of skills in teaching methods and technologies.

Competence Approach to Teaching Masters of Pedagogical Specialties the Disciplines of the Mathematical Cycle

Pletenytska L.S., Mezhylovska L.Y.

Vasyl Stefanyk Precarpathian National University, Ivano-Frankivsk, Ukraine,
ulja-cool@ukr.net

In the context of the implementation of the objectives of the development of New Ukrainian School, the modern stage of preparation of masters of pedagogical specialties is marked by the search by scientists (A. Khutorskyi, A. Tykhonenko, Y. Trofymenko) and methodologists (O. Korchevska, S. Skvortsova, O. Onopriienko) for the ways of providing didactic and organizational conditions favorable for the development and self-development of the personality of the future teacher. The basis for the implementation of the competence approach in the formation of professional and methodological competencies of masters is the harmonization of the national normative educational base with the relevant international documents. Among the measures aimed at adapting masters to European educational standards, the formation of a learning system throughout the whole pedagogical activity and improving its quality, the NQF has been developed and adapted as part of the European Qualifications Framework for lifelong learning. The requirements for practical and general educational competencies of a person at various educational levels – from pre-school to post-doctoral – are described in the NQF and its European analogues.

With the masters of the specialty “Primary Education”, we use the definition of competence, according to the Tuning project of the European Commission, as a dynamic combination of knowledge, understanding of the skills, values, other personal qualities of the teacher, which describe the results of training in the educational program, acquired realizational abilities of the individual to effective activity. During the study of theoretical modules of mathematical disciplines, we teach masters to perceive and transform information into models of problem life situations, to compare action algorithms for solving mathematical problems.

The content of the practical modules involves the formation of skills and abilities to turn information into charts, tables, graphs, figures, models. Based on the basic curricula during the pedagogical practice, we offer to carry out full or partial integration of the tasks of the mathematical field with others. The variability of the content of the preparation of masters of pedagogical specialties is ensured through the introduction of special courses for the students to choose. We conduct the certification of masters in mathematical disciplines in the form of project defense. Implementation of the competence approach in the process of professional training of masters of the specialty "Primary Education" provides for the creation of such learning conditions, under which each student can maximize the theoretical knowledge, personal and creative abilities.

The developed competence-oriented methods for training masters of the pedagogical specialties constitute prospects for further research on the identified problem.

Using Maple Environment in Teaching Quantum Mechanics

Vozniak O.M.[1], Turovska L.V.[2], Prokopiv V.V.[1], Nykyruy L.I.[1]

[1]*Vasyl Stefanyk PreCarpathian National University, Ivano-Frankivsk, Ukraine, prkvv@i.ua*
[2]*Ivano-Frankivsk National Medical University, Ivano-Frankivsk, Ukraine*

In contrast to the classical branches of theoretical physics, such as classical mechanics or electrodynamics, which are quite visual, quantum physics is largely abstract, and it is often difficult to imagine a physical picture of quantum phenomena. At the same time, in recent decades a number of software packages of so-called “computer mathematics” have been developed, which can greatly facilitate the carrying out complex, long and routine calculations, visualize obtained results, and in many cases, implement problem solving.

One of such mathematical packages is Maple computer algebra system, which was developed several decades ago and is continuously being improved. Due to its simple and convenient interface and powerful software, it is widely used not only for educational purposes, but also as a research tool. Therefore, when teaching future specialists, it is important to make this tool familiar to them in their future professional activity.

In this paper, we have considered a number of problems of quantum mechanics, in which the package is used for illustration of the main points of quantum mechanics course, solving exactly solvable problems by means of symbolic mathematical transformations, for which the result can be obtained in analytical form, numerical implementation of finding the solution of problems and graphical presentation of results. A sufficient amount of information on the basic features of Maple computer math package has been presented, which allows the student to actively use the mentioned package and to deepen the skills of its use through self-education.

1. Vozniak O.M., Prokopiv V.V., Nykyruy L.I. Using Maple environment to solve quantum mechanics problems: навчальний посібник. Ivano-Frankivsk: Vasyl Stefanyk Precarpathian National University, 2018. 156 p.

School on the Properties of the Principality the Use of Innovative Technologies of the New Ukrainian

Vysochan L.M.

Vasyl Stefanyk Precarpathian National University, Ivano-Frankivsk, Ukraine,
lesjavusochan@gmail.com

The new Ukrainian school is a key reform of the Ministry of Education and Science. The main purpose of this is to create a school in which children will be pleased to learn and give them not only theoretical knowledge, but also the ability to apply them in life [3]. She needs to help form conscious motivation for learning, self-organization and self-development. One of the features of the modern education system is the coexistence of two strategies for organizing learning - traditional and innovative [1, c.58]. Innovation in translation from Greek means "updating, novelty, change". With regard to the pedagogical process, innovation means the introduction of new in the purpose, content, methods and forms of education and education, the organization of the joint activities of teachers and students [4, c. 25]. I. Kotlyarova gives the following definition: "innovation - a phenomenon in the field of education that objectively arises or is projected and characterized by the creation, development, testing, the introduction of educational innovation, which contributes to improving the quality of education in broad sense (favorable to human changes in its intellectual, emotional, spiritual and physical spheres); which manifests itself in the emergence of fundamental changes in the content of education, in the course of educational processes, in educational relations, in the properties of subjects of innovation, in educational means or educational space [2, c.16. Currently, the school needs such an organization of its activities, which would ensure the development of individual abilities and creative attitude to the life of each student, the introduction of various innovative educational programs, the implementation of the principle of a humane approach to children.

1 Dichkivska I.M. Innovative pedagogical technologies. K., 2004. 352 p.
2. Kotlyarova I.O. The systematization of innovation management in an educational institution. Chelyabinsk: YUr-GU, 1998. - 129p.
3. New Ukrainian School: Web site.URL: /http://nus.org.ua/tags/114/
4. Taraduk N.V. Panasyuk O.P. Innovative Technologies: Creative and Educational Aspect: Monograph, Lutsk: Tverdinya, 2009. 164 p.

Fractality and Innovative Concepts of Teaching Natural Sciences at Higher Educational Institutions and Universities

Yurkovych Nataliya, Mar'yan Mykhaylo, Seben Vladimir *

Uzhhorod National University, Uzhhorod, Ukraine, nataliya.yurkovych@uzhnu.edu.ua
**University of Presov, Presov, Slovakia*

At the present stage of the development of science education and information technology, their integration, complementarity and implementation are extremely important. Therefore, the search of methods of teaching natural sciences, based on the principles of self-organization and computer modeling, corresponds to the immediate tasks of the present [1,2].

The possibility of applying the fractal approach in the study of natural sciences are foundated. Features of fractals - self-similarity on spatial and temporal scales, integrity and algorithmic self-sufficiency, as adequate and acceptable for description and information representation of physical processes is considered. The iterations of the fractal structure on the example of studying sections of physics "Geometric optics" and "Wave optic" elaborated. It is shown that each iteration is characterized by a synergy - adding new iteration provides a qualitative perception of the new information. The possibility of using this approach in other sections of natural sciences, and research fields related to physics has been demonstrated. It manifests the formation of a fractal structure and the corresponding iterations, reflecting the integrity and spontaneity of information perception. Based on the proposed synergistic approach to the use of subject areas of knowledge and computer modeling, the fractal structure is formed on an intuitive level. The functioning of this structure manifests itself in a qualitative transition to self-sufficiency of students, which involves the use of a creative approach and the desire to apply the received information in radically new fields [3]. The ways of implementation an innovative fractal approach to the study of natural sciences, taking into account the synergy between different sciences and disciplines are considered.

References

1. Yurkovych, N., Seben, V., & Mar'yan, M. (2017). *Computer modeling and innovative approaches in physics: optics.* - Presov: Prešovska univerzita v Prešove. 113 P.
2. Yurkovych, N., Seben, V., & Mar'yan, M. (2017). Fractal approach to teaching physics and computer modeling. *Journal of Science Education*, 18(2), 117-120.
3. Mar'yan M., Seben V., & Yurkovych N. (2018). *Synergetics and Fractality in Science Education.* Presov: University of Presov in Presov Publishing, 168 P.

Assessment Technologies of Social-Oriented Management in Educational Institutions

Blahun N.M.

Vasyl Stefanyk Precarpathian National University, Ivano-Frankivsk, Ukraine,
n.blahun@gmail.com

Domestic and foreign scientists consider educational technology as an important means of improving the quality of identity formation.

Its subject matter brings together a clash of several opposing points of view. Some scientists consider teaching as a complex technology of modern teaching aids, others – as a process of communication. There is also a separate group of scholars who consider the concept of "Educational Technology" as means and processes of learning. The formation of Educational Technology as a science took place in the 60-s of the twenties century. However, some of the scientists identified the concepts of "Learning Technology" and "Educational Technology" as equal. A multidimensional approach to the concept of "educational technology" has been formed gradually. According to our point of view, the most complete definition of this concept was provided by P. Mitchell in his "*Encyclopedia of Educational Media Communications and Technology"*. "As Educational Technology is not synonymous with "teaching aid", it served as an interdisciplinary conglomerate, which concerns virtually all aspects of education: P. Mitchell describes Educational Technology as, "an area of study and practice (within education) concerned with all aspects of the organization or educational systems and procedures whereby resources are allocated to specified and potentially replicable educational outcomes". In 1979, the US Association for Educational Communication and Technology published the «official» definition of Educational Technology as, "a complex, integrated process involving people, procedures, ideas, devices and organization for analyzing problems and devising, implementing, evaluating and managing solutions to those problems involved in all aspects of human learning". The US scientists define Educational Technology as, "not mere research in the field of using technical aids or computers, this investigation aims to identify the principles and develop methods of optimizing the educational process by analyzing the factors that confirm their effectiveness through the establishment and implementation of techniques and materials, and using assessment methods.

Domestic and foreign literature review of "Educational Technology" definitions allows us to draw the following conclusions:

– technification of "intellectual production" what education stands for, is an objective, logical and irreversible process, a means of boosting students' educational level;

– variety and variability is traced in the theory and teaching practice, which are determined by educational theories, scientific approaches, concepts, principles, specific key aspects and components of pedagogical process;

– technologies of educational process are characterized by multidimensionality, due to the peculiarities of the content, methods and means of interaction between the parties of the learning process;

– structure of educational technology includes: a) conceptual framework;

b) content part (goals, content); c) procedural part — work activity.

New Technique of Progressive Spiral Scratch Test

Zakiev V.I.[1], Zakiev I.M.[1], Voloshko S.M.[2], Vladimirskiy I.A.[2]

[1] *National Aviation University, Kyiv, Ukraine, zakiev@ukr.net*
[2] *National Technical University of Ukraine "Igor Sikorsky KPI", Kyiv, Ukraine*

Scratch test is one of the most simple and widely used techniques for assessing adhesion strength of film/substrate systems. The test is based on generating of controlled scratch with indenter on a selected area. Coating will start to fail at a certain critical load which can be detected according to the changing of tangential force or using optical microscope. This test gives ability to characterize scratch resistance and adhesion strength only along scanning path. To empower this method and characterize strength portrait of the surface we propose technique of progressive spiral scratching which is realized on the multifunctional micro/nano indentation tester «Micron-gamma» [1]. It is based on generating of spiral scratch with gradually increasing and then decreasing load on the indenter ***P*** with recording of tangential force during the test. Spiral scratching is realized by simultaneous specimen rotation with speed ***w*** and linear movement of the indenter ***L*** (fig. 1, a).

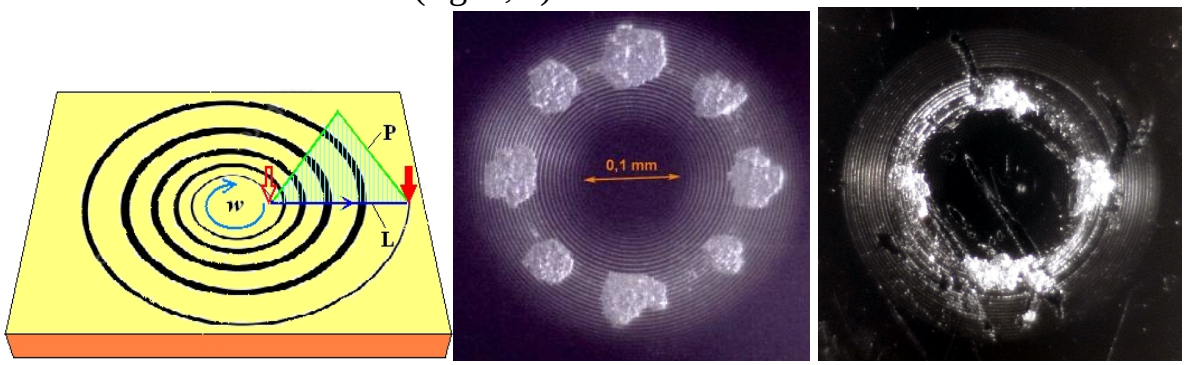

a *b* *c*

Figure 1 Schematic of the progressive spiral scratch test (a), uncoated single-crystal Si with maximum load 25 gf (b) and Ni/Cu/Cr nanoscale system deposited onto Si (100) single-crystal substrates with maximum load 120 gf (c) after progressive spiral scratching using Vickers indenter.

Obtained results show that brittle fracture of single-crystal Si (fig. 1, b) starts along crystallographic planes with maximum load on indenter 20-25 gf. Deposited by DC magnetron sputtering Ni/Cu/Cr nanoscale system with 25 nm thickness of each layer onto Si(100) single-crystal substrates increase resistance to brittle fracture in several times (fig. 1, c). It will start to fail with maximum load on indenter 120 gf. Proposed method can be used to characterize adhesion and strength portrait of the surface.

1. Ignatovich S.R., Zakiev I.M. Universal Nano-Hardness Tester "Micron-Gamma". *Zavodskaya laboratoriya. Diagnostika materialov*. 2005. vol. 77, № 1, pp. 61-67.

[335]Photoluminescence Properties and Photostability of CdSe Quantum Dots Doped with Silver and Copper Ions

Borkovska L.V.[1], Korsunska N.O.[1], Stara T.R.[1], Rachkov A.E.[2]

[1]*V. Lashkaryov Institute of Semiconductor Physics, 41 Prosp. Nauky, 03028 Kyiv, Ukraine, bork@isp.kiev.ua*

[2]*Institute of Molecular Biology and Genetics of NAS of Ukraine, 150 Zabolotnogo Str., 03680, Kyiv, Ukraine, oleksandr_rachkov@yahoo.com*

Significant progress achieved in the last decade in the development of the methods for synthesis of luminescent quantum dots (QDs) has opened wide prospects for their application in a variety of optoelectronic devices, as well as in biology and medicine. The doping of QDs with metal impurities is one of the methods for control of their photoluminescence (PL) spectrum. However, photostability of doped QDs was not studied sufficiently.

In this report, the results of the investigations of PL and photostability of nano-composites of undoped and doped with copper and silver ions CdSe QDs embedded in gelatine and polyvinyl alcohol films (PVA) films are presented. The QDs were synthesized in an aqueous solution and transferred after dialysis to the solution of corresponding polymer. The doping of QDs was carried out in the process of their synthesis.

The PL spectra of undoped QDs show a band edge PL and a wide band caused by PL of intrinsic defects of QDs. The doping of QDs results in complete suppression of band edge PL and a shift of defect-related band to the short-wavelength spectral region. The latter, apparently, is due to appearance of characteristic PL of corresponding impurities. The PL excitation spectra show that several ensembles of QDs are formed in the case of Ag doping. The QDs embedded in gelatine demonstrate the PL bands of higher intensity and shifted to shorter wavelengths as compared to the QDs in PVA.

An irradiation of the nano-composites with light corresponded to band-to-band absorption in the QDs produce significant changes in the PL spectra. In particular, the PL spectra of undoped QDs show a decrease in the intensity of the defect-related PL and an increase in the intensity of the band edge PL accompanied with a shift of its maximum to the long-wavelength spectral region. These changes are considerably larger for the QDs in PVA. In turn, the irradiation of Ag doped QDs embedded in PVA results in darkening of the film and, as a consequence, a decrease in the intensity of defect-related PL. It is proposed that some silver compounds, presumably of metallic silver, are formed on the surface of QDs under light irradiation. At the same time, the nano-composites with Cu doped QDs do not change their optical characteristics under prolonged irradiation. The obtained results indicate that the QDs in gelatine are more photostable than the QDs in PVA, and the Cu doped QDs are more photostable than the Ag doped ones.

[336]Advances in Laser Nanostructuring of Metal Surfaces

Gnilitskyi Iaroslav[1] and Orazi Leonardo [2]

[1]*NoviNano Lab LLC, 79000, Lviv, Ukraine*
[2] *DISMI, University of Modena and Reggio Emilia (UNIMORE), 41122, Reggio Emilia, Italy*
E-mail: iaroslav.gnilitskyi@novinano.com

Formation of laser-induced periodic surface structures (LIPSS) under laser irradiation is of high interest for the nanostructure-demanding applications [1]. Recently, the possibility to obtain a high regularity at high processing velocities was demonstrated on Cr, Ti and Si [2] in the regime of laser-induced oxidation.

Conversely, we demonstrate in this work the formation of highly-regular nanostructures LIPSS (HR-LIPSS) at the surface of several materials, in the regime of ablation. The experimental parameters leading to the formation of HR-LIPSS on large area at high velocity are provided for a number of materials such as Mo, various types of steel alloys, Ti and alloys, Zr, and Si [3,4].

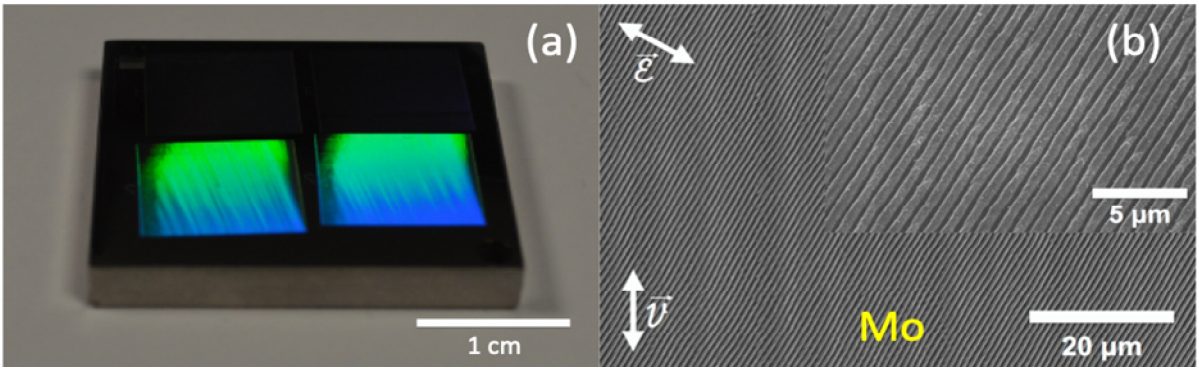

a b

Fig. 1. (a) Macrophoto of stainless steel sample treated by nanostructures LIPSS. (b) SEM image of highly regular LIPSS-based nanopatterning .

This work helps to bring a better control in the formation of laser-induced periodic structure in ablation regime. A competitive process for industrial applications based on nanostructuring can be envisionned [3-4].

[1] J. Bonse, S. Hohm, S. V. Kirner, A. Rosenfeld & J. Kruger, "Laser-Induced Periodic Surface Structures – a Scientific Evergreen" *IEEE Journal of Selected Topics in Quantum Electronics 1, xxxxx* (2016).

[2] I. Gnilitskyi, T. J.-Y. Derrien, Y. Levy, N. M. Bulgakova, T. Mocek, L. Orazi, "High-speed manufacturing of highly regular femtosecond laser-induced periodic surface structures: physical origin of regularity", Nature:Sci.Rep 7, 8485 *(2017)*

[337]Bimetallic Nanocatalysts PtCu and PtNi for Fuel Cells

Chernikova O.M.[1], Ogorodnik Y.V.[2]

[1]*Kryviy Rih National University, Kryviy Rih, Ukraine, hmchernikova@gmail.com*
[2]*Radiation Monitoring Devices, Inc. USA*

Of particular interest are fuel cells (PEs), which are an integral part of energy devices. As a catalytic component in PE, as a rule, use platinum. Its main disadvantages include degradation during long-term work in the PE, as well as high cost. The solution of these problems is associated with the development of multi-component catalytic systems based on platinum with the inclusion of other metals. The strategies of their development really depend on a detailed understanding of the mechanisms of oxidation of fuel and the recovery of oxygen [1].

We review the physical mechanisms of heterogeneous catalytic oxidizing reactions methanol oxidation with using bimetallic film layered mechanically strained PtNi and PtCu-based catalysts. The main research methods are theoretical calculations based on the density functional theory and the ″ab initio″ pseudopotential method. The work illustrates that the mechanical stress and the presence of dissociated oxygen have the greatest impact on increasing electron bimetallic catalyst activity during the oxidation of methanol with using bimetallic layered mechanically strained PtNi and PtCu-based catalysts. The compression of the platinum film pushes the electron density outside the film and it gives the density an elongated form and increases the chemical and absorption activity of the film.

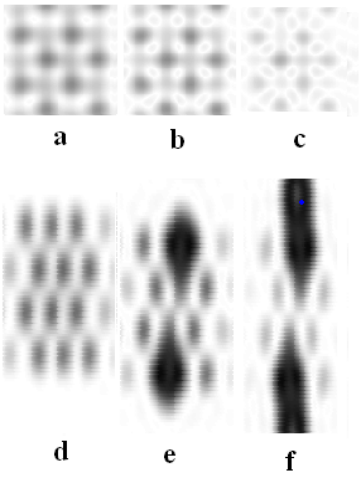

Fig. 1 Intersections of spatial density distributions of valence electrons in planes (110) and (100) 32-atoms film Cu atom of methanol on the surface (the center of the molecule is located above void between atoms on surface layer of catalyst) and the oxygen atom of the molecule of O_2 is dealt face up in the position between the surface atoms of Cu catalysts: (a, d) film Cu; (b, e) film Cu with the addition of the atom O; (c, f) Cu film with atom O and molecule of methanol.

1. Yoshiyuki Show, Yutavo Ueno Formation of platinum catalyst on corbon black using on in-liquid plasma method for fuel cells// J. Nanomaterials, 2017, V.7, pp. 31-40.

AUTHORS INDEX

Наукове видання

ФІЗИКА І ТЕХНОЛОГІЯ ТОНКИХ ПЛІВОК ТА НАНОСИСТЕМ
Збірник тез XVII Міжнародної Фреїківської конференції

МКФТТПН-XVII

PHYSICS AND TECHNOLOGY OF THIN FILMS AND NANOSYSTEMS
Abstract Book of XVII International Freik Conference

ICPTTFN-XVII

Відповідальний за випуск *Любомир Никируй*

Усі тези подано у авторський редакції

Підписано до друку 22.04.2019.
Формат 60x84/$_{16}$. Ум. др. 23,5 арк. Гарнітура «Times New Roman».
Папір офсетний, друк цифровий. Тираж 300 примірників.

Видавець
ДВНЗ «Прикарпатський національний університет
імені Василя Стефаника»,
вул. С. Бандери, 1, м. Івано-Франківськ, 76000.
Тел. (0342) 71-56-22.
E-mail: vdvcit@pu.if.ua

Свідоцтво суб'єкта видавничої справи
ДК №2718 від12.12.2006.